OPTIMUM USAGE AND ECONOMIC FEASIBILITY OF ANIMAL MANURE-BASED BIOMASS IN COMBUSTION SYSTEMS

A Dissertation

by

NICHOLAS THOMAS CARLIN

Submitted to the Office of Graduate Studies of
Texas A&M University
in partial fulfillment of the requirements of the degree of

DOCTOR OF PHILOSOPHY

May 2009

Major Subject: Mechanical Engineering

OPTIMUM USAGE AND ECONOMIC FEASIBILITY OF ANIMAL MANURE-BASED BIOMASS IN COMBUSTION SYSTEMS

A Dissertation

by

NICHOLAS THOMAS CARLIN

Submitted to the Office of Graduate Studies of
Texas A&M University
in partial fulfillment of the requirements of the degree of

DOCTOR OF PHILOSOPHY

Approved by:

Chair of Committee, Kalyan Annamalai
Committee Members, Jerald Caton
Warren Heffington
John Sweeten
Head of Department, Dennis O'Neal

May 2009

Major Subject: Mechanical Engineering

ABSTRACT

Optimum Usage and Economic Feasibility of Animal Manure-Based Biomass in Combustion Systems. (May 2009)

Nicholas Thomas Carlin, B.S., The University of Texas at Austin;

M.S., Texas A&M University

Chair of Advisory Committee: Dr. Kalyan Annamalai

Manure-based biomass (MBB) has the potential to be a source of green energy at large coal-fired power plants and on smaller-scale combustion systems at or near confined animal feeding operations. Although MBB is a low quality fuel with an inferior heat value compared to coal and other fossil fuels, the concentration of it at large animal feeding operations can make it a viable source of fuel.

Mathematical models were developed to portray the economics of co-firing and reburning coal with MBB. A base case run of the co-fire model in which a 95:5 blend of coal to low-ash MBB was burned at an existing 300-MW_e coal-fired power plant was found to have an overall net present cost of $22.6 million. The most significant cost that hindered the profitability of the co-fire project was the cost of operating gas boilers for biomass dryers that were required to reduce the MBB's moisture content before transportation and combustion. However, a higher dollar value on avoided nonrenewable CO_2 emissions could overrule exorbitant costs of drying and transporting the MBB to power plants. A CO_2 value of $17/metric ton was found to be enough for the MBB co-fire project to reach an economic break-even point.

Reburning coal with MBB to reduce NO_x emissions can theoretically be more profitable than a co-fire project, due to the value of avoided NO_x emissions. However, the issue of finding enough suitable low-ash biomass becomes problematic for reburn

systems since the reburn fuel must supply 10 to 25% of the power plant's heat rate in order to achieve the desired NO_x level. A NO_x emission value over $2500/metric ton would justify installing a MBB reburn system.

A base case run of a mathematical model describing a small-scale, on-the-farm MBB combustion system that can completely incinerate high-moisture (over 90%) manure biomass was developed and completed. If all of the energy or steam produced by the MBB combustion system were to bring revenue to the animal feeding operation either by avoided fueling costs or by sales, the conceptualized MBB combustion system has the potential to be a profitable venture.

DEDICATION

To my lovely wife, Ann Marie

ACKNOWLEDGEMENTS

I would like to thank my committee chair, Dr. Kalyan Annamalai, for his guidance, and committee members, Dr. Warren Heffington, Dr. Jerald Caton, and Dr. John Sweeten. I would also like to thank Dr. Wyatte Harman of the Texas A&M Blackland Research and Extension Center in Temple, Texas for his invaluable guidance on Engineering Economics throughout my research.

Thanks to my friends and colleagues at the Texas A&M University Coal and Biomass Laboratory: Mi Amigo Dr. Gerardo Gordillo Ariza, Dr. Hyukjin Oh, Mr. Ben Lawrence, Sergeant Patsky Gomez, and Mr. Udayasarathy Arcot Vijayasarathy. Thank you as well to our exchange student workers from Germany: Witold, Chris, and Andreas. Thank you all for your support and friendship. I wish you and your families all the best, and I trust you will find joy and success in all your careers and endeavors.

Also, I would like to show my appreciation to the Texas Commission on Environmental Quality (TCEQ) and the United States Department of Energy, National Renewable Energy Laboratory (DOE-NREL) at Golden, Colorado for funding this research. Thank you to Mr. Cliff Clark of Luminant Power (formerly TXU) for allowing us to tour the Oak Grove Power Plant near Franklin, Texas. Thank you also to members of our Industrial Advisory Committee for the DOE project, including members from Texas Cattle Feeders Association, Texas Association of Dairymen, Panda Energy, Luminant Power, Xcel Energy, Texas Farm Bureau, and Animal-Agricultural Consulting, Inc. Thanks also to our collogues Dr. Mukhtar, Dr. Capareda, Dr. Auvermann, Mr. Kevin Heflin, and the rest of our colleagues at the Department of Biological and Agricultural Engineering, Texas A&M University and the AgriLife Research and Extension Center at Amarillo, Texas.

Most special thanks to my parents, Patrick and Sylvia. I owe everything to you. A lucky man would have good parents. So I must be the luckiest man in the world.

Thank you and congratulations to my sister, Petty Officer Second Class Anna Alicia Nelson and to her new husband Petty Officer Second Class Mike Nelson.

Welcome to the family Mike! We had a great time at the wedding. And please, both of you return home safely when your service to our country is complete. Thank you to the rest of my family, my grandmothers—Mrs. Beverly Carlin and Mrs. Esperanza Trevino—my aunts, my uncles, and my cousins. Thanks especially to my uncle, Dr. Thomas Carlin, for reminding me when my enthusiasm momentarily waned, that "Dr. Nicholas Carlin" has a nice ring to it. Thank you all for your unending care and support.

Finally, to my wife Ann Marie: You are beautiful. Your family is beautiful. And never was my life more beautiful until you arrived. There is so much love in my heart for you that I might write another 500 pages about how much you mean to me. If only I had the time. If only there were enough words. When you are with me, I am never afraid.

Thank you all. In my time at Texas A&M University, I have found that the most important thing in life is to surround yourself with good people. I have been around some very good people. I have learned nothing more important than that.

TABLE OF CONTENTS

Page

Page

Page

Page

LIST OF FIGURES

Page

Page

Page

Page

Page

Page

Page

Page

Page

Page

Page

LIST OF TABLES

Page

Page

Page

1. INTRODUCTION

Over the past 50 years, the rural landscape of the United States has changed from one that contained an abundance of relatively small, scattered farms to one that struggles to hold onto a few, extremely large concentrated animal feeding operations (CAFOs). The industrialization of American agriculture has come about due to low commodity prices, federal funding, high competition between farmers, and a large fast food industry. Currently, fewer than five million Americans live on farms, and only about half of them keep any farm animals on their land. However, for those who do house dairy cows, beef cattle, hogs, chickens, and other traditional farm animals, the amount of manure produced from the hundreds, sometimes thousands, of animals on the farm is a significant undertaking (Centner, 2004). Figure 1.1 is a photograph of a typical large feedlot operation. These CAFOs show the potential for water, soil, and air pollution, yet the concentration of the manure (Figure 1.2) makes this low heat value feedstock a viable source of fuel for combustion and emission control systems either at nearby power plants or in smaller energy conversion systems on or near the farm.

Figure 1.1 Feedlot cattle on large confined animal feeding operation (FactoryFarm.org, 2007)

This dissertation follows the style of the *International Journal of Green Energy*.

Figure 1.2 Solid manure generated from an animal feeding operation (FactoryFarm.org, 2007)

1.1. Industrialization of Agriculture

From a global perspective, larger, more homogenized agricultural operations have become necessary to compete with cheaper, foreign commodities. Lower prices on food stuffs and most other agricultural products have made smaller, less efficient farms even more obsolete in the modern industrial agricultural system. Even operators of large CAFOs have difficulty satisfying the economic bottom lines of their farms. It is estimated that 55% of American farms have an operator, an operator's spouse, or both working a secondary job, off the farm, to generate additional revenue. Usually, in order for his/her survival, the operator must expand the operation and keep more animals or grow more crops to keep the farm competitive. Indeed thousands of farms have shutdown, even in the past 10 years. For example, in Figure 1.3 it can be seen that the overall number of operations that housed dairy cows was over 120,000 in 1997;

however, by 2007 only about 70,000 farm operations kept dairy cows. At the same time, the number of dairy operations with more than 500 head increased by 38% to over 3,200 (NASS, 2008).

The domination by larger animal feeding operations in the dairy industry is further illustrated in Figure 1.4. Seventy-six percent of the 71,500 dairy operations in the US each house less than 100 milk cows, but these smaller farms only contain about 23% of all milk cows in the country and produce only about 19% of the country's milk. About half of all dairy cows, 49%, in the US are kept on the relatively few dairy farms with more than 500 head each. These large farms also produce 54% of the country's milk. Similarly, the 601,000 feed cattle operations with less than 50 head only contain about 10% of all cattle on feed in the nation. See Figure 1.5. Almost a third, 31%, of all feed cattle are kept on large feedlot operations with over 1,000 head each. However, this trend of dominance from large CAFOs is perhaps most perceptible when considering hog or swine farms. See Figure 1.6. Fifty-six percent of all hogs and pigs are kept on large 5,000-plus head operations, which only make up about four percent of all swine feeding operations in the US. The smallest 61% of swine operations keep only one percent of all swine in the country.

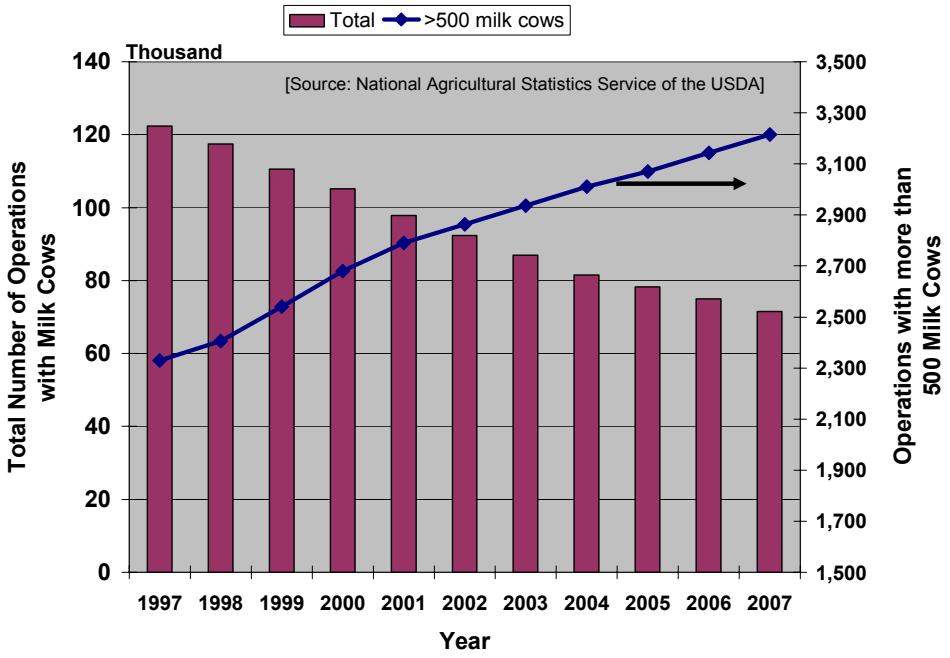

Figure 1.3 Change in number of operations with milk cows and growth of large dairy operations in the US from 1997 to 2007 (NASS, 2008)

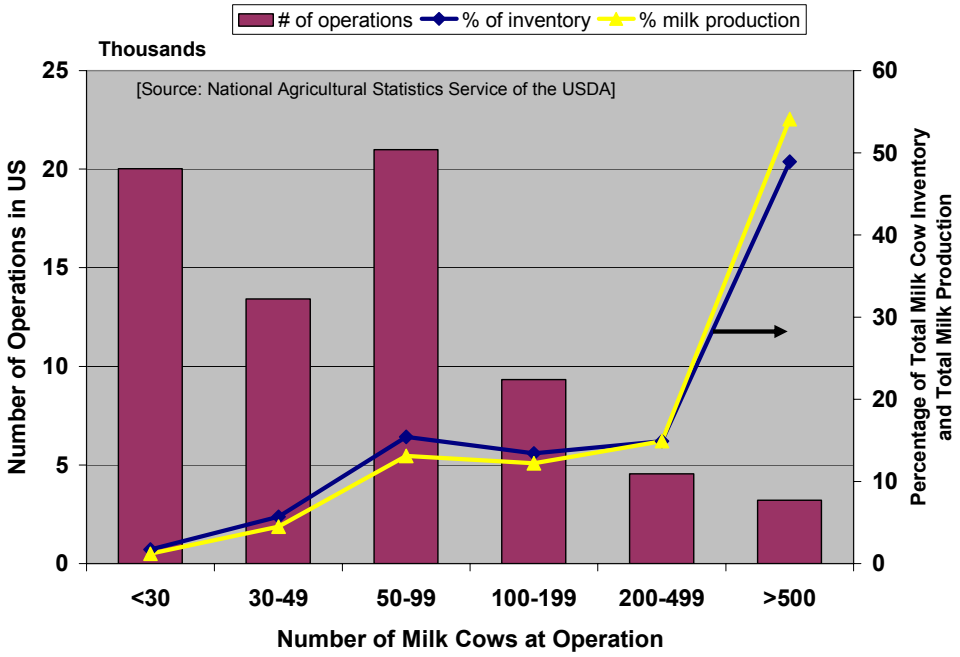

Figure 1.4 Number of operations with milk cows, milk cow inventory percentage, and milk production percentage in 2007 vs. size category of operation, Total operations in US = 71,510 (NASS, 2008)

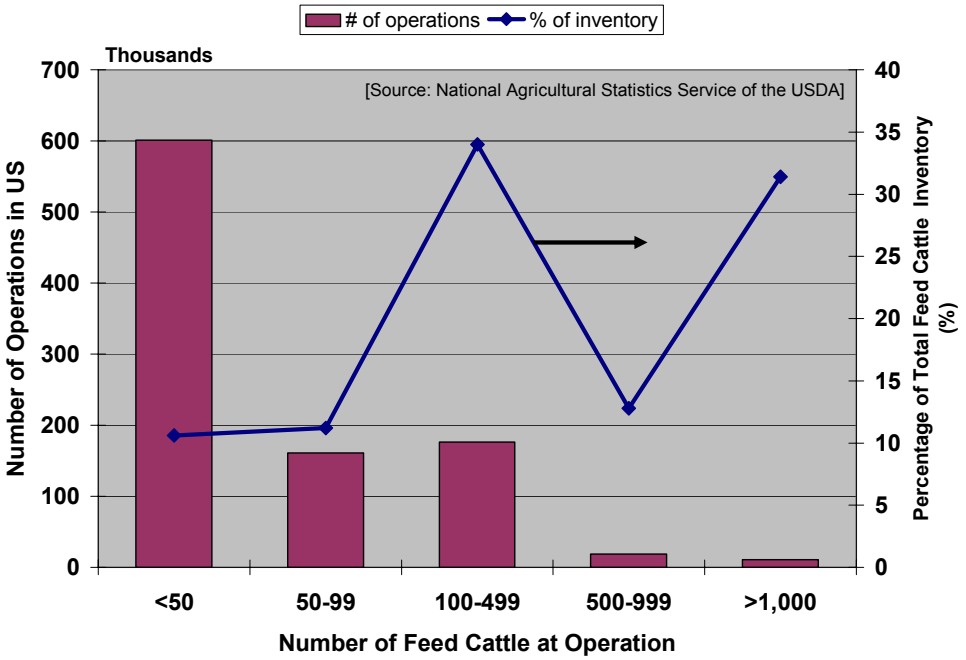

Figure 1.5 Number of operations with feed cattle and feed cattle inventory percentage in 2007 vs. size category of operation, Total operations in US = 967,540 (NASS, 2008)

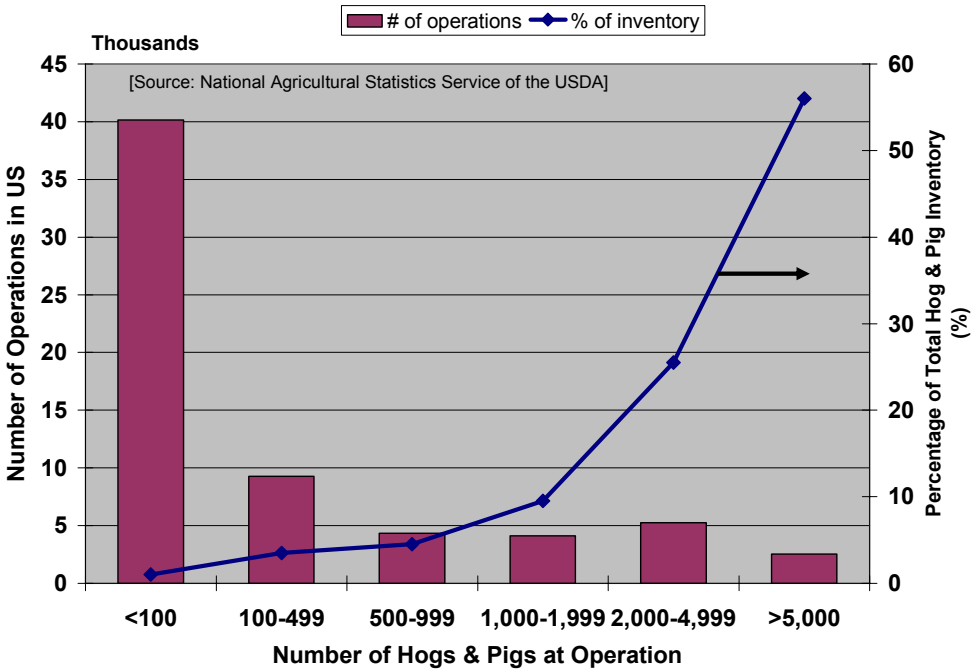

Figure 1.6 Number of operations with hogs & pigs and hog & pig inventory percentage in 2007 vs. size category of operation, Total operations in US = 65,640 (NASS, 2008)

Due to this dominance, a relative few, large animal feeding operations can control the values of agricultural products, such as milk and beef prices. Large farms can flood the market with animal-based products and lower prices, causing difficulty for smaller, family farms to stay competitive. Since family farm operators are also residents of rural communities, hundreds of ancillary businesses in small American towns have also suffered. As farmers have obtained less disposable income or have simply moved away to urban and suburban areas, American rural economies as a whole have suffered (Centner, 2004).

In general, all agricultural operations, not just animal farms, have been increasing in size and concentration for most of the 20th Century and into the 21st Century. Basically, there have been two forces behind this growth: (1) state and federal funding and (2) competition between farmers. Since the creation of the United States Department of Agriculture (USDA) and the Land Grant University System in 1865, research and development in agricultural equipment and practices have made the American Agricultural System the most productive and least labor intensive agriculture system in the world. See Figure 1.7. American Agriculture has become an increasingly mechanized and specialized system capable of growing more food on less land. Consequently, many smaller, family oriented farms that tended to grow a variety of crops and keep a diverse population of animals have disappeared. In order to stay competitive, most farmers have had to specialize in one or two crops or keep one type of animal. Growing single monocultures and keeping one animal type has allowed farmers to produce more food more efficiently (Centner, 2004).

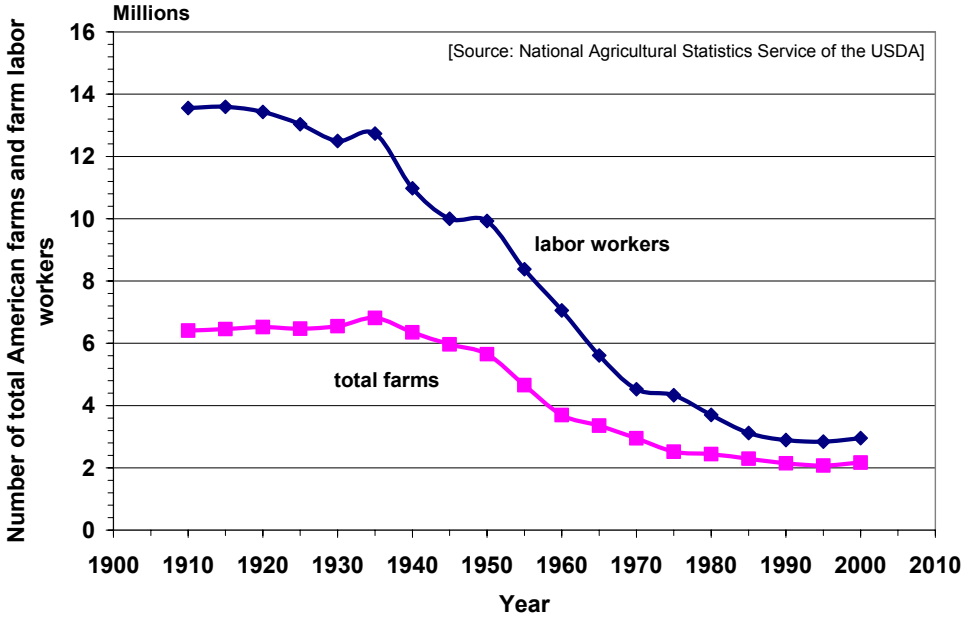

Figure 1.7 Number of total American farms and farm labor workers vs. year (NASS Census, 2002)

In the 1930s, New Deal legislation offered safety nets and funding for American farmers. Many similar funds are still available to farmers even today. However, many of the larger agricultural producers have joined to create conglomerates and politically powerful congressional lobbies, causing much of the available state and federal funding to go to larger operations. A 1999 study by the General Accounting Office in Washington D.C. showed that 52% of federal funds for agriculture were paid to the largest 8% of American farms. Small farms, which make up about 76% of the number of farms in the United States, received only 14% of these funds. Consequently, many larger operations have the ability to buy out smaller farms which may be competing with them. Yet even though most American farms are considered "small", most of the country's agricultural production comes from "superfarms" that concentrate on eight major crops: wheat, corn, barley, oats, sorghum, rice, cotton, and oilseeds (soybeans). About 3% of the country's largest farms produce about half of the entire agricultural commodities in the United States (Centner, 2004). Large CAFOs also benefit from government subsidies of these major crops because feed grains are included with these

specialized products. Hence, cheap grain allows owners of large CAFOs to feed many animals; however, other aspects of keeping animals, such as bedding application and waste handling, remain expensive and physically demanding.

For this study, animal farms, particularly large CAFOs, are of most concern. All of the trends of the growing industrial agricultural system are especially true for these large farms. CAFOs, which include cattle feedlots and dairy operations, are a cornerstone of the agricultural economy of the United States, particularly in Texas and neighboring states in the Southern Great Plains. The US is the largest producer of beef and the third largest producer of pork products. Yet, a consequence of this success has been the high amounts of manure and associated wastes from animal feeding operations. CAFOs in the US produce more than 350 million dry tons of manure per year (USDA, 2003).

Animal feeding operations have not only become larger, but also more concentrated. Part of the reason for keeping more animals in smaller spaces is the decrease in available labor and higher labor costs. In Figure 1.7, it can be seen that not only are the numbers of labor workers dropping on American farms, but also the average number of workers per farm is decreasing. In 1950, there were about 1.75 workers per farm (this includes animal farms and crop farms); however, by 2000 this ratio dropped 22% to 1.36 workers per farm. Proper waste disposal is made more challenging and expensive due to the concentration of animals, and hence manure.

Large CAFOs have been cited as major point sources for potential air, soil, and water pollution, while land application of manure, as fertilizer, has been cited as a non-point source for water contamination (TNRCC, 2001). Dairy farmers (Matthews *et al*., 2003), feedlot farmers (Sweeten, 1990), and swine farmers (Reisner, 2005; Anderson *et al*., 2006) have come under pressure to address the impacts their operations have on the environment. Large rainfall events, poorly maintained manure storage structures such as lagoons, and over application of manure as fertilizer on nearby parcels of land are all potential causes of nutrient leaching and contamination of water sources. Too much nutrients, such as phosphorus and nitrogen, in rivers, streams and coastal waters can

cause algal blooms, which can destroy fish. Aquatic life may also be harmed from high ammonia concentrations in waterways near animal feeding operations. Nutrient contamination can also make water unsafe to drink in towns and cities near CAFOs. Moreover, high quantities of the greenhouse gases nitrous oxide (N_2O) and methane (CH_4) come from large animal farms. Odors and possible exposure of nearby food sources to pathogens are also risks incurred by CAFOs.

The possible seepage of manure nutrients to surface and ground water sources has been a major concern. The high cost of transporting manure solids from feeding operations to composting sites and application fields, together with relatively shallow top soil and high intensity rainfall, limit the ability to properly distribute the manure. Moreover, the amount of manure to be applied is usually determined by the amount of nitrogen contained in the solids. Sometimes this can lead to an overloading of phosphorus on the land. Only recently have farms begun to switch to P-based land application and composting (Osei *et al*., 2000), (Keplinger *et al*., 2004), (McFarland *et al*., 2006).

Moreover, when wet and composting manure streams decompose or anaerobically digest in relatively uncontrolled settings, such as poorly maintained manure storage lagoons, methane (CH_4) and malodorous odors can form, reducing the quality of life near the farm (Mukhtar, 1999).

Yet, there is little doubt that larger and more concentrated animal feeding operations have made the production of beef, pork, dairy, and poultry products more efficient. However, as other aspects of animal farming, such as feeding, breeding, and slaughtering, have become more industrialized and automated, manure disposal has generally not advanced beyond usage of manure as fertilizer, compost, or simple disposal of the manure in landfills. Due to the concentration of manure at CAFOs, it is possible that manure-based biomass (MBB) can be used for fossil fuel supplementation.

1.2. Coal-fired Power Plants and Their Emissions

Energy production facilities, particularly coal-fired power plants, may benefit from MBB as bio-fuel feedstock. The recent increased concern over CO_2 emissions and global warming is only the latest in a seemingly perpetual call to reduce the amount of fossil fuels used for heat and electrical energy and the resulting emissions from fossil fuel power plants. Nitrogen oxides (NO_x), sulfur oxides (SO_x), mercury (Hg), and particulates have all been regulated emissions from coal-fired power plants, and restrictions on these products of combustion will probably continue to tighten.

About 50% of the electrical energy generated in the United States comes from burning coal. Most coal consumed in the US is burned in utility coal power plants. Almost every state in the country obtains at least some of its electrical energy from coal plants, and, with the exception of the New England States and the Pacific States, coal is generally the primary source of electricity. Table 1.1 is a list of the number of coal-fired units, electrical capacity, coal consumption, average coal price and average coal heat value for each state. Note that each coal plant may have more than one coal-fired unit. The East North Central Region of the US, including Ohio, Indiana, and Illinois, consumes the most coal of any region; about 232 million metric tons of coal in 2006. Texas burned almost 100 million metric tons of coal in 2006 and is the largest single state consumer of coal.

Table 1.1 Electric coal-fired units, electrical capacity, coal consumption, average coal prices, and average coal heat value in 2006 for each state in the US

Census Region, State	Number of Electric Coal-fired Units[a]	Total Electrical Capacity[a] (MW)	Coal Consumption[b] (10^3 metric tons)	Average Price of Coal Delivered to End Use[b] ($/GJ$_{th}$)	Average Heat Value of Coal[b] (kJ/kg)
New England	**17**	**2,817**	**7,961**	**2.53**	**27,667**
Connecticut	3	553	2,037	NR	23,389
Maine	2	85	133	NR	29,734
Massachusetts	8	1,651	4,309	2.64	26,854
New Hampshire	4	528	1,482	2.43	30,692
Rhode Island	0	0	0	--	--
Vermont	0	0	0	--	--
Middle Atlantic	**123**	**24,006**	**63,493**	**2.16**	**27,765**
New Jersey	10	2,124	4,205	2.59	29,701
New York	35	3,474	8,543	2.27	26,943
Pennsylvania	78	18,408	50,745	1.63	26,652
East North Central	**362**	**78,025**	**210,245**	**1.39**	**23,282**
Illinois	64	15,822	48,933	1.19	20,786
Indiana	79	19,532	54,960	1.29	24,742
Michigan	70	11,781	31,685	1.59	23,200
Ohio	97	22,224	53,165	1.61	26,805
Wisconsin	52	8,666	21,502	1.25	20,875
West North Central	**180**	**36,589**	**132,931**	**1.00**	**19,483**
Iowa	45	6,520	19,265	0.88	20,030
Kansas	17	5,323	18,937	1.13	20,019
Minnesota	34	5,074	17,757	1.04	20,726
Missouri	52	11,218	41,371	0.95	20,486
Nebraska	16	3,858	11,686	0.76	19,802
North Dakota	14	4,121	22,043	0.83	15,469
South Dakota	2	476	1,872	1.43	19,849
South Atlantic	**284**	**70,438**	**162,157**	**2.16**	**28,332**
Delaware	7	1,043	1,986	NR	28,843
District of Columbia	0	0	0	--	--
Florida	31	10,693	25,179	2.43	28,241
Georgia	33	13,262	35,281	2.06	25,570
Maryland	16	4,912	10,558	2.15	29,082
North Carolina	77	13,046	27,630	2.55	28,534
South Carolina	31	7,160	14,298	2.00	29,269
Virginia	50	5,686	12,877	2.32	29,287
West Virginia	39	14,636	34,349	1.58	27,833
East South Central	**140**	**37,432**	**105,869**	**1.93**	**24,553**
Alabama	40	11,647	33,719	2.00	25,303
Kentucky	57	14,709	38,046	1.61	26,905
Mississippi	10	2,677	9,415	2.62	20,842

Table 1.1, continued

Census Region, State	Number of Electric Coal-fired Units[a]	Total Electrical Capacity[a] (MW)	Coal Consumption[b] (10^3 metric tons)	Average Price of Coal Delivered to End Use[b] ($/GJ$_{th}$)	Average Heat Value of Coal[b] (kJ/kg)
Tennessee	33	8,399	24,690	1.48	25,163
West South Central	**72**	**36,950**	**137,712**	**1.28**	**19,418**
Arkansas	6	4,458	13,258	1.39	20,416
Louisiana	10	4,349	14,821	1.47	19,084
Oklahoma	14	5,216	19,222	0.93	20,344
Texas	42	22,927	90,412	1.35	17,828
Mountain	**117**	**31,861**	**104,095**	**1.21**	**22,826**
Arizona	15	5,736	18,603	1.22	23,261
Colorado	29	5,893	17,878	1.21	22,798
Idaho	0	0	0	--	--
Montana	11	2,497	10,253	0.74	19,602
Nevada	12	3,038	3,164	1.64	26,736
New Mexico	12	3,940	15,387	1.48	21,589
Utah	15	4,606	15,068	1.29	25,540
Wyoming	23	6,152	23,741	0.87	20,254
Pacific	**21**	**2,748**	**6,895**	**1.23**	**23,247**
Alaska	NR	105	370	NR	NR
California	18	503	816	NR	28,338
Hawaii	NR	180	653	NR	25,452
Oregon	1	556	1,315	1.23	19,353
Washington	2	1,404	3,742	NR	19,844
United States Total	**1,316**	**320,866**	**931,357**	**1.65**	**24,064**

[a]Source: 2006 National Electric Energy Data System (NEEDS) of the Environmental Protection Agency, Integrated Planning Model (IPM). Includes approved new units. See (USEPA, 2007a) in the reference section.
[b]Source: Energy Information Agency (EIA), 2006 United States Electricity Profiles

NR: Not Reported

Recently, CO_2 emissions from fossil fuel combustion have garnered the most attention due to the threat of global warming caused by higher concentrations of CO_2 in the atmosphere. In the US, 36% of CO_2 emissions in 2006 came from the combustion of coal. See Figure 1.8. Ninety-one percent of all CO_2 emissions from burning coal are emitted from electric power plants. Currently, there are no commercially available technologies that can reduce CO_2 emissions after combustion. The only feasible way to reduce CO_2 emissions, at this time, is to obtain electricity from alternative sources such as nuclear, hydro-electric, solar, wind, and biomass combustion or to burn other fossil fuels that emit less CO_2 per unit energy, such as natural gas. However, in most parts of the country, coal is both cheaper and more available than any alternative form of energy. Plus, coal is generally cheaper than most other fossil fuels per unit energy. The average price of natural gas for electricity producers in 2006 was \$6.74/GJ_{th} (\$7.11/MMBtu) (EIA, 2007b). However, from Table 1.1 it can be seen that the price of coal in all states is much lower than this price.

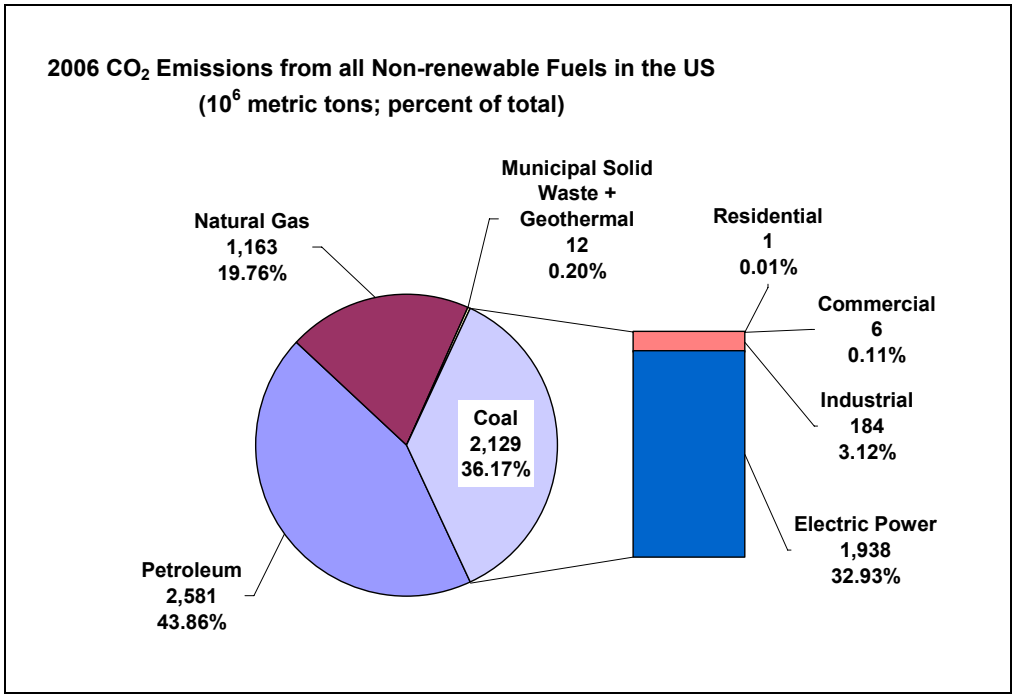

Figure 1.8 CO_2 emissions from all nonrenewable fuels in the US (EIA, 2007a)

Moreover, there are no mandatory CO_2 cap-and-trade laws or carbon taxes in most of the US, giving little incentive for developing carbon-neutral alternatives or developing carbon sequestration technologies. The one exception is the Regional Greenhouse Gas Initiative, which held its inaugural CO_2 allowance auction in September 2008. However, only 10 Northeastern states were required to participate, including New York, Connecticut, Delaware, Maine, Maryland, Massachusetts, New Hampshire, New Jersey, Rhode Island, and Vermont (RGGI, 2008). From Table 1.1, it can be seen that most of these states are already among the lowest consumers of coal, thus CO_2 allowance auctions need to be extended to other parts of the country before there is a significant impact on CO_2 emissions from electric coal plants.

Since there are no commercial technologies that can capture carbon post-combustion, CO_2 emissions from coal are usually a good indicator of coal consumption. In Figure 1.9, the coal consumption of the top 20 CO_2-emitting states in 2004 is compared to the CO_2 emissions of those same states. The trend is generally the same, states that burned more coal, emitted more CO_2. However, since the carbon content and average heat value of coal vary from state to state, the relationship is not exactly one-to-one.

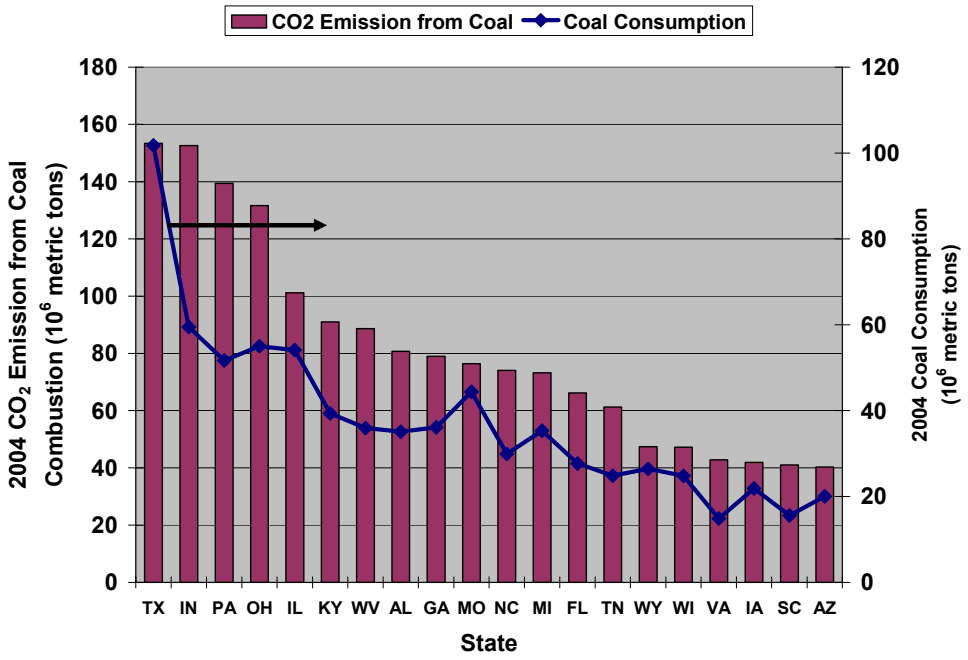

Figure 1.9 Top 20 states that emitted CO_2 from coal combustion in 2004 and their respective coal consumption (EIA, 2007c)

However, some other emissions from coal combustion have been successfully reduced in recent years due to cap and trade laws and emission control technologies. Figure 1.10 shows how NO_x and SO_x emissions from conventional power plants (burning fuels including coal, natural gas, and petroleum) and combined heat-and-power plants have decreased since 1995. Sulfur oxides (SO_x) dropped by nearly 30% since a high of 13.5 million metric tons in 1997. This reduction is partly attributed to the installation of Flue Gas Desulphurization (FGD) systems on fossil-fueled steam-electric generators. As of 2005, 248 fossil-fueled units had a FGD system, which is a 28% increase since 1995 (EIA, 2007c). Scrubber efficiencies from FGD systems are usually about 95% for large steam-electric generators (USEPA, 2007a). Moreover, lower SO_x emissions allowances, under the American Clean Air Interstate Rule, have recently increased the demand for low sulfur, sub-bituminous coal, mined mostly out of the Powder River Basin (Global Energy Decisions, 2006).

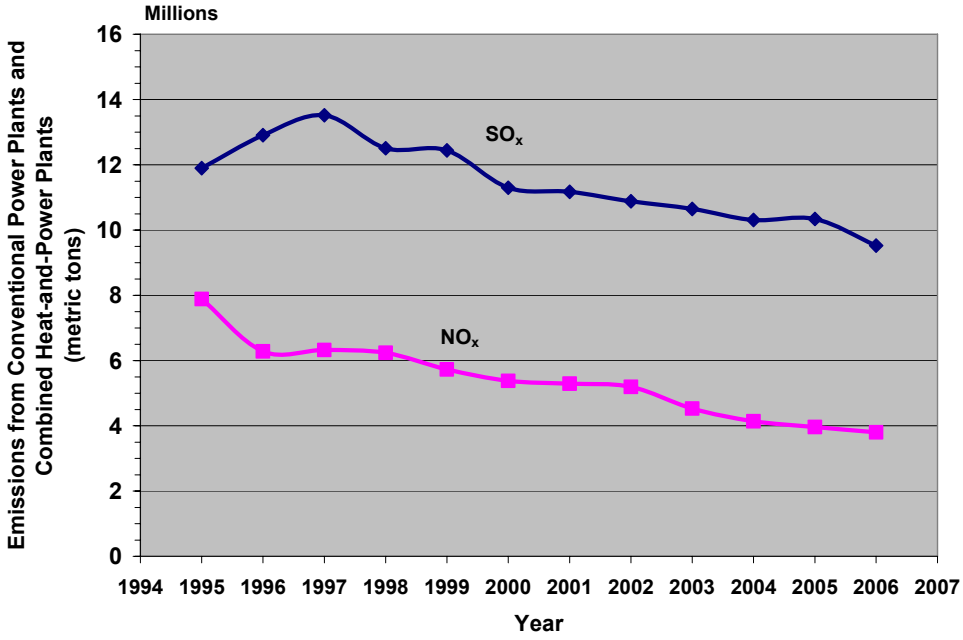

Figure 1.10 NO_x and SO_x emissions from conventional power plants and combined heat-and-power plants in the US from 1995 to 2006 (EIA, 2007c)

Nitrogen oxides (NO_x) have also been reduced by nearly 52% since 1995. These reductions are mostly due to primary combustion controls, including low-NO_x burners and air staging, now installed in most existing coal-fired power plants. Moreover, post-combustion NO_x controls such as selective catalytic reduction (SCR) and selective non-catalytic reduction (SNCR) have also been installed on many fossil-fueled power plants. As of 2005, over 150 coal-fired units utilized SCR technology (Srivastava *et al*, 2005). Currently, the best primary NO_x controllers can lower NO_x levels down to about 60 g/GJ_{th} (0.14 lb/MMBtu), while SCR systems, which are generally more expensive, can lower NO_x down to 26 g/GJ_{th} (0.06 lb/MMBtu) (USEPA, 2007a). However, caps on regional NO_x emissions continue to decline, making NO_x allowances more expensive. Therefore research into cheaper and more effective ways to reduce NO_x from fossil fuel combustion has continued.

1.3. Problem Statement

Based on these understandings of large industrial CAFOs and fossil fueled power plants, there seems to be an opportunity for a more symbiotic relationship between animal farmers and energy producers, or at least for animal farmers to become energy producers themselves. If burning MBB can alleviate the waste disposal issues found on some large animal farms and generate more jobs and activity to rural economies, while at the same time displacing a fraction of the fossil fuels that are burned for energy generation, then perhaps MBB can be added to the list of renewable and carbon-neutral energy production technologies that will eventually supplement fossil fuel combustion.

Co-combustion of coal and MBB has been found to reduce NO_x emissions, increase the oxidation of elemental mercury emissions, and reduce the amount of nonrenewable CO_2 emissions from coal combustion. This claim will be warranted and explained in the following sections of this dissertation. However, the primary purpose of this study is to investigate the economic feasibility of processing and transporting MBB to existing energy production facilities and subsequently burning the biomass. Can the avoided costs of coal and emissions balance out the costs of processing and transporting the MBB, as well as any additional operation and maintenance costs involved in burning MBB? If so, what are the limiting factors of a successful co-combustion system? If not, can MBB still be utilized on smaller, on-the-farm combustion systems for waste disposal and possible energy production for the farm? The following study will attempt to answer these questions, but first, a deeper understanding of the properties of coal and MBB and the supply of MBB must be obtained.

2. BACKGROUND INFORMATION

2.1. Fuel Supply and Properties

This study will focus on MBB utilization at nearby coal plants or smaller scale on-the-farm combustion facilities. Emissions, flame temperatures, and heat energy outputs from burning biomass are required to determine the effectiveness and profitability of biomass energy conversion systems. However, in order to estimate these outputs, fuel properties of both coal and biomass must be known. The following is a review of the fuel properties of coals and some manure-based biomasses. A brief discussion of the supply of manure biomasses will also be included.

2.1.1. Coal

The type of coal consumed for a particular power plant usually depends on what type of coal is mined at nearby coal fields; although, recently many plants around the country have begun to import low-sulfur sub-bituminous coal from the Powder River Basin. Figure 2.1 is a map of the major coal fields in the United States. The largest coal deposits are in the Powder River Basin, the North Dakota or Fort Union Region, the Four Corners or Southwest Region, the Appalachian Basins and the Illinois Basins (Probstein, 2006a). The rank of the coal is usually determined by the carbon content. Higher ranked coals have higher percentages of carbon on a dry, ash-free basis, and generally have a greater higher heating value, or calorific value. A proximate analysis of the fuel can provide the moisture, ash, fixed carbon, and volatile matter contents of the fuel. Volatile matter is the part of the solid fuel that will vaporize, or pyrolize, in an inert environment when heated. Fixed carbon is material that will not vaporize in inert environments, but will oxidize when a reactant (usually air or oxygen) is heated along with the fuel. The ash is the inert portion of the solid fuel that is left even after the reaction with the oxidizer. Yet, for this study, an ultimate analysis of the fuels, which includes the elemental contents of the fuel (Carbon, Hydrogen, Nitrogen, Oxygen, and

Sulfur) along with moisture and ash, will be required for emissions and energy release calculations.

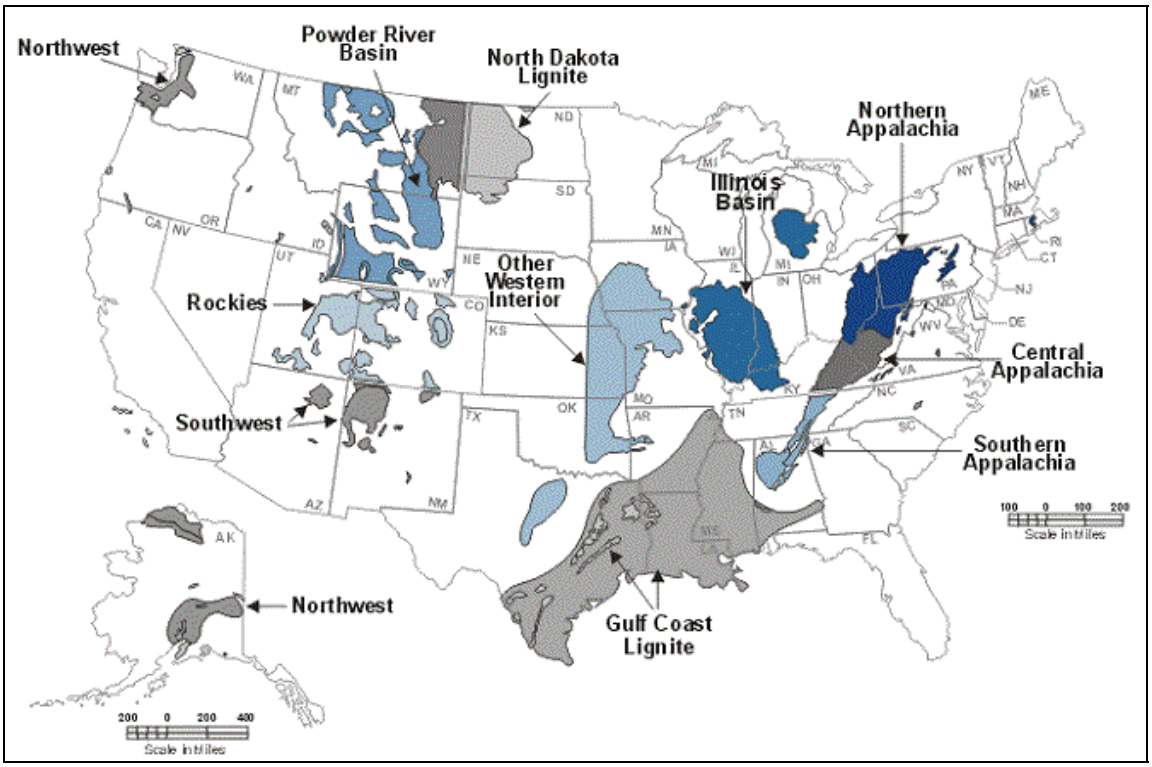

Figure 2.1 Coal fields in the United States (EIA, 2005)

Table 2.1 Ultimate and heat value analyses of major coals mined in the US (Probsein et al., 2006a)

	Fort Union Lignite	Powder River Basin Sub-bituminous	Four Corners Sub-bituminous	Illinois C Bituminous	Appalachia Bituminous
(by mass)			**As received**		
Moisture	36.2	30.4	12.4	16.1	2.3
Ash	8.6	7.8	25.6	7.4	9.7
Carbon	39.9	45.8	47.5	60.1	73.6
Hydrogen	2.8	3.4	3.6	4.1	4.9
Nitrogen	0.6	0.6	0.9	1.1	1.4
Oxygen	11	11.3	9.3	8.3	5.3
Sulfur	0.9	0.7	0.7	2.9	2.8
HHV (kJ/kg)	15,600	18,400	19,600	24,900	31,200
			Dry, ash-free		
Moisture	0	0	0	0	0
Ash	0	0	0	0	0
Carbon	72.3	74.1	76.6	78.6	83.6
Hydrogen	5.1	5.5	5.8	5.4	5.6
Nitrogen	1.1	1.0	1.5	1.4	1.6
Oxygen	19.9	18.3	15.0	10.8	6.0
Sulfur	1.6	1.1	1.1	3.8	3.2
HHV (kJ/kg)	28,261	29,773	31,613	32,549	35,455

Ultimate analyses of several representative coals in the US are presented in Table 2.1 on both an as-received basis and a dry, ash-free basis. These coals follow the general trend for ranking coal. Lignite coals generally have less carbon, but more oxygen, than higher ranked sub-bituminous and bituminous coals on a dry, ash-free basis. Heat values also increase for higher ranked coals. For the present study, a closer look into coals burned at Texas steam-electric power plants will be conducted later. Fuel analyses of Texas lignite from the Gulf Coast lignite field and Wyoming sub-bituminous from the Powder River Basin will be used during simulations. The ultimate, proximate and heat value analyses of these coals are presented in Table 2.2.

Table 2.2 Ultimate, proximate, and heat value analyses of coals modeled in this study (TAMU, 2006)

	Texas Lignite	Wyoming Sub-bituminous
(by mass)	**As received**	
Moisture	38.3	32.9
Ash	11.5	5.6
Fixed Carbon	25.4	33.0
Volatile Matter	24.8	28.5
Carbon	37.2	46.5
Hydrogen	2.1	2.7
Nitrogen	0.7	0.7
Oxygen	9.6	11.3
Sulfur	0.6	0.3
HHV (kJ/kg)	14,290	18,194
	Dry, ash-free	
Moisture	0.0	0.0
Ash	0.0	0.0
Fixed Carbon	50.6	53.7
Volatile Matter	49.4	46.3
Carbon	74.1	75.7
Hydrogen	4.2	4.4
Nitrogen	1.4	1.1
Oxygen	19.1	18.4
Sulfur	1.2	0.4
HHV (kJ/kg)	28,467	29,594

As part of determining coal properties, a thermal gravimetric analyzer/ differential scanning calorimeter (TGA/DSC) instrument can provide information on the moisture and combustible volatile matter released during pyrolysis and early gasification processes. Tests were performed using a TA Q600 TGA/DSC and discussed by Lawrence (2007) and Carlin *et al*. (2008). The purge gases typically used are N_2 for pure pyrolysis and air for oxidation reactions. The instrument monitored temperature, particle mass, and heat flow versus time. The pyrolysis temperature was found to be approximately 350 °C (650 °F) and the ignition temperature was about 320 °C (620 °F) for Texas lignite.

Much of the present study will also require some understanding of the processing of solid fuels before combustion, particularly drying. Abhari *et al*. (1990) studied the drying kinetics of lignite, sub-bituminous, and bituminous coals. Strezov *et al*. (2004)

discussed several correlations for computing the specific heat (heat capacity) of coals on a dry, ash-free basis, given the temperature and volatile matter content of the coal. Priyadarsan (2002) discussed the specific heat of coal ash. He reported that the specific heat of coal ash varied only slightly with temperature and had values of 1.28 – 1.46 kJ/kg K from temperatures ranging from 900 K to 1200 K. Priyadarsan also reported that the dry, ash free specific heat of coal ranged between 32.69 and 34.21 kJ/kg K at the same temperature range. Higher ash contents in coal lower the composite specific heat of the combined coal and ash solid.

2.1.2. Dairy Biomass

There are certain areas of the country, such as the Bosque River Watershed near Waco, Texas and many parts of California that contain dozens of large dairy operations, each with over 500 milking cows. See Figure 2.2. The dairy cows in the Bosque River Watershed make up about 25% of the total number of dairy cows in Texas. The Californian counties of Tulare (26%), Merced (14%), and Stanislaus (10%), house about 50% of the 1.74 million dairy cows in California (CDFA, 2006).

Full-grown milking cows can produce 7 to 8% of their body weight in manure per day; roughly 7.3 dry kg (16 lb) per animal per day according to Schmidt *et al*. (1988). The American Society of Agricultural Engineer (ASAE) standard, as excreted, manure production from a full grown lactating cow is 8.9 dry kg (20 lb) per animal per day. The manure is roughly 87% moisture when excreted (ASAE, 2005). If about 70% of this manure can be collected, then 21.2 million dry metric tons (23.3 million tons) of dairy manure per year can be utilized in the US. Texas dairy cows produce about 890,000 dry metric tons (980,000 tons) of manure per year. If dairy manure solids are roughly 40% ash on average, and the dry ash-free heating value of the manure is about 20,000 kJ/kg, then the thermal energy conversion of dairy manure in the US can potentially produce about 255 million GJ/yr (242 million MMBtu/yr).

The term “cattle biomass (CB)” will refer to both feedlot and dairy manure in general. Manure from feedlots will be termed feedlot biomass (FB) and manure from dairies will be termed dairy biomass (DB).

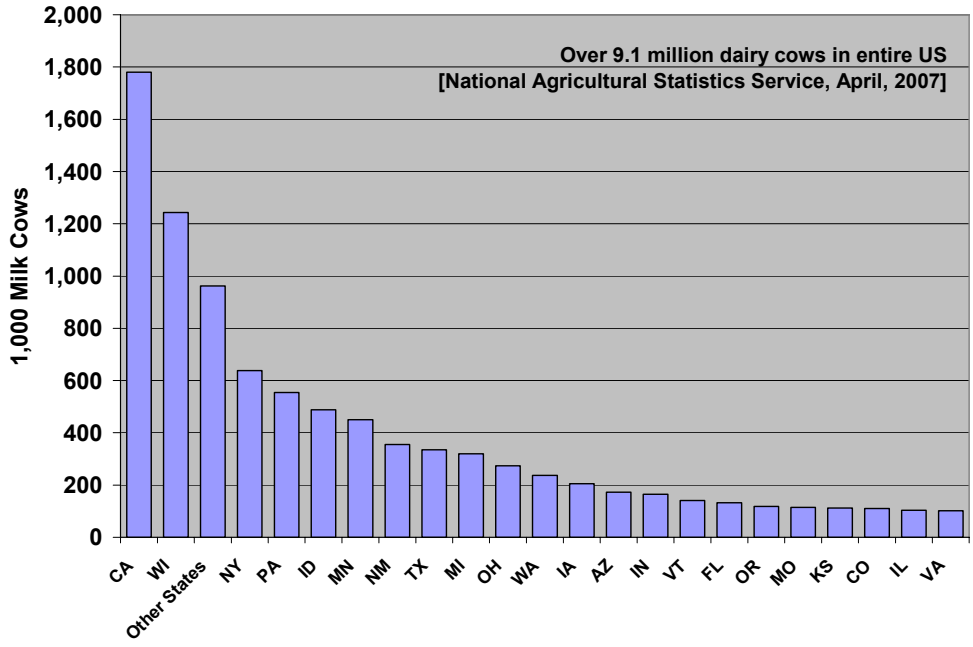

Figure 2.2 Average numbers of dairy cows in the US (not including heifers) for 2006 (NASS, 2007 and USDA, 2007)

Figure 2.3 is an illustration of some of the most common ways DB and FB is collected, treated, and used at most animal feeding operations. Feedlot biomass will be discussed in the next section. The manure collection processes at dairies generally depend on how the animals are kept. Most dairies keep cows primarily in open lots or corrals paved with soil. Manure is periodically removed by scraping the corrals with a tractor and box blade, usually when the cows are at the milking center. However, large amounts of dirt and other inert material is also scraped along with the manure, making the DB from open lot dairies high in ash and unsuitable for most direct combustion processes. Scraping manure from soil surfaced open lots can produce 16.1 dry kg (35.5 lb) of recoverable solids per animal per day. About 43% of these solids are inert material or ash. The moisture percentage of scraped solids from soil surfaced lots can

range between 39 and 69% (ASAE, 2005). Hybrid dairy facilities have open lots plus free stalls. Free stalls are covered, open air barn structures, typically paved with concrete. Bedding, which can be straw, sand, or composted manure, is usually placed on the concrete floor for the animals' comfort. Sometimes loafing beds are placed on the concrete floors to further increase the animals' comfort level as well (Mukhtar *et al.*, 2008).

Manure may be removed from free stall barns in several ways. The manure, along with the bedding material can be washed or flushed with water, which usually flows downhill from one end of the free stall barn to the other. At the bottom end of the barn, some dairies have solid separators that remove some of the solids from the liquid flushed manure. The separated solids are either stored or composed and are eventually used as fertilizer on nearby plots of land or discarded at landfills. The remaining wastewater from the separator is typically sent to a treatment pond or lagoon, where the remaining solids are diluted and broken down by anaerobic biological processes. See Figure 2.3. Any inorganic matter in the wastewater will sink to the bottom of the lagoon and create a layer of sludge. After treatment, the water in the lagoon is typically used for further flushing in the free stall, or as irrigation water (Mukhtar, 1999). Alternatively, a vacuum machine can collect the manure and bedding into a "slurry wagon." After manure is vacuumed, it is taken either to fields and used as fertilizer or spread and dried. If flushing or vacuum systems are not available, free stalls can be also be scraped to remove manure (Mukhtar *et al.*, 2008). About 11.2 dry kg (24.7 lb) of manure per animal per day can be recovered when scraping concrete surfaces. Whereas only 5.36 dry kg (12 lb) per animal per day can be recovered from flushed DB slurry. The slurry will be roughly 92% moisture (ASAE, 2005).

The makeup of the combustible or dry ash-free portion of the manure biomass is largely determined by the feed or the ration that the animals eat. In Table 2.3, the mean proximate, ultimate and heat value analyses of the cattle feed, as excreted manure, and aged manure solids are listed for a number of dairies in Texas obtained by Mukhtar *et al.* (2008). On an as received basis and on a dry basis (i.e. all moisture removed) the heat

value of the excreted manure was less than the heat value of the original rations that were feed to the animals. However, on a dry, ash free basis, the heat values for excreted manure and cattle feed was very similar. On a dry basis, it may also be seen that the heat value for aged solids was lower compared to the excreted manure. This decrease in heat value was predominantly due to the loss of volatiles during composting or storage of manure solids.

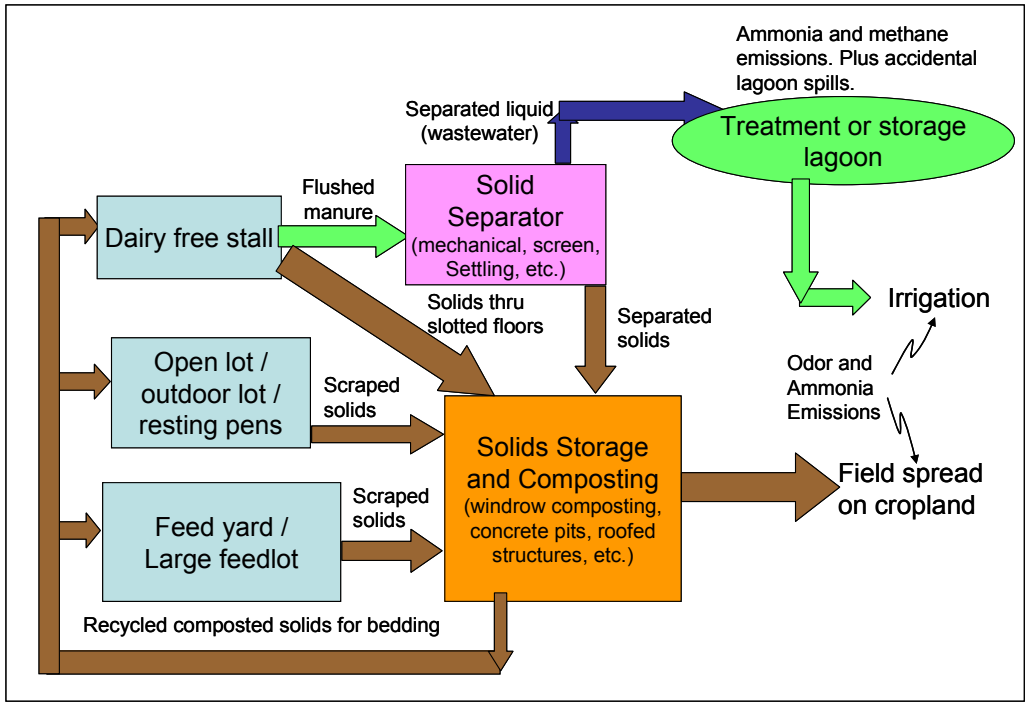

Figure 2.3 Current dairy and feedlot manure disposal (adapted from Schmidt *et al*., 1988)

Table 2.3 Averaged ultimate, proximate, and heat value analyses of dairy cow feed, as-excreted manure, and aged solids for various dairies in Texas (Mukhtar et al., 2008)

	Dairy Cattle Feed	As Excreted Dairy Manure	Aged Solid Dairy Manure
(by mass)		**As received**	
Moisture	41.4	84.1	36.2
Ash	5.2	3.2	41.7
Fixed Carbon	11.2	2.3	0.7
Volatile Matter	42.2	10.4	21.4
Carbon	26.3	6.8	11.1
Hydrogen	3.2	0.8	1.2
Nitrogen	1.5	0.4	1.0
Oxygen	21.7	4.7	8.6
Sulfur	0.2	0.0	0.3
HHV (kJ/kg)	9,159	1,161	2,810
		Dry	
Moisture	0.0	0.0	0.0
Ash	8.9	20.1	65.4
Fixed Carbon	19.1	14.5	1.1
Volatile Matter	72.0	65.4	33.5
Carbon	44.9	42.8	17.4
Hydrogen	5.5	5.0	1.9
Nitrogen	2.6	2.5	1.6
Oxygen	37.0	29.6	13.5
Sulfur	0.3	0.0	0.5
HHV (kJ/kg)	15,792	7,354	4,519
		Dry, ash free	
Moisture	0.0	0.0	0.0
Ash	0.0	0.0	0.0
Fixed Carbon	21.0	18.1	3.2
Volatile Matter	79.0	81.9	96.8
Carbon	49.3	53.5	50.2
Hydrogen	6.0	6.3	5.4
Nitrogen	2.8	3.1	4.5
Oxygen	40.6	37.0	38.9
Sulfur	0.4	0.0	1.4
HHV (kJ/kg)	16,644	16,788	13,045

In Table 2.4, the ultimate, proximate, and heat value analyses for dairy manure solids collected by various methods are presented from the same study by Mukhtar *et al.* (2008). Scraped DB solids were collected at open lots and hybrid lots in both central Texas and the Texas Panhandle region. Separated solids from flushed systems on hybrid

lots were also collected in these two Texas regions. Vacuumed DB solids were collected from two hybrid lots in central Texas as well. First, notice the moisture percentage on an as received basis. Scraped DB, which was once 80% moisture as excreted, mixes with either bedding or soil in open lots and is dried in the sun to about 40% moisture; however, on a dry basis the DB's ash percentage increases from 20% as excreted to about 36%, on average, when scraped. Scraped solids can be as high as 70% ash on a dry basis, depending on the open lot surfacing and the care taken by the box blade operator when collecting the manure.

On the other hand, mechanically and gravitationally separated solids are extremely high in moisture as they are screened or settled from streams of high moisture flushed dairy manure. Mechanically separated solids were found to be very low in ash, as much of the inert material in the DB is made-up of smaller particles that pass through screen meshes more easily than the combustible, organic material. This data confirms the same hypothesis by Carlin (2005) and Carlin *et al*. (2007a), who found that separated DB solids from a dairy in Hico, Texas were only 11% ash on a dry basis. However, gravitationally separated solids are higher in ash since the small inert particles settle to the bottom of settling basins along with the combustible material.

Table 2.4 Averaged ultimate, proximate, and heat value analyses for dairy manure solids collected by various methods for various dairies in Texas (Mukhtar et al., 2008)

	Scraped Dairy Solid Manure	Mechanically Separated Dairy Solids	Gravitationally Separated Dairy Solids	Vacuumed w/ Sand Bedding	Vacuumed w/ Compost Bedding
(by mass)			**As received**		
Moisture	40.8	83.2	69.9	52.0	83.6
Ash	21.2	1.3	12.4	38.6	3.6
Fixed Carbon	5.3	10.5	8.5	6.7	5.6
Volatile Matter	32.7	5.0	9.2	2.7	7.2
Carbon	18.8	8.0	12.0	5.9	6.8
Hydrogen	2.2	0.9	1.4	0.7	0.8
Nitrogen	1.3	0.3	0.5	0.3	0.4
Oxygen	13.8	6.2	8.2	2.4	4.7
Sulfur	0.3	0.1	0.1	0.1	0.1
HHV (kJ/kg)	6,433	2,554	3,777	2,258	2,740
			Dry		
Moisture	0.0	0.0	0.0	0.0	0.0
Ash	35.8	7.7	41.2	80.4	22.0
Fixed Carbon	9.0	62.5	28.2	14.0	34.1
Volatile Matter	55.2	29.8	30.6	5.6	43.9
Carbon	31.8	47.6	39.9	12.3	41.5
Hydrogen	3.7	5.4	4.7	1.5	4.9
Nitrogen	2.2	1.8	1.7	0.6	2.4
Oxygen	23.3	36.9	27.2	5.0	28.7
Sulfur	0.5	0.6	0.3	0.2	0.6
HHV (kJ/kg)	11,361	15,480	11,452	4,854	14,813
			Dry, ash free		
Moisture	0.0	0.0	0.0	0.0	0.0
Ash	0.0	0.0	0.0	0.0	0.0
Fixed Carbon	13.9	67.7	48.0	71.3	43.8
Volatile Matter	86.1	32.3	52.0	28.7	56.3
Carbon	49.5	51.6	67.8	62.8	53.1
Hydrogen	5.8	5.8	7.9	7.4	6.3
Nitrogen	3.4	1.9	2.8	3.2	3.1
Oxygen	36.3	40.0	46.3	25.5	36.7
Sulfur	0.8	0.6	0.6	1.1	0.8
HHV (kJ/kg)	17,667	16,788	18,255	23,949	19,130

The type of material used as bedding in free stalls and open lots plays a significant role in how much inert material is collected along with the DB. In Table 2.4, fuel analyses for vacuumed DB solids are also presented. It can be seen that vacuumed solids from free stalls with sand bedding had significantly higher ash contents than from

free stalls with compost bedding. According to Sweeten and Heflin (2006), this higher ash content from free stalls bedded with sand is also true for flushed manure and the related separated solids. In general, sand bedding causes ash contents in manure to be extremely high, no matter what collection technique is employed, and thus making the DB unsuitable for most any thermo-chemical conversion process. On a dry basis, the results for vacuumed manure from free stalls with compost bedding seem promising, with a mean ash percentage of only 22%. Vacuum machines can collect almost all of the manure from the free stalls, along with the bedding.

On a dry, ash free basis, the compositions and heat values of each of the manure samples in Table 2.3 and Table 2.4 should be similar; however, since these numbers are averages of samples taken from several dairies in different parts of Texas, there seems to have been some variation in the combustible contents of the DB samples. In Table 2.5, ultimate and heat value analyses are presented for a dairy in Comanche, Texas. The low-ash DB sample was taken from separated solids from a free stall using composted manure as bedding. The high-ash sample is from scraped DB from an open lot at the same dairy. The combustible contents of these two samples on a dry, ash free basis seem similar, although the heat value for the high ash sample is significantly lower, even on a dry, ash-free basis. This lower heat value for higher ash manure samples has been observed on several occasions over the course of this study and previous work; however, physically the low-ash and high-ash samples should be almost identical on a dry, ash-free basis if the manure samples are from the same feeding operation and the animals are given the same ration. The discrepancy may be from the fuel testing itself. Higher heat values are typically determined from bomb calorimeters, and it may be that part of the combustible content is shielded or diluted in the high ash content of the fuel and not burned during the calorimetry test. Ash analyses of these fuels as well as other coals and agricultural based biomasses can be found at the Texas A&M Coal and Biomass Energy Laboratory website (TAMU, 2006).

Table 2.5 Ultimate and heat value analyses of dairy manure from a dairy in Comanche, Texas (Sweeten and Heflin, 2006)

	Low-ash Dairy Manure	**High-ash Dairy Manure**
(by mass)	As received	
Moisture[a]	25.3	12.2
Ash	14.9	59.9
Fixed Carbon	13.0	3.9
Volatile Matter	46.9	24.0
Carbon	35.2	18.0
Hydrogen	3.1	1.6
Nitrogen	1.9	1.2
Oxygen	19.2	6.9
Sulfur	0.4	0.2
HHV (kJ/kg)	12,843	4,312
	Dry	
Moisture	0.0	0.0
Ash	20.0	68.2
Fixed Carbon	17.4	4.4
Volatile Matter	62.8	27.3
Carbon	47.1	20.5
Hydrogen	4.2	1.8
Nitrogen	2.6	1.3
Oxygen	25.6	7.9
Sulfur	0.6	0.2
HHV (kJ/kg)	17,183	4,912
	Dry, ash-free	
Moisture	0.0	0.0
Ash	0.0	0.0
Fixed Carbon	21.7	14.0
Volatile Matter	78.4	86.0
Carbon	58.9	64.6
Hydrogen	5.2	5.7
Nitrogen	3.2	4.1
Oxygen	32.0	24.9
Sulfur	0.7	0.6
HHV (kJ/kg)	21,475	15,467

[a]Moisture in manure samples is low due to solar drying prior to fuel analysis, typically 80% moisture for low-ash dairy manure before drying, moisture of scraped high-ash solids is variable before drying

Yet, as far as the use of DB as a fuel for thermo-chemical conversion technologies is concerned, there may be a problem with the availability of low-ash DB feedstock. The vast majority of DB from large CAFOs is scraped. A very small fraction

of the total DB produced from large dairy operations is the low-ash separated solids from flushed free stall barns that is ideal for energy conversion. One reason for the short supply of low-ash feedstock is that many dairy operators have chosen to not to switch to hybrid or free stall systems at their dairies. Free stalls are usually built in parts of the country where there is a lot of rain fall or inclement weather, which causes mud problems in open lots. Therefore, in dryer parts of the country, such as the Texas Panhandle, most dairies have remained dry open lots. In central Texas the climate is marginal and the rate of water evaporation minus the amount of average rain fall (moisture deficit) is between 50 and 130 cm (20 and 50 inches). Dairy operators must make difficult decisions to either continue running their dairies as dry open lots or convert to hybrid lots (Stokes *et al*., 1999).

Other reasons to convert to free stall barns are environmental regulations of wastewater runoff and herd profitability. Free stall operations offer a more controlled environment for the dairy cows, and hence more milk production. However, water consumption by the farm usually does increase for free stalls due to the flushing systems. Plus, manure management becomes a very different process compared to open lots. Labor costs may also increase due to bedding management (Stokes *et al*., 1999). Even when dairy operators convert to free stall systems, if sand is used as bedding, the DB produced from the dairy will be very high in ash. So, the ability to secure enough low-ash DB for energy conversion is a challenge in and of itself.

The two fuel analyses shown in Table 2.5 will be used later in modeling studies of MBB combustion and its associated economic feasibility and impacts.

For DB, as well as FB and other MBB, the moisture and ash percentages of the biomass significantly affect the fuel's heat value. Plotting heating value against moisture and ash percentage allows some estimation of the required moisture and ash percentage necessary for combustion in boilers, gasification chambers, and other combustors. From Figure 2.4, it can be deduced that CB fuels with ash percentages greater than 40%, on a dry basis, would be unsuitable for suspension coal-fired boilers, but may be acceptable for fluidized bed combustion. It can also be seen from the figure

that, even for lower ash CB with ash contents of 10 to 20% (dry basis); pre-drying processes may be required for raw CB fuels which may contain 60 to 85% moisture as received. Ikeguchi *et al*. (1997) studied the mass transfer of moisture and ammonia from manure in free stall barns. They found heat transfer correlations for manure biomass in terms of air velocity and compared the mathematical correlations to experimental data found in a testing wind tunnel. Carlin (2005) also investigated maximum allowable ash and moisture contents of DB for small-scale, on-the-farm combustion schemes.

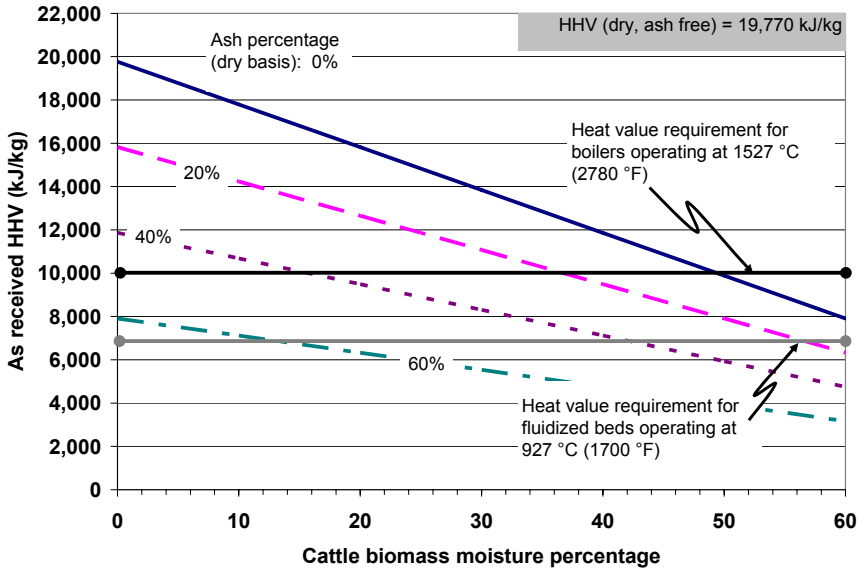

Figure 2.4 Higher heating value of cattle biomass vs. moisture and ash percentage (assuming a dry, ash free HHV of 19,770 kJ/kg)

From TGA experiments, pyrolysis temperatures were found to be 60 to 70 °C less for pure CB fuels than Texas lignite (Lawrence, 2007 and Carlin *et al*., 2008). Finally, in Figure 2.5, the nitrogen, sulfur, and chlorine contents of DB, FB, lignite, and Wyoming sub-bituminous coal are compared on an energy basis. Nitrogen contents of DB and FB are about 2 to 3 times those of lignite and sub-bituminous coal, which suggest higher NO_x emissions if the biomass fuels are burned under fuel lean conditions. Sulfur contents of DB and FB seem to be slightly lower than that of lignite; however, Wyoming sub-bituminous has the lowest sulfur content of all. Moreover, chlorine

content of DB is much greater than either lignite or sub-bituminous coal, which suggests the possibility of higher mercury (Hg) oxidation during coal and biomass co-combustion (Arcot Vijayasarathy, 2007).

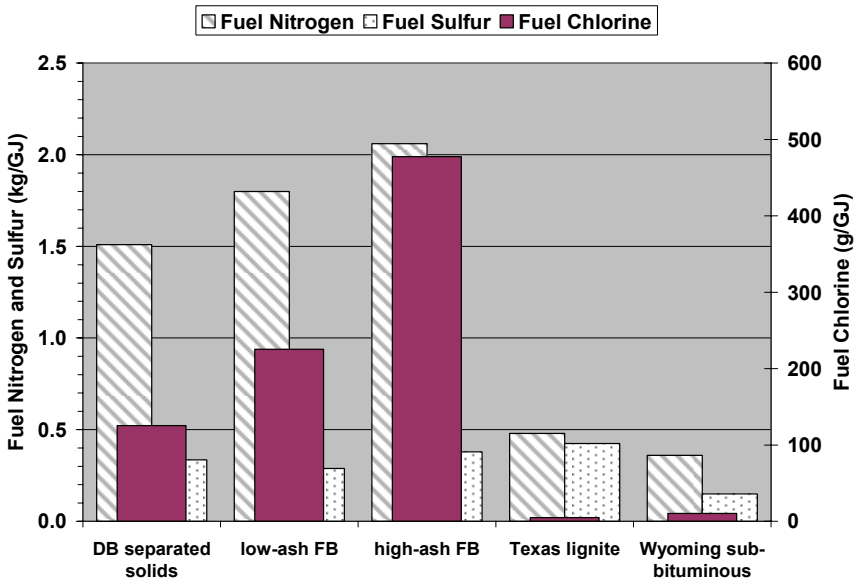

Figure 2.5 Nitrogen, sulfur, and chlorine contents of DB, FB, Texas lignite, and Wyoming sub-bituminous (adapted from TAMU, 2006 and Arcot Vijayasarathy, 2007)

Properties of MBB, such as density and specific heat, are also essential for this study, since drying and transporting models require at least some estimates of these traits. Most of the research into the thermal properties of MBB was conducted in the 1970s and 80s. Houkom *et al*. (1974) and Chen (1982 and 1983) studied the effect of moisture content on the bulk density, specific heat, thermal conductivity, and thermal diffusivity of FB. Both authors conducted experiments and provided curve fitted equations for their data. Houkom's work was also reviewed in a textbook by Mohsenin (1980). Later, Bohnhoff *et al*. (1987) conducted experiments and developed similar curve fitted equations for separated DB solids. Bohnhoff *et al*. also studied the effect of volatile matter content on the average dry particle density of DB solids. Finally Achkari-Begdouri *et al*. (1992) conducted their own study of the thermal properties of high-moisture dairy manure from dairies in Morocco. Achkari-Begdouri *et al*. also

reviewed all the other previous work into the thermal properties of MBB. Since the results for FB and DB were found to be quite similar according to these studies, the properties of both will be discussed here and compared.

Bohnhoff *et al*., Chen, and Achkari-Begdouri *et al*. all published their estimates of average dried manure particle density, which are listed in Table 2.6. Brohnhoff *et al*. also modeled particle density as a function of volatile solids percentage. A plot of the fitted line produced by their experiments is shown in Figure 2.6. According to the expression, the particle density increases when less volatile content is present in the manure. However, Brohnhoff *et al*. did not distinguish between fixed carbon and inert ash as was done earlier in Table 2.4. The term "fixed solids" refers to the combined total of fixed carbon and ash. Yet, presumably less volatile solids means higher ash content in the manure, meaning that high-ash manures are denser and heavier than low-ash solids. This relation between ash percentage and density corroborates some personal discussion with Heflin (2008) who demonstrated, to the current author, that higher ash feedlot manure at an experimental feedlot facility in Bushland, Texas was generally heavier than low-ash feedlot manure.

Table 2.6 Measured mean dry particle density for manure-based biomass from various sources.

mean dry particle density, $\rho_{p,MBB}$ (kg/m^3)	Source	Notes
1524	Chen (1982)	Average particle density from beef cattle manure samples. Standard deviation = 110 kg/m^3.
1576	Bohnhoff *et al*. (1987)	Average particle density from separated dairy manure solids samples. Range: 1534 to 1626 kg/m^3. Standard deviation = 29 kg/m^3. Also modeled mean particle density as a function of volatile solids percentage.
1690	Achkari-Begdouri *et al*. (1992)	Average particle density from high-moisture (%M > 85) dairy manure samples. Range: 1424 to 1902 kg/m^3. Standard deviation = 102 kg/m^3.

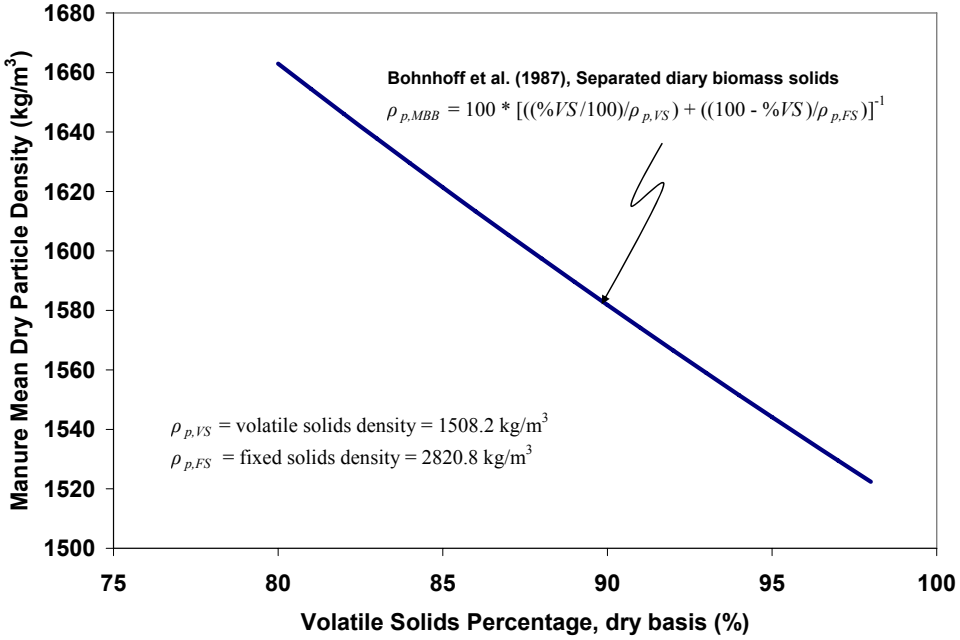

Figure 2.6 Manure-based biomass mean dry particle density vs. volatile solids percentage

One problem with the work conducted by Bohnhoff *et al*. was the extremely high volatile solids percentage found in separated dairy manure solids. They found that raw separated dairy manure had volatile percentages of about 94% and composted dairy manure had volatile percentages between 85% and 90%. These numbers are much higher than those seen in the previous tables. In fact, even on a dry, ash-free basis, no manure samples in the literature were shown to have such high volatile matter contents, except for the averaged volatile matter content of aged DB solids on a dry, ash-free basis presented in Table 2.3. In Table 2.4, separated dairy manure solids were shown to have a volatile matter percentage of just 30% on a dry basis and about 32% on a dry, ash-free basis, far less than what was reported by Bohnhoff *et al*. In Table 2.5, low-ash separated DB was found to have 62.8% volatile matter on a dry basis and 78.4% on a dry, ash-free basis. Similarly in a previous study by Carlin (2005), separated DB solids were found to have 69.7% volatile matter on a dry basis and 78.5% on a dry, ash-free basis. It is not clear if the modeling equation used in Figure 2.6 can be applied to manure with

significantly lower volatile matter, since the density of the fixed solids may change when the proportion of the fixed carbon and inert ash change relative to each other.

Bulk density was also measured for different moisture contents. The results from Chen (1983) and Houkom *et al*. (1974) are shown in Figure 2.7. Bulk density is of special importance when estimating hauling costs of transporting MBB to combustion facilities. Depending on the collection process and weather conditions, the moisture percentage, along with the bulk density, of the MBB can vary greatly.

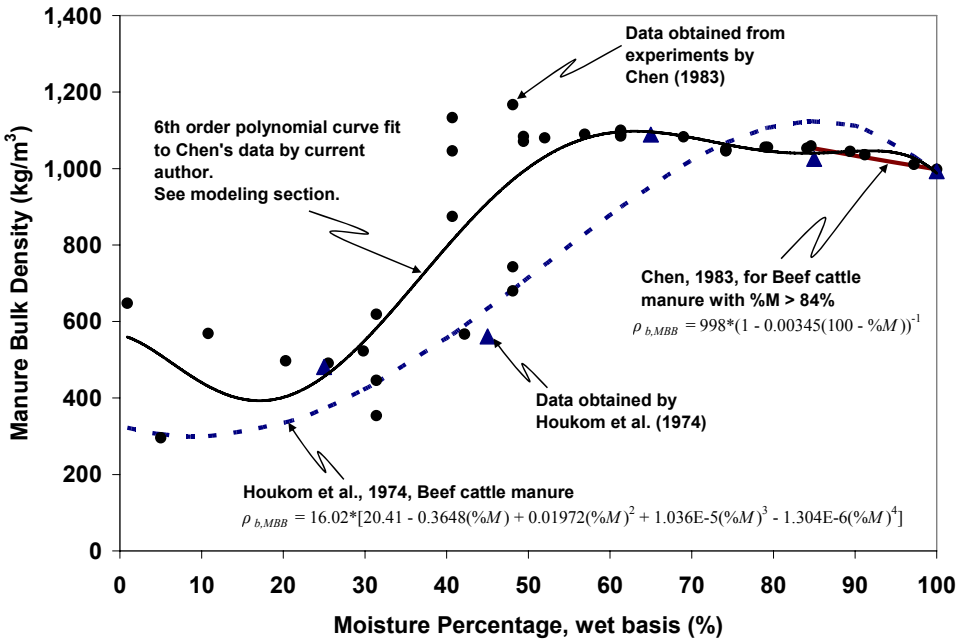

Figure 2.7 Measurements and fitted curves for bulk density of manure-based biomass from various sources.

At very high moisture contents the density of MBB approaches that of water, but as the moisture content decreases the density increases steadily as the manure remains in a liquid phase with dense manure particles. At about 80 or 85% moisture, the manure becomes a dense, high-moisture solid. The density of freshly separated dairy manure solids is greater than the density of the liquid manure entering the mechanical solids separator. However, at about 50 or 60% moisture, the density of the MBB drops steeply as the moisture evaporates leaving numerous void volumes among the manure particles.

The solid manure particles are still dense, but the void volumes in between the particles make the MBB, in bulk, a relatively light solid.

The specific heat of MBB is also highly dependant on moisture content. In Figure 2.8, data from Chen (1982), as well as curve fits from various other researchers, show a linear relationship between specific heat and moisture percentage. Curve fitted lines by Chen (1982), Bohnhoff *et al*. (1987), and Achkari-Begdouri *et al*. (1992) predict that the specific heat of MBB at close to 100% moisture is very close to that of pure water (4.197 kJ/kg K). However, at the other extreme at 0% moisture, the different equations do not exactly agree, and predict that the specific heat of dry MBB will be between 0.92 and 1.44 kJ/kg K.

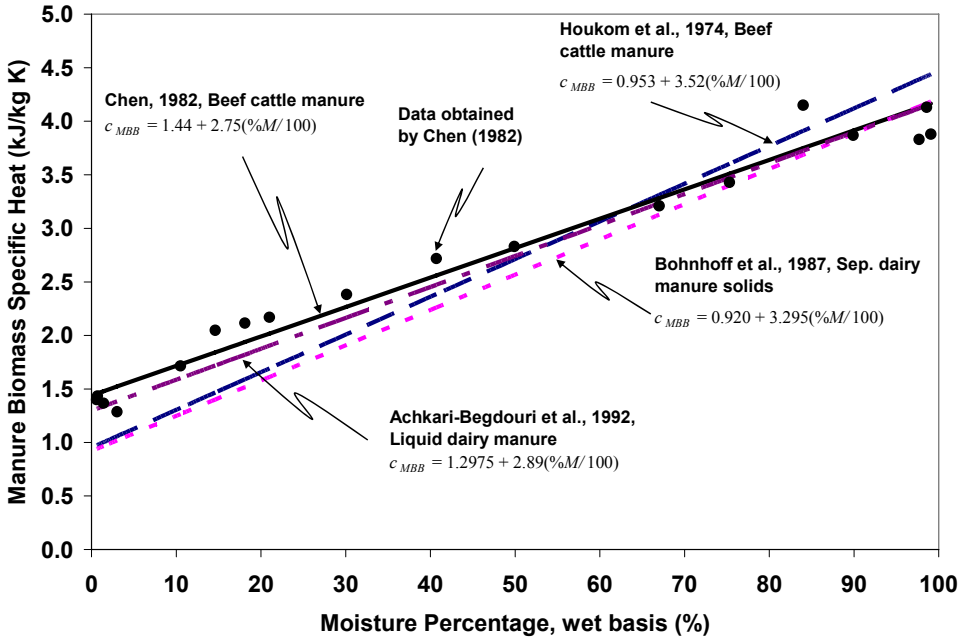

Figure 2.8 Measurements and fitted curves for specific heat of manure-based biomass from various sources.

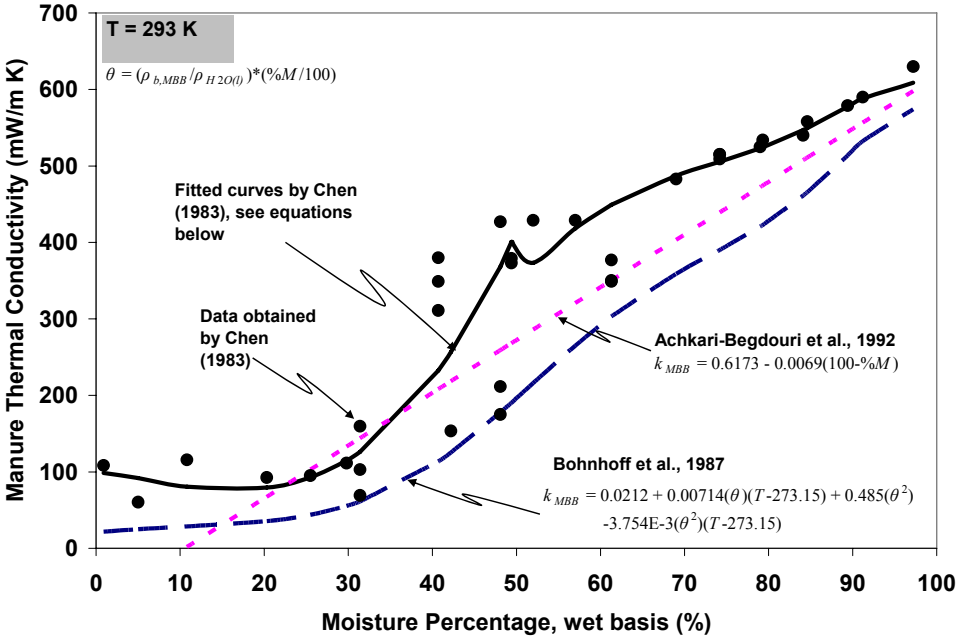

Figure 2.9 Measurements and fitted curves for thermal conductivity of manure-based biomass from various sources.

Thermal conductivity can also be plotted against moisture percentage; however, most of the studies reviewed here, with the exception of Achkari-Begdouri *et al*. (1992), did not fit thermal conductivity curves to moisture percentage. Bohnhoff *et al*. (1987) fitted thermal conductivity to four parameters: bulk density, the density of water, the temperature, and the moisture percentage. See Figure 2.9. Chen (1983) fitted thermal conductivity with different parameters depending on the range of moisture and density of the MBB. For MBB with < 49% moisture:

$$k_{MBB} = 706 * \exp(-3.06 * \varepsilon) \tag{2.1}$$

where ε is the porosity or the void volume of the biomass. For MBB with >49% moisture and a bulk density less than that of water:

$$k_{MBB} = 119.5 - 0.372\rho_{b,MBB} + 0.00066\rho_{b,MBB}^2 \tag{2.2}$$

If the bulk density is greater than that of pure water, then:

$$k_{MBB} = \rho_{b,MBB}\left[0.607 - 0.0051(100 - \%M)\right] \tag{2.3}$$

Thermal diffusivity of MBB can be computed with the following expression:

$$\alpha_{MBB} = \frac{k_{MBB}}{\rho_{b,MBB} c_{MBB}} \tag{2.4}$$

Chen (1983) and Bohnhoff *et al*. (1987) also plotted thermal diffusivity against various parameters.

Finally, for MBB in solid states, it is also helpful to know the size distribution of the particles. Houkum (1974) used number 4, 8, 16, 30, 50, 100, and 140 sized sieves to measure the size distribution of particles of both high moisture (85%) and low moisture (25%) beef cattle manure. The results of these experiments are shown in Table 2.7. Meyer *et al*. (2007) conducted similar experiments for as-excreted dairy cow manure for lactating cows, heifers, and calves. The results for adult lactating cows are shown in Table 2.8 along with results for partially composed separated dairy cow manure used for coal-MBB co-firing experiments by Lawrence (2007).

Table 2.7 Results of sieve analyses of beef cattle manure

Sieve No.	Particle Size (μm)	% on Sieve	Cumulative % greater than stated size
Beef cattle manure with a 25% moisture content (Houkum, 1974)			
4	4750	3.80	3.80
8	2380	35.40	39.20
16	1190	27.80	67.00
30	541	18.30	85.30
50	282	9.50	94.80
100	149	3.40	98.20
140	104	1.00	99.20
Pan		0.80	100.00
Beef cattle manure with an 85% moisture content (Houkum, 1974)			
4	4750	3.20	3.20
8	2380	7.10	10.30
16	1190	11.90	22.20
30	541	9.70	31.90
50	282	7.90	39.80
100	149	3.60	43.40
140	104	1.30	44.70
Pan		55.30	100.00

Table 2.8 Results of sieve analyses for dairy cow manure

Sieve No.	Particle Size (μm)	% on Sieve	Cumulative % greater than stated size
Low-ash partially composted separated solids, after being solar dried and coarsely ground (Lawrence, 2007)			
10	2000	0.04	0.04
16	1190	0.26	0.30
20	840	0.84	1.14
50	300	21.82	22.96
100	150	31.45	54.41
200	75	22.88	77.29
325	45	9.60	86.89
Pan		13.11	100.00
As-excreted lactating dairy cow manure (Meyer *et al*., 2007)			
10	2000	30.00	30.00
18	1000	7.00	37.00
35	500	6.00	43.00
60	250	5.00	48.00
120	125	3.00	51.00
Pan*		49.00	100.00

*Includes feces and urine

The DB used by Lawrence was solar dried in a green house, finely ground and partially crushed by Kevin Heflin at the Texas A&M AgriLife Research and Extension Center in Amarillo, Texas before the sieve analysis.

The distributions of all of these MBB samples are compared to each other in the log-log plot in Figure 2.10. Rosin-Rammler distribution equations can be fitted to the data from the sieve analyses to predict the particle size distribution at all particle sizes. The Rosin-Rammler distribution equation has the following form:

$$\begin{pmatrix} Mass\ percentage \\ less\ than\ the\ indicated \\ particle\ size \end{pmatrix} = D\left(d_p\right) = 100 * \left\{1 - \exp\left[-\left(\frac{d_p}{d_c}\right)^n\right]\right\} \qquad (2.5)$$

where d_c is the characteristic particle size of the distribution and n is a shape parameter. In the case of the Rosin-Rammler distribution, d_c is the particle size at which 63.2% of the mass of the particles are smaller in size than d_c. From the figure, it can be seen that the characteristic particle size was 274 μm for high moisture beef cattle manure,

2180 µm for low moisture beef cattle manure, 963 µm for as-excreted dairy manure, and 246 µm for air dried, coarsely ground DB. The Rosin-Rammler distribution is discussed further by Brown *et al*. (1995) and Hinds (1999). Lawrence (2007), as well as Thien (2002), applied the distribution equation to coals and MBB for co-fire experiments. The current author applied the distribution to the data from Houkum (1974) and Meyer *et al*. (2007).

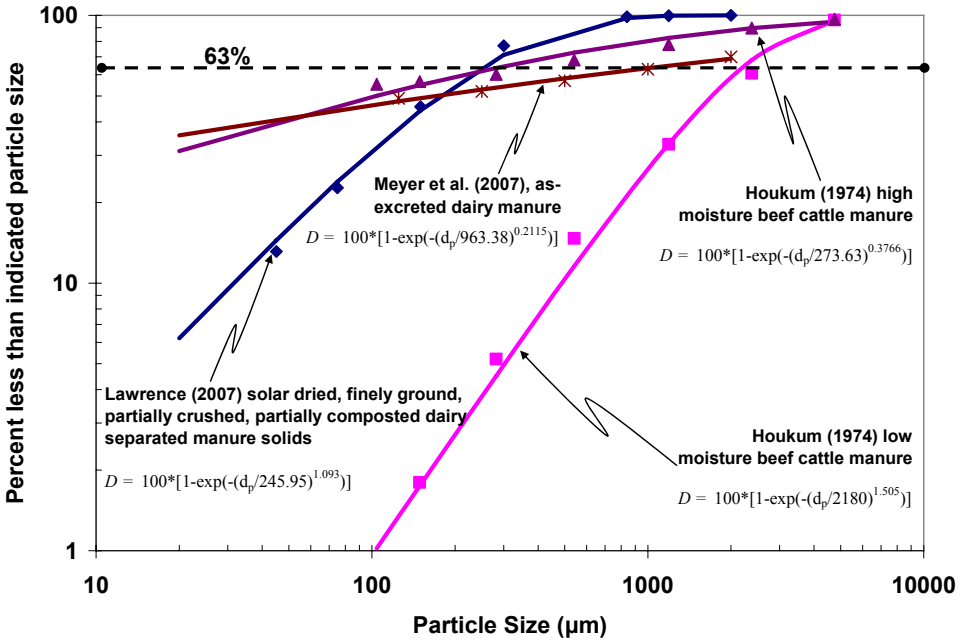

Figure 2.10 Particle size distributions of beef cattle and dairy cow manure from various sources plus Rosin-Rammler distribution equations generated by Lawrence (2007) and the current author

It is somewhat surprising that higher moisture MBB would have a more even distribution and lower characteristic diameter size than lower moisture solids. The comparative results from these studies seem to suggest that high moisture solids, including as-excreted solids which can be about 80% moisture, are relatively fine. During drying, the particles seem to agglomerate together to form a broader distribution of particle sizes, with a greater characteristic size, making dried manure more coarse than fresh manure. Only after grinding, is the characteristic size decreased, however, the broad size distribution still remains, as seen by the data from Lawrence (2007).

Alternatively, the MBB can be characterized by the mass mean diameter, which can be computed with the following expression:

$$d_{mm} = \frac{\sum m_i d_i}{M} \tag{2.6}$$

where m_i can be read from column 3 in Table 2.7 or Table 2.8, d_i can be read from column 2, and M in this case would be 100%. Masses of each group and the total mass, M, can also be used instead of percentages (Hinds, 1999).

2.1.3. Feedlot Biomass

The population of feedlot cattle on large operations in the US is illustrated in Figure 2.11. The three largest cattle states are Texas, Kansas and Nebraska, respectively. These three states produce more feedlot cattle than the other 47 states combined. Most of the Texas feedlots are concentrated in the Panhandle region of the state (NASS, 2007). Feedlots in the Texas and Oklahoma Panhandle regions can range between 5,000 and 75,000 head (Harman, 2004). Moreover, feedlot cattle can produce 5 to 6% of their body weight in manure each day; roughly 5.5 dry kg (12 lb) per animal per day (DPI&F, 2003). According to the ASAE (2005) standard, full grown beef cattle excrete 6.6 dry kg (15 lb) of manure per animal per day. However, only about 5.0 dry kg (11 lb) per animal per day is collectable when scraped from earthen lots. Beef cow manure from earthen lots can range between 53 and 87% ash (dry basis), and 24 and 42% moisture. Thus, nearly 18 million dry metric tons (19.8 million tons) of cattle manure per year comes from large feedlot CAFOs. Texas alone produces over 27% of this annual total. If the manure is roughly 70% ash (dry basis), and the dry ash-free heating value of the manure is roughly 20,000 kJ/kg, the thermal energy conversion of the collectable manure from large feedlot operations in the US can produce about 109 million GJ/yr (103 million MMBtu/yr).

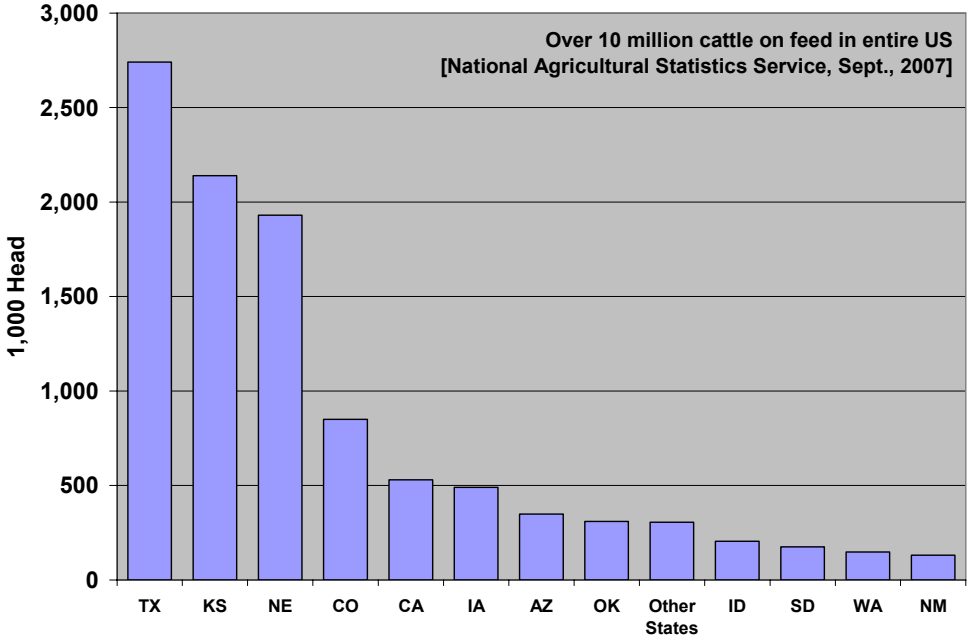

Figure 2.11 Feedlot cattle on large 1,000+ head operations in the US (NASS, 2007 and USDA, 2007)

In Table 2.9, ultimate and heat value analyses are presented for cattle feed ration, low-ash feedlot manure, and high-ash feedlot manure collected at an experimental feedlot facility at Bushland, Texas by Mr. Kevin Heflin. Just as with DB, the primary concern with FB is the ash content in the manure. Hence, the way the manure is collected and how the feed cattle are kept is important. Most cattle on feed at large feedlot operations are kept in large feed yards or corrals, similar to open lots discussed previously for dairies. The important distinction between feedlots that produce low-ash FB and feedlots that produce high-ash FB is the type of surfacing of the feed yards. Feedlots that are not paved or only paved with soil tend to produce high ash manure, about 45% on a dry basis according to Table 2.9. Although ash contents can be much greater from unpaved lots if less care is taken when scraping the corrals. As illustrated in Figure 2.12, inert material can be mixed with the excreted manure by the animals when they shuffle their hooves and from box blade scrapers collecting soil along with the manure. Problems with mud in open lots also causes soil (ash) entrainment, which leads to collecting FB higher in ash. On the other hand, as seen in Figure 2.13, feedlots

paved with either cement or fly ash byproduct from coal combustion can produce FB that is very low in ash. Further discussion of paved and un-paved feedlots was undertaken by Sweeten *et al.* (2006).

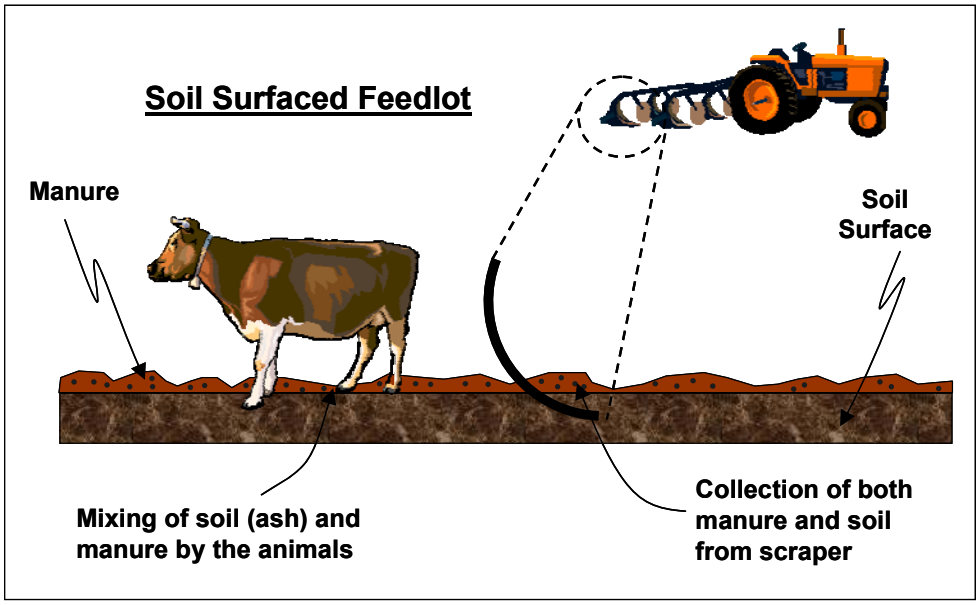

Figure 2.12 Feedlot biomass collection at soil surfaced feed yards

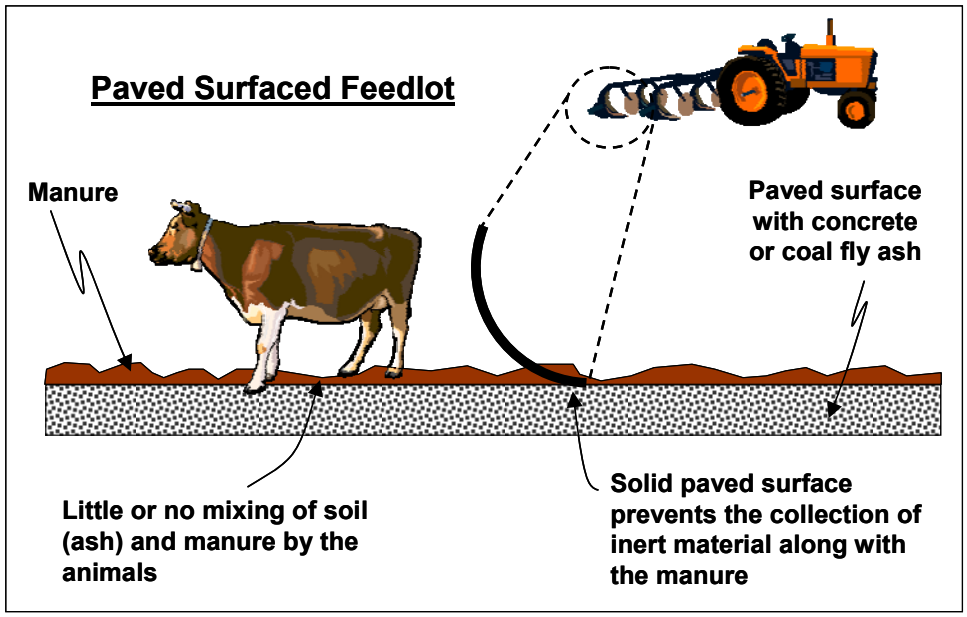

Figure 2.13 Feedlot biomass collection at paved surfaced feed yards

Table 2.9 Ultimate and heat value analyses of cattle feed ration and feedlot manure from Bushland, Texas

	Cattle Feed Ration[b]	Low-ash Feedlot Manure[c]	High-ash Feedlot Manure[c]
(by mass)		**As received**	
Moisture[a]	19.8	29.3	27.3
Ash	3.6	9.6	32.9
Fixed Carbon	17.9	12.9	7.3
Volatile Matter	59.5	48.0	32.5
Carbon	35.9	35.1	23.5
Hydrogen	5.0	4.2	2.8
Nitrogen	1.6	2.4	1.7
Oxygen	34.0	19.1	11.5
Sulfur	0.1	0.4	0.3
HHV (kJ/kg)	14,700	13,222	8,189
		Dry	
Moisture	0.0	0.0	0.0
Ash	4.5	13.6	45.2
Fixed Carbon	22.3	18.2	10.0
Volatile Matter	74.2	67.9	44.7
Carbon	44.8	49.6	32.3
Hydrogen	6.2	5.9	3.9
Nitrogen	2.0	3.3	2.3
Oxygen	42.4	27.0	15.8
Sulfur	0.1	0.5	0.4
HHV (kJ/kg)	18,329	18,688	11,266
		Dry, ash-free	
Moisture	0.0	0.0	0.0
Ash	0.0	0.0	0.0
Fixed Carbon	23.4	21.2	18.4
Volatile Matter	77.6	78.5	81.7
Carbon	46.9	57.4	59.1
Hydrogen	6.5	6.8	7.0
Nitrogen	2.1	3.9	4.2
Oxygen	44.4	31.3	28.9
Sulfur	0.1	0.6	0.8
HHV (kJ/kg)	19,191	21,626	20,572

[a]Moisture in manure samples is low due to solar drying prior to fuel analysis

[b]Sweeten *et al*., 2003

[c]Sweeten and Heflin, 2006

Sweeten *et al*. (2003) reported that the higher heating value (HHV) of FB on a dry, ash-free basis tends to generally be between 18,000 and 22,000 kJ/kg depending on

the animal's feed ration. In Figure 2.14, it may be seen that raw FB, partially composted (PC) FB, fully/finished composted (FC) FB, and cattle ration (cattle feed) all fall under this dry, ash-free (DAF) HHV range. Similar results are also found when blending 5% crop residues with each FB fuel.

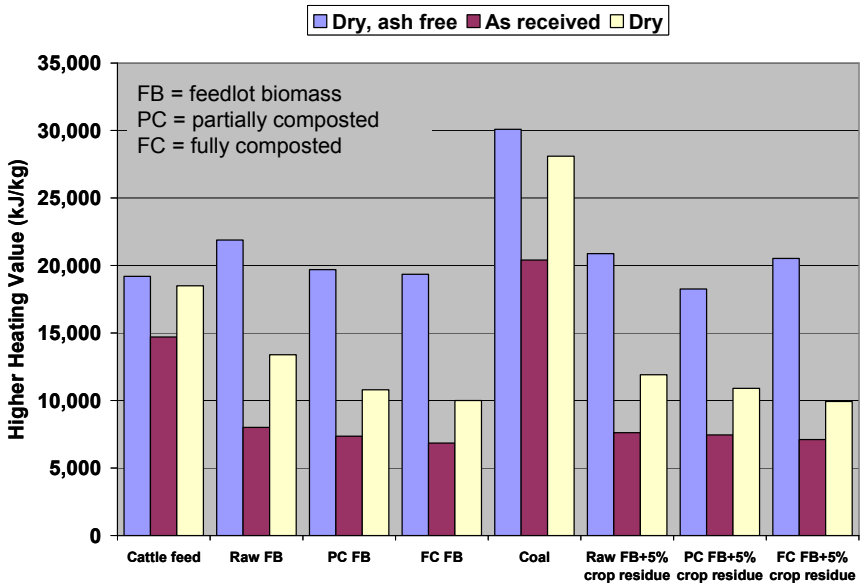

Figure 2.14 Higher heating values for cattle ration, raw FB, partially composted FB, finished composted FB, coal, and respective FB+5% crop residue blends (adopted from Sweeten *et al*., 2003)

On a dry, ash-free basis, the combustible contents of low-ash FB and high-ash FB are similar to the feed ration given to the animals, just as was the case for dairy cows. However, also like dairies, very few feedlots produce low-ash biomass, because the vast majority of feedlots are unpaved. There are concerns of how the hard surfaces of paved lots will affect the animals. Moreover, paving feedlots is expensive, and since many operations are so large, a tremendous amount of concrete or coal ash would be needed to completely convert an entire feedlot operation to paved surfaces. Over time, maintenance and repaving may also be required, since the animals are heavy and generate a great amount of force when they stomp on the ground. This in turn may add to the cost of operating the feedlot (Heflin, 2008).

Previous TGA experiments by Martin *et al*. (2006) found similar ignition temperature results for FB as with DB, discussed earlier. Pure FB samples had an average ignition temperature of 474 °C (885 °F), while biomass blends with Texas lignite coal had an average ignition temperature of 292 °C (560 °F). The lower ignition temperatures in coal-FB blends are generally due to the high amount of fixed carbon in coal that is not present in pure biomass fuels. Ignition temperature did not vary appreciably between high ash FB and low ash FB. Nor did it vary significantly with average particle size or coal:FB blend ratio. Additional TGA analyses of FB pyrolysis are also provided by Raman *et al*. (1981a). A study by Rodriguez *et al*. (1998) showed that drying at 100 °C (212 °F) did not significantly affect the heating value of cattle biomass fuels. Moreover, additional information of biomass fuel properties and heating values can be found by Annamalai *et al*. (2006) and Annamalai *et al*. (1987b).

2.1.4. Hog or Swine Biomass

Most of the discussion in this dissertation will center on cattle manure. However, much of the same findings and modeling equations presented here can be used for hog or swine MBB in combustion systems as well. In 2007, Iowa had the largest inventory of hogs and pigs with over 19 million head. This was almost twice as much as the second largest state inventory, which belonged to North Carolina with about 10 million head. Minnesota, Illinois, and Indiana were the next largest swine states in 2007. In Table 1.1, the East North Central census region of the US was shown to be the largest coal consuming region. Four of these states (Illinois, Indiana, Michigan, and Ohio) are all among the states with the largest swine inventories. Figure 2.15 is a graph of hog and pig inventory by state in 2007.

The ultimate, proximate, and heat value analyses from three different studies of swine manure may be found in Table 2.10. Like cattle manures, swine manure is 70 to 80% volatile matter with a dry, ash free higher heating value of about 20,000 kJ/kg. Swine manure is also, at many times, flushed from indoor piggeries and stalls, and very high in moisture, as can be seen in the table. However, the ash content of this high

moisture swine manure is about 30 to 35% on a dry basis, which is slightly higher than low-ash dairy manure, which is also generally flushed from free stall barns.

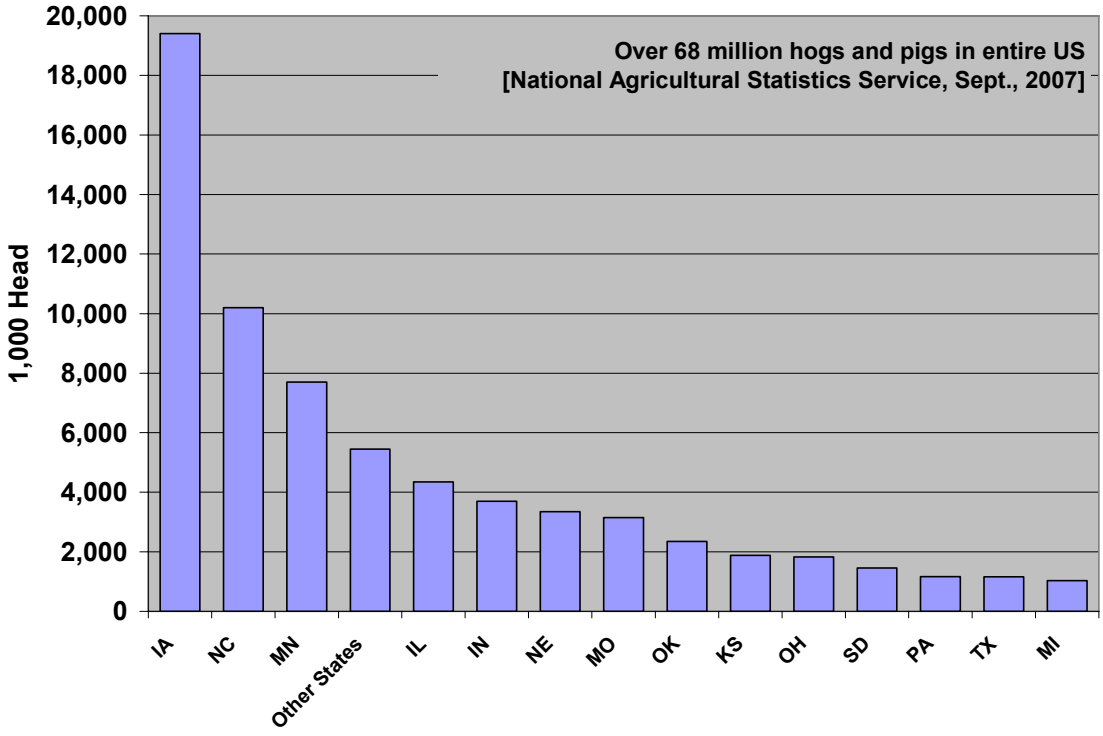

Figure 2.15 Total inventory of hogs and pigs by state in the US in 2007 (NASS, 2007)

Table 2.10 Ultimate, proximate, and heat value analyses of various hog or swine manures

	Air-dried Raw Hog Manure[a]	High Moisture Swine Manure[b]	High Moisture Pig Manure[c]
(by mass)		**As received**	
Moisture	7.2	72.57	92.1
Ash	29.1	NR[d]	2.8
Fixed Carbon	11.3	NR[d]	1.0
Volatile Matter	52.3	23.94	4.1
Carbon	34.3	12.53	2.8
Hydrogen	5.0	1.77	0.3
Nitrogen	3.5	0.95	0.2
Oxygen	27.4	8.59	1.7
Sulfur	0.7	0.1	NR
HHV (kJ/kg)	14,511	NR	1,089
		Dry	
Moisture	0.0	0.0	0.0
Ash	31.4	NR	35.4
Fixed Carbon	12.2	NR	12.7
Volatile Matter	56.4	87.3	51.9
Carbon	37.0	45.7	35.4
Hydrogen	5.4	6.5	3.8
Nitrogen	3.7	3.5	2.8
Oxygen	29.5	31.3	21.5
Sulfur	0.7	0.4	NR
HHV (kJ/kg)	15,640	NR	13,785
		Dry, ash-free	
Moisture	0.0	0.0	0.0
Ash	0.0	0.0	0.0
Fixed Carbon	17.8	NR	19.6
Volatile Matter	82.2	NR	80.4
Carbon	53.9	NR	54.9
Hydrogen	7.9	NR	5.9
Nitrogen	5.5	NR	4.3
Oxygen	43.0	NR	33.3
Sulfur	1.0	NR	NR
HHV (kJ/kg)	22,798	NR	21,353

[a]Jensen *et al*., 2003

[b]He *et al*., 2000

[c]ECN, 2003

[d]Ash + fixed carbon is 3.49% on an as received basis

NR: Not reported

According to the ASAE (2005) standard, gestating sows excrete about 0.5 dry kg (1.1 lb) of manure per animal per day, lactating sows excrete 1.2 dry kg (2.5 lb) of manure per animal per day, and boars excrete about 0.38 dry kg (0.84 lb) of manure per animal per day. About 0.32 dry kg (0.70 lb) of manure per animal per day is collectable from flushed manure from indoor piggeries. Liquid flushed manure from indoor piggeries is generally about 98% moisture. Roughly 7.9 million dry metric tons (8.7 million tons) of swine manure can be collected every year in the US. If the manure solids are 40% ash on average, then the thermal energy conversion of swine manure can potentially generate about 95 million GJ/yr (90.3 million MMBtu/yr).

2.2. Manure-based Biomass's Effect on Emissions from Coal Combustion

The average baseline NO_x levels for wall and tangentially-fired boilers, using both bituminous and sub-bituminous coals, have decreased from 1995 to 2003, primarily due to the usage of low-NO_x burners and air staging. The nitrogen contained in a solid fuel is released to the gas phase during combustion and can either form NO or N_2 depending on the combustion conditions. Fuel nitrogen is typically released as a mixture of HCN, NH_3 and N_2 from coal and biomass, see Figure 2.16. During homogeneous combustion, these gases will form NO mostly under lean conditions when O_2 is available; however, under fuel rich conditions, N_2 will form, as there is a limited amount of O_2 to form NO. The amount of NO that is converted to N_2 depends on the proportion of NH_3 to HCN, with higher NH_3/HCN ratios providing greater conversion. The NO_x generated from fuel nitrogen compounds is termed as fuel NO_x, while the NO_x from atmospheric N_2 is referred as thermal NO_x. For most coal-fired units, thermal NO_x contributes about 25% of the total NO_x emission, and fuel NO_x contributes the other 75% of the total (DOE, 1999).

Although MBB such as cattle biomass contains high amounts of fuel nitrogen, much of the nitrogen is released very rapidly during combustion along with the rest of the volatile matter. Researchers at Texas A&M University have hypothesized that much of the fuel nitrogen from biomass is also released in the form of NH_3. If this is true, then

MBB has the potential to be an effective reburn fuel that can, not only reduce NO_x by releasing hydrocarbon fragments in rich secondary combustion regions as in reburning with natural gas, but also release NH_3 that can also react with existing NO_x emissions from coal combustion in primary burn zones, thereby reducing NO_x more effectively than other reburn fuels that have been studied in the past. In the next section of this dissertation, a more detailed description of coal-biomass co-combustion technologies will be made.

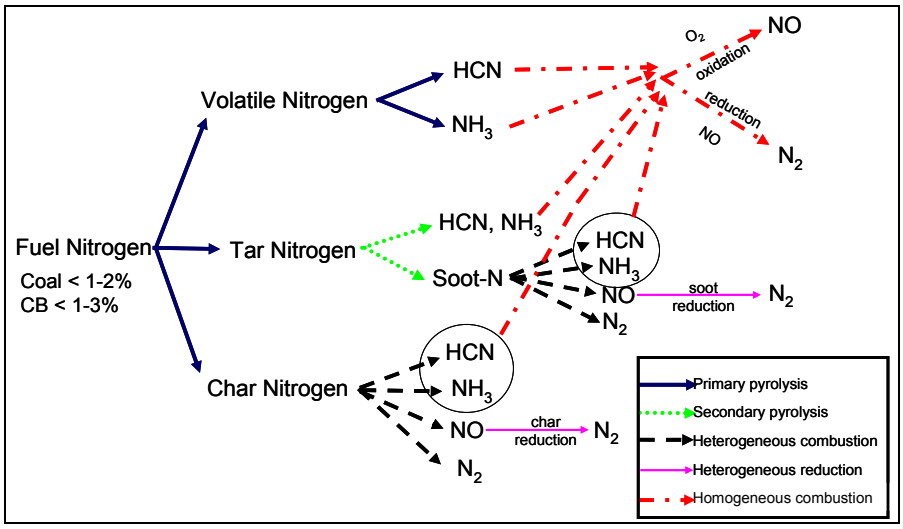

Figure 2.16 Fuel nitrogen paths to NO and N_2 (adapted from Di Nola, 2007)

Co-combustion of coal and cattle biomass can also reduce the amount of nonrenewable CO_2 emissions from coal-fired power plants. Coal combustion accounted for 36% of the roughly 5.9 billion metric tons of CO_2 released by anthropogenic sources in the US during 2006. Of course, burning coal with cattle biomass, alone, will not reduce CO_2 emissions to acceptable levels; however, as discussed by Pacala *et al.* (2004), biomass combustion can be one of many wedges of development in alternative technologies that can create an energy economy capable of sustaining our climate and our way of life. See Figure 2.17. Most of these technologies, such as nuclear power, solar energy, and bio-fuel combustion, are already well understood, but they still must be further implemented into our current energy production systems.

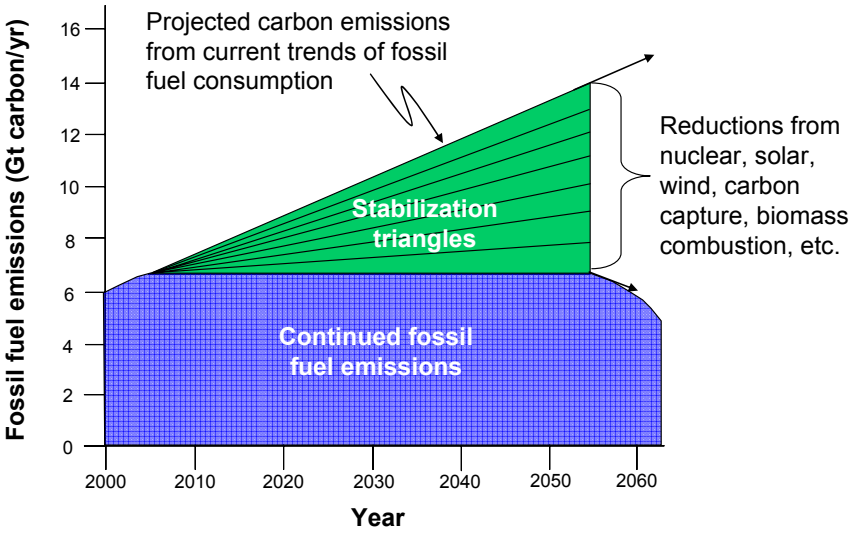

Figure 2.17 Stabilization triangles of avoided emissions and allowed emissions (adapted from Pacala *et al*., 2004)

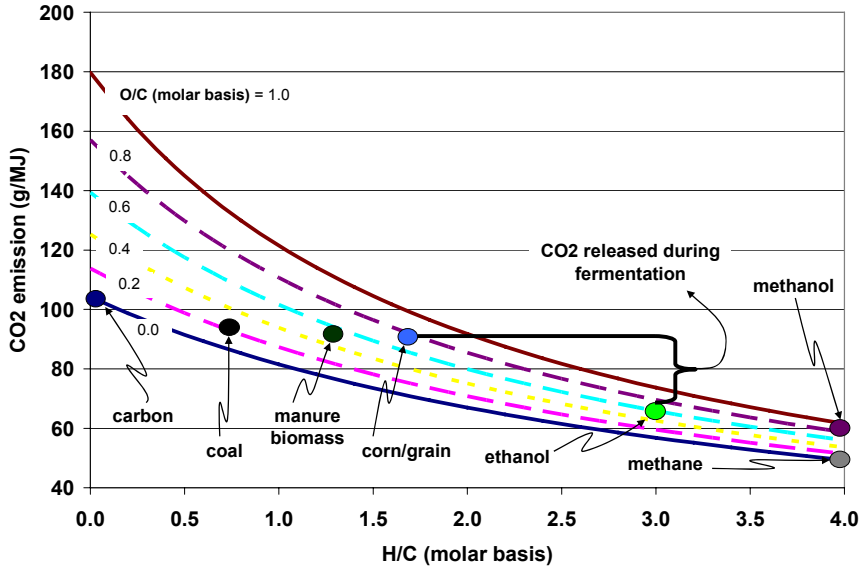

Figure 2.18 CO_2 emission vs. O/C and H/C ratios, with various fuels indicated (Carlin *et al.*, 2008)

Carbon emissions from a fuel are directly related to the hydrogen-carbon (H/C) ratio and the oxygen-carbon (O/C) ratio, as can be seen in Figure 2.18. Note that this

figure shows total CO_2 emission (both for renewable and non-renewable fuels). Plotting CO_2 emissions in this way can provide an estimation of carbon released during synthetic gas (e.g. methane) and value added liquid fuel (e.g. ethanol) processing. For instance, CO_2 released by the generation of ethanol from corn or grain through fermentation is indicated on Figure 2.18. This difference of CO_2 emission between corn (approximately the same as coal) and ethanol must be accounted for when determining carbon savings and footprints. Ideally, this difference in CO_2 emission should also come from a renewable source when generating value added liquids and gases.

The drive for cleaner air has also caused an increased concern for control of toxic metal emissions from coal combustion systems. In particular, mercury has been targeted for control due to its unique characteristics such as high volatility, bio-accumulation and other toxic properties. To date, there are no post combustion treatments which can effectively capture elemental mercury vapor. The Environmental Protection Agency (EPA) has released a Clean Air Mercury Rule, which caps the mercury emission from coal-fired power plants from a current rate of 158 tons per year to 15 tons per year by 2018. Elemental mercury (Hg^0), due to its volatile nature, exists in vapor phase in the flue gases which escapes into the atmosphere without being captured in any environmental emission capturing devices currently available, while an oxidized form of mercury (Hg^{2+}, e.g. $HgCl_2$) can be captured in commonly used Flue Gas Desulphurization (FGD) units, since oxidized mercury is soluble in water. Moreover, particulate mercury (Hg_p), which is found in fly ash, can be captured in bag houses and electrostatic precipitators (ESP). See Figure 2.19. The objective of this aspect of the research is to use cattle biomass and coal/biomass blends as fuel to effectively convert Hg^0 to its oxidized form which can be captured more easily when using traditional environmental devices. The high chlorine content of CB, particularly DB, may allow more Hg^0 to be converted to Hg^{2+}.

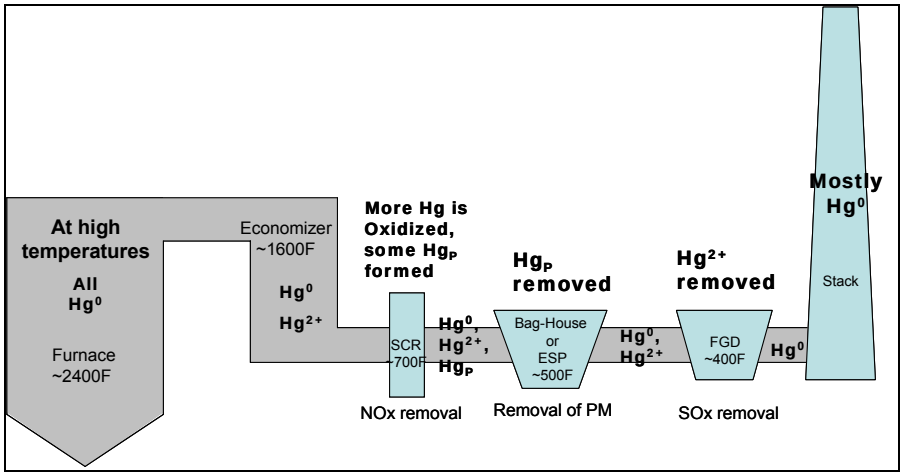

Figure 2.19 Mercury reduction co-benefits from secondary combustion controls (adapted from Arcot Vijayasarathy, 2007)

Yet, due to the high amount of fuel-bound nitrogen in CB fuels, it is critical to determine what happens to this nitrogen during combustion. Otherwise, any reductions in CO_2 and Hg may be overruled by higher NO_x emissions. In following sections of this paper, CB co-firing, reburning, and gasification experiments will be reviewed. This review includes most of the work conducted at the Coal and Biomass Laboratory of Texas A&M University as well as limited literature review. There will also be a brief review of biological gasification processes for high moisture manure.

2.3. Energy Conversion Technologies

Five different paths for energy production from manure based-biomass (MBB) are illustrated in Figure 2.20. From the high moisture MBB exiting free stall barns, open lots, and feed yards, the remaining liquid stream from mechanical (screen) separation can be sent through an anaerobic digestion system, which will be referred to as Path 1. Anaerobic digestion allows for methane capture from natural biological decomposition of manure wastes. The resulting CH_4/CO_2 gas mixture (usually termed biogas) can then be burned in gas turbines, internal combustion engines, or heat furnaces for energy production.

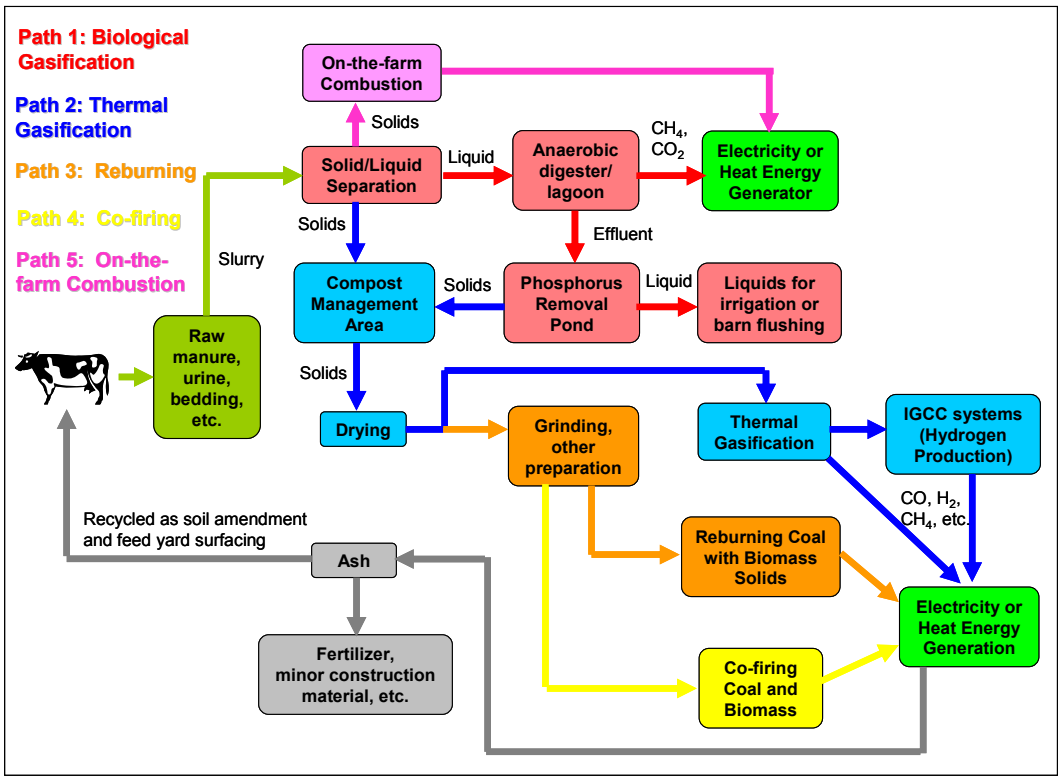

Figure 2.20 Five paths to heat and electrical energy production from MBB (adapted from Annamalai *et al.*, 2007)

The remaining manure solids from the mechanical separation can be dried, ground, and either gasified or fully combusted. Path 2 in the present discussion will be thermal gasification of MBB either with air or air-steam mixtures to produce low to medium-calorific value gases which can then be utilized in a variety of different combustion processes. Moreover, gasification allows the usage of coarser, higher ash, and higher moisture MBB solids. Path 3 will be burning coal in a primary burn region and then reburning the coal with MBB in a secondary or reburn zone of an existing coal-fired power plant. The primary purpose of reburning is to reduce NO_x emissions. Path 4 will be co-firing coal with MBB in the primary burn region of a coal-fired power plant. In Paths 3 and 4 MBB is utilized as a supplementation to coal, which can reduce the amount of non-renewable CO_2 emissions from large coal plants; however, both of these applications generally require drying and fine grinding of both coal and MBB fuels. Finally, Path 5 is the direct firing or incineration of manure wastes on or very near the

farm. The primary purpose of Path 5 is to dispose of manure while reducing the need of transporting large quantities of raw manure off the farm or land application of unprocessed solids as fertilizer. Electrical or heat energy is an additional benefit of Path 5 systems.

In this section, there will first be a brief discussion of anaerobic digestion. Anaerobic digestion is the most commercially available energy conversion system involving MBB. Investigators at Texas A&M have studied Paths 2 through 5 extensively for research and development purposes. Results from experimental research on gasification, reburning, and co-firing (Paths 2, 3, and 4, respectively) are presented in order to show how CB can reduce coal consumption, NO_x emissions, and Hg emissions. The economic viability of installing a co-combustion system on an existing coal plant is the main topic of discussion for this dissertation, along with computational models and system designs for Path 5. However, information about Paths 1 through 4 will be presented first.

2.3.1. Biological Gasification of Manure-based Biomass

To date, most of the research on energy conversion systems that involve high moisture and/or high ash animal biomass have dealt with capturing methane (CH_4) or biogas (mixture of CH_4, CO_2, and other trace gases) biologically produced from anaerobic digesters. The biological conversion of MBB to biogas can occur anaerobically (absence of oxygen) in three different steps. First, hydrogen-producing acetogenic bacteria consume organic acids in the liquid manure to produce hydrogen, CO_2, formate, and acetate. Secondly, homoacetogenic bacteria form more acetate from H_2, CO_2, and formate. Finally, methanogenic bacteria produce CH_4. There may be an initial hydrolysis step to break down lignocellulosic material, but this step is primarily used when digesting crop residues. In contrast to plant or crop-based biomass, manure typically does not contain enough lignin to make an initial hydrolysis step cost effective (Probstein *et al*., 2006c).

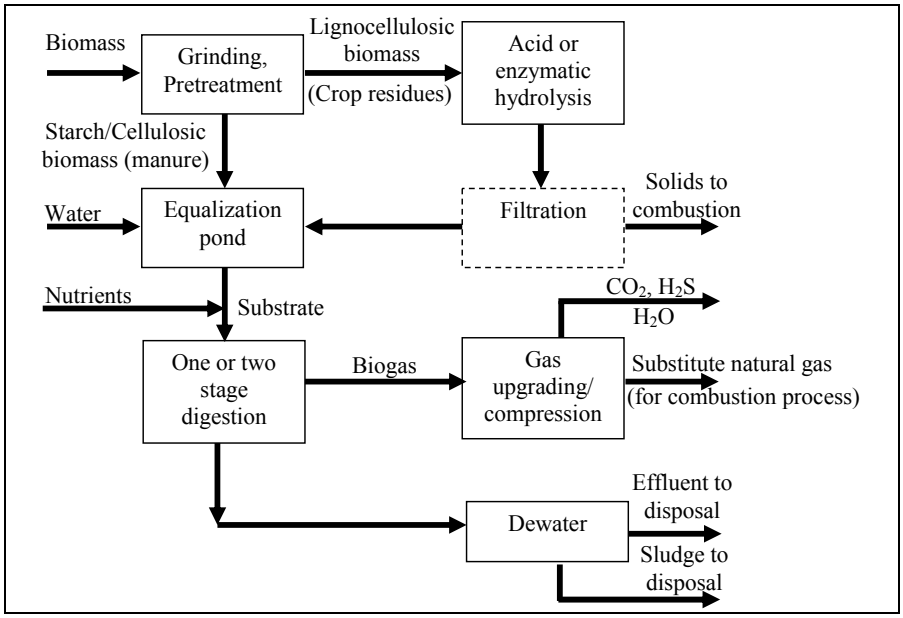

Figure 2.21 Simplified anaerobic digestion flow diagram (adopted from Probstein *et al*., 2006c)

Ideally all three steps should occur in separate reactors; however, as shown in Figure 2.21, manure is usually first sent to an equalization pond so that a mixture of biomass, water and nutrients can form a homogeneous substrate before entering a digester. Sometimes the digester will be divided into two stages, with mechanical mixing occurring in the first stage, although mixing may be found not to be energy efficient. Wen *et al*. (2007) found that treating the manure before sending it to the digester, and thereby increasing its organic strength, had more of an effect on biogas production and organic matter removal than mixing. Plug flow reactors and completely mixed reactors performed very similarly when the manure was treated before entering the digester. It was also found that liquid manure from storage lagoons did not produce as much biogas as liquid manure created from as-excreted manure plus fresh tap water (1:4 and 1:2, by weight, mixtures of manure and tap water were investigated). Reduction of total solids in the manure varied between 27 and 48% and reduction of volatile solids varied between 26 and 47%, with higher reductions being found for the 1:2 mixture of excreted manure to tap water.

Depending on whether the desired end product is a low, medium, or high calorific value gas, the biogas can be upgraded by removing undesirable contaminants, such as hydrogen sulfide (H_2S), and neutral gases, such as CO_2 and water vapor. Generally, both of these products must be removed to various extents in order to provide an adequate natural gas substitute. Hydrogen sulfide and CO_2 are usually removed from a product gas through liquid absorption (Kohl *et al*., 1974). However, if the biogas is to be burned in a conventional, industrial IC engine for electric power, on or very near the animal feeding operation (*in situ*), usually only particulate matter and water vapor removal from the raw biogas are required.

The bacteria involved in anaerobic digestion can also be divided into the temperature range in which they thrive. Psychophilic bacteria thrive at near ambient temperatures (25 °C or 77 °F), mesophyllic bacteria dominate at about 35 °C (95 °F) and thermophyllic bacteria dominate at higher temperatures of 57 °C (135 °F). The selection of operating temperature determines which bacteria group will thrive, and hence also determines the percentage of CH_4 in the biogas, the conversion rates, the residence time of the substrate in the digester, and the overall cost of the system (Probstein *et al*., 2006c). Typically biogas can contain between 55 to 70% CH_4 and 30 to 45% CO_2; although, there have been reports of biogases with as much as 90% CH_4, even without upgrading (Krich *et al*., 2005).

Nutrients such as nitrogen, phosphorus, and alkali metals must be present for anaerobic bacteria to survive, thus manure, which contains all of these, is an ideal feedstock for these systems. Yet, very high ammonia (NH_3) concentrations may be toxic. Therefore, the carbon to nitrogen ratio in animal biomass is critical. Dairy manure has a higher than average C/N ratio, approximately 20 as can be derived from data in Table 2.4. Higher C/N ratios make retention times relatively short. However, in batch processes, there is a limit to C/N ratio in which anaerobic digestion will stop. Nitrogen concentrations are usually higher in the effluent after digestion, making the effluent an even more valuable fertilizer (Probstein *et al*., 2006c), (Monnet, 2003), (Wen, *et al*., 2007).

The percentage of CH_4 may be reasonably predicted using atom conservation equations for the reaction between digestible solids and H_2O. Krich *et al*. (2005) and Probstein *et al*. (2006c) presented this atom balance generalized as cellulose as follows:

$$\left(-C_6H_{10}O_5-\right)+H_2O \xrightarrow{bacteria} 3CO_2+3CH_4 \tag{2.7}$$

From this equation an ideal methane production of 0.3 kg CH_4 per kg of biomass may be expected. Krich *et al*. (2005) also conducted atom balances for wastes containing proteins ($C_{10}H_{20}O_6N_2$, which produces a CH_4:CO_2 ratio of about 55:45) and fats or triglycerides ($C_{54}H_{106}O_6$, which produces a ratio of about 70:30). The actual CH_4:CO_2 ratio produced from manure, however, depends on a number of other factors such as temperature in the digester, residence time, pretreatment of the substrate, etc.

Moreover, Carlin (2005) and Annamalai *et al*. (2006) conducted atom balances from ultimate analysis of manure biomass with the following chemical balance equation:

$$CH_hN_nO_oS_s + N'_{H_2O}H_2O_{(l)} \xrightarrow{bacteria} N'_{CH_4}CH_{4(g)} + N'_{CO_2}CO_{2(g)} + N_nS_{s(solid)} \tag{2.8}$$

From here, methane concentrations and higher heating values of the resultant biogas can be estimated in terms of the C/N and C/O ratios. See Figure 2.22 (a) and (b). Also, note that the water in these reaction equations is very small compared to the amount of water entering the digester. The effluent contains nearly all of the water that was present in the substrate. The remaining material in the effluent can sometimes be further processed to make fertilizer. Effluent can also be recycled back to make more substrate; however, this recycling is limited because toxins may build up in the system and harm the methane producing bacteria. The pH level of the digester should be maintained between 6.6 and 7.6 (Probstein *et al*., 2006c), (Monnet, 2003), (Ghaly, 1996). An overall mass and energy balance for CB digestion was presented by Probstein *et al*. (2006c), based on results found by Chen, *et al*. (1980), and is summarized in Table 2.11.

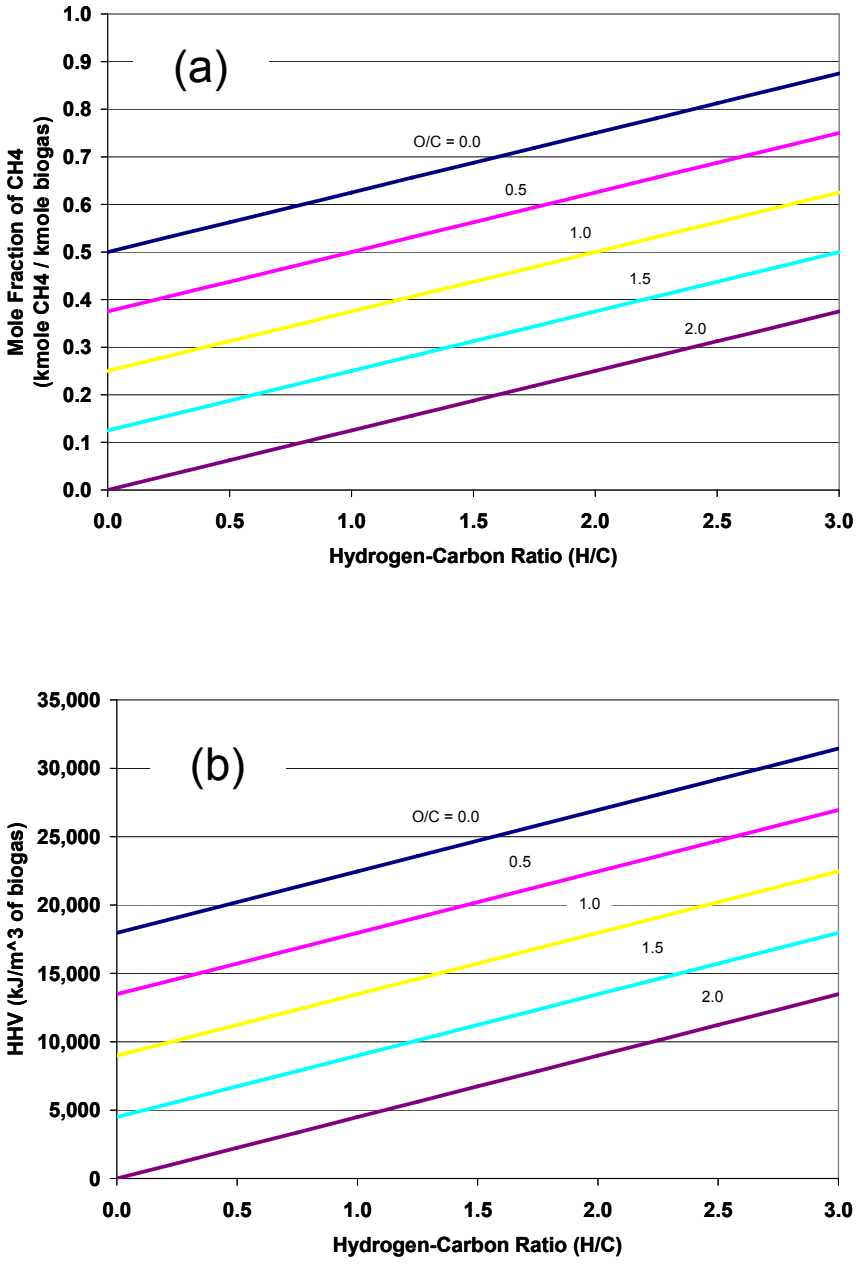

Figure 2.22 (a) Mole fraction of methane in biogas vs. H/C and O/C ratios in flushed DB (b) HHV of biogas vs. H/C and O/C ratios in flushed DB (adopted from Carlin, 2005)

Table 2.11 Material and thermal balance for anaerobic digestion of cattle manure (adopted from Probstein *et al*., 2006c)

	Mass, kg	Heat Content, MJ/kg	Heat, MJ	Heat, % of Total
IN				
Cattle Manure (dry)	100†	13.4	1340	84.7
Dilution water (10% solids)	900	--	--	--
Substrate heating‡	--	--	157	9.9
Mixing energy	--	--	55	3.5
Gas scrubbing	--	--	21	1.3
Methane compression (to 1 MPa)	--	--	9	0.6
Total	1000		1582	100.0
OUT				
Methane (21 m^3)	15	55.6	834	52.7
Carbon dioxide	41	--	--	--
Moisture in gas§	6	--	--	--
Effluent water	888	--	--	--
Sludge (dry) and losses (by difference)	50	--	748	47.3
Total	1000		1582	100.0

$$Thermal\ efficiency = \frac{834}{1582} * 100 = 53\%$$

†About 22 bovine-days worth

‡Assuming 50% heat recovered from the effluent

§Assuming gas saturated at 55 deg C and 101 kPa

However, despite being the most commercial energy conversion systems for manure biomass, digestion systems installed on animal feeding operations are not very common in the United States. There were only 41 operational systems in this country as of November 2007; 29 of those systems were installed on dairy farms, 10 were installed on swine farms, one on a duck farm and one on a chicken farm (USEPA, 2007b). However, near Stephenville, Texas, the largest manure-to-natural gas plant in the United

States has recently been completed. The plant obtains manure from local dairies in Erath County and mixes it with restaurant grease and other wastes to produce biogas. The biogas is then upgraded to industry standards as a natural gas replacement fuel. It is expected that the natural gas from this plant can produce enough energy to power 11,000 homes (Associated Press, 2007).

Goodrich *et al*. (2005) studied the overall biogas production and economics of a digester system installed on an 800-cow dairy in Princeton, Minnesota. In this example, the dairy profited greatly from the production of biogas, using it to meet most of the electrical energy needs of the farm and either selling unused electricity to the utility or flaring excess biogas produced in the digester that cannot be consumed by the engine. Goodrich *et al*. (2005) do admit that most dairies may not be able to profit on the installation of an anaerobic digester, as the installation and operation & maintenance costs may be too overwhelming and feasibility is very "site specific." Long operation times and biodegradable bedding (instead of sand) are also necessities to make manure digesters profitable. However, some digesters are not installed to obtain an economic profit. Rather, they are installed to control odors and to reduce pathogens from manure storage. Relatively inexpensive digesters can be installed by simply covering a storage lagoon with a tarp and placing a flare to burn the biogas. With these systems, no economic return is expected from electricity sales; although small boilers may be installed with the flare to provide heat to buildings at or near the farm. The USEPA (2007b) also provides estimated installation costs for all current, on-the-farm operating systems, which vary from $15,000 to $1.4 million, depending on what kind of digester is installed and whether or not an engine-generator set is purchased along with the digester.

Further discussions of biological energy conversion of manure-based biomass solids can be found in the literature. These include, but are not limited to: Meyer (2003), who discussed a digester on a 700-cow dairy in Iowa; Chang (2004), who compared the efficiencies and sustainability of anaerobic digesters to non-biological, thermal gasification; Simons *et al.* (2003), who reviewed some of the initiatives for digester installations in California; Ghaly (1996), who compared the anaerobic digestion

of cheese whey and dairy manure in a two-stage reactor; and Monnet (2003), who provides a general review of digester types and operating conditions.

2.3.2. Thermal Gasification of Manure-based Biomass

Extensive literature exists on technologies used to gasify coals. These systems are very briefly summarized by Hotchkiss (2003), including fixed-bed, fluidized bed, and entrained gasifiers. More detailed discussions of coal gasification are also available by Howard-Smith (1976), Nowacki (1981), and Probstein *et al*. (2006b). Moreover, a review of common gasification technologies for wood and crop-based biomass is provided by Quaak *et al*. (1999).

However, there have been limited studies on non-biological, thermal gasification of high moisture, high ash manure biomass. An advanced gasification system discussed by Young *et al*. (2003) proposed the use of separated DB solids pressed to 70% moisture from an auger press in a high temperature, air blown gasifier to produce synthetic gas. Gasification conversion efficiencies were estimated to range between 65 and 81%, and the gasification temperature was assumed to be about 1300 °C (2370 °F). The product gas composition was found to be approximately 30.2% (molar) CO, 5.5% CO_2, 25.7% H_2, and 38.6% N_2, with a heating value of 7,140 kJ/kg (3,076 Btu/lb). The gas could then be fired in an internal combustion engine to generate electrical power. The dairy would be able to produce twice its electrical energy requirement from the synthetic gas.

Experiments are being performed by investigators at Texas A&M University on gasification of coal and CB. Furthermore, modeling results on gasification of FB with air and air-steam mixtures as oxidizing agents have also been generated (Sami *et al*., 2001), (Priyadarsan *et al*., 2005a), (Gordillo, 2008).

There has also been extensive work and application on thermal gasification of CB in fluidized bed combustors. Sweeten *et al*. (1986) conducted several experiments on a 0.305 m (1.0 ft) diameter pilot plant fluidized bed combustor. It was found that when bed and vapor space temperatures exceeded 788 °C and 927 °C (1450 °F and 1700 °F), respectively, severe ash agglomeration and plugging occurred in the vapor space

transition duct and hot cyclone. However, ash agglomeration, plugging and slagging could be avoided if the combustor was operated on a re-circulating bed mode, which lowered vapor space temperature to 649 °C (1200 °F). Annamalai *et al*. (1987a) found that on a 0.15 m (0.5 ft) diameter fluidized bed combustor with bed temperatures ranging from 600 °C to 800 °C (1112 °F to 1472 °F), gasification efficiencies ranged from 90 to 98% and combustion efficiencies ranged from 45 to 85%. Moreover, Raman *et al*. (1981b) developed a mathematical model to describe FB gasification in fluidized bed combustors. It was assumed that initial volatilization of the biomass fuel was nearly instantaneous and only secondary reactions including char gasification and water-gas shift reaction were modeled. The resulting calculations suggested that the water-gas shift reaction was the most dominant reaction. However, when comparing computational results to experimental data, it was found that reactions involving volatiles from devolatilization (pyrolysis) should be included.

The applications of CB gasification have proven to be beneficial as a renewable source of energy. For example, Panda Ethanol, Inc., based out of Dallas, Texas, has recently completed a bubbling fluidized bed gasification plant near Hereford, Texas, which will convert FB from local feedlot operations to synthetic gas. The gases can then be burned in a combustor to produce steam, which is necessary to process corn into ethanol. See Figure 2.23 for an overview of this system. A by-product of the ethanol production process is wet-distiller grains and solubles (WDGS), which can be used as an additive in cattle feed ration. The bubbling sand bed is operated at low temperatures to avoid ash agglomeration and fouling (Panda Ethanol, 2007). The disposal of ash from manure gasification has proven to be one of the more challenging aspects because unlike ash from coal combustion, manure ash is not suitable as a replacement for Portland cement or as aggregate in Portland cement concrete. However, there are alternative uses for manure ash such as road base, flowable fills, and soil amendments (Megel *et al*., 2007).

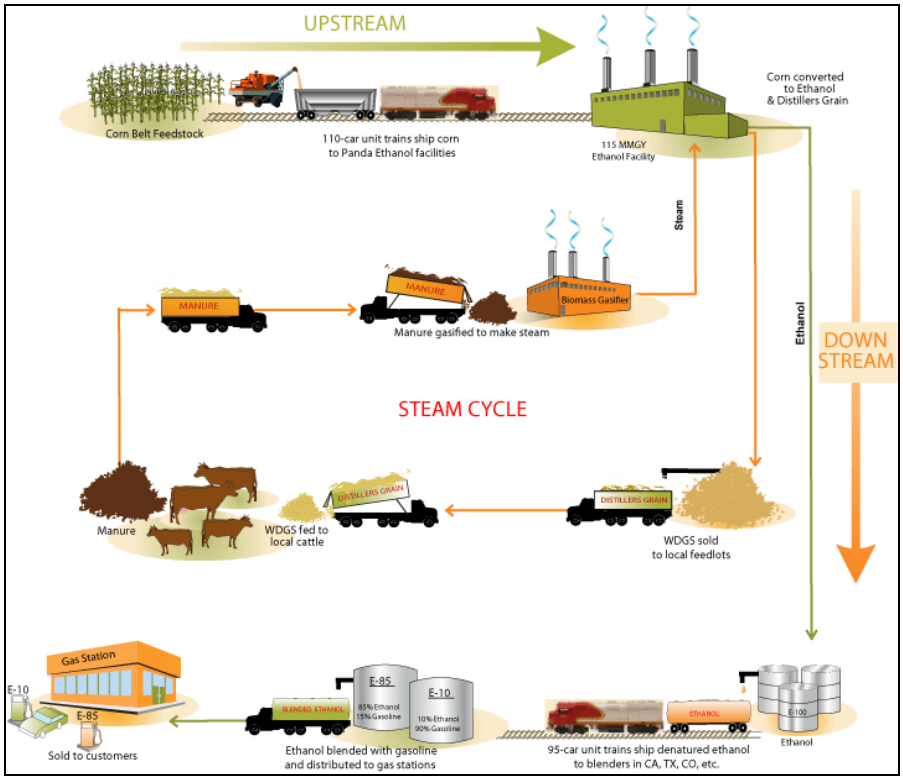

Figure 2.23 Cattle manure gasification for corn ethanol production (Panda Energy, 2007)

Recent experimentation at the Texas A&M University Coal and Biomass Laboratory has concentrated on fixed-bed gasification of MBB, which may be particularly suitable for small-scale energy conversion operations, because fixed-bed gasifiers have a high thermal efficiency and require little pre-treatment of the solids before gasification (Hobbs *et al.*, 1992). For fixed bed gasification, the products from thermal gasification are emitted at different zones in the gasifier's chamber. The different zones that the CB, or any solid fuel, encounters during the gasification process, as well as the main expected product gas species from coal and biomass gasification, are listed in Figure 2.24. In the drying zone, with temperatures of 25 – 130 °C (78 – 265 °F), the fuel's moisture is vaporized. In the pyrolysis section, 130 – 330 °C (265 – 630 °F), the fuel is broken down into volatile gases and solid char. The char, carbon dioxide, and water vapor undergo reactions in the reduction zone in which carbon monoxide (CO) and hydrogen (H_2) are produced. The remaining char is burned in the oxidation zone providing heat, carbon dioxide, and water vapor for the reduction zone. Reduction

and oxidation zones generally occur at temperatures of 330 – 1050 °C (630 – 1920 °F) (Gordillo *et al*., 2008).

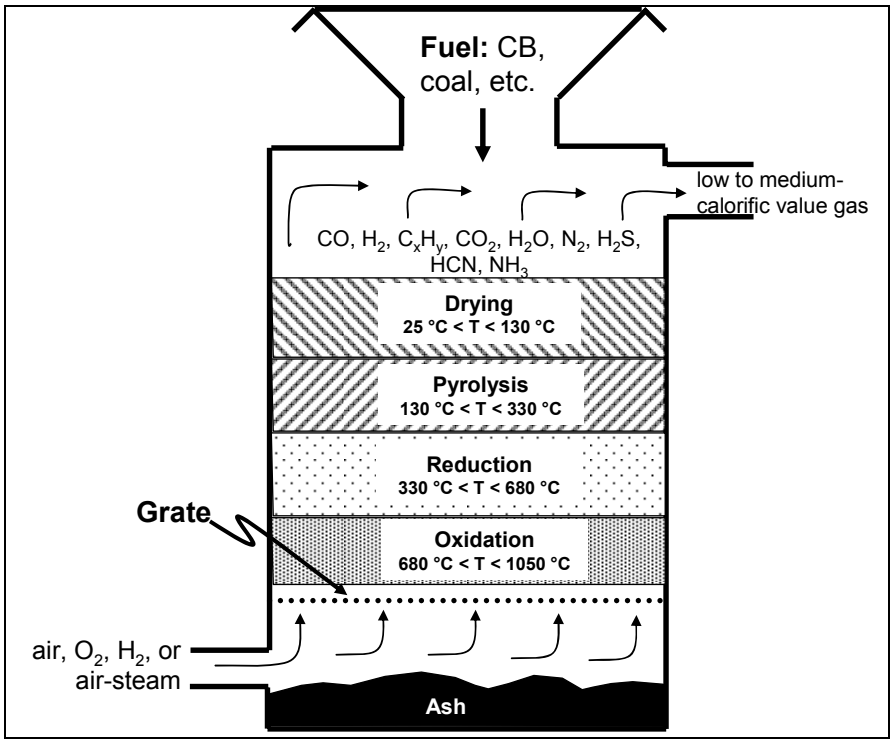

Figure 2.24 Different zones in an updraft, fixed-bed gasifier (adapted from Priyadarsan *et al*., 2005b)

Gasification experiments were conducted and discussed by Priyadarsan (2002), Priyadarsan *et al*. (2005a), Priyadarsan *et al*. (2005b), and Priyadarsan *et al*. (2005c). In these experiments FB, chicken litter biomass (LB), blends of LB with FB, and blends of LB and FB with coal were each used as fuel for an updraft, fixed-bed gasifier. The experiments were performed on a 10 kW (30,000 Btu/hr) counter-current fixed bed gasifier using air as the oxidizing agent. The experimental setup in Figure 2.25 is similar to that used by Priyadarsan *et al*., except that steam is added to the reactant air in current experiments. The grate has also been fitted with a linear vibrator so that ash can be continuously removed from the gasifier, thus allowing for uninterrupted operation and constant location of the peak temperature of the bed.

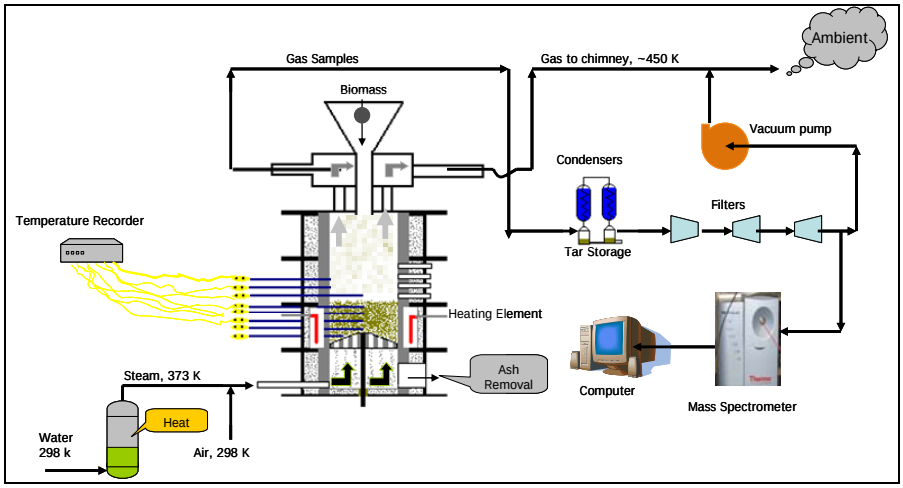

Figure 2.25 Schematic of 10 kW (30,000 Btu/hr) fixed-bed counter flow gasifier (Gordillo *et al*., 2008)

Figure 2.26 shows the species compositions measured at different distances over the grate, and the bed temperature profile from FB gasification experiments obtained by Priyadarsan (2002) in a study of fixed gasification at normal pressure. Here, results for experiments performed at 45 SCFM (76.5 m^3/hr) are presented. The figure shows that the maximum production of CO (31%) is reached at half an inch (12.7 mm) above the grate and starts to stabilize through the grate at about 27%. On the other hand, the H_2, CO_2, and CH_4 concentrations increase continuously, indicating the presence of pyrolysis throughout the bed. However, the increased rate of the production of CO_2 and H_2 is higher than the production of CH_4. Also, the experimental results show that the maximum production of H_2 (8%) and CO_2 (10%) are reached at the top of the bed (7 inch, 178 mm). Beyond two and a quarter inches (57 mm) above the grate, there is a rapid increase in the production of H_2 and CO_2 marking the drying and devolatilization zone in the bed. It should be noted that, although there seems to be devolatilization taking place over the entire bed, the oxidation and gasification reaction's maximum contribution to the product gas species is near the base of the bed. The bed temperature data curve shows a peak at two and a quarter inches (57 mm) indicating that, before this point, oxidation and gasification occur and after this point, drying and devolatilization processes occur. Typically, the gas composition data is correlated with the peak temperature in fixed bed gasification. Additional information on animal biomass

gasification and co-gasification of animal biomass fuels with coals can be found by Priyadarsan *et al*. (2005b) and Priyadarsan *et al*. (2005c).

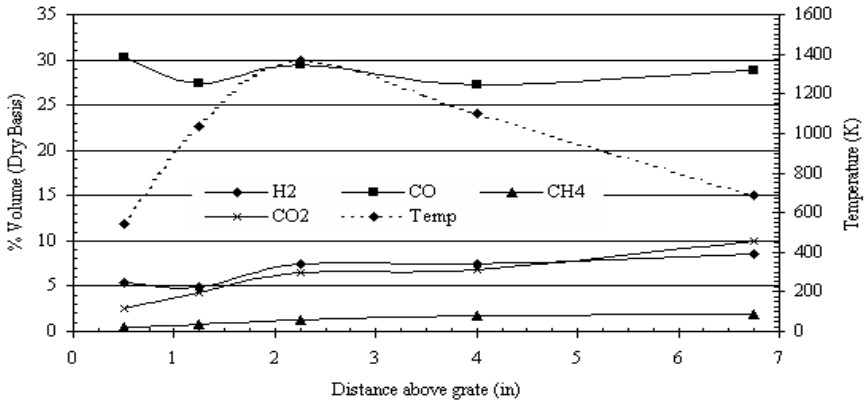

Figure 2.26 Gas species profiles for FB at air flow rate of 45 SCFH (adopted from Priyadarsan, 2002)

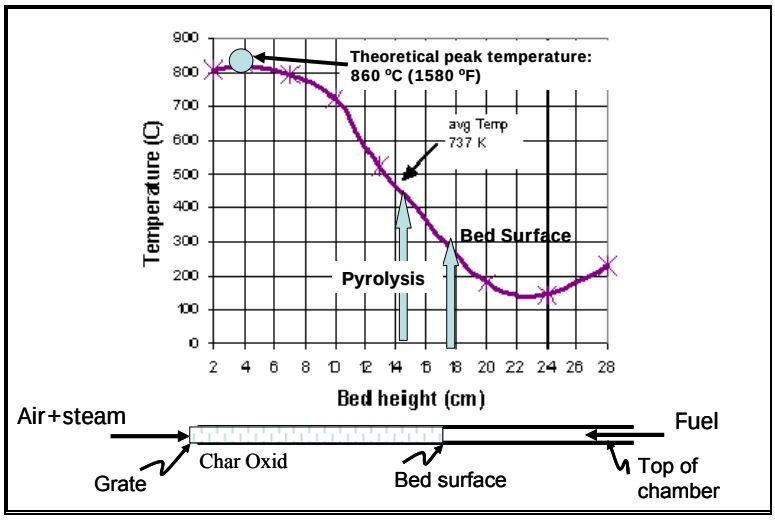

Figure 2.27 Experimental bed-temperature profile for DB at a time interval of 140 minutes with equivalence ratio of 1.8 and ASR of 0.38 (Carlin *et al*., 2008)

Experiments on the gasification of CB with air and air-steam mixtures as oxidizing agents are currently underway. In Figure 2.27, a temperature profile of a DB gasification experiment with equivalence ratio (ER) of 1.8 and air steam ratio (ASR) of

0.38 is presented. The peak temperature of 860 °C occurs near the grate. More discussion of these experiments may be found in a paper by Gordillo *et al*. (2008).

One other form of gasification that can possibly be an energy conversion process for MBB, particularly high moisture MBB, is high-pressure catalytic gasification. A patent by Elliot *et al.* (1997) describes the process as: maintaining a liquid organic mixture and an effective amount of metal catalyst (ruthenium, rhodium, osmium, iridium, or mixtures thereof) in a pressure reactor at 300 – 450°C and at least 130 atmospheres for an effective amount of time to produce a gas consisting of methane, carbon dioxide and hydrogen. Water is the only oxidizer. The process is basically steam reforming, and Elliot *et al.* (2004) reported that the percentage of carbon recovered as gas was close to 100% for most of the bench-scale test experiments performed. The percentage of methane in the product gas varied between 52 and 61% (by volume).

Ro *et al.* (2007) continued work on wet catalytic gasification on animal manure and municipal wastes by conducting overall energy balances and economic analyses. A high efficiency heat recovery system would be needed in order for wet gasification of municipal solid wastes and feedlot manure from unpaved lots (i.e. high-ash feedlot manure) to generate positive energy returns. High sulfur contents in the feedstock can cause poisoning and decrease the life of the catalysts. Partly due to the catalyst and pretreatment of feedstock, wet catalytic gasification was found to be considerably more expensive than anaerobic lagoon gasification.

2.3.3. Co-firing Coal and Manure-based Biomass in Primary Burn Zones

Cattle biomass can also be used as a fuel by mixing it with coal and firing it in the primary burn zone of an existing coal suspension fired combustion system. This technique is known as co-firing. The high temperatures produced by the coal allow the biomass to be completely burned. Previous work concerned with co-firing FB with coal may be found in papers by Annamalai *et al*. (2007), Sweeten *et al*. (2003), Frazzitta *et al*. (1999), Arumugam *et al*. (2005), Annamalai *et al*. (2003a), and Annamalai *et al*. (2003b). Di Nola (2007) conducted co-firing experiments for coal-chicken litter

biomass blends. Most co-firing experimental results obtained when using coal and finely ground CB seem to indicate that NO_x emissions did not increase and sometimes even decreased when co-firing coal and animal biomass.

Co-firing experiments have been conducted with two primary objectives: (1) to access the feasibility of using CB to reduce NO_x and (2) to measure the mercury emissions when co-firing coal with CB. Co-firing experiments at Texas A&M were conducted using a 30 kW_{th} (100,000 Btu/hr, approximately 15 lb or 6.80 kg of coal/hr) small scale furnace capable of firing most types of ground fuels.

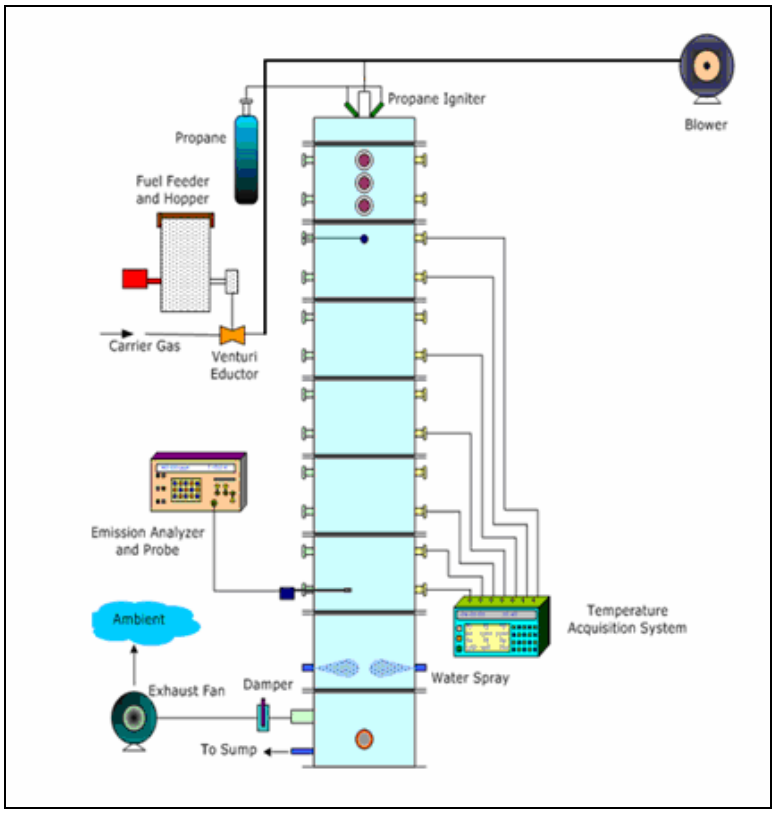

Figure 2.28 Schematic of small-scale 30 kW (100,000 Btu/hr) co-firing experimental setup

A schematic of the furnace used at Texas A&M is shown in Figure 2.28. The combustion air was split between primary (~20%) and secondary (~80%) air. Primary air was necessary to propel the solid fuel through the fuel line and into the furnace. A blower provided the secondary air. Before being injected into the furnace, the air passed

through a pre-heater to heat the air to approximately 150 °C (300 °F). Propane and natural gas were used to heat the furnace to the operating temperature of 1100 °C (2000 °F). Type-K thermocouples were present along the axial length of the furnace. These thermocouples provided a detailed profile of the temperature of the furnace throughout the combustion zone. A solid fuel hopper fed coal and coal/biomass blends during experiments. Solid fuel exited the solid fuel line as a finely ground powder lightly dispersed in the primary air stream. Combustion gas compositions were measured using an E-Instruments 8000 Flue Gas Analyzer. The instrument measured the dry volume percentages of CO, CO_2, O_2, SO_2, NO, NO_2, and combined NO_x. Another method for detecting NO_x with laser sensors is discussed by Thomas *et al*. (2006). At the furnace's final port, a probe was used to sample the flue gases. Just after the final port, exhaust gases passed through a water cooling spray to significantly lower the temperature of the gases. The water was pumped out of the furnace by a sump pump. More details are provided by Annamalai *et al*. (2007), Annamalai *et al*. (2003a), and Annamalai *et al*. (2003b). A study on fouling during co-firing may be found by Annamalai *et al*. (2003c).

Results from the study by Annamalai *et al*. (2003b) are shown in Figure 2.29. These co-firing experiments were conducted on the same boiler described above. The figure shows that even for fuel lean (excess oxygen) conditions, NO_x emissions for a 90:10 coal to FB blend were lower than those for burning pure coal. However, similar experiments conducted by Arumugam *et al*. (2005) (Figure 2.30) seem to suggest that lower NO_x emissions are not seen until 20% (by mass) biomass is blended with coal. Residence time, fuel particle size, and other factors may have caused the slight difference between the two results.

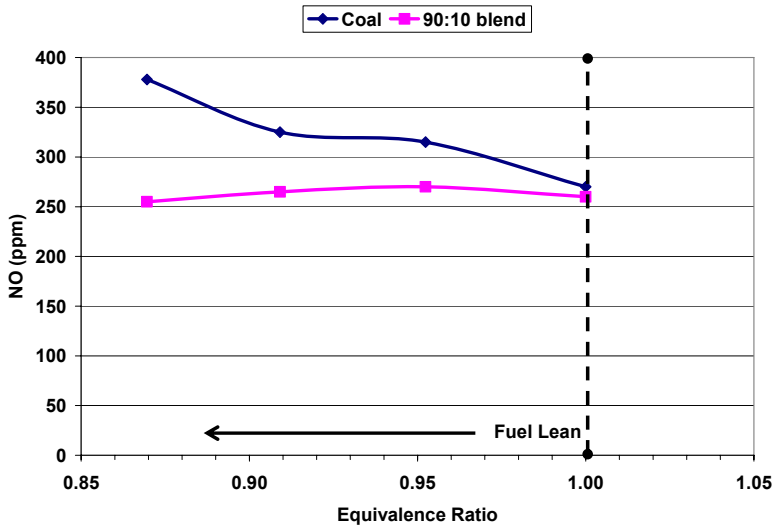

Figure 2.29 NO emission from coal and 90:10 coal-FB blends (adopted from Annamalai *et al*., 2003b)

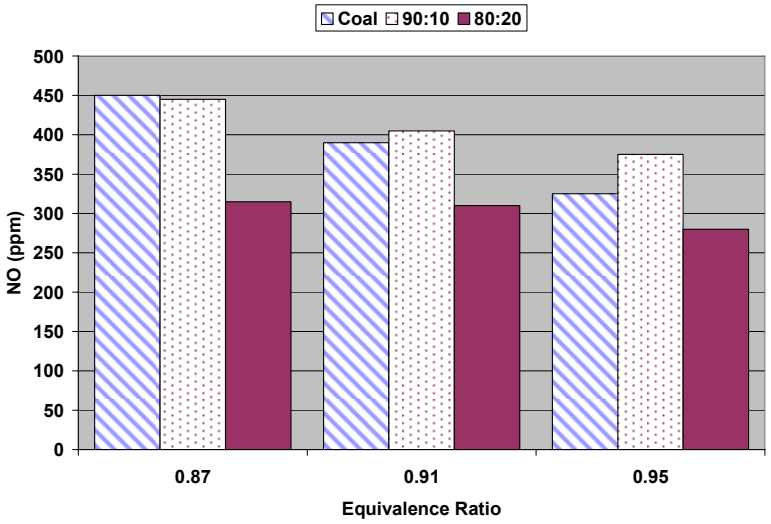

Figure 2.30 NO emission for coal, 90:10, and 80:20 blends of coal and FB vs. equivalence ratio (adapted from Arumugam *et al*., 2005)

Experiments at the Texas A&M Coal and Biomass Laboratory continue the work begun by Annamalai *et al*. Experiments in which pure Wyoming Powder River Basin coal, Texas Lignite coal, and blends of each coal with partially composted separated DB solids were burned have been conducted. Each coal was blended in 95:5, 90:10, and

80:20 (by mass) blends with DB. Experiments were performed for equivalence ratios of 0.8, 0.9, 1.0 (stoichiometric), 1.1, and 1.2. The results of these experiments may be found in a thesis by Lawrence (2007).

In principle, it is difficult to hypothesize whether or not NO_x emissions, particularly during lean (low ER) combustion, will be lower for coal-CB blends. Since CB has more fuel-bound nitrogen, one may conclude that more NO_x would be formed if oxygen is available. However, since CB has a higher volatile content that is released quicker than the volatiles in coal, the oxygen might react more quickly to the nitrogen in the volatile matter, creating local fuel rich areas where NO reduction can take place, even during an overall lean combustion process. This reduction would be intensified if the fuel N in the CB was released as NH_3. Moreover, the size of the FB particles is significant. Smaller FB particles can release volatile matter during combustion more quickly than larger particles. In both studies by Annamalai *et al*. (2003b) and Arumugam *et al*. (2005), the fuels were ground to similar sizes. Seventy percent of the FB particles in each study passed through a 170 μm sieve.

The manure contains two forms of nitrogen (N): (1) Less stable inorganic (ammonium) N present as urea in urine (50% of total N) and (2) more stable organic N present in the feces, which is released more slowly (USDA *et al*., 2007). The organic N is a mixture of proteins, peptides, etc. of undigested feed. While the N slightly decreases during composting, the heat value decreases much faster and as such N per GJ increases with composting (Sweeten *et al*., 2003) since the stable organic N decomposes very slowly. Thus it is hypothesized that more stable N is released at high temperatures. However, no measurements have yet been published to determine nitrogen percentage released as NH_3, HCN and other forms when co-firing coal with CB.

One other way to investigate NO_x emissions from coal-CB blends is to compute the fuel nitrogen conversion efficiency to NO_x. The fuel nitrogen converted to NO_x can be estimated with the following equation:

$$N_{CONV} = \frac{(c/n) * X_{NO}}{X_{CO_2} + X_{CO}} \tag{2.9}$$

where c/n is the ratio of fuel carbon to fuel nitrogen, X_{NO} is the mole fraction of NO, X_{CO_2} is the mole fraction of CO_2 and X_{CO} is the mole fraction of CO in the combustion products. The results for N conversion efficiency for coal, 90:10, and 80:20 blends of coal and FB can be found in Figure 2.31. In general, N conversion efficiency to NO_x was lowest for the 80:20 blend of coal and FB. However, conversion efficiency for 90:10 blends was higher than pure coal combustion except for leaner combustion at equivalence ratio of 0.87. Yet for all operating conditions, the conversion efficiency of fuel-N to NO_x was never significantly higher than efficiencies found when burning pure coal. The greatest difference between pure coal combustion and 90:10 combustion was only a 3% increase seen at ER of 0.95. These results, at least ease some concern over producing significantly more NO_x when blending FB (a higher nitrogen containing fuel) with coal. In fact, the 80:20 results imply that if FB had a similar nitrogen content to that of coal, it may produce less NO_x than pure coal. For more discussion on fuel nitrogen conversion efficiency please refer to work by Annamalai *et al*. (2003b) and Lawrence (2007).

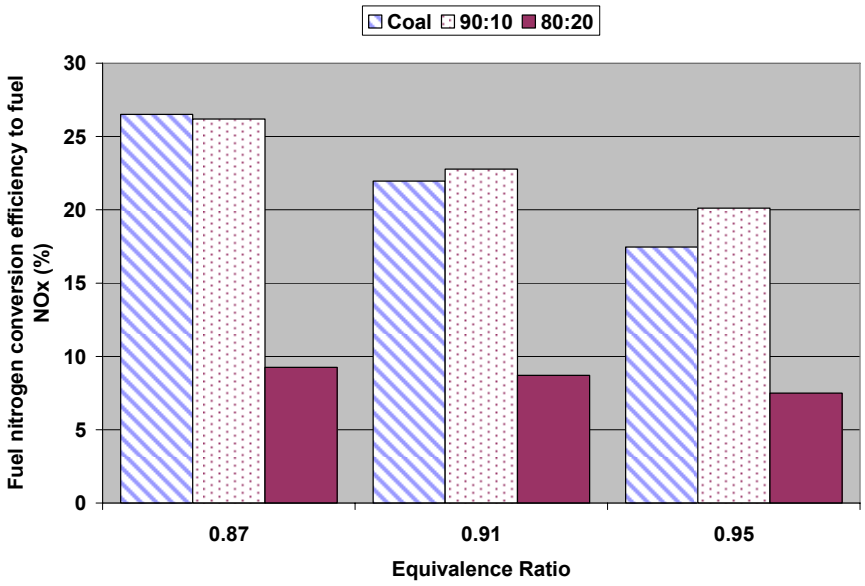

Figure 2.31 Fuel nitrogen conversion efficiency to fuel NO_x for coal, 90:10, and 80:20 blends of coal and FB (computed by Carlin *et al*., 2008 from data found by Arumugam *et al*., 2005)

During the recent co-firing experiments with Wyoming sub-bituminous coal-FB blends, mercury measurements were also taken. Elemental Mercury measurements were taken using a Mercury Instrument VM 3000 based on the cold vapor atomic absorption principle. The oxidized mercury was measured using the wet chemistry method. To better understand the speciation of mercury compounds, this wet chemistry based flue gas conditioning system was developed which is based on a modified Ontario Hydro Method for online detection. The results presented in Figure 2.32 are promising, as they indicate greater reductions of elemental Hg when more DB is blended with both Texas lignite and Wyoming sub-bituminous. For a full discussion of mercury emissions during co-firing experiments, please refer to a thesis by Arcot Vijayasarathy (2007).

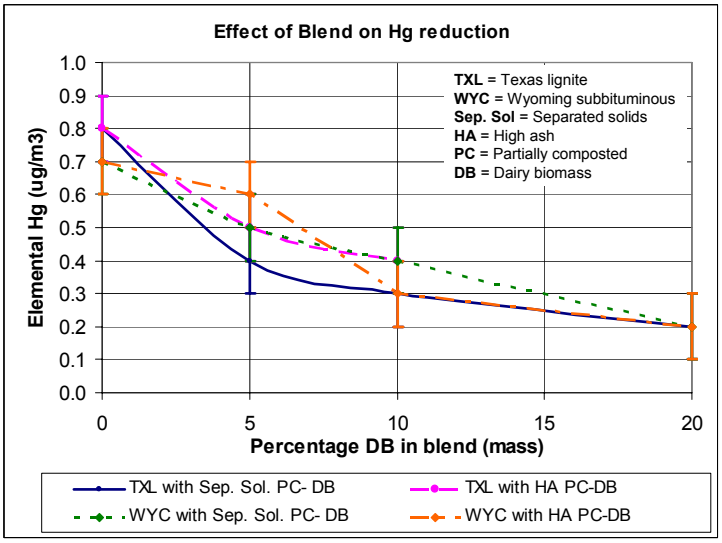

Figure 2.32 Elemental Hg reductions while co-firing coal with cattle biomass (adopted from Arcot Vijayasarathy, 2007)

2.3.4. Reburning Coal with Manure-based Biomass

During co-firing experiments NO_x was reduced slightly when coal was co-fired with FB at many operating conditions, possibly due to significant release of fuel-bound nitrogen in the form of NH_3. Therefore, experiments have also been performed to determine FB's effectiveness as a reburn fuel for NO_x reduction in coal fired power

plants. The basic reburn technology in coal-fired plants uses two separated combustion zones: the primary combustion zone where primary fuel is fired (e.g. coal) and the reburn combustion zone where the additional fuel (typically natural gas) is fired in order to reduce NO_x produced in the main burner. In the primary zone, coal is fired under normal to low excess air conditions with 70 to 90% of the total heat input, whereas in the reburn zone, the reburn fuel along with the products of combustion from the primary zone are burned with a deficient amount of air.

In the case of natural gas reburn fuels that do not contain fuel-bound nitrogen, 10 to 30% less NO_x is produced simply because 10 to 30% (by heat) of the primary coal fuel is displaced by the reburn fuel. Moreover, in the reburn zone, while operating in a fuel-rich regime, the natural gas molecules break down to hydrocarbon fragments which react with NO_x to form hydrogen cyanide (HCN) and NH_3. These nitrogen compounds then react with other nitrogen-containing species to form N_2. Similar processes also occur when reburning with nitrogen containing fuels such as coal, oil, and biomass. See Figure 2.33 for a general illustration of the reburning process. The optimal equivalence ratio (ER) in the reburn zone is 1.18 to 1.05 (stoichiometric ratio of 0.85 to 0.95, respectively) (DOE, 1999). The reburn fuel produces 10 to 30% of the total heat input. Over fire air (OFA) is typically used downstream of the reburn zone to create a burnout zone for complete combustion.

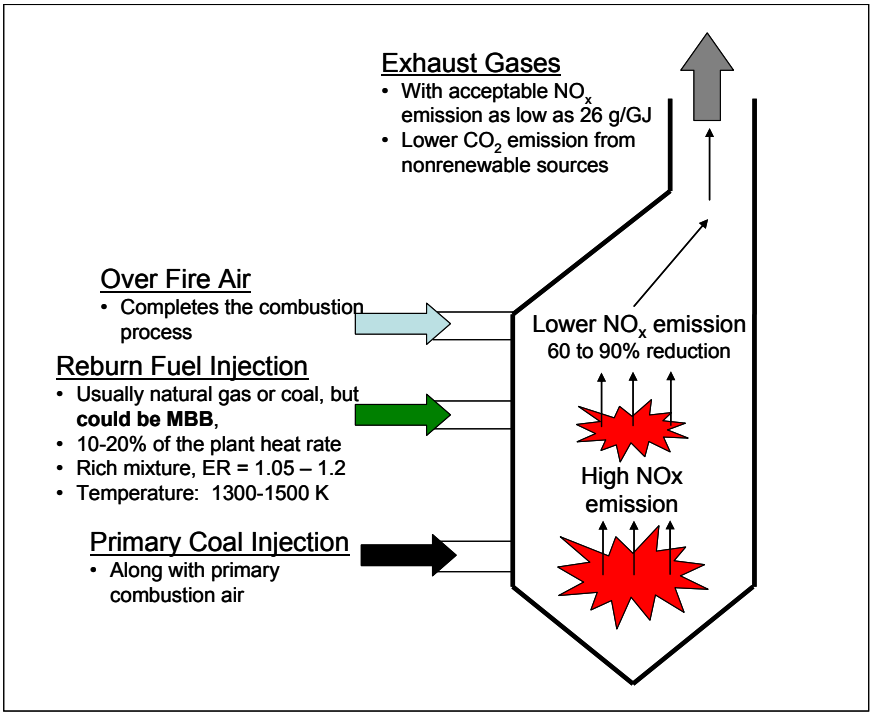

Figure 2.33 Simplified schematic of the reburn process

Nitrogen oxide (NO_x) reduction while reburning with OFA using a down-fired pilot-scale (300 kW) combustion facility was examined for the effect of metal-containing compounds by Lissianski *et al*. (2001). Natural gas was used as the main fuel and the reburn fuel. Metal-containing compounds such as sodium carbonate, potassium carbonate, calcium acetate, and fly ash were injected with the main fuel or the reburn fuel. Reburning resulted in a 50% reduction of SO_2. The baseline NO_x level was 600 ppm. Reburning with natural gas alone provided a 66% NO_x reduction, while injection of 100 ppm of the metal compounds provided a 4 – 7% additional reduction in NO_x.

Yang *et al*. (1997) investigated NO reduction when coal was reburned with more coal in the reburn zone. Eight different bituminous coals were used as reburn fuel. A maximum NO_x reduction of 65% was found, as well as an optimum residence time of 450 ms. Base NO_x levels of 600 ppm from the primary burn zone were simulated by burning a mixture of propane and NH_3. Reburn zone stoichiometry and the volatile matter content of the reburn fuel were found to influence the reburn performance the most. However, fuel nitrogen content of the reburn fuel was found not to be as

important as most of the other operating conditions of the experiments. Yet the nitrogen content of the reburn fuel may become significant in cases where the NO concentration from the primary zone is very low, such as cases when low-NO_x burners and air staging are installed. Yang *et al*. (1997) suggests that at some point (about 150-170 ppm) NO-forming mechanisms overtake NO-reducing reactions, causing a net increase in NO_x. This places a limitation on the practicality of reburning with nitrogen containing fuels such as coal, oil and MBB.

Table 2.12 is a summary of various reburn experiments and existing systems and their bottom line NO_x reduction performances. Some descriptions of the experimental parameters are also indicated; however, please refer to each source for a full explanation of the tested systems.

Table 2.12 Reburn systems and experimental results with various reburn fuels

Primary Fuel	Reburn Fuel	NO_x Reduction Results	Source	Comments
Coal	Straw, miscanthus (type of grass), natural gas, and wood	Measured NO_x levels between 125 to 150 ppm	Rudiger *et al.* (1996)	300 kW_{th} total heat input. Reduction zone residence time varied from 1.0 to 1.6 seconds. Under same conditions coal reburning only achieved a NO_x level of 250 ppm.
Coal	Pyrolysis gases from coal and miscanthus (with and without tars)	Measured NO_x levels as low as 100 ppm	Rudiger *et al.* (1997)	Best results were from coal pyrolysis gases with tars produced at 800 °C. Gas composition, stoichiometry, and residence time in the reburn zone all influenced the NO_x reduction results.
Propane + NH_3	8 different bituminous coals	Up to a 65% reduction from a base level of 600 ppm	Yang *et al.* (1997)	NH_3 in primary fuel is used to simulate base NO_x level. Reburn fraction was varied between 10 and 35%. Reburn stoichiometry was found to be the most significant factor for NO_x reduction. Optimum reburn zone residence time was found to be 450 ms. Smaller particles with higher volatile matter improve reduction.
Natural gas and coal	Fir lumber wood waste, coal, coal pond fines, carbonized refuse derived fuel, orimulsion (bitumen-based fuel)	Up to 70% reduction from basic reburning (20% heat input), 85 to 95% reduction from advanced reburning (10% heat input)	Maly *et al.* (1999)	Base NO_x levels were varied between 200 and 1300 ppm. Fuel N content, volatile content, and ash content significantly affected reductions. Most effective promoters during advanced reburning were alkalis, such as sodium compounds.
Coal	Coal and micronized coal	25 to 55% reduction	DOE (1999), Srivastava *et al.* (2005)	Survey of coal reburning applications on US coal-fired boilers. Four applications in total. Three applications were still operational as of 2005.
Coal	Natural gas	40 to 68% reduction	DOE (1999), Srivastava *et al.* (2005)	Survey of gas reburn applications on US coal-fired boilers. 22 operations in total. All operations, as of 2005, were decommissioned or not operating, except for one application at the Somerset plant in New York that also had a selective non-catalytic reduction system.

Table 2.12, continued

Primary Fuel	Reburn Fuel	NO_x Reduction Results	Source	Comments
Natural gas and Illinois and Ohio coals	Natural gas, coal, furniture waste, willow wood and walnut shells	60% reduction from gas and biomass reburning, 50% reduction from coal reburning	Zamansky *et al.* (2000)	Base NO_x levels were varied from 400 to 900 ppm. Fibrous willow wood was the most difficult biomass fuel to prepare for combustion. Economics was also discussed.
Natural gas and Illinois and Ohio coals	Advanced reburning with above fuels and nitrogen agent injection	83 to 90% reductions	Zamansky *et al.* (2000)	Three advanced reburn technologies tested: injection of nitrogen agent with over fire air, injection of nitrogen agent in rich reburn zone, and SNCR reagent injected downstream of over fire air.
Natural Gas+NH_3	Natural Gas	66% reduction from a base level of 600 ppm	Lissianski *et al.* (2001)	Reburn fuel was 25% of total heat rate. NH_3 in primary fuel is used to simulate base NO_x level.
Natural Gas+NH_3	Natural Gas+100 ppm Na, K, or Ca	70 - 73% reduction from base level of 600 ppm	Lissianski *et al.* (2001)	Reburn fuel was 25% of total heat rate. 15 - 20% reduction when Ca injected alone without natural gas.
Propane + NH_3	Coal, feedlot cattle manure biomass, 90:10 and 50:50 blends of coal and biomass	Up to a 40% reduction with coal, up to 80% reduction with pure biomass from a base level of 600 ppm	Annamalai *et al.* (2001, 2005)	It was speculated that most of the nitrogen in FB exists as NH_3, and volatile matter of FB (little fixed carbon) is twice that of coal and hence FB serves as a better reburn fuel in controlling the NO_x emissions.
Natural gas+NH_3	Low-nitrogen switch grass and high-nitrogen alfalfa	Up to 70% reduction from a base level of 500 ppm	Sweterlitsch *et al.* (2002)	Initial O_2 percentage varied between 1 and 6% and reburn fraction varied from 0 to 23% (heat). Two reburn fuel carrier gases were investigated: N_2 and steam.
Propane + NH_3	Coal, feedlot cattle manure biomass, 90:10 and 50:50 blends of coal and biomass	Up to 14% reduction with coal, up to a 62% reduction with pure biomass from a base level of 600 ppm	Arumugam (2004)	Equivalence ratio varied from 1.0 to 1.2. Circular jet and flat spray nozzel injectors were used.

A study by Annamalai *et al*. (2001, 2005) showed that 80% NO_x reductions were possible when reburning with pure FB. See Figure 2.34. Again, base NO_x levels from the primary zone were about 600 ppm. Greater reductions were seen with higher (more fuel rich) equivalence ratios, except for pure FB reburning which did not vary as significantly with ER. The reductions from pure FB reburn fuels were found to be greater than those for coal reburning or reburning with blends of coal and FB.

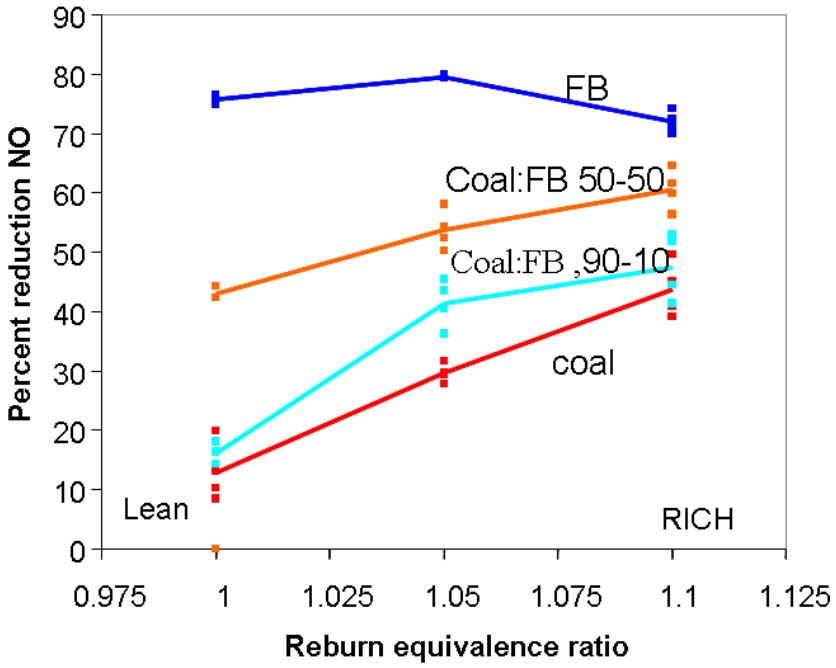

Figure 2.34 NO reduction percentage with coal, feedlot biomass and blends of coal and FB from a base level of 600 ppm NO (adopted from Annamalai *et al*., 2001 and Annamalai *et al*., 2005)

The small scale facility used for on-going reburn experiments at the Texas A&M University Coal and Biomass Laboratory is discussed in detail by Annamalai *et al*. (2001). The small-scale facility has a capacity of 30 kW_{th} (100,000 Btu/hr). The facility, illustrated in Figure 2.35, also simulated primary NO_x levels by burning a mixture of propane and NH_3. Pulverized reburn fuels were injected into the reburn zone through a hopper. Temperature distribution along the boiler was measured, as were emissions. Results for reburning with Texas Lignite (TXL) coal and Wyoming coal were used as a base case for subsequent experiments involving biomass. NO_x emissions

from reburning with pure TXL, TXL:low-ash partially composted FB blends, TXL:high ash partially composted FB blends, pure WY coal, and WY coal:low ash partially composted FB blends were obtained. Some of these results are presented in Figure 2.36. Experiments with pure high ash partially composted FB were not performed due to severe amounts of slag built up in the area near the reburn injectors in the furnace. A study by Oh *et al*. (2007) investigated ash fouling from reburning with CB. The level of NO_x emissions in the exhaust decreased with increased equivalence ratio and CO percentage in the exhaust gases. With increased equivalence ratio, the oxygen in the combustion zone was depleted quickly and hence more CO was formed. Low levels of oxygen slowed down the NO formation reaction and allowed the NO reduction reaction to be dominant in the combustion zone. Studies by Annamalai *et al*. (2001, 2005) and Arumugam (2004) found that one of the greatest influences on NO_x emission levels was equivalence ratio in the reburn zone. Greater NO_x reduction from cattle biomass fuels compared to lignite is clearly shown in Figure 2.36, but at the expense of higher CO emissions. Greater amounts of burn-out air injected after the reburn zone will be required when reburning with CB.

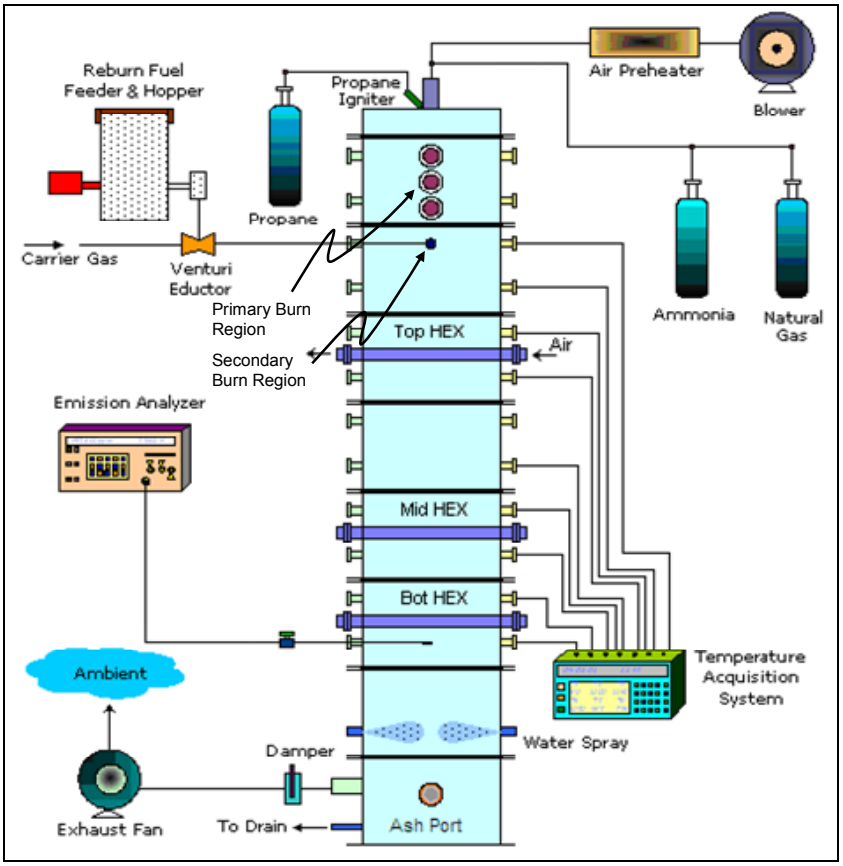

Figure 2.35 Schematic of small-scale 30 kW (100,000 Btu/hr) coal reburn facility

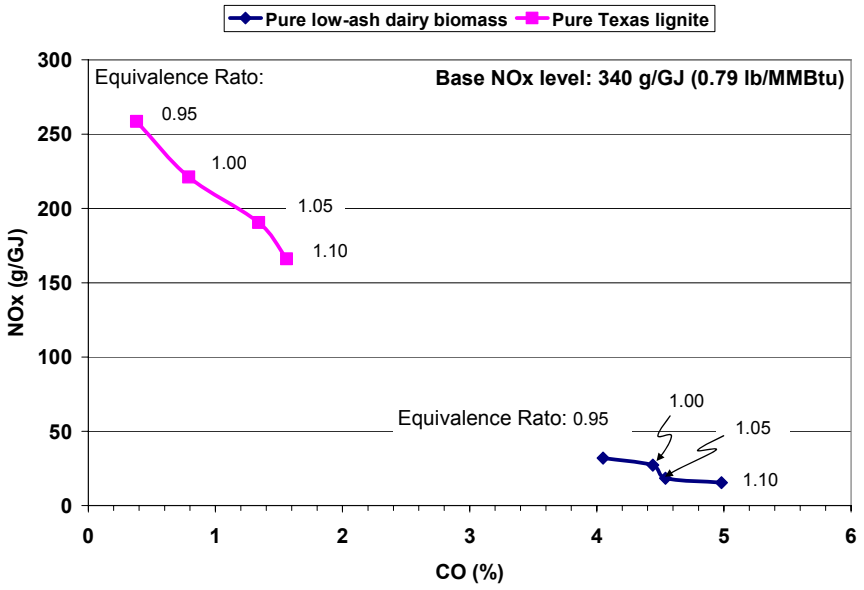

Figure 2.36 NO_x vs. CO for two reburn fuels from a base NO_x level of 340 g/GJ (0.79 lb/MMBtu)

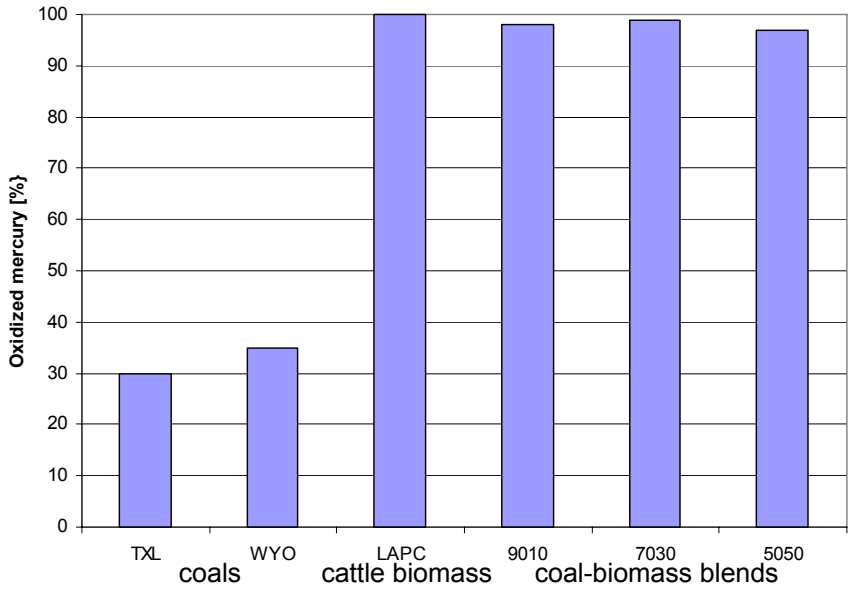

Figure 2.37 Numerical simulation of Hg oxidation from reburning coal with various fuels (adopted from Colmegna, *et al*., 2007)

With a longer residence and reaction time, more NO_x reduction is possible. The estimation of the mixing time for the lateral injection was 0.32 seconds when a linear mixing model was used with a mixing length of 30.48 cm (12 in). The vitiated air reduced oxygen concentration by dilution while better mixing reduced oxygen concentration by mixing with the main combustion stream. Better mixing also caused the fuel to combust faster and thus reduced the oxygen levels. The reduced oxygen levels inhibited NO_x formation mechanisms.

Oxidized mercury (Hg^{2+}) measurements for CB reburning have not yet been conducted on the small-scale experiments discussed above. However, Hg^{2+} emissions were numerically simulated by Colmegna *et al*. (2007). The simulation accounted for the high amounts of Cl in cattle biomass, allowing for very high mercury oxidation. This may be seen in Figure 2.37, which is a plot of oxidized mercury percentage of total mercury emitted during combustion. Similar oxidation was also predicted for coal-CB blended reburn fuels. It can be deduced that CB helps the oxidation of mercury, which

in turn, signifies that mercury can be captured more effectively at the exhaust by flue gas desulphurization-type environmental controls.

2.4. Competing NO_x Control Technologies

Perhaps the most promising application of MBB in coal-fired power plants is reburning. Experiments have shown that reburning coal with MBB can reduce NO_x emissions by over 90%, which rivals the most effective commercially available NO_x reduction technologies. However, in the United States, there are not many potential reburn applications at coal-fired power plants. According to the National Electric Energy Data System of the USEPA (2007a), of the over 1300 coal steam units existing in the US or recently approved for construction, 70% of them utilize some type of low-NO_x burner, over fire air, or other primary NO_x control technology to reduce NO_x. The NO_x levels achieved by these primary controllers are usually low enough to meet current emissions standards, plus the NO_x levels are usually so low that reburning with nitrogen containing fuels, such as MBB, becomes impractical. Of the roughly 400 coal steam units that do not have primary NO_x controllers, 68 of them are fluidized-bed combustors that can achieve emission standards without any primary NO_x controls. Ten of these fluidized-bed combustors also use selective non-catalytic reduction (SNCR) systems to reduce NO_x after combustion. Another 25 coal steam units without primary NO_x controllers have selective catalytic reduction (SCR) systems, which essentially eliminates the need for other NO_x control technologies. Seven other coal steam units without primary controllers utilize SNCR. Therefore, of the 1300 coal steam units, only about 22% can potentially utilize a reburn system with a nitrogen containing fuel like MBB, because they do not have primary or secondary NO_x controllers and are not fluidized-beds.

According to Srivastava *et al*. (2005), 29 US coal-fired boilers have utilized reburn technology since 1988. As of 2003, only four of these reburn systems were still operating. Most had been decommissioned because natural gas was used as the reburn fuel, and prices of natural gas had become too high to justify continued operation of the

reburn systems. Other reburn systems were only demonstration projects that were not continued as part of the regular operation of the power plants. In this section, competing NO_x control technologies such low-NO_x burners, SCR, and SNCR will be discussed.

2.4.1. Primary NO_x Controls

The primary NO_x controls on coal-fired power plants typically consist of either low-NO_x burners, over fire air (OFA), or a combination of both. These controls are widely used in coal-fired plants throughout the US. The more common primary control technologies and their NOx reduction efficiencies are listed in Table 2.13. Low-NO_x burners delay the complete mixing of fuel and air as long as possible in order to reduce oxygen in the primary flame zone, reduce flame temperature, and reduce residence time at peak temperatures. An illustration of the slower air and fuel mixing in low-NO_x burners may be seen in Figure 2.38. The effectiveness of a LNB depends on several factors such as the properties of the coal and the size of the furnace. Higher rank coals, that do not have high volatile matter and nitrogen contents, do not inhibit NO_x formation in local fuel-rich environments as well as low rank coals. Long flames from the LNB may impinge on furnace walls (Srivastava *et al*, 2005).

Table 2.13 NO_x reduction performance of primary control technology applications on coal-fired boilers (adopted from Srivastava et al., 2005)

Boiler Type*	Coal Type	Primary Control Technology	2003 Average Controlled NO_x Emission (g/GJ)	Average NO_x Reduction Efficiency from 1995 Levels (%)	Range of NO_x Reduction Efficiencies (%)	Number of Boilers
Wall-fired	Bituminous	LNB	177	39.2	8.6-70.1	62
Wall-fired	Bituminous	LNBO	151	53.3	32.7-71.9	16
Wall-fired	Sub-bituminous	LNB	121	45.5	19.4-80.3	16
Wall-fired	Sub-bituminous	LNBO	60	63.4	40.0-80.9	4
Tangential-fired	Bituminous	LNC1	168	35.0	17.2-65.4	26
Tangential-fired	Bituminous	LNC2	134	36.6	23.3-70.8	15
Tangential-fired	Bituminous	LNC3	108	54.9	38.1-72.2	19
Tangential-fired	Sub-bituminous	LNC1	90	45.4	11.3-74.4	18
Tangential-fired	Sub-bituminous	LNC2	99	45.6	33.9-65.4	3
Tangential-fired	Sub-bituminous	LNC3	60	60.5	48.2-77.2	23

Notes: LNB = low-NO_x burner; LNBO = LNB with over fire air; LNC1 = LNB with close-coupled OFA; LNC2 = LNB with separated OFA; and LNC3 = LNB with both close-coupled and separated OFA. *All boilers are dry-bottom type.

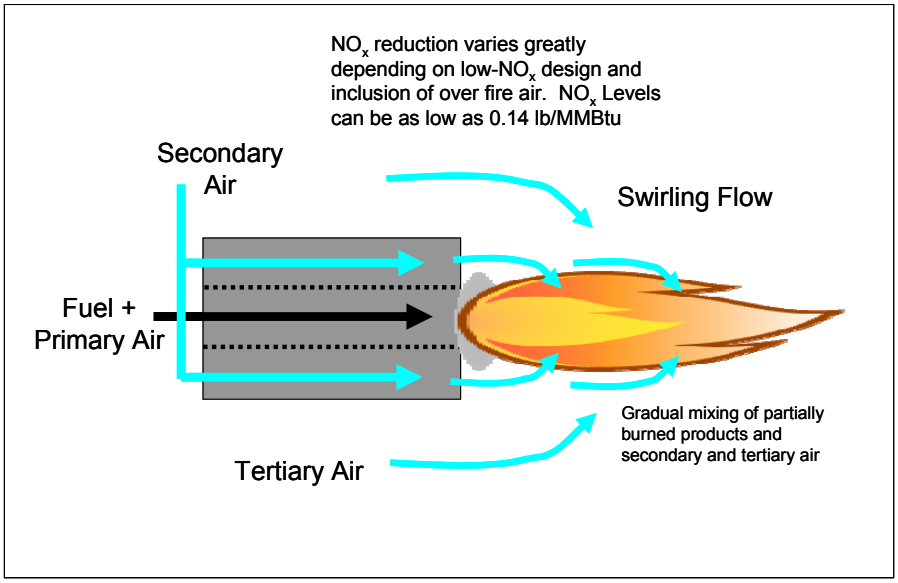

Figure 2.38 Delayed fuel-air mixing in low-NO_x burners

Moreover, unburned carbon levels typically increase when low-NO_x burners are installed. High unburned carbon levels affect boiler efficiency and the salability of ash. The amount of unburned carbon in fly ash, typically referred to loss on ignition (LOI), is limited to 6% by ASTM C618 for cement replacement in ready-mix concrete. Low-NO_x burners can increase LOI by 2-5% points (Srivastava *et al*, 2005). Additional information and case studies on reducing LOI in wall fired and tangentially fired units can be found in (Conn *et al*, 2005).

Over fire air is typically used as a supplementary technology to low-NO_x burners in which 5-20% of the combustion air is diverted and injected downstream from the primary combustion zone. The diverted air is used to complete the combustion process when burners are operated at low air-fuel ratios. When over fire air is added to low-NOx burners in wall-fired furnaces, NO_x reductions can increase 10-25%. Over fire air in tangentially-fired boilers can reduce NO_x by more than 50%. Enhancements to these primary NO_x controls such as multilevel over fire air and rotating opposed fire air can also be found in a paper by Srivastava *et al*. (2005). Li *et al.* (2007) reviewed newer designs for swirl burner technology for low-grade coal combustion.

2.4.2. Selective Catalytic Reduction

One of the most common and effective ways to reduce NO_x emissions, post combustion, is selective catalytic reduction (SCR). A schematic of a SCR system may be seen in Figure 2.39. Ammonia (NH_3) (aqueous or anhydrous) or some other reagent is injected downstream from the combustion zone at flue gas temperatures of 340-400°C (650-750°F), in the presence of a catalyst to reduce NO_x. Selective catalytic reduction systems can have reductions between 80 and sometimes greater than 90%, depending on the catalyst, the flue gas temperature and the amount of NO_x present in the combustion gases exiting the primary burn zone (Srivastava *et al*, 2005).

Currently, most commercial SCR systems do not reduce NO_x further beyond 25.8 g/GJ (0.06 lbs/MMBtu) (USEPA, 2004). However, if economics allowed, SCR systems could theoretically reduce NO_x emissions by 100% (Mussatti *et al*, 2000b).

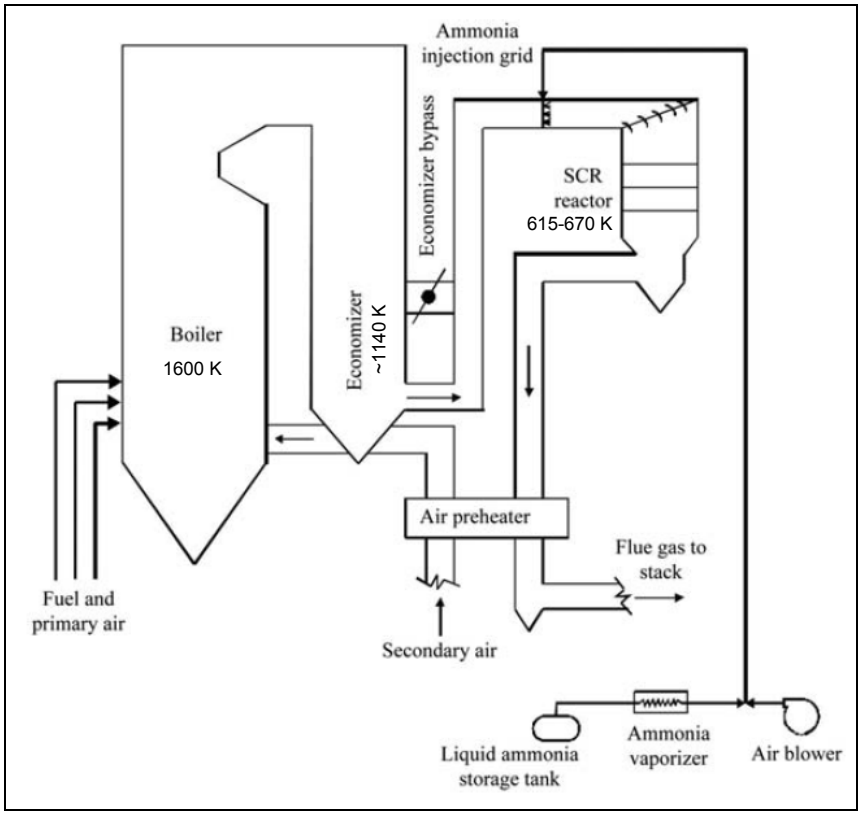

Figure 2.39 Schematic of a SCR application (adapted from Srivastava *et al*., 2005)

The major operational factors for SCR systems include:

- Reaction temperature range,
- Residence time available for reduction,
- Mixing between the reagent (NH_3) and the combustion gases,
- Molar ratio of injected reagent to uncontrolled NO_x in the combustion gases,
- Uncontrolled NO_x concentration level,
- Ammonia slip (amount of reagent escaping with exhaust gases),
- Catalyst activity, selectivity, deactivation, pitch, management, and
- Pressure drop across the catalyst.

The most common reagent is NH_3. Usually the NH_3 is transported in an aqueous solution (either 19% or 29.4% ammonia in water) due to required permits on handling and storing pressurized anhydrous NH_3. In Figure 2.40, a comparison of cost for different reagents is presented for both all year operation and ozone season operation. As can be seen, anhydrous ammonia tends to be cheaper for all boiler sizes (ratings) because more energy is spent on electric vaporizers when preparing aqueous ammonia for injection. Moreover, a greater amount of aqueous ammonia must be delivered to the plant to inject the equivalent amount of ammonia into the SCR system. However, since there are fewer regulatory restrictions on aqueous ammonia, it tends to be the most common. Yet urea-to-NH_3 conversion seems to be an option that is both cheaper than importing large amounts of aqueous ammonia and has fewer restrictions in transporting and storing than anhydrous ammonia (Salib *et al*, 2005).

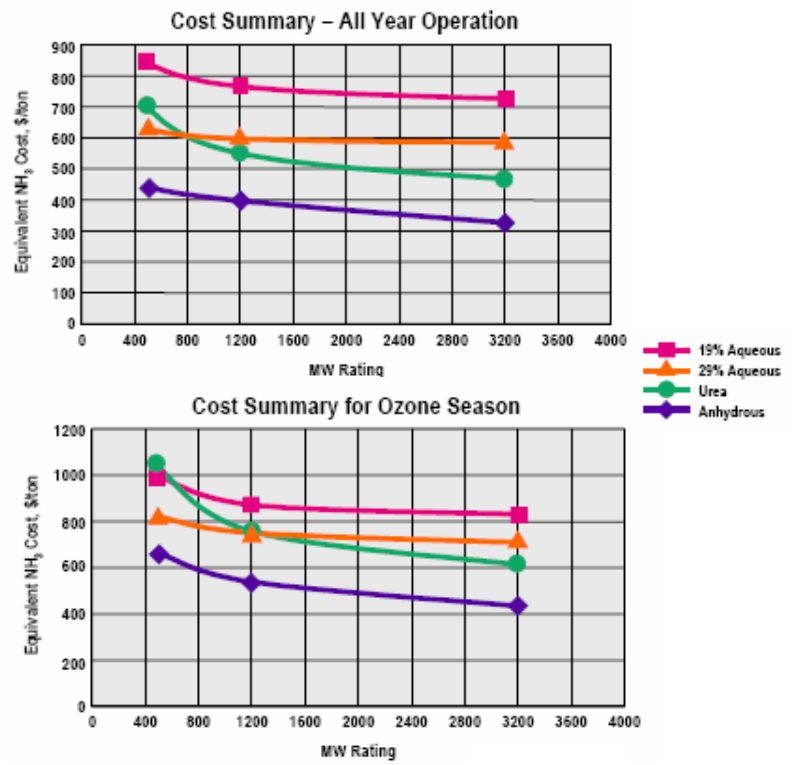

Figure 2.40 Comparative costs for different reagents in SCR applications (Salib *et al*., 2005)

The catalyst is typically made of a metal oxide such as molybdenum oxide (MoO_3) or vanadia (V_2O_2) deposited on various materials including titanium oxide (TiO_2) and Zeolite. The catalysts may be configured as a ceramic honeycomb or coated parallel metal plates in which the surface promotes the reaction between the NH_3 and NO_x molecules to form nitrogen (N_2) and nitrous oxide (N_2O) (Srivastava *et al*, 2005). For coal-fired plants, the catalyst operating life is between 10,000-30,000 hours (about 1-3 years). Sometimes the manufacturer of the catalyst will reactivate or recycle components of the catalyst for other uses. Otherwise, the facility operator must dispose of the catalyst in a landfill; however, catalyst formations are not considered hazardous in the US. There are several reasons for catalyst deactivation (Mussatti *et al*, 2000b). Some of these are:

- Poisoning: fuel constituents such as calcium oxide and magnesium oxide occupy active pores in the catalyst. This is typically the main factor for catalyst deactivation.
- Thermal Sintering: high flue gas temperatures change pore structure.
- Other factors: blinding, fouling, plugging, erosion, and aging of the catalyst.

Currently, more than 200 existing and planned coal steam units in the US have or will have SCR systems (USEPA, 2007a). Of the more than 40 units in Texas, 10 already have or will have SCR systems installed by 2009.

2.4.3. Selective Non-catalytic Reduction

Selective non-catalytic reduction (SNCR) is a similar post combustion technology to SCR, except that the NH_3 or urea is injected without the presence of a catalyst and at higher temperatures of 980-1150°C (1800-2100°F) (Srivastava *et al*, 2005). However, reductions for SNCR are rarely over 35% for large boilers with heat rates greater than 880,000 kWh/hr (3,000 MMBtu/hr) due to mixing problems. Therefore, SNCR systems are typically present in smaller units, less than 200 MW in capacity, due to their relatively low capital costs and better reductions up to 65% (Mussatti *et al*, 2000a and USEPA, 2004). A schematic of a SNCR system may be seen in Figure 2.41. The major operational factors for SNCR are generally the same as SCR except for those dealing with the catalyst.

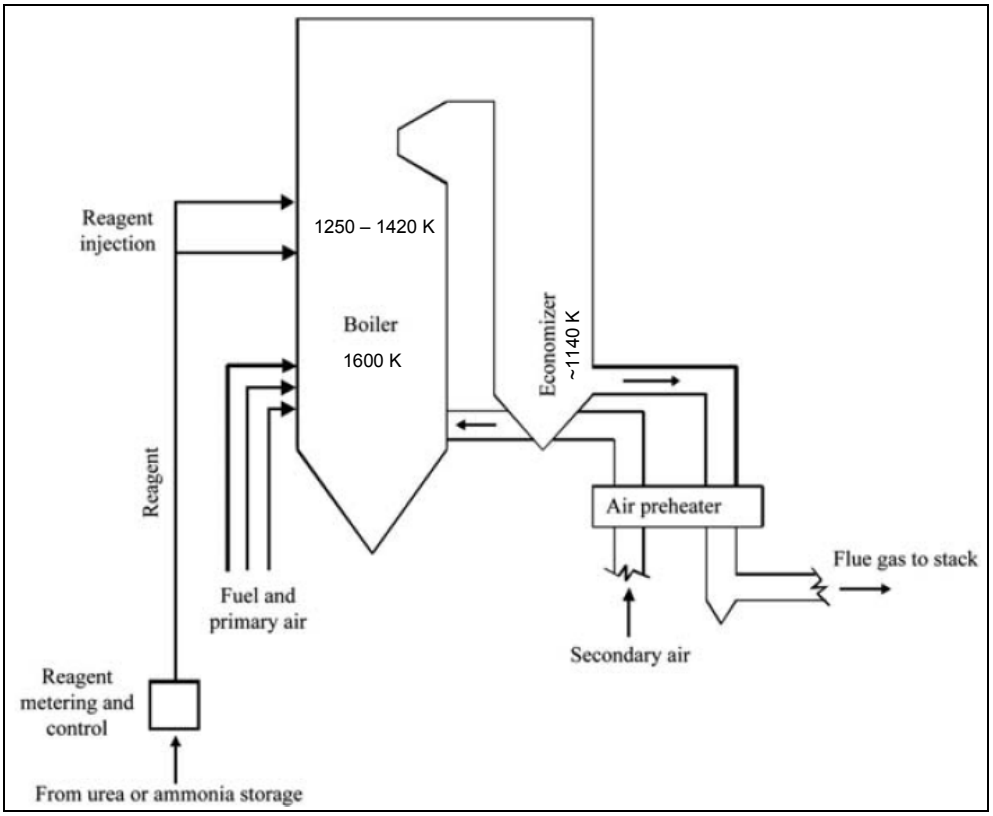

Figure 2.41 Schematic of a SNCR application (adapted from Srtivastava *et al*., 2005)

The reagents for SNCR are typically aqueous ammonia or a 50% solution of urea and water. Anhydrous ammonia is usually not used for SNCR due to restrictions and required permits. Yet between aqueous ammonia and urea, urea is more commonly used in SNCR applications because it is non-toxic and safer to transport and store. Also, urea droplets can penetrate further into the exhaust gases when it is injected, which enhances mixing (Mussatti *et al*, 2000a).

Despite the lower capital cost and relative ease to install, SNCR technology has not been as prolific in coal-fired boilers as low-NO_x burners and SCR. This is greatly attributed to the technology's unreliability and relative uncontrollability. Moreover, boiler design and operation parameters, for example lower flame temperatures from low-NO_x burners, have made SNCR impractical for many applications (Mussatti *et al*, 2000a). Furthermore, SCR systems have a few advantages over SNCR. For example, since SCR can occur at lower and broader temperature ranges, SCR systems can be

installed at various positions downstream from the main furnace (i.e. before or after an electrostatic precipitator) without the need for too much reheating. Currently, over 100 SNCR systems exist or are planned for construction in US coal steam units; however, there are no SNCR systems installed in coal-fired plants in Texas (USEPA, 2007a).

2.5. Competing Uses for Manure-based Biomass

In addition to competing emissions control technologies, there are also competing uses for the manure itself. The most common current use for manure is fertilizer or a supplement to fertilizer. Just as market food prices of crops like corn and sorghum can affect the price of ethanol and other bio-fuels, or vice versa, the price of chemical fertilizers and nitrogen can affect the price of manure. That is, fertilizer prices can affect the price that an animal farm operator will ask for, if an energy producer requests to haul away manure for co-firing or reburning operations. This asking price would then be added to the cost of transporting and processing the manure, which can possibly make the value of manure more expensive than coal or other fossil fuels. Hence, the coal-manure co-combustion facility or the small-scale, on-the-farm combustion system may become impractical.

Texas Cattle Feeders Association (TCFA) does have a program on the internet that computes the value of manure based on the nutrient content of the manure and the going prices of nitrogen and phosphorus. The program can also be used to compare the total annual cost of using fertilizer alone to the total annual cost of using manure and fertilizer in combination based on the manure collection cost, hauling distance, and specifics about the crops being fertilized (Weinheimer, 2008).

3. LITERATURE REVIEW

The primary purpose of this dissertation is to determine if utilizing MBB on large scale combustion facilities is economically feasible and to determine if MBB can be used on smaller scale on-the-farm energy conversion systems. The following section will be a brief review of these two areas. Much of the information discussed here will be used in the development of computational models, which will be discussed in a later section.

3.1. Previous Economic Studies

3.1.1. Co-firing Coal with Biomass

Although there have not been many studies on burning manure biomass in large combustion facilities, there have been co-combustion studies of other solid biomass fuels such as wood-based biomass. In fact, there have even been several recent biomass co-firing tests and proposals. For example, in 2005, American Electric Power, the largest electric generator and coal consumer in the US, successfully displaced 10% of the coal consumed at the 100 MW Picway coal plant near Columbus, Ohio with wood chips and wood waste-based biomass (Electric Power Daily, 2005). In 2007, as part of a proposal to approve the construction of a 750 MW plant, LS Power proposed to co-fire switch grass, cornstalks, and ethanol production wastes to supplement coal (Waterloo Courier, 2007). In the United Kingdom, the electric generator, Drax, is aiming to co-fire coal with 10% olive cake and elephant grass biomass at a 4,000 MW power plant in Yorkshire by 2009. Doing so would displace 1 million tons of coal and save 2 million tons of CO_2 per year. It was estimated that the delivery cost of the biomass would be 2 to 5 times that of coal, but benefits from renewable obligation certificates (ROCs) would justify the additional fueling costs (Froley, 2007).

In 2004, the US Department of Energy (DOE) conducted a fairly expansive study on co-firing coal with biomass. The study centered on the success of a pilot co-firing

test at the DOE Savannah River Site in Aiken, South Carolina. The DOE facility is composed of two stoker boilers that generate steam for heating applications. The facility is relatively small compared to most utility coal steam electric power plants, and consumes about 11,145 tons of coal per year. At the time of the study, the as delivered price of coal was $50 per ton. The facility also generated about 280 tons of scrap paper and cardboard per year. The waste paper and wood products were converted to "process engineered fuel" cubes and co-fired along with the coal. Twenty percent of the coal was offset by the biomass cubes. The project resulted in a net annual savings of about $254,000. These savings were computed after subtracting the cost of processing the wood and paper wastes. The total investment of the project was $850,000, which was paid back in approximately four years. The 10-year, net present worth of the system was determined to be $1.1 million (DOE, 2004).

There are several reasons why this specific co-firing application was so profitable. First, the cost of coal was relatively high. Secondly, the biomass that was used was generated from the facility itself, so the avoided costs of discarding the paper and wood waste in a landfill were added to the overall savings of the project. Although the DOE study sites various examples of successful co-firing applications on all types of boilers, it did say that stoker boilers are uniquely suited for co-firing because very little investment is required to accommodate most biomass fuels (DOE, 2004). Moreover, unlike manure biomass, wood biomass generally has very little moisture, ash, and sulfur, making it much more suitable for many direct combustion applications. Overall the study seemed to suggest that the eastern part of the US is particularly suited for co-firing applications because as delivered coal prices tend to be higher in eastern states, see Table 1.1. Also landfill tipping fees are generally more expensive in eastern states, giving added incentive to utilize waste-based biomasses in alternative ways.

For the purposes of this study, the most difficult cost to estimate is the capital investment cost of making the necessary modifications to the power plant site to process and handle the new biomass fuel. Several studies of biomass co-firing have quoted estimates of the investment costs of a co-fire project. Some of these studies are listed in

Table 3.1. Note that capital costs are listed as dollars per kW_e generated from the biomass.

Table 3.1 Capital investment costs of installing a biomass co-firing system on an existing coal-fired power plant, taken from various sources

Capital Cost, η ($/kW$_e$ from biomass)	**Source**	**Notes**
	CO-FIRING	
60	(Robinson *et al*, 2003)	Mode co-firing rate for <2% biomass on an energy basis. Range: 40 - 100 $/kW biomass. Wood and agriculture residue
200	(Robinson *et al*, 2003)	Mode co-firing rate for >2% biomass on an energy basis, separate stream and injection required. Range: 150 - 300 $/kW biomass. Wood and agriculture residue
175 - 200	(Hughes, 2000)	Co-firing with separate feeder. Wood waste, short rotation crops, and switch grass biomass
109	(USEPA, 2007c)	>500 MWe pulverized coal plant. Probably wood and crop based biomass
218	(USEPA, 2007c)	201 - 500 MWe pulverized coal plant. Probably wood and crop based biomass
251	(USEPA, 2007c)	<200 MWe pulverized coal plant. Probably wood and crop based biomass

Robinson *et al*. (2003), along with the DOE (2004) study, suggested that a major factor in the capital investment cost of a co-firing project was the percentage of biomass that the boiler would use. If less than 2% biomass were to be utilized, then the investment costs would be significantly lower because existing equipment used to process the coal may also be used at the same time to process the biomass. The coal and biomass would be directly mixed before grinding and conveying to the burner. Figure 3.1 illustrates the new equipment that would be required to process the biomass under this scenario. However, this may not be true for some pulverized coal power plants, which have equipment specifically designed to micronize coal and not biomass, which may be more difficult to grind.

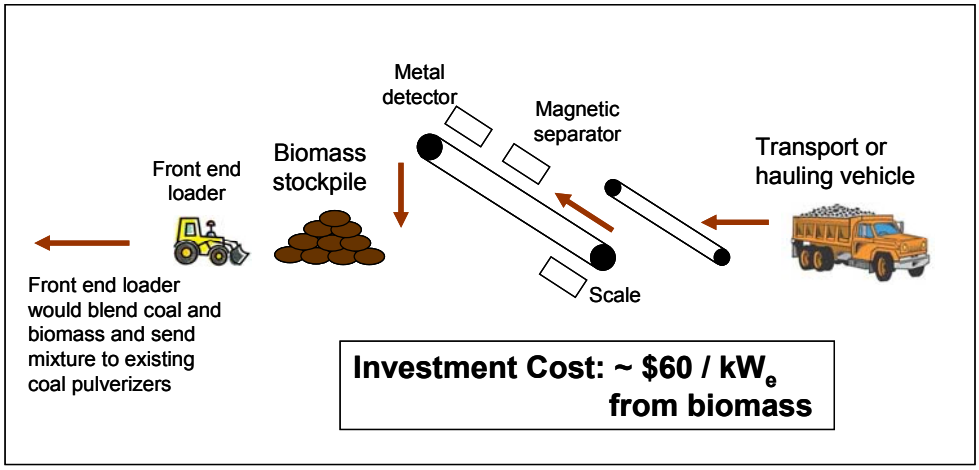

Figure 3.1 Schematic of a blended-feed co-firing arrangement for a pulverized coal boiler (adapted from DOE, 2004)

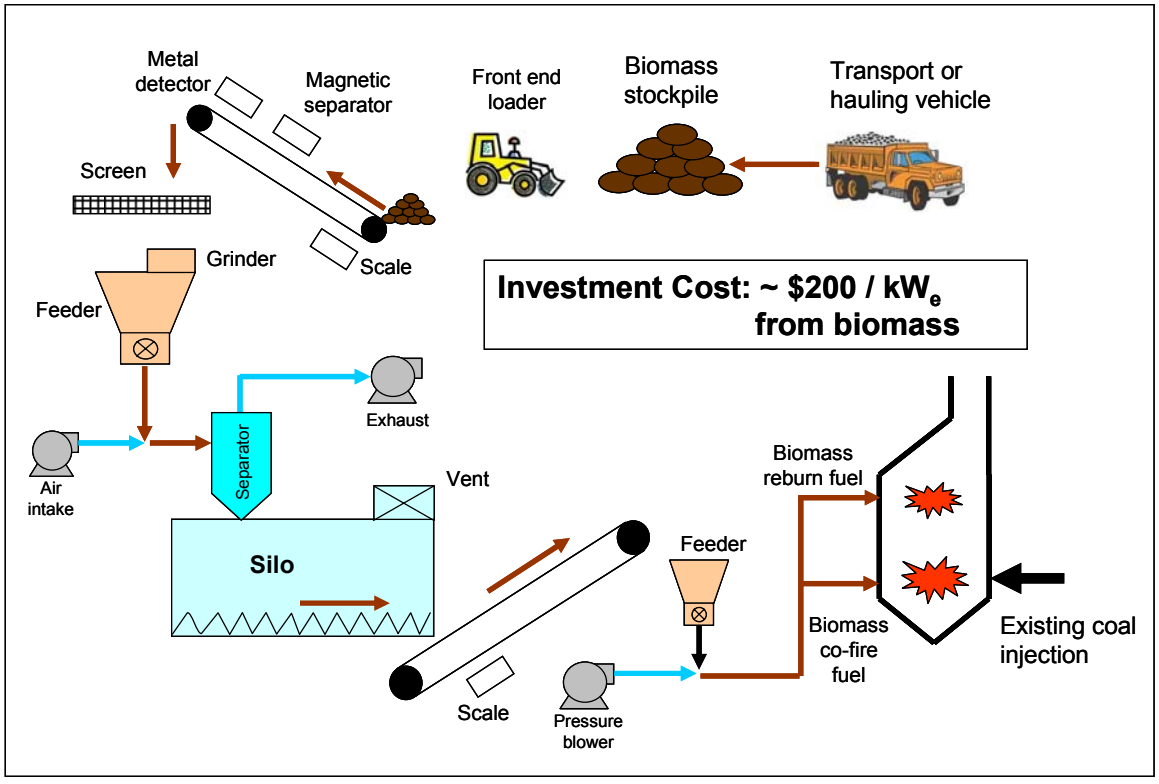

Figure 3.2 Schematic of a separate-feed co-firing arrangement for a pulverized coal boiler (adapted from DOE, 2004)

If more than 2% biomass were to be utilized, then additional processing equipment would be necessary, adding to the overall investment cost. Figure 3.2 illustrates the greater amount of new equipment that must be purchased if separate equipment were used to handle the biomass. However, keep in mind that these projected additions to coal-fired facilities are for wood-based biomass. Manure-based biomass may require different equipment.

The USEPA (2007c) study, listed in Table 3.1, also provided estimates for the annual operation and maintenance costs. According to the study, the fixed operation and maintenance cost for operating the additional biomass processing equipment was estimated to be approximately \$7.63 per kW_e from biomass per year. Additional values were given to estimate the cost of transporting the biomass to the combustion facility.

3.1.2. Reburning Coal with Biomass

As discussed earlier, there have been relatively few reburn tests at coal-fired power plants in the US. Most of these tests included reburning coal with natural gas and only four or five power plants reburned coal with more micronized coal. Thus, one of the challenges of this study was to estimate the cost performance of a MBB reburning system at a coal plant, even when only experimental results and pilot scale tests have been conducted for MBB reburning, and few applications of gas and coal reburning systems existed for comparison. Work by Zamansky *et al*. (2000) suggested that reburn systems utilizing furniture wastes, willow wood, and walnut shell biomass as reburn fuel have similar capital costs to coal reburning systems. An earlier USEPA (1998) report for the Clean Air Act Amendment, which was also sited by Biewald *et al*. (2000), modeled both gas and coal reburn systems, although the coal reburn model was meant only for cyclone boiler types. And since gas reburning costs are generally lower than coal reburning costs, the reburn capital cost model presented by the USEPA (1998) would only be applicable for cyclone boilers. Cyclone boilers burn coarsely crushed coal, but coal reburn systems typically require pulverized or micronized coal to avoid unburned carbon emissions. Hence, purchasing pulverizing equipment is generally

required for cyclone boiler plants that wish to install coal, or other solid fuel, reburn systems.

Table 3.2 Capital investment costs of installing a reburning system on an existing coal-fired power plant, taken from various sources

Capital Cost, η ($/kW$_e$ total plant capacity)	Source	Notes
REBURNING		
35	(Zamansky *et al*, 2000)	Same cost for both coal and biomass reburning. 300 MWe plant. Furniture, willow wood, and walnut shell biomass.
45	(Zamansky *et al*, 2000)	Same cost for both coal and biomass reburning. 300 MWe plant. Advanced reburn process.
$70.7\left(\frac{300}{P}\right)^{0.388}$	(USEPA, 1998)	Coal reburning in cyclone boilers only. P = plant capacity in MW_e
60	(Smith, 2000)	Coal reburning in cyclone boilers, 40% NO_x reduction from an 0.86 lb/MMBtu baseline emission
6 - 13	(Smith, 2000)	Pulverized coal configurations using some existing equipment for coal reburn fuel preparation
66 and 43	(Mining Engineering, 2001)	For 110 MW and 605 MW plants, respectively. 50% NO_x reduction on cyclone burners with pulverized coal for reburn fuel

Some estimates of coal and biomass reburn capital costs are presented in Table 3.2. Unlike co-firing, reburning costs are usually expressed on a "dollar per kW_e of total plant capacity" basis. Smith (2000) reported that coal reburn capital costs may be as low as $6/$kW_e$ for pulverized coal plants with existing equipment available for preparing the reburn fuel. However, MBB is significantly different from most wood and plant-based biomasses, as well as coal. The moisture and ash contents in MBB vary to greater degrees than wood biomass, although low ash cattle biomass has a comparable heat value to the biomass discussed by Zamansky *et al*. (2000). Moreover, reburn systems usually require 15 – 20% of the power plant's heat rate to be supplied by the reburn fuel. If biomass were to be used as the reburn fuel, additional processing equipment would almost certainly be required, based on the previous discussion of biomass co-firing.

Also note that capital costs for reburning in Table 3.2 do not include the capital cost of dryers and biomass hauling vehicles which will be needed for manure biomass reburning but not coal reburning. These costs must be computed separately. As for fixed operation and maintenance costs of the reburn fuel's processing equipment, the model presented by the USEPA (1998), for reburning coal with micronized coal, may be used for the current study; however, an additional correction factor that accounts for the MBB's poorer heat value, and hence greater required fueling rate, should be implemented.

3.1.3. Competing NO_x Control Technologies

In addition to modeling the economics of reburning coal with biomass, comparative estimates of other competing NO_x control technologies should also be computed. Fortunately, the economics of more common NO_x control technologies such as low-NO_x burners, SCR, and SNCR are modeled by the US EPA. The USEPA Integrated Planning Model (IPM) is a multi-regional, dynamic, deterministic linear programming model of the US electric power sector. The results from the IPM are meant to compare energy policy scenarios and governmental mandates concerning electric capacity expansion, electricity dispatch and emission control strategies. The model and base case inputs to the model are updated annually. The latest update, as of the writing of this dissertation, may be found on the USEPA (2006) website. Since a section of the IPM is concerned with evaluating the cost and emission impacts of proposed policies, it is possible to adopt these emission models to describe the economics of common primary and secondary controls, and then compare them to results for MBB reburning. However, since reburn technologies are not a significant part of the current efforts to reduce NO_x at coal-fired power plants in the US, their associated investment and operating costs were not included in the latest version of the IPM.

The NO_x control technology options modeled by the EPA IPM are low-NO_x burners (with and without over fire air), SCR, and SNCR. Capital and fixed operation

and maintenance costs were set as functions of power plant capacity, while variable operation and maintenance costs were set as functions of heat rate. Models presented by Mussatti *et al*. (2000 a & b) offer more detailed and comprehensive representations for SCR and SNCR cost components, but require more detailed inputs. The cost equations in the IPM for NO_x control technologies are based on costs for 300 MW_e sized boilers. These costs are then translated to costs for different boiler sizes with scaling factors. The cost equations and scaling factors of IPM will be discussed further in the modeling section of this dissertation.

3.1.4. Dollar Values of Emissions

Annual monetary values pertaining to NO_x, SO_x, nonrenewable CO_2, and ash revenues are also required. Values for NO_x and SO_x emission credits can be found by the South Coast Air Quality Management District (SCAQMD) (2007). In 2006, trading credits for NO_x were \$2,353/ton for the 2005 compliance year and as high as \$15,698/ton for the 2010 compliance year. For compliance years beyond 2010, the NO_x credit values were \$11,100/ton. SOx credits were traded at \$882/ton for the 2005 compliance year and \$966/ton for the 2006 compliance year. In a white paper prepared for TXU Energy (now Luminant Energy) by NERA Economic Consulting in 2004, the NO_x permit price assumption for long term strategic fuel planning was \$4,000/ton NO_x with a sensitivity range of \$2,000 to \$6,000/ton NO_x. The permit price assumption for SO_2 was \$250/ton SO_2 with a sensitivity range of \$150 to \$500/ton SO_2 (NERA, 2004).

Although most coal-fired plants in the US are currently not required to reduce CO_2 emissions, speculations may be made as to how emission taxes, cap and trade-based CO_2 allowances, or avoided sequestering costs may affect the profitability of a MBB co-fire or reburn system. The same NERA report to TXU estimated that the cost of reducing CO_2 by capture and storage would range between \$50 and \$80/ton CO_2. Comparatively, the report showed that the cost of reducing CO_2 by co-firing coal with biomass ranged between \$5 and \$15/ton CO_2. However, the biomass referred to in this study was undoubtedly wood or plant-based biomass, and was probably based on a

similar report to the DOE (2004) study on biomass co-firing discussed earlier. Moreover, ongoing results of the Regional Greenhouse Gas Initiative (RGGI, 2008) can provide some basis of the monetary value put on CO_2 in the US, even though the RGGI is in its infancy and only has jurisdiction in the northeastern part of the US. According to the RGGI website, the clearing price of CO_2 allowances in its inaugural auction in September 2008 was \$3.07/ton CO_2.

Finally, the ability of plant managers to find suitable uses for ash produced from biomass combustion as well as local buyers, could greatly affect a MBB co-fire or reburn system's overall profitability. Preliminary studies on the possible usage of ash produced from manure combustion have provided mixed results. Ash produced from manure combustion is a suitable sub-grade material for road construction, and if mixed with 10% Portland cement, can be used as a light weight concrete material with about one-third of the compressive strength of concrete. Yet the manure ash is not self-cementing and is not a suitable replacement for Portland cement. Also, chemical analyses show that manure ash is a non-hazardous, possibly reactive industrial waste which could be used for feedlot surfacing, road base, some structural building projects, and possibly fertilizer (Megel *et al*, 2006 and Megel *et al*, 2007). More information about the uses of fly ash from coal combustion was provided by the USDOT (2006). If ash is not sold, then it must be discarded, typically in local landfills, which require tipping fees.

3.2. Review of Designs for Small-scale, On-the-farm Manure-based Biomass Combustion Systems

Manure-based biomass can also be considered a possible feedstock for smaller, on-the-farm combustion systems designed to properly dispose of manure solids and wastewater. Using commercially available equipment like solid separators, augers, and dryers, MBB can be prepared for smaller combustion processes. If these systems are constructed on or near a CAFO, the benefits of reducing tremendous amounts of waste and avoiding potential environmental misfortunes can be realized with out much of the

transportation and processing costs required to burn cattle biomass in large electric utility boilers.

There have been several patents and design studies of small scale, combustion systems meant to burn manure on or near large animal farms. One such design was the gasification system discussed earlier by Young *et al*. (2003) for dairy manure biomass. The dairy manure is first reduced to about 70% moisture with an auger press and then sent through a high-temperature, entrained-flow air gasification system. A patent by Kolber (2001) was an elaborate design of an energy conversion system that could treat solid and liquid manure from confined animal feeding operations. The motivation of this study was to reduce the need for anaerobic treatment lagoons at large pig farms in North Carolina. The design is illustrated in Figure 3.3. Flushed manure wastes from growing buildings enter a waste holding tank, where the manure is either sent to a covered waste processor or held if the rest of the system is backed up. The components of the covered waste processor are shown in Figure 3.4. Wastewater is homogenized and then sent to a solids separator, after which the solids are dried and then burned or gasified in a combustor. The liquid from the separator is treated or deodorized in an ozonation tank, where organic material left in the liquids is oxidized. The liquids are then sent to a flush water reservoir. Air and hot flue gases from the manure combustion are used to dry the separated solids. Any waste gases generated from the other components of the system would also be burned in the combustor.

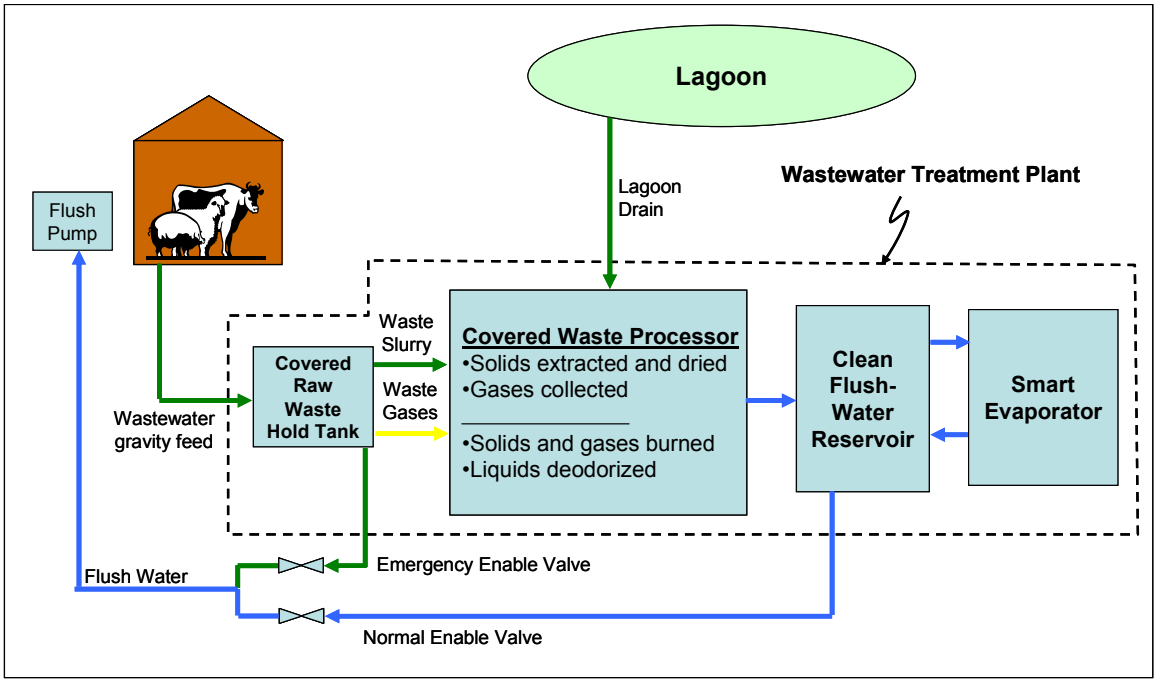

Figure 3.3 Design for a wastewater treatment plant for large confined animal feeding operations and drainage of anaerobic treatment lagoons (Kolber, 2001)

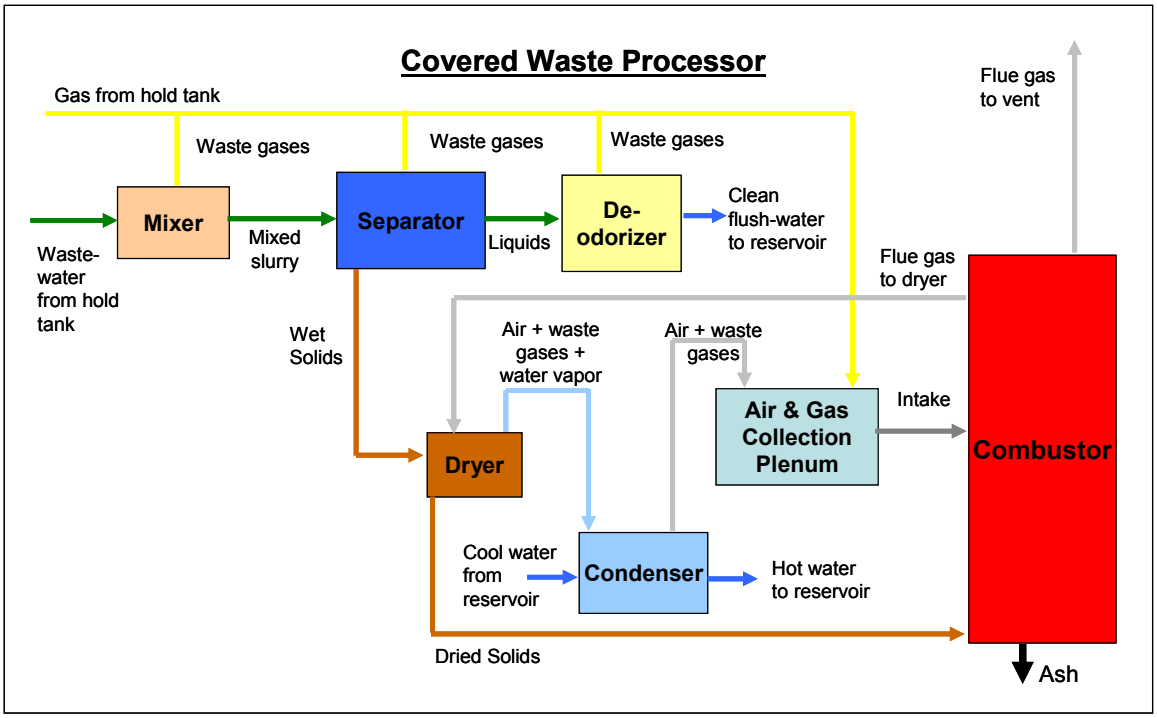

Figure 3.4 Components of the covered waste processor in the wastewater treatment plant discussed by Kolber (2001)

A solar drying system, which Kolber called a "Smart Evaporator", would evaporate any wastewater that is not treated in the covered waste processor and keep the system from overflowing. Each of these components, as well as a control system and alternative embodiments, are discussed in greater detail in Kolber's patent.

There is also a prototype system developed by Skill Associates, Inc. called Elimanure™ that can eliminate both the liquid and solids of any animal manure. The system is pictured in Figure 3.5. Waste manure up to 95% moisture enters large drying units and is mixed by large augers with hot air. The temperature in the drying units reaches 82 °C (180 °F) and the manure is dried to about 40% moisture. The water vapor is ventilated out of the drying unit, while the 40% moisture solid manure is sent to a thermal gasification boiler where it is burned at 1090 °C (2000 °F). The boiler generates steam which runs turbines to generate electricity. During the first two hours of operation, the system uses propane or some other fuel to start up, but after that, the dried manure can sustain the process. Besides water vapor from the drying process, the only byproduct is a grey powdery ash which contains the inorganic or noncombustible material in the manure. The facility was constructed at an animal farm in Greenleaf, Wisconsin in 2005 (Skill Associates, 2005), which houses 4,000 animal units (dairy cows, horses, and other animals) and produces 1,007 dry kg (2,220 dry lbs) of manure per hour. At this animal farm, the boiler produces 4500 kg (10,000 lb) of steam per hour at 2,000 kPa (300 psi). The turbine is sized to produce 600 kW_e of electricity.

An update of the Elimanure system, installed in Greenleaf, was written in Ag Nutrient Management Magazine (Caldwell, 2008). During early operation of the combustor, Skill Associates assumed that dried manure would burn (gasify) much like sawdust, however, they soon found that the higher ash content of the manure created plugging in the boiler and heat exchangers. Moreover, the ash formed "lava" in the burning bed of the combustor. In July 2008, however, Skill Associates claimed they had solved the ash problem with the combustor by "modify[ing] and improve[ing] the combustor, making it more robust." A "new, larger, and state-of-the-art" combustor

replaced the original one. The cost estimates for the system were also updated to $4.5 millions initial investment with a 3.5 year payback period. Part of the reason for the quick payback period was the fact that the animal farm originally produced 94.6 million liters (25 million gallons) of liquid manure per year, which needed to be hauled away from the farm at an annual cost of $400,000. Reducing the liquid manure to just ash greatly reduced the waste disposal cost of the farm.

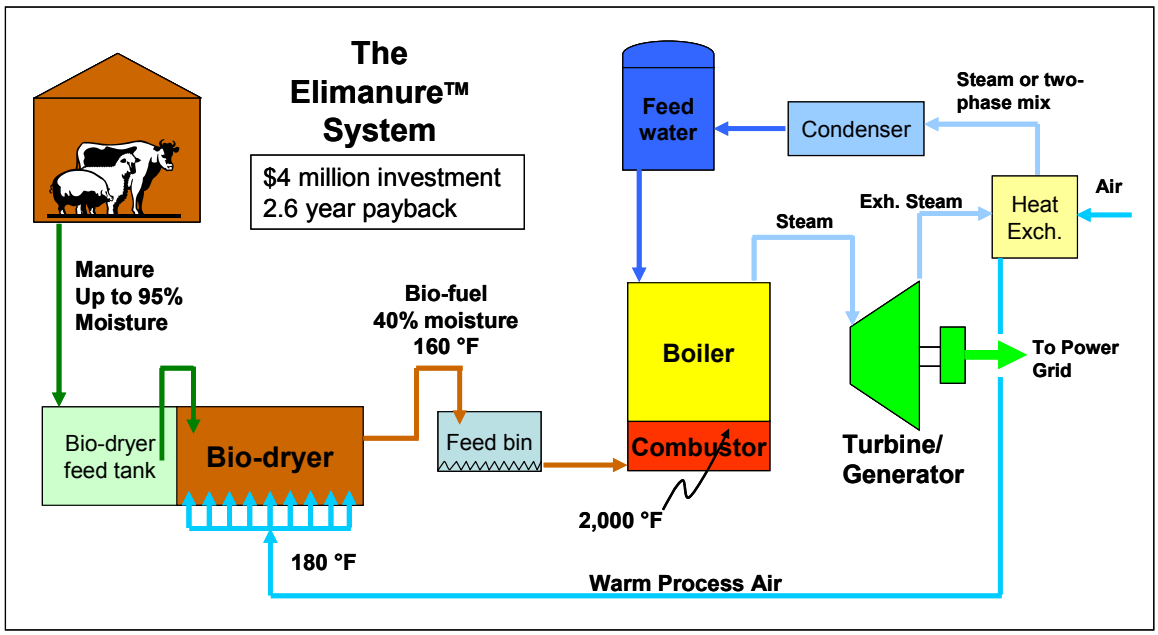

Figure 3.5 The Elimanure™ System developed by Skill Associates (2005)

On-the-farm combustion systems were also modeled by Carlin (2005) and Carlin *et al*. (2007a). Thermodynamically, a black box method was utilized to determine the greatest amount of waste that could be converted into the desired end products. This method is shown in Figure 3.6, with the inputs and outputs to the system crossing through the control volume (CV) fixed around the combustion system. A complete mass and energy balance of the system was conducted. The ash and moisture percentages were treated as variables in order to determine their required values to convert all material to combustion gases, water vapor, dry ash, and to maintain a desired system temperature (for example, 373 K).

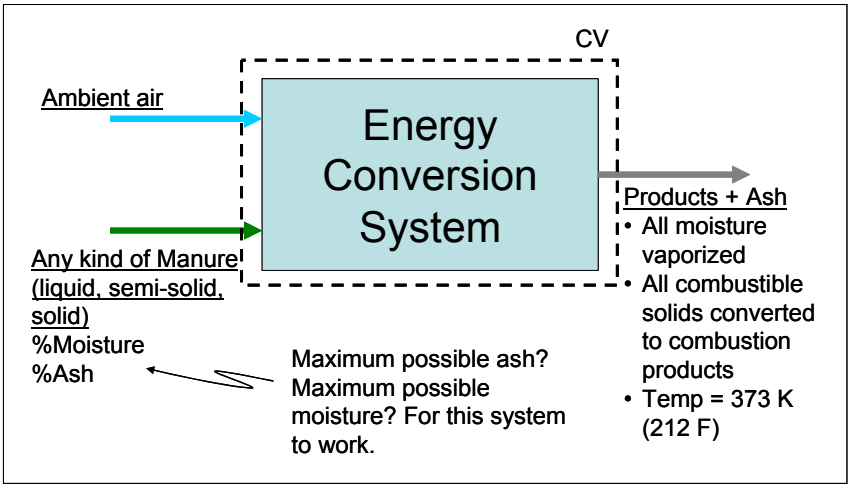

Figure 3.6 Black box thermodynamic model of a manure energy conversion system (Carlin, 2005)

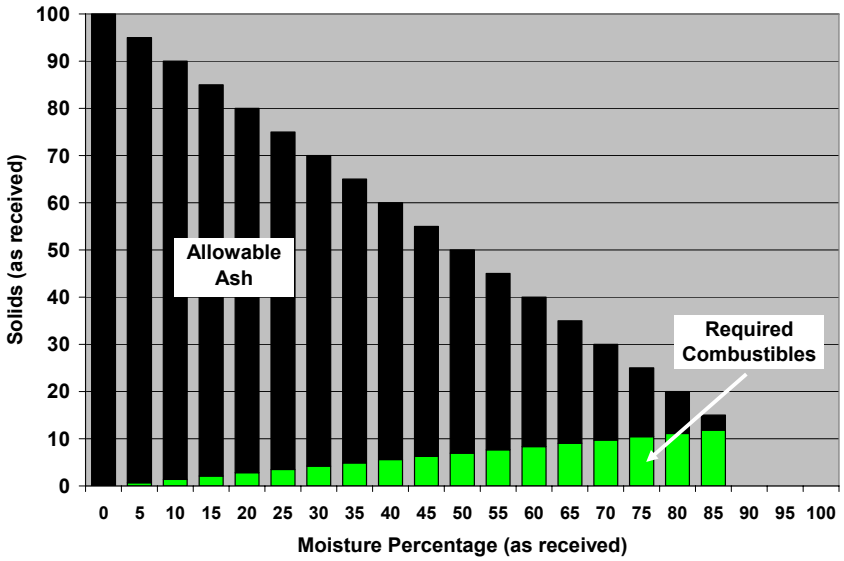

Figure 3.7 Required manure biomass solids composition needed to completely convert manure waste to combustion gases, water vapor, dry ash, and to maintain a desired system temperature of 373 K (Carlin, 2005)

Figure 3.7 displays the results of the black box methodology. According to the figure, if the flushed manure emanating from a dairy or feedlot has a moisture percentage of more than 85%, then no amount of combustible material in the solids can produce enough heat during combustion to fully vaporize all of the moisture portion

(wastewater) of the manure. However, ash also plays a limiting role in the effectiveness of independent manure combustion systems. Depending on the manure collection process, the bedding used in the dairy free stalls, or the pavement surfacing of the feed yards and open lots, the ash content of the solid manure material can make direct combustion impossible due to fowling and inadequate fuel heating value.

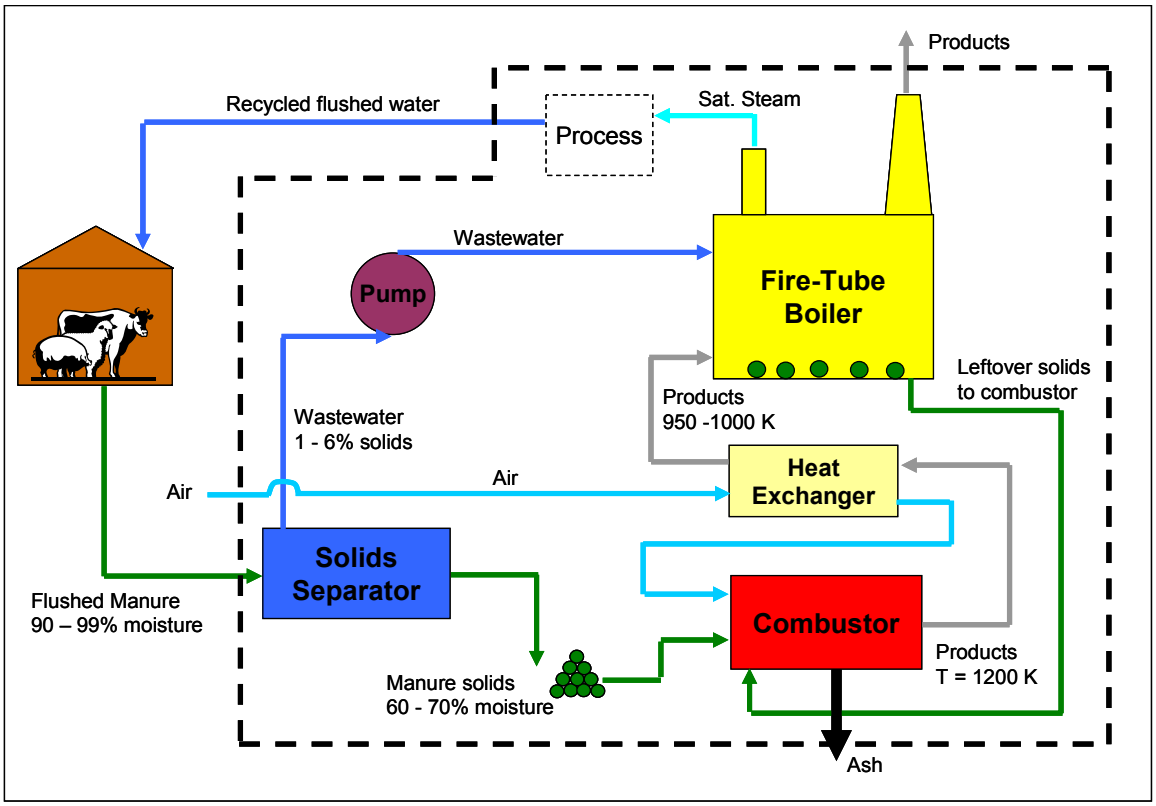

Figure 3.8 Conceptualized model for manure biomass thermo-chemical energy conversion system for a CAFO (Carlin, 2005)

The conceptualized system shown in Figure 3.8 has the potential to burn most of the manure solids and vaporize at least a portion of the wastewater stream. Again, the flushed manure is mechanically separated into solid and liquid streams. The solids are injected into a combustor, furnace, or perhaps a gasifier with a subsequent product gas burner. The combustion air is preheated in a heat exchanger by the hot products of combustion. Meanwhile, some of the remaining wastewater is sent to a fire-tube boiler

where it is sprayed onto heat pipes containing the combustion gases. The remaining solids from the wastewater can be removed periodically from the boiler (similar to blow down in conventional fire-tube boilers) and either sent back to the combustor or used as fertilizer.

This system was modeled by Carlin (2005) and Carlin *et al*. (2007a). Carlin *et al.* (2007b) added the effects of combustion air pre-heating. The steam could be used as a general heat commodity for the farm or it can be used to dry the manure solids. Figure 3.9 shows some of the results of the modeling of the system in Figure 3.8. Here, the waste disposal percentage is defined as the heat released by the combustion process, divided by the heat required to evaporate all of the manure wastewater. Waste disposal was plotted against the added amount of fuel injected into the combustor. Methane, coal and addition composted manure solids were all modeled. As can be seen, if no additional fuel is used, then the combustion process only releases about 32% of the heat required to incinerate the manure wastes. From this plot it can be seen how much additional fuel would be required to eliminate all of the manure wastes.

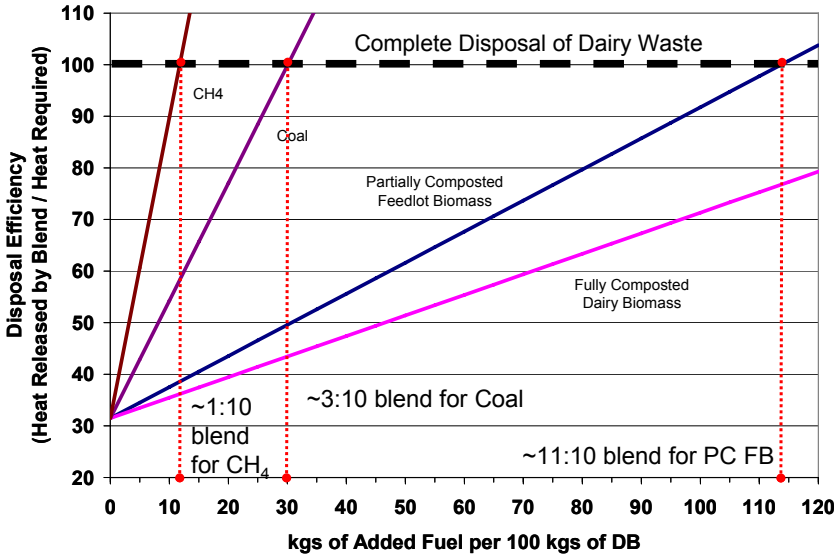

Figure 3.9 Waste disposal efficiency of conceptualized manure biomass energy conversion system vs. mass of additional fuel used for combustion (Carlin, 2005)

In addition to the combustor, one of the main design challenges of the conceptualized system in Figure 3.8 is the fire-tube boiler. There are numerous designs for wastewater evaporators such as the patented design by Gregory (1993). These evaporation tanks can handle most sludge and liquid waste streams. Kamen *et al*. (2008) patented a locally powered water distillation system for converting any wastewater, even raw sewage, to clean, potable water. The inspiration for this invention was the lack of available clean water to millions of people in developing countries in Southeast Asia, the Middle East, and Africa. The pressure vapor cycle liquid distillation system is about the size of a residential washing machine and designed to provide enough water for a family or small rural village. The design is meant to be relatively affordable for governments and individuals of third world countries, about $1,000 to $2,000 each when mass production is established. The distillation system was designed to be powered locally with easily obtainable fuels, such as "cow dung" (Schonfeld, 2006). Such a system may be scaled-up in size to handle the larger amount of wastewater from a CAFO.

For most of the energy conversion systems discussed in this section, designers assumed that high temperature gasification would be the most appropriate means by which the manure solids would be burned. However, there are some claims to directly firing manure solids such as a patent for a moving grate combustor by Mooney *et al*. (2005). See Figure 3.10. However, most of these systems are essentially two-stage gasification systems in which the released volatile gases are immediately fired, in this case, by a natural gas pilot burner. In this sense, these systems become co-firing furnaces, only now the manure is the primary fuel and the fossil fuel is an igniter.

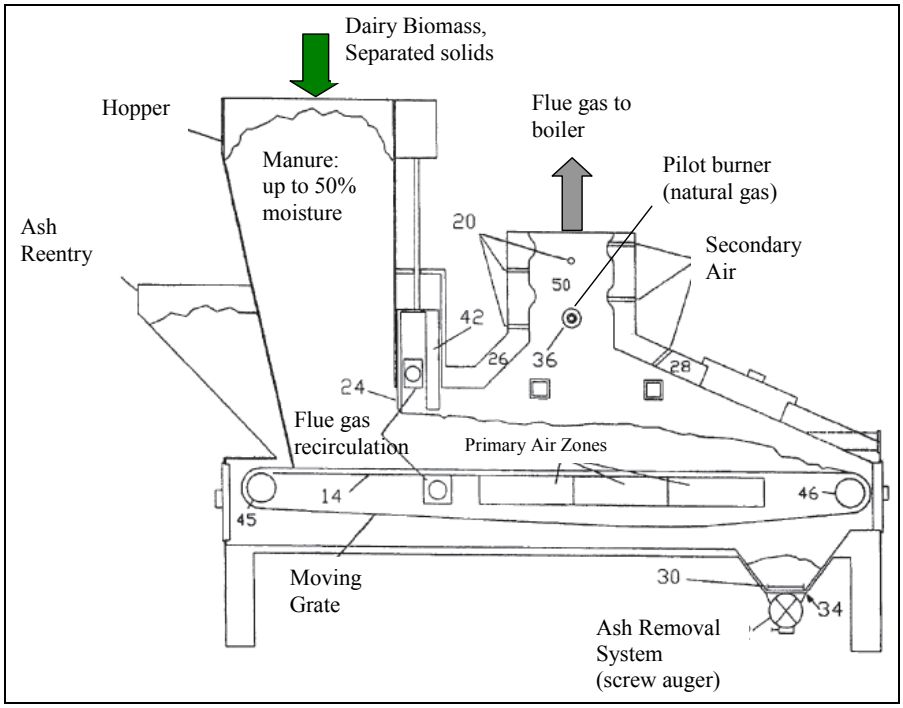

Figure 3.10 Schematic of a moving grate manure biomass combustor (adapted from Mooney *et al*., 2005)

On-the-farm MBB gasification systems might also solve many of the economic and practical issues with reburning and co-firing on larger coal-fired power plants discussed earlier. For example, synthesis gas from MBB gasification may be a viable and effective reburn fuel itself. Synthesis gas can be piped to the power plant from CAFOs or centralized gasification facilities, instead of hauled by truck. Plus, no additional ash loading would be incurred by the coal plant. Moreover, reburning with gas requires significantly less capital costs compared to solid fuel reburning systems; although, the capital cost of constructing enough gasifiers to supply a suitable amount of synthetic gas to the coal plant must be taken into account. Studies by Rudiger *et al*. (1996) and Rudiger *et al*. (1997) investigated the fuel nitrogen content in pyrolysis gases from both coal and wood and grass-based biomass that could possibly be used as reburn fuel. Future investigation into the nitrogen content and reburn effectiveness of pyrolysis gases from MBB should also be undertaken.

4. OBJECTIVE AND TASKS

In order to determine the optimum usage and feasibility of MBB in combustion systems, two objectives are hereby proposed.

1. Investigate the underlying requirements and overall emission and economic impacts of firing MBB in existing large utility coal-fired boilers, and
2. Research and develop designs for small-scale, on-the-farm combustion systems for MBB disposal and possible energy production.

In order to achieve the above objectives, the following tasks are proposed during the doctoral research.

1. Tasks under Objective 1:
    - 1.1 Determine capital expenditures for a MBB reburn and/or co-firing system including the cost of installing the reburner on an existing coal-fired power plant, the cost of purchasing transportation vehicles, and the cost of purchasing biomass processing equipment such as dryers.
    - 1.2 Determine the operation and maintenance costs that would be inherent to a MBB reburn and/or co-firing system.
    - 1.3 Estimate the NO_x and nonrenewable CO_2 savings, as well as the additional ash production and perhaps additional SO_x emissions during MBB combustion in an existing coal-fired power plant. Also account for carbon and NO_x emissions from drying and transporting biomass.
    - 1.4 Estimate the economic impacts of reducing NO_x and CO_2 and increasing ash.
    - 1.5 Determine the capital, operation and maintenance costs for other, more common NO_x control technologies such as low-NO_x burners and selective catalytic reduction (SCR), and compare to findings for MBB reburning.
    - 1.6 Compute the overall annualized cost of reducing NO_x for each NO_x control technology. Moreover, estimate the net present worth and simple payback period of a MBB reburn retrofit project on an existing coal-fired power plant.
    - 1.7 Conduct a full sensitivity analysis of the annualized cost and/or the net present worth to all significant parameters in the economic model.

1.8 Determine optimum conditions for a MBB reburn system including maximum acceptable biomass transportation distance and minimum required dollar values of CO_2 and NO_x emissions.

2. Tasks under Objective 2:

2.1 Review any current designs for on-site MBB combustion systems including biological gasification systems such as anaerobic digesters.

2.2 Expand on initial designs developed during MS research (Carlin, 2005), including ways to utilize waste heat and options for thermally drying MBB before combustion.

2.3 Investigate and suggest values for design parameters of heat exchangers, biomass dryers, combustors, and boilers, so that future experimentation and pilot-tests may be conducted.

2.4 Estimate economic costs of installing and operating a MBB combustion system on an animal feeding operation (either solid fuel burners or gasifiers with subsequent producer gas firing). Determine if on-site combustion of biomass would provide any long term financial benefits to the animal feeding operation owners.

2.5 Compare the viability of burning MBB on smaller scale, on-the-farm combustion systems to the possibility of burning in larger scale reburn or co-fired system on existing coal-fired power plants.

5. MODELING

The methodology of this study was largely based on mathematical models derived from thermodynamic, fluid mechanic, and heat transfer analyses, as well as engineering economic analysis. In this section, the derivation and general rationalization of all equations included in these models will be presented. Pre-combustion processing, including manure-based biomass (MBB) drying, grinding, and transporting, will be discussed. Next a general model for coal and MBB combustion will be generated. Then this general combustion model will be applied to both coal/MBB co-combustion in large coal plants and MBB combustion in small scale, on-the-farm combustion systems. Finally the economics of pre-combustion, combustion, and emissions from combustion processes will be modeled. Capital and operation and maintenance (O&M) costs will be included in the economics portion, as well as overall net present worth and simple payback analyses of combustion systems utilizing MBB. However, first a brief review of modeling biomass properties will be presented based on studies discussed in the Background Information Section of this dissertation.

5.1. Modeling the Properties of Manure-based Biomass

For combustion and gasification modeling, usually only the results of ultimate, proximate and heat value analyses found in Table 2.1 through Table 2.5 will be needed for both coal and MBB. However, since the current analyses will also include modeling drying processes and transportation, MBB properties such as bulk density and specific heat will also be required. Moreover, it is important to know how these parameters will change with other known parameters such as temperature and moisture percentage.

According to the study by Bohnhoff *et al*. (1987), cited earlier, the dry particle density of the MBB is a function of the volatile matter percentage. However, Bohnhoff *et al*. did not distinguish between fixed carbon percentage and ash percentage as was done in most of the proximate analyses presented in this dissertation. Thus, a

modification to the equation for dry particle density, presented by Bohnhoff *et al*., can be used for the present study.

$$\rho_{p,MBB} = 100\left(\frac{\%VS_{dry}}{\rho_{VS}} + \frac{\%FC_{dry}}{\rho_{FC}} + \frac{\%A_{dry}}{\rho_{ash}}\right)^{-1} \tag{5.1}$$

The subscript *BD* for the volatile solids (VS), fixed carbon (FC) and ash (A) denotes that the parameters must be entered on a dry basis. The densities of these three components must also be known. According to Bohnhoff *et al*., ρ_{VS} was approximately 1500 kg/m^3. Moreover, ρ_{FC} can be assumed to be approximately the density of graphite or pure carbon, 2300 kg/m^3, and ρ_{ash} can be approximated as the density of loose earth or soil, 1200 kg/m^3 (Engineeringtoolbox.com, 2008).

The bulk density, $\rho_{b,MBB}$, can be modeled by a curve fit of Chen's (1983) data in Figure 2.7 as a function of moisture percentage.

$$\begin{aligned}\rho_{b,MBB}\left[\frac{kg}{m^3}\right] = {} & 564.8745 - 4.373987(\%M) - 1.844560(\%M)^2 \\ & + 1.293383*10^{-1}(\%M)^3 - 2.800288*10^{-3}(\%M)^4 \\ & + 2.525236*10^{-5}(\%M)^5 - 8.252736*10^{-8}(\%M)^6\end{aligned} \tag{5.2}$$

The curve represented by this equation (R^2 = 0.7553) can also be seen in Figure 2.7 along with Chen's data. Alternatively, Houkom *et al*.'s (1974) equation, which is also displayed in Figure 2.7, could be used, but for consistency in this study, equation (5.2) will be used during the rest of the present discussion.

The air-filled porosity or void volume, ε_{MBB}, can also be modeled by an expression presented by Bohnhoff *et al*. (1987).

$$\varepsilon_{MBB} = 1 - \rho_{b,MBB}\left[\frac{(\%M/100)}{\rho_{H_2O_{(l)}}} + \frac{\{1-(\%M/100)\}}{\rho_{p,MBB}}\right] \tag{5.3}$$

Here, $\rho_{H_2O_{(l)}}$ is the density of liquid water.

Similarly to the expression for $\rho_{p,MBB}$, the expression for the specific heat of the dry fraction of the MBB, $c_{MBB,dry}$, can be a modification of a linear rule presented by Bohnhoff *et al*.

$$c_{MBB,dry} = c_{ash}\left(\frac{\%A_{dry}}{100}\right) + c_{FC}\left(\frac{\%FC_{dry}}{100}\right) + c_{VM}\left(\frac{\%VM_{dry}}{100}\right) \tag{5.4}$$

Again, the specific heats of ash and fixed carbon can be estimated to be those of soil and graphite, 0.80 kJ/kg K and 0.71 kJ/kg K, respectively (Engineeringtoolbox.com, 2008). According to Bohnhoff *et al*., the specific heat of MBB, on a dry basis, was 0.92 kJ/kg K when the volatile matter was 94%. Therefore the specific heat of the volatile matter component of the MBB, c_{VM}, can be back-calculated and found to be 0.93 kJ/kg K. On an as-received basis, the specific heat of the MBB is simply:

$$c_{MBB} = \left(1 - \frac{\%M}{100}\right)c_{MBB,dry} + \left(\frac{\%M}{100}\right)c_{H_2O_{(l)}} \tag{5.5}$$

where $c_{H_2O_{(l)}}$ is the specific heat of liquid water.

Although the thermal conductivity of bulk MBB does not appear in this study, it can be modeled by the following expression from Bohnhoff *et al*.

$$\begin{aligned} k_{b,MBB}\left[\frac{W}{m\cdot K}\right] = {} & 0.0212 + 0.00714\theta\left(T - 273.15\right) + 0.485\theta^2 \\ & - 0.003754\theta^2\left(T - 273.15\right) \end{aligned} \tag{5.6}$$

Here, T is in degrees K and θ is the volumetric moisture content defined as:

$$\theta = \frac{\rho_{b,MBB}}{\rho_{H_2O_{(l)}}}\left(\frac{\%M}{100}\right) \tag{5.7}$$

Finally, if the thermal diffusivity of bulk MBB must be known, then it can be computed from the following expression:

$$\alpha_{b,MBB} = \frac{k_{b,MBB}}{\rho_{b,MBB}c_{MBB}} \tag{5.8}$$

5.2. Modeling Biomass Fuel Pre-combustion Processing

5.2.1. Drying Manure-based Biomass

Solid biomass fuels can be dried by several methods, utilizing different types of dryers. Choosing the best type of dryer largely depends on the characteristics of the biomass, the drying medium, and the available sources of heat (Brammer *et al*., 1999). For this study, the operation and economic costs of two types of dryers will be modeled:

1. Conveyor belt (or band) dryers and
2. Steam-tube rotary driers.

Both dryers are suitable for handling granular, free-flowing solids such as MBB. Both dryers are also common in other agricultural applications such as conveyor belt dryers used in food processing and steam-tube rotary dryers used to dry distiller's grains, distiller's solubles, corn germ, and corn fiber feed. Rotary dryers can also handle powdery solids (particles less than 140 microns or 100 mesh), such as the finer particles in the MBB. For operation on or near feeding operations, farmers may find that rotary dryers operate similarly to rotary composting drums.

Conveyor belt dryers are suitable for accepting wet, as-harvested MBB and continuously supplying dry biomass (10-20% moisture) to co-fire and reburn systems at large-scale combustion facilities. Moreover, conveyor belt dryers can be installed at either large CAFOs, at centralized drying and composting facilities, or directly at the power plant sites or combustion facilities. If the biomass is dried at the CAFO or at a composting facility, fossil fuels such as natural gas or propane may be required to provide heat for the drying process. Solar drying is also a possibility, but there may be difficulty supplying a consistent and large enough mass flow of MBB for power plants, especially for reburn systems that would require at least a 15% heat input from the biomass if pure biomass is used as the reburn fuel. However, if the dryer is installed at the combustion site, then perhaps waste heat from the combustion processes can be used to dry the biomass. But in this case, raw manure would have to be transported and possibly stored at or near the combustion facility causing aesthetic and possibly regulatory problems.

Steam-tube rotary dryers may be more suited for the smaller scale, on-the-farm combustion systems that will be discussed later in this section, since for many cases low-quality or saturated steam will be present. However, both types of dryers could probably be used for either large scale supply to coal plants or for usage at small scale facilities. The physical modeling of these drying systems will be the basis of estimating the economics of these dryers. For example, the capital cost of conveyor belt dryers is a function of the conveyor belt area and the capital cost of rotary dryers is a function of the moisture content of the exiting biomass and the total heat transferred to the solids during drying. Thus, the underlying objective will be to compute these specific parameters. The operation costs of the dryers are dependant on gas consumption, steam consumption, and electricity consumption.

The analysis can begin by determining how many dryers will be required. If the annual amount of manure required from the combustion facility, $\dot{M}_{MBB,annum}$ (kg/yr), the annual operation hours of the dryers, OH_{dryer} (hr/yr), and the moisture content of the as-harvested biomass, $\%M_{MBB,0}$, are known, then the mass flow rate of dry MBB solids going through the dryers can be computed in kg/s.

$$\dot{m}_{MBB,dry} = \frac{\dot{M}_{MBB,annum}}{OH_{dryer}}\left(1-\frac{\%M_{MBB,0}}{100}\right)*\left(\frac{1\,hr}{3600\,s}\right) \tag{5.9}$$

Here, the subscript *dry* will denote matter on a dry basis, meaning zero moisture percentage. MBB exiting a dryer will probably not be completely dry as there will be a minimum equilibrium moisture percentage of the biomass dependant on the local temperature and relative humidity. However, in order to determine the number of dryers, $\dot{m}_{MBB,dry}$ must be compared to the maximum rated flow of dry matter through the dryer, $\dot{m}_{MBB,dry,capacity}$.

$$N_{dryers} = \begin{cases} 1, & \text{if } \dot{m}_{MBB,dry} \le \dot{m}_{MBB,dry,capacity} \\ ceiling\left|\dfrac{\dot{m}_{MBB,dry}}{\dot{m}_{MBB,dry,capacity}}\right|, & \text{if } \dot{m}_{MBB,dry} > \dot{m}_{MBB,dry,capacity} \end{cases} \tag{5.10}$$

And if $\dot{m}_{MBB,dry} > \dot{m}_{MBB,dry,capacity}$, then it will be understood that in the following equations,

$$\dot{m}_{MBB,dry} = \frac{\dot{M}_{MBB,annum} / OH_{dryer}}{N_{dryers}} \left(1 - \frac{\%M_{MBB,0}}{100}\right) * \left(\frac{1\,hr}{3600\,s}\right) \tag{5.11}$$

for the mass flow in each dryer.

Moreover, the moisture content of the MBB or the air used to dry the biomass can be expressed on a wet basis, $mf_{H_2O,i}$ (kg H_2O / kg total mass), or on a dry basis, ω_i (kg H_2O / kg dry mass). The values $mf_{H_2O,i}$, ω_i, and the moisture percentage, $\%M_i$, are related to each other by the following expression.

$$mf_{H_2O,i} = \frac{\%M_i}{100} = 1 - \frac{1}{1+\omega_i} \tag{5.12}$$

5.2.1.1. Conveyor belt biomass dryers

A process flow diagram for conveyor belt dryers is illustrated in Figure 5.1. Ambient air enters the drying system enclosed by the control volume, CV_{dryer}, and mixes with recycled air from the drying chamber enclosed by $CV_{chamber}$. The air mixture flows through a heat exchanger, where it acquires heat from steam generated from a boiler. The air mixture then enters the drying chamber where it carries moisture away from the as-harvested MBB. Some of the air is recycled, while the rest exits the dryer system.

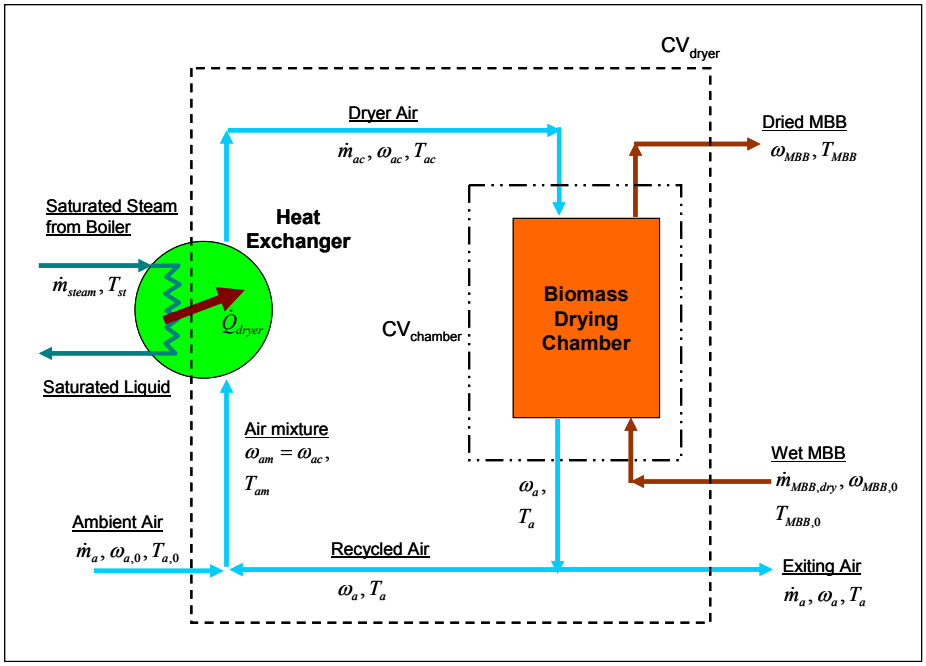

Figure 5.1 Mass and energy flow diagram for conveyor belt dryers (adapted from Kiranoudis *et al.*, 1994)

The total enthalpy of air as a function of temperature, T, and humidity ratio, ω, can be written as:

$$h_{air,i} = c_{p,air} T_i + \omega_i \left(h^0_{f,H_2O_{(g)}} + c_{p,H_2O_{(g)}} T_i \right) \tag{5.13}$$

where $c_{p,air}$ is the specific heat of dry air, $c_{p,H_2O_{(g)}}$ is the specific heat of water vapor in the air, and $h^0_{f,H_2O_{(g)}}$ is the enthalpy of formation of water vapor, which is approximately 2501.6 kJ/kg. The total enthalpy of the wet MBB can also be expressed as:

$$h_{MBB} = c_{MBB,dry} T_i + \omega_i c_{H_2O_{(l)}} T_i \tag{5.14}$$

Here, $c_{MBB,dry}$ is the specific heat of dry MBB, and $c_{H_2O_{(l)}}$ is the specific heat of liquid water, which is about 4.20 kJ/kg K. T_i is in degrees K. Note that relative humidity, ϕ, is usually known, and ω can be computed from ϕ and the temperature with the following expression:

$$\omega_{air,i} = 0.622 \frac{\phi_i P_g(T_i)}{P_{air} - \phi_i P_g(T_i)} \tag{5.15}$$

P_{air} is the air pressure (for this case approximately ambient pressure, 101,325 Pa), and P_g is the saturation pressure as a function of temperature. The Antoine Equation may be used to compute P_g from a known air temperature (Pakowski *et al*., 1991).

$$P_g = 133.322 * \exp\left[18.3036 - \frac{3816.44}{(T_i - 46.13)}\right] \tag{5.16}$$

where P_g is in Pascal (Pa) and T_i is in degrees K.

Now, a mass and energy balance can be conducted about CV_{dryer}. From the mass balance, the following expression can be found:

$$\dot{m}_a\left(\omega_a - \omega_{a,0}\right) = \dot{m}_{MBB,dry}\left(\omega_{MBB,0} - \omega_{MBB}\right) \tag{5.17}$$

And from the energy balance:

$$\dot{Q}_{dryer} = \dot{m}_a\left(h_a - h_{a,0}\right) + \dot{m}_{MBB,dry}\left(h_{MBB} - h_{MBB,0}\right) \tag{5.18}$$

A mass and energy balance can also be conducted about $CV_{chamber}$. The mass balance provides the following expression:

$$\dot{m}_{ac}\left(\omega_a - \omega_{ac}\right) = \dot{m}_{MBB,dry}\left(\omega_{MBB,0} - \omega_{MBB}\right) \tag{5.19}$$

And from the energy balance:

$$\dot{m}_{ac}\left(h_{ac} - h_a\right) = \dot{m}_{MBB,dry}\left(h_{MBB} - h_{MBB,0}\right) \tag{5.20}$$

From Figure 5.1, the following expression can also be generated from the mixing of ambient air and recycled air for the air mixture that will be sent to the drying chamber.

$$\dot{m}_{ac}h_{am} = \dot{m}_a h_{a,0} + \left(\dot{m}_{ac} - \dot{m}_a\right)h_a \tag{5.21}$$

For this analysis, the following are usually considered known parameters:

- the initial moisture content and the temperature of the MBB entering the dryer, $\omega_{MBB,0}$ and $T_{MBB,0}$,
- the desired moisture content of the MBB, ω_{MBB},
- the $\dot{m}_{MBB,dry}$ can be found from equation (5.11), and
- the properties of the ambient air entering the dryer, $\omega_{a,0}$ and $T_{a,0}$.

The following parameters are typically considered design variables for the dryer:

- the moisture content and temperature of the air exiting the dryer chamber, ω_a and T_a, and
- the air temperature drop over the drying chamber, $\Delta T_{chamber}$.

The dryer's temperature drop is defined as:

$$\Delta T_{chamber} = T_{ac} - T_a \tag{5.22}$$

Now, the following parameters must all be computed from equations (5.17) through (5.22): $\dot{m}_a$, T_{ac}, T_{MBB}, $\dot{Q}_{dryer}$, ω_{ac}, $\dot{m}_{ac}$, and T_{am}. The mass flow of air entering and exiting CV_{dryer}, $\dot{m}_a$, can be computed from equation (5.17). The temperature of the air exiting the heat exchanger and entering the drying chamber, T_{ac}, can be computed from the defined temperature drop in equation (5.22). The solution for T_{MBB} depends on how exactly the MBB is dried in the chamber. For example, if the conveyor belt dryer is a perpendicular flow dryer, as depicted in Figure 5.2, then T_{MBB} will be approximately equal to T_a. However, if the dryer is a parallel flow dryer as in Figure 5.3, then T_{MBB} is approximately equal to the wet bulb temperature, T_{wb}, which is a function of T_a and ω_a.

$$T_{MBB} \cong \begin{cases} T_a, & \text{if perpendicular flow dryer} \\ T_{wb}, & \text{if parallel flow dryer} \end{cases} \tag{5.23}$$

Please refer to Appendix B for an algorithm for computing T_{wb}. With temperatures $T_{a,0}$, T_a, $T_{MBB,0}$, and T_{MBB} either known or computed along with the moisture contents, ω, of both the MBB and air, the enthalpies can be computed at each point in Figure 5.1 with equations (5.13) and (5.14), and $\dot{Q}_{dryer}$ may be computed from equation (5.18).

Now, in order to find ω_{ac}, and $\dot{m}_{ac}$, the remaining equations (5.19) and (5.20) must be combined:

$$\frac{h_{ac} - h_a}{\omega_a - \omega_{ac}} = \frac{h_{MBB} - h_{MBB,0}}{\omega_{MBB,0} - \omega_{MBB}}$$

and arranged as:

$$h_{ac} + \frac{h_{MBB} - h_{MBB,0}}{\omega_{MBB,0} - \omega_{MBB}}\omega_{ac} = \frac{h_{MBB} - h_{MBB,0}}{\omega_{MBB,0} - \omega_{MBB}}\omega_a + h_a$$

From equation (5.13), the enthalpy of the air entering the dryer is $h_{ac} = c_{p,air}T_{ac} + \omega_{ac}\left(h^0_{f,H_2O_{(g)}} + c_{p,H_2O_{(g)}}T_{ac}\right)$. Plugging this equation into the expression above, and solving for ω_{ac}, an equation for ω_{ac} can be obtained:

$$\omega_{ac} = \frac{\left(\frac{h_{MBB} - h_{MBB,0}}{\omega_{MBB,0} - \omega_{MBB}}\right)\omega_a + h_a - c_{p,air}T_{ac}}{h^0_{f,H_2O_{(g)}} + c_{p,H_2O_{(g)}}T_{ac} + \left(\frac{h_{MBB} - h_{MBB,0}}{\omega_{MBB,0} - \omega_{MBB}}\right)} \tag{5.24}$$

With ω_{ac} computed, $\dot{m}_{ac}$ can be found with either equations (5.19) or (5.20). The enthalpy, and hence the temperature, of the air mixture, T_{am}, can be computed from equation (5.21).

Thus far, the analysis has produced solutions for drying parameters that are essential for computing operation costs of drying. For example, the value determined for $\dot{Q}_{dryer}$ can now be used to determine how much steam will be required for the heat exchanger. If the boiler is operated at a pressure, P_{boiler}, and produces saturated steam, then the steam temperature, T_{st} can be computed by rearranging the Antoine Equation:

$$T_{st} = \frac{3816.44}{18.3036 - \ln\left(P_{boiler}/133.322\right)} + 46.13 \tag{5.25}$$

The steam consumption is thus,

$$\dot{m}_{steam} = \frac{\dot{Q}_{dryer}}{\Delta h^{T_{st}}_{H_2O,fg}} \tag{5.26}$$

where $\Delta h^{T_{st}}_{H_2O,fg}$ is the latent heat of vaporization, which is a function of T_{st}. Pakowski *et al*. (1991) suggested the following polynomial equation to compute $\Delta h^{T_{st}}_{H_2O,fg}$:

$$\begin{aligned}\Delta h^{T_{st}}_{H_2O,fg} = {} & 2504.65 - 2.80701*\left(T_{st} - 273.15\right) + 1.21884e-2*\left(T_{st} - 273.15\right)^2 \\ & -1.25205e-4*\left(T_{st} - 273.15\right)^3 + 4.50499e-7*\left(T_{st} - 273.15\right)^4 \\ & -6.67186e-10*\left(T_{st} - 273.15\right)^5\end{aligned} \tag{5.27}$$

Here, $\Delta h_{H_2O,fg}^{T_{st}}$ is in kJ/kg and T_{st} is in K. The amount of fuel required, in kJ_{th}/s, to produce this steam can be computed as:

$$\dot{F}_{dryer\ fuel} = \frac{\dot{m}_{steam}\left(h_{steam}\left(T_{st}\right) - h_{fw}\left(T_{a,0}\right)\right)}{\eta_{boiler}} \tag{5.28}$$

Here, η_{boiler} is the boiler efficiency, h_{steam} is the enthalpy of the steam entering the heat exchanger, and h_{fw} is the enthalpy of the boiler feed water, which is usually a function of the ambient temperature. The capital cost of the dryer's boiler is usually a function of $\dot{m}_{steam}$.

The electrical energy consumed by the dryer's fans can be computed, in kW, with the following expression:

$$\dot{E}_{fans} = \frac{\Delta P_{chamber} * \dot{m}_{ac}}{\rho_{air}} * \left(\frac{1\ kN}{1{,}000\ N}\right) \tag{5.29}$$

where $\Delta P_{chamber}$ is the pressure drop in the drying chamber, in Pa, and ρ_{air} is the air density.

However, in order to determine the capital investment cost of a conveyor belt dryer, the conveyor belt area, A_{belt}, must be determined, and this analysis depends on whether the air flow is perpendicular to a screen mesh conveyor or if the air flow runs parallel to the conveyor belt. Expressions suitable to estimate the belt area for both of these cases will now be presented.

5.2.1.1.1 Perpendicular air flow dryer

A schematic of a parallel flow, conveyor belt dryer can be seen in Figure 5.2. Dryer air, which was heated by the steam, flows over a packed bed of MBB traveling along a conveyor of length, l, and a known width, w. The belt area, A_{belt} is simply $l*w$. There are two different ways to compute A_{belt} for perpendicular flow dryers: (1) a drying model based on an empirical drying constant, k_m, discussed by Kiranoudis *et al*. (1994)

and (2) a drying model based on a transfer number *B*, discussed by Incropera *et al*. (2002).

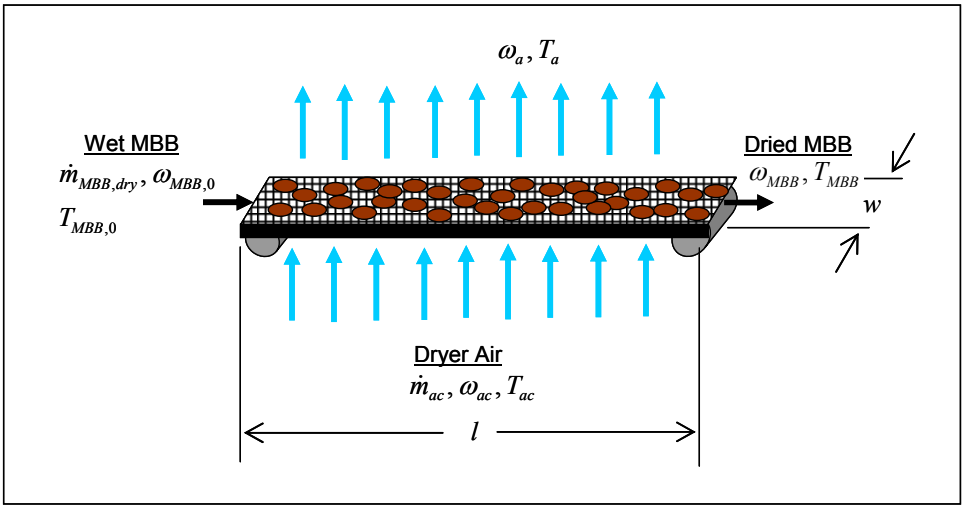

Figure 5.2 Perpendicular-flow conveyor belt dryer

Drying model with k_m:

The drying constant, k_m, is proportional to the time rate of moisture removal from the MBB, and can be defined as:

$$\frac{d\omega_{MBB}}{dt} = k_m\left(\omega_{MBB,E} - \omega_{MBB}\right) \tag{5.30}$$

Here, $\omega_{MBB,E}$ is the equilibrium moisture percentage of the MBB. This equation can be integrated:

$$\int_{\omega_{MBB,0}}^{\omega_{MBB}} \frac{d\omega'_{MBB}}{\left(\omega_{MBB,E} - \omega'_{MBB}\right)} = \int_0^t k_m dt'$$

The prime on the variables indicates a dummy variable for integration. Completing the integration with a substitution method, and solving for the final moisture percentage of the MBB, ω_{MBB}, the following expression may be obtained:

$$\omega_{MBB} = \omega_{MBB,E} + \left(\omega_{MBB,0} - \omega_{MBB,E}\right)\exp\left(-k_m t\right) \tag{5.31}$$

Here, t can be thought of as the MBB residence time in the dryer. The equilibrium moisture percentage, $\omega_{MBB,E}$, is the driest moisture percentage that can be obtained for the biomass, given the air temperature and humidity. Thus, $\omega_{MBB,E}$ is a function of T_a and the relative humidity, ϕ_a. The Guggenheim-Anderson-de Boer (GAB) Equation can be used to compute $\omega_{MBB,E}$:

$$\omega_{MBB,E} = \frac{CK\omega_m\phi_a}{\left[\left(1-K\phi_a\right)\left(1-K\phi_a+CK\phi_a\right)\right]} \tag{5.32}$$

where,

$$C = C_0 \exp\left(\frac{\Delta\bar{H}_C}{\bar{R}T_a}\right), \qquad K = K_0 \exp\left(\frac{\Delta\bar{H}_K}{\bar{R}T_a}\right)$$

$$\phi_a = \frac{\omega_a P_{air}}{\left(0.622+\omega_a\right)P_{g,air}\left(T_a\right)}$$

Here, ω_m, C_0, $\Delta\bar{H}_C$, K_0, and $\Delta\bar{H}_K$ are constants that can be found from drying experiments

The drying constant, k_m, can be expressed as an empirical constant as a function of a characteristic MBB particle size, d_c (such as the mass-mean diameter), the temperature of the exiting air, T_a, the humidity of the exiting air, ω_a, and the air velocity, U_∞.

$$k_m = k_0 d_c^{k_l} T_a^{k_T} \omega_a^{k_\omega} U_\infty^{k_U} \tag{5.33}$$

The constants k_0, k_l, k_T, k_ω and k_U are all empirical constants that can be found from experiments for different biomass solids such as MBB. The air velocity, U_∞, which is actually the upstream velocity that would exist if the packed MBB bed were not present, can be defined with the following expression:

$$U_\infty = \frac{\dot{m}_{ac}\left(1+\omega_{ac}\right)}{\rho_{air}A_{belt}} = \frac{\dot{m}_{ac}\left(1+\omega_{ac}\right)}{\rho_{air}lw} \tag{5.34}$$

One other important parameter is the biomass application load at the dryer's entrance, $\rho'_{MBB,0}$ (kg/m^2, on a wet basis). This application load is simply the product of

the MBB's as-received bulk density, $\rho_{b,MBB,0}$, and the application thickness, $a_{t,0}$ (in meters), of MBB on the conveyor belt at the entrance of the dryer.

$$\rho'_{MBB,0} \equiv \rho_{b,MBB,0} a_{t,0} = \frac{\dot{m}_{MBB,dry}\left(1+\omega_{MBB,0}\right)t}{A_{belt}} \tag{5.35}$$

The application thickness, and thus $\rho'_{MBB,0}$, can be considered a design value. However, equations (5.31), (5.33), (5.34), and (5.35) must be used to compute the following four unknowns in this analysis: U_∞, t, A_{belt}, and k_m. First, combine equations (5.31) and (5.33) to eliminate k_m and solve for U_∞:

$$U_\infty = \left[\frac{-\ln\left(\dfrac{\omega_{MBB} - \omega_{MBB,E}}{\omega_{MBB,0} - \omega_{MBB,E}} \right)}{t \cdot k_0 \cdot d_c^{k_l} \cdot \left(T_a - 273.15\right)^{k_T} \cdot \omega_a^{k_\omega}} \right]^{1/k_U} \tag{5.36}$$

Similarly, combine equations (5.34) and (5.35) to eliminate A_{belt} and solve for U_∞:

$$U_\infty = \frac{\dot{m}_{ac}\left(1+\omega_{ac}\right)}{\dot{m}_{MBB,dry}\left(1+\omega_{MBB,0}\right)} * \frac{\rho'_{MBB,0}}{\rho_{air}} * \frac{1}{t} \tag{5.37}$$

Now, equate (5.36) and (5.37) and solve for the MBB residence time, t:

$$t = \left[\frac{-\ln\left(\dfrac{\omega_{MBB} - \omega_{MBB,E}}{\omega_{MBB,0} - \omega_{MBB,E}} \right)}{k_0 \cdot d_c^{k_l} \cdot \left(T_a - 273.15\right)^{k_T} \cdot \omega_a^{k_\omega}} \right]^{1/(1-k_U)} * \left[\frac{\dot{m}_{MBB,dry}\left(1+\omega_{MBB,0}\right)\rho_{air}}{\dot{m}_{ac}\left(1+\omega_{ac}\right)\rho'_{MBB,0}} \right]^{k_U/(1-k_U)} \tag{5.38}$$

Once t is found, either equations (5.36) or (5.37) can be used to find U_∞, equation (5.33) can be used to find k_m, and finally A_{belt} can be computed from either equations (5.34) or (5.35).

This analysis can be very useful if the empirical constants in equations (5.32) and (5.33) are known for the product that is being dried, in this case MBB, and thus avoiding the use of thermo-physical properties and transport coefficients which may produce inaccurate results, especially in large scale industrial applications such as a MBB distribution system for large coal-fired power plants (Kiranoudis *et al*., 1994). However,

if these coefficients are not known, then a mass transfer model based on a transfer number, *B*, must be utilized instead.

Drying model with *B*:

An alternative model for drying biomass can be based on a presumption that the rate of evaporation is controlled by moisture transport through the boundary layer between the solid biomass particles and the dryer air. The transfer number, *B*, is the driving force for the transfer of moisture from the MBB to the dryer air. The transfer number, for this problem, can be defined as:

$$B = \frac{mf_{H_2O,\infty} - mf_{H_2O,s}}{mf_{H_2O,s} - 1} \tag{5.39}$$

Here, $mf_{H_2O,\infty}$ is the mass fraction of water in the dryer air and $mf_{H_2O,s}$ is the mass fraction of water at a point very near the biomass surface. For this problem, let the temperature of the dryer air $T_\infty = T_{ac}$, and let the $mf_{H_2O,\infty} = mf_{H_2O,ac}$, which can be computed from equation (5.12).

In order to compute $mf_{H_2O,s}$, it is necessary to know the temperature near the biomass surface, T_s. At steady state operation, it can be assumed that the process in the drying chamber is adiabatic, so that $T_s \approx T_{wb}$. The wet bulb temperature, T_{wb}, is a function of T_∞ and ω_∞. The saturated humidity ratio very near the MBB surface can then be computed as:

$$\omega_s = 0.622 \frac{P_g\left(T_{wb}\right)}{P_{air} - P_g\left(T_{wb}\right)}$$

Finally, $mf_{H_2O,s}$ can then be computed from equation (5.12).

The moisture removal rate from the MBB to the dryer air can be computed, for this case, with the following expression:

$$\dot{m}_w = \dot{m}_{ac}\left(\omega_a - \omega_{ac}\right) \tag{5.40}$$

The transfer number, *B*, is proportional to this moisture removal rate with a mass transfer conductance coefficient, *g*.

$$\frac{\dot{m}_w}{A_{MBB} \cdot l \cdot w \cdot \left(a_{t,0} + a_{belt}\right)} = gB = \left(\frac{g}{g*}\right) g*B \tag{5.41}$$

B is dimensionless and g has dimensions of kg/m^2 s. g* is the mass transfer conductance coefficient for a very small mass transfer rate. The ratio of g and g* is a strong function of B, and for turbulent flows with constant free-stream velocities and high mass-transfer rates, the ratio of g and g* can be approximated by the following expression (Annamalai *et al.*, 2006):

$$\frac{g}{g*} = \frac{\ln\left(1+B\right)}{B} \tag{5.42}$$

A_{MBB} is the wetted surface area of the biomass particles per unit volume of the packed bed of MBB on top of the conveyor belt, and has units of m^2 / m^3. Multiplying A_{MBB} with the length (l), width (w), and height of the biomass bed will produce the approximate surface area of the particles exposed to the dryer air. The height of the bed will be the sum of the application thickness, $a_{t,0}$, and the conveyor belt or screen thickness, a_{belt}. A_{MBB} can be computed with the following expression:

$$A_{MBB}\left[\frac{m^2}{m^3}\right] = \frac{6\left(1-\varepsilon\right)}{\psi \cdot d_c} \tag{5.43}$$

where, ε is the porosity of the MBB, which is defined as the void volume of the packed bed of biomass divided by the total volume of the bed. The parameter, ψ, is the sphericity factor, which is a correction for non-spherical particles. Bituminous coal has a sphericity factor between 1.05 and 1.11 and sand has a sphericity of 1.57 (Hinds, 1999).

The only parameter, aside from l, that is not known in equation (5.41) is g*. The purpose of this analysis is to find l and thus the conveyor belt area (l * w). However, first g* can be expressed in terms of the mass-transfer Stanton number (St_m). The St_m is a modification of a dimensionless concentration gradient at the surface of the MBB (or whatever product is being dried) called the Sherwood number (Sh). With this modification, inertial forces can be related to mass transfer resistance; in this case, the

resistances of moisture transfer from the MBB to the dryer air. The St_m can be defined as the following:

$$St_m = \frac{g^*}{\rho_{air} U_\infty} \tag{5.44}$$

However, for this case, in order for the St_m to be useful it must be particularly applied to the flow of air through a packed bed of particles, as in the MBB dryer. In order to do this, the Colburn j factor for mass transfer must be introduced.

$$\bar{j}_m = St_m Sc^{2/3} \tag{5.45}$$

where Sc is the ratio of momentum forces to mass diffusivities. For air at nominal temperatures, Sc is approximately 0.6. This Colburn j factor is a dimensionless mass transfer coefficient, which becomes useful for this case since it can be applied to flow over packed beds with the following equation given by Incropera *et al*. (2002).

$$\varepsilon \cdot \bar{j}_m = 2.06\, Re_{d_c}^{-0.575} \tag{5.46}$$

This expression is valid for Re_{d_c} between 90 and 4000. The Reynolds number (Re) is the ratio of inertial forces to viscous forces and for this case, the characteristic length is d_c. The Re for this problem can be expressed as the following:

$$Re_{d_c} = \frac{\rho_{air} U_\infty d_c}{\mu_{air}} = \frac{d_c}{\mu_{air}} \left[\frac{\dot{m}_{ac} (1 + \omega_{ac})}{l \cdot w} \right] \tag{5.47}$$

Since U_∞ is not yet known, it can be eliminated by inserting the definition of U_∞ from equation (5.34).

Now, combining equations (5.44), (5.45), and (5.46), an expression for the unknown g^* can be obtained:

$$g^* = 2.06 \left(\frac{\rho_{air} U_\infty}{\varepsilon} \right) Sc^{-2/3}\, Re_{d_c}^{-0.575} \tag{5.48}$$

Next, if this expression for g* is inserted into equation (5.41), along with equation (5.42) for the ratio of g over g^*, the following equation will be obtained:

$$\frac{\dot{m}_w}{A_{MBB} \cdot l \cdot w \cdot \left(a_{t,0} + a_{belt} \right)} = 2.06 \left(\frac{\rho_{air} U_\infty}{\varepsilon} \right) Sc^{-2/3}\, Re_{d_c}^{-0.575} * \ln(1 + B)$$

Then, the definitions of the Re and the U_∞, equations (5.47) and (5.34) respectively, can be plugged along with equation (5.40) for $\dot{m}_w$ to provide:

$$\frac{\dot{m}_{ac}\left(\omega_a-\omega_{ac}\right)}{A_{MBB}\cdot l\cdot w\cdot\left(a_{t,0}+a_{belt}\right)}=2.06\left(\frac{1}{\varepsilon}\right)\left[\frac{\dot{m}_{ac}\left(1+\omega_{ac}\right)}{l\cdot w}\right]\mathrm{Sc}^{-2/3}\left(\frac{d_c}{\mu_{air}}\right)^{-0.575}$$
$$*\left[\frac{\dot{m}_{ac}\left(1+\omega_{ac}\right)}{l\cdot w}\right]^{-0.575}\ln\left(1+B\right)$$

Finally, solving for *l*, gives an explicit formula for computing the length of the biomass dryer.

$$l=0.2845*\left[\frac{\dot{m}_{ac}d_c}{\mu_{air}w}\right]*\left[\frac{\left(\omega_a-\omega_{ac}\right)\cdot\varepsilon\cdot\mathrm{Sc}^{2/3}}{A_{MBB}\left(a_{t,0}+a_{belt}\right)\ln\left(1+B\right)}\right]^{40/23}*\left[\frac{1}{\left(1+\omega_{ac}\right)}\right]^{17/23}$$

Multiplying through by the width of the conveyor belt, *w*, will give an expression for the area, A_{belt}:

$$\begin{aligned}A_{belt}&=l\cdot w\\&=0.2845*\left[\frac{\dot{m}_{ac}d_c}{\mu_{air}}\right]*\left[\frac{\left(\omega_a-\omega_{ac}\right)\cdot\varepsilon\cdot\mathrm{Sc}^{2/3}}{A_{MBB}\left(a_{t,0}+a_{belt}\right)\ln\left(1+B\right)}\right]^{40/23}*\left[\frac{1}{\left(1+\omega_{ac}\right)}\right]^{17/23}\end{aligned}\quad(5.49)$$

Once A_{belt} is computed, the velocity, U_∞, and the residence time, *t*, may be found with the definitions for velocity, equation (5.34), and manure application load, $\rho'_{MBB,0}$ equation (5.35).

The pressure drop, for perpendicular flow dryers, may be estimated by the Carmen-Kozeny Equation for fluid flow through packed beds (Ergun, 1952 and Ramadan *et al*., 2007):

$$\Delta P_{chamber}=\frac{f'\rho_{air}\left(a_{t,0}+a_{belt}\right)\left(1-\varepsilon\right)U_\infty^2}{\varepsilon^3\cdot d_c}\quad(5.50)$$

where the friction factor, f', for packed beds has been found to be:

$$f'=150\left(\frac{1-\varepsilon}{\mathrm{Re}_{d_c}}\right)+1.75\quad(5.51)$$

Here, the Reynolds number is based on d_c, just as in equation (5.47).

5.2.1.1.2 Parallel air flow dryer

A schematic of MBB entering and exiting a parallel flow conveyor belt drying chamber is illustrated in Figure 5.3. The analysis for finding A_{belt} for this case is similar to that of perpendicular flow dryers, except that the solution for g^* differs.

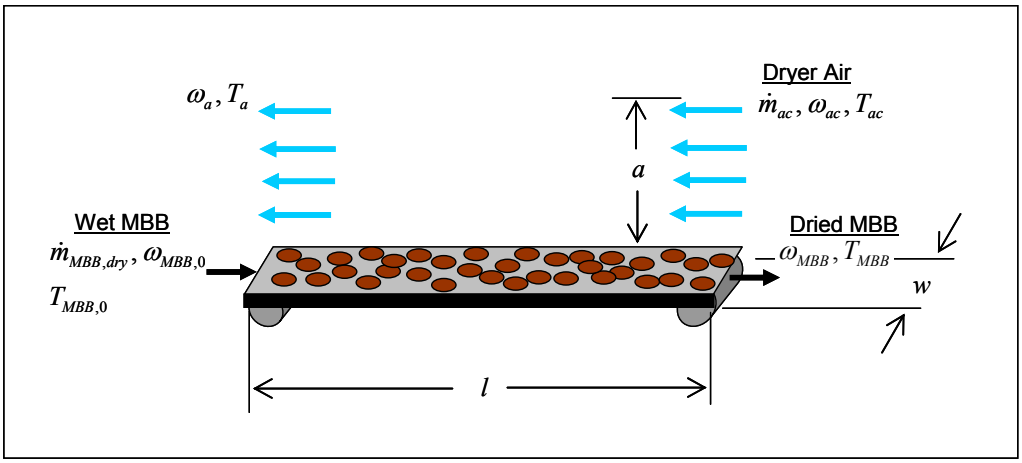

Figure 5.3 Parallel flow conveyor belt dryer

The rate of moisture removal, $\dot{m}_w$, remains the same as equation (5.40), as does the definition of B in equation (5.39) and the value of the ratio (g / g^*) in equation (5.42); however, equation (5.41) now becomes the following

$$\frac{\dot{m}_w}{lw} = gB = \left(\frac{g}{g^*}\right) g^* B \tag{5.52}$$

This problem can be estimated as drying over a flat plate, described in Kays *et al.* (2005) for laminar flow. The definition of the Sherwood number with respect to the length of the dryer's conveyor belt can be expressed as the following:

$$\mathrm{Sh}_l = \frac{g^* \cdot l}{\rho_{air} \mathcal{D}_{H_2O,air}} \tag{5.53}$$

where $\mathcal{D}_{H_2O,air}$ is the binary mass diffusion coefficient for water vapor in air. At standard pressure and temperature, $\mathcal{D}_{H_2O,air}$ is approximately 0.26 x 10^{-4} m^2/s. However, since the

flow in the dryer will probably be turbulent, an expression relating Sh_l to Re_l and Sc for turbulent flow over a flat plate can be taken from Incropera *et al*. (2002).

$$\mathrm{Sh}_l = 0.037 \cdot \mathrm{Sc}^{1/3}\, \mathrm{Re}_l^{4/5} \tag{5.54}$$

The Reynolds number for this problem, Re_l, can be defined as the following:

$$\mathrm{Re}_l = \frac{\rho_{air} l \left(U_\infty - U_{MBB}\right)}{\mu_{air}} \tag{5.55}$$

where U_∞ is now:

$$U_\infty = \frac{\dot{m}_{ac}\left(1+\omega_{ac}\right)}{\rho_{air} \cdot w \cdot a} \tag{5.56}$$

and the effective linear velocity of the MBB through the dryer is:

$$U_{MBB} = \frac{\dot{m}_{MBB,dry}\left(1+\omega_{MBB,0}\right)}{\rho_{b,MBB,0} \cdot w \cdot a_{t,0}} \tag{5.57}$$

These two velocities are added together in equation (5.55) if the flow of the dryer air is opposite, or counter-flow, to the travel direction of the conveyor belt. If the air flow is flowing in the same direction as the travel of the conveyor belt, then U_{MBB} is subtracted from U_∞. Also note that a is the height of the drying chamber as shown in Figure 5.3.

Now, equating expressions (5.53) and (5.54) and solving for g*:

$$g^* = 0.037\left(\frac{\rho_{air}\mathcal{D}_{H_2O,air}}{l}\right)\mathrm{Sc}^{1/3}\, \mathrm{Re}_l^{4/5} \tag{5.58}$$

Next, equations (5.42) and (5.58) can be inserted into equation (5.52) to obtain the following:

$$\dot{m}_w = 0.037 \ln\left(1+B\right) w \rho_{air} \mathcal{D}_{H_2O,air} \mathrm{Sc}^{1/3}\, \mathrm{Re}_l^{4/5} \tag{5.59}$$

Finally, inserting equations (5.55), (5.56), (5.57) and (5.40) into equation (5.59) and solving for the conveyor belt length, l:

$$l = 61.62\left[\frac{\dot{m}_{ac}\left(\omega_a - \omega_{ac}\right)}{\rho_{air}\mathcal{D}_{H_2O,air}\ln\left(1+B\right)}\right]^{5/4} * \frac{\mu_{air}}{\mathrm{Sc}^{5/12}w^{1/4}\left(\frac{\dot{m}_{ac}\left(1+\omega_{ac}\right)}{a} - \frac{\rho_{air}}{\rho_{b,MBB,0}}\frac{\dot{m}_{MBB,dry}\left(1+\omega_{MBB,0}\right)}{a_{t,0}}\right)}$$

Multiplying through by w, will give A_{belt}:

$$\begin{aligned} A_{belt} &= l \cdot w \\ &= 61.62\left[\frac{\dot{m}_{ac}\left(\omega_a - \omega_{ac}\right)}{\rho_{air}\mathcal{D}_{H_2O,air}\ln\left(1+B\right)}\right]^{5/4} * \frac{\mu_{air}\cdot w^{3/4}}{\mathrm{Sc}^{5/12}\left(\frac{\dot{m}_{ac}\left(1+\omega_{ac}\right)}{a} - \frac{\rho_{air}}{\rho_{b,MBB,0}}\frac{\dot{m}_{MBB,dry}\left(1+\omega_{MBB,0}\right)}{a_{t,0}}\right)} \end{aligned} \quad (5.60)$$

This equation is applicable for $\mathrm{Re}_l >> 5\times10^5$. Unlike the previous problem for perpendicular flow dryers, U_∞ does not depend on A_{belt} or l, and can be computed simply with equation (5.56). The MBB residence time in the dryer for this case is simply:

$$t = \frac{l}{U_{MBB}} = \frac{\rho_{b,MBB,0}\cdot w\cdot a_{t,0}\cdot l}{\dot{m}_{MBB,dry}\left(1+\omega_{MBB,0}\right)} \quad (5.61)$$

5.2.1.2. Steam-tube rotary biomass dryers

Another type of dryer that may be utilized to dry MBB for combustion processes is a steam-tube rotary biomass dryer. These dryers may be particularly useful when a supply of steam happens to be available, as will be the case for some of the small-scale, on-the-farm systems that will be discussed later. An illustration of a rotary steam-tube, indirect dryer is shown in Figure 5.4. The numbering system for the points in this diagram follows the numbering system for small scale combustion systems that will be discussed later. At point 2, wet as-harvested biomass enters the dryer and tumbles down an incline at angle, α, as the drum rotates with an angular velocity, N_{drum}. The inner diameter of the drum is D, while the total length of the dryer will once again be denoted

as *l*. At point 3, dry biomass exits the dryer. Pressurized saturated steam is supplied at point 9d where it resides in both an outer steam jacket and inner steam tubes of smaller diameter. This water exits the dryer at point 10 as saturated liquid, having never come into direct contact with the biomass. The drying chamber is kept open to the atmosphere so that at steady state operation vapor generated from the evaporated moisture from the biomass entrains the chamber, along with a small amount of air, and exits the dryer at point 11.

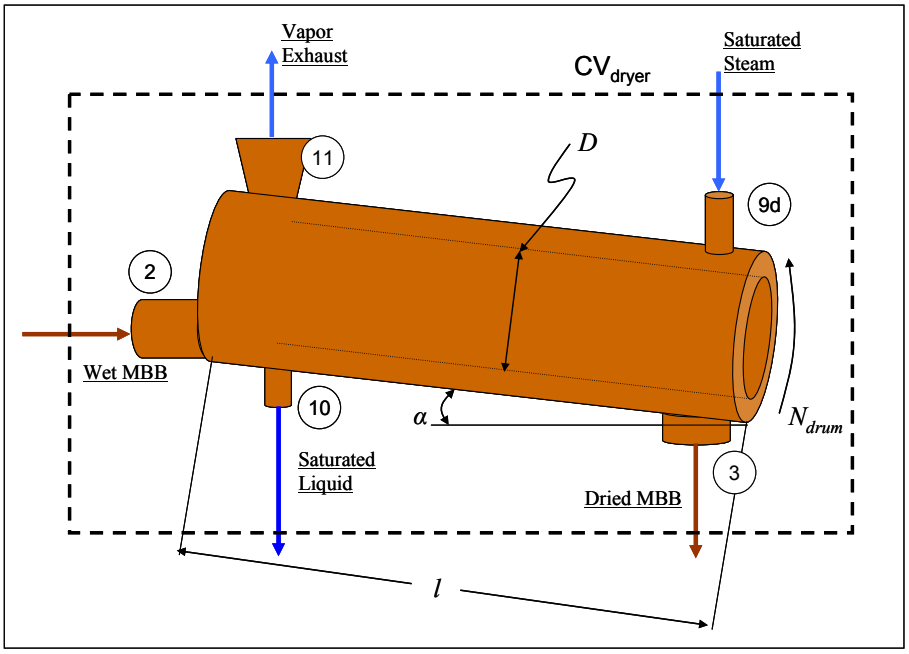

Figure 5.4 Indirect rotary steam-tube dryer for biomass

A cross-sectional view of the rotary dryer can be seen in Figure 5.5. The smaller steam tubes within the drying chamber have diameters, d_{tubes}, and the total number of these tubes in the dryer is n_{tubes}. As the drum rotates, fins scoop up the biomass particles and drop them at the top of the dryer's diameter. The biomass particles fall through the entrained vapor, where it is presumed that much of the drying occurs through forced convection as the particles free-fall back to the bottom of the drum.

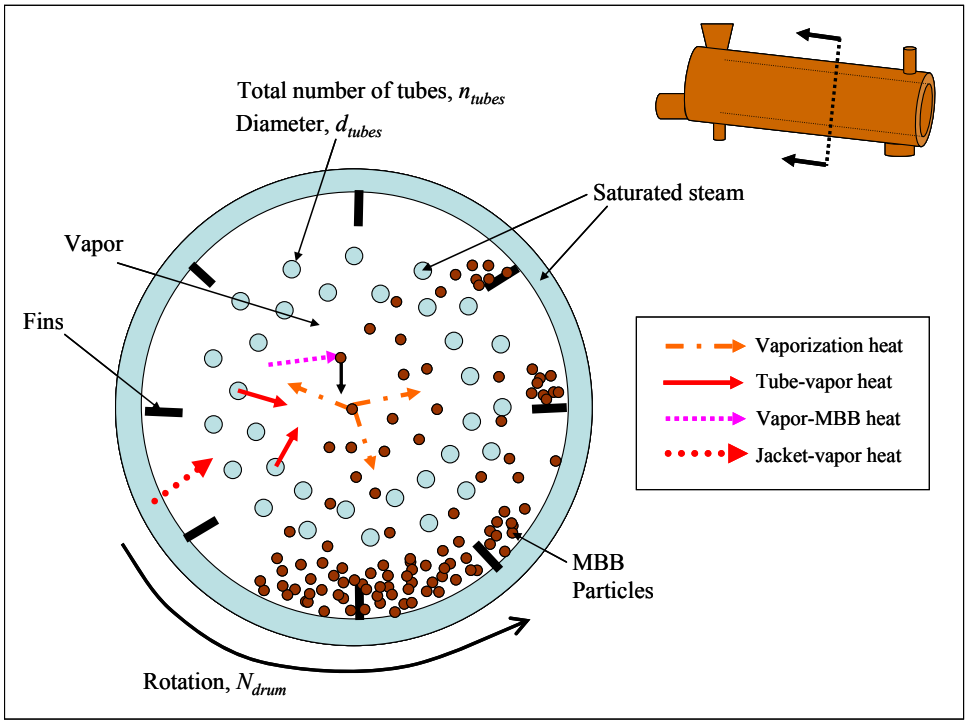

Figure 5.5 Cross-sectional view of rotary steam-tube dryer (adapted from Canales *et al.*, 2001)

There are four basic modes of heat transfer occurring during the steady state operation of these types of dryers that are considered to be the most significant:

1. Latent heat of vaporization from the biomass particles to the entrained vapor,
2. Sensible heat from the small steam tubes to the vapor,
3. Sensible heat from the vapor to the biomass particles, and
4. Sensible heat from the steam jacket to the vapor.

The processes for this dryer are divided into two sections: a heating zone in which the biomass solids are heated up to a drying temperature and a drying zone in which moisture is removed from the biomass particles. The axial direction down the length of the dryer will be denoted as the z direction. As can be seen in Figure 5.6, the temperature of the biomass, $T_{MBB,0}$, increases to $T_{MBB} = T_3$ in the heating zone at a point z'. From z' to the end of the dryer's length, l, the temperature of the MBB remains constant at T_{MBB}. In the heating zone, the moisture content of the MBB, remains constant at $\omega_{MBB,2}$, but drops down to $\omega_{MBB,3}$ in the drying zone. The temperature of the steam remains constant, T_{steam}, throughout the length of the dryer since it enters as

saturated steam and exits as saturated liquid at the same pressure. Moreover, since the pressure of the vapor generated from the moisture removal of the MBB particles is assumed to be at uniform ambient pressure throughout the drying chamber, the vapor temperature, T_{vapor}, is also considered constant throughout the length of the dryer at steady state operation.

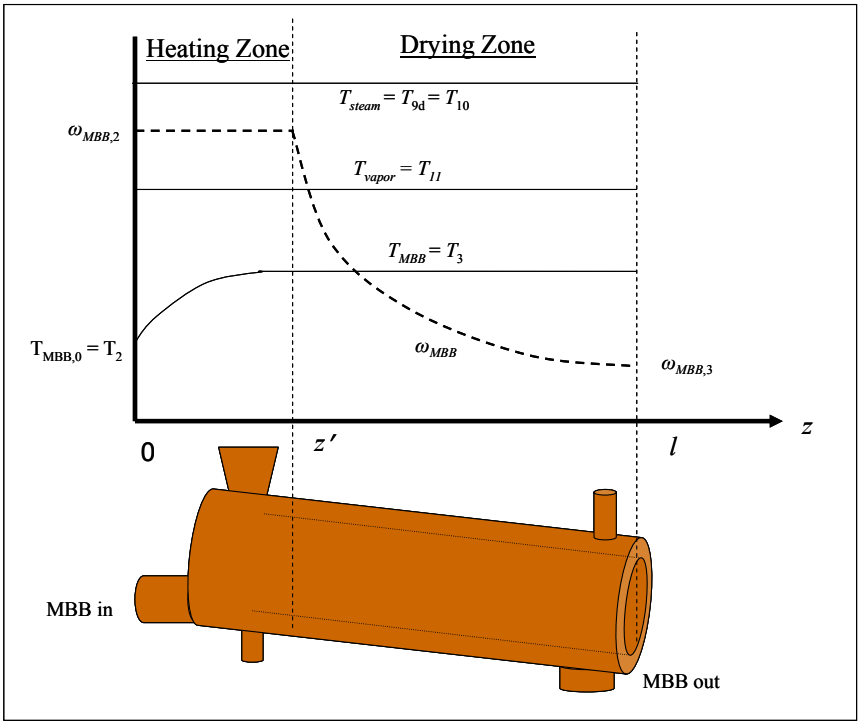

Figure 5.6 Heating and drying zones and assumed temperature and moisture content profiles for rotary steam-tube dryer (adapted from Canales *et al*., 2001)

This type of dryer has been modeled by Canales *et al*. (2001) for modeling fish meal drying and more information about these types of dryers can be found in this reference. The modeling equations and assumptions for the model are presented by Canales *et al*., but a solution for the purposes of this modeling study will be presented here. During Canales *et al*.'s study, the objective was largely to compute the final moisture content of the dried product (in their case, fish meal). However, for the current application, the final MBB moisture percentage, $\omega_{MBB,3}$, is known, and the primary

purpose will be to compute the vapor temperature, T_{vapor}, and ultimately the required steam flow rate, $\dot{m}_{steam,9d}$.

The analysis can begin by considering the Drying Zone, that is, the second part of the dryer from point z' in Figure 5.6 to point l. The moisture loss of the MBB particles can be written as:

$$\frac{d\omega_{MBB}}{dz} = \frac{R}{U_{MBB}} \tag{5.62}$$

where U_{MBB} is the effective linear velocity of the MBB down the z-axis of the dryer, while R is the rate of drying (kg water / kg MBB s). For this case, R can be computed as:

$$R = -\frac{h_{MBB-v} A_{MBB}}{\rho_{vapor} \Delta h_{H_2O,fg}^{T_{MBB}}} \left(T_{vapor} - T_{MBB} \right) \tag{5.63}$$

Here, h_{MBB-v} is the convective heat transfer coefficient between the MBB particles and the entrained vapor in the dryer chamber, A_{MBB} is the wetted area of the MBB particles exposed to the vapor. The parameter is similar to equation (5.43); however, instead of a fixed bed, the solid biomass is a percentage of the total volume of the dryer. This percentage of volume is usually referred to as the "holdup" of the dryer, χ. Equation (5.43) may be modified for the case of rotary dryers.

$$A_{MBB} = \frac{6 * \chi}{\psi d_c} \tag{5.64}$$

where χ here is inputted as a fraction. ρ_{vapor} is the density of the vapor, and $\Delta h_{H_2O,fg}$ is the enthalpy of vaporization of water and is a function of T_{MBB}. Integrating equation (5.62) for the entire length of the Drying Zone, from z' to l:

$$\int_{\omega_{MBB,2}}^{\omega_{MBB,3}} d\omega_{MBB} = \frac{R}{U_{MBB}} \int_{z'}^{l} dz$$

and inserting equation (5.63) for R, the following expression can be obtained:

$$\omega_{MBB,3} - \omega_{MBB,2} = -\frac{h_{MBB-v} A_{MBB}}{\rho_{vapor} \Delta h_{H_2O,fg}^{T_{MBB}} U_{MBB}} \left(T_{vapor} - T_{MBB} \right) \left(l - z' \right) \tag{5.65}$$

Next, an energy balance of the heat transfer in and out of the entrained vapor in the drying chamber's Drying Zone can be conducted. This can be best visualized in Figure 5.5 for the different heat transfer rates to and from the vapor.

$$\begin{bmatrix}\text{heat transfer from}\\ \text{vapor to MBB}\end{bmatrix}=\begin{bmatrix}\text{heat transfer from}\\ \text{tubes to vapor}\end{bmatrix}+\begin{bmatrix}\text{heat transfer from}\\ \text{jacket to vapor}\end{bmatrix}+\begin{bmatrix}\text{latent heat transfer from}\\ \text{moisture vaporization}\end{bmatrix}$$

$$h_{MBB-v}A_{MBB}\forall_{dryer}\left(T_{vapor}-T_{MBB}\right)=\left(h_{t-v}A_{tubes}+h_{j-v}A_{jacket}\right)\left(T_{steam}-T_{vapor}\right)+\dot{m}_{MBB,dry}\Delta h_{H_2O,fg}^{T_{MBB}}\left(\omega_{MBB,2}-\omega_{MBB,3}\right) \tag{5.66}$$

Here, h_{t-v} and h_{j-v} are the convective heat transfer coefficients for the steam tubes and the steam jacket, respectively, to the vapor. A_{tubes} and A_{jacket} are the surface areas of the tubes and the jacket, respectively, in the Drying Zone. $\forall_{dryer}$ is the volume of the Drying Zone.

$$A_{tubes}=n_{tubes}\pi d_{tubes}\left(l-z'\right) \tag{5.67}$$

$$A_{jacket}=\pi D\left(l-z'\right) \tag{5.68}$$

$$\forall_{dryer}=\frac{\pi D^2}{4}\left(l-z'\right) \tag{5.69}$$

The diameter, D, of the dryer, the ratio, $(l - z') / D$, and the rotation speed of the drum, N_{drum}, will be considered design parameters. Equations (5.65) and (5.66) will be used to solve for T_{vapor} and U_{MBB}. However, first T_{MBB} must be computed and expressions for each of the heat transfer coefficients must be found.

Since the drying occurring in the rotary steam-tube dryer is not adiabatic, the assumption that the MBB particles will be near the wet bulb temperature will not be valid, but the temperature of the MBB particles during drying still corresponds to the saturation temperature of water vaporizing at its partial pressure. Since the dryer chamber is uniformly at atmospheric pressure with a small fraction of air, the saturation pressure is:

$$P_{sat}\left(T_{MBB}\right)=P_{atm}Y_{steam,vapor} \tag{5.70}$$

where $Y_{steam,vapor}$ is the molar fraction of steam in the entrained vapor (mole steam / mole vapor). Basically, this molar fraction must be considered another design parameter for the dryer. Canales *et al*. (2001) set $Y_{steam,vapor}$ to 0.95 as the base case in their study.

Now, the convective heat transfer coefficients must be determined, beginning with h_{MBB-v}. After the MBB particles are carried up to the top of the drum, they fall through the vapor. As this happens, most of the vaporization occurs. If it is assumed that the particles reach a terminal velocity as they fall, then a Reynolds number can be determined, then a Nusselt number (Nu) can be computed, and finally h_{MBB-v} may be found. The terminal velocity of a particle in free fall depends on its drag coefficient, C_D; however, in order to compute C_D, the velocity must be known, hence this is usually an iterative problem. However, Hinds (1999) provides an empirical equation that can be used to compute a particle's terminal velocity, $V_{MBB,t}$, directly:

$$V_{MBB,t} = \left(\frac{\mu_{vapor}}{\rho_{vapor} d_c} \right) \exp\left(-3.070 + 0.9935J - 0.0178J^2 \right) \tag{5.71}$$

where J is:

$$J = \ln\left[C_D \left(\mathrm{Re}_{MBB-v} \right)^2 \right] = \ln\left(\frac{4\rho_{p,MBB}\rho_{vapor} d_c^3 g_c}{3\mu_{vapor}^2} \right)$$

Again, d_c is a characteristic MBB particle size and $\rho_{p,MBB}$ is the dry density of a MBB particle. Also, g_c is the gravitational acceleration, 9.81 m/s^2. The Reynolds number for this case is:

$$\mathrm{Re}_{MBB-v} = \frac{\rho_{vapor} V_{MBB,t} d_c}{\mu_{vapor}} \tag{5.72}$$

Once $V_{MBB,t}$ is computed with equation (5.71), $\mathrm{Re}_{MBB\text{-}v}$ can be computed. If $\mathrm{Re}_{MBB\text{-}v} > 1$, then the value for $V_{MBB,t}$ is accurate. However, if $\mathrm{Re}_{MBB\text{-}v}$ is found to be < 1 and if $d_c > 1$ μm, then Stokes law should be used instead of equation (5.71) to find $V_{MBB,t}$:

$$V_{MBB,t} = \frac{\rho_{p,MBB} d_c^2 g_c}{18\mu_{vapor}}$$

The Prandtl number, which is the ratio of momentum forces and thermal diffusivities, can be computed for the entrained vapor as:

$$\mathrm{Pr}_{vapor} = \frac{c_{p,vapor}\mu_{vapor}}{k_{vapor}} \tag{5.73}$$

Here, k_{vapor} is the thermal conductivity of the entrained vapor in the drying chamber.

Now, the Nu can be expressed as a function of $\mathrm{Re}_{MBB\text{-}v}$ and Pr_{vapor}. According to Canales *et al*. (2001) and Incropera *et al*. (2002), the following relation may be used for this case:

$$\mathrm{Nu}_{MBB-v} = 2 + \left(0.4\,\mathrm{Re}_{MBB,v}^{1/2} + 0.06\,\mathrm{Re}_{MBB,v}^{2/3}\right)\mathrm{Pr}_{vapor}^{0.4} \tag{5.74}$$

Finally, from the definition of the Nu, h_{MBB-v} can be computed:

$$h_{MBB-v} = \mathrm{Nu}_{MBB-v}\left(\frac{k_{vapor}}{d_c}\right) \tag{5.75}$$

Next, h_{t-v} must be determined. Although Canales *et al*. (2001) does not go into detail on how to find this heat transfer coefficient, a comparable relation can be found in Incropera *et al*. (2002). The steam tubes, as seen in Figure 5.5, are in a staggered arrangement around the drying chamber. As the drum rotates, these tubes move through the entrained vapor.

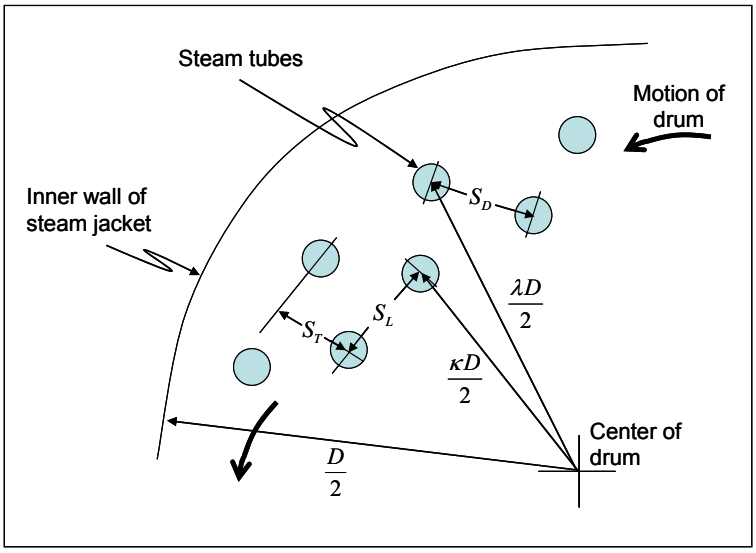

Figure 5.7 Arrangement of steam tubes in rotary dryer

The arrangement of these steam tubes is illustrated in Figure 5.7. The velocity of the steam tubes on the inner ring will be:

$$V_{inner,tube} = N_{drum}\frac{\kappa D}{2} \tag{5.76}$$

where N_{drum} is in radians/s. κ is a fraction of the drum's radius (D/2) where the inner ring of tubes is located, for example ½ or ¾. The distance between the tubes on the inner ring can be computed with the following expression, assuming that the tubes are evenly spaced:

$$S_L = \frac{\pi \cdot \kappa \cdot D}{\left(n_{tubes}/2\right)} \tag{5.77}$$

Notice that n_{tubes} must be an even number of tubes and that $(n_{tubes}/2)*d_{tubes} < \pi\kappa D$. Next, the distance, S_T may be computed with the following:

$$S_T = \left(\lambda - \kappa\right)\frac{D}{2} \tag{5.78}$$

and the diagonal distance, S_D, can be found to be:

$$S_D = \left[S_L^2 + \left(\frac{S_T}{2}\right)^2\right]^{1/2} \tag{5.79}$$

The Reynolds number for this problem is based on the maximum velocity, $V_{max,tube}$, of the fluid flow through the staggered tube arrangement, which can be computed as:

$$V_{\max,tube} = \begin{cases} \dfrac{S_T}{2\left(S_D - d_{tube}\right)} V_{inner,tube}, & if \quad S_D < \dfrac{S_T + d_{tube}}{2} \\ \dfrac{S_T}{\left(S_T - d_{tube}\right)} V_{inner,tube}, & if \quad S_D \geq \dfrac{S_T + d_{tube}}{2} \end{cases} \tag{5.80}$$

Now, the Reynolds number for this problem, Re_{tubes}, can be computed as:

$$\mathrm{Re}_{tubes} = \frac{\rho_{vapor} V_{\max,tube} d_{tube}}{\mu_{vapor}} \tag{5.81}$$

Again, the Nusselt number will be a function of Re and Pr; however, in addition to Pr_{vapor}, the Prandtl number evaluated at the temperature of the steam tubes, T_{steam}, will be required.

$$\mathrm{Pr}_{tube}\left(T_{steam}\right) = \frac{c_{p,vapor}\left(T_{steam}\right)\mu_{vapor}\left(T_{steam}\right)}{k_{vapor}\left(T_{steam}\right)} \tag{5.82}$$

Next, the Nusselt number can be expressed in the following form (Incropera *et al*., 2002):

$$\mathrm{Nu}_{t-v} = C\,\mathrm{Re}_{tubes}^{m}\,\mathrm{Pr}_{vapor}^{0.36}\left(\frac{\mathrm{Pr}_{vapor}}{\mathrm{Pr}_{tube}}\right)^{1/4} \tag{5.83}$$

where C and m are empirical constants, which can be found in Table 5.1.

Table 5.1 Constants for Nusselt number computed in equation (5.83)

Re_{tubes}	C	m
$10 - 10^2$	0.90	0.40
$10^2 - 10^3$	0.51	0.50
$10^3 - 2 \times 10^5$	$0.35*(S_T/S_L)^{1/5}$	0.60
$2 \times 10^5 - 2 \times 10^6$	0.022	0.84

Finally, $h_{t\text{-}v}$ can be found from the Nusselt number definition:

$$h_{t-v} = \frac{\mathrm{Nu}_{t-v} k_{vapor}}{d_{tube}} \tag{5.84}$$

The last convective heat transfer coefficient that must be computed is for the heat transferred from the steam jacket to the entrained vapor, $h_{j\text{-}v}$. This heat transfer problem can be estimated to be simply fluid flow through a circular pipe. The first step is to determine an effective velocity for the entrained vapor, U_{vapor}. This velocity can be related to the mass flow rate of moisture evaporation from the MBB particles.

$$U_{vapor} = \dot{m}_{MBB,dry} \frac{\left(\omega_{MBB,2} - \omega_{MBB,3}\right)}{\rho_{vapor}\left(\pi D^2/4\right)} \tag{5.85}$$

The Reynolds number for this case is simply:

$$\mathrm{Re}_D = \frac{\rho_{vapor} U_{vapor} D}{\mu_{vapor}} \tag{5.86}$$

and the Nusselt number can be computed as a function of Re and Pr (Incropera *et al*., 2002), and $h_{j\text{-}v}$ can be determined from the Nusselt definition once again:

$$\mathrm{Nu}_{j-v} = 0.023\,\mathrm{Re}_D^{4/5}\,\mathrm{Pr}_{vapor}^{0.4} \tag{5.87}$$

$$h_{j-v} = \frac{\mathrm{Nu}_{j-v} k_{vapor}}{D} \tag{5.88}$$

Now, inputting equations (5.67) through (5.69) into equation (5.66) and rearranging, the following expression may be obtained:

$$\frac{\pi D^2}{4} = \frac{\pi\left(T_{steam} - T_{vapor}\right)}{h_{MBB-v} A_{MBB}\left(T_{vapor} - T_{MBB}\right)}\left[h_{t-v} n_{tubes} d_{tubes} + h_{j-v} D + \frac{\dot{m}_{MBB,dry} \Delta h_{H_2O,fg}^{T_{MBB}} \left(\omega_{MBB,2} - \omega_{MBB,3}\right)}{\left(l - z'\right)\left(T_{steam} - T_{vapor}\right)\pi}\right] \tag{5.89}$$

The only remaining unknown in this equation is T_{vapor}, which can be solved iteratively. Notice that the left hand side of the equation is simply the cross-sectional area of the dryer, so only the right hand side must be computed iteratively for T_{vapor}. However, since T_{vapor} must be lower than T_{steam} and higher than T_{MBB}, as can be seen in Figure 5.6, the iterative process for this expression is relatively simple. But also notice that some of

the properties, such as ρ_{vapor} and μ_{vapor}, used to calculate the convective heat transfer coefficients are also functions of T_{vapor}. Once the solution for T_{vapor} is completed, then equation (5.65) can be solved for U_{MBB}:

$$U_{MBB} = \frac{h_{MBB-v} A_{MBB} \left(T_{vapor} - T_{MBB}\right)\left(l - z'\right)}{\rho_{vapor} \Delta h_{H_2O,fg}^{T_{MBB}} \left(\omega_{MBB,2} - \omega_{MBB,3}\right)} \tag{5.90}$$

In order to find the total length of the dryer, l, and not just the length of the Drying Zone, (l - z'), the Heating Zone must be evaluated. The rate of temperature increase of the MBB solids can be found to be:

$$\frac{dT_{MBB}}{dz} = \frac{h_{MBB-v} A_{MBB} \left(\pi D^2/4\right)}{\dot{m}_{MBB,dry} \left(c_{MBB,dry} + c_{H_2O_{(l)}} \omega_{MBB,2}\right)} \left(T_{vapor} - T_{MBB}\right) \tag{5.91}$$

Integrating this expression from 0 to z' and $T_{MBB,0}$ to T_{MBB}, the following equation for z' may be obtained:

$$z' = \frac{\dot{m}_{MBB,dry} \left(c_{MBB,dry} + c_{H_2O_{(l)}} \omega_{MBB,2}\right)}{h_{MBB-v} A_{MBB} \left(\pi D^2/4\right)} \ln\left(\frac{T_{vapor} - T_{MBB,0}}{T_{vapor} - T_{MBB}}\right) \tag{5.92}$$

The total length is then:

$$l = \left(l - z'\right) + z'$$

With U_{MBB}, the required tilt or slope of the rotary dryer, α, can be computed. However, empirical holdup equations for rotary dryers must be used for this computation. Friedman *et al*. (1949) suggested the following equation for the residence time, t, of solids in a rotary dryer:

$$t = \frac{l \cdot \chi}{\dot{F}_{MBB}} = \frac{\xi \cdot l}{N_{drum}^{0.9} D \tan\alpha} \tag{5.93}$$

where χ is the holdup, or the percentage of the dryer's volume that is full of biomass, or whatever solids are being dried. ξ is an empirical constant that must be determined experimentally for each dryer arrangement. Also, $\dot{F}_{MBB}$ is the volumetric feed rate of the MBB with units of m^3/s per m^2 of dryer cross-section. For this case, $\dot{F}_{MBB}$ can be computed in terms of the mass flow rate:

$$\dot{F}_{MBB} = \frac{4\dot{m}_{MBB,dry}\left(1+\omega_{MBB,2}\right)}{\rho_{b,MBB,0}\pi D^2} \tag{5.94}$$

$\dot{F}_{MBB}$ can now be used find α with the following equation.

$$\tan\alpha = \frac{\dot{F}_{MBB}\xi}{\chi N_{drum}^{0.9} D} \tag{5.95}$$

The holdup and volumetric flow rate can also be related to U_{MBB},

$$U_{MBB} = \frac{l}{t} = \frac{\dot{F}_{MBB}}{\chi} = \frac{N_{drum}^{0.9} D\tan\alpha}{\xi} \tag{5.96}$$

Friedman *et al*. (1949) suggested that χ values between 3 and 7% of the dryer's volume are usually preferable. Also, for computing t in seconds, a value of 10.584 for ξ was found to agree well with experiments for direct contact rotary dryers; however, experiments would have to be conducted with steam-tube dryers to find a more accurate value for ξ.

In order to compute the steam consumption of the dryer, an energy balance about the entire dryer, CV_{dryer} in Figure 5.4, must be conducted. The solution for the steam consumption, $\dot{m}_{steam}$, is:

$$\dot{m}_{steam} = \frac{\dot{m}_{MBB,dry}\left[\begin{array}{c} c_{MBB,dry}\left(T_3 - T_2\right) + c_{H_2O_{(l)}}\left(\omega_{MBB,3}T_3 - \omega_{MBB,2}T_2\right) \\ +\left(\omega_{MBB,2} - \omega_{MBB,3}\right)h_{vapor} \end{array}\right]}{\Delta h_{H_2O,fg}^{T_{steam}}} \tag{5.97}$$

Here, h_{vapor} is the enthalpy of the entrained vapor exiting the dryer at point 11 in Figure 5.4.

In this study, steam-tube rotary dryers will be mostly considered for conceptual designs of small scale, on-the-farm combustion systems. However, the economic costs of rotary dryers can be estimated for large scale applications in a similar way to conveyor belt dryers. Whereas the capital cost of a conveyor belt dryer is a function of the conveyor belt area, according to Brammer *et al*. (2002) the capital cost of a rotary dryer depends on the average moisture content of the solids, the mean temperature

difference between the solids and the drying medium (in this case, the entrained vapor), and the heat transferred to the biomass solids.

$$\begin{bmatrix} heat\ transfered\ to \\ MBB\ solids \end{bmatrix} = h_{MBB-v} A_{MBB} \forall_{dryer} \left(T_{vapor} - T_{MBB} \right) \tag{5.98}$$

5.2.2. Transporting Manure-based Biomass

Coal transportation and processing is generally well understood and practiced. Most industrial and utility operations that require coal have amortized capital and operational procedures already in place and the cost of importing coal to the plant and injecting it into the burner is pretty much set for each individual operation and type of coal burned. Therefore, for the present study, the cost of processing and importing coal will be a simple dollar per ton input or design value.

However, the cost of transporting the biomass for co-firing and reburning processes must be determined from known values of fueling rate, moisture percentage, labor, distance between plant and feeding operation and other transportation costs.

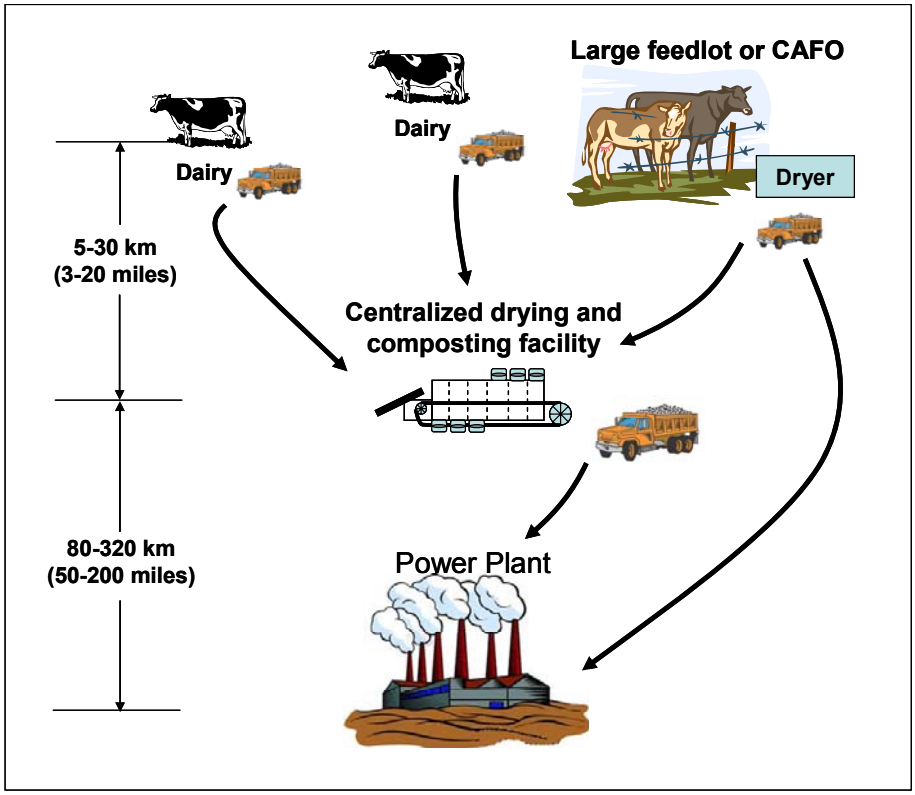

Figure 5.8 Transporting MBB from animal feeding operations to centralized drying facilities and to large power plants

The cost of transporting the dried cattle biomass to the power plant is one of the most significant cost to a biomass reburn facility. One of the most important parameters that will be considered is the average distance between the animal feeding operation(s) and the power plant, $\hat{D}$ in km. This average distance may also include the driving distance between the feeding operations and any centralized drying composting facility if drying equipment is not directly built on the feeding operations. See Figure 5.8. This distance will determine the number of hauling vehicles (trucks) required to move the biomass (N_{trucks}, trucks per trip), as well as the number of round trips that those trucks must take per year (N_{trips}) to consistently supply the biomass to the power plant.

The following hauling transportation analysis is adopted largely from a USEPA (2001) report on the economics of running confined animal feeding operations. Other parameters that must be known for the following transportation analysis are:

- the annual hours of operation of the reburn facility (OH_{reburn}), which may or may not be the same as OH_{plant},
- the biomass loading and unloading times (t_{load} & t_{unload}) in minutes,
- the average truck speed ($\hat{s}_{truck}$) in km per hour,
- the hauling schedule (HS), that is, the number of hours per day spent hauling,
- the number of hauling days per year ($N_{haul\ days}$),
- the density of the dried biomass ($\rho_{b,MBB}$), and
- the volumetric capacity of each truck ($\forall_{truck}$) in cubic meters (m^3) per truck.

The modeling of biomass transportation begins with the total annual amount of cattle biomass required for the power plant, $\dot{M}_{MBB,annum}$. Taking into account loading, unloading, and driving time, the total time (hours) for one trip must now be computed.

$$t_{trip} = \frac{\left(t_{load} + t_{unload}\right)}{60\ min/hr} + \frac{2\hat{D}}{\hat{s}_{truck}} \tag{5.99}$$

Here, $\hat{D}$ is multiplied by two in order to account for the total round trip of the haul. With the time for one trip known, the maximum annual number of trips for one truck may be determined.

$$N_{trips,max} = Ceiling\left|\frac{HS * N_{haul\ days}}{t_{trip}}\right| \tag{5.100}$$

The word "ceiling" in the equation means that the result of this computation is rounded up to the nearest integer number of trips. Moreover, the hauling capacity, in kg, for each truck can be computed from its haul volume.

$$C_{truck} = \rho_{b,MBB}\forall_{truck} \tag{5.101}$$

The total number of trucks required may be determined from $\dot{M}_{MBB,annum}$, equation (5.100), and equation (5.101).

$$N_{trucks} = Ceiling\left|\frac{\dot{M}_{MBB,annum}}{N_{trips,max}C_{truck}}\right| \tag{5.102}$$

This is the total number of trucks that the power plant must purchase to consistently supply the plant with biomass reburn fuel. The capital cost of these trucks can be a significant obstacle for implementing the retrofit on the plant, especially for larger capacity firing units.

Subsequently, once the number of trucks is determined, the actual number of trips required per year may now be computed.

$$N_{trips,actual} = Ceiling\left|\frac{\dot{M}_{MBB,annum}}{N_{trucks}C_{truck}}\right| \tag{5.103}$$

Lastly, the total annual hours each truck spends loading, unloading, and transporting biomass reburn fuel can be computed with the following expression.

$$t_{total,annual} = t_{trip}N_{trips,actual} \tag{5.104}$$

One other significant factor in determining the number of trucks and hauling time during MBB transport is the decision of whether to dry the biomass before transportation or to transport raw, wet manure and dry the biomass at the power plant. Drying the manure at the power plant might save considerable dryer fueling costs if waste heat from the coal-fired boiler is used to dry the biomass. However, transporting raw manure would mean higher diesel consumption for the transport vehicles because the hauling vehicles would also transport a considerable amount of moisture with the manure solids. As far as equations (5.99) through (5.104) are concerned, the parameter that will change with this decision is the total mass of MBB that must be transported, $\dot{M}_{MBB,annum}$. If raw manure is transported, then $\dot{M}_{MBB,annum}$ is considerably greater, and hence, N_{trucks}, $N_{trips,actual}$, and $t_{total,annual}$ will all be greater as well.

The annual fuel consumption of all the transport vehicles can be computed in liters with the following expression.

$$\dot{F}_{diesel} = \frac{2\hat{D}N_{trips,actual}N_{trucks}}{\left(Truck's\ fuel\ economy\ in\ km/liter\right)} \tag{5.105}$$

5.2.3. Grinding and Processing of Manure-based Biomass

As discussed in the literature review, the operation and maintenance costs for processing biomass for co-firing and reburning facilities has been modeled previously by the DOE (2004), the USEPA (2007c), and during the earlier reburn model conducted by the USEPA (1998). In order to utilize the estimations from these previous studies, only the plant capacity or the hourly consumption of MBB (co-fire or reburn fuel) is required to compute an annual dollar cost of operating and maintaining grinders, silos, and conveyor belt systems at the power plant to handle the biomass before combustion.

However, it is possible that the grinding and processing cost of manure biomass may deviate from that of coal or wood-based biomass discussed by the previous studies. In particular, it is not known if MBB can be grinded in the same equipment used to grind coal, particularly in pulverized coal plants. All experiments and pilot scale tests for MBB reburning and co-firing that have been conducted by the Texas A&M Coal and Biomass Laboratory were done with manure that had been pulverized with a hammer mill and a subsequent impact mill at the Texas A&M University System, Bushland Research and Extension Center in Bushland, Texas. However, these mills are not necessarily the type of mills used at pulverized coal plants. Hammer mills are used to chop solids that are more fibrous than coal, such as MBB, into coarsely ground particles. The coarse particles can then be pulverized by blasting them in an impact mill (Heflin, 2008).

Ideally, an experimental study should be conducted to compare the electricity consumption of hammer mills and impact mills processing coal, wood-based biomass, and MBB. From these experiments, anticipated maintenance and labor costs should also be estimated. Shi *et al*. (2003) conducted an energy-based model for swing hammer mills at coke oven feed burners, but the modeling equations in this study have empirical constants that require experimental results for each specific hammer mill tested.

For the sake of the current modeling study, the estimations from the DOE (2004), the USEPA (2007c), and the earlier reburn model conducted by the USEPA (1998) will

be used along with a gross estimation of the electric consumption of the hammer mill and impact mill used at the Bushland facility.

5.2.4. Emissions from Pre-combustion Processing of Biomass

In addition to the cost of operating and maintaining drying and transportation equipment for manure biomass, there may also be indirect costs from gaseous emissions resulting from drying and transporting. Here, the more significant emission is CO_2 from both gas boilers for the manure dryers and diesel combustion for the hauling vehicles. Of course, carbon emissions from pre-processing will only be economically significant if there is a monetary value placed on CO_2 from nonrenewable sources. In fairness, this monetary value would also be applied to these emissions from dryers and trucks, which may detract from the emissions savings seen when burning MBB in the place of coal. In cases when MBB is used as reburn fuel in existing coal plants for NO_x reduction, NO_x emissions from transport vehicles may also be significant and must be accounted for during emission savings calculations.

The CO_2 levels from drying depend on what fuel is burned to generate the heat energy in the boilers. If natural gas is burned, then the CO_2 emissions can be estimated to be the same as carbon emissions from burning methane (CH_4). The CO_2 level from burning methane, $\mathcal{L}_{CO_2,drying}$, is 49.4 kg CO_2 / GJ. If propane is used instead of natural gas, then $\mathcal{L}_{CO_2,drying}$ will be 59.5 kg / GJ. The annual emission of CO_2, in metric tons, from drying the manure biomass can be computed with the following expression:

$$\mathcal{E}_{CO_2,drying} = \mathcal{L}_{CO_2,drying} * \dot{F}_{dryer,fuel} * OH_{dryer} * N_{dryers} * \left(\frac{1\,metric\ ton}{1,000\,kg}\right) * \left(\frac{1\,GJ}{10^6\ kJ}\right) * \left(\frac{3600\,s}{1\,hr}\right) + \mathcal{E}_{CO_2,dryer\ fans} \quad (5.106)$$

The fuel consumption, $\dot{F}_{dryer,fuel}$, can be computed with equation (5.28). Notice, that the biomass dryers will also consume electricity, predominantly from fans and blowers. The annual CO_2 emission from electricity consumption can be estimated from the electricity

consumption from the fans, $\dot{E}_{fans}$, which was computed earlier in equation (5.29), along with the CO_2 levels from burning coal, which will be discussed in a later section. Since about half of the electricity consumed in the US is generated from burning coal, carbon emissions from coal combustion may be a worst case estimate for the actual carbon footprint of fans and blowers in manure dryers. However, other estimates of the carbon emission from electricity consumption may be made if electricity is known to come from other sources.

Carbon dioxide will also be emitted from hauling vehicles, which are typically fueled with diesel. If diesel can be estimated as $C_{12}H_{26}$, then about 2.64 kg of CO_2 is emitted for every liter of diesel (22 lb CO_2 / gallon) that is burned, assuming that the density of diesel is approximately 0.85 kg/liter. So, the annual emission of CO_2 from the vehicles can be computed with the following expression.

$$\dot{\mathcal{E}}_{CO_2,trucks} = \mathcal{L}_{CO_2,diesel}^{\mathcal{C}} * \dot{F}_{diesel} * \left(\frac{1\ metric\ ton}{1,000\ kg} \right) \tag{5.107}$$

where, $\mathcal{L}_{CO_2,diesel}^{\mathcal{C}}$ for this case is simply 2.64 kg/liter and $\dot{F}_{diesel}$ was computed in equation (5.105).

Nitrogen oxides from biomass transportation may also be significant. If the average distance from feeding operations, is long enough, then over time the NO_x emitted by the hauling trucks may become significant compared to the controlled amount of NO_x from the power plant. Currently, most diesel powered vehicles limit NO_x with exhaust flue gas recirculation (EGR) systems, oxidation catalysts, and special injection timing to meet lower NO_x limits of about 0.93 g/MJ (2.5 g/bhp-hr). However, to meet 2007 standards of 0.075 g/MJ (0.2 g/bhp-hr), diesel powered trucks are to be equipped with special NO_x absorbers and selective catalytic reduction (SCR) systems (Krishnan *et al*., 2005). Therefore the NO_x emission level from each of the trucks will be:

$$\mathcal{L}_{NO_x,truck} = \begin{cases} 0.2\,\dfrac{g}{bhp \cdot hr}, \textit{if SCR is installed} \\ 2.5\,\dfrac{g}{bhp \cdot hr}, \textit{without SCR} \end{cases} \tag{5.108}$$

The total annual hours spent hauling the manure can be computed as:

$$t_{driving} = \frac{2\hat{D}N_{trips,actual}N_{trucks}}{\hat{s}_{truck}} \tag{5.109}$$

If the typical percent load factor for the trucks is $\%L_{truck}$ and the rated horsepower is hp_{truck}, then the annual NO_x emission from hauling manure biomass to existing coal plants can be computed with the following expression.

$$\mathcal{E}_{NO_x,truck} = \mathcal{L}_{NOx,truck} * \left(\frac{\%L_{truck}}{100}\right) * hp_{truck} * t_{driving} * \left(\frac{1\,metric\ ton}{10^6\ g}\right) \tag{5.110}$$

5.3. General Modeling of Coal and Biomass Oxidation

5.3.1. Direct and Complete Combustion of Coal and Biomass Fuels

Modeling the combustion of coal or MBB can begin with determining an empirical chemical formula quantifying the elements in the combustible material of the fuel—carbon (C), hydrogen (H), oxygen (O), nitrogen (N), and sulfur (S). This empirical formula can be derived from an ultimate analysis of the fuel. Moreover, the systems that are modeled in this study involve variations of the moisture and ash percentages (%*M* and %*A*, respectively) of MBB. For example, different MBB collection techniques at animal feeding operations partly determine the ash content of the as-fired biomass and solid separators; and dryers change the moisture percentage of MBB before combustion. Cleaning and drying processes also alter the %*M* and %*A* of coals. Therefore, during this analysis, the combustible elements must be expressed in terms of %*M* and %*A* for both coal and MBB.

$$
\begin{aligned}
C\left[\frac{\text{kmol C}}{\text{100 kg of as received fuel}}\right] &= \frac{(100-\%M-\%A)*DAF_C}{12.01} \\
H &= \frac{(100-\%M-\%A)*DAF_H}{1.008} \\
N &= \frac{(100-\%M-\%A)*DAF_N}{14.0067} \\
O &= \frac{(100-\%M-\%A)*DAF_O}{15.997} \\
S &= \frac{(100-\%M-\%A)*DAF_S}{32.064}
\end{aligned}
\tag{5.111}
$$

Here, the numbers DAF_k are the dry, ash-free fractions (kg element per kg of dry, ash-free fuel) of each element in the fuel and the constants in the denominators are the elemental molecular weights.

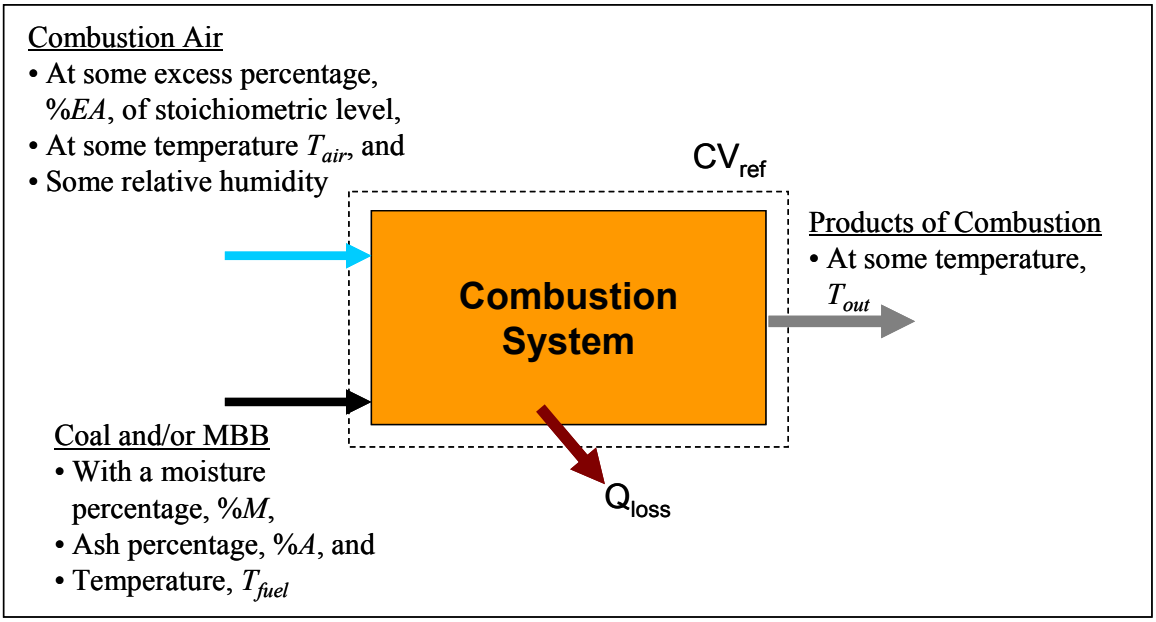

Figure 5.9 General combustion process for coal and manure-based biomass

Consider the generalized combustion system for coal and/or MBB fuels in Figure 5.9. Fuel, with a certain amount of moisture and ash, is injected into the system along with air and is burned completely, generating heat and products of combustion (CO_2, H_2O, SO_2, N_2, and O_2). The empirical formula of the combustible material in the fuel

($C_C H_H N_N O_O S_S$) can be used in the following chemical reaction equation, derived from a balance of species entering and exiting the control volume about the combustion system, to determine the amount of each product of combustion. Since this particular analysis will be utilized several times throughout this section, the control volume in Figure 5.9 will be referred to as the reference control volume (CV_{ref}).

$$\begin{aligned}\left(C_C H_H N_N O_O S_S + w H_2O_{(l)} + \text{Ash}\right) \\ + a\left(O_2 + \frac{79}{21}N_2 + y_{H_2O,air}\left(1+\frac{79}{21}\right)H_2O_{(g)}\right) \\ \rightarrow b CO_2 + c H_2O_{(g)} + d N_2 + e SO_2 + f O_2 + \text{Ash}\end{aligned} \tag{5.112}$$

Here, w is the number of kmoles of liquid water per 100 kg of as received fuel and $y_{H_2O,air}$ is the mole fraction of water vapor in the combustion air. The water vapor mole fraction can be found with the following equation:

$$y_{H_2O,air} = \frac{\phi P_g(T_{air})}{P_{air} - \phi P_g(T_{air})} \tag{5.113}$$

where ϕ is the known relative humidity of the air, P_{air} is the air pressure, and P_g is the saturation pressure as a function of temperature found in equation (5.16).

Note than the water, c, in the right hand side of equation (5.112) includes the liquid water in the fuel, the water vapor initially in the combustion air, and the water produced during the combustion process. Moreover the ash in this chemical balance equation is assumed to be inert and does not contribute to the chemical balance equation; however, the inert ash will play some role in determining flame temperatures and heat transfer rates later in the analysis and so, is included here for completeness. Since there are six unknowns in equation (5.112): a, b, c, d, e, and f, and only five elemental balance equations from the five elements present in the reaction (C, H, N, O, and S), another input parameter and equation must be introduced in order to solve the chemical reaction equation. Determining this equation can begin by considering the stoichiometric reaction equation describing the case in which an ideal amount of air is used in the combustion process so that no O_2 remains in the products of combustion.

$$\left(C_C H_H N_N O_O S_S + wH_2O_{(l)}\right) + a_{st}\left(O_2 + \frac{79}{21}N_2 + y_{H_2O,air}\left(1+\frac{79}{21}\right)H_2O_{(g)}\right) \rightarrow bCO_2 + cH_2O_{(g)} + dN_2 + eSO_2 \quad (5.114)$$

where a_{st} is the stoichiometric amount of air required to completely burn the fuel. Now, conducting an atom balance for equation (5.114).

Carbon:

$$b = C \quad (5.115)$$

Hydrogen:

$$c = \frac{H}{2} + w + a_{st} y_{H_2O,air}\left(1+\frac{79}{21}\right) \quad (5.116)$$

Sulfur:

$$e = S \quad (5.117)$$

Oxygen:

$$O + w + 2a_{st} + a_{st} y_{H_2O,air}\left(1+\frac{79}{21}\right) = 2b + c + 2e$$

Inserting equations (5.115), (5.116), and (5.117), and solving for a_{st}:

$$a_{st} = C + \frac{H}{4} + S - \frac{O}{2} \quad (5.118)$$

The excess air percentage can now be defined as the following:

$$\%EA = \left(\frac{a}{a_{st}} - 1\right) * 100 \quad (5.119)$$

$\%EA$ can now be treated as a design variable and is the extra input parameter required for this analysis. Solving equation (5.119) for a and inserting equation (5.118):

$$a = \left(\frac{\%EA}{100} + 1\right)\left(C + \frac{H}{4} + S - \frac{O}{2}\right) \quad (5.120)$$

With a known, equation (5.112) can now be solved. Note that b, c, and e are the same as in equations (5.115), (5.116), and (5.117).

Oxygen:

$$O + w + 2a + ay_{H_2O,air}\left(1 + \frac{79}{21}\right) = 2b + c + 2e + 2f$$

$$f = \frac{\%EA}{100}\left(C + \frac{H}{4} + S - \frac{O}{2}\right) \tag{5.121}$$

Nitrogen:

$$N + 2a\left(\frac{79}{21}\right) = 2d$$

$$d = \frac{79}{21}\left(\frac{\%EA}{100} + 1\right)\left(C + \frac{H}{4} + S - \frac{O}{2}\right) + \frac{N}{2} \tag{5.122}$$

Now, with equations (5.115) through (5.117) and equations (5.120) through (5.122), the number of kmoles of each species, N_k, entering and leaving CV_{ref} can be determined. The number of kmoles entering the CV_{ref} as fuel, excluding ash, are:

$$\begin{aligned} N_{fuel,DAF} &= 1 \quad \text{and} \\ N_{H_2O(l),fuel} &= w \end{aligned} \tag{5.123}$$

The number of kmoles entering the CV_{ref} as the combustion air are:

$$\begin{aligned} N_{O_2,air} &= \left(\frac{\%EA}{100} + 1\right)\left(C + \frac{H}{4} + S - \frac{O}{2}\right), \\ N_{N_2,air} &= \frac{79}{21}\left(\frac{\%EA}{100} + 1\right)\left(C + \frac{H}{4} + S - \frac{O}{2}\right), \\ N_{H_2O(g),air} &= y_{H_2O,air}\left(1 + \frac{79}{21}\right)\left(\frac{\%EA}{100} + 1\right)\left(C + \frac{H}{4} + S - \frac{O}{2}\right) \end{aligned} \tag{5.124}$$

The number of kmoles exiting the CV_{ref} as products of combustion, excluding ash, are:

$$
\begin{aligned}
&N_{CO_2,out} = C,\\
&N_{H_2O(g),out} = \frac{H}{2} + w\\
&\qquad + y_{H_2O,air}\left(1+\frac{79}{21}\right)\left(\frac{\%EA}{100}+1\right)\left(C+\frac{H}{4}+S-\frac{O}{2}\right),\\
&N_{N_2,out} = \frac{79}{21}\left(\frac{\%EA}{100}+1\right)\left(C+\frac{H}{4}+S-\frac{O}{2}\right)+\frac{N}{2},\\
&N_{SO_2,out} = S, \quad \text{and}\\
&N_{O_2,out} = \frac{\%EA}{100}\left(C+\frac{H}{4}+S-\frac{O}{2}\right).
\end{aligned}
\tag{5.125}
$$

Equations (5.123) through (5.125) can also be expressed in terms of %M and %A if equation (5.111) is plugged in. Moreover, the liquid moisture and the ash in the fuel can be expressed with the following equations.

$$w = \frac{\%M}{18.02} \tag{5.126}$$

$$m_{ash,\,fuel} = m_{ash,out} = \%A \tag{5.127}$$

The next step in this analysis is to conduct an energy balance about CV_{ref}. This conservation analysis will be done for two general cases: one in which Q_{loss} in Figure 5.9 is zero so that an adiabatic flame temperature can be calculated and secondly, where Q_{loss} is the heat transferred from the furnace to a process, for example heat to boil water to generate steam.

The fist case is shown in Figure 5.10. Here, coal or MBB solids will be directly fired in a furnace, producing heat and products of combustion. Since there is no heat lost by the system, the temperature of the products exiting the system, T_{out}, is approximately the same as the flame temperature, T_{flame}.

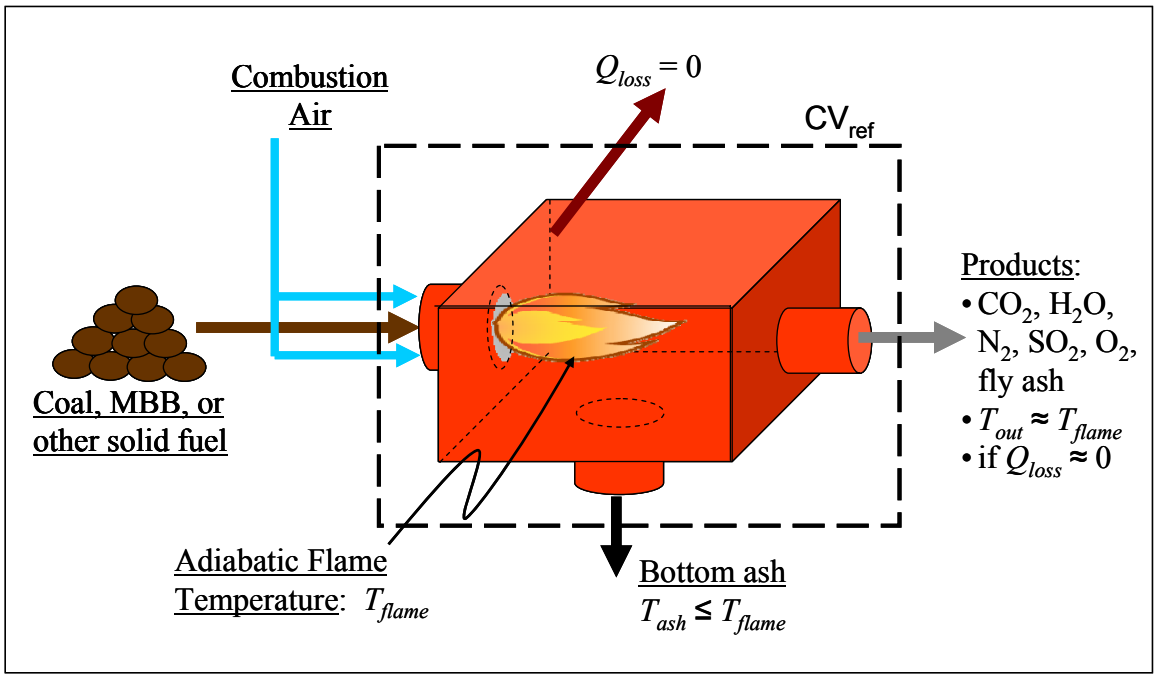

Figure 5.10 Energy conservation for computing adiabatic flame temperature

The energy balance equation for this system can be written as:

$$\begin{aligned} 0 = {} & N_{fuel,DAF}\bar{h}_{fuel,DAF} + w\bar{h}_{H_2O(l),fuel} + m_{ash}c_{p,ash}\left(T_{fuel} - 298\right) \\ & + \sum_{air,in} N_k\bar{h}_k - \sum_{products,out} N_k\bar{h}_k - m_{fly\ ash}\left\{c_{p,ash}\left(T_{out} - 298\right)\right\} \\ & - m_{bottom\ ash}\left\{c_{p,ash}\left(T_{ash} - 298\right)\right\} \end{aligned} \tag{5.128}$$

where $m_{ash,fuel} = m_{fly\ ash} + m_{bottom\ ash}$ .and $c_{p,ash}$ is the specific heat of the inert material in the fuel. The enthalpies, $\bar{h}_k$, have two components: enthalpies of formation, $\bar{h}^0_{f,298,k}$, and changes in thermal enthalpy, $\Delta\bar{h}^T_{t,k}$. The temperature 298 K (537 R, 77 °F) is assumed to be the reference temperature. The changes in thermal enthalpy are functions of temperature, in this case, either the temperature of the air or the flame temperature.

$$\bar{h}_k = \bar{h}^0_{f,298,k} + \Delta\bar{h}^T_{t,k} \tag{5.129}$$

$$\Delta\bar{h}^T_{t,k} = \Delta\bar{h}^T_{t,k}\left(T\right) = \int_{298}^{T} \bar{c}_{p,k}\left(T\right)dT' \tag{5.130}$$

In order to calculate $\Delta\overline{h}_{t,k}^{T}$, the function of $\overline{c}_{p,k}$ in terms of T must be known. Although, in cases where the flame temperature is either known or hypothesized to be at a certain range, the specific heats can be considered to be approximately constant with T, usually allowing for an analytical solution to complete combustion problems. However, for the current study, since moisture and ash percentages of MBB fuels will vary greatly, so too will the flame temperature, and thus specific heats will not be considered constant. Instead, polynomial equations for specific heats for different species will be used when determining values of $\Delta\overline{h}_{t,k}^{T}$. These polynomials are provided in Table 5.2.

Table 5.2 Polynomial equations used to compute specific heats of various species (Annamalai *et al*., 2006)

Species	Temperature range	Polynomial equation for computing specific heat ($\overline{c}_p/\overline{R}$)
CO_2	300 – 1,000 K	2.275724 + 0.09922072E-1*T - 0.10409113E-4*T^2 + 0.06866686E-7*T^3 - 0.0211728E-10*T^4
	1,000 – 5,000 K	4.453623 + 0.03140168E-1*T - 0.12784105E-5*T^2 + 0.02393996E-8*T^3 - 0.16690333E-13*T^4
$H_2O_{(g)}$	300 – 1,000 K	3.386842 + 0.03474982E-1*T - 0.06354696E-4*T^2 + 0.06968581E-7*T^3 - 0.02506588E-10*T^4
	1,000 – 5,000 K	2.672145 + 0.03056293E-1*T - 0.08730260E-5*T^2 + 0.12009964E-9*T^3 - 0.06391618E-13*T^4
N_2	300 – 1,000 K	3.298677 + 0.14082404E-2*T - 0.03963222E-4*T^2 + 0.05641515E-7*T^3 - 0.02444854E-10*T^4
	1,000 – 5,000 K	2.92664 + 0.14879768E-2*T - 0.0568476E-5*T^2 + 0.10097038E-9*T^3 - 0.06753351E-13*T^4
O_2	300 – 1,000 K	3.212936 + 0.11274864E-2*T - 0.0575615E-5*T^2 + 0.13138773E-8*T^3 - 0.08768554E-11*T^4
	1,000 – 5,000 K	3.697578 + 0.06135197E-2*T - 0.1258842E-6*T^2 + 0.01775281E-9*T^3 - 0.11364354E-14*T^4
SO_2	300 – 2,000 K	5.699 + 0.801E-3*T - 1.015E5*T^{-2}

Here, $\overline{R}$ is the ideal gas constant, 8.314 kJ/kmole K, and T is in degrees K

The enthalpy of the fuel may be computed as the following:

$$\begin{aligned}\overline{h}_{fuel,DAF} &= \overline{h}_{f,298,fuel}^{0} + c_{fuel,DAF} MW_{fuel}\left(T_{fuel} - 298\right) \\ &= HHV_{fuel,DAF} MW_{fuel} + C\overline{h}_{f,298,CO_2}^{0} + \frac{H}{2}\overline{h}_{f,298,H_2O(l)}^{0} \\ &\quad + S\overline{h}_{f,298,SO_2}^{0} + c_{fuel,DAF} MW_{fuel}\left(T_{fuel} - 298\right)\end{aligned} \tag{5.131}$$

Here, $c_{fuel,DAF}$ is the specific heat of the dry, ash-free content of the fuel. The molecular weight of the dry, ash-free fuel is simply:

$$MW_{fuel}\left[\frac{kg\ DAF\ fuel}{100\ kg\ as\ received}\ or\ \frac{kg\ DAF\ fuel}{1\ kmole\ DAF\ fuel}\right] = 12.01*C + 1.008*H + 14.0067*N + 15.994*O + 32.065*S \tag{5.132}$$

Next, expand the summations in equation (5.128) and plug in equations (5.129) and (5.131) to obtain the following energy equation for the control volume problem in Figure 5.10. Keep in mind that the values of $\overline{h}^0_{f,298,O_2}$ and $\overline{h}^0_{f,298,N_2}$ are zero.

$$\begin{aligned}
&N_{CO_2,out}\left\{\overline{h}^0_{f,298,CO_2}+\Delta\overline{h}^{T_{out}}_{t,CO_2}\right\}+N_{H_2O(g),out}\left\{\overline{h}^0_{f,298,H_2O(g)}+\Delta\overline{h}^{T_{out}}_{t,H_2O(g)}\right\}\\
&+N_{N_2,out}\left\{\Delta\overline{h}^{T_{out}}_{t,N_2}\right\}+N_{SO_2,out}\left\{\overline{h}^0_{f,298,SO_2}+\Delta\overline{h}^{T_{out}}_{t,SO_2}\right\}+N_{O_2,out}\left\{\Delta\overline{h}^{T_{out}}_{t,O_2}\right\}\\
&+m_{fly\ ash}\left\{c_{p,ash}\left(T_{out}-298\right)\right\}+m_{bottom\ ash}\left\{c_{p,ash}\left(T_{ash}-298\right)\right\}\\
&=\left\{HHV_{fuel,DAF}MW_{fuel}+C\overline{h}^0_{f,CO_2}+\frac{H}{2}\overline{h}^0_{f,298,H_2O(l)}+S\overline{h}^0_{f,298,SO_2}\right.\\
&\quad\left.+c_{fuel,DAF}MW_{fuel}\left(T_{fuel}-298\right)\right\}+w\left\{\overline{h}^0_{f,298,H_2O(l)}+\overline{c}_{p,H_2O(l)}\left(T_{fuel}-298\right)\right\}\\
&\quad+m_{ash,fuel}\left\{c_{p,ash}\left(T_{fuel}-298\right)\right\}+N_{O_2,air}\left\{\Delta\overline{h}^{T_{air}}_{t,O_2}\right\}+N_{N_2,air}\left\{\Delta\overline{h}^{T_{air}}_{t,N_2}\right\}\\
&\quad+N_{H_2O(g)}\left\{\overline{h}^0_{f,298,H_2O(g)}+\Delta\overline{h}^{T_{air}}_{t,H_2O(g)}\right\}
\end{aligned} \tag{5.133}$$

The temperature of the incoming fuel (T_{fuel}), incoming air (T_{air}), and outgoing bottom ash (T_{ash}) are considered known design variables. The only unknown in equation (5.133) is T_{out}, which is approximately equal to the flame temperature, T_{flame}. However, this variable is embedded in the polynomial equations for $\Delta\overline{h}^{T_{out}}_{t,k}=\int_{298}^{T_{out}}\overline{c}_{p,k}dT'$ and must be solved iteratively.

The second case in which the energy balance about CV_{ref} can be conducted is one in which Q_{loss} is *not* zero, but rather is defined as the heat lost by the combustion system and gained by an external process such as steam production. This case is illustrated in Figure 5.11.

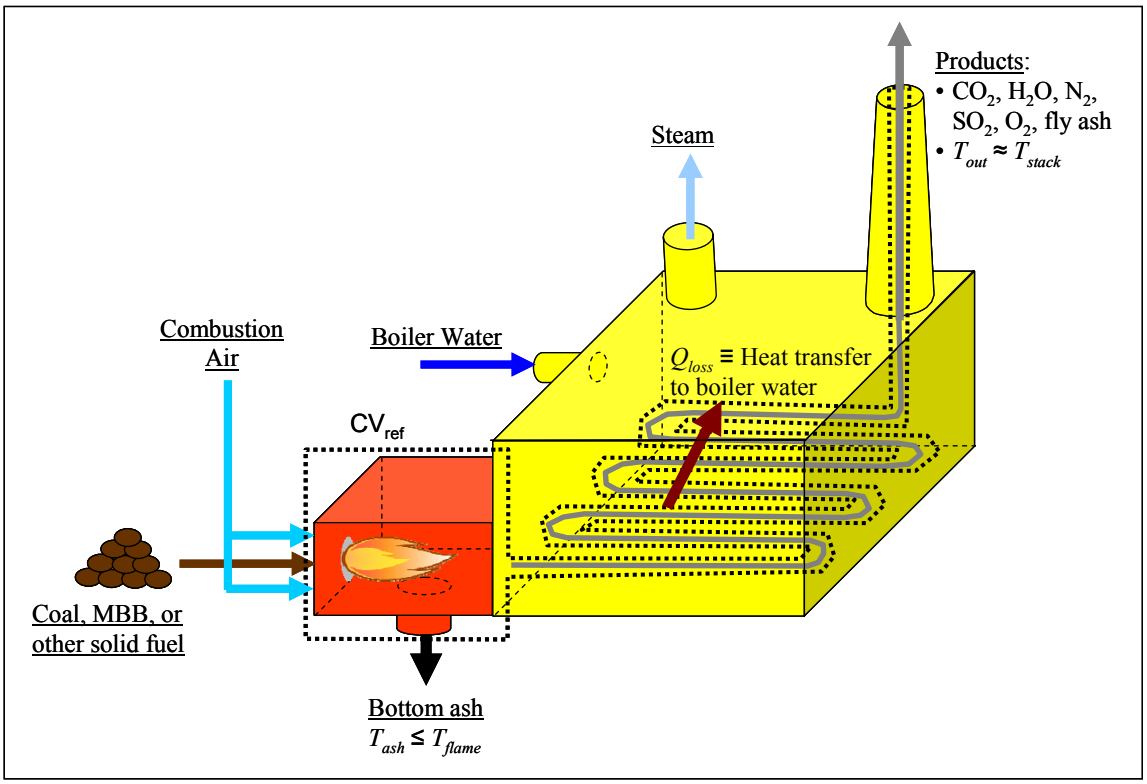

Figure 5.11 Energy conservation for computing heat lost to an external process

In this case, simply revisit equation (5.128), and include Q_{loss}.

$$\begin{aligned} Q_{loss}\left[\frac{kJ}{100\ kg\ as\ rec\ fuel}\right] = & \sum_{products,out} N_k \bar{h}_k + m_{fly\ ash}\left\{c_{p,ash}\left(T_{out}-298\right)\right\} \\ & + m_{bottom\ ash}\left\{c_{p,ash}\left(T_{ash}-298\right)\right\} \\ & - N_{fuel,DAF}\bar{h}_{fuel,DAF} - w\bar{h}_{H_2O(l),fuel} \\ & - m_{ash}c_{p,ash}\left(T_{fuel}-298\right) - \sum_{air,in} N_k \bar{h}_k \end{aligned} \tag{5.134}$$

If Q_{loss} is positive, then heat is said to be entering CV_{ref}. If Q_{loss} is negative, then heat is exiting CV_{ref} and being transferred to the desired process. Since the objective of the combustion system in Figure 5.11 is to transfer as much heat to the boiler water as possible, a more negative Q_{loss} is desirable. Hence, it can be seen how preheating the fuel and the combustion air (i.e. increasing the quantities of the last four terms in equation (5.134) on the right-hand side) would improve the amount of heat transferred from the combustion system to the external process. Lowering T_{out} as much as possible

is also desirable, although in practice this is limited due to the formation of sulfuric acids in the stack. Equation (5.134) can be expanded in much the same way as equation (5.133), only here, all temperatures—incoming fuel temperature (T_{fuel}), incoming air temperature (T_{air}), exiting bottom ash temperature (T_{ash}), and the temperature of the products of combustion exiting the stack ($T_{out} = T_{stack}$)—are considered known design variables.

5.3.2. Partial Oxidation and Gasification of Coal and Biomass Fuels

From a practical design point, there is a major issue confronting a combustion system such as the one depicted in Figure 5.11, and that is ash fouling and clogging in the fire tube as the products of combustion travel from the furnace to the stack. This problem is of particular concern for fuels with high ash contents such as MBB. Fouling and clogging from high ash inputs are also problems for steam-tube boilers (although probably not to the same extent) in which the boiler water and subsequent steam are located in the tube(s) and the hot combustion products travel over the steam tube(s).

One way to avoid much of the ash fouling and clogging on heat exchanger and boiler tube surfaces is to avoid having any fly ash in the hot products of combustion at all. It is possible to achieve this by first partially oxidizing, or gasifying, the coal and/or MBB solids generating producer gas predominantly made up of carbon monoxide (CO) and hydrogen (H_2). See Figure 5.12. The producer gas can then be fed into a gas furnace to generate heat energy. As shown in the figure, the producer gas may also be sent through a filter or clean-up system to remove any remaining inert particles before combustion.

In addition to air, steam may also be supplied to the gasifier to produce higher concentrations of H_2 in the producer gas. The objective of this analysis is to approximate the composition of the producer gas; given the fuel composition, the amount of air injected into the gasifier, the amount of steam injected into the gasifier, the pressure in the gasification chamber, and the temperature in which the gasifier is operated.

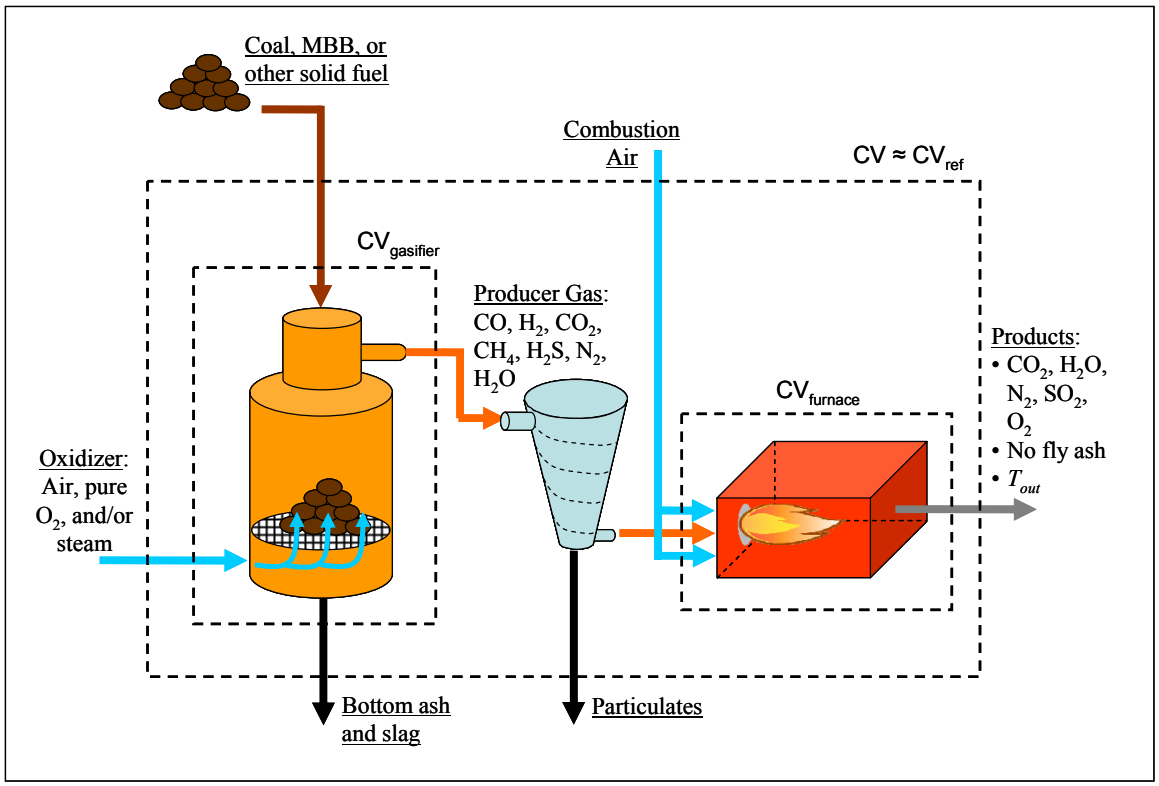

Figure 5.12 Partial oxidation of coal and biomass and subsequent burning of producer gases

The analysis may begin with the chemical balance formula for the species entering and exiting $CV_{gasifier}$.

$$\left(C_C H_H N_N O_O S_S + wH_2O_{(l)} + \text{Ash}\right) + n_{O_2,air}\left(O_2 + \frac{79}{21}N_2\right) + n_{steam}H_2O_{(g)}$$
$$\rightarrow n_{CO_2,g}CO_2 + n_{CO,g}CO + n_{CH_4,g}CH_4 + n_{H_2S,g}H_2S + n_{N_2,g}N_2 \qquad (5.135)$$
$$+ n_{H_2,g}H_2 + n_{H_2O,g}H_2O_{(g)} + \text{Ash}$$

The amount of air injected into the gasifier, unlike in the previous complete combustion case, will be less than the stoichiometric amount required to completely burn the fuel and convert all carbon present in the fuel to CO_2. Therefore, instead of defining $\%EA$, an equivalence ratio will be defined as:

$$ER = \frac{a_{st}}{n_{O_2,air}} \qquad (5.136)$$

where the definition of a_{st} for this case is the same as that in equation (5.118). Yet, %*EA* can be expressed in terms of *ER*.

$$\%EA = \left(\frac{n_{O_2,air}}{a_{st}} - 1 \right) * 100 = \left(\frac{1}{ER} - 1 \right) * 100 \tag{5.137}$$

However, for gasification, *ER* will be greater than one, making %*EA* negative, thus making it an air deficiency percentage.

For cases in which steam is injected into the gasifier along with air, a steam-air ratio is defined as the following:

$$SAR = \frac{n_{steam}}{n_{O_2,air}\left(1 + \frac{79}{21}\right)} \tag{5.138}$$

The solution to the chemical reaction equation (5.135) can begin with an atom balance, just as was done for equation (5.112).

Carbon:

$$C = n_{CO_2,g} + n_{CO,g} + n_{CH_4,g} \tag{5.139}$$

Hydrogen:

$$H + 2w + 2n_{steam} = 4n_{CH_4,g} + 2n_{H_2S,g} + 2n_{H_2,g} + 2n_{H_2O,g} \tag{5.140}$$

Oxygen:

$$O + w + 2n_{O_2,air} + n_{steam} = 2n_{CO_2,g} + n_{CO,g} + n_{H_2O,g} \tag{5.141}$$

Nitrogen:

$$N + 2n_{O_2,air}\left(\frac{79}{21}\right) = 2n_{N_2,g} \tag{5.142}$$

Sulfur:

$$S = n_{H_2S,g} \tag{5.143}$$

With equations (5.118) and (5.136), $n_{O_2,air}$ can be found to be:

$$n_{O_2,air} = \frac{1}{ER}\left(C + \frac{H}{4} + S - \frac{O}{2} \right) \tag{5.144}$$

Inserting this result into equation (5.138):

$$n_{steam} = \left(\frac{SAR}{ER}\right)\left(1+\frac{79}{21}\right)\left(C+\frac{H}{4}+S-\frac{O}{2}\right) \tag{5.145}$$

And inserting into equation (5.142):

$$n_{N_2,g} = \frac{N}{2}+\frac{1}{ER}\left(\frac{79}{21}\right)\left(C+\frac{H}{4}+S-\frac{O}{2}\right) \tag{5.146}$$

Now, the remaining unknowns are $n_{CO_2,g}$, $n_{CO,g}$, $n_{CH_4,g}$, $n_{H_2,g}$, and $n_{H_2O,g}$, but only equations (5.139), (5.140), and (5.141) remain. In order to complete this problem, two equations from chemical equilibrium analysis must be obtained. However, first these remaining equations can be reformatted and simplified by defining the total number of moles of carbon ($n_{C,in}$), hydrogen ($n_{H_2,in}$), and oxygen ($n_{O_2,in}$) entering the gasifier's chamber ($CV_{gasifier}$ in Figure 5.12) as:

$$n_{C,in} = C \tag{5.147}$$

$$n_{H_2,in} = \frac{H}{2}+w+n_{steam} \tag{5.148}$$

$$n_{O_2,in} = \frac{O}{2}+\frac{w}{2}+n_{O_2,air}+\frac{n_{steam}}{2} \tag{5.149}$$

Moreover, the mole fractions of each species in the producer gas can be defined as $y_{i,g} = n_{i,g}/n_{tot,g}$, where $n_{tot,g}$ is the total moles in the producer gas.

$$n_{tot,g} = n_{CO_2,g}+n_{CO,g}+n_{CH_4,g}+n_{H_2S,g}+n_{N_2,g}+n_{H_2,g}+n_{H_2O,g} \tag{5.150}$$

and

$$1 = y_{CO_2,g}+y_{CO,g}+y_{CH_4,g}+y_{H_2,g}+y_{H_2O,g}+\frac{n_{H_2S,g}}{n_{tot,g}}+\frac{n_{N_2,g}}{n_{tot,g}} \tag{5.151}$$

So that equations (5.139), (5.140), and (5.141) become

$$n_{C,in} = \left(y_{CO_2,g}+y_{CO,g}+y_{CH_4,g}\right)n_{tot,g} \tag{5.152}$$

$$n_{H_2,in} = \left(2y_{CH_4,g}+y_{H_2,g}+y_{H_2O,g}+\frac{n_{H_2S,g}}{n_{tot,g}}\right)n_{tot,g} \tag{5.153}$$

$$n_{O_2,in} = \left(y_{CO_2,g} + \frac{y_{CO,g}}{2} + \frac{y_{H_2O,g}}{2} \right) n_{tot,g} \tag{5.154}$$

Assuming that there is no O_2 present in the producer gas and that all the solid carbon in the coal and/or MBB fuel is converted to either CO_2, CO, or CH_4, the relevant chemical equilibrium reaction equations can be reduced to the following two (Probstein *et al*., 2006b):

I $$\mathrm{CH_4 + H_2O \leftrightarrow CO + 3H_2} \tag{5.155}$$

II $$\mathrm{CO_2 + CH_4 \leftrightarrow 2CO + 2H_2} \tag{5.156}$$

For a general reaction, $\nu_A A + \nu_B B \leftrightarrow \nu_C C + \nu_D D$, the equilibrium constant, *K*, can be computed as:

$$K(T) = \frac{y_C^{\nu_C} y_D^{\nu_D}}{y_A^{\nu_A} y_B^{\nu_B}} \left(\frac{P}{P_{ref}} \right)^{\nu_C + \nu_D - \nu_A - \nu_B}$$

where, *P* is the reactor pressure and P_{ref} is a reference pressure—usually 1 atmosphere (101.325 kPa). So, for this case the equilibrium constants are:

$$K_{\mathbf{I}}(T) = \frac{y_{CO,g} y_{H_2,g}^3}{y_{CH_4,g} y_{H_2O,g}} P^2 \tag{5.157}$$

$$K_{\mathbf{II}}(T) = \frac{y_{CO,g}^2 y_{H_2,g}^2}{y_{CO_2,g} y_{CH_4,g}} P^2 \tag{5.158}$$

These two equations are the remaining two equations required to successfully complete the analysis of $CV_{gasifier}$; however, the equilibrium constants, which are functions of temperature, must first be computed. It can be shown that $\log K = \sum \nu_i \log K_i$, so that for this case:

$$K_{\mathbf{I}}(T) = \frac{K_{CO}}{K_{CH_4} \cdot K_{H_2O}} \tag{5.159}$$

and

$$K_{\mathbf{II}}(T) = \frac{K_{CO}^2}{K_{CO_2} K_{CH_4}} \tag{5.160}$$

where,

$$K_i(T) = \exp\left(\frac{-\Delta\overline{g}^0_{f,T,i}}{\overline{R}T}\right) \tag{5.161}$$

Here, $\Delta\overline{g}^0_{f,T,i}$ is the Gibbs free energy function, which can be expressed in terms of the enthalpy of formation and a polynomial function of temperature. The ideal gas constant, $\overline{R}$, is 0.008314 kJ/mol K. Note that since the Gibbs free energy of H_2 is zero, K_{H_2} is unity, and thus does not appear in equations (5.159) and (5.160). Probstein *et al*. (2006b) suggested the following equation for $\Delta\overline{g}^0_{f,T,i}$:

$$\Delta\overline{g}^0_{f,T,i} = \overline{h}^0_{f,298,i} + c_1 T \ln T - c_2 T^2 - \left(\frac{c_3}{2}\right)T^3 - \left(\frac{c_4}{3}\right)T^4 + \left(\frac{c_5}{2T}\right) + c_6 + c_7 T \tag{5.162}$$

The constants for this equation can be found in Table 5.3.

Table 5.3 Constants for computing Gibbs free energy, $\Delta\overline{g}^0_{f,T,i}$, in equation (5.162) in kJ/mol, temperature, *T*, in degrees Kelvin (Probstein *et al*., 2006b)

Species	$\overline{h}^0_{f,298,i}$ (kJ/mol)	c_1	c_2	c_3	c_4	c_5	c_6	c_7
CH_4	-74.8	-4.620E-2	+1.130E-5	+1.319E-8	-6.647E-12	-4.891E+2	+1.411E+1	-2.234E-1
CO	-110.5	+5.619E-3	-1.190E-5	+6.383E-9	-1.846E-12	-4.891E+2	+8.684E-1	-6.131E-2
CO_2	-393.5	-1.949E-2	+3.122E-5	-2.448E-8	+6.946E-12	-4.891E+2	+5.270E+0	-1.207E-1
H_2O	-241.8	-8.950E-3	-3.672E-6	+5.209E-9	-1.478E-12	0	+2.868E+0	-1.722E-2

Now, using equations (5.151) through (5.154), (5.157), and (5.158), the chemical equilibrium problem can be solved. Combining equations (5.151) through (5.154), the mole fractions $y_{CO,g}$, $y_{CH_4,g}$, $y_{H_2,g}$, and $y_{H_2O,g}$ can be expressed in terms of $y_{CO_2,g}$ and $n_{tot,g}$:

$$y_{CO,g} = \frac{n_{C,in} - n_{H_2,in} - n_{N_2,g} + n_{tot,g}}{2n_{tot,g}} - y_{CO_2,g} \tag{5.163}$$

$$y_{CH_4,g} = \frac{n_{C,in} + n_{H_2,in} + n_{N_2,g} - n_{tot,g}}{2n_{tot,g}} \tag{5.164}$$

$$y_{H_2,g} = \frac{3n_{tot,g} - 4n_{O_2,in} - n_{C,in} - n_{H_2,in} - 2n_{H_2S,g} - 3n_{N_2,g}}{2n_{tot,g}} + y_{CO_2,g} \tag{5.165}$$

$$y_{H_2O,g} = \frac{4n_{O_2,in} + n_{H_2,in} - n_{C,in} + n_{N_2,g} - n_{tot,g}}{2n_{tot,g}} - y_{CO_2,g} \tag{5.166}$$

Next, combining equations (5.157) and (5.158):

$$\frac{K_{\mathbf{I}} y_{H_2O,g}}{y_{H_2,g}} = \frac{K_{\mathbf{II}} y_{CO_2,g}}{y_{CO,g}}$$

and plugging in equations (5.163), (5.165), and (5.166), and rearranging, a quadratic equation for $y_{CO_2,g}$ can be obtained in terms of $n_{tot,g}$:

$$\begin{aligned} 4n_{tot,g}^2\left(K_{\mathbf{I}} - K_{\mathbf{II}}\right)y_{CO_2,g}^2 - 2n_{tot,g}\left(4K_{\mathbf{I}}n_{O_2,in} + A_2K_{\mathbf{II}}\right)y_{CO_2,g} \\ + \left(4n_{O_2,in} - A_1\right)A_1K_{\mathbf{I}} = 0 \end{aligned} \tag{5.167}$$

The solution to this equation using the quadratic formula is:

$$y_{CO_2,g} = \frac{-b \pm \sqrt{b^2 - 16n_{tot,g}^2\left(K_{\mathbf{I}} - K_{\mathbf{II}}\right)\left(4n_{O_2,in} - A_1\right)A_1K_{\mathbf{I}}}}{8n_{tot,g}^2\left(K_{\mathbf{I}} - K_{\mathbf{II}}\right)} \tag{5.168}$$

where,

$$b = -2n_{tot,g}\left(4n_{O_2,in}K_{\mathbf{I}} + A_2K_{\mathbf{II}}\right)$$

$$A_1 = n_{C,in} - n_{H_2,in} - n_{N_2,g} + n_{tot,g}$$

$$A_2 = 3n_{tot,g} - 4n_{O_2,in} - n_{C,in} - n_{H_2,in} - 2n_{H_2S,g} - 3n_{N_2,g}$$

Values for $n_{tot,g}$ can be chosen in an iterative fashion, generating solutions for the mole fractions in equations (5.163) through (5.166) and (5.168). Then, checking if these solutions satisfy both equations (5.157) and (5.158), the true solution for the mole fractions and $n_{tot,g}$ may be determined; thus, establishing the composition of the producer gas exiting the gasifier chamber in Figure 5.12.

The higher heating value of the producer gas can be computed with the following expression.

$$HHV_{prod\ gas} = \sum\left(y_i * HHV_i\right) \tag{5.169}$$

Now, the analysis that was just discussed for the mass and energy balance about $CV_{gasifier}$ is really only necessary if the constituents and the heat value of the producer gas must be known. However, going back to Figure 5.12, the same reference control volume (CV_{ref}) that was used to model complete combustion (see Figure 5.9 and Figure 5.10) can be drawn around the combined process of gasification plus immediate combustion of the producer gas in a furnace. If air is the only oxidizer in the gasifier, then the gasifier-furnace system depicted in Figure 5.12 is thermodynamically equivalent to the solid burner depicted in Figure 5.10, since the same inputs (solid fuel and air) and same outputs (products of combustion and ash) flow in and out of CV_{ref} in both cases. ***Therefore, for the remainder of this paper, particularly in the discussion of small-scale on-the-farm combustion systems, the term "combustion" can either mean a solid fuel burner or a gasifier-furnace system.*** The analysis for complete oxidation of solid fuels presented in Section 5.3.1 can adequately model the mass and energy flows of both solid fuel burners and gasifier-furnace systems.

The one problem with this reasoning may come from loss on ignition (or leftover char or carbon) that may exit the gasifier with the bottom ash and slag. If this carbon loss is significant, then either the heat value of the solid fuel inputted into the model can be decreased (say by 10 to 20%) or an additional term can be written into the mass and energy balances (equations (5.112) and (5.134), respectively).

5.4. Modeling Manure-Based Biomass Combustion in Large Utility Coal-Fired Boilers

In order to model the economics of MBB combustion in large coal fired power plants, whether it be for co-firing or for reburning with coal, the power plant's operating conditions must first be known or computed. Plant operating parameters such as the capacity, the heat rate, the capacity factor, the annual operating hours, the ultimate analyses of the primary and co-fire (or reburn) fuels, the higher heating values of the fuels, and the percentage of the plant's heat rate supplied by each fuel are known or design variables. Other parameters such as the plant's overall heat energy consumption

rate, the mass fueling rates of the primary and co-fire (or reburn) fuels, the plant's overall thermal efficiency, and the various emissions can generally be computed from these inputs. Also, different blends of fuels may be assigned to the primary and reburn zones. Moreover, the moisture and ash percentages (before and after any drying and/or transportation process) of each of the fuels must be known as well.

After the plant's operating parameters and emissions are determined, then the drying, preparation and transportation of MBB can be modeled. Finally, the economics of all of these aspects to the overall biomass combustion system can be estimated.

5.4.1. Heat and Fueling Rates of Coal-fired Power Plants

Coal-fired power plants are usually defined by their electric capacity, $\mathscr{P}$, in MW. Typically, a power plant will have a number of separate units (say two or three), each with its own capacity, fuel and air injection systems, and emissions controls. Parameters that are typically known and considered design parameters are:

- the plant's heat rate, $\mathscr{K}$, is commonly expressed in Btu/kWh in the US (that is, Btu of heat supplied per kWh of electricity produced), but for this paper in which modeling equations are expressed in SI units, $\mathscr{K}$ will be expressed in kJ_{th}/kWh,
- the plant's capacity factor, %*CF*, which is the average annual percentage of capacity at which the plant is operating (i.e. actual electrical power production level divided by the electrical capacity),
- the plant's annual hours of operation, OH_{plant}, in hr/yr,
- the higher heating values of each of the fuels (coal, biomass, etc.), *HHV*, in kJ/kg, and

The power plant's overall, time rate consumption of heat, $\dot{Q}$, in kJ/s can be computed with the following expression:

$$\dot{Q} = \mathscr{K}\left(\frac{\%CF}{100}\right)\mathscr{P} * \left(\frac{1{,}000\ kJ_e / s}{MW_e}\right) * \left(\frac{1\ hr}{3600\ s}\right) \tag{5.170}$$

The plant's overall efficiency percentage may be computed as:

$$\eta_{plant} = \frac{1}{\mathcal{K}} * \left(\frac{3600\ s}{1\ hr} \right) * (100\%) \tag{5.171}$$

The required mass rate of fuel required to satisfy the plant's time rate of heat consumption, in kg/s, is:

$$\dot{m}_{coal} = \frac{\dot{Q}}{HHV_{coal,as\ fired}} = \frac{\dot{Q}}{HHV_{coal,DAF} * \left(1 - {\%M_{coal}}/{100} - {\%A_{coal}}/{100} \right)} \tag{5.172}$$

If the chemical composition of the coal (ultimate analysis) is known, then equations (5.123) through (5.125) can be used to find the amount of air required to burn the coal in the furnace, as well as the emissions of CO_2, H_2O, N_2, SO_2, and O_2 in the exhaust gas, assuming complete combustion.

5.4.2. Coal-fired Power Plant Emissions

Co-firing and reburning coal with MBB can at least affect four different emissions from coal-fired power plants: NO_x, SO_x, ash, and nonrenewable CO_2. However, before discussing MBB's impact on these emissions, some knowledge of the production of these emissions during regular operations, before any biomass is utilized, must be obtained.

5.4.2.1. NO_x from primary burn zones

In coal plants, the main source of NO_x is fuel-bound nitrogen. Seventy to 80 percent of the NO_x produced from coal combustion is generated from the oxidation of HCN and NH_3 emitted during the primary pyrolysis of volatile nitrogen, secondary pyrolysis of tar nitrogen, and heterogeneous combustion of char nitrogen.

To simplify the analysis, instead of generating an equilibrium model to estimate the NO_x emission from coal combustion, base NO_x level assumptions will be adopted from the US EPA's Integrated Planning Model (IPM) for predicting emissions, electric capacity, and economic costs of utility power generators. In Table 5.4 the levels of

uncontrolled NO_x from coal combustion ($\mathcal{L}_{uncontrolled,NOx}$), assuming that no primary controls such as low-NO_x burners are installed on the power plant, are listed for different boiler types and coal ranks in g/GJ_{th}.

Table 5.4 Uncontrolled NO_x levels for wall and tangentially fired coal-fired power plants, assuming no primary or secondary NO_x control technologies are used (USEPA, 2006)

Boiler Type	Coal Type	Uncontrolled Base NO_x Levels (g/GJ_{th}), $\mathcal{L}_{uncontrolled,NOx}$
Wall fired	Bituminous	640.20
	Sub-bituminous/lignite	348.90
Tangentially fired	Bituminous	330.16
	Sub-bituminous/lignite	217.68

However, most coal-fired boilers in the US do have special low-NO_x burners that decrease NO_x emissions from the primary burn region to more acceptable levels. The extent to which NO_x levels are reduced by primary controls depends on the type of boiler, the type of coal, and the type of low-NO_x burner and over fire air configuration. The EPA suggested the following expression for computing the average NO_x levels achieved by primary controls, $\mathcal{L}_{primary,NO_x}$, in g/GJ_{th}.

$$\mathcal{L}_{primary,NOx} = \mathcal{L}_{uncontrolled,NOx}\left[1-\left(a+b*\mathcal{L}_{uncontrolled,NOx}\right)\right] \tag{5.173}$$

The values of constants *a* and *b* are listed in Table 5.5 for different primary controls installed on wall-fired and tangentially-fired boilers.

Table 5.5 Constants for equation (5.173), used to determine NO_x levels, in g/GJ_{th}, attained by primary NO_x controls (USEPA, 2006)

Boiler Type	Coal Type	Primary NO_x Control*	*a* in equation (5.173)	*b* in equation (5.173)
Wall-fired	Bituminous	LNB	0.163	6.3263E-4
		LNBO	0.313	6.3263E-4
	Sub-bituminous/ lignite	LNB	0.135	12.5828E-4
		LNBO	0.285	12.5828E-4
Tangentially-fired	Bituminous	LNC1	0.162	7.8149E-4
		LNC2	0.212	7.8149E-4
		LNC3	0.362	7.8149E-4
	Sub-bituminous/ lignite	LNC1	0.200	16.6764E-4
		LNC2	0.250	16.6764E-4
		LNC3	0.350	16.6764E-4

*LNB = low-NOx burner; LNBO = LNB with over fire air; LNC1 = LNB with close-coupled OFA; LNC2 = LNB with separated OFA; and LNC3 = LNB with both close-coupled and separated OFA.

Nitrogen oxide emissions can also be expressed in different ways when reporting them to regulatory agencies such as the EPA. The NO_x level computed with equation (5.173) is a ratio of mass of pollutant and energy consumed, but NO_x can also be expressed as a ratio of mass of pollutant and electrical energy delivered by the plant, g/kWh.

$$\mathcal{L}'_{primary,NO_x} = \mathcal{L}_{primary,NO_x} * \mathcal{H} * \left(\frac{1\,GJ}{10^6\ kJ} \right) \tag{5.174}$$

The emission index, EI_{NOx} (g NO_x / kg fuel), can be computed with the following:

$$EI_{NOx} = \mathcal{L}_{primary,NOx} * HHV_{coal,as\ fired} * \left(\frac{1\,GJ}{10^6\ kJ} \right) \tag{5.175}$$

The annual NO_x emission, $\mathcal{E}_{NOx}$, can be computed with the following equation, in metric tons per year:

$$\mathcal{E}_{NO_x,hourly} = \mathcal{L}_{primary,NO_x} * \left(\frac{1\ metric\ ton}{10^6\ g} \right) * \dot{Q} * \left(\frac{1\,GJ}{10^6\ kJ} \right) * \left(\frac{3600\ s}{1\,hr} \right) \tag{5.176}$$

$$\mathcal{E}_{NO_x,annum} = \mathcal{E}_{NO_x,hourly} * OH_{plant} \tag{5.177}$$

In order to find the kmole (or volume) fraction of NO_x in the exhaust from the primary burn region, equations (5.125) for the number of kmoles of each element, $N_{k,out}$, in the exhaust can be used in the following equation.

$$fraction_{NO_x} = \frac{EI_{NOx} * \left(\frac{1\,kg}{1{,}000\,g} \right) * \left(100\,kg\ fired\right) / MW_{NO_2}}{\sum_{out,dry} N_{k,out}} \tag{5.178}$$

Typically, kmole fractions are reported on a dry basis, thus $N_{H_2O_{(g)},out}$ will be left out of the summation in the denominator of equation (5.178). Moreover, by convention, the molecular weight of NO_2 (MW_{NO_2} = 46) is used when reporting NO_x emissions because the species NO is quickly converted to NO_2 in the atmosphere, and NO_2 is more germane to the health effects from NO_x emissions. The fraction can also be expressed in parts per million (ppm) of NO_x.

$$ppm_{NOx} = fraction_{NOx} * 10^6 \tag{5.179}$$

Molar fractions of emissions, such as NO_x, are also reported on a standard oxygen percentage basis to avoid any distortion of pollutant emissions by diluting the exhaust with air. The standard oxygen level, $\%O_{standard}$, in the exhaust is defined as:

$$\begin{aligned} \frac{\%O_{standard}}{100} &= \frac{N_{O_2,out}}{\sum_{out,dry,standard} N_{k,out}} \\ &= \frac{N_{O_2,out}}{N_{CO_2,out} + N_{N_2,out} + N_{SO_2,out} + N_{O_2,out}} \end{aligned} \tag{5.180}$$

Inserting equations (5.125) into (5.180) and solving for $\%EA$, the equivalent excess air percentage ($\%EA_{standard}$) to the standardized oxygen percentage for a fuel with an empirical formula, $C_C H_H N_N O_O S_S$, can be computed.

$$\%EA_{standard} = \frac{\left(\frac{\%O_{standard}}{100} \right) * \left[C + \frac{N}{2} + S + \frac{79}{21}\left(C + \frac{H}{4} + S - \frac{O}{2} \right) \right]}{\left[1 - \left(\frac{\%O_{standard}}{100} \right)\left(1 + \frac{79}{21} \right) \right] * \left(C + \frac{H}{4} + S - \frac{O}{2} \right)} * 100\% \tag{5.181}$$

The standard oxygen level, $\%O_{standard}$, for coal fired utility boilers is usually either 3% or 15%. Next, plug in $\%EA_{standard}$ to equations (5.125) for $\%EA$ and compute $\sum_{out,dry,standard} N_{k,out}$. The corrected $fraction_{NOx}$ (and subsequently ppm_{NOx}) for the standard oxygen level is computed with the following expression.

$$fraction_{NOx,standard} = fraction_{NOx,actual} * \frac{\sum_{out,dry,actual} N_{k,out}}{\sum_{out,dry,standard} N_{k,out}} \tag{5.182}$$

The NO_x reduction percentage achieved by the primary NO_x controls can be computed as:

$$\%\mathcal{R}_{primary,NOx} = \frac{\left(\mathcal{L}_{uncontrolled,NOx} - \mathcal{L}_{primary,NOx}\right)}{\mathcal{L}_{uncontrolled,NOx}} * 100\% \tag{5.183}$$

and the annual NO_x reduction is simply:

$$\mathcal{R}_{primary,NO_x} = \mathcal{E}_{uncontrolled,NO_x} - \mathcal{E}_{primary,NO_x} \tag{5.184}$$

5.4.2.2. Ash from coal

The amount of ash in MBB may be the greatest obstacle when co-firing and reburning with coal in large utility coal plants. Although most coals and lignite do not contain as much ash as MBB (even low-ash MBB), it is first necessary to estimate how much ash is produced when only coal is burned. The ash production level of the power plant, $\mathcal{L}_{ash}$, may be computed, in kg/GJ, with the following expression.

$$\mathcal{L}_{ash} = \frac{\left(\%A_{coal} \big/ 100\right)}{HHV_{coal,as\ fired}} * \left(\frac{10^6\ kJ}{1\ GJ}\right) \tag{5.185}$$

The hourly and annual emission of ash may be computed in much the same way as NO_x emissions.

$$\mathcal{E}_{ash,hourly} = \mathcal{L}_{ash} * \left(\frac{1\ metric\ ton}{1{,}000\ kg}\right) * \dot{Q} * \left(\frac{1\ GJ}{10^6\ kJ}\right) * \left(\frac{3600\ s}{1\ hr}\right) \tag{5.186}$$

$$\mathcal{E}_{ash,annum} = \mathcal{E}_{ash,hourly} * OH_{plant} \tag{5.187}$$

5.4.2.3. CO_2 from coal

Again, the emission of CO_2 from burning coal may be obtained from the results of the earlier complete combustion analysis found in equation (5.125). Here, $\mathcal{L}_{CO_2}$ is expressed in kg/GJ.

$$\mathcal{L}_{CO_2} = \frac{\left(N_{CO_2,out}/100\ kg\ fired\right)}{HHV_{coal,as\ fired}} * MW_{CO_2} * \left(\frac{10^6\ kJ}{1\ GJ}\right) \tag{5.188}$$

Next, $\mathcal{E}_{CO_2}$, can be computed as was done in equations (5.186) and (5.187).

5.4.2.4. SO_2 from coal

The emission of SO_2 from burning coal may also be obtained from the results of the earlier complete combustion analysis found in equation (5.125). Here, just as with ash and CO_2, $\mathcal{L}_{SO_2}$ is expressed in kg/GJ.

$$\mathcal{L}_{SO_2} = \frac{\left(N_{SO_2,out}/100\ kg\ fired\right)}{HHV_{coal,as\ fired}} * MW_{SO_2} * \left(\frac{10^6\ kJ}{1\ GJ}\right) \tag{5.189}$$

Next, $\mathcal{E}_{SO_2}$, can be computed as was done in equations (5.186) and (5.187).

5.4.3. Co-firing Coal with Manure-based Biomass

The general idea of co-firing coal with MBB is illustrated in Figure 5.13. Depending on how much the biomass contributes to the overall heat rate of the plant, the coal and MBB can be blended and then injected into the primary burn region of the furnace or, if the mass flow rate is too great to be handled by one fuel injector, separate streams of coal and MBB can be fired simultaneously in the primary burn region. However, both of these cases are modeled the same way here. Additional biomass injection systems will only impact the economics portion of the model which will be discussed later.

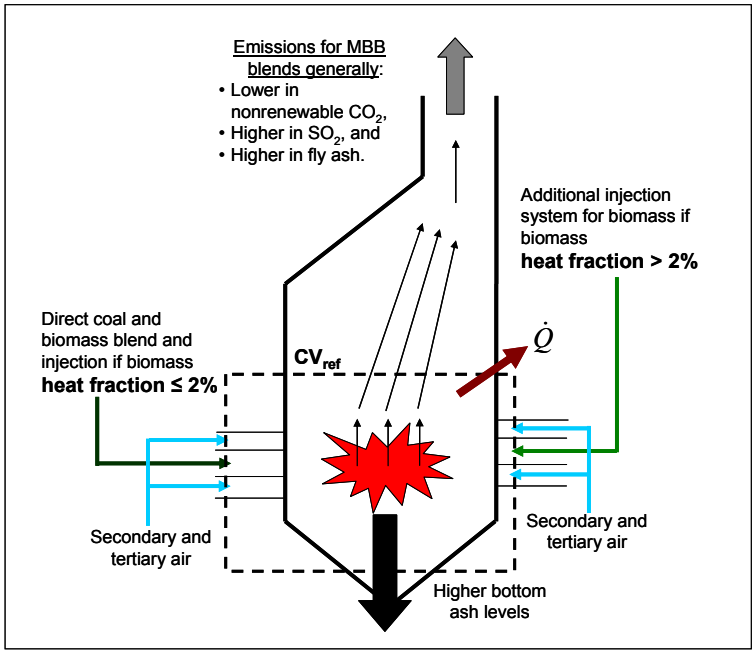

Figure 5.13 Co-firing coal with biomass

When MBB is fired along with coal in the primary burn region of an existing combustion facility, the overall fuel mass injected into the burner as well as the emissions of ash, CO_2, SO_x, and possibly NO_x will change. In order to forecast the economic cost and benefits of co-firing biomass with coal, these changes must be understood.

This analysis may begin by defining the biomass co-fire mass fraction as:

$$mf_{MBB} = \frac{\dot{m}_{MBB}}{\dot{m}_{coal} + \dot{m}_{MBB}} \tag{5.190}$$

Next, with if the moisture and ash percentage of both the MBB and coal are known, along with the dry, ash-free contents of both fuels, equations (5.111) can be computed for the two fuels fired in the boiler. Next, the moisture and ash contents of the blend can be computed:

$$\%M_{blend} = \left(1 - mf_{MBB}\right) * \%M_{coal} + mf_{MBB} * \%M_{MBB} \tag{5.191}$$

$$\%A_{blend} = \left(1 - mf_{MBB}\right) * \%A_{coal} + mf_{MBB} * \%A_{MBB} \tag{5.192}$$

Moreover, in a similar fashion to equations (5.111), the combustible content of the blend can be computed as:

$$\begin{aligned} C_{blend} &= \left(1 - mf_{MBB}\right) * C_{coal} + mf_{MBB} * C_{MBB} \\ H_{blend} &= \left(1 - mf_{MBB}\right) * H_{coal} + mf_{MBB} * H_{MBB} \\ N_{blend} &= \cdots \\ O_{blend} &= \cdots \\ S_{blend} &= \cdots \end{aligned} \tag{5.193}$$

Now, equations (5.112), (5.114), (5.118) through (5.120), and (5.123) through (5.134) can be computed with $\%M_{blend}$, $\%A_{blend}$, and C_{blend} through S_{blend} for the case in which coal is co-fired with MBB in the primary burn region of a power plant. Note that the inputs and outputs of CV_{ref} in Figure 5.13 are the same as the inputs and outputs in CV_{ref} in Figure 5.9. The higher heat value of the fuel blend can also be expressed as:

$$HHV_{blend} = \left(1 - mf_{MBB}\right) * HHV_{coal} + mf_{MBB} * HHV_{MBB} \tag{5.194}$$

Referring to equation (5.170); which is used to relate the power plant's overall consumption of heat, $\dot{Q}$, to the electric capacity, $\mathscr{P}$, capacity factor, $\%CF$, and heat rate, $\mathscr{K}$; theoretically $\dot{Q}$ should stay the same during co-firing since the $\mathscr{P}$ and $\%CF$ will be the same. That is, the electric demand on the power plant will remain the same regardless of the fuels being fired or the blend's mass fraction mf_{MBB}. However, in reality, it is possible that $\mathscr{K}$ may increase (and hence η_{plant} decrease) with mf_{MBB}, since MBB has higher ash content than coal, which will cause fouling of heat exchanger surfaces and lower flame temperatures. If ash is not removed sufficiently, then co-firing with MBB may significantly increase $\dot{Q}$, and hence increase the power plant's fuel consumption:

$$\dot{m}_{total} = \dot{m}_{coal} + \dot{m}_{MBB} = \frac{\dot{Q}}{HHV_{blend}} \tag{5.195}$$

When MBB is blended with coal, the HHV of the blend will decrease, which will also increase the total fuel consumption, $\dot{m}_{total}$. This phenomenon can easily be described by the equations (5.194) and (5.195). On the other hand, it is more difficult to predict how

$\dot{Q}$ will change with mf_{MBB}, because this change will depend on the ash removal operations and frequency of ash removal of the plant and the general ability to prevent fouling on heat exchanger surfaces. For this study, therefore, it will be assumed that $\dot{Q}$ remains the same when co-firing, which physically means that additional ash loading on the boiler will not significantly affect $\mathcal{K}$. Yet for future work, and for specific applications, it may be possible to find how $\dot{Q}$ will increase when co-firing coal with MBB, by finding a relation such that:

$$\mathcal{K} = \mathcal{K}\left(mf_{MBB}, \%A_{MBB}, \%A_{coal}, \textit{ash removal system}, \ldots\right)$$

Moving on, it may be necessary to convert the mf_{MBB} to a heat fraction, hf_{MBB}, defined as:

$$hf_{MBB} = \frac{\dot{Q}_{MBB}}{\dot{Q}} = \frac{\dot{Q}_{MBB}}{\dot{Q}_{coal} + \dot{Q}_{MBB}} = \frac{\dot{m}_{MBB} HHV_{MBB}}{\dot{m}_{coal} HHV_{coal} + \dot{m}_{MBB} HHV_{MBB}} \tag{5.196}$$

Since, the fuel consumptions of coal and MBB can be expressed in terms of mf_{MBB}:

$$\dot{m}_{coal} = \left(1 - mf_{MBB}\right)\dot{m}_{total} \tag{5.197}$$

$$\dot{m}_{MBB} = mf_{MBB}\dot{m}_{total} \tag{5.198}$$

The heat fraction can be expressed as:

$$hf_{MBB} = \frac{mf_{MBB} HHV_{MBB}}{\left(1 - mf_{MBB}\right) HHV_{coal} + mf_{MBB} HHV_{MBB}} \tag{5.199}$$

Although there is a definite requirement of increasing the overall fueling rate when co-firing coal with MBB, the tradeoff is the possibility that emissions will have a net change that will positively affect the environment and perhaps even the bottom line economics of the power plant if cap and trade or emission taxes are in place. As discussed earlier, it is currently not clear if co-firing with MBB will increase or decrease NO_x. For now, it will be assumed that co-firing does not significantly change NO_x emissions.

Ash emissions, however, will definitely increase when co-firing with MBB. The level of ash production from co-firing, $\mathcal{L}_{ash,cofiring}$, can be found in kg/GJ:

$$\mathcal{L}_{ash,cofiring} = \frac{\left(1-mf_{MBB}\right)\left(\frac{\%A_{coal}}{100}\right)+mf_{MBB}\left(\frac{\%A_{MBB}}{100}\right)}{\left(1-mf_{MBB}\right)HHV_{coal}+mf_{MBB}HHV_{MBB}} * \left(\frac{10^6\ kJ}{1\ GJ}\right) = \frac{\left(\frac{\%A_{blend}}{100}\right)}{HHV_{blend}} * \left(\frac{10^6\ kJ}{1\ GJ}\right) \tag{5.200}$$

This level can be compared to the ash level before co-firing computed in equation (5.185) by simply computing a difference:

$$\Delta\mathcal{L}_{ash} = \mathcal{L}_{ash,cofiring} - \mathcal{L}_{ash} \tag{5.201}$$

Hourly and annual ash production rates can also be computed much the same way as was done in equations (5.186) and (5.187).

The level of total CO_2 may increase when co-firing coal with MBB, which can be expressed by the following equation:

$$\mathcal{L}_{CO_2,cofiring} = \frac{\left(1-mf_{MBB}\right)\left(\frac{C_{coal}}{100}\right)+mf_{MBB}\left(\frac{C_{MBB}}{100}\right)}{\left(1-mf_{MBB}\right)HHV_{coal}+mf_{MBB}HHV_{MBB}} * MW_{CO_2} * \left(\frac{10^6\ kJ}{1\ GJ}\right) = \frac{\left(\frac{C_{blend}}{100}\right)}{HHV_{blend}} * MW_{CO_2} * \left(\frac{10^6\ kJ}{1\ GJ}\right) \tag{5.202}$$

However, if MBB is considered a renewable fuel source in which the CO_2 generated from its combustion does not add to the overall loading in the atmosphere, then the only CO_2 that is reported are emissions from the coal.

$$\mathcal{L}_{CO_2,cofiring,reported} = \frac{\left(1-mf_{MBB}\right)\left(\frac{C_{coal}}{100}\right)}{HHV_{blend}} * MW_{CO_2} * \left(\frac{10^6\ kJ}{1\ GJ}\right) \tag{5.203}$$

The reduction percentage of non-renewable CO_2 is then computed with the following:

$$\%\mathcal{R}_{CO_2,cofiring} = \frac{\mathcal{L}_{CO_2} - \mathcal{L}_{CO_2,cofiring,reported}}{\mathcal{L}_{CO_2}} * 100\% \tag{5.204}$$

Hourly and annual reductions, $\mathcal{R}_{CO_2,cofiring}$, can also be computed from emission rates, $\mathcal{E}_{CO_2,cofiring}$.

Sulfur emissions may become a setback during co-firing and reburning if the sulfur content of the MBB is significantly higher than coal on a "per energy" basis. This is especially true when using MBB to replace low sulfur coals such as Wyoming sub-bituminous. Moreover, many coal plants that burn low sulfur coals do not have flue gas desulphurization systems, which means that any additional SO_2 released when co-firing coal with MBB will be added to the exhaust emissions of the power plant. The SO_2 emission level during co-firing operations can be computed with the following:

$$\dot{\mathcal{L}}_{SO_2,cofiring} = \frac{\left(1-mf_{MBB}\right)\left(\frac{S_{coal}}{100}\right)+mf_{MBB}\left(\frac{S_{MBB}}{100}\right)}{\left(1-mf_{MBB}\right)HHV_{coal}+mf_{MBB}HHV_{MBB}} * MW_{SO_2} * \left(\frac{10^6\ kJ}{1\ GJ}\right) \quad (5.205)$$

This level can be compared to the SO_2 level before co-firing computed in equation (5.189) by simply computing a difference:

$$\Delta\dot{\mathcal{L}}_{SO_2} = \dot{\mathcal{L}}_{SO_2,cofiring} - \dot{\mathcal{L}}_{SO_2} \quad (5.206)$$

Hourly and annual ash production rates can also be computed much the same way as was done in equations (5.186) and (5.187). However, during these calculations it is essential to account for different operating hours of the co-fire system (OH_{cofire}) and the power plant (OH_{plant}). The power plant may not co-fire coal and biomass the entire time it is operating.

5.4.4. Reburning Coal with Manure-based Biomass

With respect to the mathematical modeling in this study, reburning is simply a special type of co-firing in which NO_x emissions are significantly reduced when utilizing MBB in coal-fired power plants. The general idea of reburning is depicted in Figure 5.14. Coal is burned in the primary burn region, and then burned again with MBB (or some other reburn fuel) in a secondary burn region under fuel-rich conditions. Over-fire air is then injected to complete the combustion and avoid any CO or unburned hydrocarbon emissions. The reburn fuel (RF) provides between 10 and 20% of the power plants overall heat input. The RF is usually natural gas, but can also be oil, biomass, more coal; or any other hydrocarbon-based fuel. The primary burn region will

be referred to as the primary zone (PZ) and the secondary burn region will be referred to as the reburn zone (RZ).

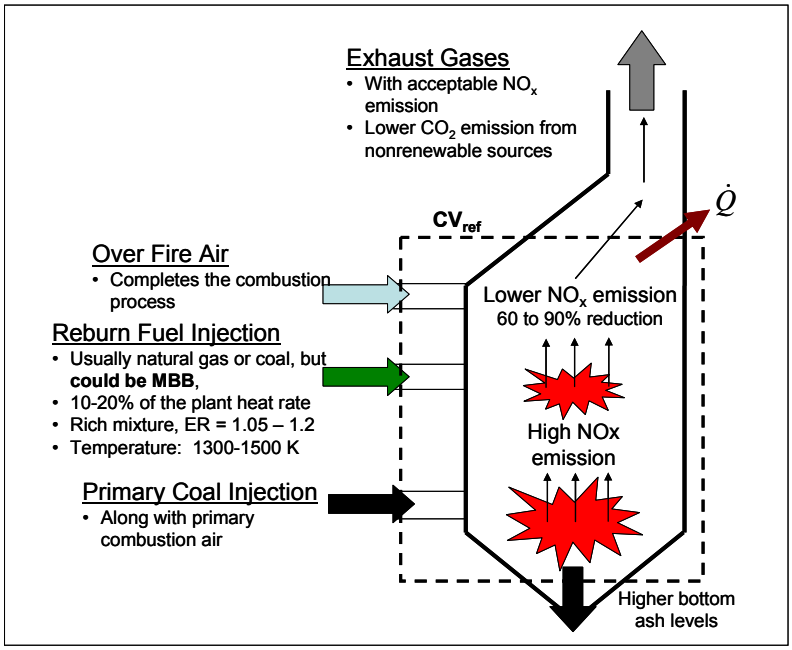

Figure 5.14 Reburning coal with biomass

Usually when discussing reburn technology, the *hf* is prescribed instead of the *mf*, but one can be converted to the other using equation (5.199). Also, variables in the reburn model will generally have subscripts RF and PF to denote reburn fuel and primary fuel. For example, the heat generated by the reburn fuel and the primary fuel are:

$$\dot{Q}_{RF} = hf_{RF}\dot{Q} \tag{5.207}$$

and

$$\dot{Q}_{PF} = \left(1 - hf_{RF}\right)\dot{Q} \tag{5.208}$$

respectively. The power plant's total heat consumption, $\dot{Q}$, may still be computed with equation (5.170). Equations (5.191) through (5.194) can also be used for reburning with the RF and PF notation, since thermodynamically co-firing and reburning are similar processes. The control volume problem, CV_{ref} introduced in Figure 5.9, is applicable to

both the reburn and co-fire analysis. Therefore, the earlier equations (5.112), (5.114), (5.118) through (5.120), and (5.123) through (5.134) may also be used, noting that %*EA* includes the over-fire air in the reburn fuel staging.

More sophisticated reburn models that attempt to predict the NO_x reductions from reburning must first contain a mass and energy balance, as well as an equilibrium analysis for both the PZ and the RZ. However, since the primary purpose of the current model is to describe the economic impacts of reburning coal with MBB at large coal-fired power plants, computations can be greatly simplified if the NO_x level achieved by reburning with MBB, $\mathcal{L}_{reburn,NO_x}$, is treated as an input to the model. As discussed in the Background Information Section of this dissertation, $\mathcal{L}_{reburn,NO_x}$ can be as low as 26 g/GJ (0.06 lb/MMBtu) when reburning with MBB. The NO_x reduction from reburning, $\%\mathcal{R}_{reburn,NOx}$, or any other secondary NO_x control technology, can be measured from either one of two data: (1) the NO_x level achieved by the primary NO_x control (e.g. low-NO_x burner) and (2) the uncontrolled NO_x level generated when neither primary nor secondary controls are used.

$$\%\mathcal{R}_{reburn,NOx} = \frac{\mathcal{L}_{primary,NOx} - \mathcal{L}_{reburn,NOx}}{\mathcal{L}_{primary,NOx}} * 100\% \tag{5.209}$$

or

$$\%\mathcal{R}_{reburn,NOx,total} = \frac{\mathcal{L}_{uncontrolled,NOx} - \mathcal{L}_{reburn,NOx}}{\mathcal{L}_{uncontrolled,NOx}} * 100\% \tag{5.210}$$

In some cases, the power plant may not utilize the reburn fuel throughout the year. For example, reburning may only be conducted during a summer ozone season, when regulations on NO_x emissions are more stringent. For this case, the annual reburn operation hours, OH_{reburn}, will be different from the plant's operating hours, and so the annual NO_x emission, in metric tons per year, can be computed as:

$$\begin{aligned}\mathcal{E}_{NOx,annum} = &\left[\mathcal{L}_{reburn,NOx} OH_{reburn} + \mathcal{L}_{primary,NOx}\left(OH_{plant} - OH_{reburn}\right)\right] * \dot{Q} \\ &* \left(\frac{1\,metric\ ton}{10^6\ g}\right) * \left(\frac{1\,GJ}{10^6\ kJ}\right) * \left(\frac{3600\,s}{1\,hr}\right)\end{aligned} \tag{5.211}$$

Ash, nonrenewable CO_2, and SO_2 emissions are computed in the same manner as with co-firing. Annual emissions of these pollutants must also take into account any differing operation hours for reburning as was done in equation (5.211).

5.4.5. Comparing Reburning to Other Secondary NO_x Control Technologies

On top of modeling MBB reburn systems installed on large coal plants, a comparison to other, more commercial secondary NO_x control technologies should also be made in order to determine if power companies and plant proprietors should opt to install biomass reburn systems over these more common reduction methods. In the US, the most common secondary NO_x control technologies are selective catalytic reduction (SCR) and selective non-catalytic reduction (SNCR).

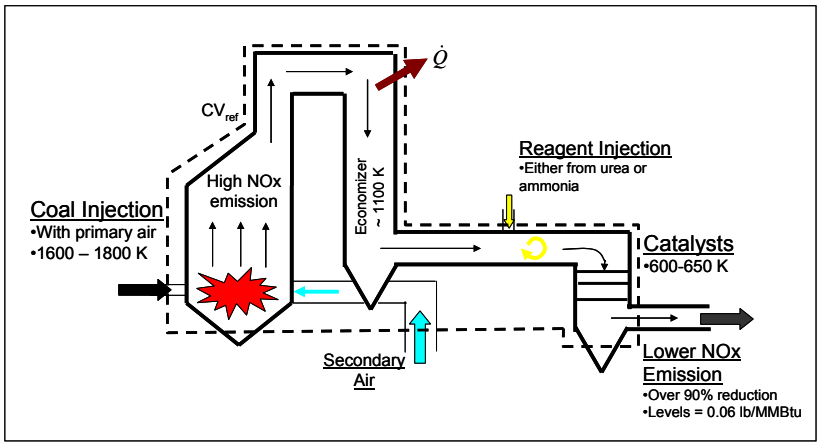

Figure 5.15 Selective catalytic reduction modeling

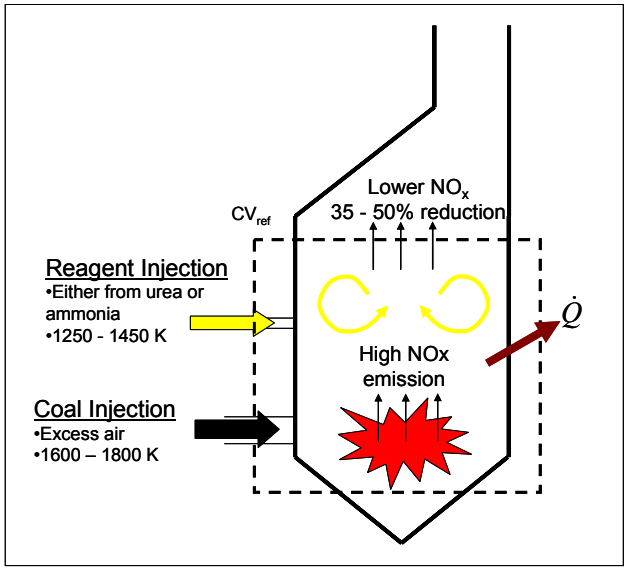

Figure 5.16 Selective non-catalytic reduction modeling

In Figure 5.15 and Figure 5.16, it can be seen that the same combustion analysis that was conducted for the control volume (CV_{ref}) problem in Figure 5.9 can be used here, except for the fact that a reagent (usually ammonia or urea) is injected into the control volume. However, for this model it will be assumed that the reagent does not significantly add to the heat input of the plant, and thus does not alter the coal consumption of the power plant. Hence, for the SCR and SNCR cases, the combustion problem is treated as if coal alone is fired, without any biomass. Equations (5.112), (5.114), (5.118) through (5.120), and (5.123) through (5.134), as well as equations (5.170) through (5.188) are still applicable for the SCR and SNCR cases, with the exception that NO_x levels will now be reduced to some level $\mathcal{L}_{SCR,NOx}$ or $\mathcal{L}_{SNCR,NOx}$. NO_x reduction percentages can then be computed as they were for MBB reburning in equation (5.210). For example:

$$\%\mathcal{R}_{SCR,NOx,total} = \frac{\mathcal{L}_{uncontrolled,NOx} - \mathcal{L}_{SCR,NOx}}{\mathcal{L}_{uncontrolled,NOx}} * 100\% \tag{5.212}$$

and

$$\mathcal{E}_{NOx,annum} = \left[\mathcal{L}_{SCR,NOx} OH_{SCR} + \mathcal{L}_{primary,NOx} \left(OH_{plant} - OH_{SCR} \right) \right] * \dot{Q} * \left(\frac{1\, metric\ ton}{10^6\ g} \right) * \left(\frac{1\, GJ}{10^6\ kJ} \right) * \left(\frac{3600\ s}{1\, hr} \right) \quad (5.213)$$

5.5. Modeling Small-Scale, On-the-farm Manure-Based Biomass Combustion Systems

Manure-based biomass may also be utilized on smaller scale combustion systems located on or very near large animal feeding operations. The primary purpose of these combustion systems would be to incinerate manure wastes not used for fertilizer, compost, or other external purposes. These systems would be particularly useful in situations were few application fields or crop lands exist near the feeding operation or when there are local environmental laws or mandates that restrict the size of manure storage structures such as anaerobic treatment lagoons. Combustion systems can also alleviate odor problems on large animal feeding operations.

As discussed in the Literature Review section of this dissertation, there have been several designs, and even at least one demonstration system, for local thermo-chemical conversion of MBB. In these systems, there have been several common aspects such as: (1) the separation of high moisture manure streams into a solid manure portion and a liquid wastewater portion, (2) aggressive usage of waste heat, (3) drying of high moisture solids, and (4) the recycling of wastewater. In addition to previous work conducted by Carlin (2005) and Carlin *et al*. (2007), these facets can be added to the system shown in Figure 3.8 to form a revised conceptual design that is inclusive of most of these aspects. Although most of the discussion here will center on the disposal of high moisture MBB, simpler systems with much of the same design characteristics can also be designed to handle lower moisture solid MBB from feedlots, large corrals, and open lot dairies.

5.5.1. Combustion System for High Moisture Manure-based Biomass

A revised conceptualized thermo-chemical conversion system for high moisture MBB is shown in Figure 5.17. This system, if installed at or near a large animal feeding operation, has the potential to burn most of the manure solids and vaporize at least a portion of the wastewater generated from the feeding operation. The flushed manure can be mechanically separated into solid and liquid streams. The solids can then be dried, in this case using an indirect rotary steam-tube dryer, which was discussed earlier. The dried solids can then be injected into a combustor, which can be a solid fuel burner but probably would have to be a gasifier-burner system due to ash fouling. However, the mass and energy balances for both these systems are equivalent (see Section 5.3.2). The combustion air may be preheated before it is injected along with the manure solids. Meanwhile, some of the wastewater from the solids separator may be sent back to the animal housing units for further flushing or to storage or treatment lagoons for later irrigation or fertilizer uses. The rest of the wastewater would be pumped to a fire-tube boiler where it can be vaporized by heat pipes containing the hot gaseous products of combustion. The remaining solids that were contained in the vaporized wastewater can be removed periodically from the boiler (similar to blow down in conventional fire-tube boilers) and either sent back to the combustor or used as fertilizer. The steam produced in the fire-tube boiler can be used for drying solids, preheating combustion air, or for external uses such as hot water generation for milking center cleanup, space heating at feeding operations located in northern states, production of cattle feed in steam flaking mills, or any other process on or near the farm that may require steam and make the combustion system profitable.

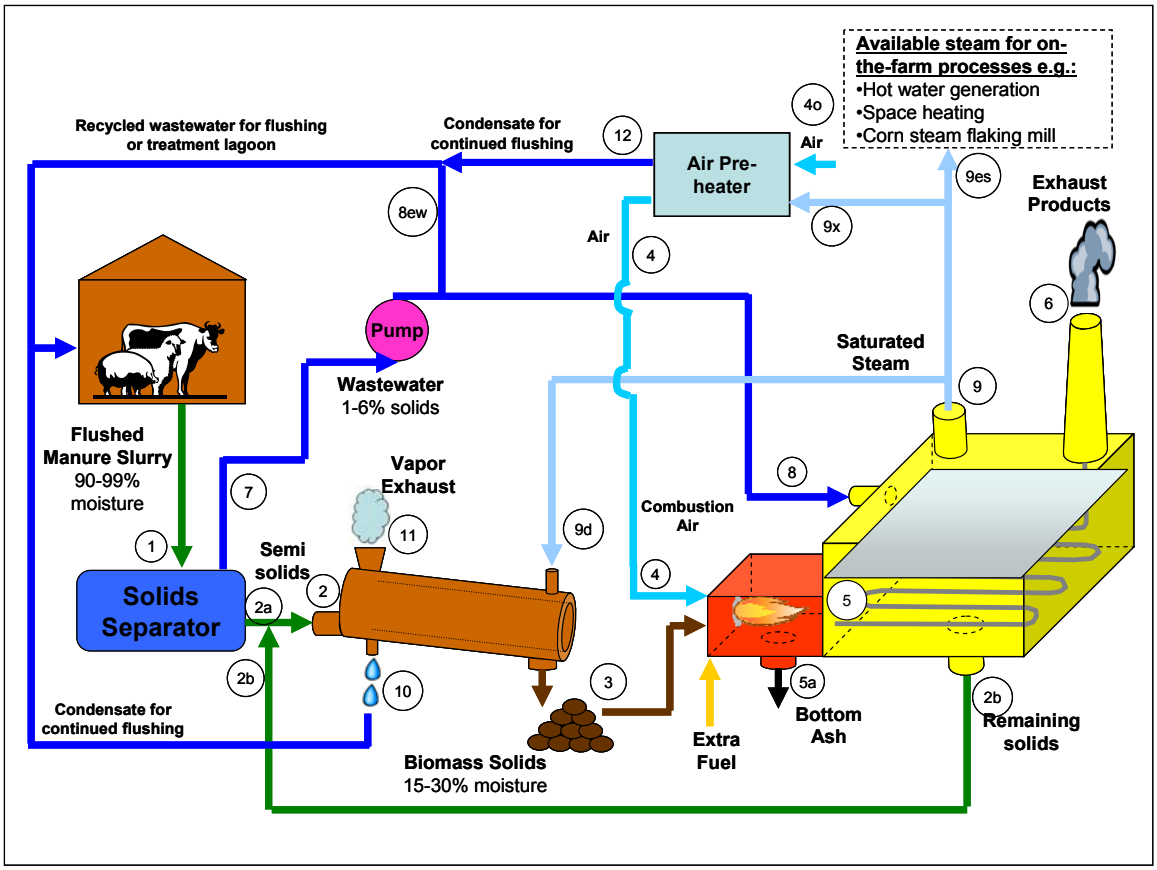

Figure 5.17 Conceptualized design of MBB thermo-chemical energy conversion system for large free stall dairies or large indoor piggeries with flush waste disposal systems

The generalized equations presented earlier for drying and burning biomass can be applied to this system, but the mass and energy balances can become complicated. Moreover, if extra fuel is added to the combustor, the analysis becomes slightly more complicated.

The analysis of this system can begin with a mass balance about the solids separator. It is important to remember that the MBB flows at points 1, 2a, and 7 in Figure 5.17 all contain solid and moisture fractions. The solid separator will probably not remove all of the solids from the flushed manure. The mass balance of dry solids entering and exiting the separator can be expressed as the following:

$$\dot{m}_{MBB,dry,1} = \dot{m}_{MBB,dry,7} + \dot{m}_{MBB,dry,2a} \tag{5.214}$$

where $\dot{m}_{MBB,dry,1}$ is the flow rate of dry biomass entering the solid separator, $\dot{m}_{MBB,dry,7}$ is the relatively small amount of biomass solids remaining in the wastewater exiting the solids separator, and $\dot{m}_{MBB,dry,2a}$ is the dry fraction of the separated solids. But each of these points also has a moisture fraction. The flow of moisture in and out of the separator can be expressed as:

$$\dot{m}_{MBB,dry,1}\omega_{MBB,1} = \dot{m}_{MBB,dry,7}\omega_{MBB,7} + \dot{m}_{MBB,dry,2a}\omega_{MBB,2a} \tag{5.215}$$

where $\omega_{MBB,i}$ is the moisture content of the MBB in each point, *i*. Recall that ω_i can be converted to a moisture percentage, $\%M_i$, or fraction, $mf_{H_2O,i}$, with equation (5.12). Also note that:

$$\begin{aligned} \dot{m}_{MBB,i} &= \dot{m}_{MBB,dry,i}\left(1+\omega_{MBB,i}\right) \\ &= \dot{m}_{MBB,dry,i}\left(\frac{1}{1-\%M_i/100}\right) \\ &= \dot{m}_{MBB,DAF,i}\left(\frac{1}{1-\%A_{dry,i}/100}\right)\left(\frac{1}{1-\%M_i/100}\right) \end{aligned} \tag{5.216}$$

Usually, $\dot{m}_{MBB,dry,1}$ and $\omega_{MBB,1}$ will be known from fuel analyses and knowledge of the number of animals on the farm or how much liquid manure must be incinerated. Moreover, $\omega_{MBB,2a}$ and $\omega_{MBB,7}$ will be known from design specifications of the solids separator.

The remaining unknowns, $\dot{m}_{MBB,dry,2a}$ and $\dot{m}_{MBB,dry,7}$, may be found by combining equations (5.214) and (5.215):

$$\dot{m}_{MBB,dry,2a} = \dot{m}_{MBB,dry,1}\left(\frac{\omega_{MBB,7}-\omega_{MBB,1}}{\omega_{MBB,7}-\omega_{MBB,2a}}\right) \tag{5.217}$$

$\dot{m}_{MBB,dry,7}$ is simply the difference between $\dot{m}_{MBB,dry,1}$ and $\dot{m}_{MBB,dry,2a}$.

Now, the prime mover for this system is the combustor. In order to determine how much wastewater can be vaporized, it is necessary to know how much heat is released during combustion, but the tools for these computations have already been discussed. First the numbers of kmoles of each species entering and exiting the

combustor must be computed just as in equations (5.123) through (5.127). The only exception might be for cases in which additional fuel such as propane, coal, or additional composted biomass is used. For this case, the same concept that was discussed for co-firing in large coal plants in Section 5.4.3 can be utilized. Namely, equations (5.123) through (5.127) will be based on the combined blend of the two fuels:

$$\begin{aligned}
\%M_{blend} &= \left(1 - mf_{EF}\right)\%M_{MBB} + mf_{EF}\%M_{EF} \\
\%A_{blend} &= \left(1 - mf_{EF}\right)\%A_{MBB} + mf_{EF}\%A_{EF} \\
C_{blend} &= \left(1 - mf_{EF}\right)C_{MBB} + mf_{EF}C_{EF} \\
H_{blend} &= \cdots \\
N_{blend} &= \cdots \\
O_{blend} &= \cdots \\
S_{blend} &= \cdots \\
HHV_{blend} &= \cdots
\end{aligned} \tag{5.218}$$

Here, mf_{EF} is defined as:

$$mf_{EF} = \frac{\dot{m}_{EF}}{\dot{m}_{fuel}} \tag{5.219}$$

where, $\dot{m}_{EF}$ is the mass flow rate of extra fuel and $\dot{m}_{fuel}$ is the total amount fuel consumed by the combustor.

$$\dot{m}_{fuel} = \dot{m}_{MBB,3} + \dot{m}_{EF} \tag{5.220}$$

It is also important to distinguish time rate flows of mass through the combustion system ($\dot{m}$) as opposed to mass flows per 100 kg of fuel fired (m). This distinction can be described by the following general equation:

$$\dot{m}_{k,i} = m_{k,i} * \dot{m}_{fuel} = N_{k,i} * \frac{MW_k}{100} * \dot{m}_{fuel} \tag{5.221}$$

for each species $k = O_2$, N_2, CO_2, etc. and point in Figure 5.17 i = 1, 2a, 2b, 3, etc.

Next, the adiabatic flame temperature, T_5, can be found with a modification of equation (5.133).

$$
\begin{aligned}
&N_{CO_2,5}\left\{\overline{h}^0_{f,298,CO_2}+\Delta\overline{h}^{T_5}_{t,CO_2}\right\}+N_{H_2O(g),5}\left\{\overline{h}^0_{f,298,H_2O(g)}+\Delta\overline{h}^{T_5}_{t,H_2O(g)}\right\}\\
&+N_{N_2,5}\left\{\Delta\overline{h}^{T_5}_{t,N_2}\right\}+N_{SO_2,5}\left\{\overline{h}^0_{f,298,SO_2}+\Delta\overline{h}^{T_5}_{t,SO_2}\right\}+N_{O_2,5}\left\{\Delta\overline{h}^{T_5}_{t,O_2}\right\}\\
&+m_{ash,5}\left\{c_{p,ash}\left(T_5-298\right)\right\}+m_{ash,5a}\left\{c_{p,ash}\left(T_{5a}-298\right)\right\}\\
&=\left\{HHV_{fuel,DAF}MW_{fuel}+C\overline{h}^0_{f,CO_2}+\frac{H}{2}\overline{h}^0_{f,298,H_2O(l)}+S\overline{h}^0_{f,298,SO_2}\right.\\
&\quad\left.+c_{fuel,DAF}MW_{fuel}\left(T_3-298\right)\right\}+w\left\{\overline{h}^0_{f,298,H_2O(l)}+\overline{c}_{p,H_2O(l)}\left(T_3-298\right)\right\}\\
&\quad+m_{ash,3}\left\{c_{p,ash}\left(T_3-298\right)\right\}+N_{O_2,air,4}\left\{\Delta\overline{h}^{T_4}_{t,O_2}\right\}+N_{N_2,air,4}\left\{\Delta\overline{h}^{T_4}_{t,N_2}\right\}\\
&\quad+N_{H_2O(g),air,4}\left\{\overline{h}^0_{f,298,H_2O(g)}+\Delta\overline{h}^{T_4}_{t,H_2O(g)}\right\}
\end{aligned}
\tag{5.222}
$$

This equation must be iterated for T_5. Note that if there is extra fuel added to the combustor, it is simply lumped with the MBB fuel at point 3. Here, the inert solid byproduct of combustion (ash) can be divided into fly ash, which will travel with the other gaseous products of combustion, through point 5, and bottom ash or slag, which will exit the combustor at point 5a. So, if the fly ash percentage of the solid byproduct is %*FA*, and the total amount of ash produced per 100 kg of fuel fired in the combustor is $m_{ash,3}$, then:

$$m_{ash,5}=\left(\frac{\%FA}{100}\right)m_{ash,3} \tag{5.223}$$

$$m_{ash,5a}=\left(1-\frac{\%FA}{100}\right)m_{ash,3} \tag{5.224}$$

Next, the heat generated from the combustion, that in turn heats the wastewater entering the boiler to produce steam, can be computed in a similar fashion to equation (5.134).

$$
\begin{aligned}
Q_{comb}\left[\frac{kJ}{100\ kg\ as\ rec\ fuel}\right]=&\sum_{products,6}N_k\overline{h}_k+m_{ash,6}\left\{c_{p,ash}\left(T_6-298\right)\right\}\\
&+m_{ash,5a}\left\{c_{p,ash}\left(T_{5a}-298\right)\right\}\\
&-N_{fuel,DAF,3}\overline{h}_{fuel,DAF,3}-w\overline{h}_{H_2O(l),fuel,3}\\
&-m_{ash,3}c_{p,ash}\left(T_3-298\right)-\sum_{air,4}N_k\overline{h}_k
\end{aligned}
\tag{5.225}
$$

Here T_6 is the stack temperature, which is usually a known design variable, dependant on the operating conditions of the boilers.

Once the quantity of heat transferred to the wastewater is known, the amount of wastewater that can possibly be vaporized in the boiler can be computed. This analysis can begin by isolating the wastewater in the boiler and conducting a mass and energy balance of that system. See Figure 5.18.

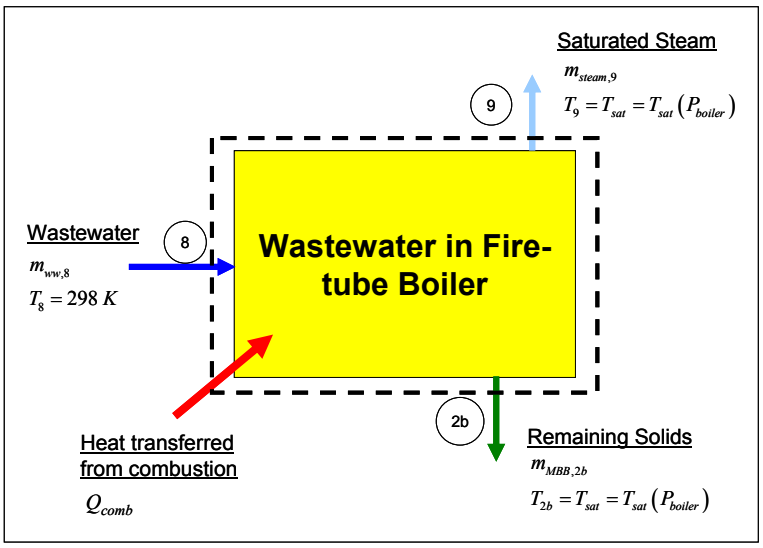

Figure 5.18 Mass and energy balance of wastewater in fire-tube boiler

So, the objective of this analysis is to find the amount of wastewater entering the fire-tube boiler per 100 kg of fuel burned in the combustor, $m_{ww,8}$. An energy balance of the wastewater system provides the following.

$$\begin{aligned} &Q_{comb} + m_{MBB,DAF,8}c_{MBB,DAF}T_8 + m_{ash,8}c_{ash}T_8 + m_{H_2O(l),8}c_{H_2O(l)}T_8 \\ &\quad = m_{steam,9}h_{sat,steam}(P_{boiler}) + m_{MBB,DAF,2b}c_{MBB,DAF}T_{2b} + m_{ash,2b}c_{ash}T_{2b} \\ &\qquad + m_{H_2O(l),2b}c_{H_2O(l)}T_{2b} \end{aligned}$$

Noting that $m_{MBB,DAF,8} = m_{MBB,DAF,2b}$ and that $m_{ash,8} = m_{ash,2b}$

$$\begin{aligned} Q_{comb} &= m_{steam,9}h_{sat,steam} + m_{H_2O(l),2b}c_{H_2O(l)}T_{2b} - m_{H_2O(l),8}c_{H_2O(l)}T_{2b} \\ &\quad + m_{MBB,DAF,8}c_{MBB,DAF}(T_{2b} - T_8) + m_{ash,8}c_{ash}(T_{2b} - T_8) \end{aligned} \tag{5.226}$$

The ash and moisture percentages at points 8 and 2b are known. The moisture percentage at 2b, which is the remaining amount of moisture in the solids coming out of the boiler in the blow down process, will be considered a design variable dependant on the specifics of the boiler's operation. In equation (5.226), $m_{MBB,DAF,8}$, $m_{ash,8}$, $m_{H_2O(l),2b}$, $m_{H_2O(l),8}$, and $m_{steam,9}$, must be expressed in terms of moisture percentage, ash percentage, and one unknown variable, such as $m_{ww,8}$, the flow of wastewater into the boiler per 100 kg of fuel burned in the combustor. The ash and the dry ash free portions of the incoming wastewater can be shown to be:

$$m_{MBB,DAF,8} = m_{MBB,DAF,2b} = \left(1 - \frac{\%A_{dry}}{100}\right)\left(1 - \frac{\%M_8}{100}\right)m_{ww,8} \tag{5.227}$$

$$m_{ash,8} = m_{ash,2b} = \left(\frac{\%A_{dry}}{100}\right)\left(1 - \frac{\%M_8}{100}\right)m_{ww,8} \tag{5.228}$$

where $\%A_{dry}$ is the ash percentage on a dry basis. The moisture percentage of the wastewater at 2b can be defined as:

$$\frac{\%M_{2b}}{100} \equiv \frac{m_{H_2O(l),2b}}{m_{MBB,DAF,2b} + m_{ash,2b} + m_{H_2O(l),2b}}$$

Inserting equations (5.227) and (5.228) into this definition provides the following:

$$m_{H_2O(l),2b} = \frac{\%M_{2b}}{\left(100 - \%M_{2b}\right)}\left(1 - \frac{\%M_8}{100}\right)m_{ww,8} \tag{5.229}$$

The moisture percentage of the incoming wastewater is simply:

$$m_{H_2O(l),8} = \frac{\%M_8}{100}m_{ww,8} \tag{5.230}$$

The steam production rate is simply the difference between $m_{H_2O(l),8}$ and $m_{H_2O(l),2b}$:

$$m_{steam,9} = \left[\frac{\%M_8}{100} - \frac{\%M_{2b}}{\left(100 - \%M_{2b}\right)}\left(1 - \frac{\%M_8}{100}\right)\right]m_{ww,8} \tag{5.231}$$

Now, inserting equations (5.227) through (5.231), the ratio of heat produced by the combustion to the amount of wastewater entering the boiler can be solved in terms of the moisture and ash percentages of the wastewater stream and the temperatures.

$$\begin{aligned}\frac{Q_{comb}}{m_{ww,8}} = &\left[\frac{\%M_8}{100} - \frac{\%M_{2b}}{\left(100-\%M_{2b}\right)}\left(1-\frac{\%M_8}{100}\right)\right]h_{sat,steam} \\ &+\left(\frac{\%M_{2b}}{100-\%M_{2b}}\right)\left(1-\frac{\%M_8}{100}\right)c_{H_2O(l)}T_{2b} - \frac{\%M_8}{100}c_{H_2O(l)}T_8 \\ &+\left(1-\frac{\%A_{dry}}{100}\right)\left(1-\frac{\%M_8}{100}\right)c_{MBB,DAF}\left(T_{2b}-T_8\right) \\ &+\left(\frac{\%A_{dry}}{100}\right)\left(1-\frac{\%M_8}{100}\right)c_{ash}\left(T_{2b}-T_8\right)\end{aligned} \tag{5.232}$$

Since, Q_{comb} has already been computed, $m_{ww,8}$ can now be found. Subsequently, values can be found for equations (5.227) through (5.231). However, it is also required to find all of these mass flows on a time rate basis, but since all of the values so far are on a "per 100 kg fired" basis, it is now necessary to compute the time rate of fuel fired in the boiler. The calculation of fueling rate involves a rather complicated mass balance since the burned separated solids, extra fuel, wastewater for the boiler, and steam used to dry the separated solids are all interconnected in the system. The following is an explanation of this mass balance.

Just before the rotary dryer, the separated solids are combined with the remaining solids from the wastewater boiler so that:

$$\dot{m}_{MBB,dry,2a} + \dot{m}_{MBB,dry,2b} = \dot{m}_{MBB,dry,2} \tag{5.233}$$

$$\dot{m}_{MBB,dry,2a}\omega_{MBB,2a} + \dot{m}_{MBB,dry,2b}\omega_{MBB,2b} = \dot{m}_{MBB,dry,2}\omega_{MBB,2} \tag{5.234}$$

The combined biomass solids will then go through the dryer, where moisture will be removed, but the dry solid fraction will remain the same. That is:

$$\dot{m}_{MBB,dry,2} = \dot{m}_{MBB,dry,3} \tag{5.235}$$

On an as received basis, the mass balance through the dryer can be expressed as the following:

$$\dot{m}_{MBB,3} = \dot{m}_{MBB,2} - \dot{m}_{vapor,11} \tag{5.236}$$

Inserting expression (5.233) for $\dot{m}_{MBB,2}$, along with an expression for the flow of vapor exhaust leaving the dryer, which is implied in equation (5.85), equation (5.236) becomes:

$$\dot{m}_{MBB,3} = \dot{m}_{MBB,2a} + \dot{m}_{MBB,2b} - \dot{m}_{MBB,dry,3}\left(\omega_{MBB,2} - \omega_{MBB,3}\right) \tag{5.237}$$

Next, inserting this expression for $\dot{m}_{MBB,3}$ into equation (5.220) for the total fuel entering the combustor:

$$\dot{m}_{fuel} = \dot{m}_{MBB,2a} + \dot{m}_{MBB,2b} - \dot{m}_{MBB,dry,3}\left(\omega_{MBB,2} - \omega_{MBB,3}\right) + \dot{m}_{EF} \tag{5.238}$$

Rearranging this equation:

$$\begin{aligned} \frac{\dot{m}_{MBB,dry,3}\left(\omega_{MBB,2} - \omega_{MBB,3}\right) - \dot{m}_{MBB,2a}}{\dot{m}_{MBB,3} + \dot{m}_{EF}} &= \frac{\dot{m}_{MBB,2b}}{\dot{m}_{fuel}} + \frac{\dot{m}_{EF}}{\dot{m}_{fuel}} - 1 \\ &= m_{MBB,2b} + mf_{EF} - 1 \end{aligned} \tag{5.239}$$

Before solving for the biomass flow rate at point three, $\omega_{MBB,2}$ and $\dot{m}_{EF}$ must be replaced with known variables. If equations (5.233) and (5.234) are combined, the following expression for $\omega_{MBB,2}$ can be found:

$$\omega_{MBB,2} = \frac{\dot{m}_{MBB,dry,2a}}{\dot{m}_{MBB,dry,3}}\omega_{MBB,2a} + \omega_{MBB,2b} - \frac{\dot{m}_{MBB,dry,2a}}{\dot{m}_{MBB,dry,3}}\omega_{MBB,2b} \tag{5.240}$$

Next, with equations (5.219) and (5.220), $\dot{m}_{EF}$ can be eliminated by finding the following expression:

$$\dot{m}_{EF} = \frac{mf_{EF}\left(1 + \omega_{MBB,3}\right)}{1 - mf_{EF}}\dot{m}_{MBB,dry,3} \tag{5.241}$$

Finally, plugging equations (5.240) and (5.241) into (5.239) and noting that $\dot{m}_{MBB,3} = \dot{m}_{MBB,dry,3}\left(1 + \omega_{MBB,3}\right)$, the following formula for $\dot{m}_{MBB,dry,3}$ can be obtained.

$$\dot{m}_{MBB,dry,3} = \frac{\dot{m}_{MBB,dry,2a}\left(1 + \omega_{MBB,2b}\right)\left(1 - mf_{EF}\right)}{\left(1 - mf_{EF}\right)C_2 - mf_{EF}\left(1 + \omega_{MBB,3}\right)C_1} \tag{5.242}$$

where,

$C_1 = m_{MBB,2b} + mf_{EF} - 1$

$$C_2 = \left(\omega_{MBB,2b} - \omega_{MBB,3}\right) - \left(1 + \omega_{MBB,3}\right)C_1$$

All the moisture contents in this equation are known, or have been computed. $\dot{m}_{MBB,dry,2a}$ was computed with equation (5.217) and $m_{MBB,2b}$ can be found with equation (5.227). With the value for $\dot{m}_{MBB,dry,3}$, $\dot{m}_{EF}$ can be computed, and hence $\dot{m}_{fuel}$ can also be found. Thus, the time rate mass flow of wastewater and left over solids flowing in and out of the fire-tube boiler can also be found, along with each reactant entering the combustor and each product of combustion exiting the stack, along with the ash production using equation (5.221).

Now, some discussion should be articulated as to the limits of applicability of the formulae derived for this model; namely, the maximum amount of extra fuel that can be added to the combustor before all of the wastewater is vaporized in the boiler. Once $\dot{m}_{fuel}$ is known, a value for the amount of wastewater that can be vaporized, $\dot{m}_{ww,8}$, can be computed, but the total amount of liquid manure coming from the solids separator, $\dot{m}_{MBB,7}$, may be computed with the following expression.

$$\dot{m}_{MBB,7} = \dot{m}_{ww,8} + \dot{m}_{ww,8ew} \tag{5.243}$$

where $\dot{m}_{ww,8ew}$ is the amount of extra wastewater from the solids separator that could not be handled by the boiler because the combustion of the fuel blend could not provide enough heat. But as mf_{EF} increases, $\dot{m}_{ww,8ew}$ will eventually become zero and $\dot{m}_{ww,8}$ will be greater than $\dot{m}_{MBB,7}$. If this is the case, then additional wastewater, not produced from the confined animal units, can be handled by the system, or the steam produced in the boiler can be superheated and not simply saturated vapor.

There are two main factors that may be used to gage the effectiveness of this conceptualized MBB combustion design. The first is the boiler efficiency, which is defined as the total amount of heat transferred to the boiler water divided by the heat released by the fuel. However, since in this case the boiler water is wastewater emanating from the solid separator, there will be a great deal of solids in the boiler water

as it is being vaporized. Thus the equation for boiler efficiency must be modified to account for these solids.

$$\eta_{boiler} = \frac{\dot{Q}_{comb} - \left(\dot{m}_{MBB,BD,2b} c_{MBB,BD} - \dot{m}_{H_2O,2b} c_{H_2O_{(l)}}\right)\left(T_{2b} - T_8\right)}{\dot{m}_{fuel,3} HHV_{fuel}} \tag{5.244}$$

Finally, the disposal efficiency is an indication of how much of the liquid flushed manure from the animal housing was incinerated. Since there will always be ash leftover from the combustion, the disposal efficiency can never be unity, but high disposal efficiencies are achieved when all of the water in the liquid manure is vaporized and all of the combustible material in the manure has been burned.

$$\eta_{disposal} = \frac{\dot{m}_1 - \dot{m}_{8,ew} - \dot{m}_{5a}}{\dot{m}_1} \tag{5.245}$$

5.5.2. Combustion System for Scraped Solids and Lower Moisture Biomass

Not all manure waste from large CAFOs is handled as a liquid or is even high in moisture. Scraped manure from open lots and feedlots, especially in areas with dry climates, will usually be lower than 30% (Heflin, 2008). For these cases, solids separators and dryer would not be needed. See Figure 5.19. Plus, instead of using wastewater in the boiler, a standard vapor-power cycle would suffice, in order to utilize heat from biomass combustion to generate steam for external processes.

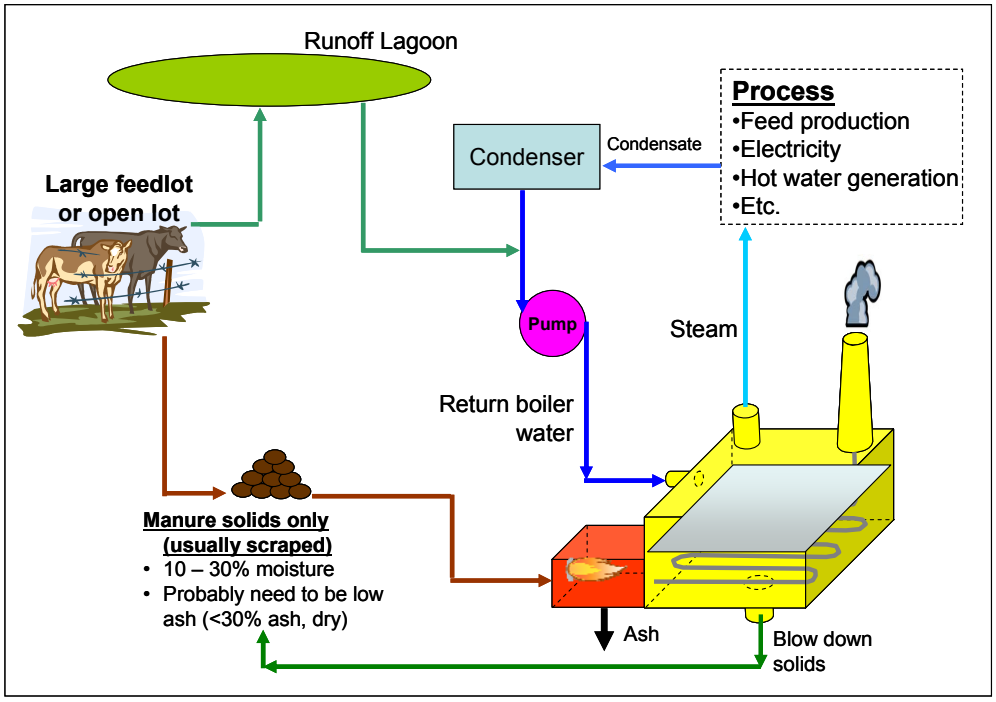

Figure 5.19 Conceptualized design of MBB thermo-chemical energy conversion system for large feedlot corrals or open lot dairies that produce low moisture manure

There are of course different ways a MBB combustion system could be designed. For instance, if the large feedlot has a lagoon that stores wastewater runoff, a fire-tube boiler could be used in a similar way to that of the flushed manure design. Also, it is possible to avoid producing steam at all, and still generate useful energy. If the MBB is gasified, as in Figure 5.12, then the producer gas can be burned in a modified internal combustion engine or a gas turbine to produce electrical energy. All of these possibilities can be modeled with the equations presented throughout this section. The use of a vapor-power cycle in manure biomass energy conversion systems, shown in Figure 5.19, was discussed by Carlin (2005) for cases where lower moisture biomass was present. However, in that report, it was thought that vacuumed manure solids would have similar moisture contents to scraped manure solids. Yet, based on the data reported in Table 2.4, this assumption may not be true for most cases. The moisture content of manure, that is not flushed or washed with water, is probably more dependant on the climate of the local geographic area.

Moreover, it should be noted that for all of these small-scale combustion systems, low-ash manure is preferred. High ash contents in manure make direct combustion processes very difficult, if not impossible. Even for gasification processes, the cost of continuously removing ash and increased maintenance to equipment can become very costly.

5.6. Modeling the Economics of Manure-based Biomass Combustion Systems

The economics of MBB combustion can now be discussed. In this section, capital, operation and maintenance (O&M) costs of drying biomass, transporting biomass, and processing and burning biomass at large-scale combustion facilities (for both co-fire and reburn processes) will be discussed. Additional fueling costs (or savings) from utilizing MBB will also be discussed. The equations for capital and O&M costs of competing NO_x control technologies will be presented for cases in which reburning with biomass will be compared to SCR and SNCR. Equations for the total dollar cost (or savings) of CO_2, NO_x, SO_x, and ash emissions from the combustion facility will then be presented.

Finally, several economic analyses that can integrate all costs and benefits from MBB utilization to determine the overall profitability of using biomass in large coal-fired power plants will be presented. These include: (1) the net present worth (NPW) of a MBB combustion project, (2) the simple payback period, (3) the rate of return (ROR) on investment of capital necessary for a MBB combustion project, and (4) an annualized cost of a MBB combustion project. Taxes on income and depreciation of capital will also be included in the economic analysis.

The scope of the economic study for co-firing coal with MBB is illustrated in Figure 5.20 and the scope for reburning with MBB is shown in Figure 5.21. The studies for both co-firing and reburning may be divided into three portions: drying MBB, transporting MBB to the power plant, and processing of MBB at the power plant. The emissions from each of these parts of the system will also enter into the model.

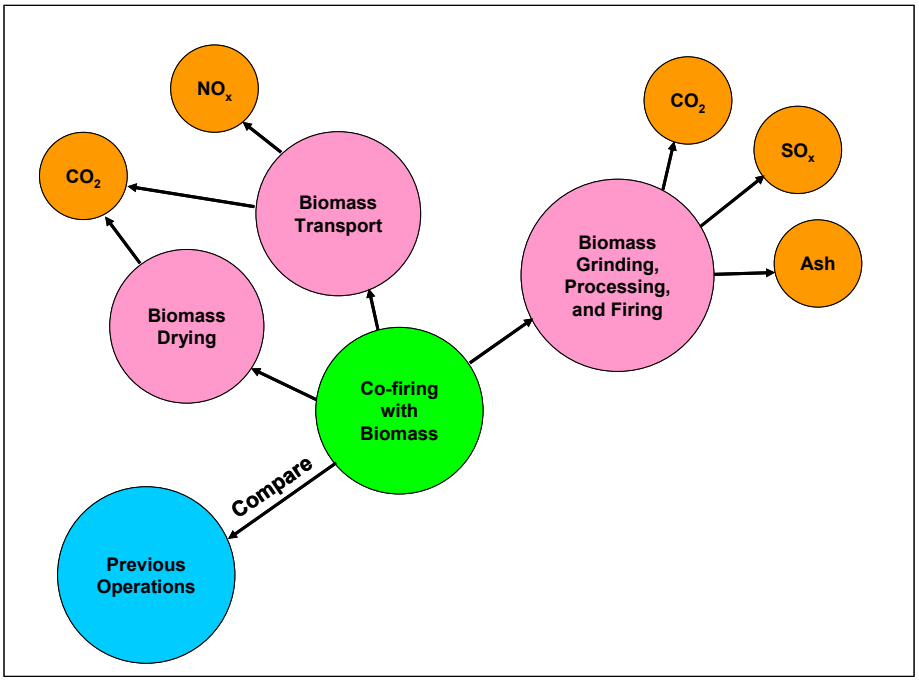

Figure 5.20 Scope of manure-based biomass co-firing economic study

The primary difference between the co-fire and the reburn models is that the operating costs for co-firing will only be compared to the status quo operation of the coal-fired power plant whereas reburning will be compared to both the status quo operation and the operating costs of other more common NO_x control technologies. Moreover, since current experimental research has not yet provided a definite idea of how co-firing coal and MBB will affect NO_x, especially in coal burners with low-NOx burners and other primary controls, NO_x emissions will be assumed unchanged during co-firing, and will not enter into the economics model.

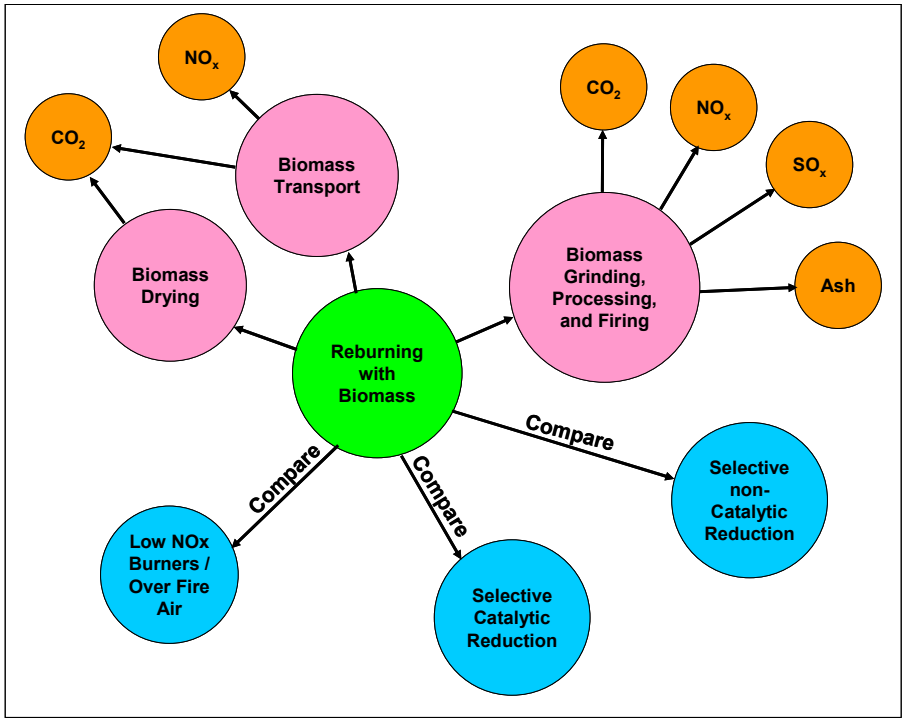

Figure 5.21 Scope of manure-based biomass reburn economic study

Finally, note that the dollar costs and savings computed from the following equations are estimates taken from literature review, government reports, and manufacturer's data. Unlike other engineering calculations involving thermodynamics or heat transfer problems, economic calculations are highly speculative and are not rooted in fundamental physical laws. Cost estimates presented here and in the literature are based on previous experiences and current market values of commodities, and since situations can vary and commodity values can change, the estimations from the equations presented here can also change. For these reasons, sensitivity analysis methods will also be discussed at the end of this section.

Before discussing the individual costs of co-fire and reburn systems, note that some fuel prices and values of emissions, as well as labor, escalate annually throughout the life of the co-fire or reburn project. The price of the commodity at any year, n, can be computed with the following expression.

$$Price_{i,n}\left[\frac{\$_n}{yr}\right] = Price_{i,year\,1} * \left(1+\left(\varepsilon_{price,i}\right)\right)^n \tag{5.246}$$

where the price of commodity *i* will be in year-*n* dollars computed from the annual escalation rate, $\varepsilon_{price,i}$.

5.6.1. Drying Cost Estimations

For the reburning and co-firing models, conveyor belt dryers will be considered the dryer of choice. The capital cost, or purchasing cost of a conveyor belt dryer is a function of the conveyor belt area, which was computed in equations (5.34) or (5.49) for perpendicular air flow dryers and in equation (5.60) for parallel air flow dryers. Brammer *et al*. (2002) suggested the following equation for the capital cost of a conveyor belt dryer.

$$Capital_{dryer}\left[\$\right] = 6,015\left(2.79A_{belt} + 52.2\right)^{0.863} \tag{5.247}$$

Each dryer receives heat energy from a steam generating boiler, the cost of which may be estimated as the following.

$$Capital_{dryer-boiler}\left[\$\right] = \frac{\$160,000}{kg/s} * \dot{m}_{steam,dryer} \tag{5.248}$$

The steam consumption of a dryer, $\dot{m}_{steam,dryer}$ was computed with equation (5.26). Other ancillary capital costs of the MBB drying system such as loaders, land, and extra manure storage bins may be computed with the following three equations.

$$Capital_{loaders}\left[\$\right] = \begin{pmatrix} loaders\ per \\ dryer \end{pmatrix} * Price_{loader}\left[\frac{\$}{loader}\right] \tag{5.249}$$

$$Capital_{land}\left[\$\right] = \begin{pmatrix} number\ of \\ drying\ sites \end{pmatrix} * \begin{pmatrix} acres\ per \\ site \end{pmatrix} * Price_{land}\left[\frac{\$}{acre}\right] \tag{5.250}$$

$$Capital_{storage}\left[\$\right] = \begin{pmatrix} number\ of \\ drying\ sites \end{pmatrix} * \begin{pmatrix} extra\ storage \\ trailers\ per\ site \end{pmatrix} * Price_{trailer}\left[\frac{\$}{trailer}\right] \tag{5.251}$$

The total capital cost of the entire drying system is simply the sum of these costs.

$$Capital_{total,drying}\left[\$\right] = \left(Capital_{dryer} + Capital_{dryer-boiler} + Capital_{loader}\right) * N_{dryer} + Capital_{land} + Capital_{storage} \quad (5.252)$$

Here, N_{dryer} is the total number of dryers required to supply the biomass, which was computed in equation (5.10).

Brammer *et al*. (2002) also suggested than the fixed operation and maintenance (O&M) cost of the dryers could be estimated to be about 4% of the capital cost. For this model, fixed O&M was estimated to be the following for the dryers.

$$FO\&M_{dryers}\left[\frac{\$}{yr}\right] = 0.04 * \left(Capital_{dryer} + Capital_{dryer-boiler} + Capital_{loader}\right) * N_{dryer} \quad (5.253)$$

There are two components to the variable O&M cost of the dryers. First, the fueling cost of the dryer can be computed with the following:

$$VO\&M_{dryer-fuel}\left[\frac{\$}{yr}\right] = \dot{F}_{dryer\ fuel} * OH_{dryer} * Price_{dryer\ fuel}\left[\frac{\$}{GJ_{th}}\right] * N_{dryers} * \frac{3600 s/hr}{10^6 kJ/GJ} \quad (5.254)$$

$\dot{F}_{dryer\ fuel}$ was computed with equation (5.28) and OH_{dryer} is the annual operating hours per year for the dryers. The second component to the variable operation and maintenance cost for the dryer is the electricity consumption of the dryer's fans, $\dot{E}_{fan}$. $\dot{E}_{fan}$ was computed with equation (5.29).

$$VO\&M_{dryer-fan}\left[\frac{\$}{yr}\right] = \dot{E}_{fan} * OH_{dryer} * Price_{electricity}\left[\frac{\$}{kWh}\right] * N_{dryers} \quad (5.255)$$

Finally, labor is based on how many operators are assumed to be employed per dryer and the price of labor, both of which are input values. Labor costs, for this model can thus be simply computed with the following expression.

$$Labor_{dryer}\left[\frac{\$}{yr}\right] = \left(\frac{operators}{per\ dryer}\right) * N_{dryers} * OH_{dryer} * Price_{labor}\left[\frac{\$}{hr}\right] \quad (5.256)$$

The total O&M cost of the drying system is simply the sum of all of these costs.

$$O\&M_{total-drying}\left[\frac{\$}{yr}\right] = FO\&M_{dryers} + VO\&M_{dryer-fuel} + VO\&M_{dryer-fan} + Labor_{dryer} \quad (5.257)$$

5.6.2. Transportation Cost Estimations

The purchasing price of the hauling vehicles is an input, therefore the total capital cost of purchasing all of the required hauling vehicles is simply:

$$Capital_{truck}\left[\$\right] = N_{trucks} * Price_{truck}\left[\frac{\$}{truck}\right] \quad (5.258)$$

The number of trucks required to haul all of the MBB, N_{trucks}, was computed with equation (5.102). The fixed operation and maintenance of the hauling vehicles is the general cost of maintaining the quality of the vehicles and is based on a dollar-per-kilometers driven value.

$$FO\&M_{truck}\left[\frac{\$}{yr}\right] = 2\hat{D}N_{trips,actual} * Price_{repair}\left[\frac{\$}{km}\right] * N_{trucks} \quad (5.259)$$

The number of trips each truck travels per year, $N_{trips,actual}$, was computed with equation (5.103). The variable operation and maintenance cost of the hauling vehicles is simply the price of fueling them with diesel.

$$VO\&M_{truck-fuel}\left[\frac{\$}{yr}\right] = \frac{2\hat{D}N_{trips,actual}N_{trucks}}{\left(\begin{array}{c} fuel\ economy, \\ km\ per\ liter \end{array}\right)} * Price_{diesel}\left[\frac{\$}{liter}\right] \quad (5.260)$$

Labor is also taken into account for the hauling vehicles. The annual number of hours spent loading, unloading, and transporting biomass, $t_{total,annual}$ was computed with equation (5.104).

$$Labor_{trucks}\left[\frac{\$}{yr}\right] = t_{total,annual} * Price_{labor}\left[\frac{\$}{hr}\right] * N_{trucks} \quad (5.261)$$

Finally, if SCR systems are installed on the hauling vehicles to reduce NO_x emissions from their tailpipes, then the additional cost of installing and maintaining these SCR systems must also be added to the overall cost hauling MBB.

$$SCR_{truck}\left[\frac{\$}{yr}\right] = Price_{SCR,truck}\left[\frac{\$}{yr}\right] * N_{trucks} \tag{5.262}$$

The total O&M cost of hauling the manure from the animal feeding operations to the power plant is the sum of the previous four equations.

$$O\&M_{total-truck}\left[\frac{\$}{yr}\right] = FO\&M_{truck} + VO\&M_{truck-fuel} + Labor_{trucks} + SCR_{truck} \tag{5.263}$$

5.6.3. Processing and Firing Cost Estimations

The cost of installing an environmental retrofit on a coal-fired power plant can be broken up into three different components: capital cost, fixed operation and maintenance costs (FO&M), and variable operation and maintenance costs (VO&M). The capital cost is the initial investment of purchasing and installing all necessary equipment so that the system is fully functional. Fixed operation and maintenance costs are generally incurred whether the system is running or not. These costs typically include labor and overhead items such as fuel feeders, grinders, and air and fuel injectors, whereas, VO&M costs include handling and delivery of raw materials and waste disposal (Newnan *et al*., 2000).

5.6.3.1. Co-firing

Some suggestions for co-firing capital costs for biomass are listed in Table 3.1. For this model, the capital costs suggested by the USEPA (2007c) will be adopted. Thus the following expression was used to compute capital costs for co-firing coal with manure. These expressions are based on the total electrical energy generated from the biomass combustion.

$$Capital_{cofire}[\$] = \begin{cases} 251\left[\frac{\$}{kW_e}\right]\dot{Q}_{MBB}\left(\frac{\eta_{plant}}{100}\right), & if\ \mathcal{P} \le 200MW_e \\ 218\left[\frac{\$}{kW_e}\right]\dot{Q}_{MBB}\left(\frac{\eta_{plant}}{100}\right), & if\ 201 < \mathcal{P} < 500MW_e \\ 109\left[\frac{\$}{kW_e}\right]\dot{Q}_{MBB}\left(\frac{\eta_{plant}}{100}\right), & if\ \mathcal{P} \ge 500MW \end{cases} \quad (5.264)$$

Here, $\dot{Q}_{MBB}$ is the heat generated from biomass combustion and can be computed from equation (5.196). The plant efficiency, η_{plant}, was computed with equation (5.171), and $\mathcal{P}$is the electric capacity of the power plant.

The fixed operation and maintenance cost of co-firing is also based on the electricity produced from biomass combustion. The USEPA (2007c) suggested the following expression, which will be adopted here.

$$FO\&M_{co-fire}\left[\frac{\$}{yr}\right] = \theta\left[\frac{\$}{kW_e \cdot yr}\right]\dot{Q}_{MBB}\left(\frac{\eta_{plant}}{100}\right) \quad (5.265)$$

The USEPA (2007c) suggested a value of \$7.63/kWe-yr for θ.

Finally, the annual cost of burning coal when co-firing con be computed with the following expression.

$$\begin{aligned} Fueling_{coal,cofiring}\left[\frac{\$}{yr}\right] = {} & \dot{m}_{coal,cofire} * Price_{coal}\left[\frac{\$}{metric\ ton}\right] * OH_{cofire} \\ & + \dot{m}_{coal,no\ cofire} * Price_{coal}\left[\frac{\$}{metric\ ton}\right] \\ & * \left(OH_{plant} - OH_{cofire}\right) \end{aligned} \quad (5.266)$$

The coal consumption rates, $\dot{m}_{coal}$, before and during co-firing operations were computed with equations (5.172) and (5.197) Here, $OH_{co\text{-}fire}$ is the number of hours per year that the power plant is co-firing with biomass. The net dollar savings from avoided coal combustion is simply:

$$Coal\ Savings\left[\frac{\$}{yr}\right] = Fueling_{coal} - Fueling_{coal,cofiring} \quad (5.267)$$

If the farmer providing the MBB to the coal plant requests some compensation for the biomass, perhaps a dollar value comparable to the biomass's value as a fertilizer, then an additional cost for purchasing the MBB must be considered.

$$MBB\ Cost\left[\frac{\$}{yr}\right] = \dot{M}_{MBB,annum}\left(1-\frac{\%M_{MBB,0}}{100}\right)*\left(\frac{metric\ ton}{1,000\ kg}\right) * Price_{MBB}\left[\frac{\$}{dry\ metric\ ton}\right] \quad (5.268)$$

5.6.3.2. Reburning and other secondary NO_x control technologies

For this study, both primary and secondary NO_x control technologies were modeled in much the same way as was done for the USEPA Integrated Planning Model (IPM). The IPM is a multi-regional, dynamic, deterministic linear programming model of the U.S. electric power sector. The results from the IPM are meant to compare energy policy scenarios and governmental mandates concerning electric capacity expansion, electricity dispatch and emission control strategies. The model and base case inputs to the model are updated annually. The latest update, as of the writing of this paper, may be found on the USEPA (2006) website. Since a section of the IPM is concerned with evaluating the cost and emission impacts of proposed policies, it is possible to adopt these emission models to describe the economics of common primary and secondary controls, and then compare them to results for MBB reburning.

The NO_x control technology options modeled by the EPA IPM are LNB (with and without over fire air), SCR, and SNCR. Capital and FO&M costs are functions of power plant capacity, while VO&M costs are functions of heat rate. Models presented by Mussatti *et al* (2000a&b) offer more detailed and comprehensive representations for SCR and SNCR cost components, but require more inputs. Economic modeling equations in the IPM for LNB are based on costs for 300 MW size boilers, listed in Table 5.6.

Table 5.6 Cost of primary NO_x combustion controls for coal boilers, 300 MW_e size (adopted from USEPA, 2006)

Boiler Type	Primary Control Technology	Capital, α ($/kW$_e$)	FO&M, β ($/kW$_e$ yr)	VO&M, γ ($/kWh$_e$)
Dry Bottom Wall-Fired	Low-NO_x Burner without Over fire Air	19.24	0.29	6.00E-05
	Low-NO_x Burner with Over fire Air	26.12	0.40	8.00E-05
Tangentially-Fired	Low-NO_x Coal-and-Air Nozzles with Close-Coupled Over fire Air	10.14	0.16	1.00E-06
	Low-NO_x Coal-and-Air Nozzles with Separated Over fire Air	14.17	0.21	2.70E-05
	Low-NO_x Coal-and-Air Nozzles with Close-Coupled and Separated Over fire Air	16.19	0.25	2.70E-05

These costs may be translated to cost for different boiler sizes with the following expressions provided by the USEPA (2006):

$$Capital_{primary}[\$] = \alpha\left(\frac{300}{\mathscr{P}}\right)^{0.359} \mathscr{P} * \left(\frac{1{,}000\ kW}{MW}\right) \tag{5.269}$$

$$FO\&M_{primary}\left[\frac{\$}{yr}\right] = \beta\left(\frac{300}{\mathscr{P}}\right)^{0.359} \mathscr{P} * \left(\frac{1{,}000\ kW}{MW}\right) \tag{5.270}$$

$$VO\&M_{primary}\left[\frac{\$}{yr}\right] = \gamma\left(\frac{\%CF}{100}\right)\mathscr{P}\left(OH_{plant}\right) * \left(\frac{1{,}000\ kW}{MW}\right) \tag{5.271}$$

Here, $\mathscr{P}$ is the power plant's electrical capacity in MW_e, $\%CF$ is the plant's capacity factor as a percentage, and OH_{plant} is the number of hours per year that the plant is operational. Similarly, SCR and SNCR may be modeled using the values in Table 5.7

Table 5.7 Cost of secondary NO_x combustion controls for coal boilers (adopted from USEPA, 2006)

Secondary Control Technology	Capital, δ ($/kW$_e$)	FO&M, ε ($/kW$_e$ yr)	VO&M, ζ ($/kWh$_e$)
SCR	111.48	0.74	6.70E-04
SNCR--Term 1	19.06	0.28	9.80E-04
SNCR--Term 2	21.74	0.33	

Similarly, the following expressions may be used to compute capital and O&M costs for SCR and SNCR (USEPA, 2006).

$$Capital_{SCR}[\$] = \delta\left(\frac{242.72}{\mathscr{P}}\right)^{0.27} \mathscr{P} * \left(\frac{1{,}000\ kW}{MW}\right) \tag{5.272}$$

$$FO\&M_{SCR}\left[\frac{\$}{yr}\right] = \varepsilon\left(\frac{242.72}{\mathscr{P}}\right)^{0.27} \mathscr{P} * \left(\frac{1{,}000\ kW}{MW}\right) \tag{5.273}$$

$$VO\&M_{SCR}\left[\frac{\$}{yr}\right] = \zeta\left(\frac{242.72}{\mathscr{P}}\right)^{0.11} \left(\frac{\%CF}{100}\right) \mathscr{P}\left(OH_{SCR}\right) * \left(\frac{1{,}000\ kW}{MW}\right) \tag{5.274}$$

$$Capital_{SNCR}[\$] = \left(\frac{\delta_1\left(\frac{200}{\mathscr{P}}\right)^{0.577} + \delta_2\left(\frac{100}{\mathscr{P}}\right)^{0.681}}{2}\right) \mathscr{P} * \left(\frac{1{,}000\ kW}{MW}\right) \tag{5.275}$$

$$FO\&M_{SNCR}\left[\frac{\$}{yr}\right] = \left(\frac{\varepsilon_1\left(\frac{200}{\mathscr{P}}\right)^{0.577} + \varepsilon_2\left(\frac{200}{\mathscr{P}}\right)^{0.681}}{2}\right) \mathscr{P}\left(\frac{1{,}000\ kW}{MW}\right) \tag{5.276}$$

$$VO\&M_{SNCR}\left[\frac{\$}{yr}\right] = \zeta\left(\frac{\%CF}{100}\right) \mathscr{P}\left(OH_{SNCR}\right) * \left(\frac{1{,}000\ kW}{MW}\right) \tag{5.277}$$

Reburn technologies were not included in the latest version of the IPM. Thus, the main challenge of this study was to estimate the cost performance of a MBB reburning system even when only experimental results and pilot scale tests have been conducted for these systems, and few applications of gas and coal reburning systems existed for comparison. Work by Zamansky *et al*. (2000) suggested that reburn systems utilizing furniture wastes, willow wood, and walnut shell biomass have similar capital costs to coal reburning systems. An earlier USEPA (1998) report for the Clean Air Act Amendment, which was also sited by Biewald *et al*. (2000), modeled both gas and coal reburn systems, although the coal reburn model was meant only for cyclone boiler types. And since gas reburning costs are generally lower than coal reburning costs, the reburn capital cost model presented by the USEPA (1998) would only be applicable for cyclone boilers. Cyclone boilers burn coarsely crushed coal, but coal reburn systems typically

require pulverized or micro-ionized coal to avoid unburned carbon emissions. Hence, purchasing pulverizing equipment is generally required for cyclone boiler plants.

Some estimates of coal and biomass reburn capital costs are presented in Table 3.2. If a value for reburn capital (η in \$/kW$_e$ of total plant capacity) is chosen from this table, the following expression may be used to compute the capital cost of a reburn system installed on a plant with a capacity $\mathcal{P}$.

$$Capital_{reburn}\left[\$\right] = \eta\mathcal{P} * \left(\frac{1{,}000\ kW}{MW}\right) \tag{5.278}$$

Note that capital costs for reburning (values for η listed in Table 3.2) do not include the capital cost of dryers and biomass hauling vehicles which will be needed for CB reburning but not coal reburning. These costs, as was discussed earlier, were computed separately. As for the FO&M cost equation, the model presented by the USEPA (1998) was used for the spreadsheet model, with the exception of an additional scaling factor that accounted for the MBB's poorer heat value and hence greater required fueling rate.

$$FO\&M_{reburn}\left[\frac{\$}{yr}\right] = \theta\left(\frac{300}{\mathcal{P}}\right)^{0.388}\mathcal{P} * \left(\frac{1{,}000\ kW}{MW}\right)\left(\frac{HHV_{coal}}{HHV_{MBB}}\right) \tag{5.279}$$

The USEPA (1998) suggested that θ = \$1.07/kW$_e$-yr. However, to describe the uniqueness of MBB reburning to other reburning facilities, VO&M costs such as biomass drying, transporting, and ash disposal were individually calculated in a previous section. The cost of burning coal when reburning with biomass can be computed in much the same way as was done for co-firing.

5.6.4. Cost of Emissions

Emission reductions when co-firing and reburning were discussed in Sections 5.4.3 and 5.4.4. Beginning with CO_2 emissions, carbon savings must include the reduction of nonrenewable CO_2 emitted from the power plant, as well as emissions from drying and hauling vehicles.

$$CO_2\ Savings\left[\frac{\$}{yr}\right]=\left[\left(\mathcal{E}_{CO_2,no\ cofire}-\mathcal{E}_{CO_2,cofiring,reported}\right)-\mathcal{E}_{CO_2,drying}-\mathcal{E}_{CO_2,trucks}\right]*Value_{CO_2}\left[\frac{\$}{metric\ ton}\right] \tag{5.280}$$

Similarly the cost or savings, depending on the sulfur content of the co-fired fuel, of SO_2 emissions may be computed with the following expression.

$$SO_2\ Cost\ or\ Savings\left[\frac{\$}{yr}\right]=\left(\mathcal{E}_{SO_2,no\ cofire}-\mathcal{E}_{SO_2,cofiring}\right)*Value_{SO_2}\left[\frac{\$}{metric\ ton}\right] \tag{5.281}$$

Ash can either be sold for external uses, such as cement production, or discarded in a landfill. The overall cost of ash disposal and ash sales can be computed with the following two equations.

$$Ash\ Disposal\left[\frac{\$}{yr}\right]=\left(1-\frac{\%Ash\ Sold}{100}\right)*\left(\mathcal{E}_{ash,cofiring}-\mathcal{E}_{ash,no\ cofire}\right)*Price_{disposal}\left[\frac{\$}{metric\ ton}\right] \tag{5.282}$$

$$Ash\ Sale\left[\frac{\$}{yr}\right]=\left(\frac{\%Ash\ Sold}{100}\right)*\left(\mathcal{E}_{ash,cofiring}-\mathcal{E}_{ash,no\ cofire}\right)*Price_{ash}\left[\frac{\$}{metric\ ton}\right] \tag{5.283}$$

However, sometimes ash may not be sold at the same rate or at all when co-firing. If this is the case, then the above two equations should be adjusted accordingly.

These annual cash flows for emissions are applicable to both co-firing and reburning. However, in this study, NO_x emission reductions are unique to reburning and are ignored for co-firing. The NO_x savings may be computed with the following expression when reburning coal with MBB.

$$NO_x\ Savings\left[\frac{\$}{yr}\right]=\left[\left(\mathcal{E}_{NO_x,no\ reburn}-\mathcal{E}_{NO_x,reburn}\right)-\mathcal{E}_{NO_x,truck}\right]*Value_{NO_x}\left[\frac{\$}{metric\ ton}\right] \quad (5.284)$$

A similar equation may also be written for NO_x emission savings from SCR and SNCR.

5.6.5. Overall Economic Analysis

To this point, the modeling equations could be used to generate many different cash flows and dollar values that vary from the purchase price of hauling vehicles to the dollar savings of CO_2 emissions. However, in order to make sense of the bottom line meaning of all the dollar figures computed to this point, there must be a system to integrate all of the dollar values computed above to form one encompassing figure or number that can indicate the bottom line economic success or inadequacy of co-firing (or reburning) coal with MBB in an existing coal plant. One of the more common ways to indicate the economic bottom line of a project is to compute a net present worth (NPW) that is the equivalent combined value of all cash flows computed throughout the life of the project in present dollars.

When modeling SCR and SNCR for the Integrated Planning Model, the USEPA assumed a project life for environmental retrofits of 30 years. Following this method, both co-fire and reburn retrofits were assumed to have a project life of 30 years as well. However, note that the same analysis can be conducted for shorter or longer project lives. Taking into account price escalations, each of the annual (dollar per year) costs and revenues for the co-fire project can be computed for each year. Cash flow diagrams, such as the one in Figure 5.22, are helpful when visualizing all of the computed cash flows.

Moreover, at year zero of the co-fire project the plant equipment and the measures required to install a biomass co-fire system, as well as the trucks and the dryers and associated equipment were all purchased in full. However, since hauling vehicles and drying equipment probably will not last the full 30 years of the project's life, an

entirely new set of trucks was assumed to be purchased at years seven, 14, and 21. Similarly, an entirely new set of dryers and all ancillary dryer equipment was assumed to be purchased at year 15, the mid-point of the project. These future capital investment cash flows are also shown in Figure 5.22. Computing the value of these future investments in real dollars is similar to the computation of future commodity prices with equation (5.246). For example, the capital cost of a dryer at year 15 can be computed with the following equation.

$$Capital_{total-drying,15}\left[\frac{\$_{15}}{yr}\right] = Capital_{total-drying,year\ 0} * \left(1+\left(\varepsilon_{price,dryer}\right)\right)^{15} \qquad (5.285)$$

The same can be done for $Capital_{truck}$ for years seven, 14, and 21.

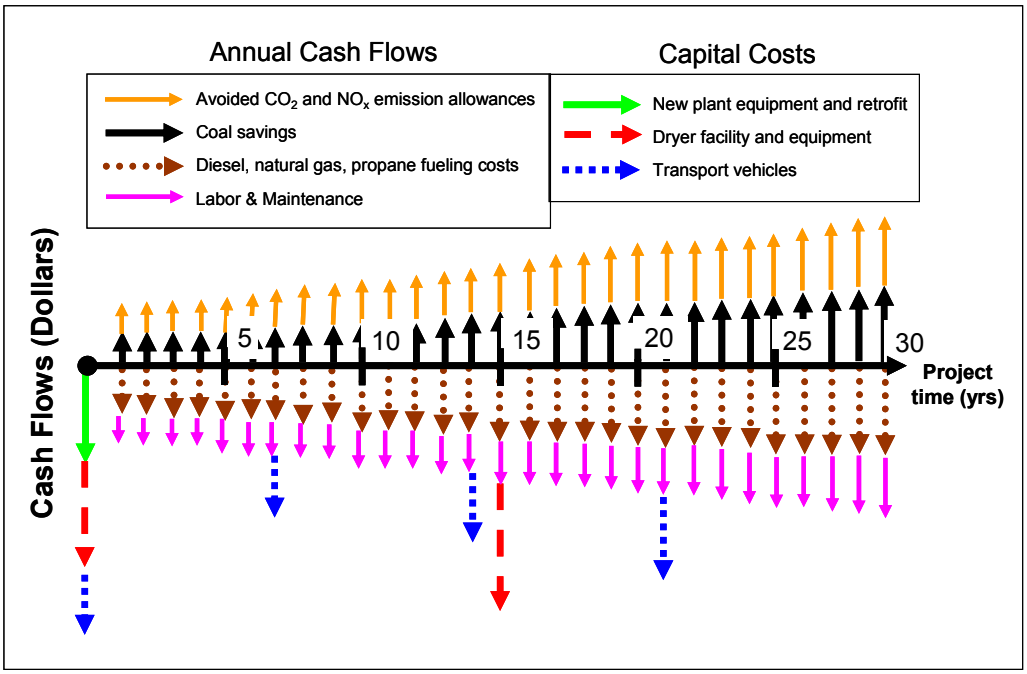

Figure 5.22 Capital and annual cash flows encountered for manure-based biomass co-fire and reburn operations and retrofit projects

Now all of the cash flows in Figure 5.22 must be converted into one net present worth. The first step in computing the NPW is to compute an Operating Cost (or revenue) for each year, *n*. This summation is shown in the following expression.

$$\begin{aligned} Operating\ Income_n = & -O\&M_{total-drying,n} - O\&M_{total-truck,n} \\ & - FO\&M_{cofire,n} + Coal\ Savings_n \\ & + CO_2\ Savings_n \pm SO_2\ Cost_n \\ & - Ash\ Disposal_n + Ash\ Sale_n \\ & + MBB\ Cost_n + NO_x\ Savings_n \end{aligned} \quad (5.286)$$

Depending on the size of the benefits versus the costs, the operating income can be positive (revenue) or negative (cost). The operating income is shown arbitrarily in the cash flow diagram in Figure 5.23

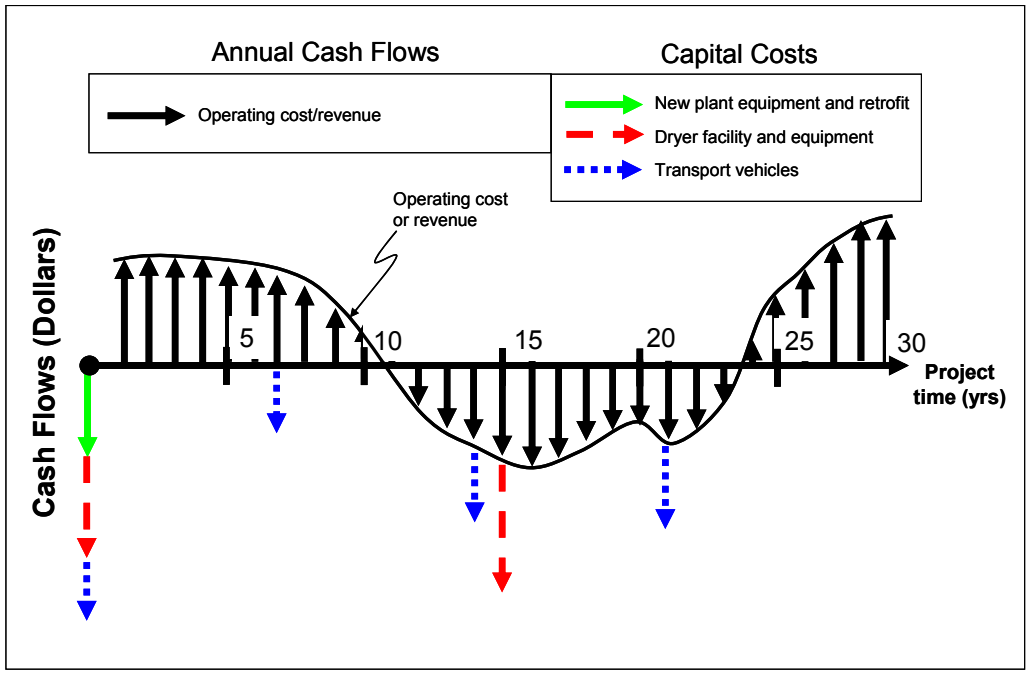

Figure 5.23 Generating an annual operating income or cost from the addition of individual cash flows for each year in the life of the co-fire or reburn project

Next, the capital investments must be added together, including the future investments in trucks and drying equipment, to produce an overall capital investment cost in present dollars. Thus, the total investment in drying equipment for the entire life of the project will be:

$$Investment_{drying} = Capital_{total-drying,year\ 0} + Capital_{total-drying,15} * \left[1 + \left(\frac{ccr}{100}\right)\right]^{-15} \quad (5.287)$$

Here, *ccr* is the capital charge rate. Similarly, the total investment in hauling vehicles can be computed with the following equation.

$$Investment_{trucks} = Capital_{truck,year\ 0} + \sum_{n=7,14,21} Capital_{truck,n}\left[1+\left(\frac{ccr}{100}\right)\right]^{-n} \quad (5.288)$$

Thus, the total investment, in present dollars, for co-firing will be:

$$Investment_{total}\left[\$_{present}\right] = Capital_{cofire} + Investment_{drying} + Investment_{trucks} \quad (5.289)$$

This translation of future capital investments to present dollars is illustrated in Figure 5.24.

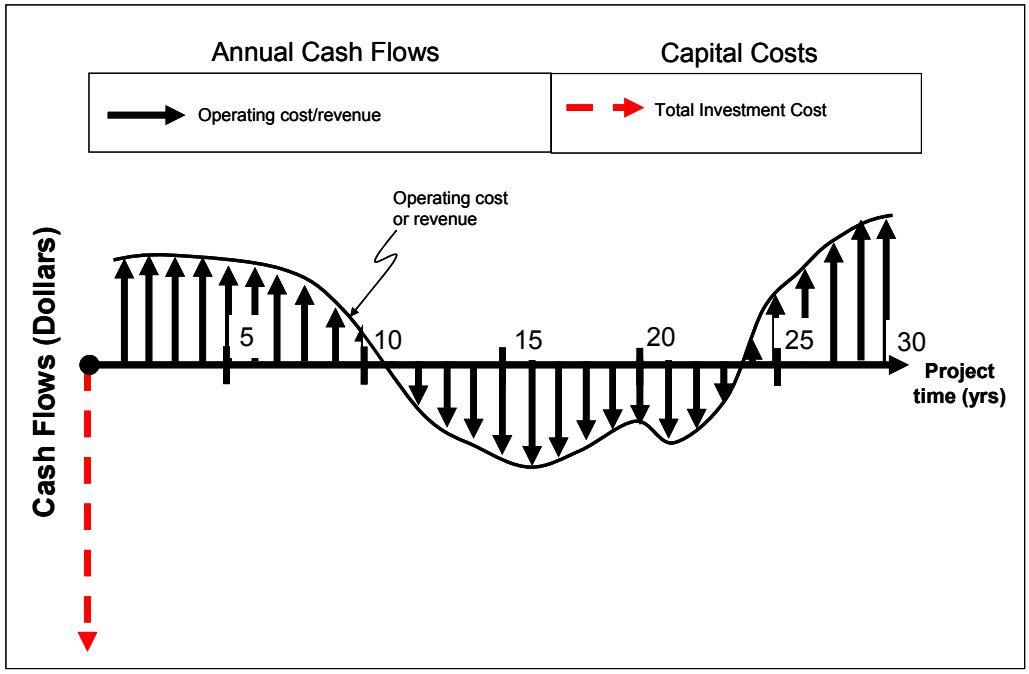

Figure 5.24 Translation of future capital costs to present dollar values

Now, before computing the NPW, depreciation of capital and taxes on income must be addressed, starting with depreciation. The depreciation method adopted for the present analysis was the modified accelerated cost recovery system (MACRS). The MACRS of depreciation schedule is a combination of declining balance depreciation and straight line depreciation. However, under the MACRS, the "property life" is usually shorter than the actual useful life; therefore, there are no salvage values of capital at the

end of the project. For the current model, dryers and their associated equipment were assumed to have useful lives of 15 years, but have a 10-year property life. Trucks had useful lives of seven years, but have a 5-year property life. Co-fire and reburn capital (as well as SCR and SNCR capital) were assumed to have useful lives of 30 years, but each had a 20-year property life. More information about the MACRS of depreciation can be found in the textbook by Newnan *et al*. (2000). A list of the applicable depreciation rates under the MACRS is given in Table 5.8.

Table 5.8 MACRS depreciation rates for 5, 10 and 20-year property life classes used for modeling biomass co-fire and reburn systems (adapted from Newnan *et al*., 2000)

	rates displayed as percentages		
Recovery Year	Trucks (5-year property life)	Dryers (10-year property life)	Co-fire and Reburn Equipment at Power Plant (20-year property life)
1	20.00	10.00	3.75
2	32.00	18.00	7.22
3	19.20	14.40	6.68
4	11.52*	11.52	6.18
5	11.52	9.22	5.71
6	5.76	7.37	5.29
7		6.55*	4.89
8		6.55	4.52
9		6.56	4.46*
10		6.55	4.46
11		3.28	4.46
12			4.46
13			4.46
14			4.46
15			4.46
16			4.46
17			4.46
18			4.46
19			4.46
20			4.46
21			2.23

*all classes convert to straight-line depreciation in the optimal year--shown with and asterisk (*)

Note: Land for the drying equipment depreciates at 2.56% throughout the 30-year life of the project.

The depreciation can be computed by simply multiplying the depreciation rate in the table above to the capital cost. Thus, the depreciation at year, *n*, for a capital cost, *i*, can be computed as:

$$\mathcal{D}_{i,n}\left[\$\right] = Capital_i * r_{\mathcal{D},i,n} \tag{5.290}$$

where $r_{\mathcal{D},i,n}$ is the depreciation rate read from Table 5.8. The total depreciation of capital for a year *n* is:

$$\mathcal{D}_{total,n} = \sum_{i=trucks,\, dryers,\, etc.} \mathcal{D}_{i,n} \tag{5.291}$$

Now, the adjusted income can be computed with the following expression:

$$Adjusted\ Income_n = Operating\ Income_n - \mathcal{D}_{total,n} \tag{5.292}$$

The adjusted income is the amount of income that will be taxed, so that:

$$Tax_n\left[\$\right] = \begin{cases} \dfrac{Tax\ Rate\left[\%\right]}{100} * Adjusted\ Income_n, & if\ Adjusted\ Income_n > 0 \\ 0, & if\ Adjusted\ Income_n \le 0 \end{cases} \tag{5.293}$$

If there were any renewable energy tax credits for co-firing or reburn systems, they would be accounted for here. The income after tax is thus:

$$Income\ after\ tax_n\left[\$\right] = Operating\ Income_n - Tax_n \tag{5.294}$$

Finally, the NPW can be computed. First, the income after tax must be discounted (or transformed) to present dollars. In order to do this, the discount rate, *DR*, must be known. The *DR* is usually divided into a non-inflated (real) rate, *DR**, and the inflation rate, *f*. A bank or a lender will usually quote a DR to a borrower (for example a power company that wants to borrow money to install a co-fire system at one of its power plants). The lender usually quotes a DR that includes the inflation rate. However, if only *DR** is known, then the following expression can be used to compute *DR*.

$$DR = DR^* + f + DR^* * f \tag{5.295}$$

The income after tax will be discounted by a factor:

$$Discount\ factor_n = \left(1 + DR\right)^n \tag{5.296}$$

And the discounted income in present dollars is simply:

$$Discounted\ Income_n\left[\$_{present}\right] = \frac{Income\ after\ tax_n}{Discount\ \ factor_n} \tag{5.297}$$

Finally, the NPW can be computed with the following expression.

$$NPW\left[\$_{present}\right] = \sum_{n=1}^{30} Discounted\ Income_n - Investment_{total} \tag{5.298}$$

If the NPW is positive, then it is usually referred to as the net present value (NPV), while negative NPWs are called net present costs (NPC). The net present worth is displayed graphically in Figure 5.25.

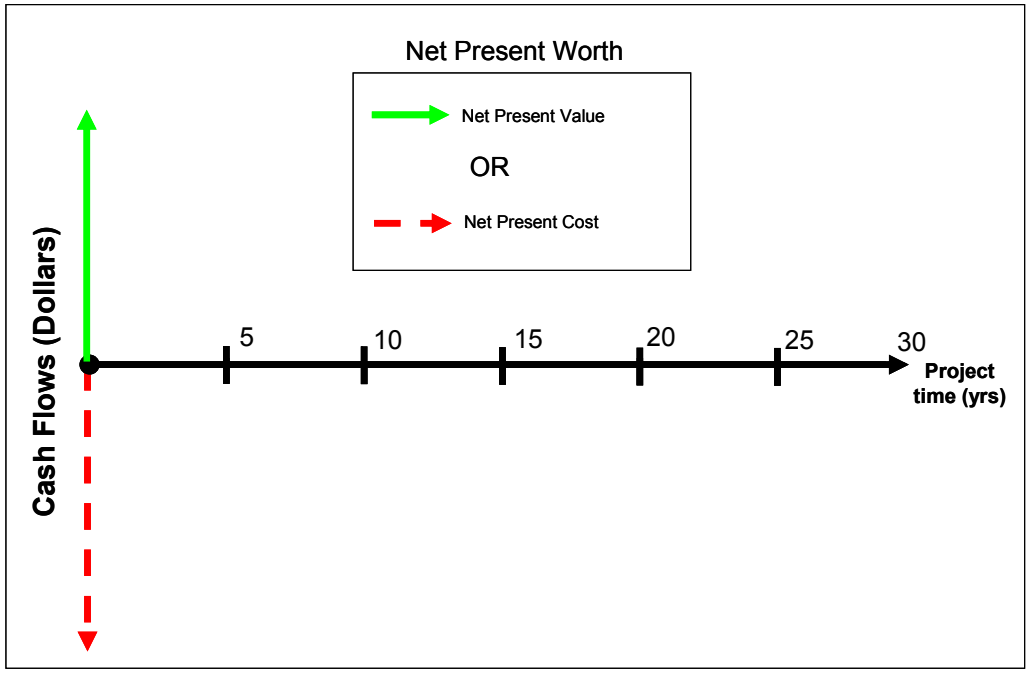

Figure 5.25 Integrating capital investment costs with annual operating incomes to generate an overall net present worth of a co-fire or reburn system

Sometimes, the NPW can be expressed as an annualized cost leveled throughout the life of the project (see Figure 5.26). For this case,

$$Annualized\ Cost\ /\ Revenue\left[\frac{\$}{yr}\right] = NPW * \left[\frac{DR(1+DR)^{30}}{(1+DR)^{30}-1}\right] \tag{5.299}$$

From here, the leveled annual cost can be expressed with other parameters specific to the co-fire or reburn model. For example, the specific CO_2 reduction cost can be computed with annualized cost with the following:

$$Specifc\ CO_2\ Reduction\left[\frac{\$}{metric\ ton\ CO_2}\right] = \frac{Annualized\ Cost}{\left[\left(\mathcal{E}_{CO_2,no\ cofire} - \mathcal{E}_{CO_2,cofiring,reported}\right) - \mathcal{E}_{CO_2,drying} - \mathcal{E}_{CO_2,trucks}\right]} \tag{5.300}$$

A similar calculation may be made for Specific NO_x Reduction Cost. Or a cost based on the electrical energy output of the power plant can be computed as well.

$$Cofire\ Cost\left[\frac{\Leftrightarrow}{kWh_e}\right] = \frac{Annualized\ Cost}{\mathcal{P}\left(\frac{\%CF}{100}\right)\left(OH_{plant}\right)\left(\frac{1{,}000\ kW}{1\ MW}\right)} * \left(\frac{100}{\$}\right) \tag{5.301}$$

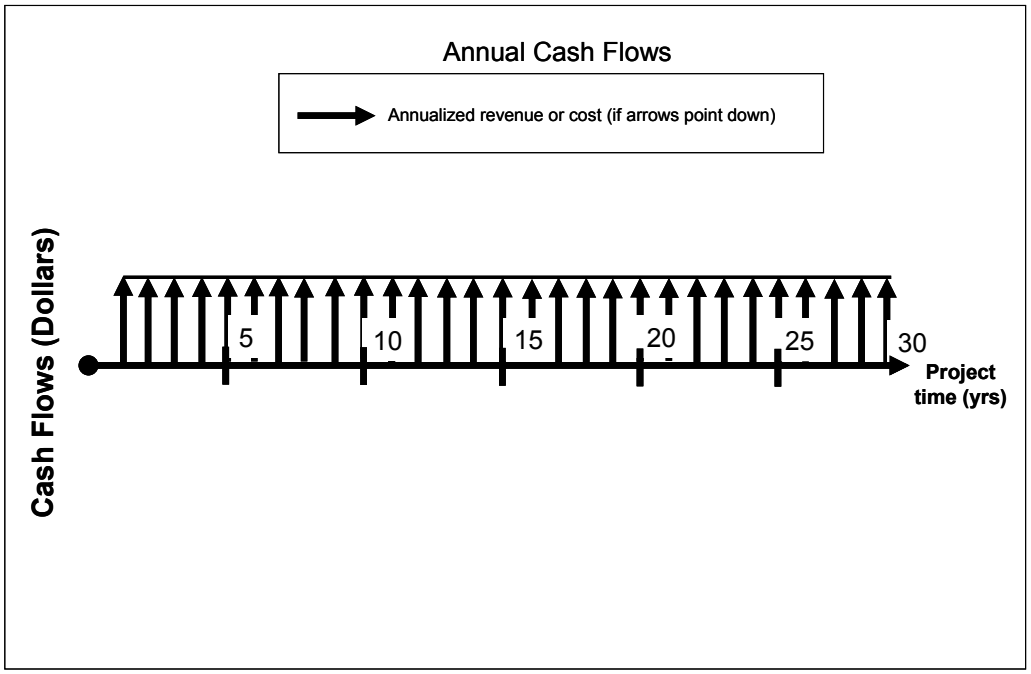

Figure 5.26 Generating a overall annualized cost from the net present worth

Other ways to display the overall economics of a project are the rate of return (*ROR*):

$$ROR = DR, \quad such\ that\ NPW = 0 \tag{5.302}$$

and the simple payback period:

$$Simple\ payback\left[years\right]=\frac{Investment_{total}\left[\$\right]}{Average\ Income\ after\ Tax\left[\$/yr\right]} \tag{5.303}$$

However, the simple payback does not account for the *DR* or the time value of money in anyway.

5.6.6. Economics of Small-scale, On-the-farm Systems

Some estimation of the economic costs for the small-scale system discussed in Section 5.5.1 may also be made as well. Brammer *et al*. (2002) provided the following two capital cost equations for rotary dryers and gasifiers, respectively.

$$Capital_{rotary\ dryer}\left[\$\right]=7072\left[\left(\frac{0.971}{\%M_{MBB,mean}^{2}}-\frac{0.479}{\%M_{MBB,mean}}+11\right)*\frac{\dot{Q}_{to\ MBB}}{\left(T_{vapor}-T_{MBB}\right)}+93.2\right]^{0.863} \tag{5.304}$$

$$Capital_{gasifier}\left[\$\right]=10,300,000\left(\dot{m}_{fuel,3}\right)^{0.698} \tag{5.305}$$

Here, $\%M_{MBB,mean}$ is the mean moisture percentage of the manure passing through the dryer, while $\dot{Q}_{to\ MBB}$ is the heat transferred to the MBB while in the drying drum. The capital cost of the gasifier is simply a function of the fuel flow rate.

Moreover, Mou *et al*. (2002) suggested the following equation for the capital cost of the heat exchanger.

$$Capital_{heat\ exchanger}\left[\$\right]=11,000+302*A_{HX} \tag{5.306}$$

The heat transfer area of the heat exchanger, A_{HX}, may be computed with the following expression.

$$A_{HX}=\frac{\dot{Q}*\ln\left[\frac{T_9-T_{4,o}}{T_9-T_4}\right]}{U_{HX}*\left[\left(T_9-T_{4,o}\right)-\left(T_9-T_4\right)\right]} \tag{5.307}$$

where U_{HX} is the overall heat transfer coefficient and $\dot{Q}$ is the heat transferred to the air. Since the fire-tube boiler may be the more innovative component of the system, its capital cost will be treated as an input for this study.

The fixed O&M cost of the system as a whole can be assumed to be a percentage of the total capital cost. However, the rest of the annual cash flows and savings due to the small scale system may depend heavily on the specific animal feeding operation at which the system is being installed.

6. RESULTS AND DISCUSSION

The modeling equations presented in the previous section can be compiled into spreadsheet or other computer-based programs. The resulting estimates of energy consumption from dryers, fuel consumption from hauling vehicles, firing rates of coal and biomass at the power plant utilizing the biomass, and emission reductions will be presented in this section. Subsequently, a discussion of overall costs and benefits of the use of manure-based biomass (MBB), based on these results, in existing power plants for co-firing and reburning applications will be conducted. Finally, there will be a discussion of how a smaller-scale, on-the-farm system, such as the one presented previously, may perform compared to larger applications. First, the results for MBB drying system models will be discussed.

6.1. Biomass Drying Models

Equations (5.13) through (5.29) describe the overall heat and mass balance of the drying system chosen to dry the MBB (see Figure 5.1), and are applicable to both the perpendicular flow conveyor belt dryer and the parallel flow conveyor belt dryer. Two main parameters that are computed from these equations are the air mass flow rate in the drying chamber ($\dot{m}_{ac}$) and the dryer's heat consumption rate ($\dot{Q}_{dryer}$). These parameters are particularly important for economic analyses. First, $\dot{m}_{ac}$ largely determines the air velocity in the drying chamber (U_{∞}) which in turn affects the pressure drop ($\Delta P_{chamber}$) and the electricity consumption ($\dot{E}_{dryer}$) of the dryer. On the other hand, $\dot{Q}_{dryer}$ exclusively determines the steam consumption of the dryer, and if conventional fuels such as natural gas or propane are used to generate this steam, then the dryer's fuel consumption (equation (5.28)) is greatly dependant on $\dot{Q}_{dryer}$.

The variables in equations (5.13) through (5.29) that are typically known are the ambient temperature, ambient relative humidity ($T_{a,0}$ and $\phi_{a,0}$, respectively), and the

initial temperature of the MBB ($T_{MBB,0}$), which can usually be assumed to be equal to $T_{a,0}$. The dry mass flow of MBB traveling through the dryer will, in this case, be determined by how much biomass is needed to fuel a co-fire or reburn system at a particular power plant of a known electric capacity and heat rate. The initial moisture content of the MBB will also be considered a known input value in this analysis. Moreover, the desired moisture content of the MBB ($\%M_{MBB,0}$) is also determined by the needs of the power plant.

However, there are three main design variables, inherent to the dryers themselves, which greatly affect the air mass flow rate and the heat consumption. These variables are: the temperature drop in the drying chamber ($\Delta T_{chamber}$); the temperature of the air exiting the drying chamber (T_a); and the relative humidity of the air exiting the drying chamber (ϕ_a). Ideally, in order to reduce fan power costs and fueling costs, it is necessary to find a combination of these three design variables that will lower both $\dot{m}_{ac}$ and $\dot{Q}_{dryer}$ as much as possible. Beginning with $\dot{m}_{ac}$, Figure 6.1 is a plot of the air mass flow rate in the chamber vs. T_a and ϕ_a at a fixed value for $\Delta T_{chamber}$ of 10 K. Increasing T_a and ϕ_a will decrease the flow rate. Similarly, Figure 6.2 is a plot of $\dot{m}_{ac}$ vs. T_a and $\Delta T_{chamber}$ at a fixed value for ϕ_a of 20%. Again here, $\dot{m}_{ac}$ decreases with higher values of T_a and $\Delta T_{chamber}$.

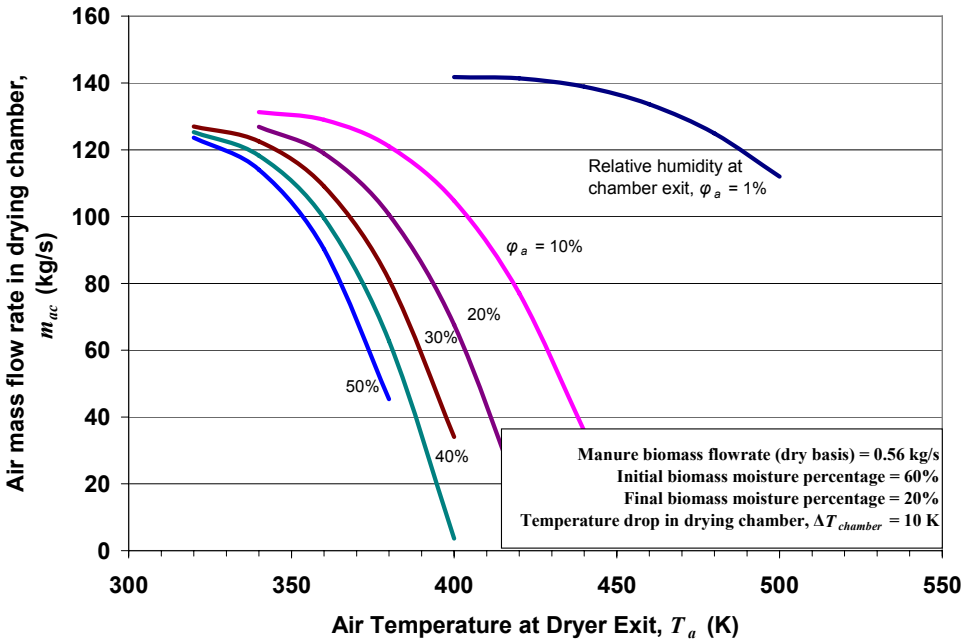

Figure 6.1 Dryer air flow rate vs. air exit temperature and exit relative humidity at fixed chamber temperature drop, $\Delta T_{chamber}$ = 10 K. MBB being dried from 60% to 20% moisture at a rate of 0.56 kg/s (2 metric tons/hour)

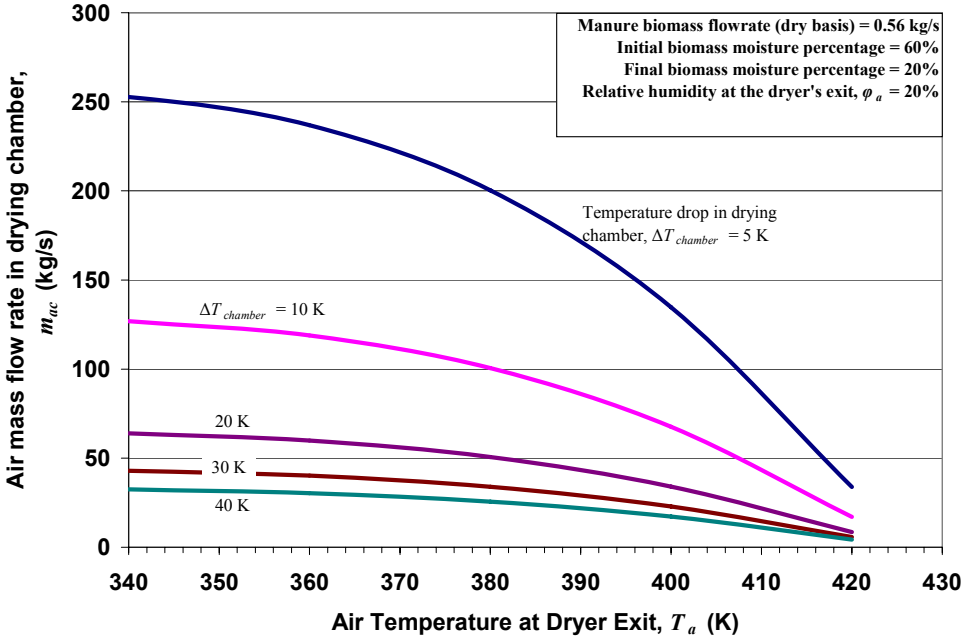

Figure 6.2 Dryer air flow rate vs. air exit temperature and drying chamber temperature drop at fixed exit relative humidity = 20%. MBB being dried from 60% to 20% moisture at a rate of 0.56 kg/s (2 metric tons/hour)

However, in practice a person operating a dryer does not have direct control of T_a, ϕ_a, and $\Delta T_{chamber}$. Instead, the air flow rate and the amount of air that is recycled through the heat exchanger and drying chamber, $\left(\dot{m}_{ac} - \dot{m}_a\right)$, can be controlled with dampers and controlling the air fans. But in the context of designing the dryer (or dryers) for providing a predetermined amount of biomass at a required moisture content to a power plant, T_a, ϕ_a, and $\Delta T_{chamber}$ can be treated as the variables, similarly to the analysis by Kiranoudis *et al*. (1994). For example, suppose that two metric tons/hour of biomass is required per dryer, and that the biomass must be dried from 60% moisture to 20% moisture. From the above figures, a set of base case values can be selected. A low flow rate is desired; therefore, $\Delta T_{chamber}$ should be at least 20 K. The temperature of the exiting air cannot be too high since MBB, which is assumed to leave the dryer at a temperature equal to T_a (see equation (5.23)), may begin to rapidly de-volatilize at temperatures over 470 K (386 °F) (Lawrence, 2007). Rodriguez *et al.* (1998) reported that there was a 4.6% loss in heating value when drying cattle manure at 377 K (219 °F) for 360 minutes. Therefore, T_a should certainly be lower than 470 K, and if it is between 370 and 470 K, then the residence time of the MBB in the dryer should be as limited as possible.

To reduce energy costs, a significant amount of the exiting drier air should be mixed with incoming fresh air and recycled back to the heat exchanger and drying chamber. Doing this will keep ϕ_a high, at least to 20%, but recycling the process air will also increase T_a between 360 K and 380 K. The plot of recycled air flow vs. T_a and $\Delta T_{chamber}$, in Figure 6.3, shows that this recycled flow rate peaks between 360 and 380 K for $\Delta T_{chamber}$ greater than 10 K.

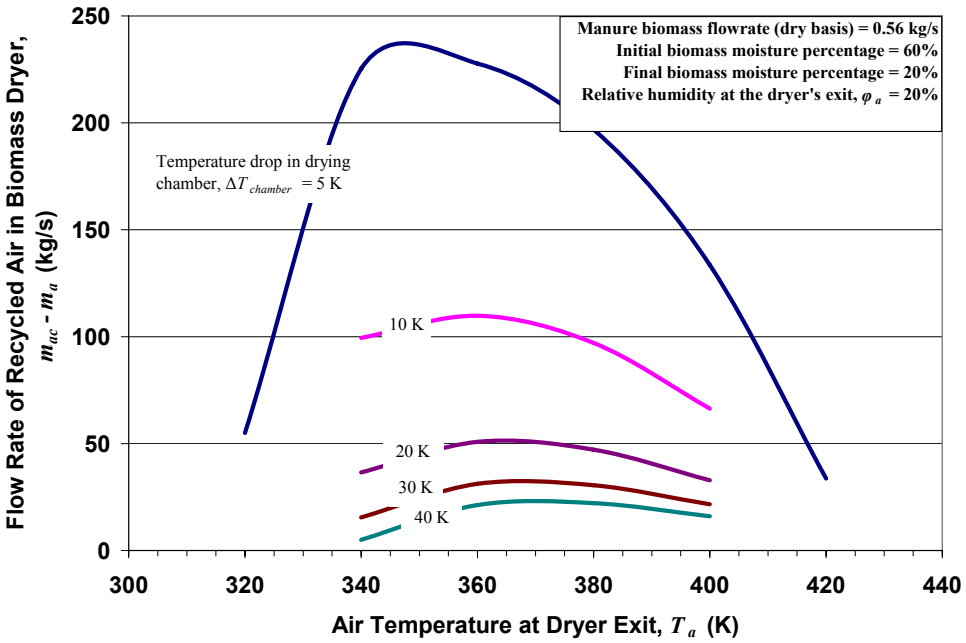

Figure 6.3 Recycled dryer air flow rate vs. air exit temperature and drying chamber temperature drop at fixed exit relative humidity = 20%. MBB being dried from 60% to 20% moisture at a rate of 0.56 kg/s (2 metric tons/hour)

Yet, there is a greater reason why T_a should be kept between 360 and 380 K. Ultimately, the most important parameter that must be found from equations (5.13) through (5.29) is $\dot{Q}_{dryer}$, which is independent of the physical dimensions of the dryer such the conveyor belt area (A_{belt}) and only weakly dependant on whether the air flow is perpendicular or parallel to the conveyor belt by equation (5.23). Moreover, $\dot{Q}_{dryer}$ is independent of $\Delta T_{chamber}$. In Figure 6.4, $\dot{Q}_{dryer}$ decreases asymptotically below 2,000 kW at exit temperatures above 380 K, for ϕ_a greater than 10%. Fixing T_a at 380 K or above ensures that a minimum amount of heat will be consumed by the dryer.

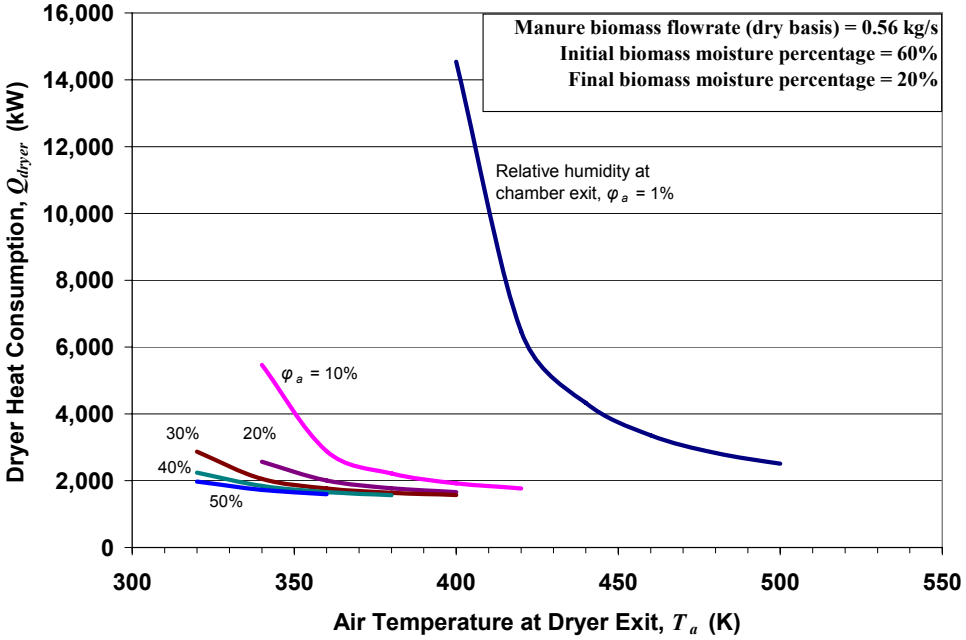

Figure 6.4 Dryer heat consumption vs. air exit temperature and exit relative humidity. MBB being dried from 60% to 20% moisture at a rate of 0.56 kg/s (2 metric tons/hour)

Thus, base values for T_a, ϕ_a, and $\Delta T_{chamber}$ of 380 K, 20%, and 30 K, respectively, can be chosen so that $\dot{Q}_{dryer}$ and $\dot{m}_{ac}$ remain low. Next, the MBB handling capacity of the dryer can be increased to investigate how heat consumption and air flow rate will change. This plot is shown in Figure 6.5.

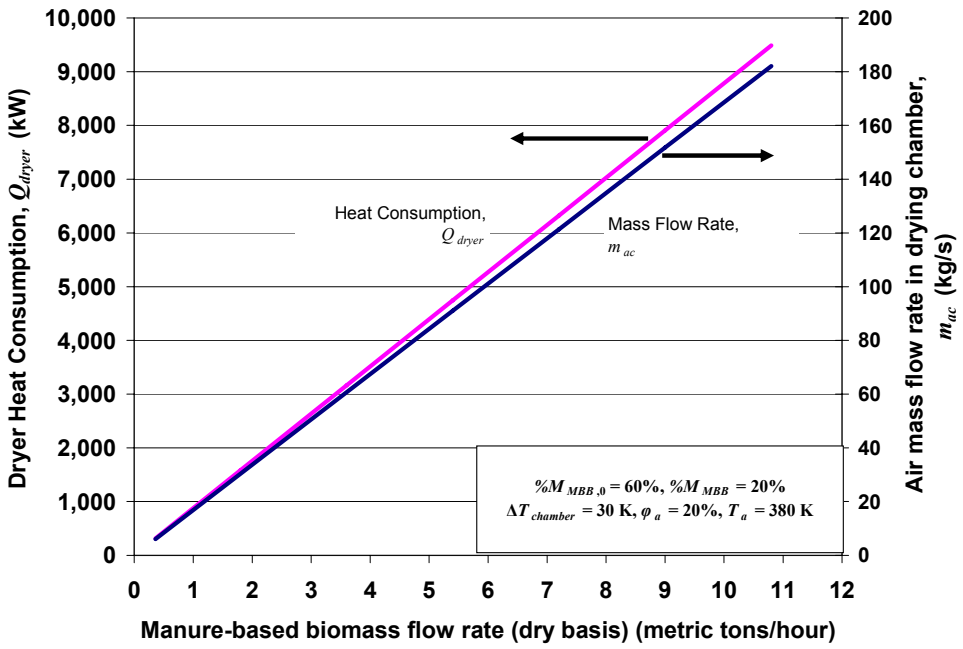

Figure 6.5 Dryer heat consumption and air mass flow rate in drying chamber vs. rate of manure-based biomass

After finding the heat consumption and air flow rate in the drying chamber, the next step in the drying analysis is to find the pressure drop over the conveyor belt, $\Delta P_{chamber}$, and the required area of the conveyor belt, A_{belt}. The pressure drop is needed to compute the electrical energy consumption of the fans in equation (5.50), while A_{belt} is needed to compute the capital investment cost of the dryer. Both of these parameters are significant when computing the overall cost of drying MBB. Other parameters such as the MBB residence time in the dryer (t) and the velocity of the dryer air (U_∞) can be computed after finding A_{belt}.

The conveyor belt area, unlike $\dot{Q}_{dryer}$ and $\dot{m}_{ac}$, is dependant on whether the dryer air flows perpendicular or parallel to the conveyor belt. Perpendicular flow dryers are covered in Section 5.2.1.1.1 , while parallel flow dryers are covered in Section 5.2.1.1.2. For the economic analysis that will follow later in this part of the dissertation, the focus will be on perpendicular flow dryers. The discussion of parallel flow dryers is included mostly for completeness.

Within the discussion of perpendicular flow dryers in Section 5.2.1.1.1, two separate models were presented for determining A_{belt}: one based on a drying rate constant (k_m) defined in equation (5.30) and one based on a transfer number (B) defined in equation (5.39). The drying constant (k_m) model requires empirical constants in equations (5.32) and (5.33). The following table is a list of these constants for several drying experiments on different processed foods.

Table 6.1 Empirical constants required for drying constant (k_m) model for perpendicular air flow dryers

	onions	peppers	potatoes	carrots	tomatoes
k_0 (s^{-1})	5.83E-08	1.11E-08	1.72E-07	9.44E-08	NR
k_l	-0.8080	-0.9820	-1.5100	-1.4800	NR
k_T	1.5500	1.5400	0.3210	0.5710	NR
k_ω	0.2480	0.0903	0.0359	0.1110	NR
k_U	-0.1190	0.2930	-0.1440	-0.0624	NR
ω_m (dry basis)	0.2020	0.2110	0.0870	0.2120	0.1820
C_0	2.30E-05	1.46E-05	1.86E-05	5.94E-05	1.99E-05
$\Delta\bar{H}_C$ (kJ/kmol)	32,500	33,400	34,100	28,900	34,500
K_0	5.79E-02	5.56E-02	5.68E-02	8.03E-02	5.52E-02
$\Delta\bar{H}_K$ (kJ/kmol)	6,430	6,560	6,750	5,490	6,700

NR: Not reported

Data adopted from Kiranoudis *et al*. (1992) and Kiranoudis *et al*. (1993)

On the other hand, the transfer number (B) model is dependant on non-dimensional numbers such as the mass transfer Stanton number (St_m) and the Colburn j factor ($\bar{j}_m$) and relationships between these numbers such as equations (5.44) through (5.46). Both the k_m and the B-models are highly dependant on the characteristic particle size of the MBB (d_c) and the initial manure application thickness on the conveyor belt at the dryer's entrance ($a_{t,0}$). In order to choose which model should be integrated into the overall economic model, these models should be compared against each other to see if there is any agreement between them. One way to compare the two models is by plotting Reynolds number (Re_{d_c}) for each of them. The Reynolds number for this case is defined in equation (5.47) and directly incorporates $\dot{m}_{ac}$, A_{belt}, and d_c. This plot can be seen in Figure 6.6. The solid-lined data are results from the B-model, while the dotted-

lined data are results from the k_m-model. The Reynolds number is plotted against d_c and the sphericity factor, ψ, for the B-model, and for the k_m-model, it is plotted against d_c for carrots and potatoes.

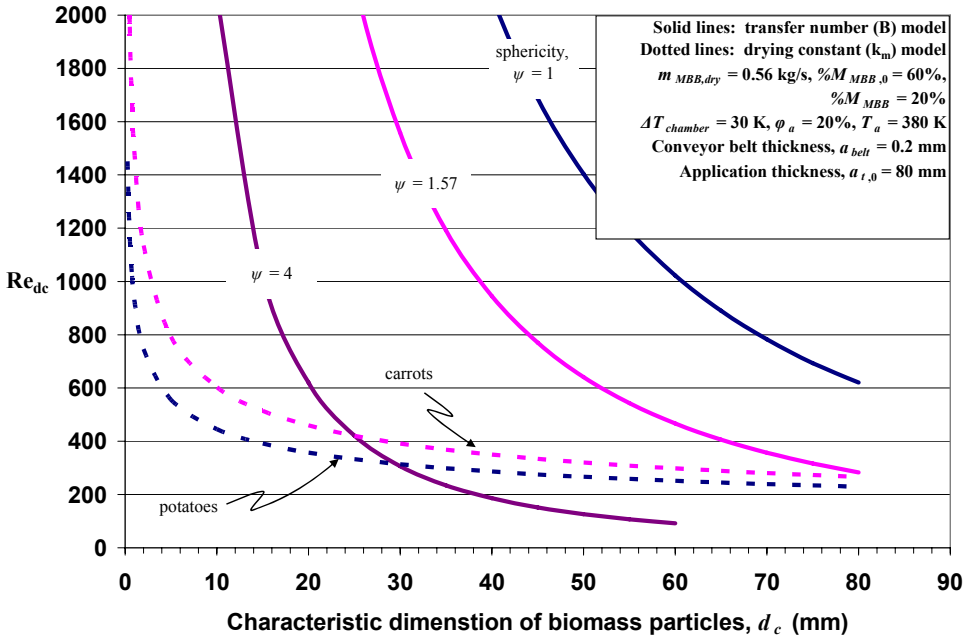

Figure 6.6 Comparison of two drying models for perpendicular air flow dryers by monitoring Reynolds number against characteristic biomass particle size and sphericity. Biomass application thickness on conveyor belt = 80 mm

First of all, the curves seem to have the same general shape for both models, indicating that Re_{d_c} increases steeply as d_c decreases. This relationship may seem counter-intuitive at first, since in equation (5.47), Re_{d_c} is directly proportional to d_c; however, Re_{d_c} is also inversely proportional to A_{belt} (= l * w). From equation (5.49), it may be seen that A_{belt} is also proportional to not only d_c, but also $\dot{m}_{ac}$. Thus d_c and $\dot{m}_{ac}$ cancel out of the Reynolds equation when equation (5.49) is plugged into (5.47). The reason why Re_{d_c} still changes with d_c is because the wetted surface area of the biomass particles (A_{MBB}) is inversely proportional d_c as well. Subsequently plugging equation (5.43) into (5.47) will show that:

$$\mathrm{Re}_{d_c} \propto \left(\frac{1}{\psi \cdot d_c} \right)^{40/23} \tag{6.1}$$

Thus, Re_{d_c} increases quickly with lower d_c, especially for spherical particles ($\psi \approx 1$). Physically, this relationship means that collections of smaller particles with greater surface areas dry quicker, and thus require a smaller conveyor belt area and residence time.

These smaller belt areas in turn increase the air velocity (U_∞) as can be seen in equation (5.34). Ultimately, for this drying problem, high Reynolds numbers suggest high air velocities in the dryer. High velocities are problematic however, because manure particles would be blown off of the conveyor belt as they travel through the dryer and hit the fans. Earlier in Section 2.1.2, the Rosin Rammler characteristic particle size of dried cattle manure was shown to be 2.18 mm (0.086 inches). At this particle size, the Re_{d_c} is beyond the 4000 limit of equation (5.46). However, for the k_m-model assuming constants for potatoes, the Reynolds number is predicted to be 726 and U_∞ is predicted to be 9 m/s (about 20 mph).

There are two possible reasons for the quantitative disagreement of the models in Figure 6.6. (1) Perhaps the food particles studied by Kiranoudis *et al*. truly had high sphericity factors. Higher values of ψ dampen the relationship between Re_{d_c} and d_c in equation (6.1), and bring the curves of the two models to better agreement (see curve for ψ = 4 in Figure 6.6). However, such high values for ψ in all of the foods tested by Kiranoudis *et al*. are unlikely. A cubic particle has a sphericity factor of 1.08; a cylindrical particle with an axial ratio of 10 has a sphericity of 1.58, at most (Hinds, 1999). (2) The disagreement between the empirical k_m-model and the *B*-model are more likely due to the inherent limits to the Colburn j factor relationships in equations (5.45) and (5.46). These equations are probably more suited to flows over larger particle sizes. Thus the constants and exponents in equations (5.45) and (5.46) may need to be altered, in effect changing the exponent of 40/23 in equation (6.1). Thus, for the remainder of this discussion and the discussion of the economics model, the k_m-model will be used to

estimate A_{belt}. The models did not vary significantly between the different foods listed in Table 6.1, so, for brevity in the remaining figures, the constants for potatoes will be used from now on. However, there is still value in the *B*-model in that a greater physical understanding of the drying problem is gained as the k_m-model (equation (5.33)) is simply a fit to experimental data.

The Reynolds number, and hence the air velocity, is also a function of the application thickness of the manure on the conveyor belt at the dryer's entrance ($a_{t,0}$). Figure 6.7 is a plot of Re_{d_c} against d_c and $a_{t,0}$ at a constant $\psi = 1.11$. According to the plot, Re_{d_c} increases with $a_{t,0}$. The quantitative disagreement between the k_m and the *B* models can be seen here as well.

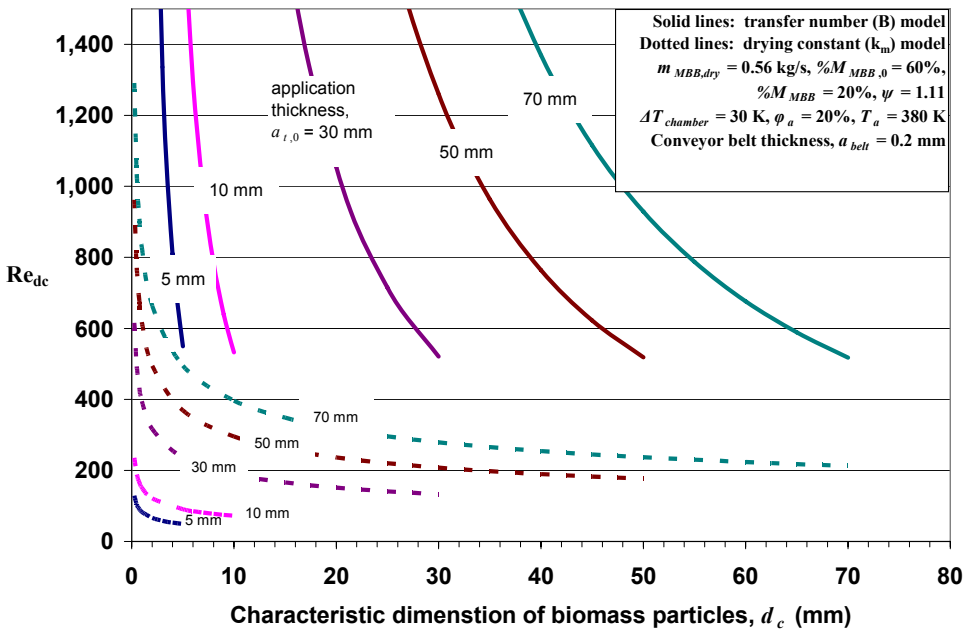

Figure 6.7 Comparison of two drying models for perpendicular air flow dryers by monitoring Reynolds number against characteristic biomass particle size and biomass application thickness on conveyor belt

During the operation of the conveyor belt dryer, it is necessary to determine the appropriate manure application thickness ($a_{t,0}$). Thicker applications increase the required U_∞ and the pressure drop in the chamber ($\Delta P_{chamber}$) which in effect increase the

electrical consumption of the dryer fans. However, thicker applications also reduce the required conveyor belt area, which reduces the capital investment cost of the dryer (i.e. smaller dryers require thicker applications of manure in order to handle the same throughput and achieve the desired moisture percentage). Thus, a compromise must be made between the two costs. In Figure 6.8, A_{belt}, $\Delta P_{chamber}$, and U_{∞} are plotted against $a_{t,0}$. The data for this case, suggests that an application thickness of 30 to 50 mm (1.18 to 1.96 inches) would be most appropriate, because both A_{belt} and $\Delta P_{chamber}$ are relatively low at this range. At a 40 mm thickness, the k_m-model for potatoes predicts a required belt area of 9.55 m^2 (about 100 ft^2), an air velocity of 4.89 m/s (about 11 mph), a MBB residence time of about 5 minutes, and a required fan power of 331 kW.

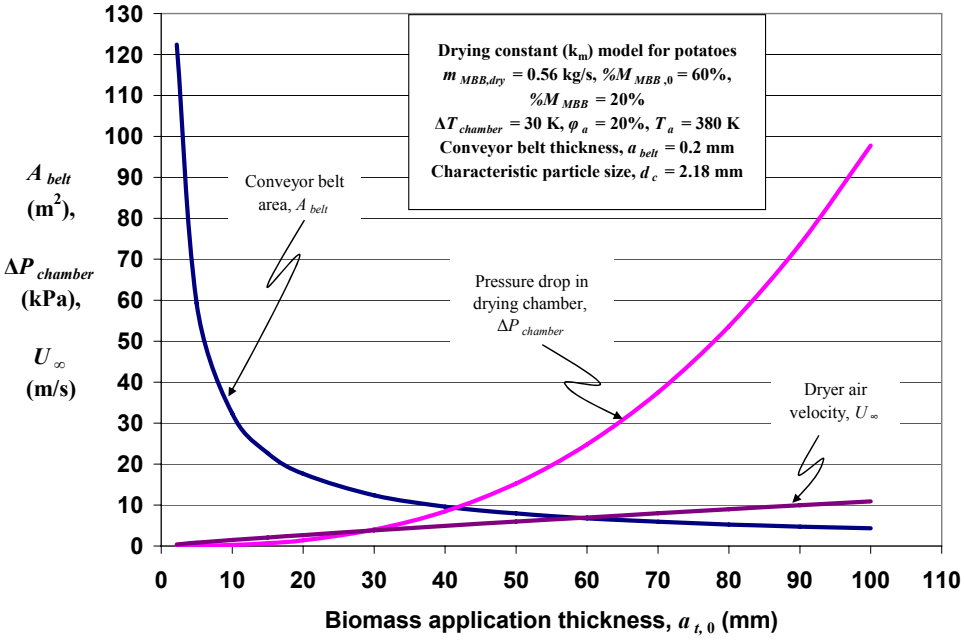

Figure 6.8 Determination of appropriate manure-based biomass application thickness

Another option for drying the MBB would be to use a conveyor belt dryer with air blowing parallel to the belt as discussed in Section 5.2.1.1.2. However, for the manure throughput and moisture reduction required for this drying problem, equation (5.60) predicts extremely large belt areas even at very thin application thicknesses ($a_{t,0}$).

These large areas may be reduced if the cross sectional area of the drying chamber is reduced (i.e. reducing *a* and *w* in equation (5.60)). However, if cross-sectional area is decreased, the air velocity becomes too great. From these results, perpendicular flow conveyor belt dryers may be more appropriate for drying manure at a scale large enough to supply coal-fired power plants than parallel flow dryers.

The one advantage to parallel dryers is that the conveyor belt does not have to be a screen, since air flows over the belt and biomass and not through them. Solid, non-screen conveyor belts may be helpful since the biomass particles have a wide range of sizes; smaller particles may fall through the screen causing major design issues for the dryer when handling granular solids of non-uniform size.

However, as stated before, conveyor belt size becomes an issue with these parallel flow conveyor belt dryers. An alternative to conveyor belt dryers are rotary dryers. Rotary dryers can handle granular solids with smaller particle sizes such as powders (< 100 mesh) (Brammer *et al*. (1999)), and remain relatively compact compared to conveyor belt dryers. Partly for this reason, rotary steam-tube dryers were modeled for drying biomass solids in Section 5.2.1.2. However, in this study, rotary dryers were modeled for small-scale MBB combustion designs, which will be discussed later. Yet, the performance of the rotary dryer can still be compared to the conveyor belt dryer. A list of base parameters for running the rotary dryer model is presented in Table 6.2. Again, a biomass throughput of 2 metric tons/hour (dry basis) can be assumed, as was done for the conveyor belt dryer. The same initial and desired moisture percentages are also assumed for this case.

Table 6.2 Base case parameters for rotary steam-tube manure-based biomass dryer

Parameter	Base Value (unit)
Mass flow of MBB through the dryer	0.56 kg/s (2 metric tons/hr)
Initial moisture percentage of biomass	60%
Desired moisture percentage of biomass	20%
Dryer drum diameter	1 m
Drying zone length to drum diameter ratio	5 (m/m)
Rotation speed of drum	35 rpm
Steam tube diameters	0.04 m
Number of steam tubes[a]	36
Characteristic particle size of MBB	2.18 mm
Sphericity factor	1.11
Holdup	5%
Molar fraction of steam in vapor phase	0.9
Boiler pressure	350 kPa, gage
Boiler efficiency	85%

[a]The steam tubes are arranged in two concentric rings around the drum's center. The first is half the distance from the center of the drum to the steam shell, the second is located 80% of the distance from the center of the drum to the shell. See Figure 5.7

From the base case results it was found that at 2 metric tons/hour, a rotary steam-tube dryer would consume about 16% less heat energy, and thus consume 16% less fuel a if similar 350 kPa (gage) boiler were to provide steam to both dryers. Figure 6.9 is a graph of fuel consumption versus biomass flow rate for both a conveyor belt dryer and a rotary dryer. Energy savings become more noticeable at higher biomass throughputs, according to the results of the dryer models. Moreover, the length of the rotary dryer was computed to be 5.29 m (about 17.5 ft). With a rotation speed of 35 rpm, the drum would need to be tilted 0.8 degrees (0.014 m/m) from horizontal and the biomass particles would travel through the drum at about 0.03 m/s (about 6 ft/minute) and have a residence time in the rotary dryer of 2.7 minutes.

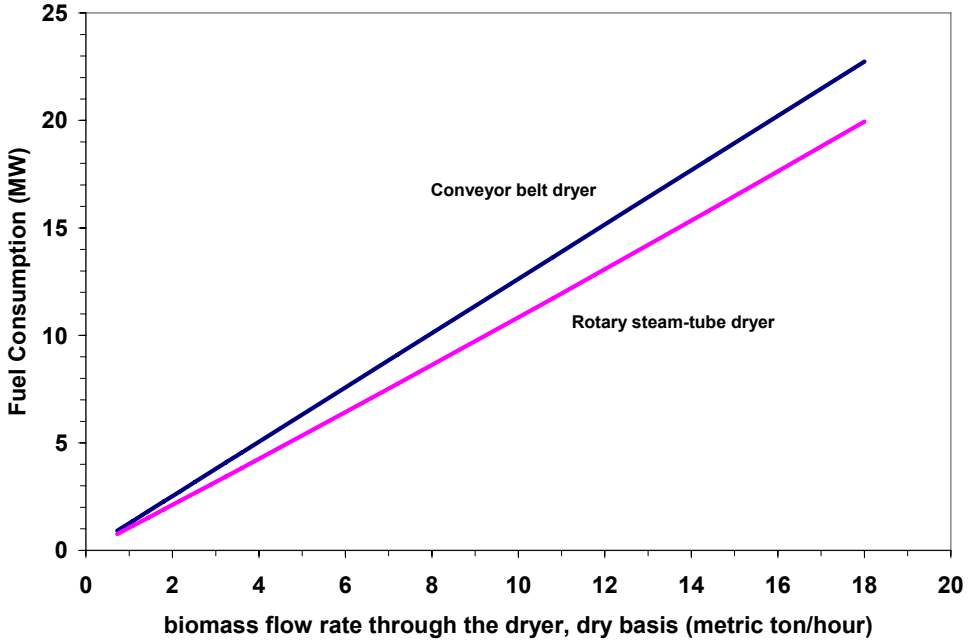

Figure 6.9 Comparison of fuel consumption between conveyor belt dryer and rotary steam-tube dryer

Another point of interest for these dryers may be the vapor temperature and the temperature of the biomass in drying zone (see Figure 5.6). For this model, the temperature at which the biomass dries is solely determined by the molar fraction of steam in the vapor phase, $Y_{steam,\ vapor}$. The drying temperature of the biomass is then used to determine the vapor temperature, the length of the heat-up zone of the dryer, and the steam consumption. Figure 6.10 is a plot of these temperatures versus $Y_{steam,vapor}$. This plot agrees fairly well with a similar plot made by Canales *et al*. (2001); however, the vapor temperature computed here seems to be two or three degrees below what Canales *et al*. computed. This difference is probably due to a slightly lower boiler pressure (and thus lower steam temperature) for this case.

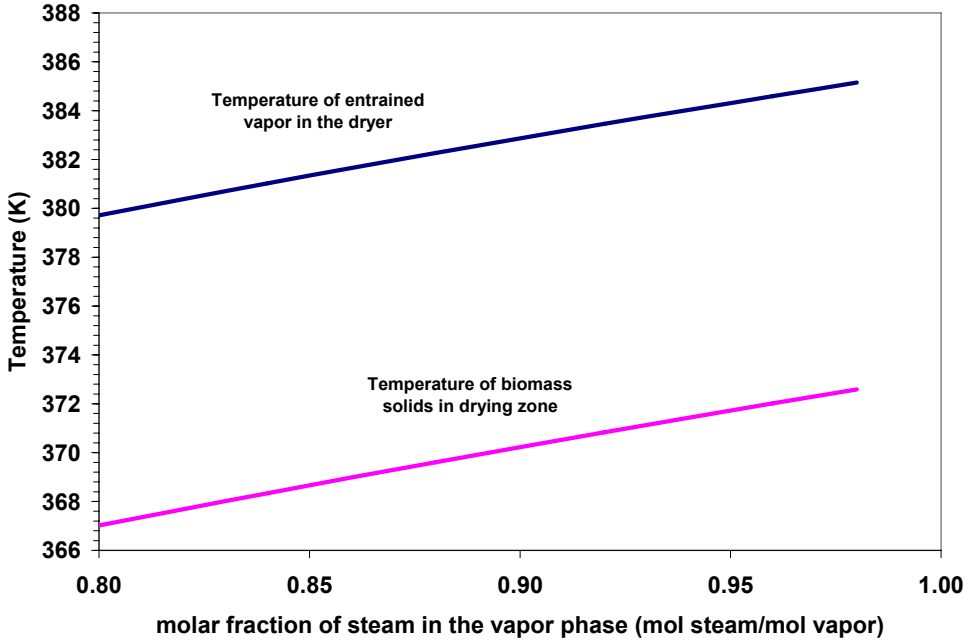

Figure 6.10 Temperature of entrained vapor and temperature of biomass solids in the drying zone vs. molar fraction of steam in vapor phase

The vapor temperature is also very dependant on biomass particle size, as can be seen in Figure 6.11. Larger particles require more time to heat up to the biomass drying temperature, thus the required length of the dryer is predicted to be slightly longer for larger particles. Since the flow rate of the vapor is fixed by the desired moisture percentage, the vapor spends slightly more time in the dryer heated by the steam tubes and steam shell, and the vapor's temperature begins to approach the temperature of the steam tubes and shell.

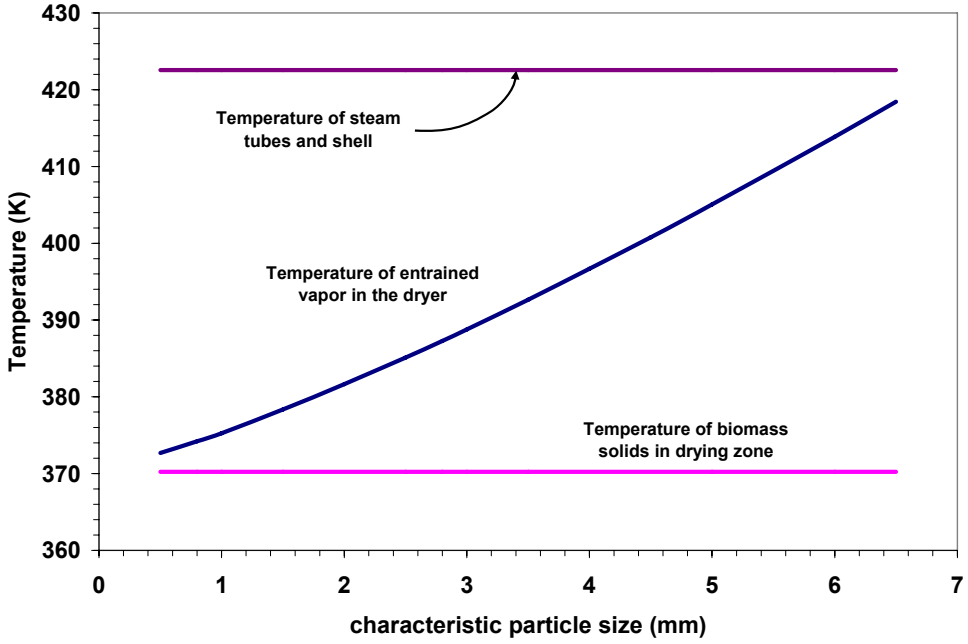

Figure 6.11 Temperature of entrained vapor vs. characteristic particle size of biomass solids

One other parameter unique to the rotary dryer is the holdup. Increasing the holdup in the dryer changes most of the operating conditions of the dryer. For example, in Figure 6.12, the slope of the drum, the residence time of the biomass and the linear speed at which the biomass solids travel through the drum are plotted against holdup. A greater holdup means that there are more solids in the dryer at any given time. More solids require longer residence times, thus the slope of the dryer must decrease and the biomass must move through the dryer slower.

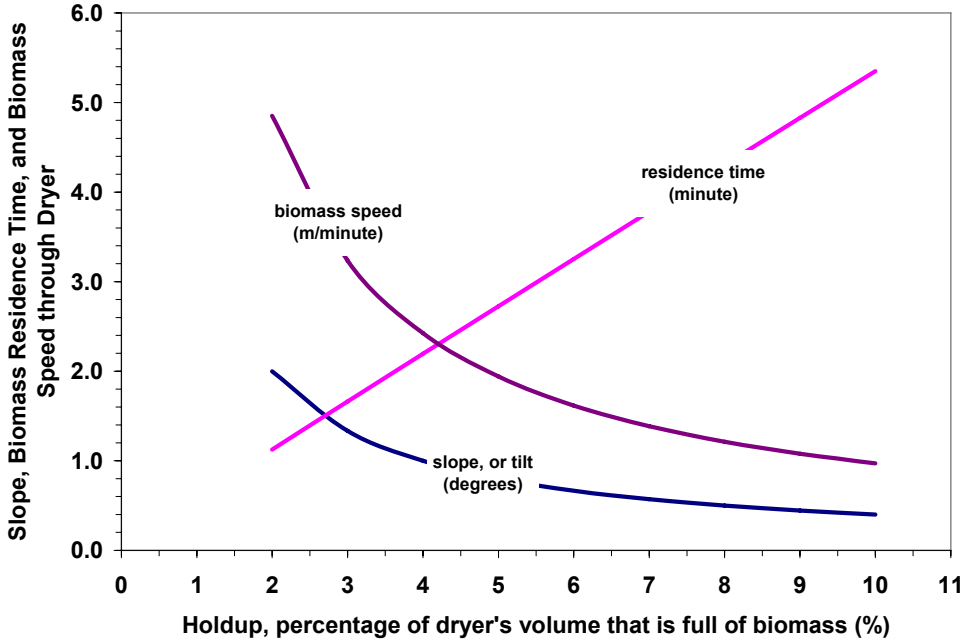

Figure 6.12 The effect of holdup on the slope, biomass residence time, and biomass speed through a rotary steam-tube dryer

6.2. Biomass Transportation Model

The manure based biomass (MBB) may be transported before or after drying. The decision of when to dry the MBB may greatly affect the transportation costs because the liquid water in the manure is added weight that must also be transported and because the bulk density of the manure is a function of the moisture percentage. The benefit of transporting wet MBB and drying it at the power plant is that waste heat from the plant's combustion processes may be used for drying manure instead of using natural gas or propane. From equation (5.2) and Figure 2.7, the bulk density of the MBB decreases as moisture is reduced below 60%. The transportation analysis discussed here was first presented in a USEPA (2001) report for transporting composted solids from feeding operations. However, changes in density were not mentioned in that report and are unique to the analysis presented here. In the USEPA report, densities were assumed to be roughly the same as the density of water (998 kg/m^3).

So, there are seemingly two components when considering transportation costs vs. MBB moisture percentage: if the manure is transported when it is high in moisture, more weight must be carried from the feeding operations to the combustion facility, but the manure will be denser, hence hauling vehicles with fixed carrying volumes (see Figure 6.13) can carry more of it. On the other hand, if the manure is transported after drying, when moisture is low, less weight must be transported, but the dried solids will not be as dense and each truck with a fixed carrying volume will not be able to carry as much biomass (assuming no compaction or compression equipment is used to artificially increase the density of the dried MBB).

Figure 6.13 Montone 33.6 m^3 (44 yd^3) dump trailer (Montone Trailers, LLC., 2008)

For example, suppose that 76,000 dry metric tons per year is required by a particular power plant. This is approximately the amount of low-ash dairy biomass that would be required for a 300 MW_e coal plant co-firing a 95:5 blend of Wyoming sub-bituminous coal and MBB. Moreover, suppose the biomass must be transported 50 km (31 miles) to the power plant, that each truck has a carrying volume of 30.6 m^3 (40 yd^3), and that the average truck speed is 80.5 km/hr (50 mile/hr). Manure hauling is assumed to be conducted 16 hours per day and 320 days per year, and loading and unloading times are assumed to be 25 minutes each. In Figure 6.14, the number of trucks required

(equation (5.102)) and the hauling weight per truck (equation (5.101)) are plotted against the moisture percentage of the MBB when it is transported. These results seem to suggest that even with more liquid mass being hauled for high moisture biomass, the number of trucks required to haul this additional mass will not change significantly due to the increase of bulk density. There is no significant difference in capital or purchasing costs for hauling vehicles once the MBB has been dried below 70% moisture. However, the figure does show that hauling liquid manure, such as flushed manure from free stalls, at 90% moisture would be significantly more expensive.

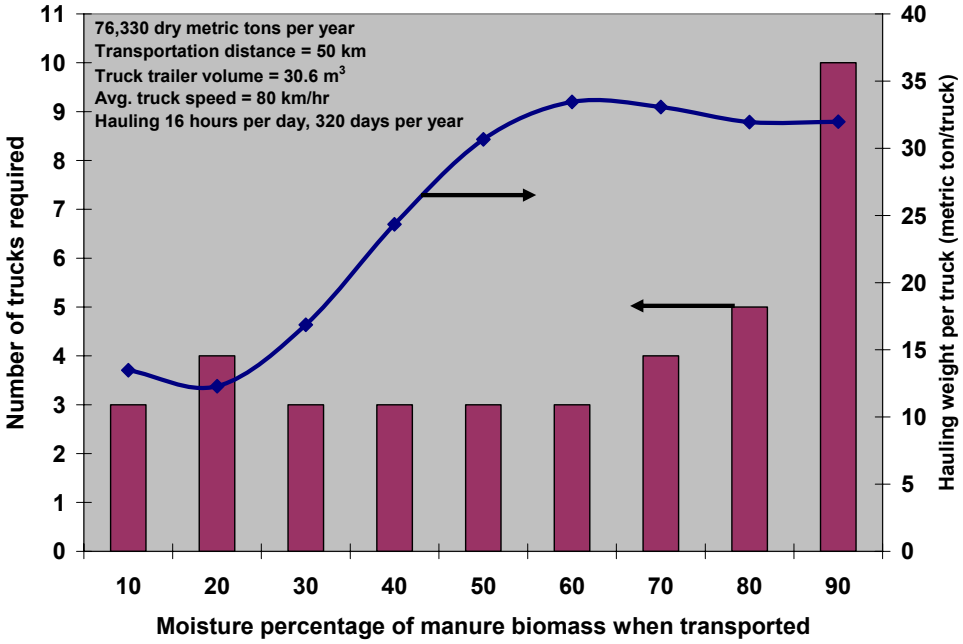

Figure 6.14 Number of hauling vehicles and hauling weight vs. moisture percentage of transported manure based biomass

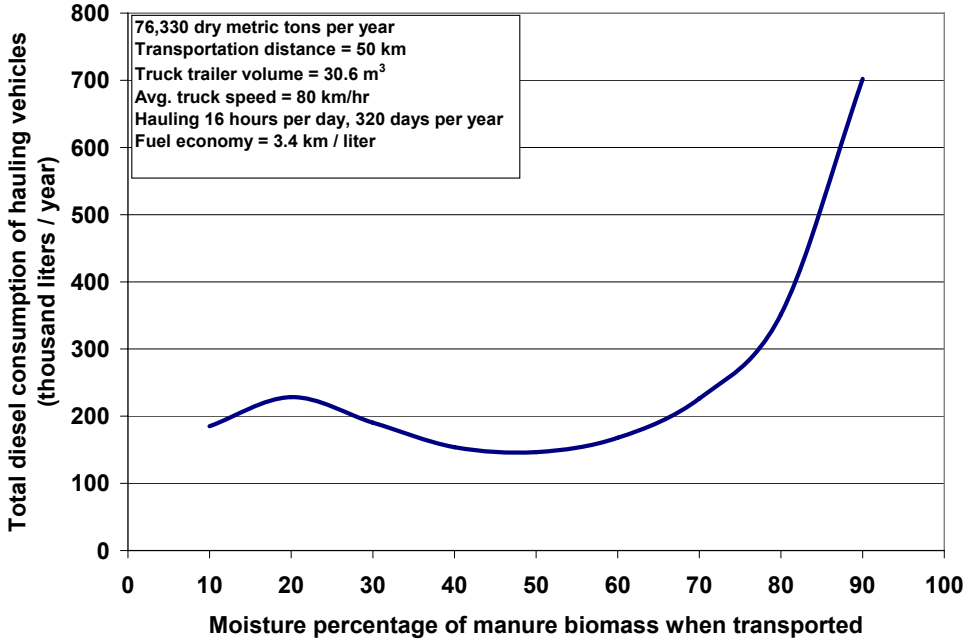

Figure 6.15 Total diesel fuel consumption from hauling vehicles vs. moisture percentage of transported manure based biomass

The same analysis can be extended to the fueling costs of the transport vehicles. Figure 6.15 is a plot of total diesel consumption of the vehicles (equation (5.105)) vs. the moisture percentage of the MBB when it is hauled. This curve is similar to the data in the previous figure for the number of required trucks. Again, there seems to be no significant difference in fuel consumption between hauling manure with 10% moisture and hauling manure with 70% moisture. In fact, there seems to be a slight minimum in fuel consumption at approximately 50% moisture. However, fuel consumption does increase dramatically if the moisture content is above 85 or 90%. It should also be noted that these calculations do not take into account any difference in fuel economy for vehicles hauling heavier loads when the manure has higher moisture content, but the aerodynamics and mechanics of the vehicle usually have a greater influence on fuel economy than the haul weight.

Moreover, there are other factors, aside from the number of vehicles required and the fuel consumption that may affect the decision of when to transport the manure. Power plant operators may have reservations to the idea of accepting wet, as-received

MBB and drying it at or near the plant due to odor, health, and environmental issues. Also loading and unloading times, as well as the general ease of handling the MBB when it is wet instead of dried, will certainly play into the decision making. Composting and outdoor drying can reduce the MBB's moisture content to an equilibrium value between 20 and 30%. However, natural composting and drying without external heat may not be able to produce enough dried biomass to consistently supply a co-combustion operation at a large coal-plant. This may be especially true for reburn systems, which would require at least 10% of the plant's heat rate to be supplied by biomass reburn fuel, although, biomass storage or stockpiling operations may be a solution. For the base case run of the economics calculations, which will be discussed later in this section, manure will be assumed to be dried with natural gas before transport to the power plant. During sensitivity analysis, cases where it is not necessary to dry MBB with fossil fuel combustion will also be considered.

Other aspects can affect the transportation cost of hauling MBB to power plants. Figure 6.16 is a graph of total diesel fuel consumption vs. the distance between the animal feeding operations supplying the MBB and the power plant for the same general conditions described above. Biomass moisture percentage was set at 20%. The number of trucks that would be required to transport all of the biomass is also indicated. As expected, both the fuel consumption and the number of trucks that must be utilized increase when the biomass must be hauled greater distances. These calculations were also conducted for different trailer volumes: 30.6 m^3 (40 yd^3), 19.11 m^3 (25 yd^3), and 11.47 m^3 (15 yd^3) trailers.

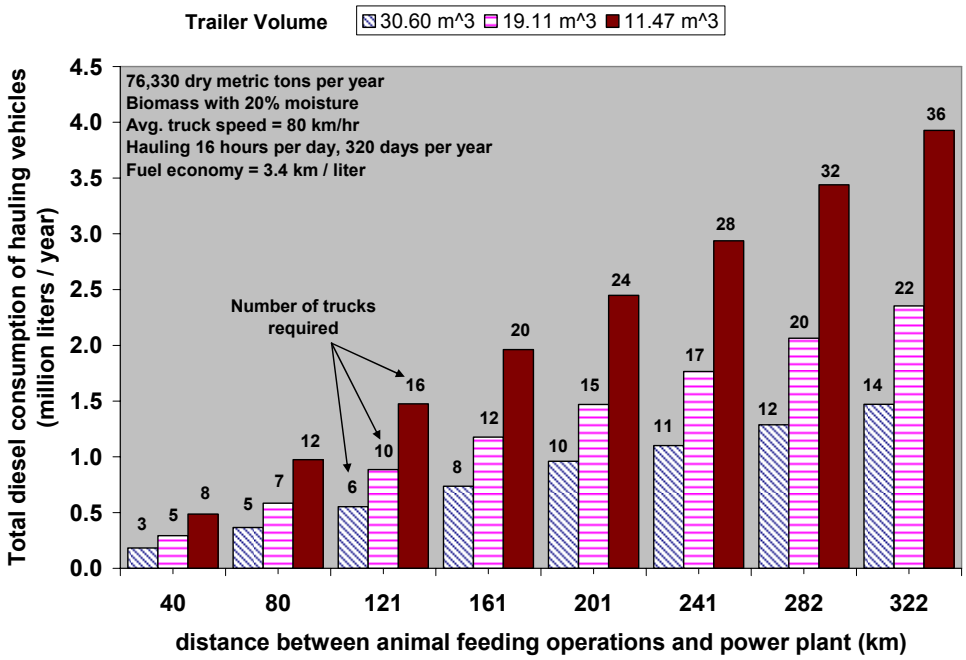

Figure 6.16 Total diesel fuel consumption and number of trucks required vs. biomass transport distance and trailer volume

One other major factor in determining the expense of transporting MBB from animal feeding operations to power plants is the time spent hauling the manure. Large electric utility coal-fired boilers generally run constantly; 24 hours per day, 365 days per year; as they provide the base load of the electrical grid. These power plants only make scheduled stops in operation for maintenance and up-grades. However, the transportation system that supplies MBB to the power plants may not run constantly, and may only run a small fraction of each day or each year. Figure 6.17 is a plot of the number of trucks required vs. the number of hours spent hauling manure each day and the number of days per year spent hauling. Again, the same other conditions were assumed for this plot as in the previous figures. One interesting result from this plot is that there seems to be a greater difference between hauling for one 8-hour shift and two 8-hour shifts (i.e. 16 hours) versus the difference between hauling for two shifts and three 8-hour shifts (i.e. 24 hours per day). This larger margin between these three hauling schedules is probably due to the fact that in the calculations, the total annual amount of MBB required and the volume of each truck are fixed. Thus, in some cases

for the shorter hauling schedules, some of the trucks at the end of the schedule may be hauling below their capacity.

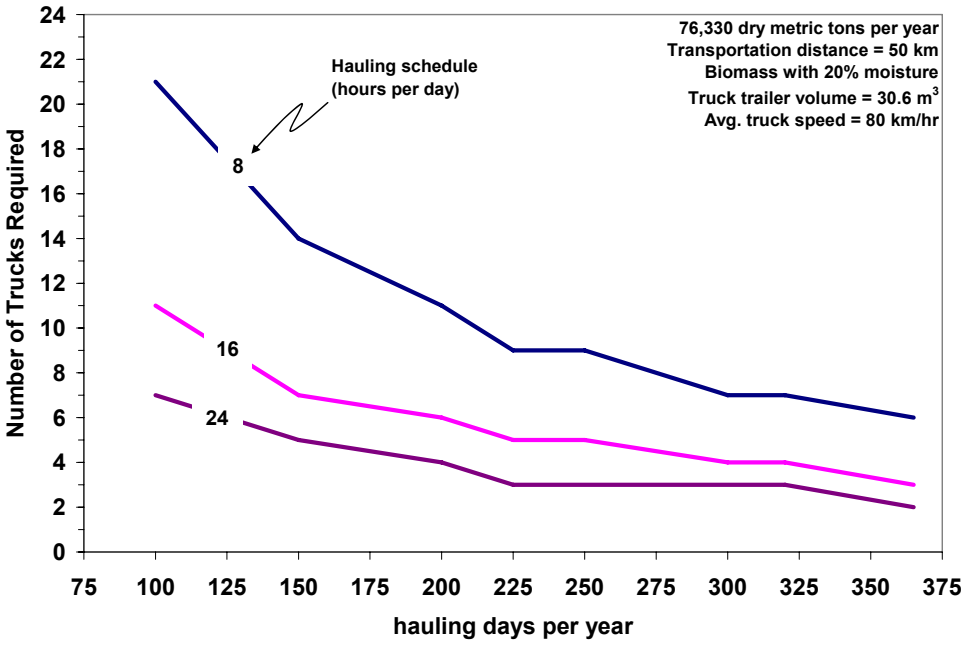

Figure 6.17 Number of trucks required for hauling MBB vs. hauling schedule and annual number of hauling days

6.3. Economics of Manure-based Biomass Combustion in Large-scale Coal-fired Power Plants

The equations presented in the modeling section of this paper were integrated into three large computer spreadsheet programs: one for computing the overall economics of co-firing coal with MBB at an existing coal plant, another for the overall economics of reburning coal with MBB, and a third for computing the general performance of a small-scale system operating at a concentrated animal feeding operation. These spreadsheet programs were useful tools for studying the feasibility and cost of utilizing MBB in combustion systems. They were also used for parametric studies to determine the limiting factors that may reduce the success of manure biomass

combustion. First, in this part of the dissertation, the results of the co-fire model will be discussed, followed by the reburn model.

6.3.1. Co-firing

An outline of the co-fire model is presented in Figure 6.18. The program can be divided into three main computing blocks: (1) for estimating the fueling, emissions and costs when burning coal alone, before any co-firing, (2) for computing the same costs when co-firing coal with biomass plus any addition O&M, transporting and drying costs, and (3) for comparing the two operating conditions with an economic analysis.

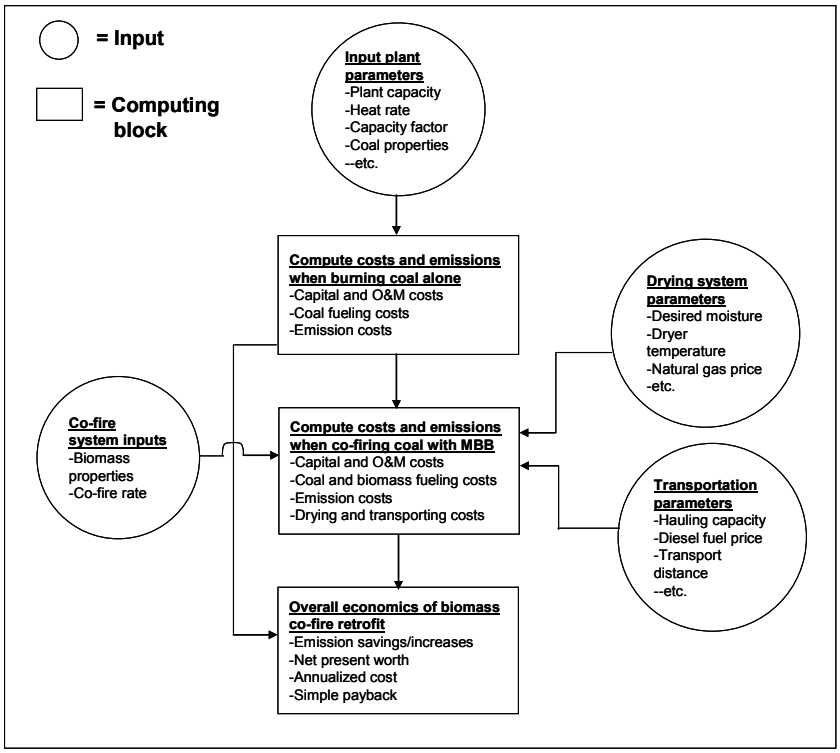

Figure 6.18 Flow diagram of computer spreadsheet model for coal/manure-based biomass co-firing system on an exiting coal-fired power plant

6.3.1.1. Base case inputs and results

To demonstrate the usage of the economic spreadsheet model for co-firing, some base case input parameters were chosen. Most of these parameters are best guess values taken from research and literature review. This set of inputs acted as a reference point for parametric study and sensitivity analysis. Table 6.3 through Table 6.7 are lists of all base case input parameters pertinent to modeling the installation and the operation of the MBB co-firing system. However, these base case inputs are not set. These numbers can and should be changed to accommodate different situations and facilities. In fact, variations of many of these input parameters were made to study the sensitivity of the overall net present worth and annualized cost. This discussion will follow a brief review of the base case findings.

Table 6.3 Base case input parameters for coal-fired power plant operating conditions and emissions

Input	Value (unit)	Source	Notes
Plant capacity	300 MW_e		
Heat rate	10,290 kJ_{th}/kWh_e (9750 Btu/kWh)		About 35% plant efficiency, average for most coal-fired power plants
Capacity factor	80%		
Operating hours[a]	8760 hr/yr		1 year = 8760 hours. Non-stop utility operation.
Primary fuel	WYPRB coal	(TAMU, 2006)	See Table 2.2, Moisture percentage for coal when fired is 30%
Boiler type	Tangentially-fired		
Coal cost	$38.58/metric ton	(EIA, 2007d)	As delivered cost for WY Powder River Basin Sub-bituminous coal in Texas.
Farmer's asking price for MBB	$0/dry metric ton		For the base case, the MBB will be assumed to be free of charge.
CO_2 price	$3.85/metric ton	(RGGI, 2008)	Slightly higher than the clearing price of CO_2 allowances at the September 2008 auction of the Regional Greenhouse Gas Initiative.
SO_x credit/allowance	$970/metric ton	(SCAQMD, 2007)	Average annual price for Compliance Year 2005.
Ash sale price	$27.56/metric ton	(Robl, 1997)	Range: $27.56 - 33.07/metric ton
Ash disposal cost	$33.07/metric ton	(ACAA, 2006)	Range: $22.05 - 44.09/metric ton. Landfill tipping fees for non-hazardous waste.
Percentage of ash sold[b]	20%	(Robl, 1997)	For coal, 61% of solid byproduct is fly ash which can be sold for outside use. On average, only 11% of solid byproduct is sold.

[a]For base case, reburn, SCR and SNCR systems are assumed to operate during all plant operating hours

[b]For base case run, ash sold during reburning is the same, by mass, as that sold when only primary controls are used

Note: metric tons = 1,000 kg = 1.1 ton

Table 6.4 Base case input parameters for co-firing and SO_x controls

Input	Value (unit)	Source	Notes
Co-fired fuel	LADB	(Sweeten *et al*, 2006)	See Table 2.5
Co-firing Rate	5% (by mass)	(DOE, 2004), (USEPA, 2007c)	Range: 2 - 15%. Generally power plants greater than 500 MW capacity co-fire at 2% biomass. Plants with capacities between 201 and 500 MW co-fire at 10% biomass. And smaller plants, less than or equal to 200 MW co-fire at 15% biomass.
Co-fire capital cost	Variable, See Notes	(USEPA, 2007c)	If capacity of power plant is >500 MW_e, then \$109/kW_e supplied by biomass. If capacity is 201 - 500 MW_e, then \$218/kW_e. If capacity is <200 MW_e, then \$251/kW_e.
Co-fire fixed O&M	\$7.63/kW supplied by the co-fired fuel per year	(USEPA, 2007c)	Does not include transportation costs of biomass if co-firing rate is larger than the standard rate. For example, if a 500 MW plant has a co-firing rate greater than 2%, then additional transportation costs must be added to the total O&M costs since more biomass is required to satisfy the desired co-firing rate. In the case of manure-based biomass, this does not include drying costs.
SO_x control	Flue gas desulphurization system **is** installed		
SO_x reduction efficiency[a]	95%	(USEPA, 2004)	Typical for Limestone Forced Oxidation (LSFO), which can reduce SO_x down to about 0.06 lb SO_x/MMBtu and is applicable to plants with greater than 100 MW capacities

[a]For the base case run, the SO_x reduction efficiency during co-firing is assumed to be the same, by percent, as the reduction efficiency during normal operations when only coal is burned.

Table 6.5 Base case input parameters for manure-based biomass drying system

Input	Value (unit)	Source	Notes
Biomass moisture percentage before drying	60%	(Carlin, 2005)	Typical for partially composted separated dairy biomass solids from flushing system
Biomass moisture percentage after drying	20%	(Annamalai *et al*., 2003a), (Annamalai *et al*., 2005)	Approximate moisture percentage of biomass during co-firing and reburn experiments
The biomass is dried before it is transported to the power plant	--		The biomass can possibly be dried at the power plant by using waste heat from the combustion processes at the plant. However, this may increase the cost of transporting the biomass and it may not be allowable to have as received manure biomass at the power plant.
Capacity of single biomass dryer	2 metric tons (2.2046 tons)		Smaller scale dryer such as those discussed by Brammer *et al*. (2002)
Height of drying chamber	0.5 m (1.64 ft)	(Brammer *et al*, 2002)	
Width of drying chamber	0.5 m (1.64 ft)	(Brammer *et al*, 2002)	
Number of drying days	300 days/yr		Approximately 6 days per week, minus holidays
Drying schedule	20 hrs/day		2 1/2 eight hour shifts
Dryer operators	0.4 employees/dryer		Employees operate loaders and maintain the dryers
Number of loaders	0.2 loaders/dryer	(GSNet.com, 2007)	3.86 - 4.63 m^3 (5 - 6 yd^3) capacity per loader. Loaders carry biomass from dryer to transport vehicles. Capital cost of each loader is about $200,000.
Characteristic particle size of manure	2.18 mm (0.09 inches)	(Houkum, 1974)	Characteristic size for Rosin-Rammler distribution of low moisture beef cattle biomass particles
Temperature of biomass entering the dryer	25 °C (77 °F)		Same as ambient air temperature, see next item
Ambient air temperature	25 °C (77 °F)		Annual average day time temperature for central Texas
Ambient relative humidity	50%		Annual average day time relative humidity for central Texas
Temperature of air exiting the dryer	107 °C (224 °F)	(Rodriguez *et al*., 1998)	Can be, at most, 195 °C (383 °F) before rapid de-volatilization occurs. Moreover, at drying temperatures over 100 °C (212 °F), drying times should also be limited to less than five minutes to preserve the biomass's heating value.
Relative humidity of air exiting the dryer	20%		

Table 6.5, continued

Input	Value (unit)	Source	Notes
Air temperature difference in dryer	30 °C (54 °F)		Difference between temperature of air entering and exiting the drying chamber. Generally determined by the air flow through the dryer.
Boiler pressure	345 kPa (gage) (50 psig)		Capital cost of each boiler is approximately \$44/(kg/hr) or \$20/(lb/hr) of steam production
Boiler efficiency	85%		
Labor cost for dryer operators	\$15/hr		
Cost of electricity	\$0.09/kWh_e	(EIA, 2007e)	Average retail price for 2006 commercial consumers
Natural gas price	\$7.36/GJ (\$7.76/MMBtu)	(EIA, 2007b)	Average 2006 price for electricity producers
Land requirement	4 hectares per drying site		Note: 1 hectare = 10,000 m^2. It was estimated that one drying site of this size could house 5 dryers
Land cost	\$12,350/hectare (\$5,000/acre)		This cost may also include general overhead costs such as small office buildings and parking lots at the drying sites.
Extra storage structures	four 30.6 m^3 storage trailers		122.3 m^3 (160 yd^3) of total extra biomass storage (about 2 days extra capacity) in case of inclement weather.

Table 6.6 Base case input parameters for manure-based biomass transportation system

Input	Value (unit)	Source	Notes
Loading & unloading times	25 min each	(USEPA, 2001)	
Average distance between plant and animal feeding operations	80 km (50 miles)		This distance should be an average distance weighted by the amount of biomass from each animal feeding operation contributing to the power plant's fueling
Number of hauling days	300 days/yr		Approximately 6 days per week, minus holidays
Hauling schedule	16 hrs/day		2 eight hour shifts
Truck capacity	30 m^3 (40 yd^3)	(GSNet.com, 2007)	30 m^3 (40 yd^3) trailers cost roughly $40,000 each, and the truck tractors hauling the trailers cost approximately $150,000 each.
Truck maintenance	$0.31/km ($0.50/mile)	(USEPA, 2001)	
Labor cost for biomass haulers	$15/hr		
Diesel fuel price	$0.79/liter ($3.00/gal)		
Average truck speed	80.5 km/hr (50 mph)	(Krishnan *et al.*, 2005)	Fuel economy for the hauling vehicles was assumed to be 3.4 km/liter (8 mpg)
Rated truck horse power	373 kW (500 hp)	(Peterbilt.com, 2009)	
Truck load factor	70%	(Krishnan *et al.*, 2005)	
Truck SCR cost	$3,120/yr	(Krishnan *et al.*, 2005)	Includes O&M and annualized capital costs. SCR can meet 74.5 g/GJ (0.2 g/bhp hr) NO_x levels; 2007 standards

Table 6.7 Base case economics input parameters

Input	Value (unit)	Source	Notes
Book Life	30 years	(USEPA, 2004)	Balance sheet for corporate financing structure for environmental retrofits
Real (non-inflated) Discount Rate	5.30%	(USEPA, 2006)	"
Inflation Rate	4.00%		
Capital Charge Rate	12.10%	(USEPA, 2006)	Balance sheet for corporate financing structure for environmental retrofits
Tax Rate	34.00%	(Turner, 2001)	Omnibus Reconciliation Act of 1993: Marginal tax rate for taxable incomes between $335,000 and $10,000,000
Assumed annual rates of price escalation based on data from the US Bureau of Labor Statistics from 1998 to 2007			
Transport vehicles	0.00%	(US Bureau of Labor Statistics, 2008)	Estimated from the combined average annual rate of price increase for truck tractors and trailers between 1998 and 2007 (computed from Producer Price Commodity Indexes). Truck trailers increased in price by about 2.66% annually, but truck tractors decreased in value by about 0.73% between 1998 and 2007.
Dryers	3.90%	(US Bureau of Labor Statistics, 2008)	Estimated from the average annual rate of price increase for industrial food production machinery (e.g. dryers) between 1998 and 2007 (computed from Producer Price Commodity Indexes)
Coal	3.77%	(US Bureau of Labor Statistics, 2008)	Estimated from the average annual rate of price increase for bituminous coal and lignite between 1998 and 2007 (computed from Producer Price Commodity Indexes)
Natural gas	5.00%		The prices of natural gas and propane have increased by about 10% and 20% annually, respectively on average, from 1998 to 2007. The assumed values are more optimistic because such high annual price increases would certainly make any co-fire or reburn project economically unfeasible if prices were to increase at these rates throughout the life of the project.
Propane	5.00%		"
Electricity	3.71%	(US Bureau of Labor Statistics, 2008)	Estimated from the average annual rate of price increase for industrial electrical power between 1998 and 2007 (computed from Producer Price Commodity Indexes)

Table 6.7, continued

Input	Value (unit)	Source	Notes
Diesel fuel	5.00%		The price of diesel has increased by 20% annually, on average from 1998 to 2007. The assumed value of 5% is more optimistic because such a high annual price increase would make transporting biomass unfeasible if the price were to increase at this rate throughout the life of the project. Moreover, the rate computed from the Producer Price Commodity Indexes is somewhat skewed due to the large price increase of oil and petroleum products in 2007.
Labor	1.50%	(US Bureau of Labor Statistics, 2008)	
CO_2 allowances	5.25%	(Sekar *et al*., 2005)	The estimated annual increase of the value of CO_2 under the proposed McCain-Libermann bill of 2003
SO_2 allowances	4.00%	(SCAQMD, 2007)	
Ash sales	1.00%		
Ash disposal (tipping fees)	1.00%		

From the base case inputs, a resulting reference run was completed. The base case results for fueling and emission rates for a 300 MW_e coal-fired power plant, before any co-fire or reburn system is implemented, are summarized in Table 6.8. These rates may be compared to those in Table 6.9 for fueling and emissions when the same power plant is fueled with a 95:5 blend (by mass) of coal and MBB. The annual energy consumption was found to increase by about 259,000 GJ per year when co-firing with MBB. This includes the energy consumed by drying equipment and transportation vehicles. The heat energy released by the MBB when burned at the power plant (i.e. 794,800 GJ/yr in Table 6.9) was found to be 535,000 GJ more than the energy needed to dry it and transport it to the plant.

Table 6.8 Base case fueling and emissions results for a 300 MW_e coal plant operating before any co-firing or reburning system is installed

		Coal only (burned with primary NO_x controls and FGD)
Fueling rate	GJ/yr	21,625,812
	metric ton/yr	1,137,322
CO_2 emission	g/GJ	93,497
	metric ton/yr	2,021,983
SO_2 emission	g/GJ	15
	metric ton/yr	324
Ash emission	g/GJ	3,093
	metric ton/yr	66,897
NO_x emission	g/GJ	84
	metric ton/yr	1,822

Total CO_2 emissions when co-firing with MBB, including carbon emissions from biomass drying and transportation, were found to be 58,600 metric tons per year less than CO_2 emissions before implementing co-firing. However, this estimate assumes that all of the electricity used to run the dryer's fans was generated completely from coal combustion. Moreover, SO_2 emissions were found to increase slightly when co-firing, but this is mostly because a flue gas desulphurization system was assumed to be installed whether MBB was being burned or not. Otherwise, higher sulfur contents in the biomass compared to the Wyoming sub-bituminous coal may have been more of a

factor. Finally, ash emissions were found to increase by about 10% when co-firing with only 5% MBB under the base case run, even though the MBB was of the low-ash variety.

Table 6.9 Base case fueling and emissions results for a 300 MW_e coal plant operating while co-firing manure-based biomass (5% by mass)

Number of drying sites	1
Number of dryers (each rated at 2 dry metric tons/hr)	5
Number of dryer operators	2
Total hectares required for drying site(s)	4
Total extra storage trailers	4
Number of hauling vehicles required (30.6 m^3 each)	3
Number of cows required (6.35 dry kg/cow/day)	21,000

		Primary fuel (coal)	Co-fired fuel (MBB)	Dryers (natural gas)	Dryers (electricity for fans)[a]	Hauling vehicles (diesel)	Total
Fueling rate	GJ/yr	20,831,030	794,782	213,423	36,931	9,091	21,885,256
	metric ton/yr	1,095,524	57,693	4,268	2,169	189	n/a
CO_2 emission	g/GJ	90,063	3,681	55,005	93,497	64,290	n/a
	metric ton/yr	1,947,672	79,655	11,709	3,453	584	1,963,418[b]
SO_2 emission	g/GJ	14.43	1.23	n/a	n/a	n/a	n/a
	metric ton/yr	312	27	n/a	n/a	n/a	338
Ash production	g/GJ	2,980	426	n/a	n/a	n/a	n/a
	metric ton/yr	64,439	9,220	n/a	n/a	n/a	73,659

[a]Electricity for fan operation is assumed to come entirely from coal. Fueling and emission rates are for the equivalent amount of coal required to produce the electricity in a power plant with an overall efficiency of 35%.
[b]Excluding CO_2 emissions from renewable fuels such as the MBB co-fired fuel

Yet economically, co-firing coal and MBB was found to be 2.3% more expensive than burning coal alone, under base case assumptions. A list of cost components at Year 1 and the overall sum of these costs and revenues for both firing coal alone and burning coal with MBB under the base case assumptions are juxtaposed in Table 6.10. The major increase in cost of co-firing MBB comes from the variable O&M increase, largely due to biomass drying operations. However, this is partly offset by combined (coal and biomass) fuel delivery savings of about $990,000. Yet, increased fixed O&M cost and $223,700 more in ash disposal costs (even when the co-fire rate is only 5%, by

mass) make co-firing coal with MBB more expensive, at Year 1, under base case assumptions.

Table 6.10 Comparison of base case Year 1 costs for power plant operation before and during manure-based biomass co-firing (300 MW_e plant, 5% biomass by mass)

Year 1 Costs	Coal Combustion only	Co-firing Coal with Biomass
Fixed O&M Cost	0	67,261
Variable O&M Cost[a]	0	2,155,166
Biomass Delivery Cost	0	620,100
Coal Delivery Cost	43,878,448	42,265,847
CO_2 Penalty	7,800,913	7,574,966
SO_2 Penalty	314,864	329,081
Ash Revenue	(368,704)	(368,601)
Ash Disposal Cost	1,769,781	1,993,493
Annualized Capital Cost	0	594,887
TOTAL COST (w/o capital)	53,395,301	54,637,314

[a]For MBB, variable O&M includes the cost of drying the biomass

In order to compute the net present worth (NPW) (equation (5.298)) of a MBB co-fire implementation project, the cash flows throughout the life of the project must be computed. This analysis requires knowledge of the discount (non-inflated) rate, inflation rate, price escalation rates, and the project life. The base case values of these parameters are listed in Table 6.7. Usually an economically attractive project would generate annual revenue in order to payoff the initial investment of the project. In the case of the co-fire project, the hope is that avoided CO_2 emission costs (allowances, taxes, avoided sequestering and/or storage costs) and avoided coal fueling costs will overrule the additional costs of drying and transporting the biomass, grinding and burning the biomass at the plant, and the cost of disposing ash emitted when burning MBB. However, at least for the base case run, this payoff was found not to occur. The total operating cost (or revenue) at year one can be computed by taking the difference of the total costs listed in Table 6.10 (i.e. \$54,600,000 – \$53,400,000 = \$1,200,000). Even though the value of carbon and the price of coal were assumed to escalate annually by 5.25% and 3.77%, respectively; the price of natural gas, electricity, and diesel fuel,

which are all necessary to supply the biomass under the base case assumptions, escalate as well at similar rates.

Thus, the operating cost of the co-fire project only grows throughout the project life without any return, as can be seen in Figure 6.19. The discounted values of the operating costs are also displayed in present dollars. The total initial investment of the project was found to be $5.9 million dollars. After adding the discounted operating costs throughout the project, the 30-year NPW for the base case run was found to be negative $22.6 million (i.e. net present cost). Distributing this NPW evenly through all 30 years with equation (5.299) showed that the annualized cost of co-firing would be $2.30 million per year. With equation (5.300), the specific CO_2 reduction cost was found to be $35.68/ton CO_2. Dividing the annualized cost by the electricity output of the plant (equation (5.301)) showed that co-firing coal with MBB would cost 0.11 ¢/kWh_e.

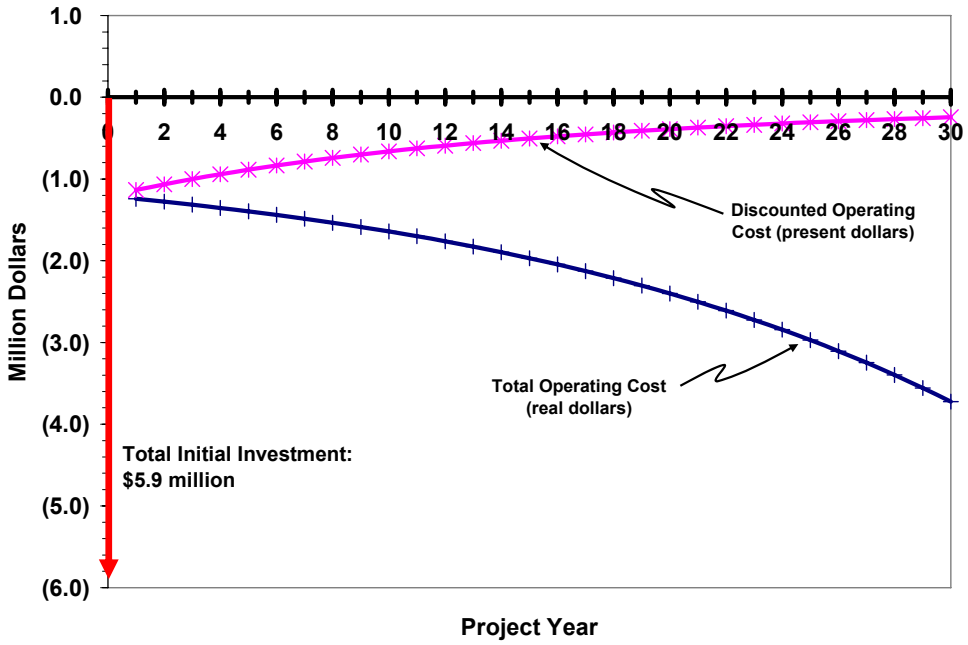

Figure 6.19 Overall cash flows for the base case run of the manure-based biomass co-fire economics model

These results will act as the base case for the remainder of this discussion on the economics of co-firing coal and MBB. Each parameter will be varied while holding all

other parameters fixed at their respective base values. Some of the more significant parameters such as transport distance and diesel price will be discussed presently; however, in Appendix C a full sensitivity analysis of the NPW for all base case values is presented.

6.3.1.2. Biomass and coal fueling

The amount of MBB burned along with the coal can greatly influence the overall cost of the system. However, whether an increase in co-fire rate will increase or lower the overall cost may not be intuitively clear, since transport and drying costs will go up, but revenue from avoided CO_2 and avoided coal will also increase. Yet in Figure 6.20, drying and transport cost seem to dominate even at higher co-fire rates. The annualized cost of the co-fire system rises steadily with higher co-fire rates.

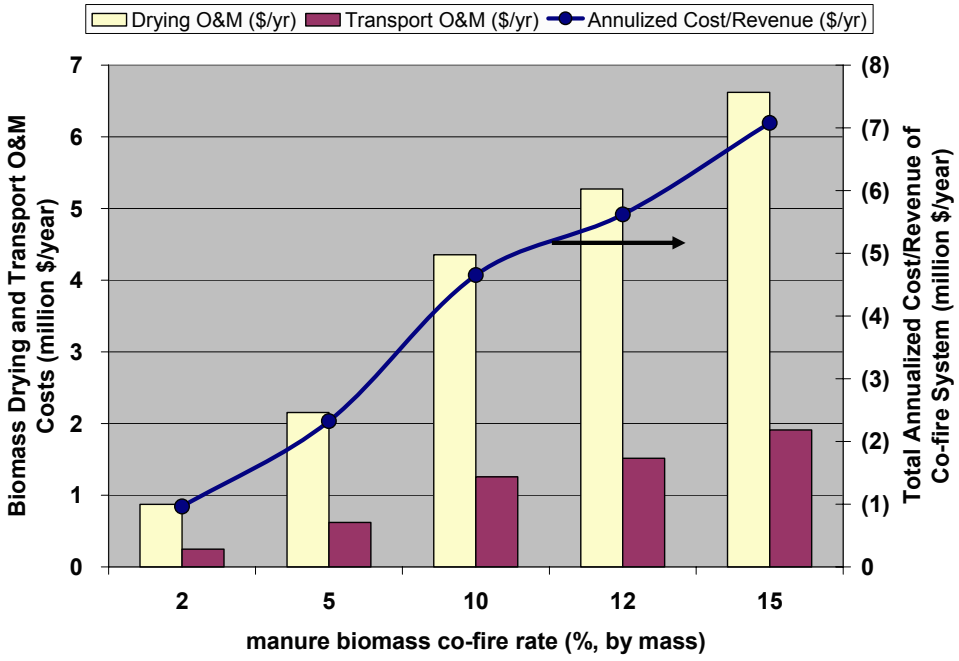

Figure 6.20 Biomass drying and transportation cost and annualized cost/revenue of biomass co-fire system vs. the biomass co-fire rate

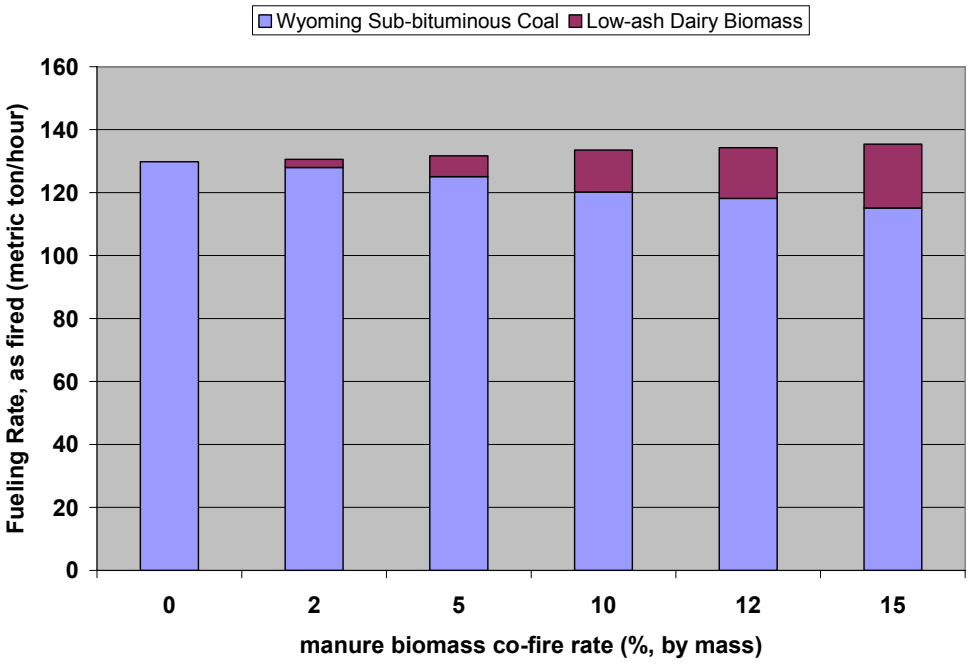

Figure 6.21 Fueling rates for Wyoming sub-bituminous coal and low-ash dairy biomass vs. co-fire rate

The MBB displaces some of the coal that must be purchased by the plant operator as seen in Figure 6.21; although, the overall fuel mass injected into the boiler increases with higher co-fire rates. For this reason, the profitability of co-firing coal with MBB is extremely sensitive to the price of the displaced coal as may be seen in Figure 6.22. If the coal is inexpensive, then there is little economic return on its displacement. This may be particularly troublesome when co-firing MBB in a plant that exclusively fires relatively cheap sub-bituminous or lignite coals from nearby mines. However, displacing higher rank, more expensive coals or even lower rank coals that must be transported long distances to the plant that consumes them may provide a better situation for MBB combustion. Coals obtained from underground mines also tend to be more expensive than coals taken from surface mining. The base case year 1 value of coal was $38.58/metric ton ($35/ton), but if the value of coal at year 1 were to be $60.63/metric ton ($55/ton), then the annualized cost would drop by 56%.

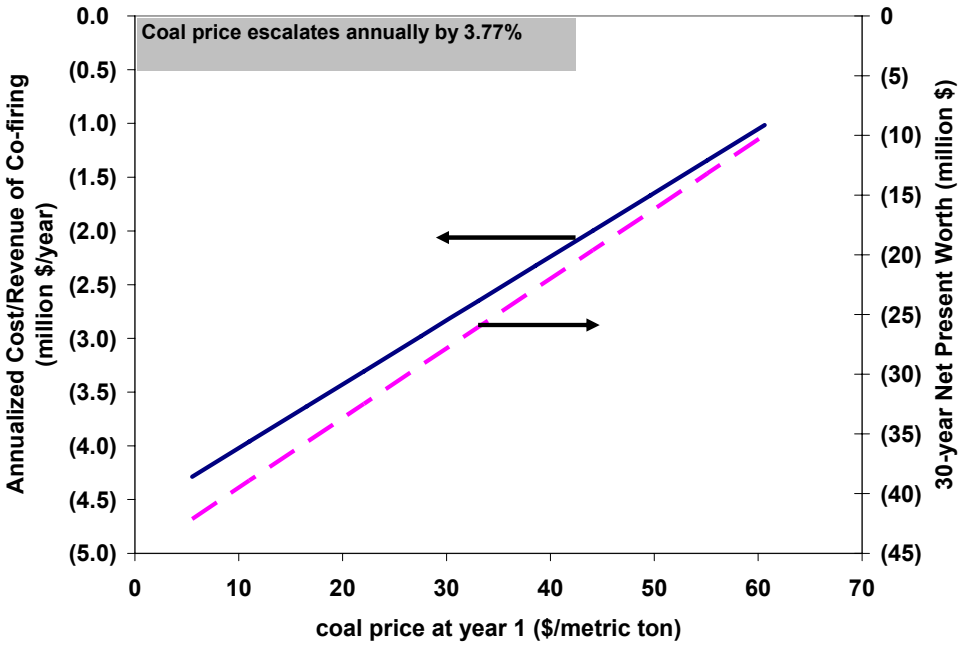

Figure 6.22 Annualized cost/revenue and net present worth vs. year 1 coal price

For the base case, the MBB was assumed to be given to the power plant facility free of charge by the farmer; however, if this is not the case, then the additional cost of buying manure from animal farm operators will adversely affect the NPW of the co-fire system, as can be seen in Figure 6.23. A MBB price of $10/dry metric ton can decrease the NPW of co-firing by 29%, if the price is also assumed to escalate by 3% annually.

Figure 6.23 Annualized cost/revenue and net present worth vs. year 1 farmer's asking price for manure

6.3.1.3. CO_2, SO_x, and ash emissions

Changes in fueling also bring changes in the plant's emissions. Since co-firing with MBB was assumed not to significantly affect NO_x emissions for this study (although some current experimentation at the Texas A&M Coal and Biomass Laboratory on co-firing manure with coal in a low-NO_x burner may prove otherwise), the primary source of revenue for co-firing must come from avoided CO_2 emissions. If the dollar value placed on CO_2 is large enough from taxes, cap and trade policies, or capture and sequestering operations, then the overall worth of a co-firing installation project may prove to be acceptable. Figure 6.24 is a plot of annualized cost and net present worth against the year 1 dollar value of a metric ton of CO_2. At the base case value of $3.85/metric ton ($3.50/ton), the net present worth and annualized value are decidedly negative, making a co-firing retrofit project economically undesirable. However, if all other base values remain the same, and the value of CO_2 were to increase to about $25/metric ton, then a break even point may be met. CO_2 values higher than

$25/metric ton would make the investment of co-firing with MBB in an existing coal plant profitable.

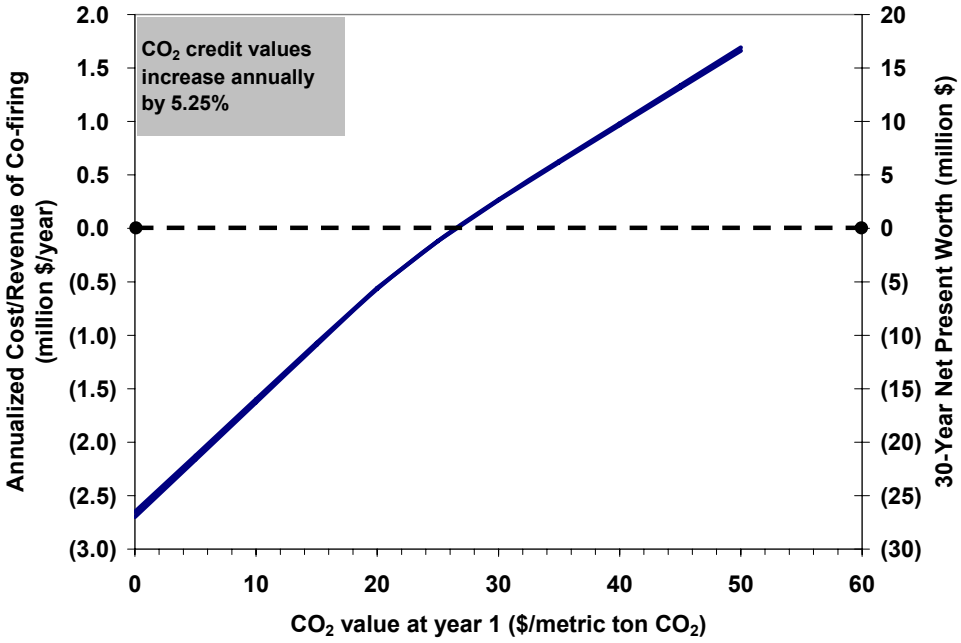

Figure 6.24 Annualized cost/revenue and net present worth vs. the value of CO_2

Another way to view the relationship between the value of CO_2 and the net present worth of the system is to divide the annualized cost/revenue by the total reduction of nonrenewable CO_2 from co-firing with MBB (equation (5.300)). Thus, a dollar per metric ton value can be obtained that is representative of every aspect of installing and operating a co-fire system. This value can then be compared to the going market value of CO_2. This comparison is illustrated in Figure 6.25. The plot can be divided into three different sections. If the specific CO_2 reduction value falls under Section 1, then the cost of reducing CO_2 through co-firing with MBB is more expensive than simply paying the market value of CO_2. If the results from the co-fire model fall under Section 2, then the cost of reducing CO_2 through co-firing is less than the market value. Finally, in extremely fortunate cases, the specific cost of reducing CO_2 by co-firing with MBB could under Section 3, which suggests that co-firing with MBB would

be even more profitable than selling CO_2 allowances; hence the going market value would be considered too low.

The plot was also generated at different CO_2 escalation rates. If the price of CO2 is expected to increase throughout the life of the co-firing project, then co-firing with MBB would become more profitable. The base case escalation rate of CO_2 was 5.25%. At this rate, a year-1 CO_2 value of over $17/metric ton would be considered enough to stimulate a profitable MBB co-firing project at an existing power plant.

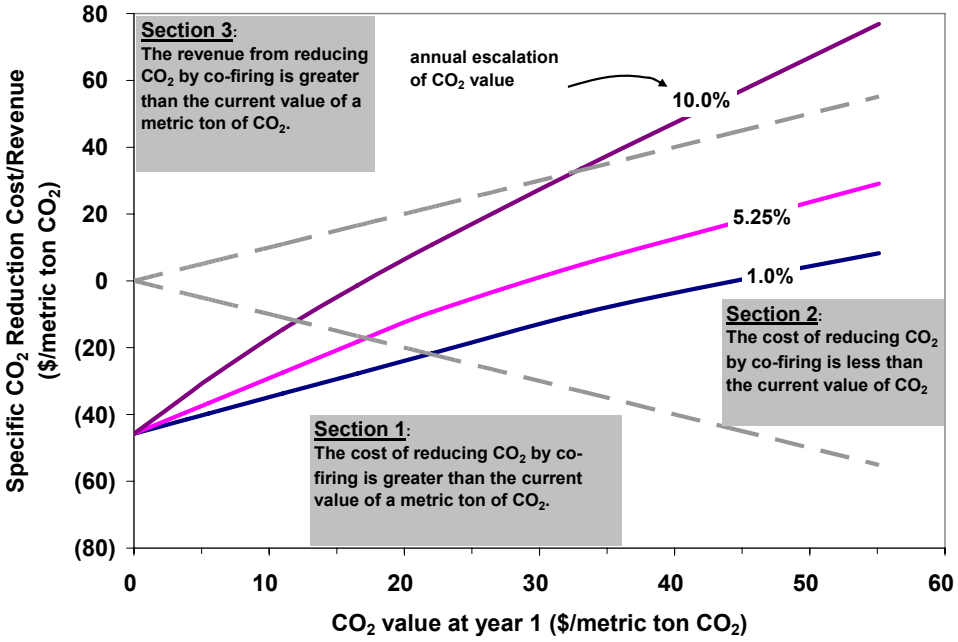

Figure 6.25 Specific CO_2 reduction cost/revenue vs. the value of CO_2

Another emission that can affect the profitability of a co-firing project is SO_2. However, the significance of sulfur depends on two issues: (1) the amount of sulfur contained in the MBB compared to the coal this being replaced and (2) whether or not there is a flue gas desulphurization (FGD) system installed at the power plant. The effect these two issues have on the annualized cost of co-firing coal with MBB is illustrated in Figure 6.26. From Table 2.5, the amount of sulfur in low-ash dairy biomass can be found to be 32.6 kg/GJ, whereas Wyoming sub-bituminous coal contains

13.5 kg/GJ, from Table 2.2. Therefore, when substituting Wyoming coal with low-ash dairy biomass, having a FGD system reduces the annualized cost by about 17%. On the other hand, Texas lignite contains about 42.2 kg sulfur/GJ. Not having a FGD seems to actually benefit a MBB co-fire system if the biomass were to replace Texas lignite. However, usually power plants that burn low-sulfur coals such as Wyoming sub-bituminous do not have FGD systems, whereas many plants that burn Texas lignite do have FGD systems to reduce SO_2 emissions post combustion.

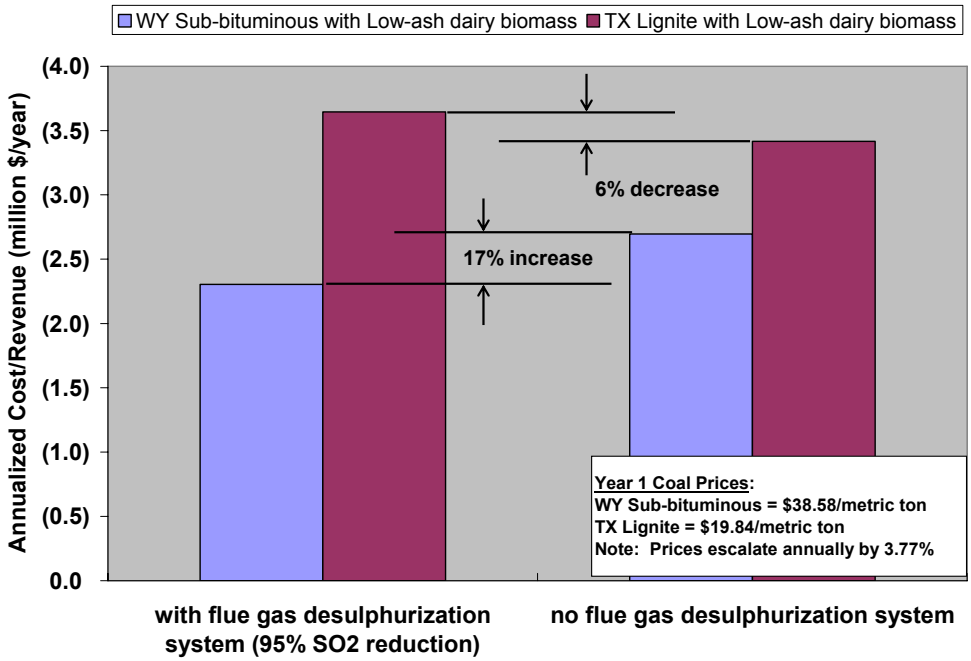

Figure 6.26 Effect of flue gas desulphurization on the annualized cost/revenue of co-firing manure-based biomass with coal

Moreover, the price of the coal is usually related to the amount of sulfur it contains. For example, Wyoming sub-bituminous coal is transported long distances to power plants in Texas such as Tolk Station, Harrington, and WA Parish because those plants do not have FGD (USEPA, 2007a). These long transport distances make Wyoming sub-bituminous coal expensive, at least in Texas. However, any dollar savings from replacing the Wyoming coal with MBB might be partly overruled by the additional cost of SO_2 emissions from burning manure instead of low-sulfur coal.

Another emission that will certainly be detrimental to co-firing with MBB is ash. Ash in MBB is a drag on the co-firing system (or reburning system) at every level. Ash adds to transportation costs as it means moving more mass for less energy content. Ash is also a heat sink during drying, making drying high ash biomass slightly more expensive than drying low ash biomass. Most significantly, ash adds to the O&M cost of co-firing because it must be removed from the power plant and then sold or disposed of off site. Figure 6.27 is a diagram of ash emission from coal and biomass for different co-fire rates when Wyoming coal is replaced by low-ash biomass. Figure 6.28 is a similar graph for Texas lignite replacement with low-ash biomass, and Figure 6.29 is for Texas lignite replacement with high-ash feedlot biomass.

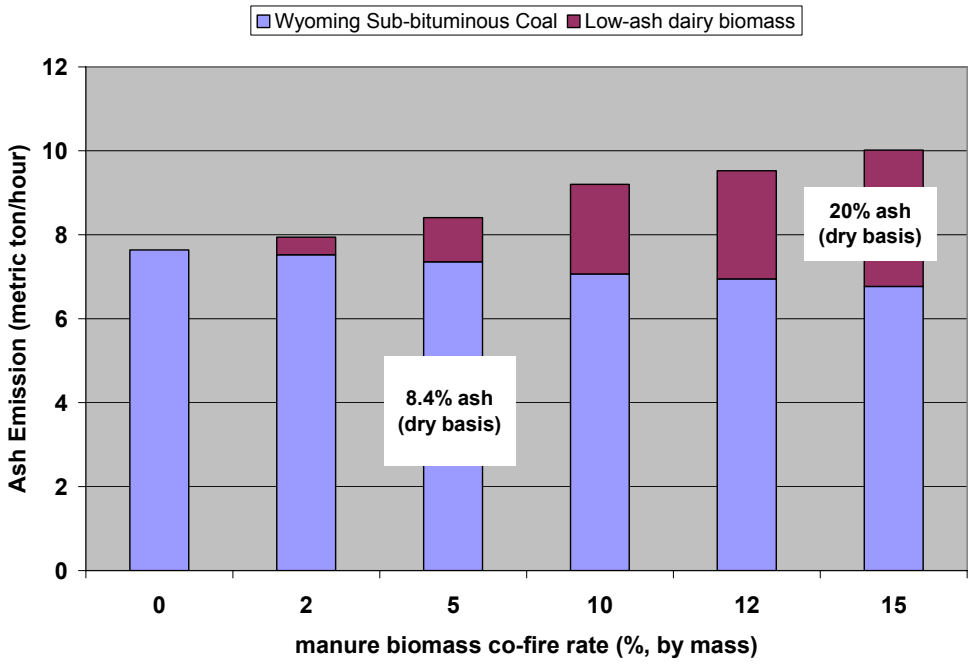

Figure 6.27 Ash emission vs. co-fire rate when replacing Wyoming sub-bituminous coal with low-ash dairy biomass

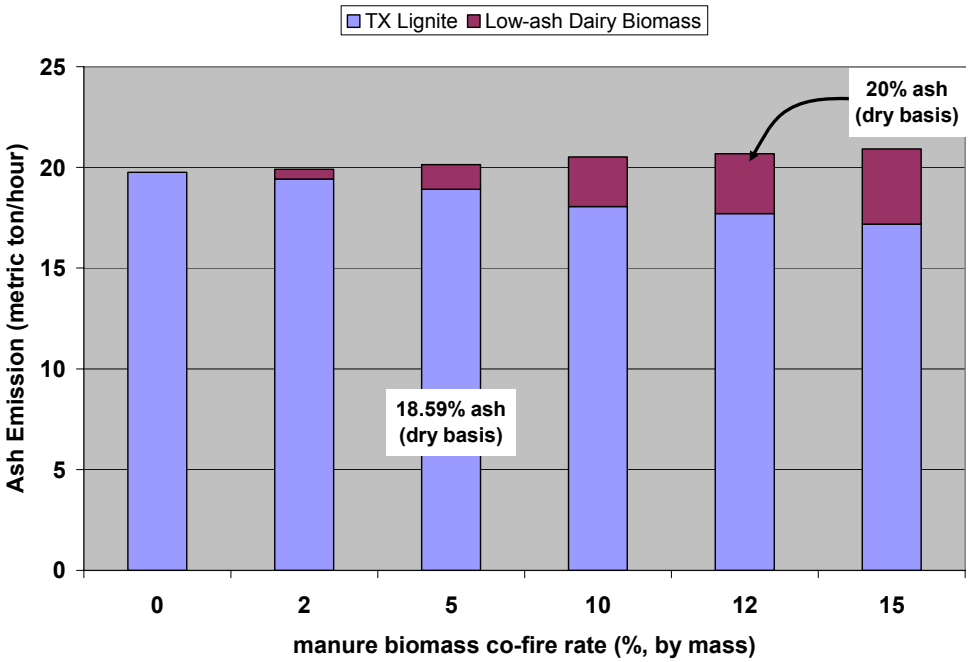

Figure 6.28 Ash emission vs. co-fire rate when replacing Texas lignite with low-ash dairy biomass

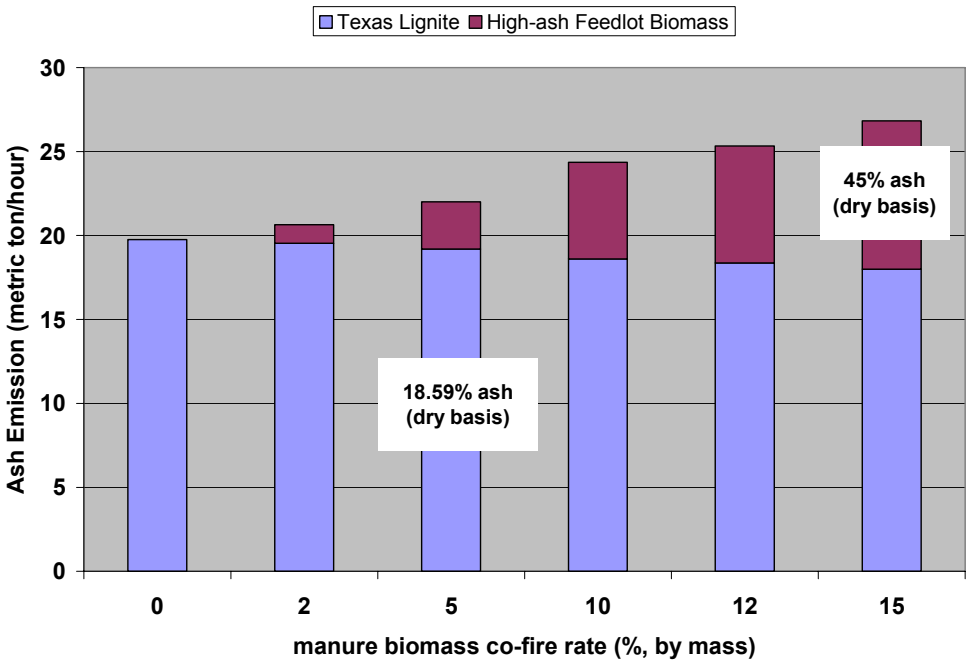

Figure 6.29 Ash emission vs. co-fire rate when replacing Texas lignite with high-ash feedlot biomass

Just as with sulfur, the significance of ash content on the profitability of co-firing with MBB is heavily dependant on the amount of ash in the MBB relative the ash content in the coal it is replacing. If low ash MBB replaces the relatively low ash Wyoming coal, ash emissions would increase from 7.64 metric tons/hr to 8.41 metric tons/hr (about 10%) when co-firing 5% biomass. However, if low-ash MBB were to replace lignite, which is higher in ash than Wyoming coal, at the same 5% rate, ash emission would increase from 19.76 metric tons/hr to 20.13 metric tons/hr (only about 1.9%).

These high ash emissions are troubling, given that studies by Megel *et al*. (2006 and 2007) reported that manure ash was not suitable as a cement replacement on its own. However, it is not clear if the same problems would occur when manure is fired with coal, as would be the case with co-firing MBB. Also, manure ash may be utilized in other ways, as discussed previously. The responsibility of finding local markets and buyers for the ash produced by MBB would probably fall on plant operators and managers.

6.3.1.4. Biomass drying and transporting

In order to co-fire coal with MBB at an existing power plant, some important logistical issues should be considered. An important logistical parameter was found to be the average distance between the plant and the animal feeding operations that supply the biomass. The power plant should be near or in a geographical area of high agricultural biomass density. Figure 6.30 is an illustration of how power plant facilities and possible supply regions of MBB fuel can be matched. Goodrich *et al*. (2007) studied manure production rates and precise rural transportation routes between coal plants and feeding operations in Texas.

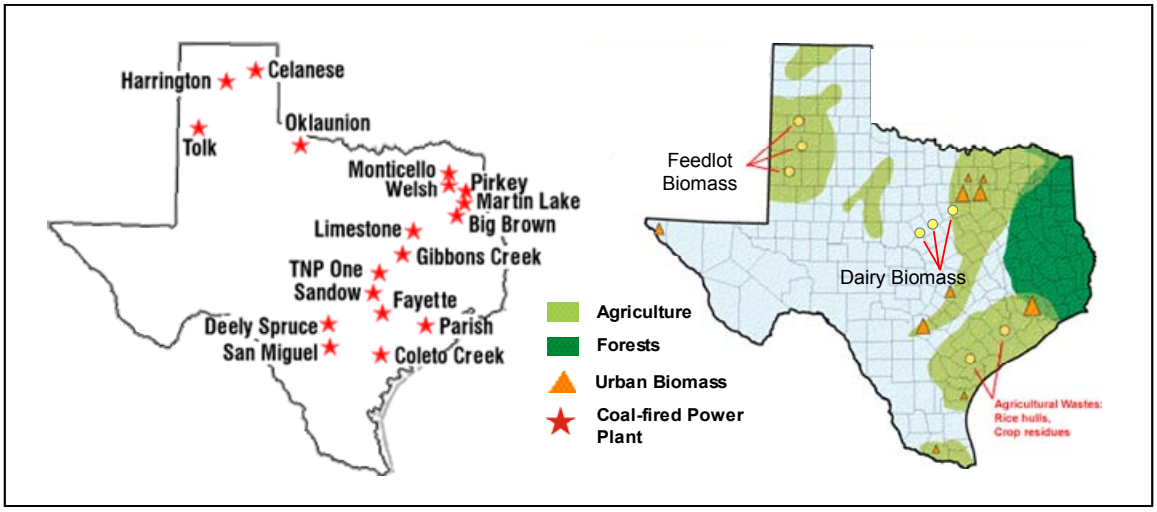

Figure 6.30 Matching coal-fired power plants and areas with high agricultural biomass densities, adapted from (Virtus Energy Research Associates, 1995) and (Western Region Ash Group, 2006)

The importance of logistics can be seen further in Figure 6.31 and Figure 6.32. These figures depict the co-firing O&M (grinding and other associated costs of burning biomass at the plant), the transportation O&M, the drying O&M, and the respective capital costs versus the distance to the feeding operations. Drying MBB was found to be the dominate O&M cost. However, if the average distance between the plant and the feeding operations that supply it were to be over 160 km (100 miles), then transportation costs would become as significant. For longer transport distances, the number of possible round trips to and from the feeding operations that hauling vehicles must make per day decreases. Hence, more trucks must be purchased for longer distances to adequately maintain the desired co-fire rate.

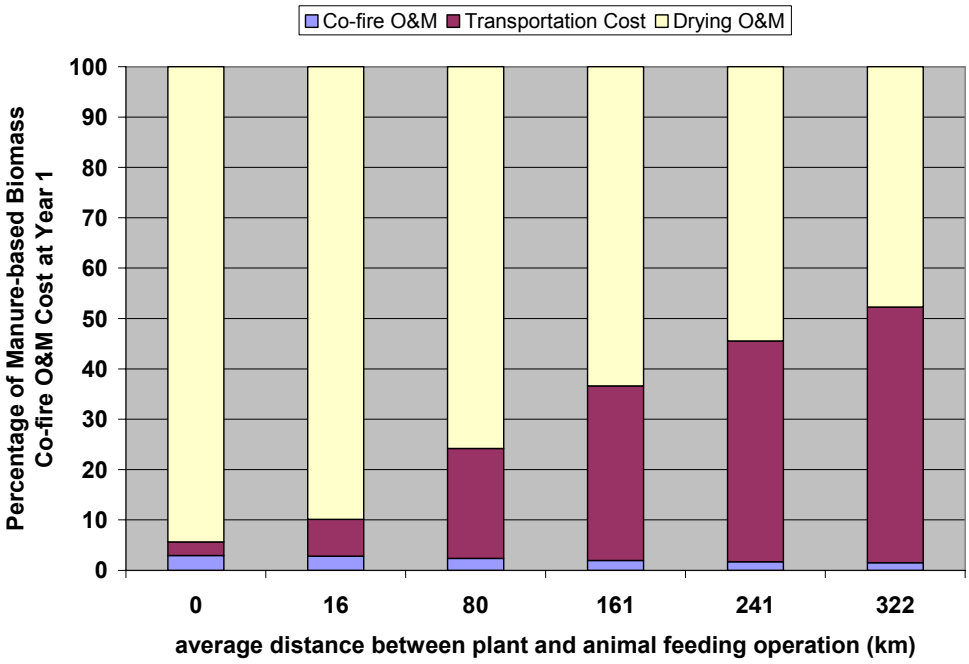

Figure 6.31 Manure-based biomass co-fire O&M cost components vs. distance between plant and animal feeding operations

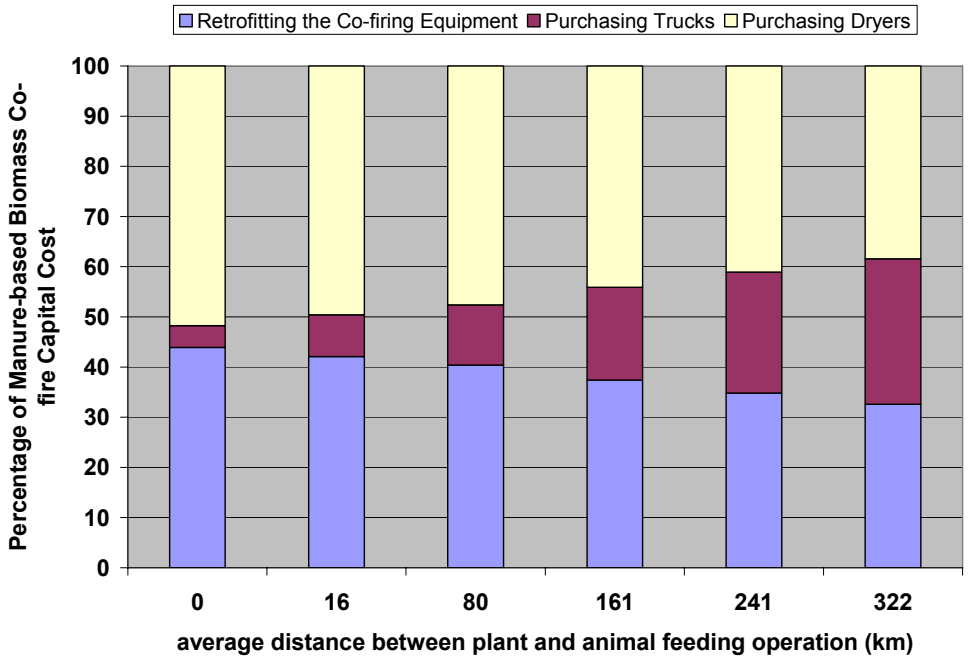

Figure 6.32 Manure-based biomass co-fire capital cost components vs. distance between plant and animal feeding operations

Figure 6.33 is a plot of annualized cost and net present worth against MBB transportation distance. If the cost of drying biomass were less significant, the transportation distance could be the deciding factor of whether co-firing with MBB was profitable or not. The most effective MBB transport systems should be closely knit networks of animal feeding operations surrounding one or two coal plants in areas within a 160 km (100 mile) radius. Short transport distances would also allow some flexibility to some of the other base case input parameters such as coal cost and ash disposal cost. Moreover, it may be possible to use ash from coal and biomass combustion to pave more feed yards in nearby feedlots which would increase the amount of low-ash feedlot biomass available for reburning facilities and other combustion processes. Currently, the only realistic CB feedstock would have to come from free stall dairies with composted manure-based bedding and flushing systems. For many cases, there may simply not be enough low-ash biomass near the plant to sustain a co-fire rate of more than a few percent.

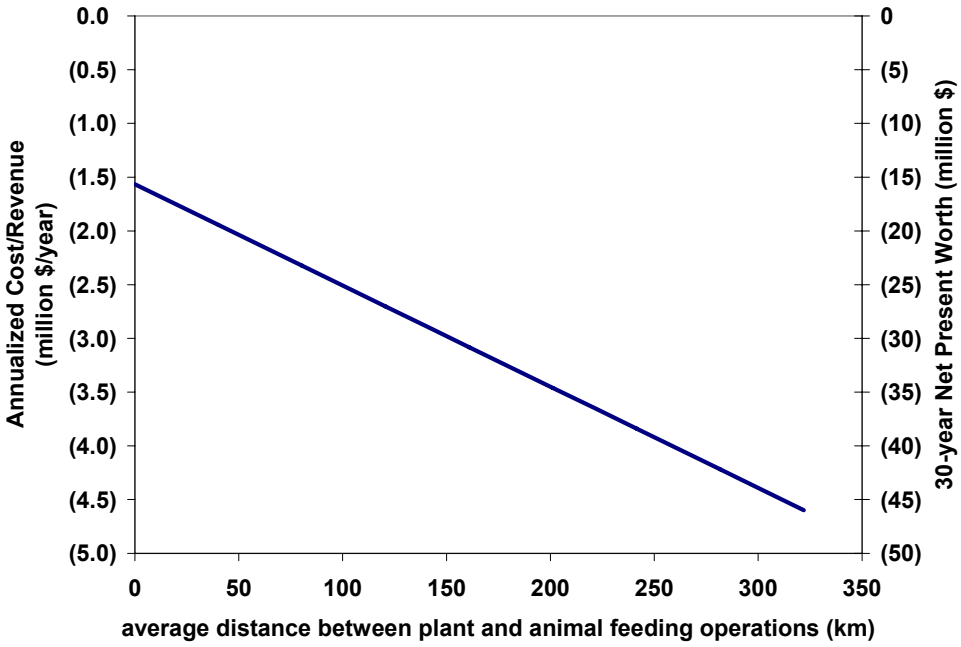

Figure 6.33 Annualized cost/revenue and net present worth vs. manure-based biomass transport distance

Yet for shorter transportation distances, the O&M cost of co-firing is dominated by the cost of drying the biomass. For the base case run of the co-firing model, drying constitutes 76% of the total cost. Of this cost, 73% is due to purchasing natural gas for generating steam for the biomass dryers. Another 15% is due to running the dryers' fans. Moreover, if the biomass must be dried before being sent to the power plant, natural gas is probably the cheapest fuel to use. Both propane and electric driers would probably be more expensive. Figure 6.34 is a plot of annualized cost against natural gas price and annual escalation of gas price. If natural gas was free, or not needed, to dry the biomass, then a break even point for the cost of co-firing would be reached, that is if all other base case values remained the same. If the price of natural gas is too high, or if the escalation is expected to be high, then a profitable scenario may be out of reach.

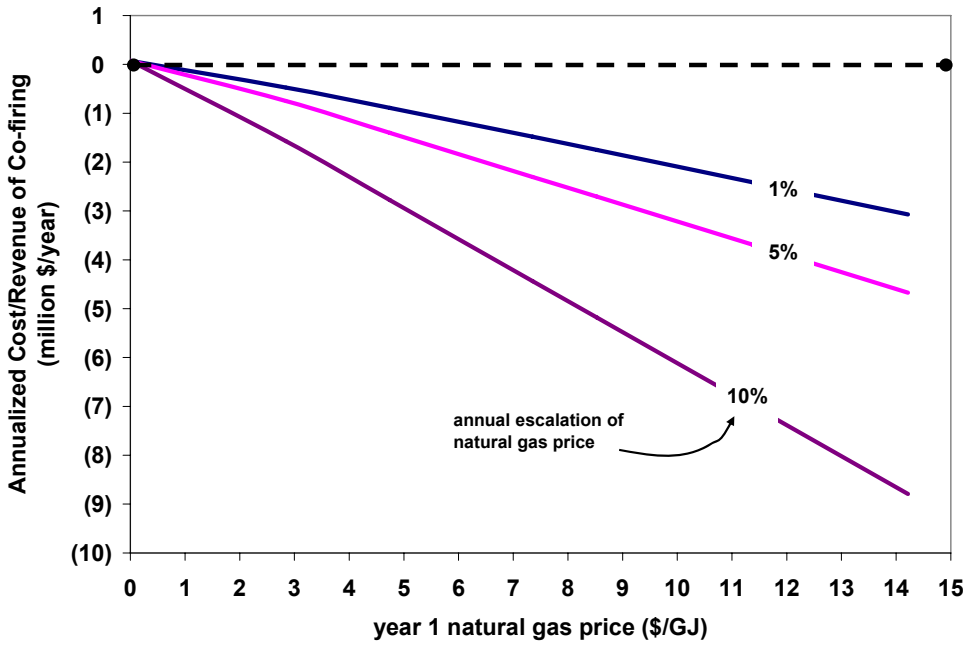

Figure 6.34 Annualized cost/revenue vs. natural gas price

However, there may not always be a need to use expensive conventional fuels to dry MBB. If power plant operators are willing to receive wet MBB, then waste heat

from coal combustion could be used to dry the biomass instead natural gas. Or if the MBB is from a more arid region where the relative humidity is low, the moisture content of the biomass, when harvested, might be low enough to forgo any drying at all. According to Heflin (2008), the moisture percentage of scraped feedlot biomass collected in the Texas Panhandle is rarely over 30%, as harvested, even after heavy rainfall. This is particularly true for low-ash solids from paved feedlots. Figure 6.35 is a graph of overall delivery cost for Texas lignite, Wyoming sub-bituminous, and low-ash dairy biomass at three drying scenarios. The first scenario is such that the biomass is dried using natural gas, just like the base case. The overall as-delivered cost of the biomass for this case is $3.95/GJ ($4.16/MMBtu), over twice the price of Wyoming sub-bituminous. If the MBB is transported to the power plant and then dried with waste heat, then the delivery price of the biomass was found to drop by 55%. If the biomass is inherently dry, say less than 30% moisture, and no additional drying is required, then the delivery price drops by 81% to $0.76/GJ ($0.80/MMBtu), which is actually cheaper than the Wyoming and Texas lignite coals.

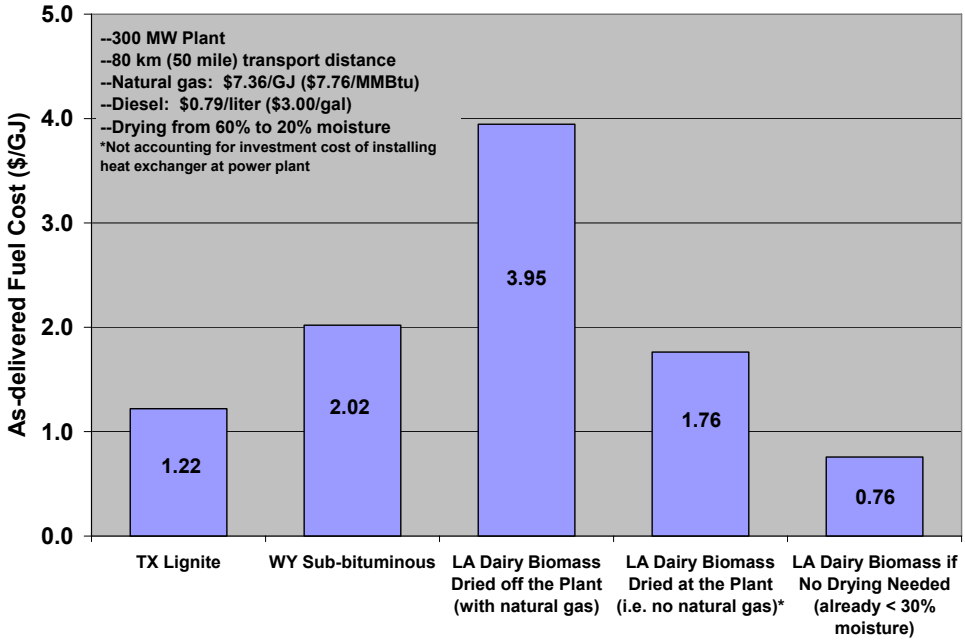

Figure 6.35 Overall fuel costs for coals and low-ash dairy biomass at different drying requirements

Yet, as stated before, currently the greatest supply of low-ash MBB may be from dairies with flushing systems or perhaps from indoor swine farms. Separated solid manure from these facilities would probably be high in moisture and require drying before combustion. Most scraped manure from feedlots and open dairy lots is high in ash since most of these lots are unpaved.

For the base case 300 MW power plant, if each cow, on average, were to produce 6.35 dry kg of manure per day (14 lb/cow/day), then about 21,000 dairy cows would be required to sustain a co-fire rate of 5% (by mass). The Bosque and Leon River Watersheds in north central Texas have about 150,000 dairy cows in over 150 dairies. Therefore, one 300 MW_e plant would require approximately 14% of all cattle manure produced by these farms. Hence, the availability of suitable, low-ash MBB, as well as the coordination between farmers, centralized composting facilities, and plant operators easily come into question when trying to apply this low heat value biomass to large electric boilers.

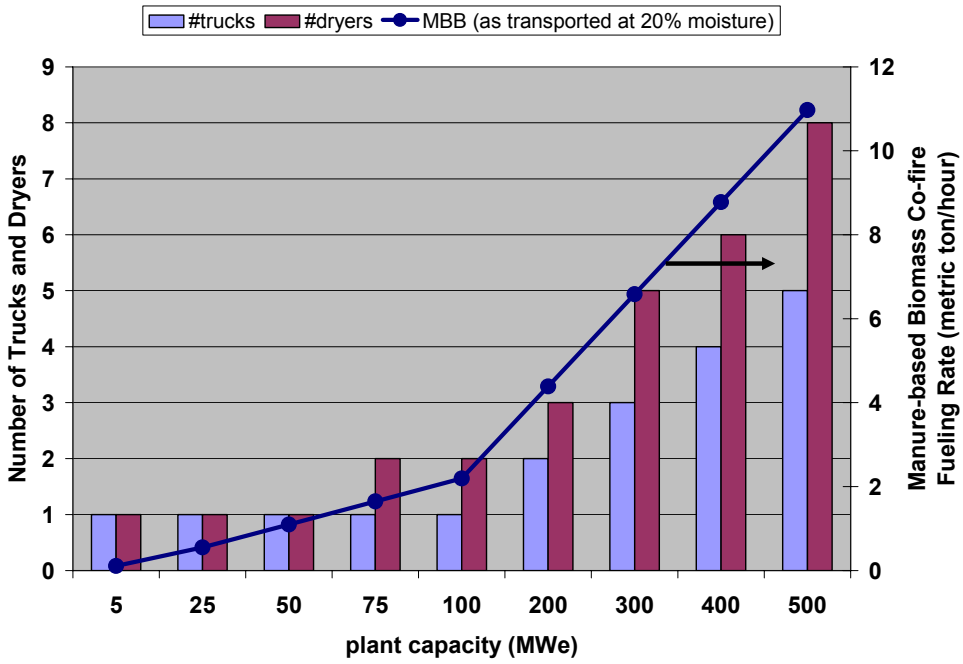

Figure 6.36 Number of trucks and dryers and manure-based biomass fueling rate vs. power plant capacity

To handle these issues, several methods such as storage and reserve stockpiles of ready-to-fire MBB can be kept near the power plant. In Figure 6.36, the number of required trucks and dryers are plotted against power plant capacity. A 500 MW_e plant would require at least 8 two-metric ton conveyor belt dryers where as a 100 MW_e plant would only require 2 dryers. Concentrating research and development of animal biomass utilization on smaller, more dispersed power facilities may be more helpful. Power plants with 50 to 100 MW_e capacities would seem to be the best candidates for co-firing coal with MBB.

6.3.2. Reburning

Modeling a MBB reburn system is very similar to the previous model for co-firing. The main difference is NO_x emissions. The revenue generated from avoided NO_x emissions adds another dimension to the analysis, and in theory makes a MBB reburn system more profitable than a simple co-firing operation. However, reburn systems require anywhere between 10 and 20% reburn fuel (in this case, biomass) on a heat basis. For the case of replacing Wyoming sub-bituminous coal with low-ash dairy biomass at 20% moisture, this range is equivalent to about 13 and 26% by mass, which is far greater than the 5% co-fire rate discussed for the base case in the previous section.

An outline of the reburn computational model is presented in Figure 6.37. The layout of the program is similar to the co-firing model, except that baseline NO_x levels must be computed both for cases with primary NO_x controls and without primary controls. Then, NO_x emission reductions can be computed for secondary controls such as reburning, SCR, and SNCR. The biomass drying and transportation sections of the model are left relatively unchanged, except for the fact that more biomass must be dried, transported, and processed at the power plant.

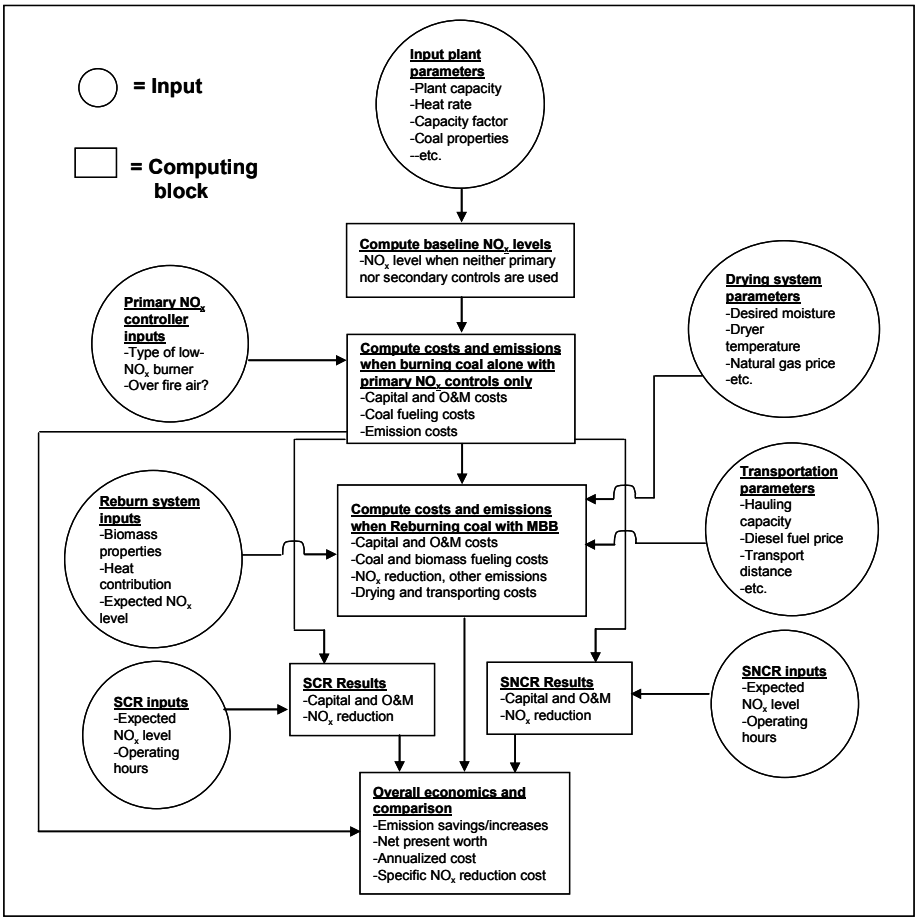

Figure 6.37 Flow diagram of computer spreadsheet model for reburning coal with manure-based biomass in an exiting coal-fired power plant along with comparisons to SCR and SNCR systems

6.3.2.1. Base case inputs and results

All base case inputs will remain the same for the reburning discussion except for those listed in Table 6.11. For the base case, the 300 MW_e coal power plant will be equipped with a primary NO_x controller (low-NO_x burner with closed coupled over fire air) capable of lowering NO_x levels to 84.2 g/GJ (0.196 lb/MMBtu). The secondary NO_x controls such as MBB reburning and SCR will be installed and operated along with the primary controls. The reburn model can be set up so that the coal is reburned with MBB without any primary controls present; however for this discussion, since low-NO_x burners, over fire air and other primary controllers are presently installed in most existing coal plants, the secondary technologies will add to the NO_x reductions already

achieved by the primary controls. Thus, all dollar savings for NO_x are acquired for reductions from the 84.2 g/GJ level.

Table 6.11 Additional base case inputs for reburning coal with manure-based biomass

Input	Value (unit)	Source	Notes
Primary NO_x control	Low-NO_x coal and air nozzles with closed-coupled OFA		See primary control NO_x level (next item)
Primary NO_x control level	84.23 g/GJ (0.1959 lb/MMBtu)	(Srivastava, 2005)	about 50% average reduction efficiency for these primary controls when burning sub-bituminous coals
Reburn fuel	LADB	(Sweeten *et al*, 2006)	See Table 2.5
Heat contribution from reburn fuel	10%		Range: 10 – 30%
Reburn NO_x control level	25.9 g/GJ (0.06 lb/MMBtu)	(Colmegna *et al*, 2007), (Oh, *et al*., 2008), (Annamalai *et al*., 2005)	
Reburn capital cost	$35/kWe	(Zamansky *et al*., 2000)	
Reburn fixed O&M	$1.07/kWe yr	(Biewald, *et al*., 2000), (USEPA, 1998)	Scaled for different plant capacities and firing cattle biomass
SCR NO_x control level	25.9 g/GJ (0.06 lb/MMBtu)	(USEPA, 2004)	>90% reduction, but current commercial systems are usually limited to 25.9 g/GJ
SNCR NO_x control level	64.6 g/GJ (0.15 lb/MMBtu)	(Srivastava, 2005)	~35% reduction for larger coal plants
NO_x credit/allowance	$2,590/metric ton reduced	(SCAQMD, 2007)	Average annual price for Compliance Year 2005. Assume credits gained for reductions beyond primary control levels
NO_x allowances	4.50%	(SCAQMD, 2007)	

For the reburn base case, the reburn fuel was pure low-ash dairy biomass, which contributed 10% of the power plants overall heat rate (about 13% by mass). The reburn model can be setup so that blends of coal and MBB can be the reburn fuel; however, according to Oh *et al*. (2008) and Annamalai *et al*. (2005), the greatest NO_x reductions are achieved when pure biomass is used as the reburn fuel. Manure-based biomass reburning and SCR were presumed to achieve the same NO_x level of 25.9 g/GJ

(0.06 lb/MMBtu), whereas SNCR was assumed to only achieve a level of 64.6 g/GJ (0.15 lb/MMBtu). Both SCR and SNCR use ammonia or urea as reagents, which do not contribute to the overall heat rate of the power plant; therefore, coal consumption and other emissions aside from NO_x are presumed to be the same for SCR and SNCR as for the case of burning pure coal alone.

Just as with the co-fire model, the base case inputs for reburning were used to generate a reference run of the reburn model. The base case results for fueling and emission rates for burning coal alone with primary NO_x controls are listed in Table 6.8. These rates may be compared to those in Table 6.12 for fueling and emissions when reburning coal with MBB. Again, the total annual fueling (energy) consumption was found to be about 709,000 GJ more per year when reburning with MBB. This increase in total fueling is almost three times that for the co-firing base case. Yet this is predominantly due to the fact that more diesel and natural gas are required to prepare enough biomass for reburning. The heat energy released by the MBB in the reburn zone of the boiler burner (i.e. 2.16 million GJ/yr in Table 6.12) was found to be 1.46 million GJ more than the energy needed to dry and transport it to the plant. However, this may not be the case if transportation distances were greater, or if more biomass was required to obtain desired NO_x levels.

Table 6.12 Base case fueling and emissions results for a 300 MW_e coal plant operating while reburning coal with manure-based biomass (10% by heat)

Number of drying sites	2
Number of dryers (each rated at 2 dry metric tons/hr)	12
Number of dryer operators	5
Total hectares required for drying site(s)	8
Total extra storage trailers	8
Number of hauling vehicles required (30.6 m^3 each)	8
Number of cows required (7.7 dry kg/cow/day)	47,000

		Primary fuel (coal)	Reburn fuel (MBB)	Dryers (natural gas)	Dryers (electricity for fans)[a]	Hauling vehicles (diesel)	Total
Fueling rate	GJ/yr	19,463,231	2,163,816	582,264	100,510	24,800	22,334,620
	metric ton/yr	1,023,590	157,400	11,644	5,046	515	n/a
CO_2 emission	g/GJ	84,147	10,043	55,005	93,497	64,290	n/a
	metric ton/yr	1,819,785	217,316	31,944	9,398	1,594	1,862,721[b]
SO_2 emission	g/GJ	13.48	3.34	n/a	n/a	n/a	n/a
	metric ton/yr	291	72	n/a	n/a	n/a	364
Ash production	g/GJ	2,784	1,162	n/a	n/a	n/a	n/a
	metric ton/yr	60,208	25,154	n/a	n/a	n/a	85,361
NO_x emission	g/GJ	26	n/a	n/a	n/a	74,501	n/a
	metric ton/yr	557	n/a	n/a	n/a	2	559

[a]Electricity for fan operation is assumed to come entirely from coal. Fueling and emission rates are for the equivalent amount of coal required to produce the electricity in a power plant with an overall efficiency of 35%.
[b]Excluding CO_2 emissions from renewable fuels such as the MBB reburn fuel

Total CO_2 emissions for reburning, including carbon emissions from MBB drying and transportation, were found to be 159,000 metric tons/yr less than emissions for primary control operation only. Again, since much more biomass would be required for reburning than the 5% (by mass) for the co-fire base case, CO_2 reduction was almost 3 times as much as carbon reduction from co-firing. However, ash emissions greatly increased for the MBB reburn system under the base case run by 27.6%. Lastly, since the hauling vehicles were assumed to meet 2007 NO_x standards with catalytic converter systems, the NO_x emitted by the vehicles only inhibited MBB reburn NO_x reductions by

about two metric tons/year, compared to a 1,260 metric ton/year reduction beyond primary control levels.

Despite the increase in ash emissions, economically, the MBB reburn system was found to be only 0.61% more expensive for the first year than operating with primary controls alone, under base case assumptions. The full list of cost components and the overall annualized results for the four possible NO_x reduction scenarios are compared in Table 6.13. The major increase in overall cost for the MBB reburn system, was found again to come from the variable O&M increase, largely due to biomass drying operations. However, this increase was offset by combined (coal and biomass) fuel delivery savings of $2.70 million/yr, avoided CO_2 penalty of $615,000/yr, and $3.71 million/yr in additional NO_x credits (or savings).

Table 6.13 Comparison of base case Year 1 costs of selected NO_x control technology arrangements (300 MW_e plant, 10% biomass by heat for reburn case)

Year 1 Costs	Primary control only	Primary control + manure-based biomass reburn	Primary control + SCR	Primary control + SNCR
Fixed O&M Cost	63,000	506,995	272,657	119,664
Variable O&M Cost[a]	56,765	5,876,452	1,433,709	2,118,293
Biomass Delivery Cost	0	1,691,040	0	0
Coal Delivery Cost	43,878,448	39,488,099	43,878,448	43,878,448
NO_x Credits[b]	0	(3,271,151)	(3,275,800)	(1,106,857)
CO_2 Penalty	7,800,913	7,186,025	7,800,913	7,800,913
SO_2 Penalty	314,864	353,717	314,864	314,864
Ash Revenue	(368,704)	(368,550)	(368,704)	(368,704)
Ash Disposal Cost	1,769,781	2,380,425	1,769,781	1,769,781
Annualized Capital Cost	531,647	2,735,890	4,481,734	1,007,622
TOTAL COST (w/o capital)	53,515,066	53,843,052	51,825,867	54,526,402

[a]For MBB, variable O&M includes the cost of drying the biomass

[b]NO_x credits are assumed to be earned for all reductions beyond those obtained from primary controls

Compared to the other secondary control options, MBB reburning was found to be more expensive than SCR, yet cheaper than SNCR. In fact, SCR was found to be about 3.2% cheaper for the year 1 total cost, than sole primary control operation. However, SCR was found to have the highest annualized capital cost, mostly due to the catalyst installation, which can constitute up to 20% of the initial investment of this type

of control system (Mussatti *et al*., 2000b). SNCR was found to have the most expensive year 1 total cost mostly due to a poorer NO_x level than that achieved by either MBB reburning or SCR. Since SCR and MBB reburning were assumed to have similar NO_x reductions, the comparisons made in this section will mostly be made between these two.

The same discount, inflation, and escalation rates, as well as project life, were assumed for the reburn model. The overall cash flow diagram for the base case run of the MBB reburn model is presented in Figure 6.38. The overall operating income begins as a net cost from years 1 through 7, but as the combined escalation of coal, CO_2 and NO_x prices overtakes that of natural gas, electricity, and other prices and costs, the operating income becomes positive after year 7. However, after adjusting the operating income for depreciation of capital, a net positive income is not seen until after year 23, thus income tax does not become a factor until this time. The major difference in this analysis compared to simple co-firing is the dollar savings from avoided NO_x emissions. Despite the requirement of larger amounts of MBB, along with more trucks and dryers needed to process it, the net present worth of the MBB reburn system, under base case assumptions, was found to be negative $19.1 million (i.e. net present cost), which is a slightly lower cost than for the simpler co-firing case discussed earlier. However, the NO_x credits are still not enough to achieve a positive net present worth or a payback under base case assumptions.

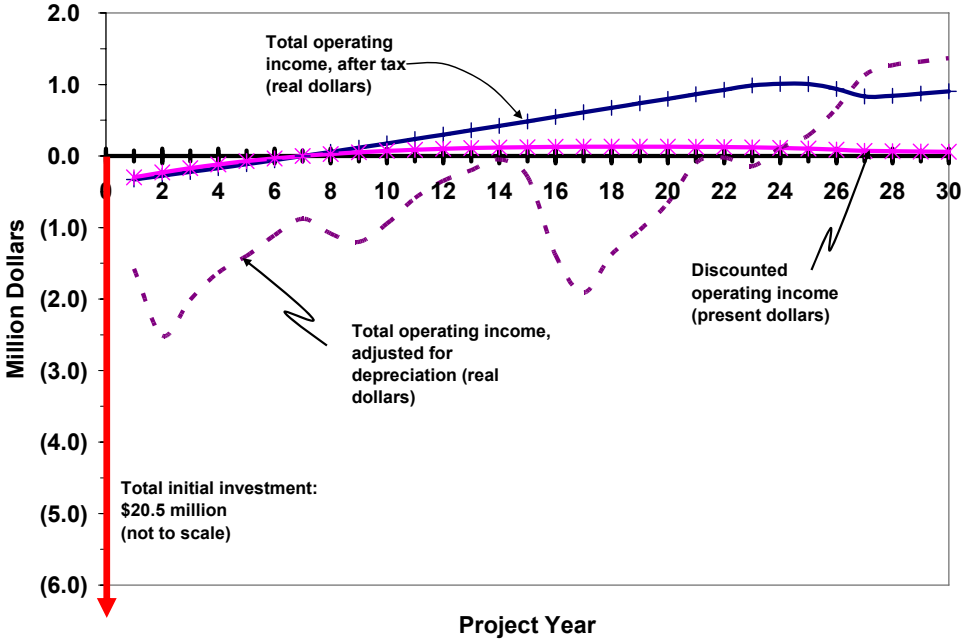

Figure 6.38 Overall cash flows for the base case run of the manure-based biomass reburn economics model

On the other hand, the total operating income for SCR was found to be positive throughout the 30 year life of the project, as can be seen in Figure 6.39. Yet, the net present worth of the SCR system, for the base case, was still found to be slightly negative at minus $4.6 million. The simple payback period, which does not account for the time value of money, was found to be about eight and half years and the rate of return for SCR at the base case was found to be 8.2%. The main reason for the relative success of SCR compared to MBB reburning at the base case is due to the fact that the same NO_x reductions can be achieved with SCR without having to pay high variable O&M costs of importing MBB. However, in the remaining part of this section, the net present worth of the MBB reburn system will be monitored for variations of certain base values to determine if reburning with MBB could ever be as profitable as SCR, or justifiable as a NO_x reduction technology on an exiting coal-fired power plant with primary NO_x controllers. A full sensitivity analysis for MBB reburning may be found in Appendix D.

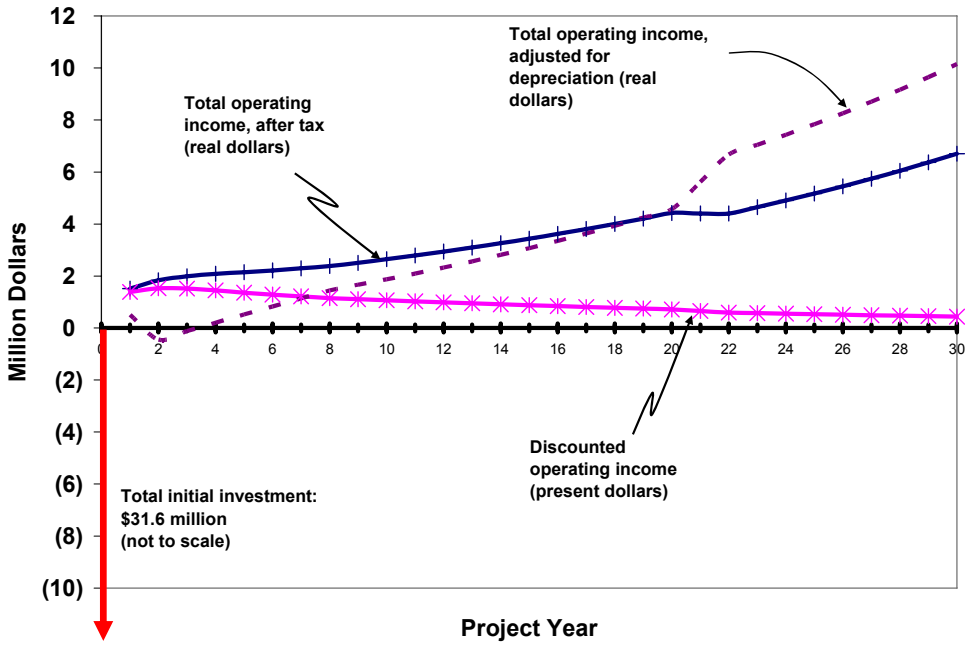

Figure 6.39 Overall cash flows for the base case run of the SCR economics model

6.3.2.2. Biomass and coal fueling

The overall negative net present worth for MBB reburning was mostly attributed to the relative expense of importing biomass, with an inferior heat value, to meet a set percentage of the plant's heat rate (for the base case, 10% by heat). Since the ammonia, urea, or other reagents imported for SCR do not add to the fueling of the plant, O&M costs for this competing technology can stay relatively low for the same targeted NO_x level. If MBB reburn systems are ever to be installed in coal plants, plant operators and engineers must find a perfect balance between lowering the biomass contribution to the heat rate, saving on coal, and still maintaining targeted NO_x levels. In Figure 6.40, the rise in MBB drying and transport O&M can be seen as more of the plant's heat rate is supplied by the biomass reburn fuel. Also, the annualized costs of MBB reburning steadily increases with greater biomass reburn contributions.

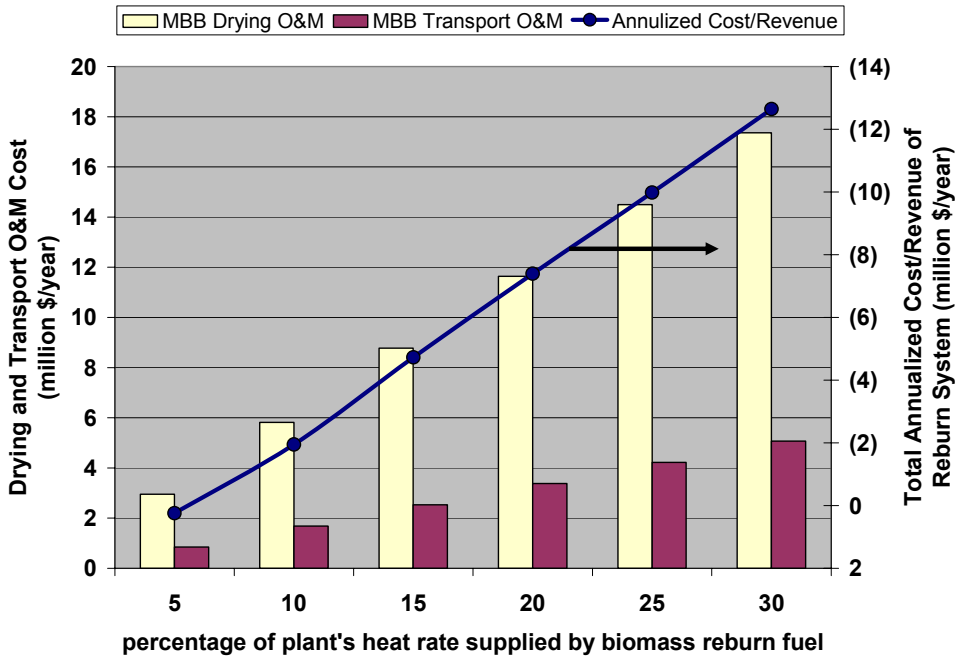

Figure 6.40 Drying and transport O&M costs and annualized cost/revenue vs. percentage of plant's heat rate supplied by manure-based biomass reburn fuel

The displacement of coal by the biomass is even more significant during reburning. The decrease of coal consumption, along with the overall increase in total fuel injection into the power plant can be seen in Figure 6.41 for different heat rate contributions from the biomass. Moreover, the significance of coal price is displayed in Figure 6.42. If the price of coal were to increase to $50/metric ton for the first year of the project, then the net present worth and annualized cost of the reburn system would be the same as SCR's.

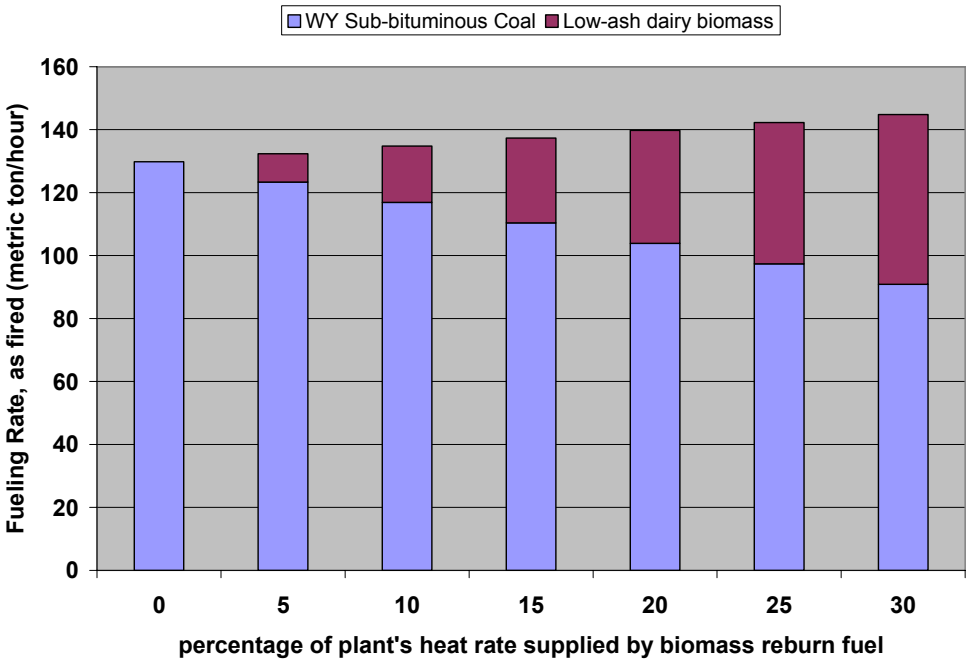

Figure 6.41 Fueling rates of Wyoming sub-bituminous coal and low-ash dairy biomass vs. percentage of plant's heat rate supplied by the biomass reburn fuel

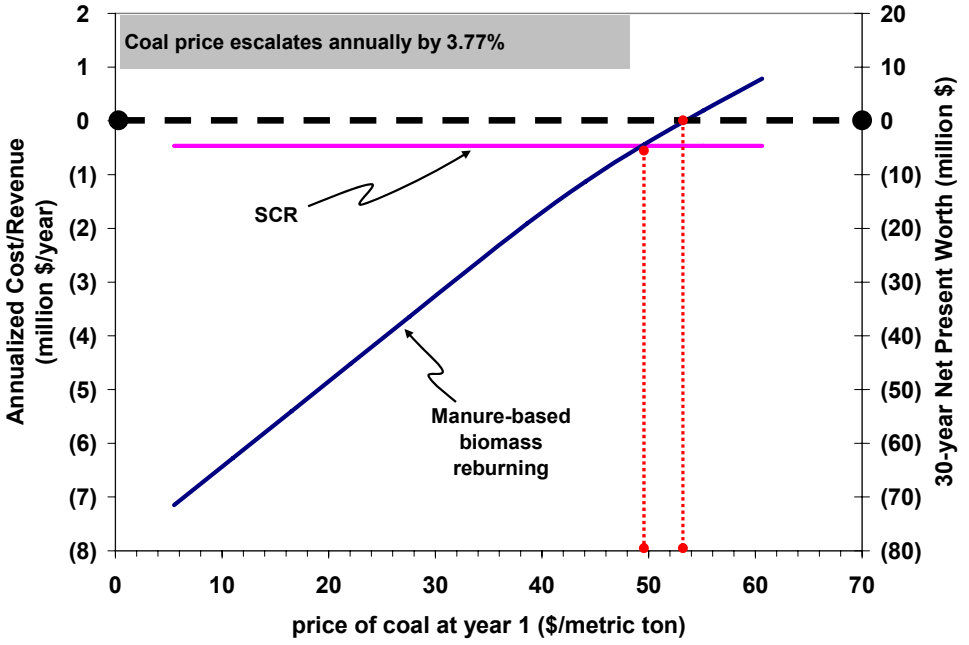

Figure 6.42 Annualized cost/revenue and net present worth of manure-based biomass reburning and SCR vs. coal price

6.3.2.3. CO_2, NO_x, SO_x, and ash emissions

Carbon emissions affect the net present worth of the MBB reburn system just like avoided coal costs. An increase in the value of CO_2 improves the profitability of a MBB reburn system tremendously, perhaps more than any other parameter other than the dollar value of NO_x. A CO_2 value beginning at \$12/metric ton would make reburning coal with MBB economically competitive to SCR. See Figure 6.43.

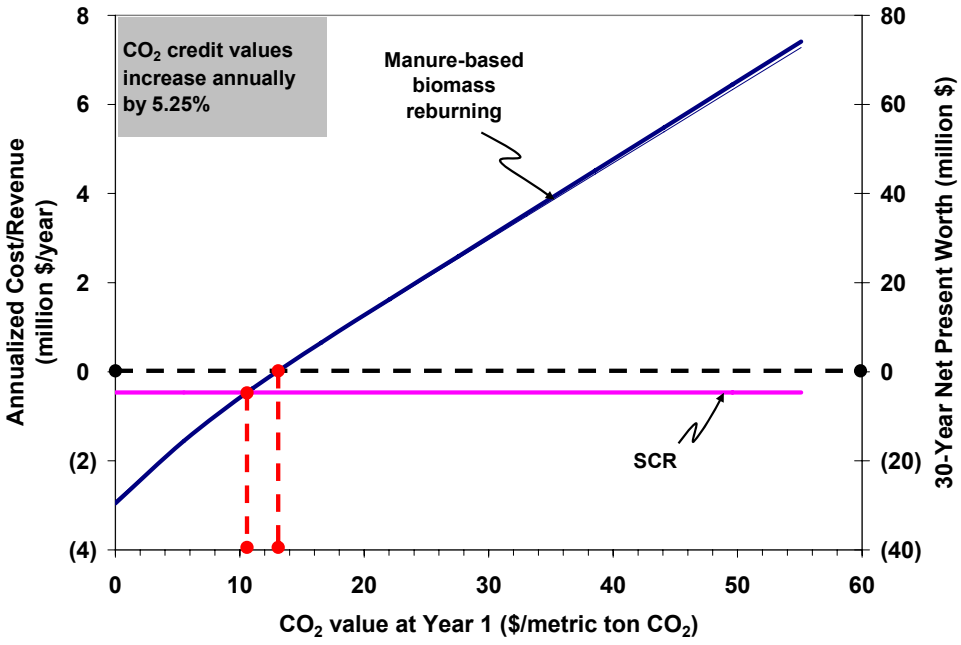

Figure 6.43 Annualized cost/revenue and net present worth vs. the value of CO_2

A similar plot is shown in Figure 6.44 for the dollar value of NO_x. If the escalation rate of the dollar value of NO_x remains the same as the base value, 4.5%, then SCR reaches an economic break even point at a year 1 NO_x value of a little less than \$3,000/metric ton, whereas MBB reburning would require a year 1 value of about \$4,000/metric ton.

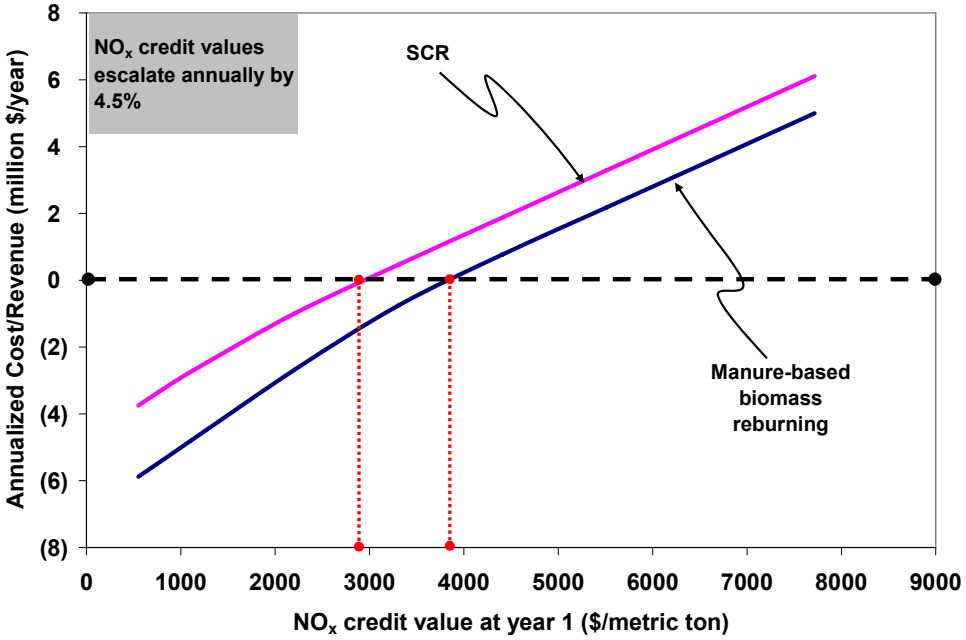

Figure 6.44 Annualized cost/revenue for both MBB reburning and SCR vs. the value of NO_x

Yet more importantly, the profitability of MBB reburning was found to be very sensitive to the effectiveness of the primary NO_x control technology already installed at the power plant. On top of competing with SCR, MBB reburning must also compete with these existing low-NO_x burners and over fire air. Figure 6.45 is a plot of annualized cost against the NO_x level achieved by primary controls. In many instances, coal-fired power plants have already installed very effective low-NO_x burners that can achieve levels as low as 60.2 g/GJ (0.14 lb/MMBtu) (Srivastava *et al*, 2005). For these plants, gaining enough revenue from NO_x credits to payoff the capital of drying and transporting biomass reburn fuel would be difficult.

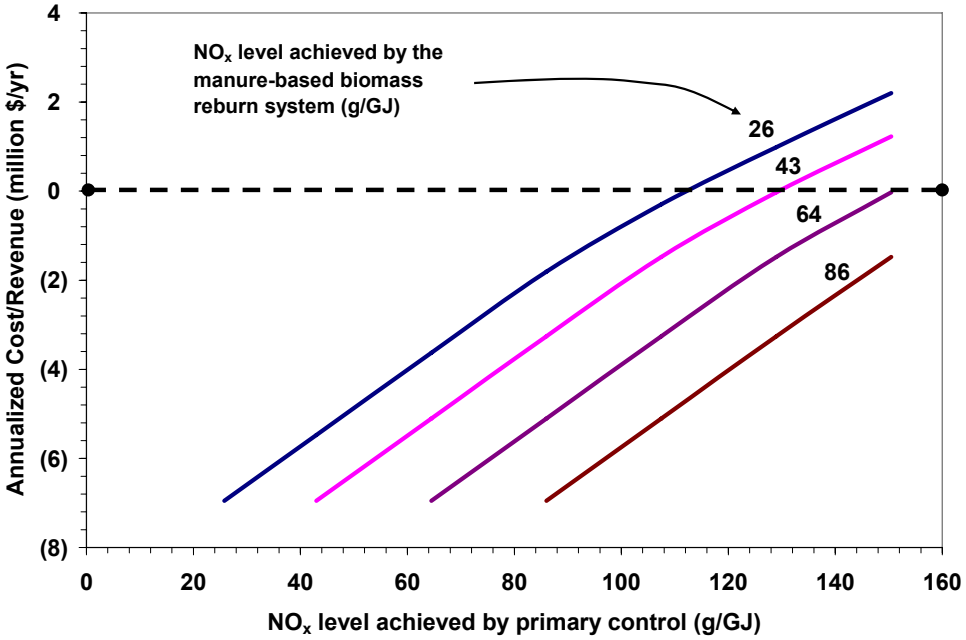

Figure 6.45 Annualized cost/revenue vs. NO_x levels achieved by primary NO_x controllers

Moreover, the success of a MBB reburn system can also be tested against the going value of NO_x, just as co-fire systems were tested against the current value of CO_2. Figure 6.46 is a similar plot to Figure 6.25, only for NO_x values. At an escalation rate of 4.5%, a current NO_x value of $2,500/metric ton would justify a MBB reburn system if this standard were to be used. However, reburning would still not be as attractive as SCR.

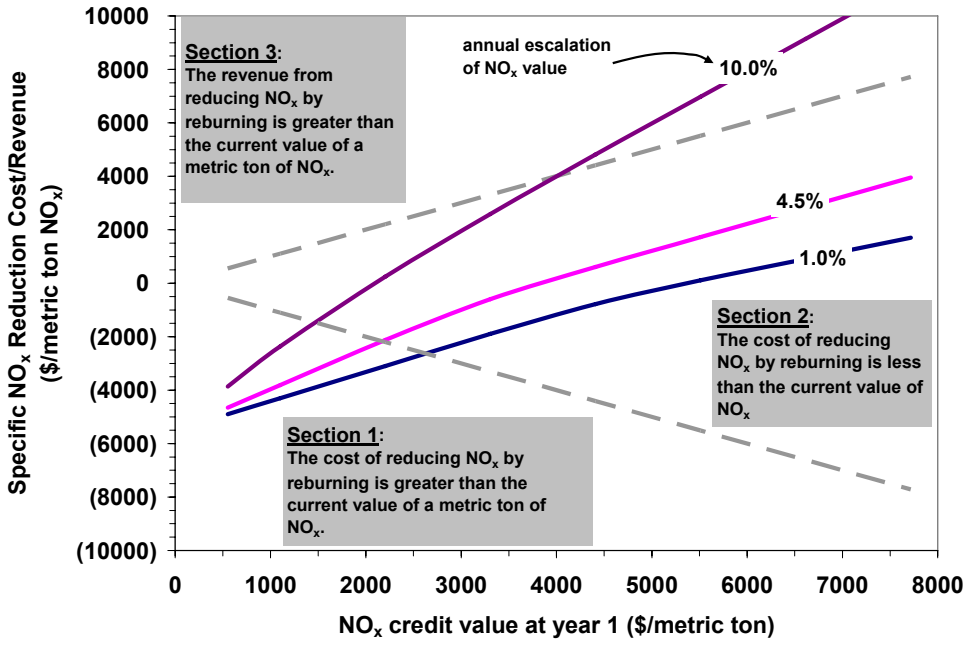

Figure 6.46 Specific NO_x reduction cost/revenue for manure-based biomass reburning vs. the value of NO_x

Emissions of SO_2 (Figure 6.47) and ash (Figure 6.48) were found to affect a reburn system in much the same way as they would a co-fire system. Supplying 10% of the heat rate through MBB reburning was found to increase ash production from 7.6 metric tons/hr (when burning coal only) to 9.7 metric tons/hr (about a 28% increase). If the heat contribution from biomass reburn fuel were to be higher at 20%, the ash level would exceed 11.8 metric tons/hr, with almost half of the ash coming from the MBB reburn fuel. Again, the high ash emissions are troubling, given the studies on the salability of manure ash by Megel *et al*. (2006 and 2007).

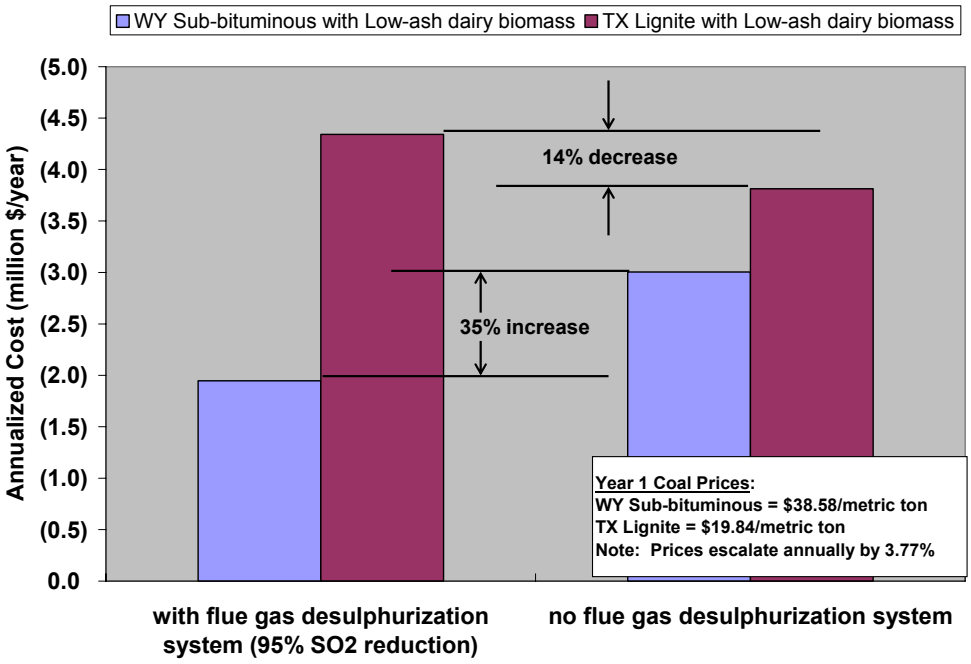

Figure 6.47 The effect of sulfur emissions on annualized cost during reburning

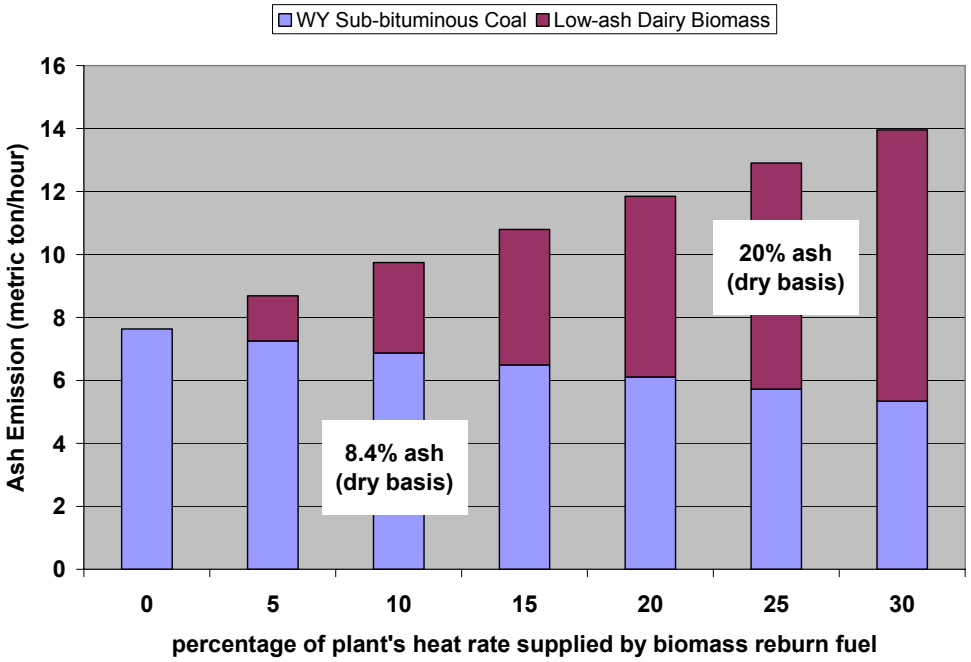

Figure 6.48 Ash emission vs. heat rate supplied by biomass reburn fuel for Wyoming sub-bituminous coal being replaced by low-ash dairy biomass

6.3.2.4. Biomass drying and transporting

The same discussion about MBB drying and transporting can be made for reburning as was done for co-firing. Since the only change for the drying and transportation sections of the economics model was the amount of biomass required for reburning, the trends during sensitivity analysis remain largely the same. However, the relationship of parameters, such as transport distance, to reburning's competitiveness to SCR should be noted. For example, in Figure 6.49, MBB reburning was found to have a similar net present worth if transport distances were shorter than 20 km (12 miles), despite the same high natural gas fueling costs involved with drying the biomass.

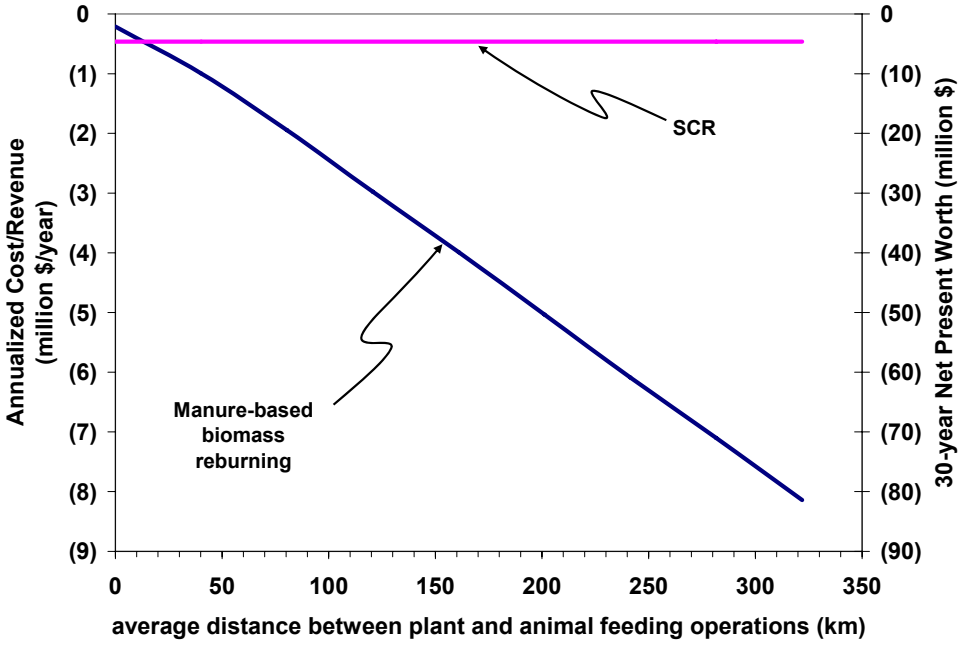

Figure 6.49 Annualized cost and net present worth of both reburning and SCR vs. manure-based biomass transport distance

During co-firing operations, the plant operator is free to burn coal with any fraction of MBB, so long as the combustion can be maintained and there is an adequate supply of co-fire fuel. However, with reburning, the amount of reburn fuel that is required is essentially fixed due to the desired NO_x emission levels. According to Oh *et*

al. (2008), lower amounts of reburn fuel will hinder NO_x reductions. Thus, the problem of finding enough low-ash biomass suitable for burning in a power plant may be an even greater challenge for reburning. For the base case 300 MW power plant, about 57,000 dairy cows, each producing about 6.35 dry kg of manure per day would be required to supply the reburn facility if the biomass reburn fuel supplied 10% of the overall heat rate. This amount of manure is roughly 38% of all the manure produced in the Bosque and Leon River Watersheds in Texas. So, even though the economics models presented for this research predict that MBB reburning would be a better investment than MBB co-firing, the feasibility of reburning coal with MBB is seemingly more doubtful.

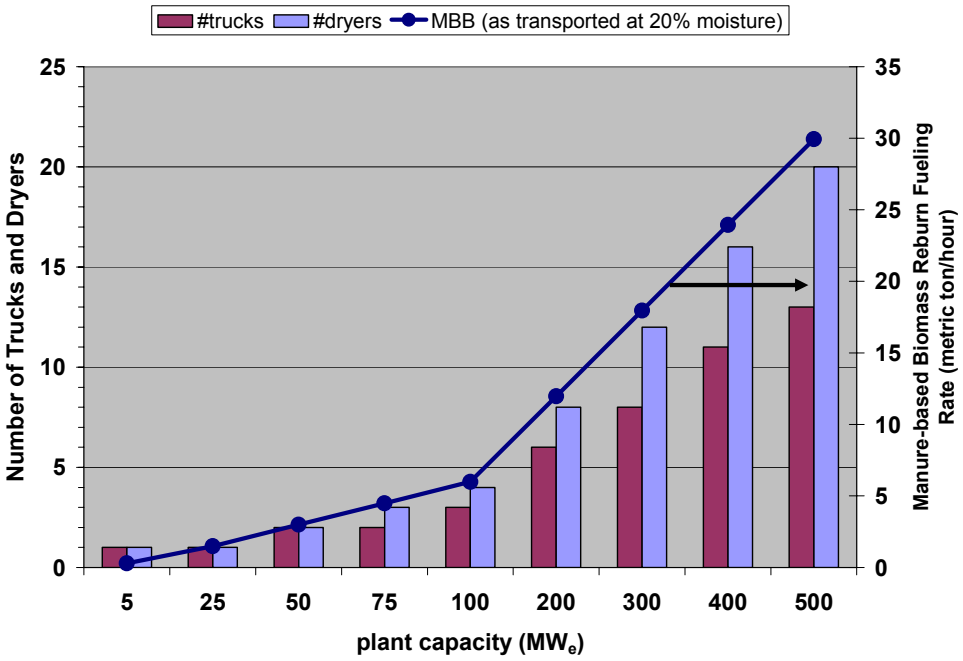

Figure 6.50 Number of required trucks and dryers and biomass fueling rate vs. plant capacity

In Figure 6.50, the number of trucks and dryers required to supply the biomass reburn fuel are plotted against power plant capacity. A 500 MW plant would require at least 20 two-metric ton/hr conveyor belt dryers where as a 100 MW plant would only require 4 dryers. Once again, the applicability of MBB reburn technology may be limited to smaller sized power plants. As state and federal governments decide how to

increase the overall electrical power capacity in the country, instead of constructing extremely large power plants dependant on nonrenewable (although readily available) fossil fuels, steps ought to be made to construct a greater number of smaller plants. These new plants can be strategically placed near areas with higher concentrations of agricultural biomass to promote reburning and co-firing coal with carbon neutral feedstock, such as MBB. Infrastructure such as smaller sized power plants could curb NO_x and CO_2 emissions, boost rural economies, minimize the environmental load from large concentrated animal feeding operations, and develop stronger business ties between the agriculture and energy sectors of the US.

6.4. Combustion at Smaller-scale, On-the-farm Systems

However, if energy producers find that utilizing manure-based biomass in existing coal-fired power plants is simply not feasible, then perhaps the biomass would be better utilized in smaller scale combustion systems installed on or near the animal feeding operations themselves. A conceptual design of a combustion system capable of handling high moisture MBB from free stall dairy barns or indoor piggeries with manure flushing systems was discussed in great detail in Section 5.5.1. Mass and energy balances were conducted to predict the combustion system's effectiveness at incinerating the manure and the amount of steam that can be generated for use as a thermal commodity for operations at or near the feeding operation.

6.4.1. Base Run

The base case parameters chosen for the small-scale combustion system are listed in Table 6.14. Suppose the combustion system is installed at a 500-cow dairy with each cow excreting about 8 dry kg of manure per day. The manure from all 500 animals is flushed from the free stall housing to the solid separator and is 95% moisture when it reaches the separator. The fire-tube boiler produces saturated steam at 300 kPa(gage).

Ten percent, preheated excess air is used to burn the dried manure solids. The base case parameters for the dryer are similar to those discussed earlier in Section 6.1.

The equations for the combustion model were, once again, compiled into a computer spreadsheet program. The resulting mass flows and temperatures at each point in the system for the base run are shown in Figure 6.51. The spreadsheet program helped tremendously in visualizing the mass flows of the system during parametric analyses.

Table 6.14 Base case values for modeling the small-scale on-the-farm MBB combustion system

Parameter	Base Value (unit)
Moisture percentage of flushed manure	95%
Type of biomass	low-ash dairy biomass, 20% ash, (dry basis)[c]
No extra fuel	--
Number of animals	500
Manure production	7.73 dry kg/cow/day
Moisture percentage of separated solids	80%
Percent solids remaining in the separated wastewater	3%
Desired moisture percentage of dried solids[a]	20%
Excess air percentage	20%
Pre-heated combustion air[b]	Yes
Boiler pressure	300 kPa,gage
Stack temperature	420K
Moisture percentage of remaining solids from boiler (blowdown solids)	70%

[a]Please see Table 6.2 for base case values for rotary dryer

[b]Heat exchanger for pre-heating air is 99% effective

[c]For base run, all ash is assumed to exit the combustion system as bottom ash

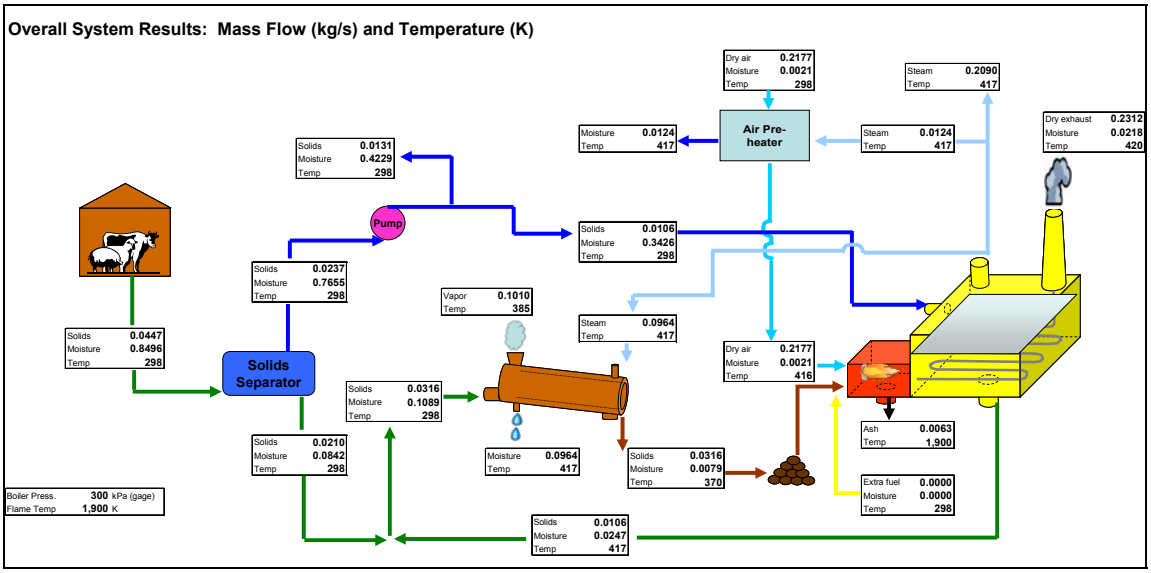

Figure 6.51 Sample output from computer spreadsheet model of small-scale on-the-farm manure biomass combustion system

For the base case, the system was found to produce 753 kg/hr of steam that would be available for thermal processes at or near the farm. The adiabatic flame temperature was found to be 1900 K and the corrected boiler efficiency (equation (5.244)) was found to be 82%. The disposal efficiency was found to be about 50% during the base case run when the only fuel that was burned was the dried separated MBB solids. This disposal efficiency (equation (5.245)) is much improved from the 34% reported by Carlin (2005) and Carlin *et al*. (2007a). This improvement is attributed mostly to the drying of the separated solids and the pre-heating of combustion air in this revised system. However, as was discussed by Carlin et al., since the moisture of the flushed solids was so high, at 95%, obtaining disposal efficiency close to 100% was not possible without the help of additional fuel. Aside from the additions of drying and pre-heating, the analysis of the system is much improved from these earlier studies. Carlin *et al*. estimated that the water leaving the solid separator was pure water and that the remaining solids in the boiler water were negligible. Thus the boiler efficiency was not adjusted for the possibility of having more solids remaining in the separated wastewater stream. Moreover, constant specific heats of combustion gases and dry combustion air

were also assumed under the earlier studies. Here both those assumptions were not made.

The system can be scaled for different sized animal feeding operations and for different manure excretion rates per animal, as can be seen in Figure 6.52.

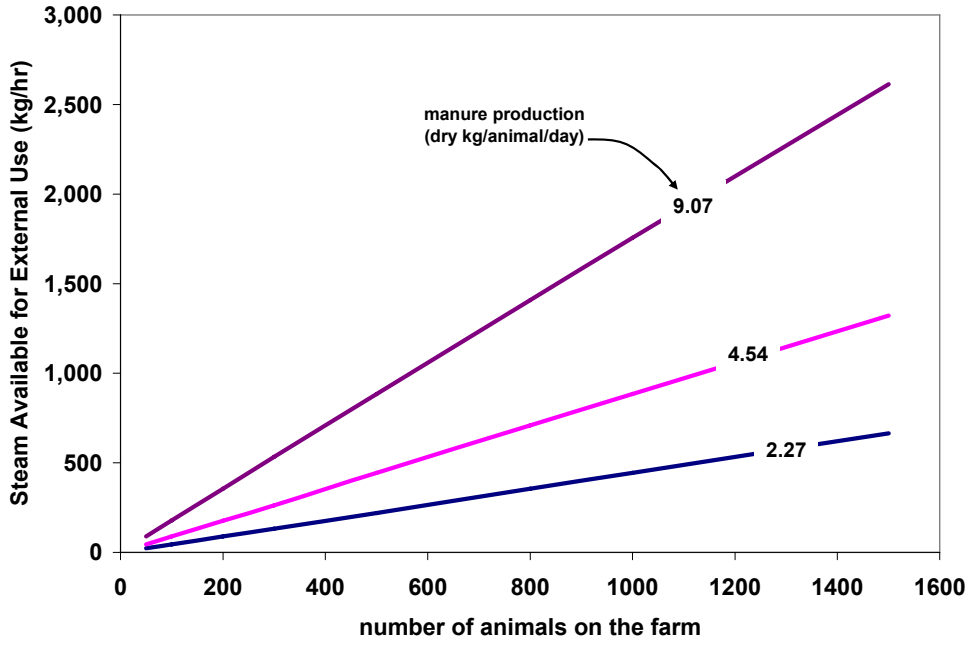

Figure 6.52 Usable steam produced from combustion system vs. number of animals housed at the feeding operation

The steam production, boiler efficiency and disposal efficiency can vary greatly when the base values are altered. The following discussion will be of parametric studies in which some of the base values were changed in order to view the sensitivity of the steam production, disposal efficiency and other important parameters.

6.4.2. Flushing Systems and Solids Separation

First, the performance of the combustion system is greatly dependant on how much moisture is in the flushed manure to begin with. The amount of wastewater that cannot be incinerated by the combustion system can increase greatly if the moisture

percentage of the flushed manure approaches 99%. See Figure 6.53. Not only is the load on the boiler greater, but the amount of fuel is depleted when the flushed moisture percentage is extremely high.

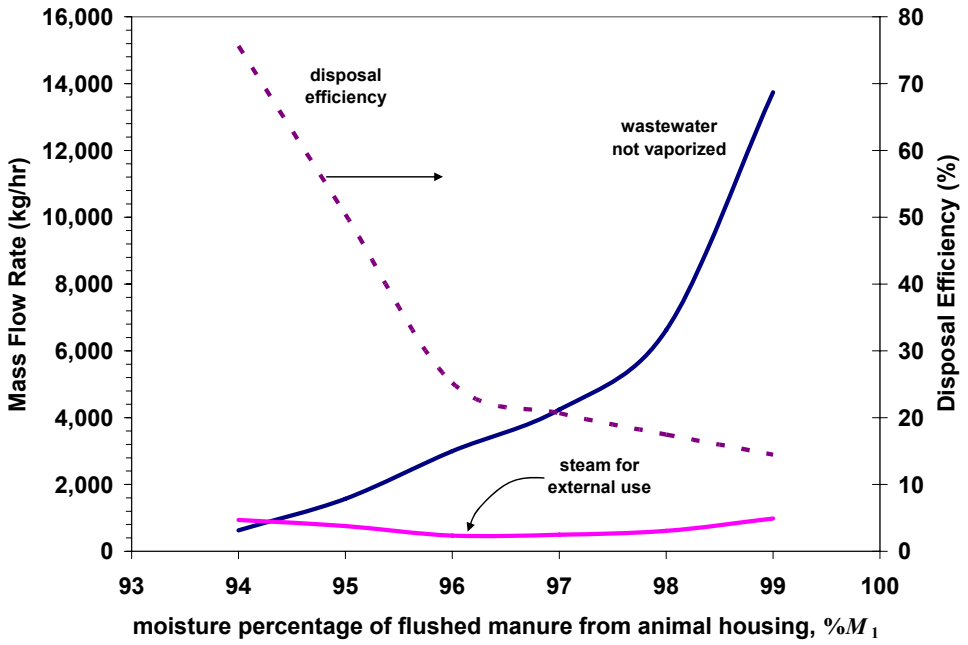

Figure 6.53 Usable steam, remaining wastewater, and disposal efficiency vs. moisture percentage of the flushed manure

The effectiveness of the combustion system is also dependant on the ability of the solid separator to screen out solids from the flushed stream. Figure 6.54 is a representation of how steam production and disposal efficiency change with increasing moisture percentage of the separated solids. Although the steam production decreases for wetter separated solids, the disposal efficiency actually increases. This is because the rotary dryer must consume more steam and transfer more heat to the separated solids in order to dry them to the desired moisture percentage of 20%. So, less steam is available for external use. However, essentially more of the wastewater is exiting the system at the vapor exhaust valve of the rotary dryer (point 11 in Figure 5.17) and less is being sent to the boiler. This may indicate that the rotary dryer is more effective at removing

moisture from the solids than the steam tube boiler, since the net effect is greater disposal efficiency.

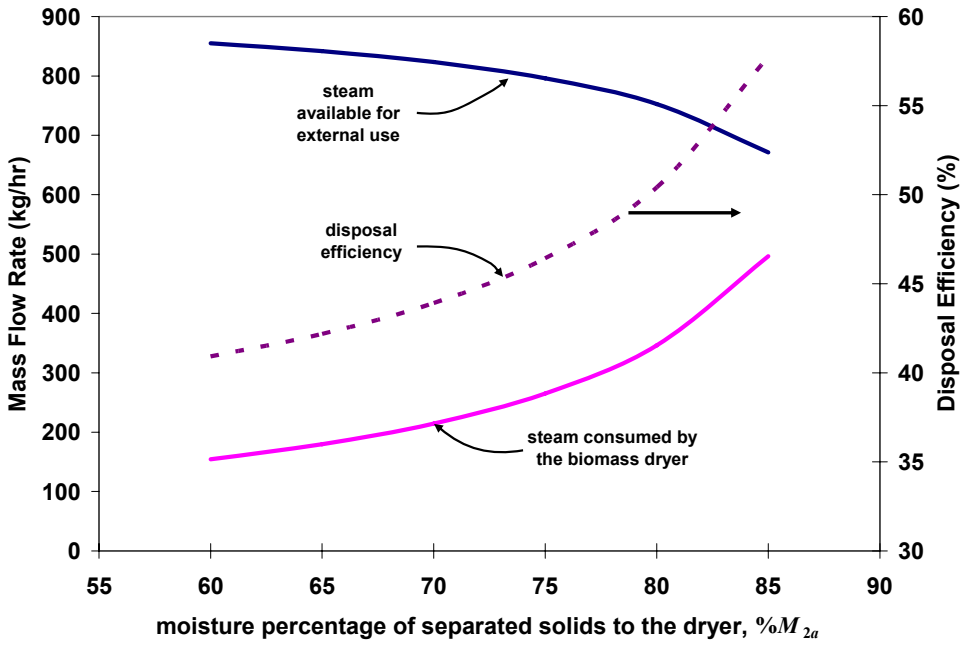

Figure 6.54 Disposal efficiency and steam production vs. moisture content of the separated MBB solids

The solids remaining in the flushed manure are mostly detrimental to the boiler efficiency. When more solids enter the drying chamber at point 8, more heat from the combustion goes to heating up these remaining solids, which are eventually sent back to the dryer, but the heat energy used to bring them to the steam temperature is essentially wasted. Thus, having more solids in the boiler water is detrimental to both boiler efficiency and the disposal efficiency as can be seen in Figure 6.55.

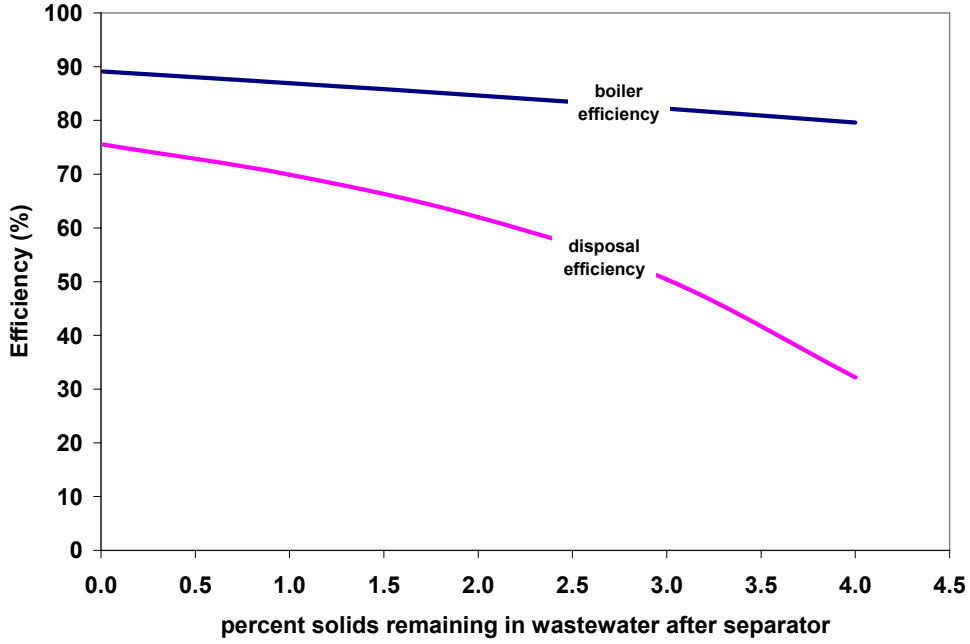

Figure 6.55 Boiler and disposal efficiency vs. the amount of solids remaining in the wastewater after the solid separator

6.4.3. Effect of Drying Solids Before Combustion

Drying the manure separated solids before combustion was the most significant addition to the small-scale system discussed by Carlin (2005). Figure 6.56 shows how drying the solids can improve flame temperature and increase the amount of wastewater that is vaporized in the boiler. Although the dryer must consume more steam to dry the manure to lower moisture percentages, the overall amount of steam that is generated in the boiler increases, causing a net increase in usable steam for external thermal processes. See Figure 6.57.

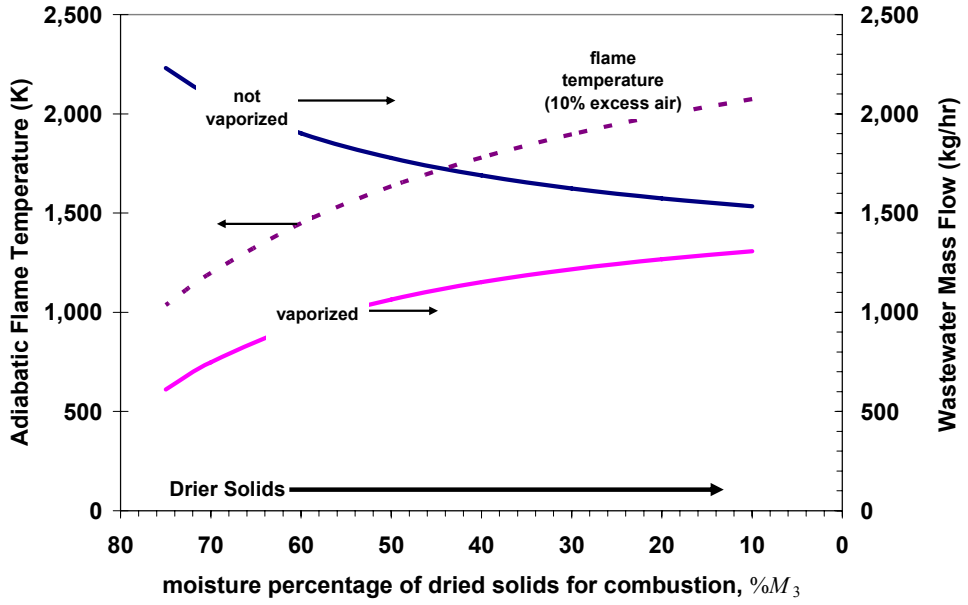

Figure 6.56 Adiabatic flame temperature and wastewater mass flow vs. moisture percentage of the dried solids

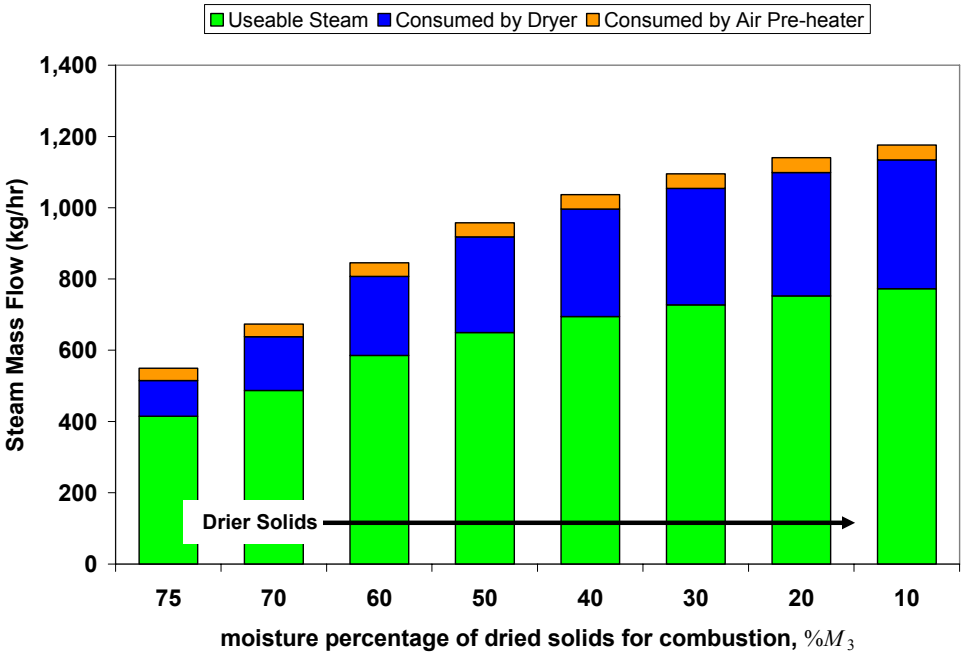

Figure 6.57 Steam production and use vs. moisture percentage of the dried solids

6.4.4. Combustion of Dried Biomass Solids

The addition of combustion air preheating was not quite as significant as drying, but still made some difference to the boiler and disposal efficiencies as can be seen in Figure 6.58. The effects of pre-heating the air are really limited by the steam temperature (and thus the boiler pressure, if the steam is saturated). The effectiveness of the heat exchanger heating the air was assumed to be 99% for the base case run. This assumption provides the hottest air possible for the combustion as the air cannot exceed the steam temperature due to the Second Law of Thermodynamics.

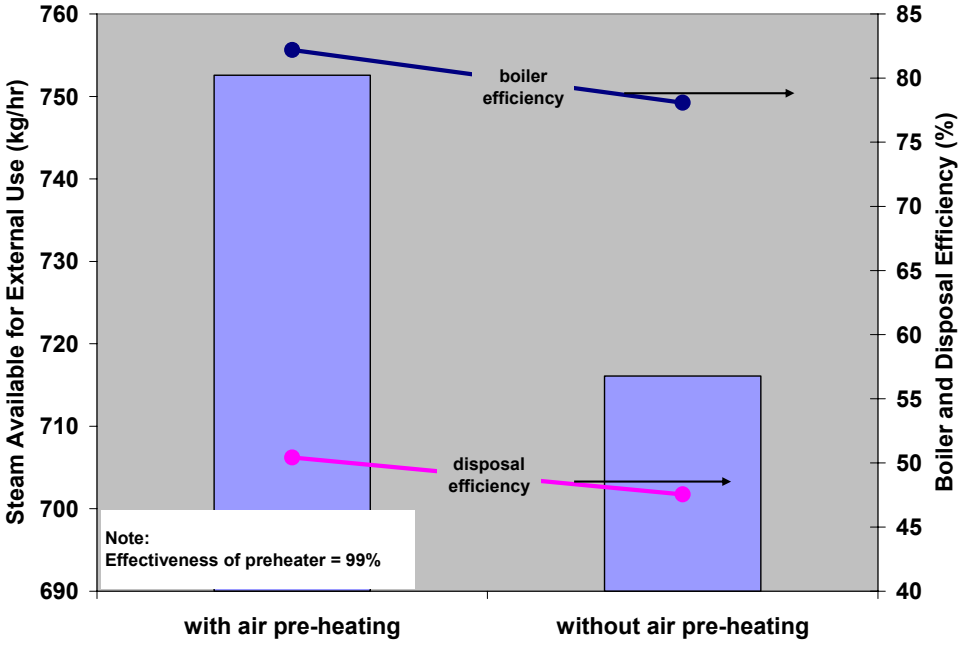

Figure 6.58 Effects of preheating combustion air

However, the pre-heating of combustion air did have a peculiar effect on both boiler efficiency (Figure 6.59) and disposal efficiency (Figure 6.60). At lower stack temperatures, both of these efficiencies actually increased with excess air percentage. Typically, both efficiencies drop with excess air percentage; however, due to the way

they were defined for this study, the heat energy added to the combustion air is seen as an addition to the system. However, at higher stack temperatures, the efficiencies were found to drop with excess air percentage as usual.

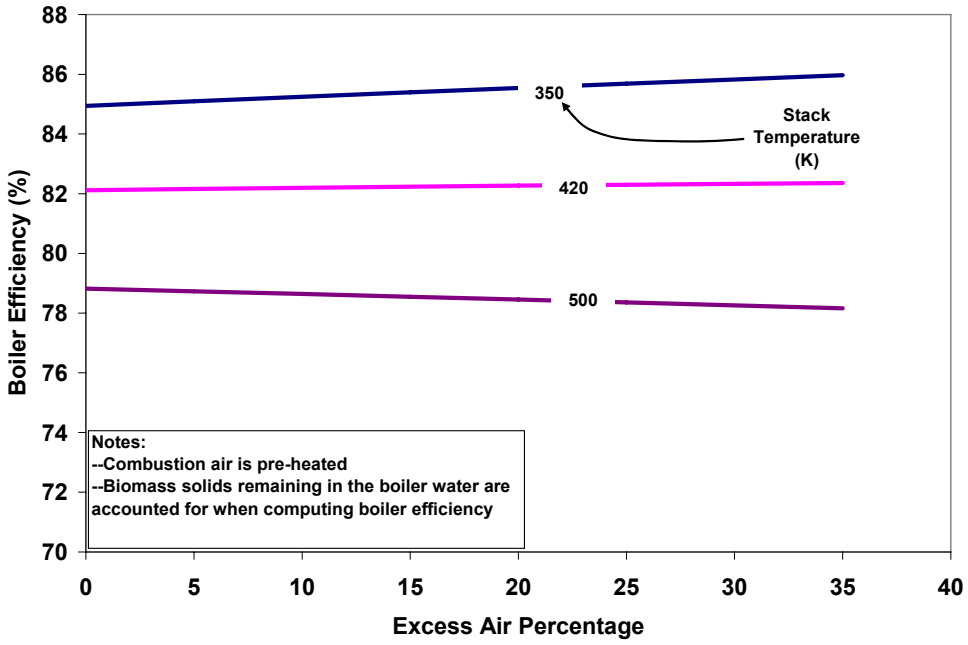

Figure 6.59 Boiler efficiency vs. excess air percentage and stack temperature

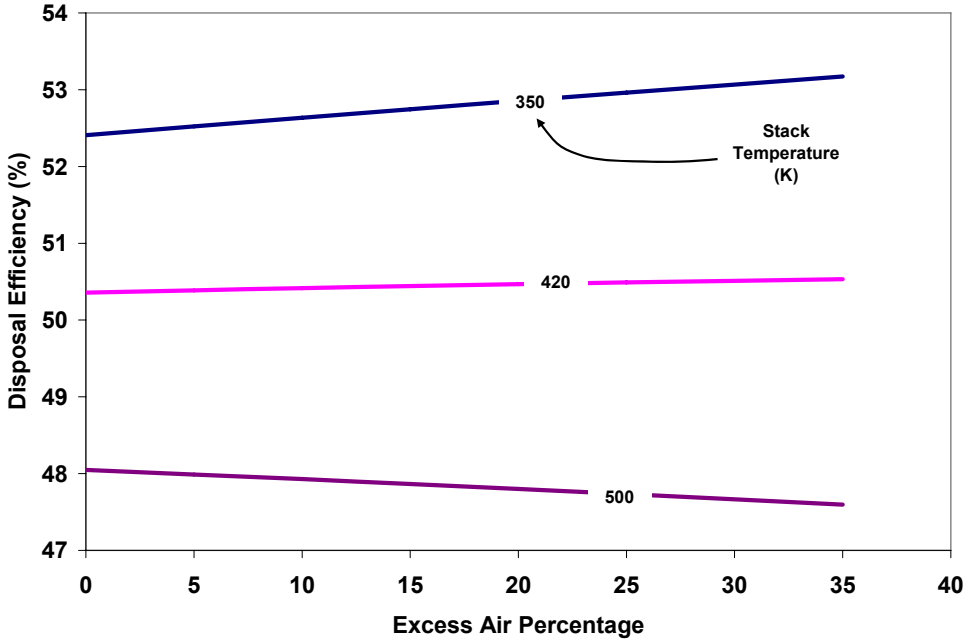

Figure 6.60 Disposal efficiency vs. excess air percentage and stack temperature

As has been the case throughout this study of MBB combustion, the ash content in the biomass fuel is detrimental to the system in every aspect. Figure 6.61 is a graph of flame temperature, steam production, and steam consumption plotted against the ash percentage of the biomass. Figure 6.62 is a plot of disposal efficiency and the remaining amount of wastewater against ash percentage. If the manure biomass has an ash content of 40%, disposal efficiency drops to about 35%, which negates the improvements obtained from drying solids and pre-heating air.

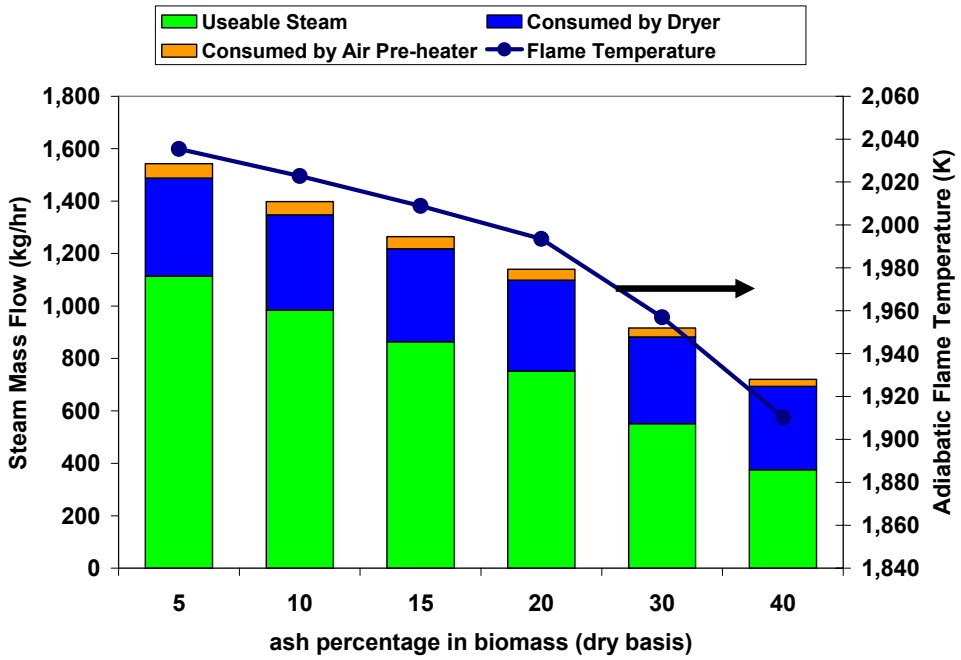

Figure 6.61 Flame temperature, Steam production, and steam usage vs. ash percentage in the MBB solids

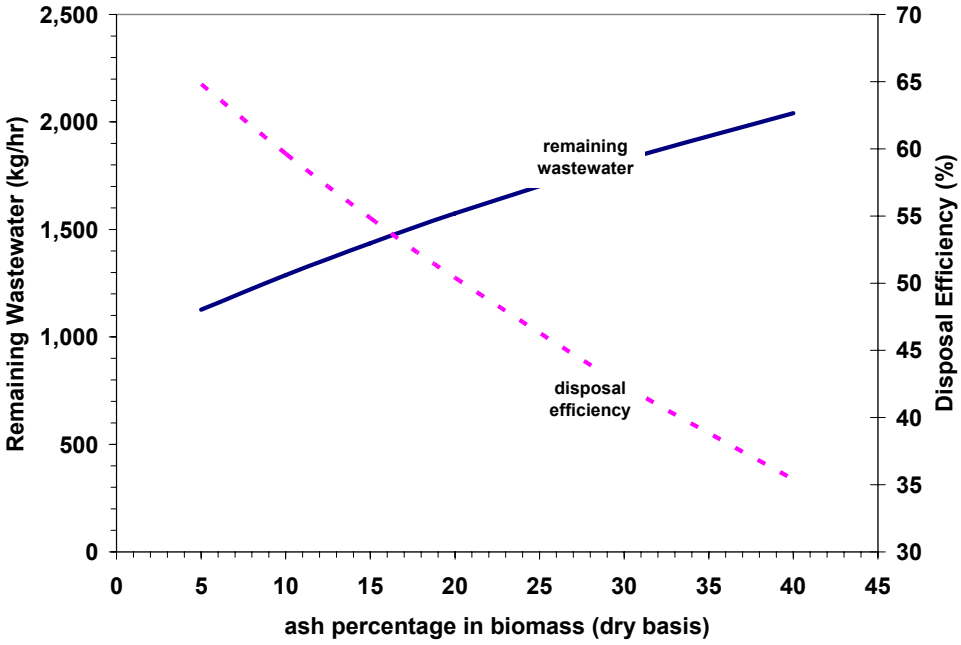

Figure 6.62 The effect of ash percentage in the MBB solids on disposal efficiency

6.4.5. Operation of Fire-tube Boiler

The greatest design issue of the conceptualized combustion system is the fire-tube boiler, which must accept heat from the combustion of a low grade fuel (MBB) and vaporize wastewater that many times can be heavy in impurities and solid material that would otherwise be used to further fuel the boiler's burner. The mechanical design of the boiler, as well as other design issues such as fowling and scaling of the fire-tube, are unfortunately not covered here. These issues are left to future work.

However, one parameter pertaining to the operation of the boiler can be investigated, and that is the degree to which the remaining solids and impurities in the boiler water (wastewater) are dried in the boiler's chamber. Figure 6.63 is a plot of usable steam and the disposal efficiency against the moisture percentage of the remaining solids (or the blow down solids). If the remaining solids leave the boiler high in moisture, then a lesser amount of wastewater was converted to steam. Thus, the amount of usable steam decreases. However, once again, the disposal efficiency was found to increase as the remaining solids are returned to the dryer, and the wastewater is eventually vaporized there instead of the boiler. This finding suggests that if disposal efficiency is the only important parameter, the operator of this system may be better served to simply produce just enough steam to run the dryer and vaporize as much of the wastewater in the dryer as possible. However, doing this (i.e. allowing the moisture percentage of the blow down solids to be left high) would greatly reduce the amount of usable steam produced by the boiler.

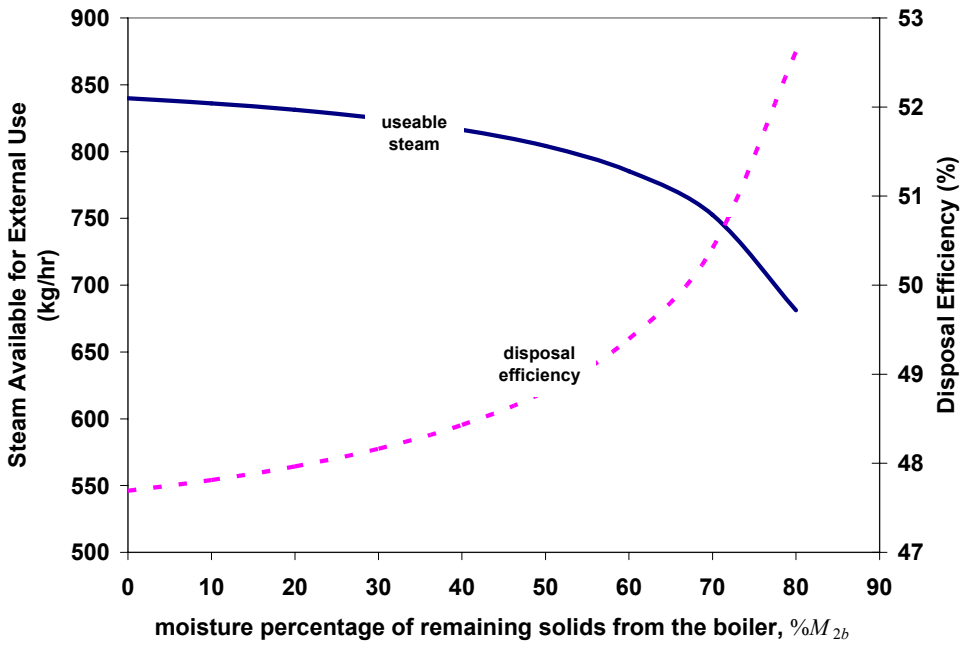

Figure 6.63 Steam production and disposal efficiency vs. moisture percentage of boiler blow down solids

6.4.6. Additional Fueling for Complete Wastewater Disposal

For high moisture flushed systems, all of the wastewater drained from the free stall barn cannot be incinerated if the only fuel that is used to generate heat energy is the separated MBB solids. In order to completely incinerate the waste coming from the barn, additional fuel must be burned in the furnace or gasifier. Figure 6.64 is a plot of disposal efficiency against a growing amount of additional fuel injection into the boiler burner. Methane, propane, and Texas lignite were modeled, but there did not seem to be much difference between these fuels as far as disposal efficiency. Due to the way disposal efficiency was defined in equation (5.245), an efficiency of 100% can never be obtained because there will always be some ash from the biomass combustion remaining. However, for all fuels modeled, the maximum disposal efficiency was found to be obtained when the additional fuel was about 18 to 20% of the total fuel burned.

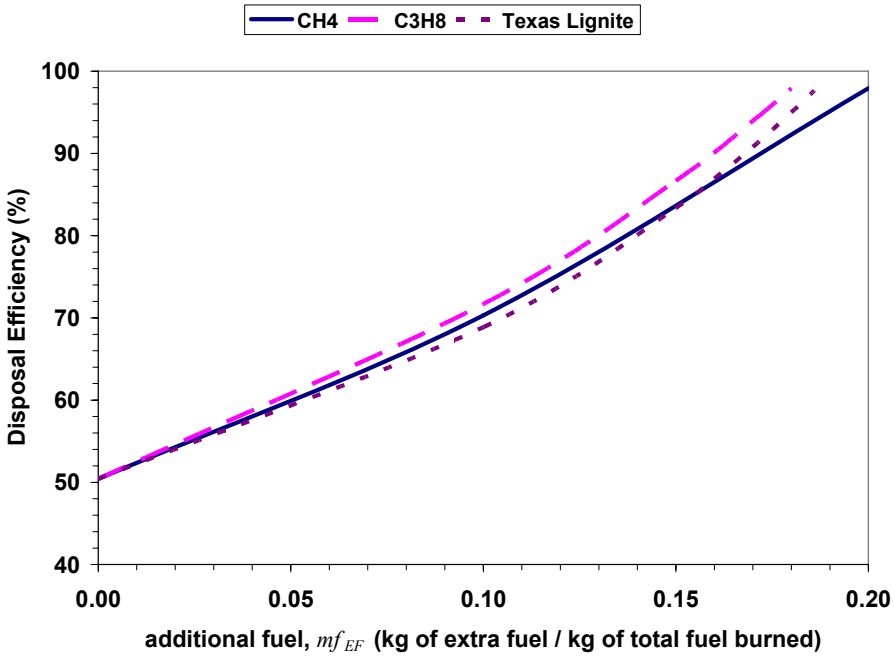

Figure 6.64 The effect of additional fueling on the disposal efficiency

6.4.7. Economic Estimations for Small-scale Manure-based Biomass Systems

The discussion of economics for small-scale MBB combustion systems will not be covered as extensively here as the economics for large-scale co-fire and reburning projects on existing coal-fired power plants. However, the results of the modeling equations suggested in the literature review and presented in Section 5.6.6 will be shown here. Under the base case input parameters, the capital cost of the rotary dryer was found to be about $1 million. If the combustor in the conceptualized model is assumed to be a gasifier and subsequent producer gas burner, then the capital investment cost of a gasifier capable of handling the amount of manure from a 500-cow farm was found to be $924,000. The air pre-heater was found to be about $11,000 when the overall heat transfer coefficient was set at 3.5 kJ/s m^2 K.

The circumstance of how these investments would be paid off depends greatly on the procedures of the animal feeding operation before the combustion system is installed. The Elimanure System discussed earlier in Section 3.2 was said to be profitable partly

because the animal farm was transporting many gallons of liquid wastewater off the farm before the installation of the disposal system. The avoided cost of hauling manure plus the profits from electricity generation were claimed to be enough to pay off the $4.5 million investment and have a 3.5 year simple payback period.

This scenario can be roughly tested for the conceptual system presented here. Keeping with the same input parameters in Table 6.14, suppose that a 500-cow dairy hauls all of its liquid manure, at 95% moisture, 50 km (about 30 miles) off site. Moreover, assume that the animal farm, or a nearby business, can somehow use the steam generated in the fire-tube boiler and avoid having to pay a fueling cost (for example propane) to generate the steam. If the conceptualized MBB combustion system is installed it will save on manure transportation costs and generate revenue from the sale or avoided fueling cost of the steam. Also assume that a solid separator is already available at the dairy and that the boiler runs continuously every day of the year. Perhaps the greatest unknown is the capital cost of the fire-tube boiler, but for now, assume that it will cost $1 million just like the dryer. The total capital cost of the system is then about $2.9 million for a system disposing waste from 500 animals. The Elimanure System was said to be $4.5 million for a 4,000-head animal farm which included dairy cows, horses, and pigs (Skill Associates, 2005), (Caldwell, 2008).

The results of this base case run are presented in Table 6.15. The combustion system was found to save the animal feeding operation $137,000 per year, even without the use of additional fuel to completely incinerate the wastewater. The manure transportation equations discussed in Section 5.2.2 were used here to estimate the cost of hauling manure (both before and after installation of the combustion system) and the resulting ash from the combustion. The labor cost was computed such that 1.5 workers were operating the combustion system at $15 per hour; that is, there was always one or two workers monitoring and maintaining the combustion system throughout the year.

Table 6.15 Base case run for the economics of the small-scale MBB combustion system when no additional fuel is burned

Cash flows before installation	
Hauling liquid manure--labor	(37,655)
Hauling liquid manure--diesel	(20,654)
TOTAL ($/yr)	(58,309)
Cash Flows after installation	
Fixed O&M of system	(118,300)
Hauling remaining liquid manure--labor	(18,403)
Hauling remaining manure--diesel	(10,094)
Hauling ash--labor	(255)
Hauling ash--diesel	(140)
Fuel Savings from boiler	423,470
Labor for system operation	(197,213)
System extra fuel (propane) cost	0
TOTAL ($/yr)	79,066
ANNUAL SAVINGS	137,375
Total capital cost of the system ($)	2,957,506
Simple Payback (years)	21.53

The payback for this base run was found to be 21 ½ years, which is usually unacceptable for a small scale project such as this. However, suppose that additional propane is injected into the burner so that all of the wastewater and MBB from the dairy is incinerated. This was the case for the Elimanure System as well. These results are presented in Table 6.16. For this case, the payback period was found to be only four year, much more comparable to the 3.5 payback period for the Elimanure System.

Table 6.16 Economic results for the small-scale MBB combustion system when additional fuel is used to completely vaporize all waste from the animal feeding operation

Cash flows before installation	
Hauling liquid manure--labor	(37,655)
Hauling liquid manure--diesel	(20,654)
TOTAL ($/yr)	(58,309)
Cash Flows after installation	
Fixed O&M of system	(137,221)
Hauling remaining liquid manure--labor	0
Hauling remaining manure--diesel	0
Hauling ash--labor	(340)
Hauling ash--diesel	(186)
Fuel Savings from boiler	1,129,805
Labor for system operation	(197,213)
System extra fuel (propane) cost	(400,885)
TOTAL ($/yr)	794,845
ANNUAL SAVINGS	853,154
Total capital cost of the system ($)	3,430,537
Simple Payback	4.02

However, these findings are all dependant the presumptions and estimations that were made, none of which is probably more significant than the capital cost of the fire-tube boiler, as can be seen in Figure 6.65.

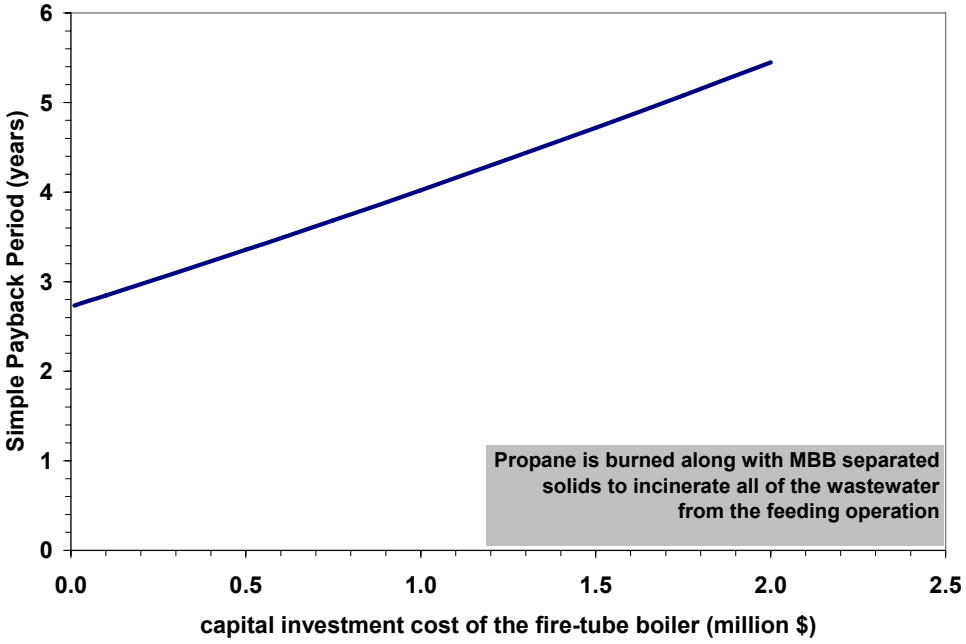

Figure 6.65 Simple payback period vs. the capital investment of the fire-tube boiler of the small-scale MBB combustion system

7. SUMMARY AND CONCLUSIONS

7.1. Drying and Transportation

The discussion of the biomass drying and transportation models can be summarized with the following main points.

1. Increasing air temperature in a conveyor belt dryer lowers the heat consumption (and hence the fuel consumption) of the dryer, but only to a certain extent. The main factor that affects the heat consumption for a fixed mass flow of manure-based biomass (MBB) of a fixed desired moisture percentage is the air flow rate.
2. A drying model for conveyor belt dryers based on an empirical drying constant, was chosen for integration into subsequent economics models over a more textbook model based on a mass transfer number. This choice was mostly based on the inability of the transfer model to describe situations where the product had a small characteristic particle size, such as MBB's at 2.18 mm. For small particle sizes, the transfer number model predicted high mass transfer rates and hence small conveyor belt areas and high air flow rates, which probably gave erroneous results.
3. The fuel consumption of biomass dryers was found to be one of the most significant factors when preparing MBB for co-combustion at large scale coal-fired power plants. The fuel consumption was found to be similar for both conveyor belt and rotary steam-tube dryers.
4. Surprisingly, MBB transportation costs were not significantly affected by the moisture content of the manure until the moisture percentage was 80% or greater. This was found to be the case because low-moisture MBB is less dense than high-moisture biomass. Unless dried manure is compressed so that its density is artificially increased, more hauling vehicles will be required to transport it. However, at moisture percentages above 80%, the additional mass of water in the biomass overtakes any variation in density. The optimum moisture percentage to transport manure, based on diesel consumption of the hauling vehicles, was found to be about 50%.

7.2. Economics of Co-firing

Co-firing MBB in large coal-fired power plants can be profitable, but a lot has to happen. The manure must be low in ash, coal prices must be high, CO_2 values must be high and expected to escalate, and the use of high-grade fuels such as natural gas during drying operations should be avoided. The following points summarize the discussion of co-firing coal with MBB.

1. A base case run of the MBB co-fire economics model for a MBB co-fire system installed on an existing 300-MW_e coal-fired power plant burning a 95:5 blend of coal to biomass showed that overall fuel energy consumption (including coal, biomass, diesel fuel, natural gas for drying, and electricity) would increase by 259 GJ/yr.
2. Burning a 95:5 blend of coal to low-ash MBB was found to lower CO_2 emissions by 58,600 tons/year (this value was calculated when accounting for CO_2 emitted during drying and transporting of MBB to the coal plant).
3. However, ash production from the plant was found to increase by 10% when burning a 95:5 blend, even when low-ash biomass was fired.
4. From base case parameters, an overall net present cost of $22.6 million was computed for the co-fire system at the 300-MW_e power plant. Operating income was never positive throughout the 30-year life of the co-fire project, causing zero return on investment, at least for the base case run. The most significant cost that hindered the profitability of the co-fire project was the cost of natural gas needed to fuel biomass dryers that could reduce the MBB's moisture content from 60% to 20%.
5. However, a higher value on avoided nonrenewable CO_2 emissions could overrule exorbitant costs of drying and transporting the MBB to power plants. A CO_2 value of $17/metric ton was found to be enough for the MBB co-fire project to reach an economic break even point.

6. The price of coal was also found to be significant to the overall profitability of the co-fire project. Since the biomass partly displaces the coal burned at the power plant, more expensive coal was found to lead to greater savings.
7. Although monetary compensation for the MBB would certainly benefit the owner of the animal feeding operation, a payment for obtaining biomass from farms could significantly decrease the profitability of a co-fire system. A MBB price of $10/dry metric ton can decrease the NPW of co-firing by 29%, if the price is also assumed to escalate by 3% annually.
8. Depending on the relative sulfur content of the MBB compared to the coal it is replacing, SO_2 emissions can become a significant factor in the economics of the co-firing project, especially if a flue gas desulphurization system is not installed at the coal plant. Sulfur is a greater detriment to the profitability when the biomass must replace a coal with very low sulfur content, such as Wyoming sub-bituminous coal.
9. Ash in MBB is a drag on the co-firing system (or reburning system) at every level. Ash adds to transportation costs as it means moving more mass for less energy content. Ash is also a heat sink during drying, making drying high ash biomass slightly more expensive than drying low ash biomass. Most significantly, ash adds to the O&M cost of co-firing because it must be removed from the power plant and then sold or disposed of off site.
10. For the base case run of the co-firing model, drying constituted 76% of the total cost. Of this cost, 73% was due to purchasing natural gas for generating steam for the biomass dryers. Another 15% was due to running the dryers' fans.
11. If scraped MBB can be both low in ash and low in moisture due to dry weather and low relative humidity, the ability to use MBB as a co-fire fuel at coal-fired power plants greatly increases.
12. Due to the low amount of suitable low-ash MBB, simply finding enough biomass to satisfy desired co-fire rates or required reburn rates for co-combustion projects at large coal-fired power plants may be challenging.

7.3. Economics of Reburning

The discussion on reburning coal with MBB in large coal-fired power plants can be summarized by the following three points.

1. Emitting NO_x is expensive. Therefore, a retrofit project in which coal is reburned with MBB (10% heat rate supplied by MBB) to reduce NO_x emissions can theoretically be more profitable than a co-fire project. However, the problem of finding enough suitable low-ash biomass becomes even more problematic for reburn systems because in order for NO_x reductions to be maintained, 10 to 25% of the plant's heat rate must be satisfied by the reburn fuel, and the highest reductions have been found to occur when the reburn fuel is pure MBB.
2. Under base case assumptions the net present cost of a MBB reburn project for an existing 300-MW_e coal-fired power plant was found to be $19.1 million. Comparatively, a selective catalytic reduction (SCR) project for a similar sized power plant with the same base case assumptions was found to be $4.6 million.
3. If the value of NO_x were to escalate annually at 4.5%, a current NO_x value over $2500/metric ton would justify installing a MBB reburn system. However, a reburn project would not be more justified, at least economically, than an SCR retrofit. In order for MBB reburning to be more profitable than SCR, a CO_2 tax or avoided cost of over $10/metric ton would be needed if the value of CO_2 was expected to escalate at 5.25% annually

7.4. On-the-farm Combustion

Given the high cost of transporting and preparing MBB for combustion in large scale coal plants, as well as the lack of available low-ash biomass, burning MBB in smaller scale combustion facilities on or near animal feeding operations may be preferable at this time. The discussion of small scale on-the-farm combustion of MBB may be summarized with the following main points.

1. A base case run of a mathematical model describing a small-scale, on-the-farm MBB combustion system that can completely incinerate high moisture (over

90%) manure biomass was completed. In the conceptualized model, liquid manure is sent to a solid separator where the separated solids are dried and then burned. The remaining wastewater is sent to a fire-tube boiler and vaporized to produce steam that can then be consumed by the dryer or a combustion air pre-heater. Some remaining steam can also be used for external thermal processes on or near the farm to make the system profitable.

2. The conceptualized MBB combustion system, under base assumptions, could potentially incinerate about 50% of all the high moisture manure waste emanating from a 500-cow dairy, while producing over 750 kg/hr of 300 $kPa_{(gage)}$ saturated steam that could be used for external thermal processes.
3. The ability of the solid separator to strain solids out of the wastewater was found to be critical, as remaining solids in the wastewater reduce the boiler efficiency and ability of the combustion system to vaporize the wastewater.
4. Drying separated solids and pre-heating combustion air greatly improve the efficiency of the MBB combustion system and increase the amount of usable steam that can be produced.
5. Higher ash contents in the MBB solids (greater than 30% on a dry basis) were found to be detrimental to the performance of the small-scale combustion system.
6. Interestingly, the results from the parametric study of the small-scale MBB combustion system seem to suggest that the rotary steam-tube dryer removes moisture from the manure waste stream more effectively than the fire-tube boiler.
7. Co-firing the dried MBB separated solids with 20% natural gas, propane, or coal can generate enough heat to completely incinerate all of the wastewater from the animal feeding operation.
8. If all of the steam produced by the small-scale MBB combustion system were to bring revenue to the animal feeding operation either by avoided fueling cost or by sales, the conceptualized MBB combustion system has the potential to be a profitable venture.

8. SUGGESTED FUTURE WORK

From the results of the present modeling study of the feasibility and economics of utilizing MBB in combustion systems, the following items are highly suggested as tasks for future work.

1. Mercury emissions may also affect the economics of MBB co-fire and reburn facilities installed at existing coal-fired power plants. The USEPA's Integrated Planning Model does model mercury emission reductions from activated carbon injection and from co-benefits from other secondary emission controllers such flue gas desulphurization systems. Future modeling of co-fire and reburn economics should take mercury into account as well.
2. When investigations into NO_x emissions during the co-firing of coal and MBB with low-NO_x burners are complete, the economic impacts of NO_x emissions should be added to the overall economic analysis for co-firing, as was done for reburning.
3. Moreover, the economics discussion for large scale MBB combustion in existing coal-fired power plants has concentrated on the economic benefits to the power plant facility, yet there are numerous benefits to farmers and others in the agricultural sector. Removing large quantities of manure from concentrated animal feeding operations decreases the possibility of phosphorus overloading and subsequent soil and water pollution by reducing the required capacity of manure storage structures such as anaerobic lagoons. Future work should also include investigations into the regional benefits such as job creation and rural economic development related to manure-based biomass combustion.
4. Other costs and benefits can be added to the overall economics model. For example, tax incentives and renewable energy credits can also be put forward to improve the economic outlook of burning MBB in large-scale settings.
5. The economic analysis presented here can also be extended to forecast the viability and profitability of thermal energy conversion of other biomass fuels such as

municipal solid waste, human fecal-based waste, plant or crop-based waste, other animal wastes, and various other agricultural-based residues and wastes.

6. If the small-scale conceptualized combustion model for MBB is to ever become reality, then the detailed design of the fire-tube boiler must be undertaken. This research may involve experimentation into the degree and difficulty of scaling from vaporized liquid manure. Similar evaporators and distillers have been developed and used for many years, however, to the author's knowledge, there has not been a machine that pressurizes liquid manure and then vaporizes it while removing remaining solids and residue.
7. A more detailed study of the possible uses of steam produced from small-scale combustion systems at animal farms may also be undertaken in the future. Possible uses of steam, or other thermal commodities, may include electrical power generation, animal feed production from steam flaking mills, hot water generation for dairies, space heating in operations located in northern states, etc.
8. As concentrated animal feeding operations continue to grow in size in the US, and in other parts of the world, more situations may arise where incineration of the manure-based waste from these facilities becomes more critical. Future work on this subject could center on investigating new possible applications of MBB combustion on or near the farm. Making manure combustion systems standard on new animal feeding operations could allow for further industrialization and automation of the American Agricultural system. On-the-farm manure combustion may also extend the operating life of concentrated animal feeding operations which are sometimes limited by sludge buildup in anaerobic treatment lagoons.

REFERENCES

Abhari R. and Isaacs L. L. (1990). Drying kinetics of lignite, sub-bituminous coals, and high-volatile bituminous coals. *Energy & Fuels* 4:448-452.

ACAA. (2006). Frequently asked questions. American Coal Ash Association. Available online at: http://acaa.affiniscape.com/displaycommon.cfm?an=1&subarticlenbr=5. (Accessed on September 2007).

Achkari-Begdouri A. and Goodrich P. R. (1992). Bulk density and thermal properties of Moroccan dairy cattle manure. *Bioresource Technology* 40: 225-233.

Anderson, M. E. and Sobsey M. D. (2006). Detection and occurrence of antimicrobially resistant E. coli in groundwater on or near swine farms in eastern North Carolina. *Water Science & Technology* 54(3): 211-218.

Annamalai, K., Ibrahim, M. Y., and Sweeten, J. M. (1987a). Experimental studies on combustion of cattle manure in a fluidized bed combustor. *Journal of Energy Resource Technology* 109: 49-57.

Annamalai, K., Sweeten, J. M., and Ramalingam, S.C. (1987b). Estimation of the gross heating values of biomass fuels. *Transactions of the Society of Agricultural Engineers* 30: 1205 1208.

Annamalai, K. and Thien, B. (2001). Feedlot manure as reburn fuel for NO_x reduction in coal fired plants. National Combustion Conference, Oakland, CA, March 25-27.

Annamalai, K., Sweeten, J. M., Mukhtar, S., Thien, B., Wei, G., et al. (2003a). Co-firing coal: feedlot and litter biomass (CFB and CLB) fuels in pulverized fuel and fixed bed burners. Final Department of Energy Report, DOE-Pittsburgh Contract #40810.

Annamalai, K., Thien, B., and Sweeten, J. M. (2003b). Co-firing of coal and cattle feedlot biomass (FB) fuels, Part II: performance results from 100,000 Btu/hr laboratory scale boiler burner. *Fuel* 82(10): 1183-1193.

Annamalai, K., Freeman, M., Sweeten, J., Mathur, M., Gilbert, et al. (2003c). Co-firing of coal and cattle feedlot biomass (FB) fuels, Part III: fouling results from a 500,000 Btu/hr pilot plant scale boiler burner. *Fuel* 82(10): 1195-1200.

Annamalai, K. and Sweeten, J. M. (2005). Reburn system with feedlot biomass. U. S. Patent #6,973,883 B1.

Annamalai, K. and Puri, I. (2006) *Combustion science and engineering*. Orlando, Florida: Taylor and Francis.

Annamalai, K., Priyadarsan, S., Arumugam, S., and Sweeten, J. M. (2007). Energy conversion: principles for coal, animal waste, and biomass fuels. *Encyclopedia of Energy Engineering and Technology* 1(1): 476-497.

Arcot Vijayasarathy, U. (2007). Mercury emission control for coal fired power plants using coal and biomass. MS Thesis. Texas A&M University: College Station, Texas.

Arumugam, S. (2004). Nitrogen oxides emission control through reburning with biomass in coal-fired power plants. MS Thesis. Texas A&M University: College Station, Texas.

Arumugam, S., Annamalai, K., Thien, B., and Sweeten, J. M. (2005). Feedlot biomass co-firing: a renewable energy alternative for coal-fired utilities. *International Journal of Green Energy* 2: 409-419.

ASAE. (2005). Manure production and characteristics: ASAE standard. American Society of Agricultural Engineers. ASAE D384.2 MAR2005.

Associated Press. (2007). Texas plant uses dairy waste to make natural gas. By Brown, A. K., Associated Press Writer. The Associated Press State and Local Wire, Business News Section, November 5, 2007.

Biewald B, Cavicchi J, Woolf T, Allen D. (2000). Use of selective catalytic reduction for control of NO_x emissions from power plants in the US. Prepared for the OntAlRio Campaign.

Bohnhoff D. R. and Converse J. C. (1987). Engineering properties of separated manure solids. *Biological Wastes* 19: 91-106.

Brammer J.G. and Bridgwater A.V. (1999). Drying technologies for an integrated gasification bio-energy plant. *Renewable and Sustainable Energy Reviews* 3: 243-89.

Brammer J.G. and Bridgwater A. V. (2002). The influence of feedstock drying on the performance and economics of a biomass gasifier-engine CHP system. *Biomass & Bioenergy* 22: 271-81.

Brown W. K. and Wohletz K. H. (1995). Derivation of the Weibull distribution based on physical principles and its connection to the Rosin-Rammler and lognormal distributions. *Journal of Applied Physics* 78(4): 2758-2763.

Caldwell E. (2008). Roast your compost: EcoCombustion Energy Systems Corporation has commercialized a manure-burning system dubbed Elimanure. *Ag Nutrient Management* Magazine by Progressive Dairy Publishing. August 2008.

Canales E. R., Borquez R. M. and Melo D. L. (2001). Steady state modeling and simulation of an indirect rotary dryer. *Food Control* 12: 77-83.

Carlin, N. T. (2005). Thermo-chemical conversion of dairy waste based biomass through direct firing. MS Thesis. Texas A&M University: College Station, Texas.

Carlin, N., Annamalai, K., Sweeten, J., and Mukhtar, S. (2007a). Thermo-chemical conversion analysis on dairy manure-based biomass through direct combustion. *International Journal of Green Energy* 4(2): 133-159.

Carlin, N., Annamalai, K., Sweeten, J. M., and Mukhtar,S. (2007b). Utilization of latent heat derived from vaporized wastewater in high moisture dairy manure combustion schemes. International Symposium on Air Quality and Waste Management for Agriculture, September 15-19, 2007: Broomfield, Colorado.

Carlin NT, Annamalai K, Oh H, Gordillo Ariza G, Lawrence B, et al. (2008). Co-combustion and gasification of coal and cattle biomass: a review of research and experimentation. Submitted to *Progress in Green Energy* on December 2007, Accepted and Revised on January 2008.

CDFA. (2006). California dairy facts. California Dairy Research Foundation of the California Department of Food and Agriculture. Available online at: http://www.cdrf.org. (Accessed on November 2007).

Centner, T. J. (2004). *Empty pastures: confined animals and the transformation of the rural landscape*. Urbana and Chicago, Illinois: University of Illinois Press.

Chang, F. H. (2004). Energy and sustainability comparisons of anaerobic digestion and thermal technologies for processing animal waste. 2004 ASAE/CSAE Annual International Meeting, Fairmont Chateau Laurier, The Westin Government Centre, Ottawa, Ontario, Canada, August 1-4, 2004.

Chen Y. R. (1982). Engineering properties of beef cattle manure. 1982 Summer Meeting of the ASAE at the University of Wisconsin-Madison, June 27-30. Paper No. 82-4085. ISSN: 0149-9890.

Chen Y. R. (1983). Thermal properties of beef cattle manure. *Agricultural Wastes* 6: 13-29.

Chen, Y. R., Varel, V. H., and Hashimoto, A. G. (1980). Chemicals from cellulosic materials. *Ind. & Eng. Chem. Prod. Res. and Dev*. 19: 471-477.

Colmegna G., K. Annamalai, and Udayasarathy A.V. (2007). Modeling of Hg reduction during reburn process with the use of cattle biomass as a reburn fuel. Third International Green Energy Conference (IGEC-III), June 17-21, Västerås, Sweden.

Conn R. E., J. Shan, and J. Vatsky. (2005). Low NO_x combustion systems for minimizing NO_x and fly ash LOI: wall-firing petcoke and T-firing severe slagging coal.

NETL of the DOE. 2005 Proceedings. Available online at: http://www.netl.doe.gov/publications/proceedings/05/UBC/pdf/Conn_paper.pdf. (Accessed on August 2006).

Di Nola, G. (2007). Biomass fuel characterization for NO_x emissions in co-firing applications. Doctoral Thesis. Delft University of Technology: Delft, The Netherlands. Available online at: http://repository.tudelft.nl/file/521100/372250. (Accessed on November 2007).

DOE. (1999). Clean coal technology: reburning technologies for the control of nitrogen oxides emissions from coal-fired boilers. United States Department of Energy Topical Report Number 14. Available online at: http://www.fossil.energy.gov/programs/powersystems/publications. (Accessed on October 2007)

DOE. (2004). Biomass co-firing in coal-fired boilers, federal technology alert: A new technology demonstration publication. Federal Energy Management Program (FEMP) of the United States Department of Energy. Paper No. DOE/EE-0288. Available online at: http://www1.eere.energy.gov/femp/pdfs/fta_biomass_cofiring.pdf. (Accessed on December 2008)

DPI&F. (2003). Feedlot waste management series: manure production data. Department of Primary Industries and Fisheries. Government of Queensland, Australia. Available online at: http://www.dpi.qld.gov.au/environment/5166.html. (Accessed on September 2005).

ECN. (2003). Phyllis: the composition of biomass and waste. Energy Research Centre of the Netherlands. Available online at: http://www.ecn.nl/phyllis/. Last updated in May 2003. (Accessed on January 2009).

EIA. (2005). Annual coal report: 2004. Energy Information Administration of the US Department of Energy. Available online at: http://tonto.eia.doe.gov/FTPROOT/coal/05842004.pdf. (Accessed on February 2009).

EIA. (2006). U.S. coal consumption by end use sector, by census division and state, Average price of coal delivered to end use sector by census division and state, receipts and Quality of coal by rank delivered for electricity generation. Energy Information Administration of the US Department of Energy. Available online at: http://www.eia.doe.gov/cneaf/coal/page/acr/table26.html, http://www.eia.doe.gov/cneaf/coal/page/acr/table34.html, and http://www.eia.doe.gov/cneaf/electricity/epm/table4_15.html. (Accessed on February 2009).

EIA. (2007a). US carbon dioxide emissions from energy sources 2006 flash estimate. Energy Information Administration. Available online at: http://www.eia.doe.gov. (Accessed on February 2009).

EIA. (2007b). Natural gas: US price data. Energy Information Administration of the US Department of Energy. Available online at: http://www.eia.doe.gov/oil_gas/natural_gas/info_glance/natural_gas.html. (Accessed on February 2009).

EIA. (2007c). Emissions from energy consumption at conventional power plants and combined-heat-and-power plants. Energy Information Administration of the US Department of Energy. Available online at: http://www.eia.doe.gov/cneaf/electricity/epa/epat5p1.html. (Accessed on February 2009).

EIA. (2007d). Average price of coal delivered to end use sector by census division and state: US price data. Energy Information Administration of the US Department of Energy. Available online at: http://www.eia.doe.gov/cneaf/coal/page/acr/table34.html. (Accessed on February 2009)

EIA. (2007e). Average retail price of electricity to ultimate customers: total by end-use sector: US price data. Energy Information Administration of the US Department of Energy. Available online at: http://www.eia.doe.gov/cneaf/electricity/epm/table5_3.html. (Accessed on February 2009).

Electric Power Daily. (2005). "American Electric Power (AEP), nations largest electric generator and coal user, exploring the possibility of reducing CO_2 by burning biomass." 24 May 2005.

Elliot D. C., Sealock Jr. L. J., Baker E. G. (1997). Method for the catalytic conversion of organic materials into a product gas. US Patent Number 5,616,154.

Elliot D. C., Neuenschwander G. G., Hart T. R., Butner R. S., Zacher A. H., Engelhard M. H., et al. (2004). Chemical processing in high-pressure aqueous environments. 7. Process development for catalytic gasification of wet biomass feedstocks. *Ind. Eng. Chem. Res.* 43: 1999-2004.

Engineeringtoolbox.com. (2008). Material properties - density, heat capacity, viscosity and more - for gases, fluids and solids. Available online at: http://www.engineeringtoolbox.com/material-properties-t_24.html. (Accessed on March 2009).

Ergun S. (1952). Fluid flow through packed columns. *Chemical Engineering Progress* 68: 89.

FactoryFarm.org. (2007). Archived pictures. Available online at: http://www.factoryfarm.org/home.php. (Accessed on January 2009).

Frazzitta, S., Annamalai, K., and Sweeten, J. M. (1999). Performance of a burner with coal and coal:feedlot manure blends. *Journal of Propulsion and Power* 15: 181-186.

Friedman S. J. and Marshall, Jr. W. R. (1949). Studies in rotary drying: Part I – Holdup and dusting. *Chemical Engineering Progress* 45(8): 482-573.

Froley A. (2007). "UK generator Drax aims to have 10% biomass co-firing at a 4,000 MW plant in Yorkshire by 2009." *Platts International Coal Report*. 12 March 2007.

Ghaly, A. E. (1996). A comparative study of anaerobic digestion of acid cheese whey and dairy manure in a two-stage reactor. *Bioresource Technology* 58: 61-72.

Global Energy Decisions. (2006). Coal view interactive: short-term forecast for 16 coals. Available online at: http://www.globalenergy.com. (Accessed on November 2007).

Goodrich L. B., Mukhtar S., Capareda S., Harman W. (2007). Characterization and transportation analysis of dairy biomass for co-firing in coal-fired power plants. Texas A&M University. Unpublished paper.

Goodrich, P. R., Schmidt, D., and Haubenschild, D. (2005). Anaerobic digestion for energy and pollution control. *Agricultural Engineering International*: the CIGR Ejournal. Manuscript EE 03 001, Volume VII.

Gordillo, G., Annamalai, K., and Arcot V, U. (2008). Gasification of coal and animal waste using an air-steam mixture as oxidizing agent. 19th National and 8th ISHMT-ASME, Heat and Mass Transfer Conference, January 3-5, JNTU Hyderabad, India.

Gregory M. W. (1993). Wastewater evaporation system. US Patent No. 5,240,560.

GSNet.com. (2007). The largest source of machinery listings online. Available online at: http://www.gsnet.com. (Accessed on November 2007).

Harman, W. L. (2004). Pen cleaning costs for dust control, Southern Great Plains feedlots. Texas Agricultural Experiment Station, Texas A&M University, Blackland Research Center Report No. 04-01.

He B. J., Zhang Y., Yin Y., Funk T. L., and Riskowski G.L. (2000). Operating temperature and retention time effects on the thermochemical conversion process of swine manure. *Transactions of the ASAE* 43(6): 1821-1825.

Heflin K. (2008). Personal contact. Extension Associate. Texas AgriLife Extension Service, Amarillo and Bushland, Texas.

Hinds W. C. (1999). *Aerosol technology: properties, behavior, and measurement of airborne particles, second edition*. New York: John Wiley & Sons, Inc.

Hobbs M. L., Predrant T., Radulovic, and Douglas Smoot L. (1992). Modeling fixed-bed coal gasifier. *AIChe Journal* 38: 681-702.

Hotchkiss, R. (2003). Coal gasification technologies. Proceedings of the Institution of Mechanical Engineers, Part A, *Journal of Power and Energy* 217(A1): 27-33.

Houkom R. L., Butchbaker A. F., and Brusewitz G. H. (1974). Effect of moisture content on thermal diffusivity of beef manure. *Transactions of the ASABE* 17: 973-977.

Howard-Smith, I. (1976). *Coal conversion technology*. Noyes Data Corporation/Noyes Publications: Park Ridge, New Jersey.

Hughes E. (2000). Biomass co-firing: economics, policy and opportunities. *Biomass & Bioenergy* 19: 457-465.

Ikeguchi A. and Kamo M. (1997).Mass transfer of moisture and ammonia from manure and manure litter mixture in free-stall housing. *Transactions of the ASAE* 40(4): 1191-1197.

Incropera F. P. and D. P. DeWitt. (2002). *Fundamentals of heat and mass transfer, fifth edition*. New York, NY: Wiley & Sons.

Jensen M. D., Timpe R. C., Laumb J. D. (2003). Advanced heterogeneous reburn fuel from coal and hog manure. Final report to the US Department of Energy – National Energy Technology Laboratory (DOE-NETL). Award No. DE-FG26-02NT41551.

Kamen D., Demers J. A., and Owens K. (2008). Locally powered water distillation system. US Patent No. 7,340,879 B2.

Kays W., Crawford M., and Weigand B. (2005). *Convective heat and mass transfer, fourth edition, international edition*. New York, NY: McGraw-Hill.

Keplinger, K., Tanter, A., and Hauck L. (2004). Manure transportation and application: model development and a general application. Texas Institute for Applied Environmental Research (TiAER), Tarleton State University: Stephenville, TX. Available online at: http://www.tiaer.tarleton.edu. (Accessed on October 2007).

Kiranoudis C. T., Maroulis Z. B., and Marinos-Kouris D. (1992). Model selection in air drying of foods. *Drying Technology* 10(4): 1097-1106.

Kiranoudis C. T., Maroulis Z. B., Tsami E., and Marinos-Kouris D. (1993). Equilibrium moisture content and heat of desorption of some vegetables. *Journal of Food Engineering* 20: 55-74.

Kiranoudis C. T., Maroulis Z. B., Marinos-Kouris D. (1994). Modeling and design of conveyor belt dryers. *Journal of Food Engineering* 23: 375-96.

Kohl, A. and Riesenfeld, F. (1974). *Gas purification, 2nd edition*. Houston, Texas: Gulf Publishing Co.

Kolber, S. N. (2001). Treatment of waste produced by farm animals raised under confined conditions. United States Patent #6,190,566.

Krich, K., Augenstein, D., Batmale, J. P., Benemann, J., Rutledge, B., Salour, D. (2005). Biomethane from dairy waste: a sourcebook for the production and use of renewable natural gas in California. Prepared for The Western United Dairymen, Funded in part through USDA Rural Development.

Krishnan R. and Tarabulski T. J. (2005). Economics of emission reduction for heavy duty trucks. DieselNet Technical Report. Available online at: http://www.dieselnet.com/papers/0501krishnan/. (Accessed on October 2007).

Lawrence, B. D. (2007). Co-firing of coal and dairy biomass in a 100,000 Btu/hr furnace. MS Thesis. Texas A&M University: College Station, Texas.

Lissianski, V. V., Zamansky, V. M., and Maly, P.M. (2001). Effect of metal-containing additives on NOx reduction in combustion and reburning. *Combustion and Flame* 125(3): 1118-1127.

Li Z. Q., Chen Z. C., Sun R., and Wu S. H. (2007). New low NO_x, low grade coal fired swirl stabilized technology. *Journal of the Energy Institute* 80(3): 123-130.

Maly, P. M., Zamansky, V. M., Ho, L., and Payne, R. (1999). Alternative fuel reburning. *Fuel* 78: 327-334.

Martin, B., Annamalai, K., Sweeten, J. M., and Heflin, K. (2006). Pyrolysis, ignition, and fuel characteristics of coal, feedlot biomass, and coal:feedlot biomass blends. Submitted to the Texas Commission on Environmental Quality.

Matthews, M. C., G. Carpenter, L. Cooperband, W. A. Darling, N. DeBoom, et al. 2003. Strategies for increasing implementation and fostering innovation in dairy manure management. National Dairy Environmental Stewardship Council. Available online at: http://www.suscon.org/dairies/ndesc.asp. (Accessed on June 2005).

McFarland, A. and Millican, J. (2006). Assessment of preexisting and post-implementation effects for the North Bosque River Watershed: Clean Water Act section 319 report. Texas Institute for Applied Environmental Research (TiAER), Tarleton State University: Stephenville, TX. Available online at: http://www.tiaer.tarleton.edu. (Accessed on November 2007).

Megel A. J., Parker D. B., Mitra R., Sweeten J. M. (2006). Assessment of chemical and physical characteristics of bottom, cyclone, and baghouse ashes from combustion of manure. Presented at the ASABE Annual Meeting, Portland, Oregon, June 2006.

Megel, A. J., DeOtte, R. E., and Robinson, C. A. (2007). Investigation of economically viable coproducts developed from ash from the combustion of manure. 2007 ASABE Annual International Meeting, Minneapolis Convention Center, Minneapolis, Minnesota, June 17-20, 2007.

Meyer, D. (2003). Digesters on the farm: making electricity from manure. *BioCycle: Journal of Composting & Organics Recycling* 44(1): 52-55.

Meyer D., Ristow P. L., and Lie M. (2007). Particle size and nutrient distribution in fresh dairy manure. *Applied Engineering in Agriculture* 23(1): 113-117.

Mining Engineering. (2001). Clean coal technology project cuts NO_x emissions. *Mining Engineering* 53(2): 24-25.

Mohsenin N. N. (1980). Thermal conductivity, diffusivity, and unit surface conductance of foods and agricultural materials. In *Thermal properties of foods and agricultural materials*, pg. 188-189. London: CRC, Gordon and Breach.

Monnet, F. (2003). An introduction to anaerobic digestion of organic wastes: final report. Remade Scotland. Available online at: http://www.remade.org.uk/Organics/organics_documents/IntroAnaerobicDigestion.pdf. (Accessed on October 2005).

Montone Trailers, LLC., (2008). 44 cubic yard dump trailer. Montone Trailers, LLC.: Dillon, South Carolina. Available online at: http://www.montonetrailers.com/home.html. (Accessed on Februrary 2009).

Mooney, R., Mooney, D., and Latulippe, D. (2005). Method and apparatus for the gasification and combustion of animal waste, human waste, and/or biomass using a moving grate over a stationary perforated plate in a configured chamber. United States Patent #6,948,436 B2.

Mou C. and Qvale, B. (2002). The consequences of unpredictable development of economic conditions on heat exchanger network configurations and economic results. *Energy Conversion and Management* 43: 1549-1562.

Mukhtar, S. (1999). Proper lagoon management to reduce odor and excessive sludge accumulation. Texas A&M University, Texas Agricultural Extension Service. Available at: http://tammi.tamu.edu/pdf%20pubs/lagoonmanagement.pdf. (Accessed on October 2005).

Mukhtar S., Goodrich B., Engler C., and Capareda S. (2008). Dairy biomass as a renewable fuel source. AgriLife Extension, Texas A&M System, L-5494, 02-08.

Mussatti D. C., R. Srivastava, P. M. Hemmer, and R. Strait. (2000a). EPA Air Pollution Control Cost Manual – Sixth Edition. Section 4, Chapter 1, Selective Non Catalytic Reduction. Available online at: http://www.epa.gov/ttn/catc/products.html. Scroll down to "EPA Air Pollution Control Cost Manual Chapters & Information". (Accessed on June 2006).

Mussatti D. C., R. Srivastava, P. M. Hemmer, and R. Strait. (2000b). EPA Air Pollution Control Cost Manual – Sixth Edition. Section 4, Chapter 2, Selective Catalytic Reduction. Available online at: http://www.epa.gov/ttn/catc/products.html. Scroll down to "EPA Air Pollution Control Cost Manual Chapters & Information". (Accessed on June 2006).

NASS. (2007). Farms, land in farms, and livestock operations: 2006 summary. National Agricultural Statistics Service of the United States Department of Agriculture. Available online at: http://usda.mannlib.cornell.edu/usda/nass/FarmLandIn//2000s/2007/FarmLandIn-02-02-2007.pdf. (Accessed on January 2009).

NASS. (2008). Farms, land in farms, and livestock operations: 2007 summary. National Agricultural Statistics Service of the United States Department of Agriculture. Available online at: http://usda.mannlib.cornell.edu/usda/nass/FarmLandIn//2000s/2008/FarmLandIn-02-01-2008_revision.pdf. (Accessed on January 2009).

NASS Census. (2002). The census of agriculture: 2002 census publications. Available online at: http://www.agcensus.usda.gov/Publications/2002/index.asp#.html. (Accessed on January 2009).

NERA. (2004). TXU activities regarding actual and potential US air emissions and climate changing policies, a white paper for TXU. Prepared by NERA Economic Consulting in collaboration with Marc Goldsmith & Associates LLC.

Newnan D. G., Lavelle J. P., and Eschenbach T. G. (2000). *Engineering economic analysis. 8th ed*. Austin, Texas: Engineering Press.

Nowacki, P. (1981). *Coal gasification processes*. Park Ridge, New Jersey: Noyes Data Corporation.

Oh, H. (2008). Reburning renewable biomass for emissions control and ash deposition effects in power generation. Ph.D. Dissertation. Texas A&M University: College Station, Texas.

Oh, H., Annamalai, K., and Sweeten, J. M. (2007). Investigations of ash fouling with cattle wastes as reburn fuel in a small boiler burner under transient conditions. Submitted to the *Journal of Air and Waste Management Association* on March 14.

Osei, E., Gassman, P. W., Jones, R. D., Pratt, S. J., Hauck, L. M., et al. (2000). Economic and environmental impacts of alternative practices on dairy farms in an agricultural watershed. *Journal of Soil and Water Conservation* 55(4): 466-472.

Pacala, S. and Socolow R. (2004). Stabilization wedges: solving the climate problem for the next 50 years with current technologies. *Science Magazine* 305: 968-972.

Pakowski Z., Bartczak Z., Strumillo C., and Stenstrom S. (1991). Evaluation of equations approximating thermodynamic and transport properties of water, steam and air for use in CAD of drying processes. *Drying Technology* 9(3): 753-773.

Panda Ethanol Inc. (2007). Manure gasification: using renewable fuel to create renewable fuel. Available online at: http://pandaethanol.com/gas/index.html. (Accessed on November 2007).

Peterbilt.com. (2009). Trucks by Peterbilt: a PACCAR Company. Company headquarters in Denton, Texas. More information online at: http://www.peterbilt.com/showroom.aspx. (Accessed on February 2009).

Priyadarsan, S. (2002). Fixed bed gasification studies on coal-feedlot biomass and coal-chicken litter biomass under batch mode operation. MS Thesis. Texas A&M University: College Station, Texas.

Priyadarsan, S., Annamalai, K., Sweeten, J., and Holtzapple, M. (2005a). Co-gasification of blended coal with feedlot and chicken litter biomass. *Proceedings of the Combustion Institute* 30: 2973-2980.

Priyadarsan, S., Annamalai, K., Thien, B., Sweeten, J. M., and Mukhtar, S. (2005b). Animal waste as a source of renewable energy. In *Agriculture as a producer and consumer of energy*. Edited by Outlaw, J *et al*. CABI Publishing.

Priyadarsan, S., Annamalai, K., Sweeten, J. M., Mukhtar, S., and Holtzapple, M. T. (2005c). Fixed bed gasification of feedlot and poultry litter biomass. *Transactions of the ASAE* 47(5): 1689-1696.

Probstein, R. F. and Hicks, R. E. (2006a). *Synthetic fuels*, Chapter 1: Introduction. Mineola, New York: Dover Publications, Inc.

Probstein, R. F. and Hicks, R. E. (2006b). *Synthetic fuels*, Chapter 4: Gas from coal. Mineola, New York: Dover Publications, Inc.

Probstein, R. F. and Hicks, R. E. (2006c). *Synthetic fuels*, Chapter 8: Biomass conversion. Mineola, New York: Dover Publications, Inc.

Quaak, P., Knoef, H., and Stassen, H. (1999). Energy from biomass: a review of combustion and gasification technologies. World Bank Technical Paper No. 422. Washington, D.C.: The World Bank.

Ramadan M. R. I., El-Sebaii A. A., Aboul-Enein S., and El-Bialy E. (2007). Thermal performance of a packed bed double-pass solar air heater. *Energy* 32: 1524-1535.

Raman, P., Walawender, W. P., Fan, L. T., and Howell, J. A. (1981a). Thermogravimetric analysis of biomass. Devolatilization studies on feedlot manure. *Ind. and Eng. Chem. Process Des. and Dev*. 20: 630-636.

Raman, P., Walawender, W. P., Fan, L. T., and Chang, C. C. (1981b). Mathematical model for the fluid-bed gasification of biomass materials. Application to feedlot manure. *Ind. and Eng. Chem. Process Des. and Dev.* 20: 686-692.

Reisner A. E. (2005). Newspaper coverage of controversies about large-scale swine facilities in rural communities in Illinois. *Journal of Animal Science* 83: 2705-2712.

RGGI. (2008). Regional greenhouse gas initiative: an initiative of the Northeast and Mid-Atlantic states of the US. Information available online at: http://www.rggi.org/home. (Accessed on September 2008).

Ro K. S., Cantrell K., Elliot D., and Hunt P. G. (2007). Catalytic wet gasification of municipal and animal wastes. *Ind. Eng. Chem. Res.* 46: 8839-8845.

Robinson, A. L., Rhodes, J. S., and Keith, D. W. (2003). Assessment of potential carbon dioxide reductions due to biomass-coal cofiring in the United States. *Environmental Science and Technology* 37(22): 5081-89.

Robl T. L. (1997). We are running out of fly ash: the nature of regional supply problems. Prepared for NETL of the DOE. Third Annual Conference on Unburned Carbon on Utility Fly Ash, Available online at: http://www.netl.doe.gov/publications/proceedings/97/97ub/robl.pdf. (Accessed on June 2006).

Rodriguez, P., Annamalai, K., and Sweeten, J. (1998). Effects of drying on heating values of biomass. *Society of Agricultural Transactions* 41: 1083-1087.

Rudiger, H., Kicherer, A., Greul, U., Spliethoff, H., and Hein, K. R. G. (1996). Investigations in combined combustion of biomass and coal in power plant technology. *Energy and Fuels* 10: 789-796.

Rudiger, H., Greul, U., Spliethoff, H., and Hein, K. R. G. (1997). Distribution of fuel nitrogen in pyrolysis products used for reburning. *Fuel* 76(3): 201-205.

Salib, R. and R. Keeth. (2005). Optimization of ammonia source for SCR applications. Washington Group International. Paper No. 46 – poster session. Available online at: http://www.ecctech.com/pdfs/CostAnalyWashGrp.pdf. (Accessed on June 2006).

Sami, M., Annamalai, K., and Wooldridge, M. (2001). Co-firing of coal and biomass fuel blends. *Progress in Energy and Combustion Science* 27: 171-214.

SCAQMD. (2007). Annual RECLAIM audit report for 2005 compliance year. South Coast Air Quality Management District. March 2, 2007 board meeting. Available online at: http://www.aqmd.gov/hb/2007/March/070334a.html. (Accessed on May 2007).

Schmidt, G. H., Van Vleck, L. D., and Hutjens, M. F. (1988). *Principles of dairy science, second edition*, Chapter 27: Dairy cattle housing. Englewood Cliffs, New Jersey: Prentice Hall.

Schonfeld E. (2006). Segway creator unveils his next act: Inventor Dean Kamen wants to put entrepreneurs to work bringing water and electricity to the world's poor. Business 2.0 Magazine and CNNMoney.com. 16 February 2006.

Sekar, R. C., J. E. Parsons, H. J. Herzog, and H. D. Jacoby. (2005). Future carbon regulations and current investments in alternative coal-fired power plant designs. MIT Joint Program on the Science and Policy of Global Change. Report No. 129, December 2005. Available online at: http://mit.edu/globalchange/www/MITJPSPGC_Rpt129.pdf. (Accessed on May 2006).

Shi F., Kojovic T., Esterle J. S., and David D. (2003). An energy-based model for swing hammer mills. *International Journal of Mineral Processing* 71: 147-166.

Simons G. and Zhang, Z. (2003). California continues push for dairy power. *BioCycle* 44(7): 63-64.

Skill Associates. (2005). Elimanure™. Available online at: http://www.burnmanure.com/management/elimanure.html. (Accessed on February 2008).

Smith D. J. (2000). Coal reburning reduces NO_x emissions. *Power Engineering* August 2000: 66-67.

Srivastava, R. K., Hall, R. E., Khan, S., Culligan, K., and Lani, B. W. (2005). Nitrogen oxides emissions control options for coal-fired electric utility boilers. *Journal of Air & Waste Management Association* 55: 1367-1388.

Stokes, S. and M. Gamroth. 1999. Freestall dairy facilities in central Texas. Texas A&M University, Texas Agricultural Extension Service. Available at: http://animalscience.tamu.edu/ansc/publications/dairypubs/l5311-freestalldairies.pdf. (Accessed on October 2005).

Strezov V., Lucas J. A. Evans T. J., and Strezov L. (2004). Effects of heating rate on the thermal properties and devolatilisation of coal. *Journal of Thermal Analysis and Calorimetry* 78:385-397.

Sweeten. J. M. (1990). Cattle feedlot waste management practices for water and air pollution control: water pollution and wastewater management. Texas Agricultural Extension Service, Texas A&M University System. B-1671.

Sweeten, J. M., Annamalai, K., Thien, B., McDonald, L. (2003). Co-firing of coal and cattle feedlot biomass (FB) fuels, Part I: feedlot biomass (cattle manure) fuel quality and characteristics. *Fuel* 82(10): 1167-1182.

Sweeten, J. M. and Heflin, K. (2006). Preliminary interpretation of data from proximate, ultimate and ash analysis, results of June 7, 2006, samples taken from feedlot and dairy biomass biofuel feedstocks at TAES/USDA-ARS, Bushland, TX. Amarillo/Bushland/Etter, TX: Texas A&M Agricultural Research & Extension Center.

Sweeten.J. M., Heflin K., Annamalai K., Auvermann B. W., McCollum F. T., and Parker D. B. (2006). Combustion-fuel properties of manure or compost from paved vs. un-paved cattle feedlots. Presented at the 2006 ASBAE Annual International Meeting, Portland, Oregon.

Sweeten, J. M., Korenberg, J., LePori, W. A., Annamalai, K., Parnell, C. B. (1986). Combustion of cattle feedlot manure for energy production. *Energy in Agriculture* 5: 55-72.

Sweterlitsch, J. J. and Brown, R. C. (2002). Fuel lean biomass reburning in coal-fired boilers. Final technical report to the DOE, Award number DE-FG26-00NT40811. Submitted by the Center for Sustainable Environmental Technologies, Iowa State University.

TAMU. (2006). TAMU Fuel Data Bank. Texas A&M University Coal and Biomass Energy Laboratory. Available online at: http://www1.mengr.tamu.edu/REL/TAMU%20FDB.htm. (Accessed on January 2007).

Thomas N., Lucht, A & R. P., Priyadarsan, S., Annamalai, K., and Caton, J. A. (2006). In situ measurements of nitric oxide in coal-combustion exhaust using a sensor based on a widely-tunable external-cavity GaN diode laser. *Journal of Applied Optics* 46(19): 3946-57.

TNRCC. (2001). Two total maximum daily loads for phosphorus in the North Bosque River: for segments 1226 and 1255. Prepared by the Strategic Assessment Division of the Texas Natural Resource Conservation Commission.

Turner W. C. (2001). *Energy management handbook, fourth edition*. Chapter 4, Economic Analysis. Liburn, GA: The Fairmont Press, Inc.

US Bureau of Labor Statistics. (2008). Producer price indexes: archived producer price index detailed report information. United States Bureau of Labor Statistics of the US Department of Labor. Available online at: http://www.bls.gov/ppi/ppi_dr.htm. (Accessed on November 2008).

USDA. (2003). Manure management for water quality costs to animal feeding operations of applying manure nutrients to land. United States Department of Agriculture. Available online at: http://www.ers.usda.gov/Publications/AER824/. (Accessed on October 2007).

USDA. (2007). Economics, statistics, and market information system. United States Department of Agriculture. Available online at: http://usda.mannlib.cornell.edu/. (Accessed on January 2009).

USDA, Cornell University, and the University of Vermont. (2007). Nitrogen management on dairy farms: types of N in manure. Available online at: http://www.dairyn.cornell.edu/pages/20cropsoil/250credits/251manTypes.shtml. (Accessed on November 2007).

USDOT. (2006). Fly ash facts for highway engineers. US Department of Transportation, Federal Highway Administration. Available online at: http://www.fhwa.dot.gov/pavement/recycling/fach01.cfm. (Accessed on July 2006).

USEPA. (1998). Analyzing electric power generation under the CAAA. Appendix No. 5.

USEPA. (2001). Cost methodology report for beef and dairy animal feeding operations. Engineering and Analysis Division. EPA Contract No. 821-R-01-019. Available online at: http://www.epa.gov/waterscience/guide/cafo/pdf/BDCostReport.pdf. (Accessed on June 2006).

USEPA. (2004). Standalone documentation for EPA base case 2004 (V.2.1.9) using the integrated planning model, chapter 5, emissions control technologies. Clean Air Markets Division. September 2005, EPA Contract No. 430-R-05-011. Available online at: http://www.epa.gov/airmarkets/progsregs/epa-ipm/past-modeling.html. Scroll down to the 2004 update. (Accessed on June 2006).

USEPA. (2006). Documentation for EPA base case 2006 (V.3.0) using the integrated planning model. Clean Air Markets Division of the United States Environmental

Protection Agency, EPA Contract No. 430-R-05-011. Available online at: http://www.epa.gov/airmarkets/progsregs/epa-ipm/. (Accessed on June 2007).

USEPA. (2007a). Integrated planning model. Clean Air Markets Division of the United States Environmental Protection Agency. Available online at: http://www.epa.gov/airmarkt/progsregs/epa-ipm/index.html. Scroll down to about two-thirds of the page to National Electric Energy Data System (NEEDS) 2006. Download Microsoft Excel Spreadsheet database file. (Accessed on June 2007).

USEPA. (2007b). Guide to operational systems: U.S. operating digesters by state. The AgSTAR program. United States Environmental Protection Agency. Last update November 2. Available online at: http://epa.gov/agstar/operation/bystate.html. (Accessed on November 2007).

USEPA. (2007c). EPA's updates to EPA base case v3.01 from EPA base case 2006 (v3.0) using the integrated planning model (IPM). Carbon assumption enhancements. Available online at: http://www.epa.gov/airmarkets/progsregs/epa-ipm/. Scroll down to "Documentation Supplement for EPA's Base Case (v3.01)". (Accessed on June 2007).

Virtus Energy Research Associates. (1995). Texas renewable energy resource assessment: survey, overview, and recommendations. Report for the Texas Sustainable Energy Development Council; July 1995. Available online at: http://www.infinitepower.org/pdf/re_study1995.pdf. (Big file, 50+ MB). (Accessed on July 2006).

Waterloo Courier. (2007). "LS Power seeking approval of 750 MW plant." 17 February 2007. Waterloo, IA: Courier Communications, a subsidiary of Lee Enterprises.

Weinheimer B. (2008). Texas cattle feeders association manure value calculator. Available online at: http://www.tcfa.org/forms/ManureVsFert/manure_value_calculator.html. (Accessed on December 2008).

Wen, Z., Frear, C., and Chen, S. (2007). Anaerobic digestion of liquid dairy manure using a sequential continuous-stirred tank reactor system. *Journal of Chemical Technology & Biotechnology* 82: 758-766.

Western Region Ash Group. (2006). Coal fired plants in the western USA. Available online at: http://www.wrashg.org/coalplant.htm. (Accessed on July 2006).

Yang, Y. B., Naja, T. A., Gibbs, B. M., and Hampartsoumian, E. (1997). Optimisation of operating parameters for NO reduction by coal reburning in a 0.2 MWt furnace. *Journal of the Institute of Energy* 70: 9-16.

Young, L. and Pian, C. C. P. (2003). High-temperature, air-blown gasification of dairy-farm wastes for energy production. *Energy* 28: 655-672.

Zamansky, V. M., Sheldon, M. S., Lissianski, V. V., Maly, P. M., Moyeda, D. K., et al. (2000). Advanced biomass reburning for high efficiency NOx control and biomass reburning – modeling/engineering studies. USDA Phase II SBIR, Contract #97-33610-4470 and DOE-NETL, Contract #DE-FC26-97FT-97270. Available online at: http://www.osti.gov/bridge/servlets/purl/786516-Dddr9I/native/786516.pdf. (Accessed on May 2006).

APPENDIX A

NOMENCLATURES

a	Height of drying chamber	m
A	Area	m^2
$\%A$	Ash percentage	%
A_{MBB}	Wetted surface area of MBB particles	m^2/m^3
$a_{t,0}$	Application thickness at conveyor belt entrance	m
B	Transfer number or mass transfer driving force	-
c	Specific heat	kJ/kg K
$\overline{c}$	Specific heat on a mole basis	kJ/kmol K
C	Carbon	kmol/100 kg of as received fuel
ccr	Capital charge rate	%
C_D	Drag coefficient	-
$\%CF$	Capacity factor, fraction of power plant's electrical production capacity	%
C_{truck}	Hauling capacity per truck	kg/truck
CV	Control volume	-
d	Diameter	m
D	Inner diameter of rotary dryer's drum	m
$\mathscr{D}$	Deprecation	$
$\mathscr{D}$	Mass diffusion coefficient	m^2/s
$\hat{D}$	Average distance between power plant and animal feeding operations	km
DAF_k	Dry-ash free fraction of species k	kg k/kg of dry ash free fuel
d_c	Characteristic dimension or particle size	m
d_{mm}	Mass mean diameter	m
d_p	Particle size	m
DR	Discount rate	%
DR^*	Non-inflated (real) discount rate	%
$\dot{E}$	Electricity consumption	kW_e
$\mathscr{E}$	Emission	metric tons/year or metric tons/hour
$\%EA$	Excess air percentage	%
EI	Emission index	g/kg fuel
ER	Equivalence ratio: >1 indicates fuel rich, <1 indicates fuel lean, =1 indicates stoichiometric mixture of fuel and combustion air	-
f	Inflation rate	%
f'	Friction factor	-

$\dot{F}$	Fueling rate	kJ/s
$\%FA$	Percentage of solid byproduct of combustion that is fly ash	%
$\%FC$	Fixed carbon percentage	%
$\dot{F}_{MBB}$	Volumetric feed rate of manure-based biomass	m^3/s per m^2 of dryer cross section
$FO\&M$	Fixed operation and maintenance	-
$\%FS$	Fixed solids percentage	%
g	Mass transfer conductance coefficient	kg/m^2 s
g^*	Mass transfer conductance for a small transfer rate	kg/m^2 s
$\overline{g}$	Gibbs free energy	kJ/kmol
g_c	Gravitational acceleration constant, 9.81	m/s^2
h	Enthalpy	kJ/kg
h	Convective heat transfer coefficient	W/m^2 k
$\overline{h}$	Enthalpy on molar basis	kJ/kmol
H	Hydrogen	kmol/100 kg of as received fuel
$\mathcal{H}$	Power plant heat rate	kJ_{th}/kWh_e
hf	Heat fraction	-
HHV	Higher (gross) heat value	kJ/kg
HS	Hauling schedule	hour/day
$\overline{j}_m$	Colburn j factor for mass transfer	-
k	Thermal conductivity	W/m K
K	Equilibrium constant	-
k_m	Empirical drying constant	1/s
l	Length	m
$\%L$	Load factor of haling vehicle	%
$\mathcal{L}$	Emission level	kg/GJ or g/GJ
m	Mass flow	kg/100 kg of as received fuel
$\dot{m}$	Time rate of mass flow	kg/s
$\%M$	Moisture percentage	%
$\dot{M}$	Annual mass requirement	kg/year
mf	Mass fraction on a wet basis	kg/kg total mass
MW	Molecular weight	kg/kmol
n	Indication of the project year or the project year	-
N	Number	-
N	Nitrogen	kmol/100 kg of as received fuel
N_{drum}	Angular velocity of rotary dryer's drum	rpm
n_k	Number of kmoles of species k in producer gas	kmol/100 kg as received fuel
N_k	Number of kmoles of species k	kmol/100 kg of as

		received fuel
NPC	Net present cost, negative net present worth	$\$_{present}$
NPV	Net present value, positive net present worth	$\$_{present}$
NPW	Net present worth	$\$_{present}$
n_{tubes}	Number of steam tubes in rotary dryer	-
Nu	Nusselt number	-
O	Oxygen	kmol/100 kg of as received fuel
O&M	Operation and maintenance	-
OH	Annual operation hours	hour/year
P	Pressure	Pa
$\mathscr{P}$	Electric capacity of power plant	MW_e
ppm	Parts per million	-
Pr	Prandtl number	-
Q	Heat transfer	kJ/100 kg as received fuel
$\dot{Q}$	Time rate of heat transfer	kJ/s
R	Drying rate	kg water/kg biomass/s
$\bar{R}$	Ideal gas constant, 8.314	kJ/kmol K
$\mathscr{R}$	Emission reduction	metric ton/year
$\%\mathscr{R}$	Emission reduction percentage	%
$r_{\mathscr{D}}$	Depreciation rate	%
Re	Reynolds number	-
ROR	Rate of return	-
$\hat{s}$	Average truck speed	km/hr
S	Sulfur	kmol/100 kg of as received fuel
SAR	Steam-air ratio	-
Sc	Schmidt number	-
SCR	Selective catalytic reduction	-
S_D	Diagonal spacing between steam tubes	m
Sh	Sherwood number	-
S_L	Spacing between steam tubes in inner ring	m
SNCR	Selective non-catalytic reduction	-
S_T	Spacing between inner ring and outer ring	m
St_m	Mass transfer Stanton number	-
t	Time	s
T	Temperature	K
U	Velocity	m/s
U_{HX}	Overall heat transfer coefficient	kJ/s m^2 K
V	Velocity	m/s
$\mathscr{V}$	Volume	m^3

$V_{MBB,t}$	Terminal velocity of MBB particle	m/s
$VO\&M$	Variable operation and maintenance	-
$\%VS$	Volatile solids percentage	%
w	Width	m
y	Mole fraction	kmol of species/total kmol
Y	Mole fraction	-
z	Axial coordinate of rotary dryer	m
z'	Transition point from heating zone to drying zone in rotary dryer	m

Greek Symbols

α	Capital cost of primary NO_x control for 300 MW_e power plant	$/kW$_e$
α	Thermal diffusivity	m^2/s
α	Tilt angle of rotary drum	radians or degrees
β	Fixed O&M cost of primary NO_x control for 300 MW_e power plant	$/kW$_e$ year
γ	Variable O&M cost of primary NO_x control for 300 MW_e power plant	$/kWh$_e$
δ	Capital cost of secondary NO_x control for 300 MW_e power plant	$/kW$_e$
Δ	Indicates a change of a parameter	-
ε	Fixed O&M cost of secondary NO_x control for 300 MW_e power plant	$/kW$_e$ year
ε	Porosity or void volume divided by the volume of the bulk solid	-
ε_{price}	Price escalation rate	-
ζ	Variable O&M cost of primary NO_x control for 300 MW_e power plant	$/kWh$_e$
η	Reburn system capital cost	$/kW$_e$
η_{boiler}	Boiler efficiency	-
$\eta_{disposal}$	Disposal efficiency	-
η_{plant}	Power plant efficiency	-
θ	Fixed O&M cost of co-firing or reburning	$/kW$_e$ year
θ	Volumetric moisture content	-
κ	Location of inner ring of steam tubes as a fraction of the drum's radius	-
λ	Location of outer ring of steam tubes as a fraction of the drum's radius	-
μ	Viscosity	kg/m s
ν	Stoichiometric amount of species in chemical balance equation	kmol
ξ	Empirical constant for holdup equation	-

π	Pi: the ratio of a circle's circumference to its diameter, 3.14	-
ρ	Density	kg/m^3
ρ'	Application load on conveyor belt	kg/m^2
ϕ	Relative humidity	-
χ	Holdup: fraction of drum's volume full of biomass	-
ψ	Sphericity factor: =1 when a perfect sphere	-
ω	Moisture content on a dry basis	kg/kg dry matter

Subscripts

0	Initial or ambient point
∞	Indication of the free stream flow, usually for air
a	Pertaining to air, especially at the exit of the drying chamber
ac	Pertaining to the air entering the drying chamber
air	Pertaining to air
am	Pertaining to the mixture of ambient air and recycled air
annum	Value of the parameter for the entire year
ash	Pertaining to ash content in fuel
atm	Atmospheric
belt	Pertaining to a dryer's conveyor belt
blend	Pertaining to the fuel blend of coal and biomass or biomass and extra fuel
boiler	Pertaining to the boiler in the drying system or in the small-scale combustion system
bottom	Pertaining to bottom ash
capacity	Maximum value of a parameter, especially for dryers and trucks
chamber	Pertaining to the drying chamber
coal	Pertaining to the coal burned in the primary burn zone
co-fire	Pertaining to the emission level during co-firing
comb	Combustion
d_c	Pertaining to the characteristic length of a particle
diesel	Pertaining to the diesel consumption of the hauling vehicles
dry	Parameter on a dry basis
dryer	Pertaining to the dryer or the drying system
E	Equilibrium point
EF	Extra fuel
f	Indication of enthalpy of formation
fans	Pertaining to the fans or blower of the dryers
FC	Fixed carbon content in fuel
fg	Indication of the latent heat of vaporization
flame	Pertaining to the flame temperature
fly	Pertaining to fly ash
fuel	Pertaining to the fueling of dryers and hauling vehicles
fw	Feed water
g	Indication of the saturation point or pertaining to the gas phase

(g)	Gas phase
gasifier	Pertaining to the gasifier
H_2O	Water or liquid moisture in fuel
HX	Pertaining to the heat exchanger
i	Indication of a geometric point in a diagram or a system
j-v	Interaction between the steam jacket and entrained vapor of rotary dryer
k	Indication of species in chemical reaction or chemical balance equation
l	Pertaining to the length of a conveyor belt
(l)	Liquid phase
load	Pertaining to the loading of biomass into the hauling vehicles
MBB	Pertaining to manure-based biomass
MBB-v	Interaction between the biomass and the entrained vapor in rotary dryer
p	Constant pressure
p	Particle
PF	Primary fuel
plant	Pertaining to the power plant
primary	Pertaining to the emission level achieved by primary controls
reburn	Pertaining to the emission level achieved by reburning
ref	Reference
RF	Reburn fuel
s	Indication of a point very near the surface of a particle
sat	Saturation
SCR	Pertaining to the emission level achieved by using SCR
SNCR	Pertaining to the emission level achieved by using SNCR
st	Saturation point, steam, liquid or saturated mixture
stack	Pertaining to the stack temperature
standard	Pertaining to a standard emission level or measuring point
steam	Pertaining to steam
t	Indication of thermal enthalpy
trip	Pertaining to the trips or the time spent hauling biomass to power plants
trucks	Pertaining to hauling vehicles
tubes	Pertaining to the steam tubes in the rotary dryer
t-v	Interaction between the steam tubes and entrained vapor in rotary dryer
uncontrolled	Pertaining to the uncontrolled emission level
unload	Pertaining to the unloading of biomass into the hauling vehicles
vapor	Pertaining to the entrained vapor in the rotary dryer
VS	Volatile solids content in fuel
w	Water or liquid moisture
wb	Wet bulb
ww	Wastewater

APPENDIX B

SOME HELPFUL EQUATIONS FOR MODELING THE PROPERTIES OF AIR WATER AND STEAM IN BOILING AND DRYING PROCESSES

The following equations and algorithms may be helpful for computing properties of air, liquid water, and steam when modeling drying processes and boilers. Most of these equations can be found in a review paper by Pakowski *et al.* (1991), but the equations used for modeling in the present study will be reproduced here. Pakowski *et al.* also presented alternative equations for the following properties and compared each of them for computing time and accuracy.

The saturation pressure of water or steam can be computed with the Antoine equation.

$$P_g = 133.322 * \exp\left[18.3036 - \frac{3816.44}{(T - 46.13)}\right] \tag{B.1}$$

where P_g is in Pa and the temperature, T, is in degrees K. If the partial pressure of water vapor in air is required, then T will be the dry-bulb air temperature, T_a, and P_g will be multiplied by the relative humidity of the moist air, ϕ_a. However, if saturated steam is being produced in a boiler, and the pressure is known, then equation (B.1) may be solved for T to compute the saturation temperature of the steam, T_{st}.

The latent heat of vaporization of water can be computed in terms of T_{st} with the following 5th order polynomial equation.

$$\begin{aligned}\Delta h_{H_2O,fg}^{T_{st}} = {} & 2504.65 - 2.80701 * (T_{st} - 273.15) + 1.21884e-2 * (T_{st} - 273.15)^2 \\ & - 1.25205e-4 * (T_{st} - 273.15)^3 + 4.50499e-7 * (T_{st} - 273.15)^4 \\ & - 6.67186e-10 * (T_{st} - 273.15)^5\end{aligned} \tag{B.2}$$

$\Delta h_{H_2O,fg}^{T_{st}}$ is in kJ/kg and T_{st} is in degrees K.

The density of steam or water vapor can be computed with the virial equation, which is a modification of the ideal gas law.

$$\rho_{vapor} = \frac{MW_{H_2O} * P}{\left(\bar{R}T_{vapor} - BP - CP^2\right)} \tag{B.3}$$

where,

$$B = -0.03397 + 55.306\left(\frac{1}{T_{vapor}}\right) * 10^{72000\left(\frac{1}{T_{vapor}}\right)^2}$$

and $C = 343.4493\left(\frac{1}{T_{vapor}^2}\right)B^3$. The molecular weight of water, MW_{H_2O}, is 18.02. ρ_{vapor} is in kg/m^3, P is in kPa, and T_{vapor} is in degrees K. The ideal gas constant, $\bar{R}$ is 8.314 kJ/kmol K.

The specific heat of vapor at low pressures, close to atmospheric pressure, may be computed with the following polynomial equation.

$$\begin{aligned} c_{p,vapor} = {} & 1.883 - 0.1674e-3 * T_{vapor} + 0.8439e-6 * T_{vapor}^2 \\ & - 0.26967e-9 * T_{vapor}^3 \end{aligned} \tag{B.4}$$

$c_{p,vapor}$ is in kJ/kg K and T_{vapor} is in degrees K. This equation is valid for temperatures between 293 and 1473 K.

The enthalpy of saturated steam may be computed with the following 4th order polynomial equation.

$$\begin{aligned} h_{sat\ steam} = {} & 2496.4 + 2.26541 * \left(T_{st} - 273.15\right) - 7.34808e-3 * \left(T_{st} - 273.15\right)^2 \\ & + 3.38602e-5 * \left(T_{st} - 273.15\right)^3 - 8.40676e-8 * \left(T_{st} - 273.15\right)^4 \end{aligned} \tag{B.5}$$

Here, $h_{sat\ steam}$ is in kJ/kg and T_{st} is in degrees K.

The enthalpy of low pressure (near atmospheric pressure), super heated water vapor can be computed from the value of $c_{p,vapor}$ computed in equation (B.4).

$$h_{vapor} = 2501.6 + c_{p,vapor}T_{vapor} \tag{B.6}$$

The viscosity of low pressure superheated water vapor may be computed with the following expression.

$$\mu_{vapor} = \left[263.4511\left(\frac{T_{vapor}}{647.3} - 0.4219836243 \right) + 80.4 \right] * 10^{-7} \tag{B.7}$$

where μ_{vapor} is in N s/m^2 and T_{vapor} is in K.

Moreover, the heat conductivity of low pressure super heated water vapor may be computed with the following equation.

$$\begin{aligned} k_{vapor} = {} & 0.0176 + 5.87e-5 * \left(T_{vapor} - 273.15 \right) + 1.04e-7 * \left(T_{vapor} - 273.15 \right)^2 \\ & - 4.51e-11 * \left(T_{vapor} - 273.15 \right)^3 \end{aligned} \tag{B.8}$$

where k_{vapor} is in W/m K and T_{vapor} is in K. This equation is valid for temperatures between 373 and 973 K.

The density of air can be computed with a similar modification to the ideal gas law as the density of steam.

$$\rho_{air} = \frac{MW_{air} * P}{\left(\bar{R} T_a - BP \right)} \tag{B.9}$$

Here, $B = -0.0407 + 13.116\left(\frac{1}{T_a} \right) + 1.2e+5\left(\frac{1}{T_a^3} \right)$. The molecular weight of air is 28.97, ρ_{air} is in kg/m^3, T_a is in K, and P is in kPa.

Finally, the specific heat of air may be estimated with the following 3rd order polynomial equation.

$$\begin{aligned} c_{p,air} = {} & 1.00926 - 4.04033e-5 * \left(T_a - 273.15 \right) \\ & + 6.17596e-7 * \left(T_a - 273.15 \right)^2 - 4.09723e-10 * \left(T_a - 273.15 \right)^3 \end{aligned} \tag{B.10}$$

$c_{p,air}$ is in kJ/kg K and T_a is in K.

The wet bulb temperature of moist air may be computed with the following algorithm. For a known air temperature (dry-bulb temperature), T_a, and a known relative humidity, ϕ_a, the computation can begin by computing the absolute humidity of the moist air:

$$\omega_a = 0.622 \frac{\phi_a P_g\left(T_a\right)}{P_{atm} - \phi_a P_g\left(T_a\right)}$$

Next, the total enthalpy of the air can be computed:

$$h_a = c_{p,a} T_a + \omega_a \left(h^0_{f,H_2O_{(g)}} + c_{p,H_2O_{(g)}} T_a \right)$$

The wet bulb temperature is the temperature that the air would be if enough moisture was added to the air, adiabatically, to reach the saturation point. Thus, the enthalpy h_a and the enthalpy at the saturation point, h_{sat}, must be equal.

$$h_a = h_{sat}$$

$$c_{p,a} T_a + \omega_a \left(h^0_{f,H_2O_{(g)}} + c_{p,H_2O_{(g)}} T_a \right) = c_{p,a} T_{wb} + \omega_{sat} \left(h^0_{f,H_2O_{(g)}} + c_{p,H_2O_{(g)}} T_{wb} \right) \qquad \text{(B.11)}$$

where,

$$\omega_{sat} = 0.622 \frac{P_g\left(T_{wb}\right)}{P_{atm} - P_g\left(T_{wb}\right)}; \qquad \phi_{sat} = 1$$

The wet bulb temperature, T_{wb}, can be computed by iterating equation (B.11).

APPENDIX C

A FULL SENSITIVITY ANALYSIS OF THE NET PRESENT WORTH OF A MANURE-BASED BIOMASS CO-FIRE SYSTEM

The net present worth (NPW) of a MBB co-fire system installed on an existing 300-MW_e coal-fired power plant was found to be -$22.6 million (i.e. overall net cost). The base case input parameters used to arrive at this NPW are listed in Table 6.3 through Table 6.7. The following graphs are plotted such that the percent difference of the NPW from the base value of -$22.6 million may be read from the vertical axis and the percent difference of each input parameter may be read from the horizontal axis. As each parameter was varied, all other parameters were assumed to remain at their base values.

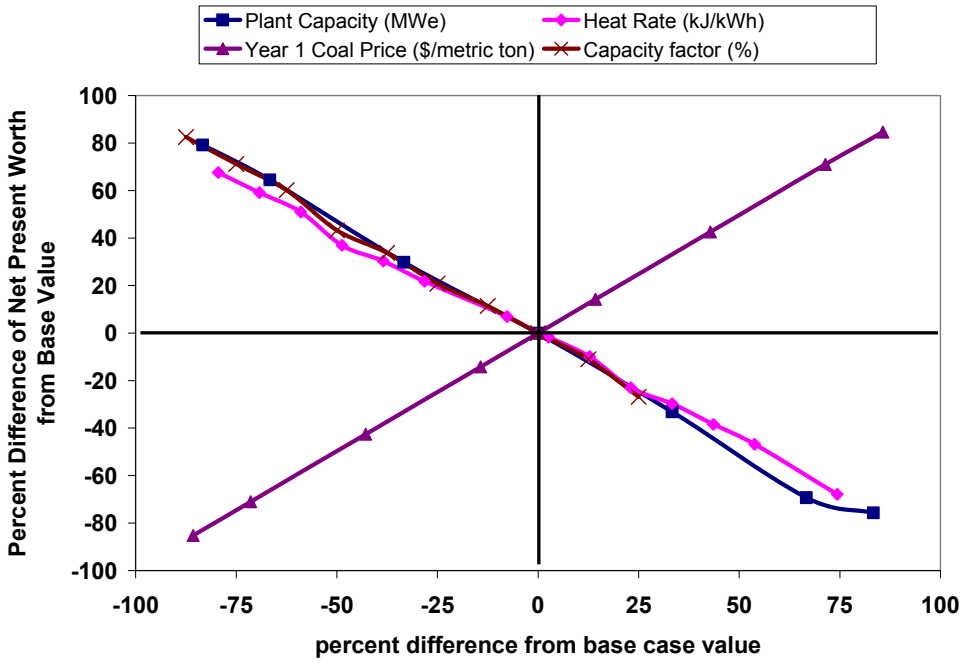

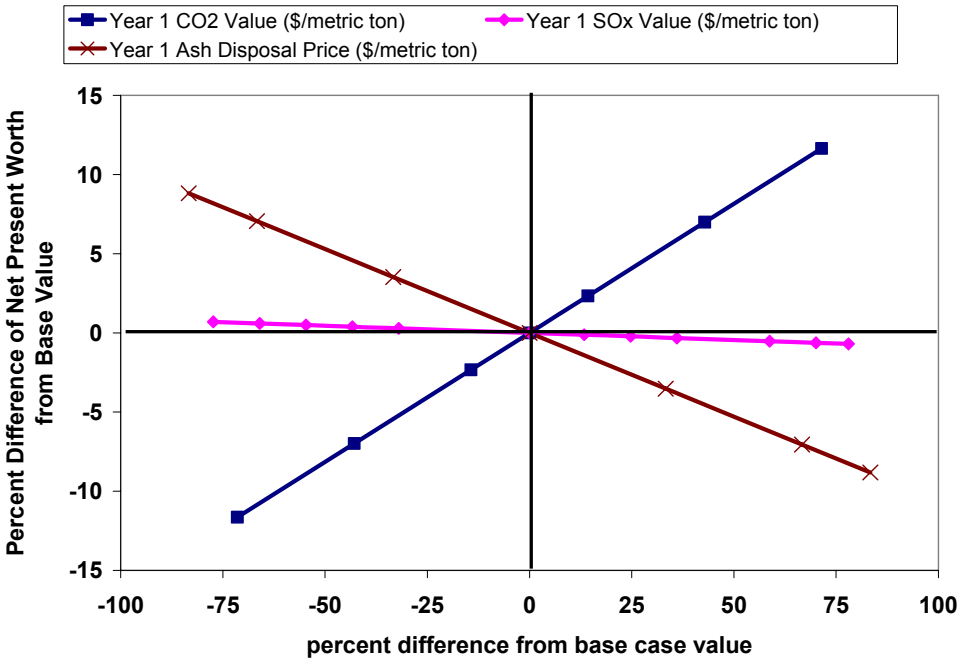
Year 1 CO2 Value ($/metric ton)
Year 1 SOx Value ($/metric ton)
Year 1 Ash Disposal Price ($/metric ton)
Percent Difference of Net Present Worth from Base Value
15
10
5
0
-5
-10
-15
-100
-75
-50
-25
0
25
50
75
100
percent difference from base case value

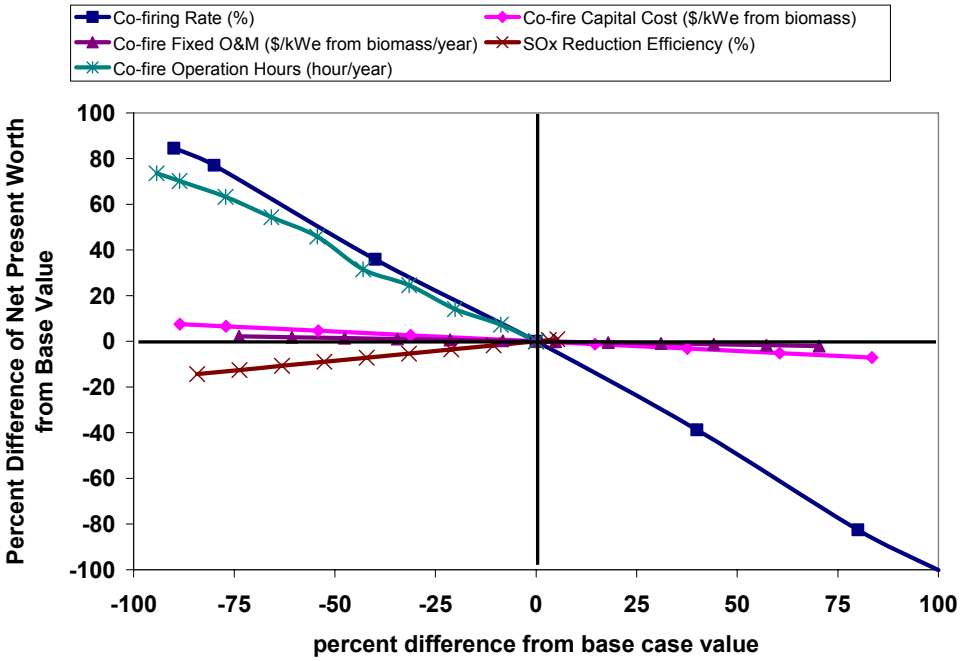
Co-firing Rate (%)
Co-fire Capital Cost ($/kWe from biomass)
Co-fire Fixed O&M ($/kWe from biomass/year)
SOx Reduction Efficiency (%)
Co-fire Operation Hours (hour/year)
Percent Difference of Net Present Worth from Base Value
100
80
60
40
20
0
-20
-40
-60
-80
-100
-100
-75
-50
-25
0
25
50
75
100
percent difference from base case value

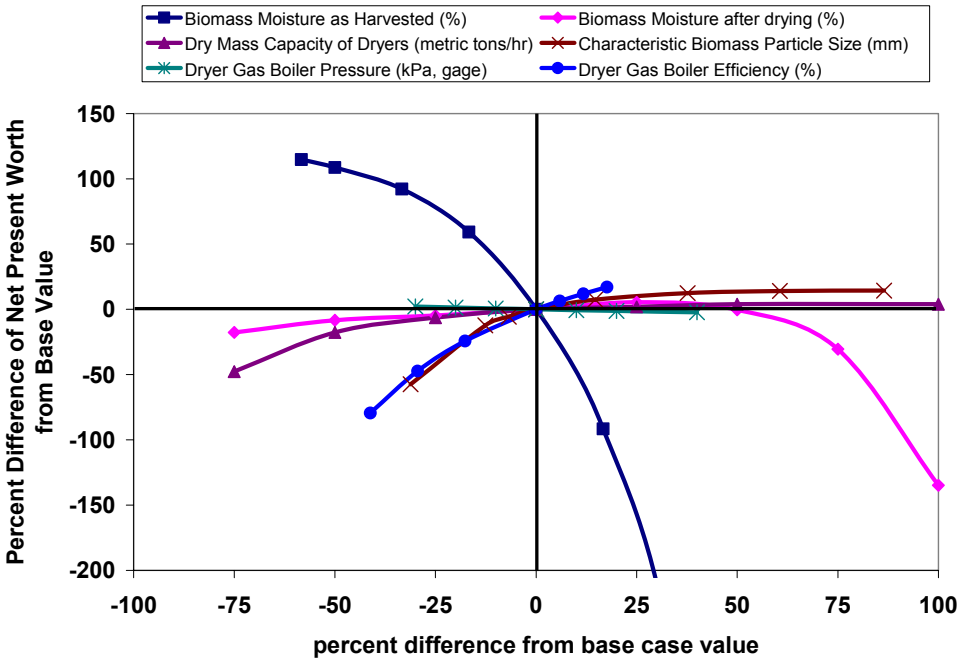
Biomass Moisture as Harvested (%)
Biomass Moisture after drying (%)
Dry Mass Capacity of Dryers (metric tons/hr)
Characteristic Biomass Particle Size (mm)
Dryer Gas Boiler Pressure (kPa, gage)
Dryer Gas Boiler Efficiency (%)
Percent Difference of Net Present Worth from Base Value
150
100
50
0
-50
-100
-150
-200
-100
-75
-50
-25
0
25
50
75
100
percent difference from base case value

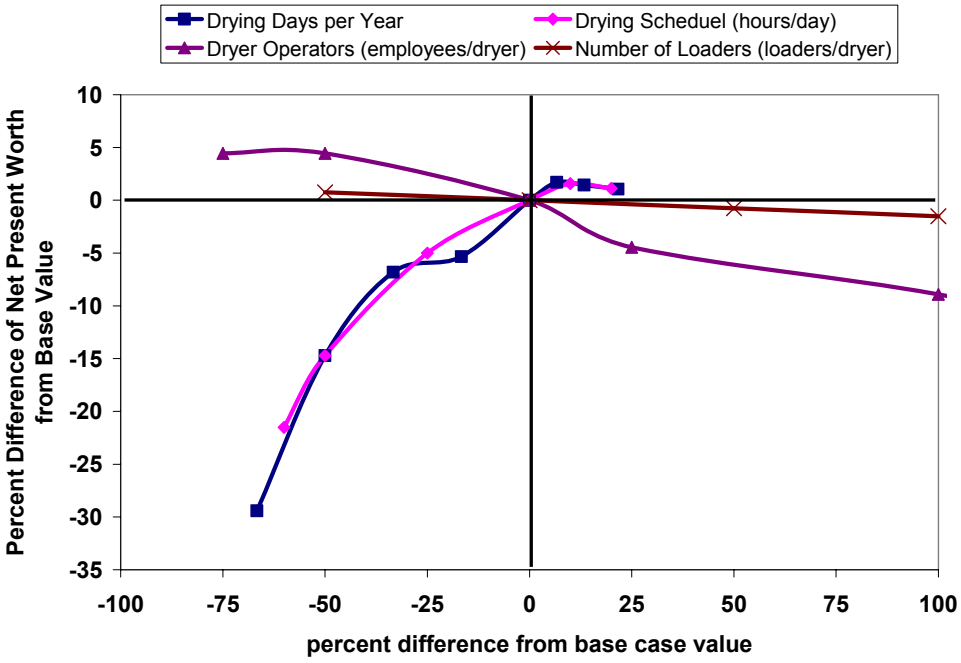
Drying Days per Year
Drying Scheduel (hours/day)
Dryer Operators (employees/dryer)
Number of Loaders (loaders/dryer)
Percent Difference of Net Present Worth from Base Value
10
5
0
-5
-10
-15
-20
-25
-30
-35
-100
-75
-50
-25
0
25
50
75
100
percent difference from base case value

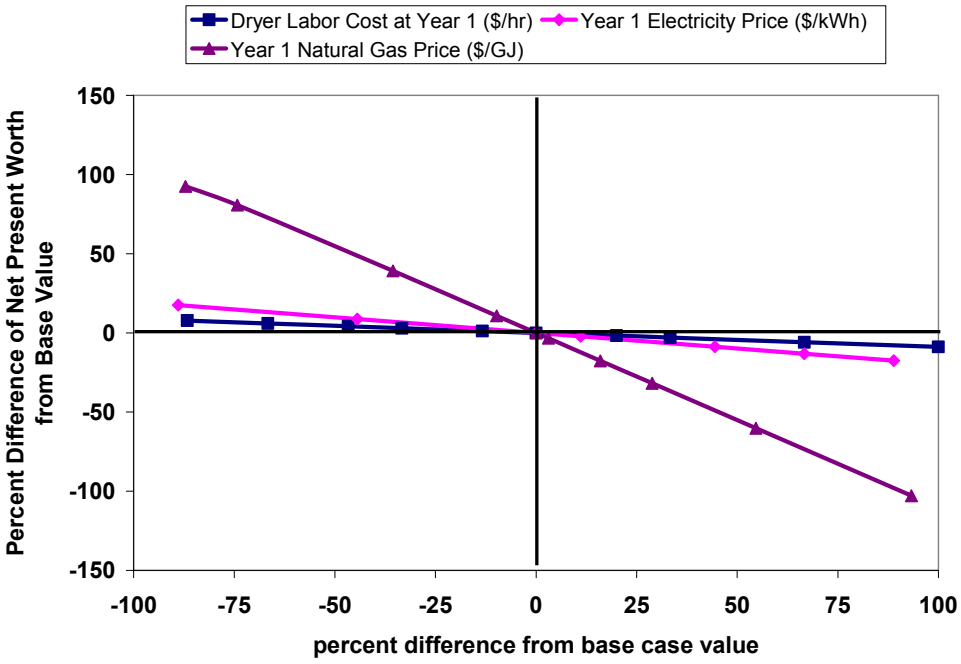
Dryer Labor Cost at Year 1 ($/hr)
Year 1 Electricity Price ($/kWh)
Year 1 Natural Gas Price ($/GJ)
Percent Difference of Net Present Worth from Base Value
150
100
50
0
-50
-100
-150
-100
-75
-50
-25
0
25
50
75
100
percent difference from base case value

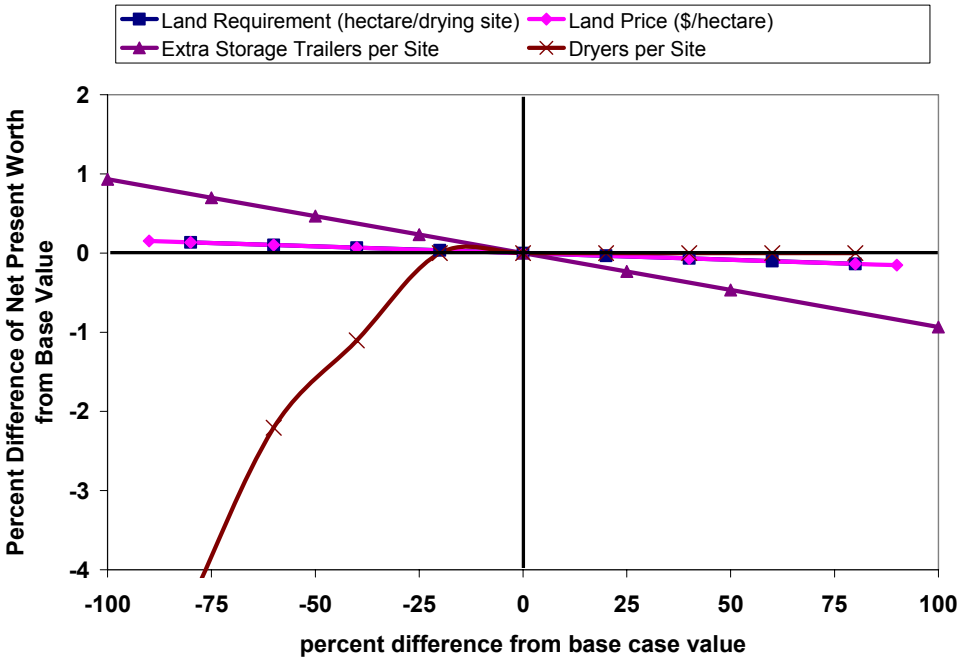
Land Requirement (hectare/drying site)
Land Price ($/hectare)
Extra Storage Trailers per Site
Dryers per Site
Percent Difference of Net Present Worth from Base Value
2
1
0
-1
-2
-3
-4
-100
-75
-50
-25
0
25
50
75
100
percent difference from base case value

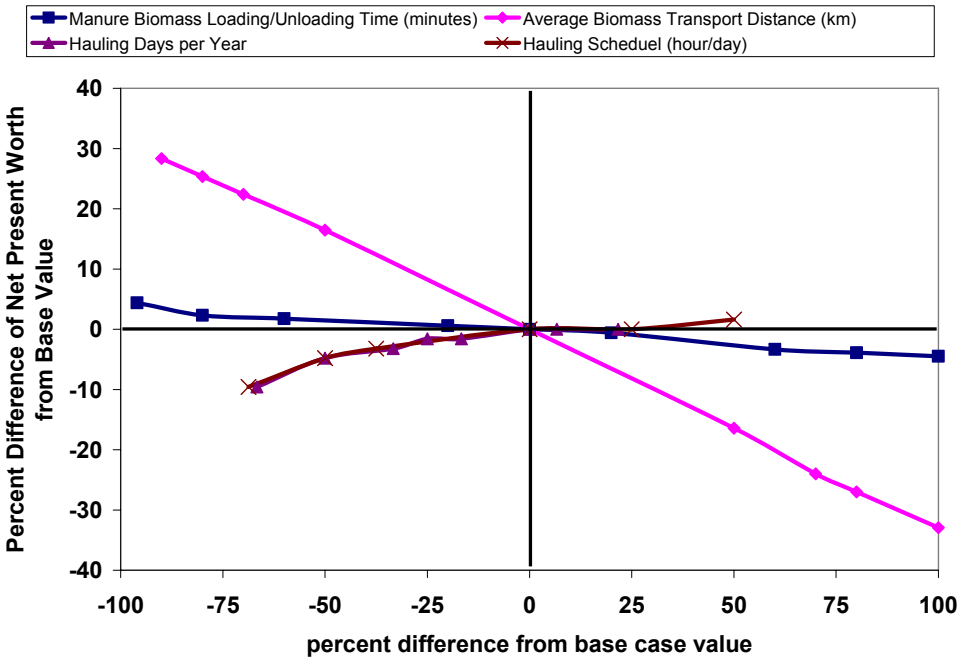
Manure Biomass Loading/Unloading Time (minutes)
Average Biomass Transport Distance (km)
Hauling Days per Year
Hauling Scheduel (hour/day)
Percent Difference of Net Present Worth from Base Value
40
30
20
10
0
-10
-20
-30
-40
-100
-75
-50
-25
0
25
50
75
100
percent difference from base case value

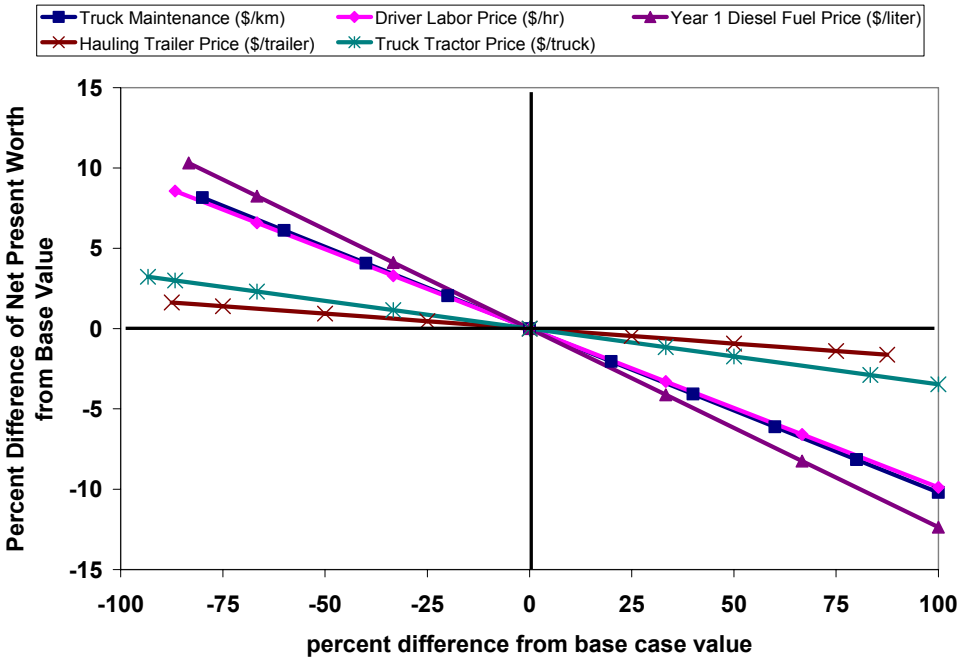
Truck Maintenance ($/km)
Driver Labor Price ($/hr)
Year 1 Diesel Fuel Price ($/liter)
Hauling Trailer Price ($/trailer)
Truck Tractor Price ($/truck)
Percent Difference of Net Present Worth from Base Value
15
10
5
0
-5
-10
-15
-100
-75
-50
-25
0
25
50
75
100
percent difference from base case value

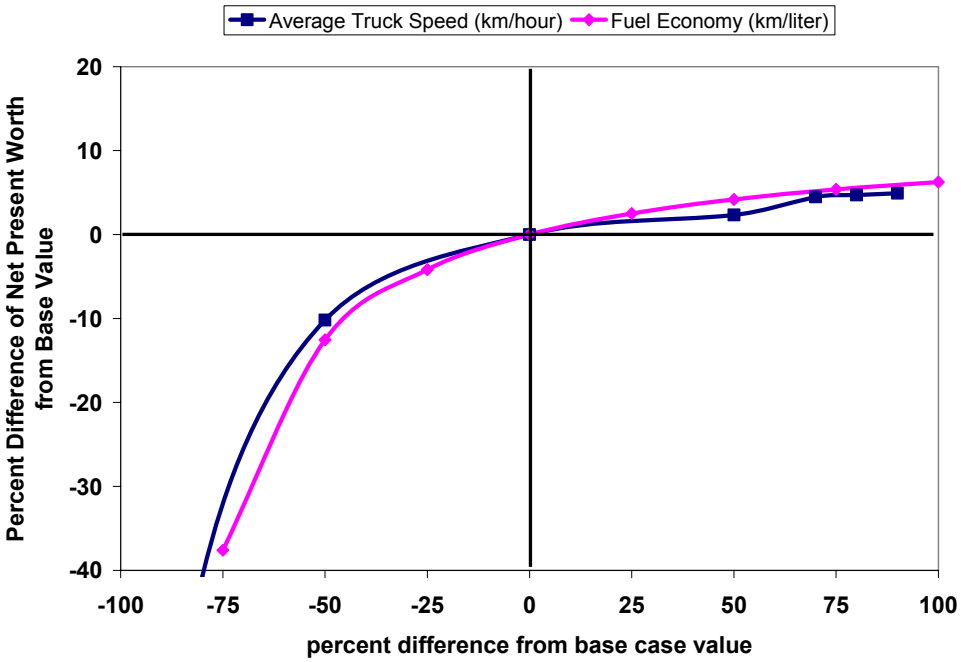
Average Truck Speed (km/hour)
Fuel Economy (km/liter)
Percent Difference of Net Present Worth from Base Value
20
10
0
-10
-20
-30
-40
-100
-75
-50
-25
0
25
50
75
100
percent difference from base case value

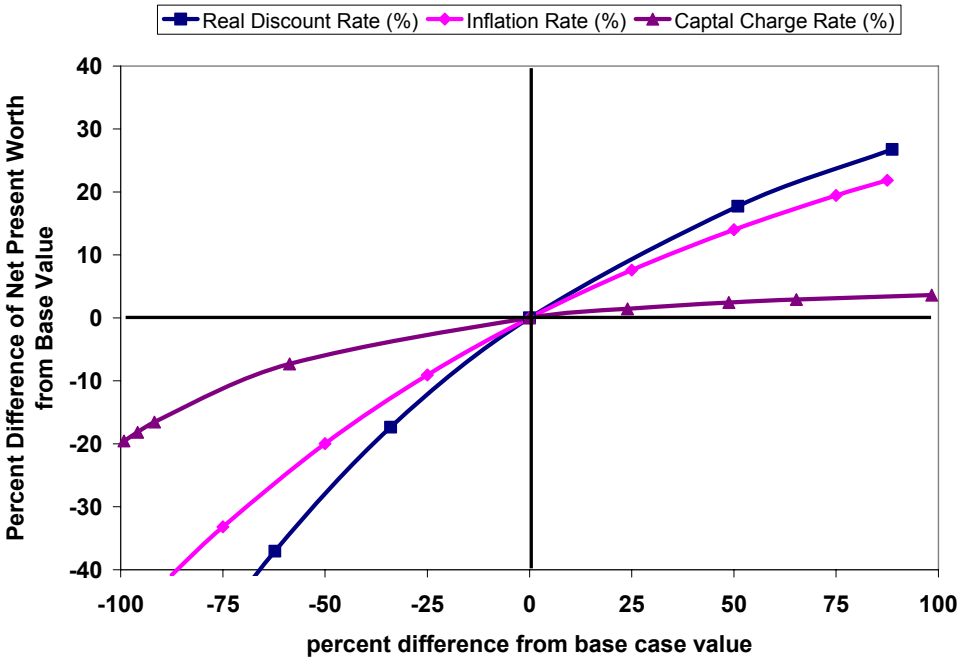
Real Discount Rate (%)
Inflation Rate (%)
Captal Charge Rate (%)
Percent Difference of Net Present Worth from Base Value
40
30
20
10
0
-10
-20
-30
-40
-100
-75
-50
-25
0
25
50
75
100
percent difference from base case value

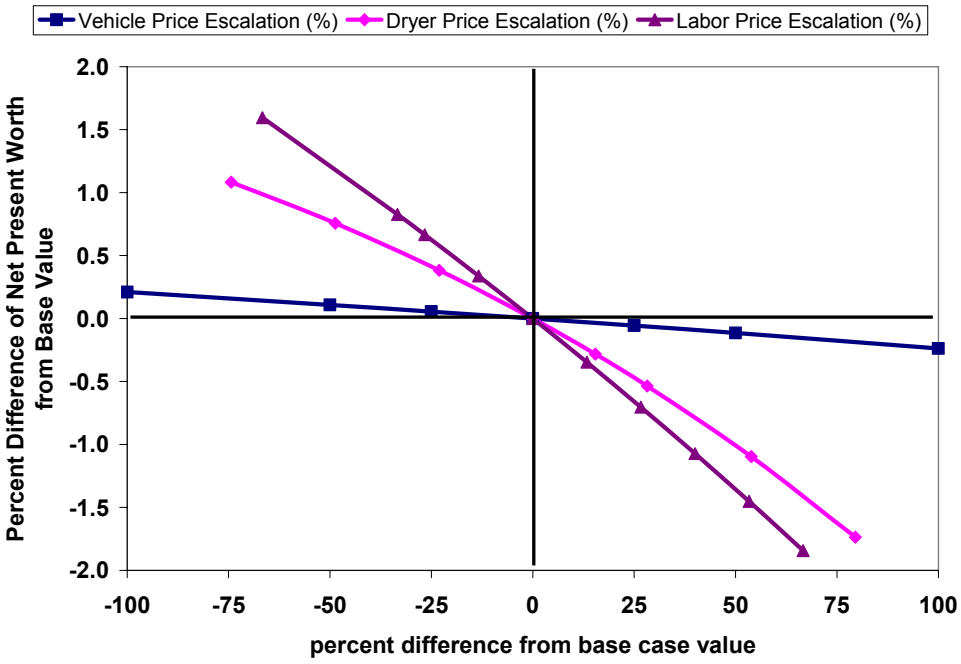
Vehicle Price Escalation (%)
Dryer Price Escalation (%)
Labor Price Escalation (%)
Percent Difference of Net Present Worth from Base Value
2.0
1.5
1.0
0.5
0.0
-0.5
-1.0
-1.5
-2.0
-100
-75
-50
-25
0
25
50
75
100
percent difference from base case value

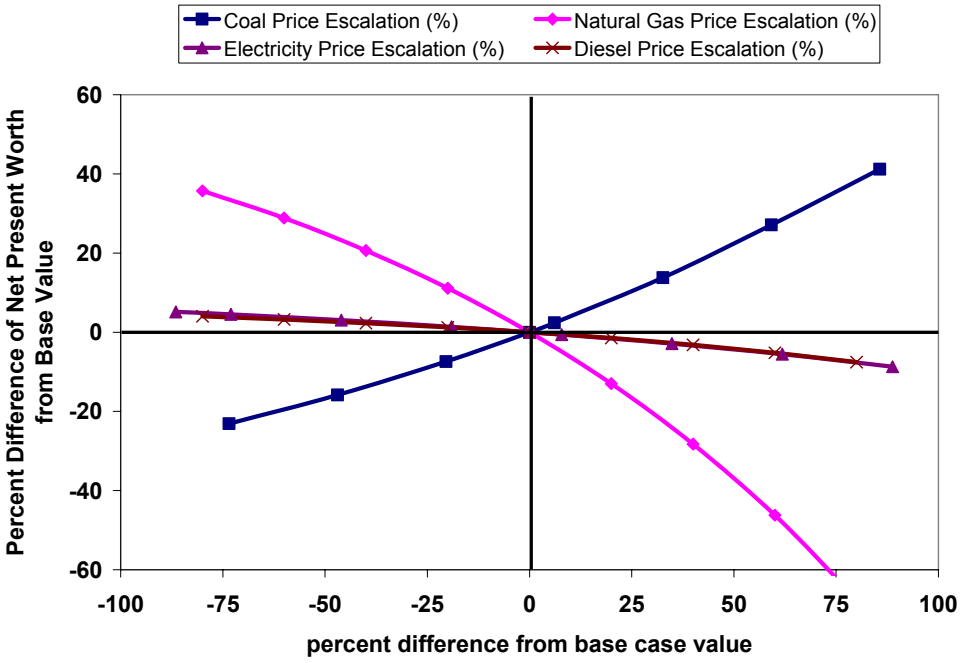
Coal Price Escalation (%)
Natural Gas Price Escalation (%)
Electricity Price Escalation (%)
Diesel Price Escalation (%)
Percent Difference of Net Present Worth from Base Value
60
40
20
0
-20
-40
-60
-100
-75
-50
-25
0
25
50
75
100
percent difference from base case value

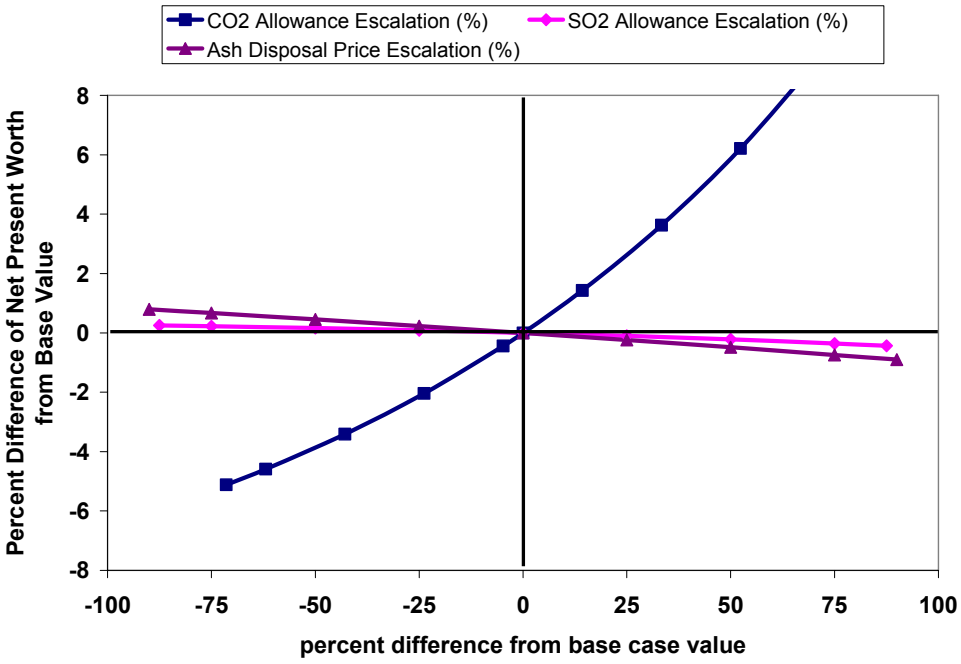
CO2 Allowance Escalation (%)
SO2 Allowance Escalation (%)
Ash Disposal Price Escalation (%)
Percent Difference of Net Present Worth from Base Value
8
6
4
2
0
-2
-4
-6
-8
-100
-75
-50
-25
0
25
50
75
100
percent difference from base case value

APPENDIX D

A FULL SENSITIVITY ANALYSIS OF THE NET PRESENT WORTH OF A MANURE-BASED BIOMASS REBURN SYSTEM

The net present worth (NPW) of a MBB reburn system installed on an existing 300-MW_e coal-fired power plant was found to be -$19.1 million (i.e. overall net cost). The base case input parameters used to arrive at this NPW are listed in Table 6.3 through Table 6.7 and Table 6.11. The following graphs are plotted such that the percent difference of the NPW from the base value of -$19.1 million may be read from the vertical axis and the percent difference of each input parameter may be read from the horizontal axis. As each parameter was varied, all other parameters were assumed to remain at their base values.

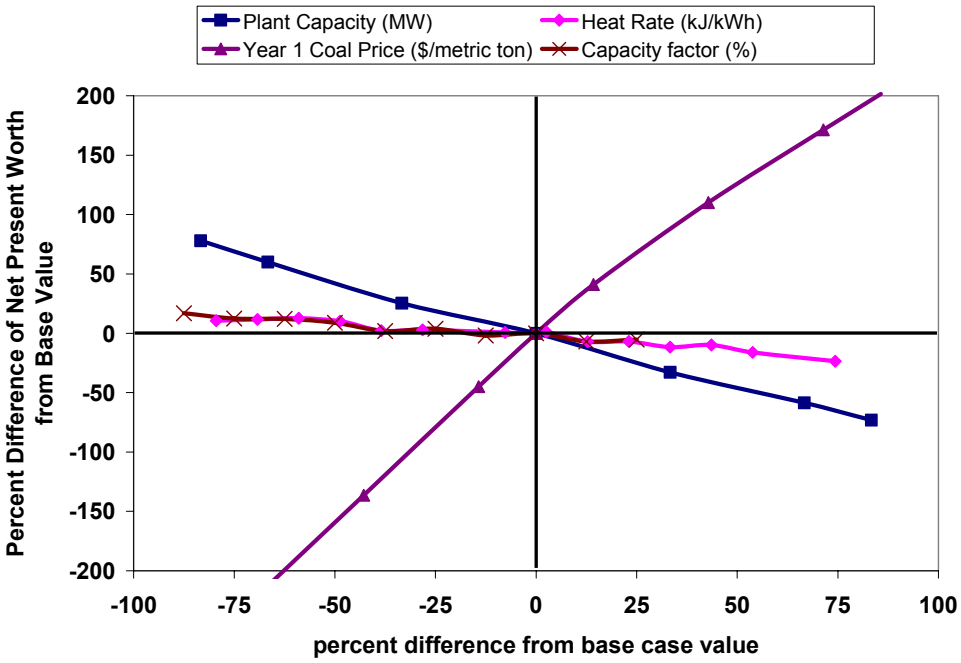

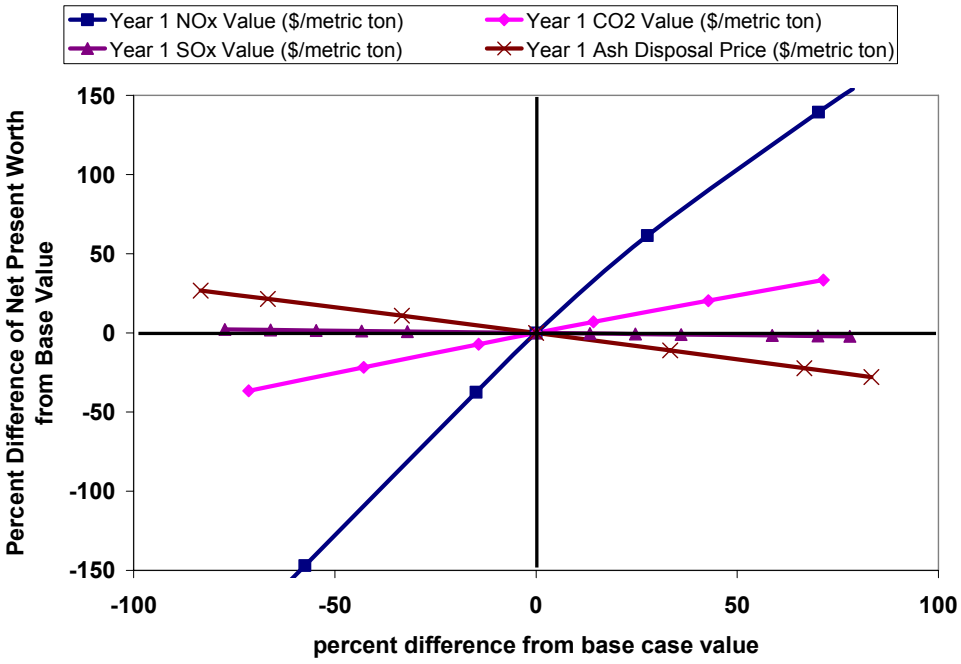
Year 1 NOx Value ($/metric ton)
Year 1 CO2 Value ($/metric ton)
Year 1 SOx Value ($/metric ton)
Year 1 Ash Disposal Price ($/metric ton)
Percent Difference of Net Present Worth from Base Value
150
100
50
0
-50
-100
-150
-100
-50
0
50
100
percent difference from base case value

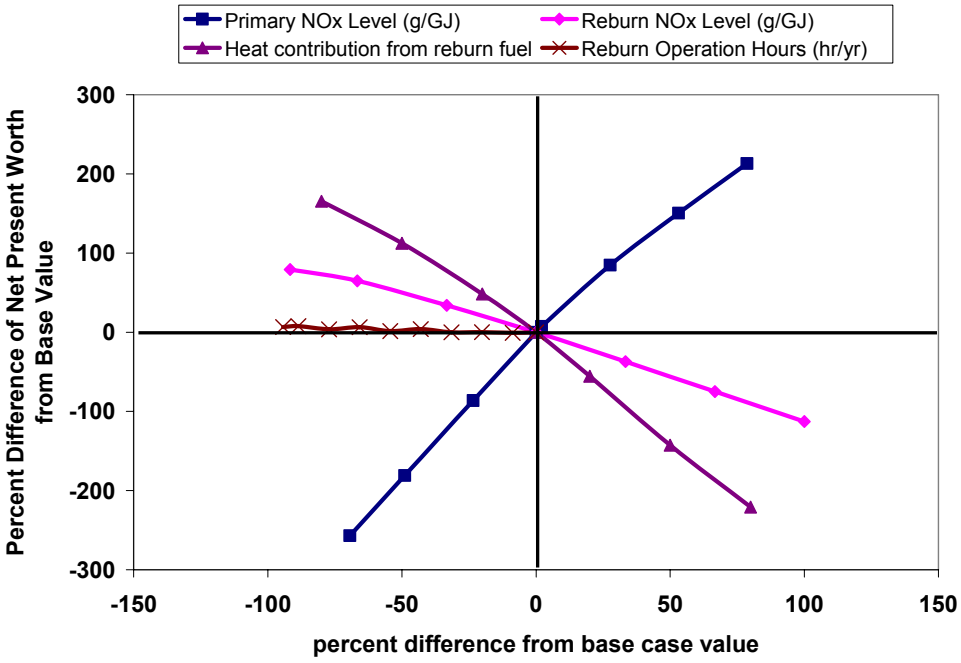
Primary NOx Level (g/GJ)
Reburn NOx Level (g/GJ)
Heat contribution from reburn fuel
Reburn Operation Hours (hr/yr)
Percent Difference of Net Present Worth from Base Value
300
200
100
0
-100
-200
-300
-150
-100
-50
0
50
100
150
percent difference from base case value

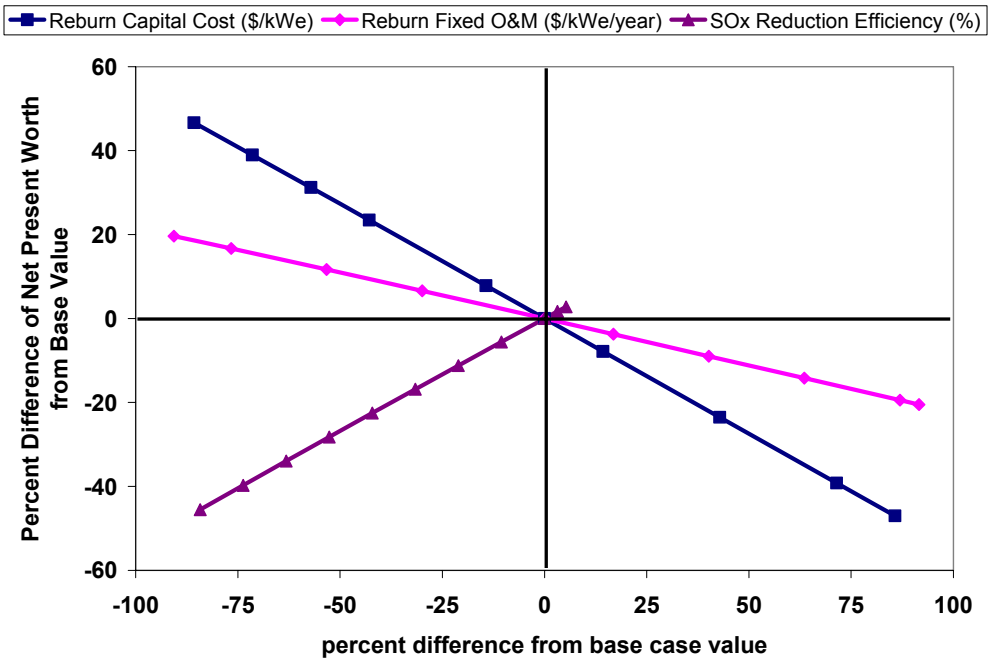
Reburn Capital Cost ($/kWe)
Reburn Fixed O&M ($/kWe/year)
SOx Reduction Efficiency (%)
Percent Difference of Net Present Worth from Base Value
60
40
20
0
-20
-40
-60
-100
-75
-50
-25
0
25
50
75
100
percent difference from base case value

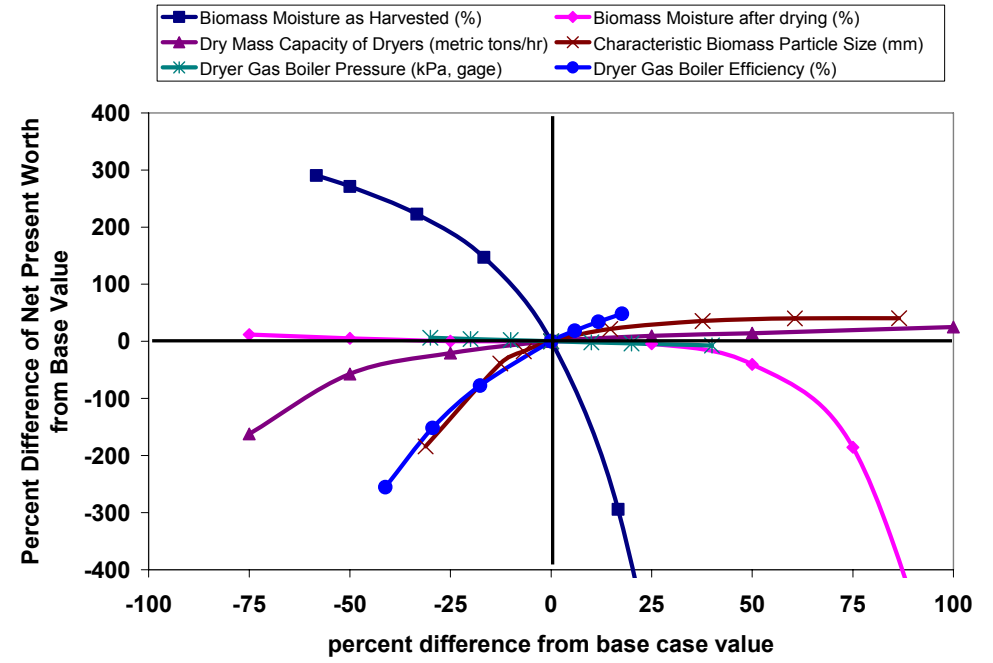
Biomass Moisture as Harvested (%)
Biomass Moisture after drying (%)
Dry Mass Capacity of Dryers (metric tons/hr)
Characteristic Biomass Particle Size (mm)
Dryer Gas Boiler Pressure (kPa, gage)
Dryer Gas Boiler Efficiency (%)
Percent Difference of Net Present Worth from Base Value
400
300
200
100
0
-100
-200
-300
-400
-100
-75
-50
-25
0
25
50
75
100
percent difference from base case value

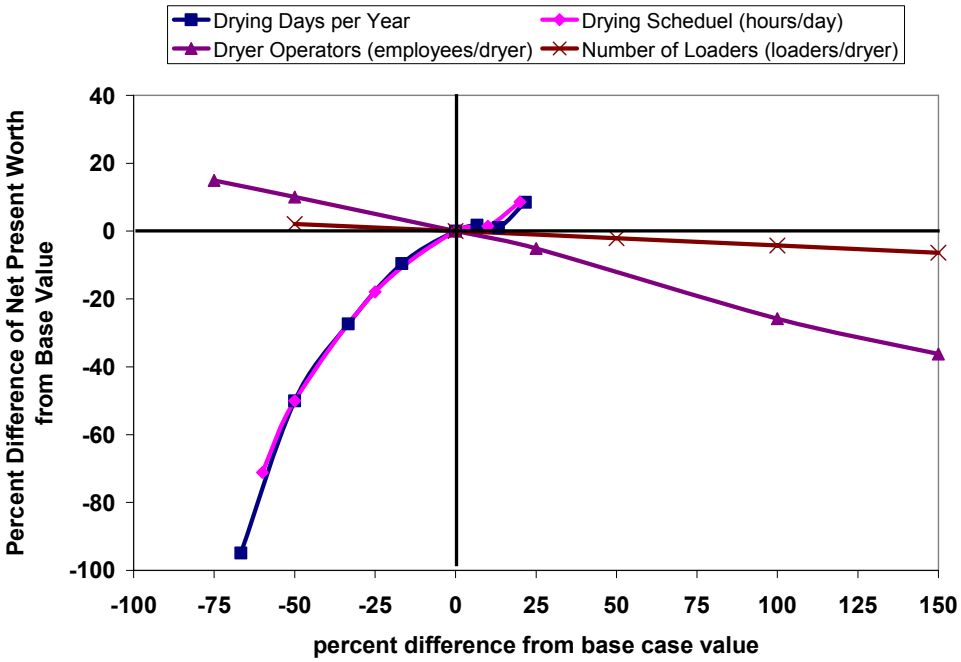
Drying Days per Year
Drying Scheduel (hours/day)
Dryer Operators (employees/dryer)
Number of Loaders (loaders/dryer)
Percent Difference of Net Present Worth from Base Value
40
20
0
-20
-40
-60
-80
-100
-100 -75 -50 -25 0 25 50 75 100 125 150
percent difference from base case value

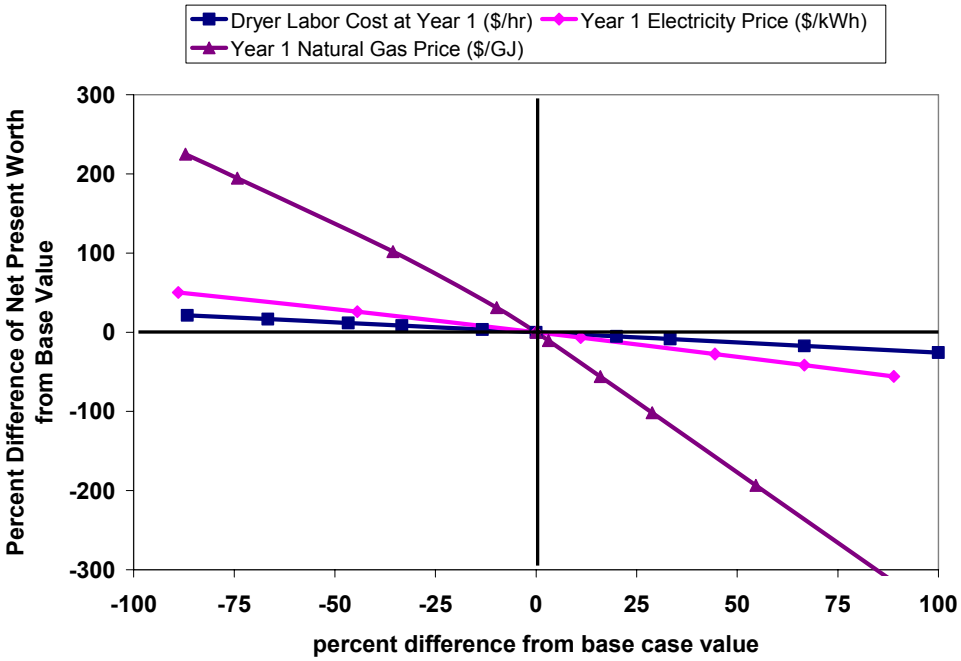
Dryer Labor Cost at Year 1 ($/hr)
Year 1 Electricity Price ($/kWh)
Year 1 Natural Gas Price ($/GJ)
Percent Difference of Net Present Worth from Base Value
300
200
100
0
-100
-200
-300
-100 -75 -50 -25 0 25 50 75 100
percent difference from base case value

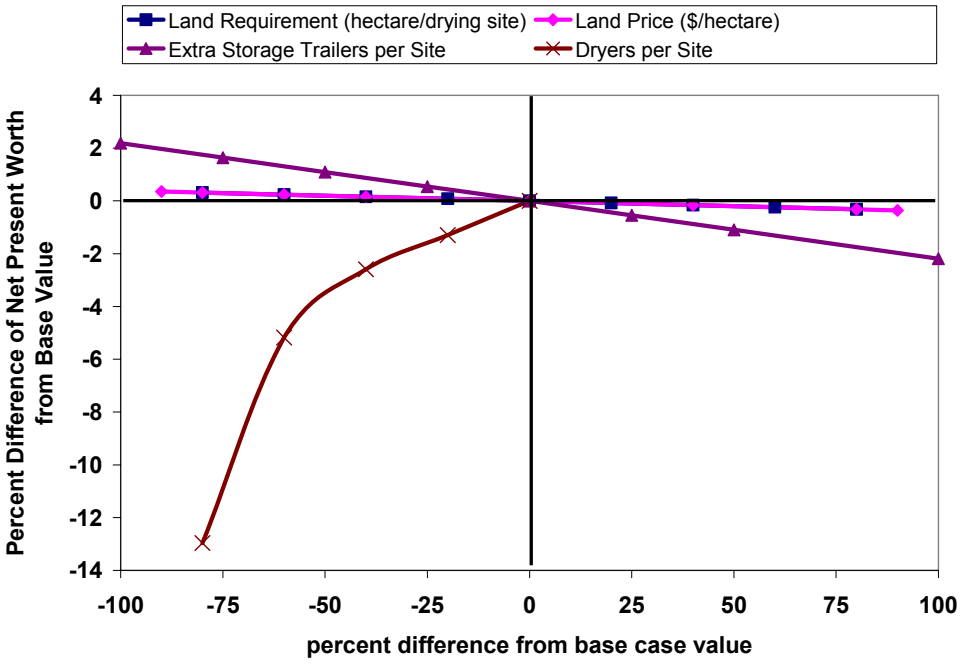
Land Requirement (hectare/drying site)
Land Price ($/hectare)
Extra Storage Trailers per Site
Dryers per Site
Percent Difference of Net Present Worth from Base Value
4
2
0
-2
-4
-6
-8
-10
-12
-14
-100
-75
-50
-25
0
25
50
75
100
percent difference from base case value

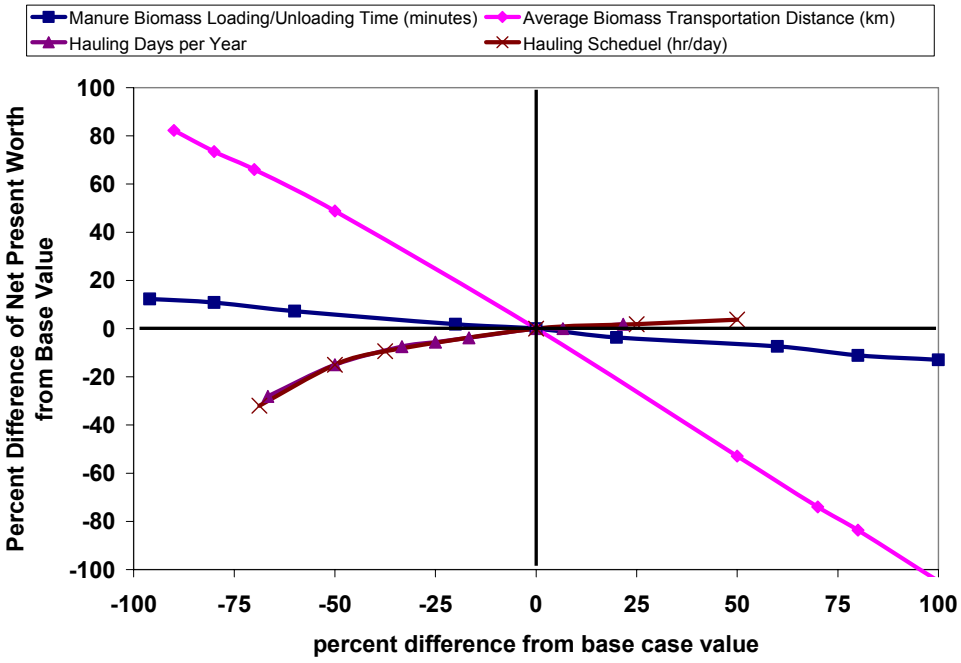
Manure Biomass Loading/Unloading Time (minutes)
Average Biomass Transportation Distance (km)
Hauling Days per Year
Hauling Scheduel (hr/day)
Percent Difference of Net Present Worth from Base Value
100
80
60
40
20
0
-20
-40
-60
-80
-100
-100
-75
-50
-25
0
25
50
75
100
percent difference from base case value

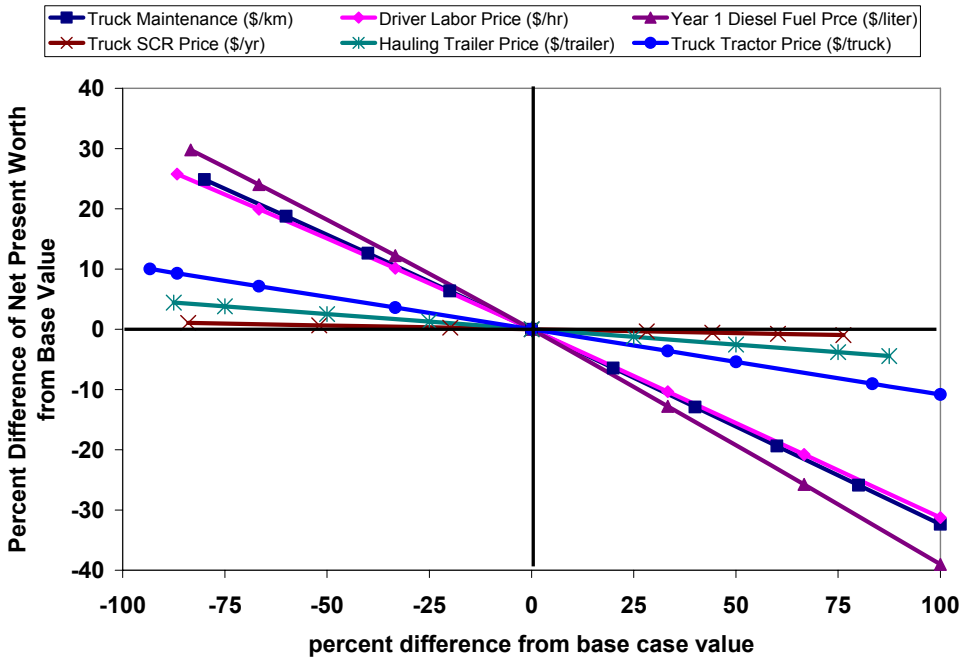
Truck Maintenance ($/km)
Driver Labor Price ($/hr)
Year 1 Diesel Fuel Prce ($/liter)
Truck SCR Price ($/yr)
Hauling Trailer Price ($/trailer)
Truck Tractor Price ($/truck)
Percent Difference of Net Present Worth from Base Value
40
30
20
10
0
-10
-20
-30
-40
-100
-75
-50
-25
0
25
50
75
100
percent difference from base case value

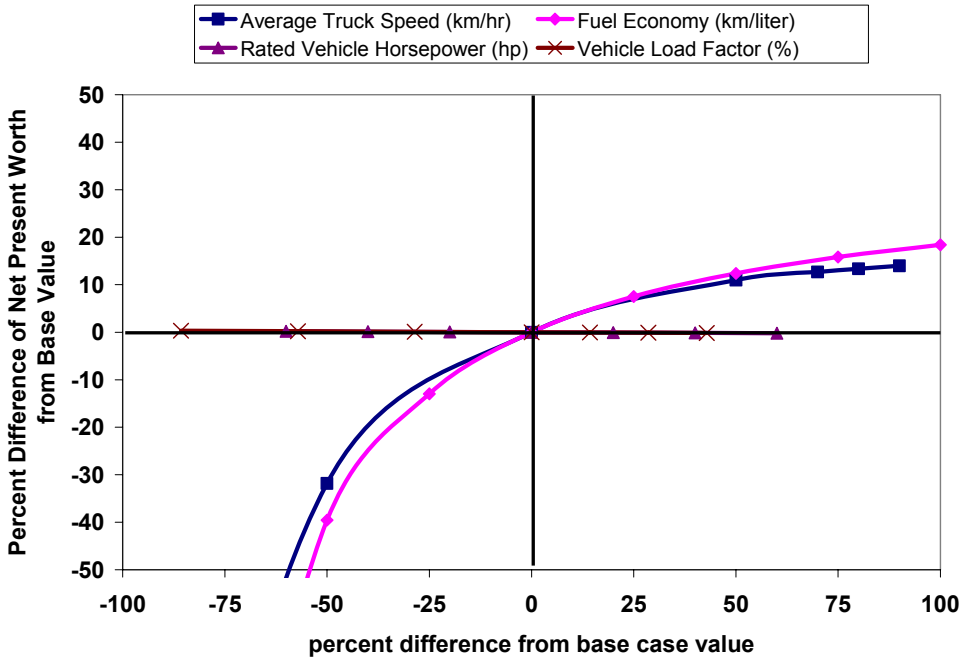
Average Truck Speed (km/hr)
Fuel Economy (km/liter)
Rated Vehicle Horsepower (hp)
Vehicle Load Factor (%)
Percent Difference of Net Present Worth from Base Value
50
40
30
20
10
0
-10
-20
-30
-40
-50
-100
-75
-50
-25
0
25
50
75
100
percent difference from base case value

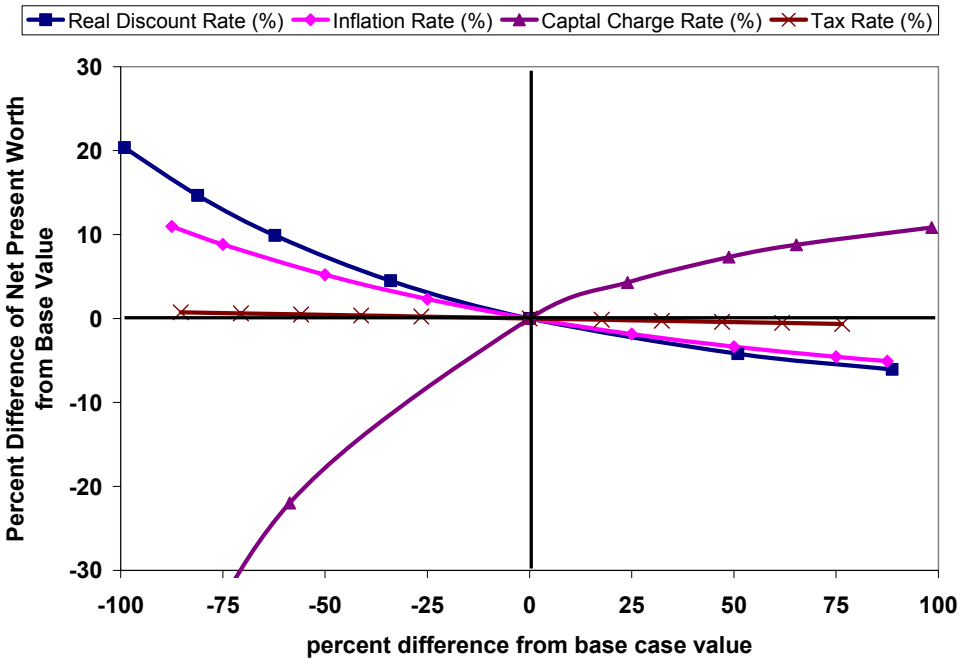
Real Discount Rate (%)
Inflation Rate (%)
Captal Charge Rate (%)
Tax Rate (%)
Percent Difference of Net Present Worth from Base Value
30
20
10
0
-10
-20
-30
-100
-75
-50
-25
0
25
50
75
100
percent difference from base case value

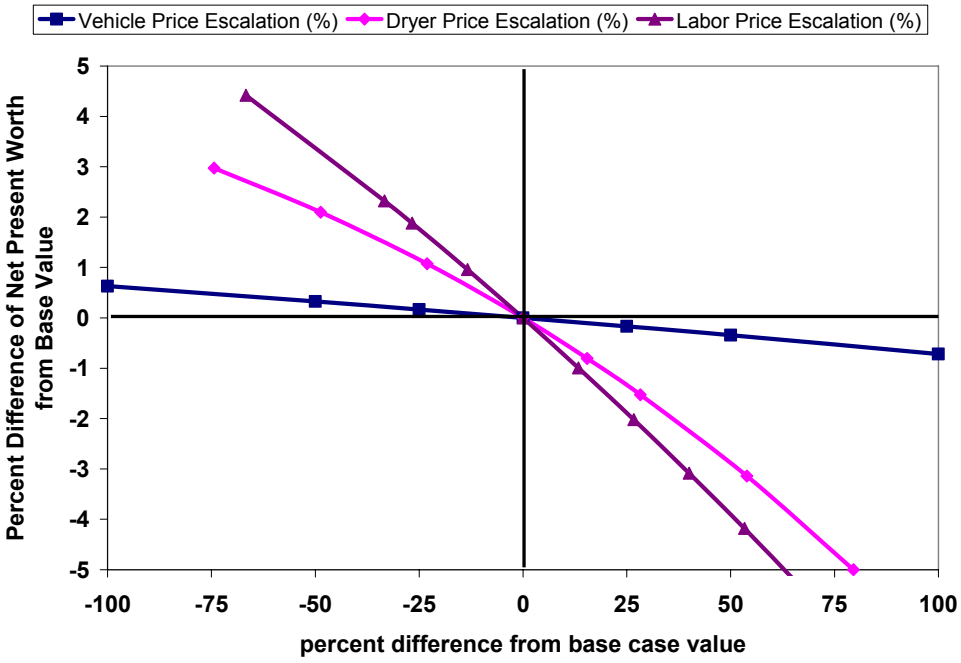
Vehicle Price Escalation (%)
Dryer Price Escalation (%)
Labor Price Escalation (%)
Percent Difference of Net Present Worth from Base Value
5
4
3
2
1
0
-1
-2
-3
-4
-5
-100
-75
-50
-25
0
25
50
75
100
percent difference from base case value

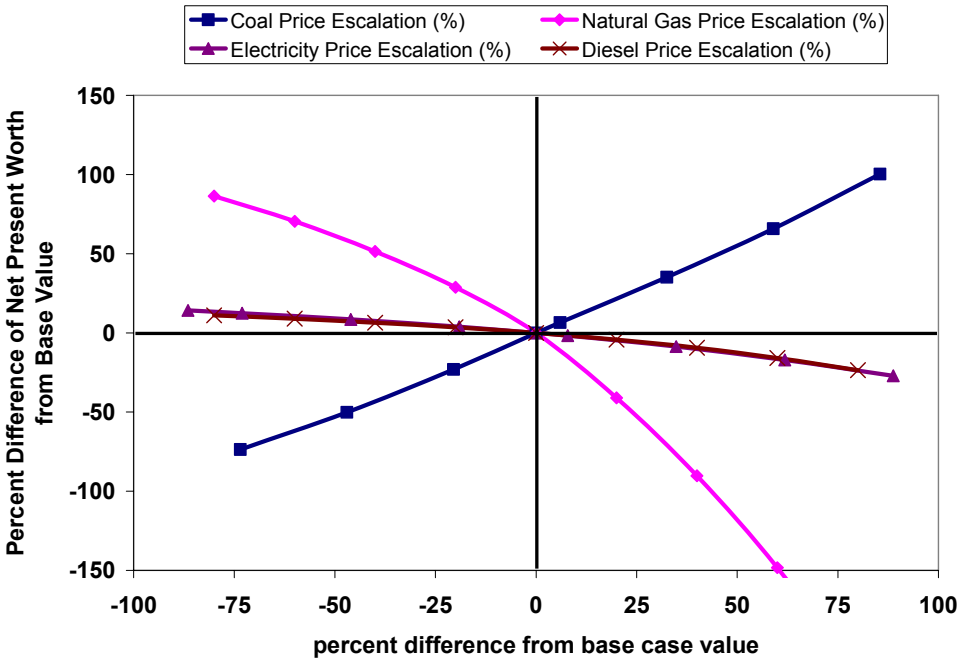
Coal Price Escalation (%)
Natural Gas Price Escalation (%)
Electricity Price Escalation (%)
Diesel Price Escalation (%)
Percent Difference of Net Present Worth from Base Value
150
100
50
0
-50
-100
-150
-100
-75
-50
-25
0
25
50
75
100
percent difference from base case value

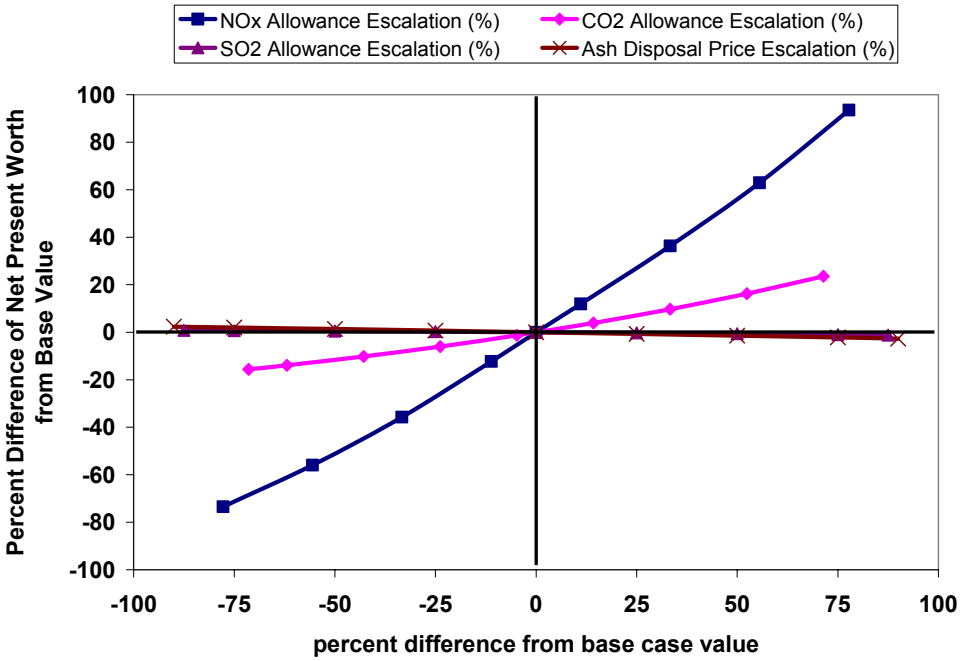
NOx Allowance Escalation (%)
CO2 Allowance Escalation (%)
SO2 Allowance Escalation (%)
Ash Disposal Price Escalation (%)
Percent Difference of Net Present Worth from Base Value
100
80
60
40
20
0
-20
-40
-60
-80
-100
-100
-75
-50
-25
0
25
50
75
100
percent difference from base case value

VITA

Name: Nicholas Thomas Carlin

Address: Texas A&M University
Department of Mechanical Engineering
3123 TAMU
College Station TX 77843-3123

E-mail Address: ncarlin50@hotmail.com

Education: B.S., Mechanical Engineering, with honors, The University of Texas at Austin
M.S., Mechanical Engineering, Texas A&M University at College Station

Publications: Carlin NT, Annamalai K, Harman W, Sweeten JM. (2009). The economics of reburning with cattle manure-based biomass in existing coal-fired power plants for NO_x and CO_2 emissions control. Accepted by *Biomass & Bioenergy* in March 2009. In press.

Carlin NT, Annamalai K, Oh H, Gordillo Ariza G, Lawrence B, *et al*. (2008). Co-combustion and gasification of coal and cattle biomass: a review of research and experimentation. Accepted by *Progress in Green Energy* in January 2008. In press.

Carlin NT, Annamalai K, Sweeten JM, and Mukhtar S. (2007). Thermo-chemical conversion analysis on dairy manure-based biomass through direct combustion. *International Journal of Green Energy* 4(2):133-159.

Carlin NT, Annamalai K, Sweeten JM, and Mukhtar S. (2007). Utilization of latent heat derived from vaporized wastewater in high moisture dairy manure combustion schemes. International Symposium on Air Quality and Waste Management for Agriculture, September 15-19, 2007: Broomfield, CO.

Annamalai K, Carlin NT, Oh H, Gordillo Ariza G, Lawrence B, *et al*. (2007). Thermo-chemical energy conversion using supplementary animal wastes with coal. Proceedings of the IMECE, 2007 ASME International Mechanical Engineering Congress and Exposition, November 11-15, 2007: Seattle, WA, USA.